Author:
Bousri, Yahia

Title:
Experimental and analytical study of reinforced concrete external beam-column subjected to cyclic loading.

EXPERIMENTAL AND ANALYTICAL STUDY OF REINFORCED CONCRETE EXTERNAL BEAM-COLUMN CONNECTIONS SUBJECTED TO CYCLIC LOADING

by

Yahia Bousri

A thesis submitted to the University

of Bristol in accordance with the requirements

for the Degree of Doctor of Philosophy

in the Faculty of Engineering

March 1994

ABSTRACT

The performance of beam-column joints in reinforced concrete structures, subjected to cyclic loading, is of critical importance in the design of structures for seismic resistance. In this thesis experiments on four sub-assemblies, representing exterior joints and subjected to cyclic loading, are presented. In particular, the performance of a new design of transverse reinforcement, consisting of overlapping U-stirrups in place of conventional stirrups, is considered. Mechanisms of joint shear resistance, suggested by others, are examined. Rules published in various design codes are also compared.

An extensive finite element study of the non-linear behaviour of reinforced concrete joints was carried out with the objectives of assessing the capability of this form of analysis under non-linear cyclic conditions, and to examine the distribution of stress and strain along the bars and in the concrete within the joint region. This study assisted considerably in understanding the behaviour of the joints under these conditions of loading.

TO MY BELOVED CHILDREN SAMI AND SARAH

AND THE MEMORY OF BOTH MY PARENTS

ACKNOWLEDGEMENTS

The research described in this thesis was carried out in the Department of Civil Engineering of the University of Bristol.

The project was carried out under the supervision of Dr J.W. Smith, and his continual guidance and encouragement is gratefully acknowledged.

The author would like to thank the technical staff of the Department of Civil Engineering who were involved in the experimental research, particularly Alun Young.

The assistance of Dr Ian Stewart from the computer centre advisory staff is acknowledged.

Financial assistance for the author was provided by the Algerian Government together with the British Council.

Finally without financial support during the writing up of this thesis from Dr. J. W. Smith, this work would not have been possible.

MEMORANDUM

The accompanying dissertation entitled "Experimental and Analytical Reinforced Concrete External Beam-Column Connections Subjected to Cyclic Loading" is submitted for the degree of Doctor of Philosophy in the Faculty of Engineering at the University of Bristol.

The dissertation is based on independent work carried out by the author between October 1988 and February 1994 under the supervision of Dr J. W. Smith.

The work and ideas are original and all contributions from others are duly acknowledged in the text by references.

This dissertation has not previously been submitted for a degree or diploma at this, or any other, University or Examining Board.

Signed .....

YAHIA BOUSRI

(March 1994)

TABLE OF CONTENTS

LIST OF FIGURES

FIGURES OF CHAPTER SIX

FIGURES OF APPENDIX A

LIST OF TABLES

NOTATION

A_b	gross area of reinforcing bar
A_g	gross cross-section area of the column
A_p	Provided anchorage length
A'_s	area of compression reinforcement
A_s	area of tension reinforcement
a	depth of equivalent rectangular stress block (*A*ppendix)
a_b	depth of equivalent rectangular stress block in the column at balanced conditions (*A*ppendix)
a_{ij}	term in a matrix *[A]* located in row *i* and column *j*
{a}	vector of nodal displacement
b	width of a section
b_b	width of beam section
b_c	width of column section
C_{colt}	compressive force in column concrete above the joint
C_{colb}	compressive force in column concrete below the joint
C_c	total compression force in concrete
C_s	compression force in compression reinforcement
D_c	diagonal compressive force in joint concrete due to direct strut mechanism
D_s	diagonal compressive force in joint concrete due to joint truss mechanism
$[D]$	global reinforced concrete stiffness matrix
$[D_c]$	uncracked concrete stiffness matrix (FE)
$[D'_c]$	cracked concrete stiffness matrix (FE)
$[D_s]$	steel stiffness matrix in local coordinates (FE)
$[D_s]$	steel stiffness matrix in global coordinates (FE)
d_b	nominal diameter of reinforcing bar

d_{eff}	effective depth of a section
d	distance from extreme compression fibre to centroid of tension reinforcement
d'	distance from extreme compression fibre to centroid of compression reinforcement
E	modulus of elasticity
E_c	elasticity modulus of concrete
E_s	elasticity modulus of reinforcement
E_s'	elasticity modulus of compression reinforcement
$\{^{e}\}$	vector relating to a single element
EPEL	elastic strain in reinforcement (FE)
EPL*A*	plastic strain in reinforcement (FE)
f_c'	concrete compressive strength
f_{cu}	concrete tensile strength
f_y	yield stress of reinforcement
f_s	stress in tension steel
f_s'	stress in compression steel
f_c	uniaxial compressive strength (FE)
f_t	uniaxial tensile strength (FE)
f_h	stress developed in reinforcing bar by standard hook
$\{f\}$	vector of nodal forces
h_c	overall depth of the column
h_b	overall depth of the beam
k	$(= x/d)$
LVDT	linear variable displacement transducer
l_c	storey height above joint
l_c'	storey height below joint
l_d	development length of reinforcing bar
$\{l\}$	vector direction cosines

M_y	beam yielding moment
M_b	moment capacity of column at ultimate balanced conditions (*A*ppendix)
M_{colb}	column bending moment below joint
M_{colt}	column bending moment above joint
M_u	ultimate resistance moment of cross-section (without material strength reduction)
N	axial force in column
N_u	applied axial load in column
N_b	column axial load to cause balanced failure (*A*ppendix)
n	$(= A_{st}/A_{sv})$ number of layers of links in a joint between the beam tension and compression reinforcement
p	applied load at the beam tip
r_1, r_2	failure surfaces' functions
s	spacing between sets of confining hoops
T	force in tension reinforcement
$[T]$	transformation matrix
U	energy dissipation
U_i	energy dissipation at cycle i
U_y	energy dissipation at yield cycle
u, v, w	displacement along x, y and z axes
V	reaction forces (shear) in column
V_b	shear force in beam at the face of column
v_{jh}	average nominal shear stress on the joint core
V_c	shear in column at the column-joint interface
V_{ch}	horizontal shear resisted by joint concrete direct strut mechanism
V_{colt}, V_{colb}	column shear above and below joint
V_{cv}	vertical shear resisted by joint concrete mechanisms

V_j	horizontal shear applied to joint core
V_{jv}	vertical shear applied to joint core
V_{sh}	horizontal shear resisted by joint truss mechanism
v_r	volume ratio of reinforcement
X, Y, Z	coordinates axes of cartesian coordinate system
x	neutral axis depth
x, y, z	cartesian coordinates
$\{i\}, x_i$	indicates quantities associated with node i
$[]^T$	transpose matrix
α	angle of orientation of plane of rupture; tension stiffening factor (FE)
α	overstrength factor applied to beam reinforcement nominal yield strength
β	joint type factor
β_c	inclination of direct concrete strut to horizontal
β_t	inclination of applied joint shear to horizontal
β	shear coefficient (FE)
β_c	shear coefficient for closed crack (FE)
β_t	shear coefficient for open crack (FE)
δ	interface normal displacement
γ, γ_{xy}	shear strain
γ	joint confinement factor
Δ_c	interstorey drift of column
ϕ	$(= U_i/U_y)$
$\Delta F_b, \Delta F_t$	force transferred from beam bars to joint core by bond at bottom and top of joint
ΔF_i	force transferred to joint core by bond from column bars adjacent to the face of joint
δ_i	displacement at cycle i

δ_y	displacement at yield cycle
ε	strain
ε^{ck}	crack strain
ε_{cr}	cracking strain in tension
ε_s	strain in tension reinforcement
ε'_s	strain in compression reinforcement
ε_u	steel ultimate strain
ε_x, ε_y, ε_z	strain (normal) components
ε_y	yield strain of reinforcement
ν	Poisson's ratio
σ	stress
σ_x, σ_y, σ_z	components of normal stresses
σ_{xp}, σ_{yp}, σ_{zp}	component of principal bi-axial stresses
σ_1, σ_2, σ_3	principal stresses
τ, τ_{xy}	shear stress
η	angle of similarity of principal stresses
θ	interface element orientation angle
θ, ϕ	rebar orientation angles
$\theta_x, \theta_y, \theta_z$	rotations about x, y and z axes
μ	$(= \delta_i/\delta_y)$, displacement ductility factor
$\Sigma\mu$	cumulative displacement ductility factor
x	neutral axis depth
x_b	neutral axis depth in the column at balanced conditions
β_1	$(= a/x)$ (Appendix)

CHAPTER ONE INTRODUCTION

1.1 BEHAVIOUR OF REINFORCED CONCRETE JOINTS IN EARTHQUAKES

In countries prone to severe earthquakes, designers of multistory buildings have long recognized the need to provide substantial lateral resistance to seismic ground motions by means of a rational structural form.

In Algeria, reinforced concrete is the most commonly used material for structures of this type, while the choice of structure lies between moment-resisting frames, shear wall structures, or some combination of those two types.

The commonly accepted philosophy of aseismic design recognizes that elastic response will be exceeded under moderately severe earthquake motions in structures designed to the base shear coefficients specified by building codes [NZS4203 (1976) and SEAOC (1973)]. Well built structures are therefore required to possess sufficient ductility (that is the ability to deform plastically without losing significant strength, to dissipate earthquake energy in a predictable and stable fashion). The guiding principle is that in a severe earthquake a building may be irreparably damaged, but should not collapse in any circumstances.

In reinforced concrete frames this ductility is usually achieved by inelastic rotation of plastic hinges in the beams, normally adjacent to the column faces as shown in Fig.1.1. The "weak beam/strong column" principle is intended to ensure that ductility is

distributed evenly throughout a building rather than concentrated unpredictably at a single floor level.

Both the philosophy and the means of achieving ductility in beam plastic hinges are well understood [Park and Paulay (1975)], and designers and codes [ACI (1977) and DZ3101 (1978)] take care to achieve this by, for example, ensuring that the ratio of compressive reinforcement to tensile reinforcement shall not be less than 0.75, and by providing generous stirruping in the critical regions (connection area) to carry the shear and to confine the flexural bars.

Having provided in the beam hinges the capacity to undergo the necessary plastic deformation in order to achieve efficient energy dissipation, the designers must further ensure the integrity of the structure by eliminating the possibility of brittle behaviour or premature failure at other less desirable locations e.g. the joint regions.

Recent experimental investigations of reinforced concrete beam-column joints have indicated that when the plastic hinges form in the members adjacent to the connections (near the column face) the joint core may be subjected to extremely high shear forces and bond stresses. Such subassemblies, when subjected to large load reversals, have been observed to undergo considerable degradation in stiffness and strength, and the plastic hinges tend to form near the column face. A plastic hinge forming at this location usually causes a loss of stiffness and strength in the joint. Under cyclic loading the concrete in the joint core may break down due to alternating diagonal tension cracks and bond forces, and the bars may slip through the

joint core due to bond deterioration. Consequently, substantial transverse reinforcement is required in the joint region to ensure its integrity.

In the design of framed structures it is commonly assumed that the beams and columns are rigidly interconnected and that the joints are as strong as the connected members. However, in the past the behaviour of beam-column connections was not taken into account. From various investigations and experience in earthquake, it has emerged, that in certain cases the strength of structural joints may be lower than that of the connected members [Nilsson Ingvar (1973), and Stroband and Kolpa (1981)]. Since the safety of framed structures is partly dependent on the behaviour of the joints, it is important that the designers should have a proper conception of this behaviour and of how the reinforcement is to be detailed.

Extensive research in many parts of the world has resulted in imposed rules governing aseismic design of reinforced concrete joints (American Concrete Institute, ACI and New Zealand Draft). However, there are several problems and uncertainties which require further investigations. These include: reinforcement congestion in joint region; need to keep beam plastic hinges away from the column face; lack of verification of effectiveness of recent design rules in major earthquakes; uncertainty about advantage or problem of axial load; uncertainty about the proportion of overall ductility in terms of rotation of connection attributed to the joint; need to improve analytical modelling of such sub-assemblies.

1.2 MECHANISMS OF JOINT SHEAR RESISTANCE

1.2.1 General

Understanding of the behaviour of reinforced concrete joints under cyclic loading has developed over many years as a result of substantial laboratory research and observations of performance in real earthquakes. The following descriptions of the mechanism of joint shear resistance is based on work done by Park (1975), Paulay (1977), Beckingsale (1980) and others.

1.2.2 Actions on Plane Frame Exterior Joint

In order to study the strength of a beam-column joint, it is necessary firstly to define the forces acting on the joint under severe seismic loading. For an exterior joint of a plane frame having plastic hinges located in the beam adjacent to the column faces, the horizontal shear force acting on the joint may be derived from the forces in the beam flexural bars, less the shear force in the column above or below the joint, as demonstrated below.

Using the notation shown in Fig.1.2, the horizontal shear force acting above a horizontal plane passing across the beam-column joint between the layers of top and bottom bars is :

$$V_{jh} = C - Vcol_t \qquad (1\text{-}1)$$

From equilibrium of the beam section to the right of the joint, the total compression force C at the top of the right-hand beam in both steel and concrete is equal to the tensile force T at the bottom of the beam.

$$C = T = A_s \cdot f_s \qquad (1\text{-}2)$$

Where :- A_s is the area of bottom reinforcement

- f_s is the stress in it.

(This is based on the assumption that $Vcol_t = Vcol_b$)

Under severe seismic loading the beam reinforcement will yield, and if the ductility demand on the plastic hinges is sufficient, some strain hardening can also be expected. To allow for possible strain-hardening, and also for the likelihood that the actual yield strength for the bars will exceed the ideal yield strength; f_y, it is prudent that the input shear for joint design should be based on a design strength for the beam bars greater than the specified yield strength. This may be achieved by applying an overstrength factor α ($\alpha = 1.25$) to the specified yield strength.

$$f_s = \alpha \cdot f_y \qquad (1\text{-}3)$$

Once an appropriate value of α has been applied, the maximum likely action of the beam flexural bars on the joint is well defined. The value of the column shear $Vcol_t$ or $Vcol_b$ is less precisely defined. Under dynamic loading the bending moment patterns in the columns of a frame may not be regular, and the distribution of beam input moments to the column section above and below the joint is uncertain. The column shear in a particular storey depends on the moments at top and bottom of the column, but for the purpose of joint design, a reasonable empirical approximation for the column shear in a regular frame is given with the notation of Fig.1.2.

$$Vcol_t = Vcol_b = \frac{M_b + 0.5\, V_b\, h_c}{0.5\,(l_c + l_c')} \qquad (1\text{-}4)$$

in the case of $l_c = l_c'$, equation (1-4) becomes

$$Vcol_t = Vcol_b = \frac{M_b + 0.5\, V_b\, h_c}{l_c}$$

Where : - l_c and l_c' are the storey heights from centre to centre of the beams above and below the joint respectively.

- h_c is the column depth.

Concurrently with the horizontal joint shear, a vertical shear, V_{jv}, is imposed on the joint due to the change in the sense of the column moments above and below the joint. This may be assessed by considering the column bars forces, the concrete compression force in the column, and the appropriate beam shear force to one side or other of the column centreline.

1.2.3 Direct Concrete Strut Mechanism

The shear applied to a beam-column joint under lateral loading of a building frame may be resisted in a variety of ways, depending on the condition of the joint and the adjacent flexural members at any given stage of loading. Fig.1.3 shows that if sufficient horizontal and vertical forces are available at the appropriate corners of the joint, then shear may be transferred across the joint by direct concrete strut, which carries a compressive force, D_c. This mechanism does not require any joint reinforcement apart from confining reinforcement to ensure that the concrete strut can sustain the

compressive stresses. Consideration of the boundary conditions necessary to sustain this mechanism shows that the vertical forces from the column are readily available, since the column is designed to remain essentially elastic throughout seismic loading. Concrete compression forces C_t and C_b within the column section due to flexure and axial load should therefore remain viable, and loss of bond strength of the column bars will be negligible. In the beams, however, the expected inelastic response of the hinges adjacent to the column faces means that the horizontal actions necessary to provide viable end conditions for the action of a concrete strut will not be so readily available once severe seismic loading has been imposed on the structure.

In elastic conditions, that is before the occurrence of significant yielding in the beam reinforcement, the concrete compression forces in the beams, C_c and the forces ΔF_t transferred from the beam bars by bond within the compressed area of the column section, will be a significant fraction of the total horizontal force to be transferred across the joint. Thus in this situation the direct diagonal strut mechanism may resist a significant proportion of the total applied horizontal joint shear, V_{jh}. However, after reversed inelastic loading has been applied, the concrete compression forces in the beam, C_c, is likely to be small (due to permanent elongation of the reinforcement leaving full depth cracks) while penetration of strains in excess of yield strain in the beam bars into the joint core means that the bond strength will be lost close to the concrete of the joint panel, and the total horizontal force available to combine with the vertical forces to allow a diagonal strut to act will therefore be small.

The inclination β_c of the strut to the horizontal may be approximated by that of the line between the centroids of concrete compression in the beam and column at diagonally opposite corners as shown in Fig.1.3. When reversed inelastic loading occurs the location of the centre of effective compression in the beam may be somewhat uncertain, and the appropriate horizontal forces may be considered to act at the centroid of the beam bars.

1.2.4 Joint Truss Mechanism

A second mechanism by which joint shear may be resisted is shown in Fig. 1.4. This mechanism consists of a truss, comprising joint horizontal reinforcement, diagonal concrete struts, and a vertical reaction supplied either by concrete compressive forces in the column, and (or) by vertical joint reinforcing. The horizontal reinforcement may consist of either horizontal joint stirrups or bars running through the joint and anchored in the beams beyond. Vertical reinforcement may consist of either vertical stirrups or column intermediate bars. In most cases it is impractical because of construction difficulties to place stirrups in both vertical and horizontal directions, and the most common configuration for joint reinforcing consists of horizontal stirrups with intermediate column bars used as vertical reinforcing. Note that the diagonal compression forces D_s carried by the concrete is additive to the diagonal force D_c caused by the direct compression strut mechanism of resistance. Study of Fig.1.4 shows that the horizontal and vertical input shears may be introduced to the truss mechanism at any location around the joint perimeter. For this reason the mechanism may be expected to provide shear resistance throughout the loading history of the structure. It should also be noted that inclusion of horizontal joint

reinforcing alone is insufficient to ensure the satisfactory performance of this mechanism. Vertical compression components must be supplied, and this is particularly important in the design of joints for which the column axial load is small, where vertical reinforcement must be provided across the joint.

1.2.5 Allocation of Applied Joint Shear to Mechanism of Resistance

It is postulated that the overall means of resistance to joint shear will be the direct concrete strut (Fig.1.3) and the truss mechanism (Fig.1.4), with the proportion of the input shear resisted by each mechanism depending on the boundary conditions.

The shear V_{jh} applied to the joint in the horizontal direction may be derived from Eqs. (1-1) to (1-4). The concrete direct strut will carry part of this horizontal shear, V_{ch} , and the truss mechanism can then be designed to carry the remaining shear V_{sh}.

$$V_{jh} = V_{ch} + V_{sh} \qquad (1\text{-}5)$$

Fig.1.3 shows that for joints for which reversible plastic hinge is expected to form in the beam immediately adjacent to the joint (i.e. where C_c is small), and for which the column axial load is small, the direct strut mechanism may not be very effective [Fenwick (1977)] under inelastic cyclic loading, and hence it is postulated that in this case the horizontal shear resisted by the joint concrete should be taken as zero.

$$V_{ch} = 0 \qquad (1\text{-}6)$$

When heavier axial loads are applied to the column, and where the column neutral axis is therefore relatively deep in the section, some bond forces may be picked up within the compressed area of the column, so that some diagonal compression may be transferred by the strut mechanism. In this case some horizontal shear resistance will be provided by the concrete strut mechanism, and Fig.1.3 shows that may be defined as

$$V_{ch} = D_c \cdot \cos\beta_c \qquad (1\text{-}7)$$

The relationship between column axial load and the shear resistance of the strut mechanism is discussed further in Chapter 6, in the light of the test results.

The horizontal reinforcing (total area of horizontal hoops) required in the joint to form the required truss mechanism is

$$A_{sh} = \frac{V_{sh}}{f_{yh}} \qquad (1\text{-}8)$$

where :- A_{sh} is the total area of horizontal reinforcement crossing the diagonal plane from corner to corner of the joint between the top and bottom layers of beam bars.

- f_{yh} is the yield strength of the joint horizontal reinforcement.

Considering the vertical shears applied to the joint, a similar equation to Eq. (1-5) may be written.

$$V_{jv} = V_{cv} + V_{sv} \qquad (1\text{-}9)$$

However concrete compression forces may be expected to be available in the column throughout the loading history, due to the absence or a very limited occurrence of yielding in the column reinforcement. The term V_{cv} therefore includes not only the vertical component of the direct strut mechanism, $D_c \sin\beta_c$, but also part of the necessary vertical action for the truss mechanism. The vertical actions, T_v, shown in Fig.1.4, can be provided both as tensile forces in vertical joint reinforcement within the joint panel, and as compressive forces acting in the column concrete at the top and bottom edges of the joint panel. Thus the availability of appropriate forces in the column sections can reduce the vertical joint reinforcement required to complete the truss, so that the total value of V_{cv} can also be expected to depend on the column axial load. The necessary vertical joint reinforcement (total area of intermediate vertical column bars) to be placed between the outer layers of column bars is

$$A_{sv} = \frac{V_{sv}}{f_{yv}} \qquad (1\text{-}10)$$

Where: - f_{yv} is the yield strength of the vertical joint reinforcement.

For design purposes a strength reduction factor ϕ_j is often applied when determining the required reinforcement in both horizontal and vertical directions, given by Eqs. (1-8) and (1-10).

1.3 PARAMETERS AFFECTING JOINT RESPONSE TO SEISMIC LOADING

1.3.1 General

The resistance of beam-column joints to the high shear forces

generated by severe seismic loading has been postulated to be a combination of joint concrete acting as a direct compression strut mechanism, and by joint reinforcement acting with the concrete to form a truss mechanism. The total shear to be resisted by a joint must be limited to prevent overstressing the concrete, which is required to carry diagonal compression in both principal mechanisms of resistance. Since the joint concrete will become extensively cracked in both diagonal directions under cyclic loading, it is obvious that the maximum stress that can be carried safely will be considerably less than the cylinder strength of the concrete. A limit may be set by restricting the maximum nominal horizontal shear stress within the joint.

The shear to be resisted by the truss mechanism is normally limited by the congestion of the necessary joint reinforcement. The resistance of the truss mechanism to joint shear depends only on the quantity of joint reinforcement and the yield strength of the reinforcing steel, as shown by Eq.(1-8).

It is therefore apparent that the assessment of the strength of the direct strut mechanism is critical for the efficient design of beam-column joints to resist seismic loading. If more shear resistance can be allocated to this mechanism then the requirement for joint reinforcement will be reduced. The strength and viability of the mechanism depends on a variety of parameters, and these are discussed individually in the following sections.

1.3.2 Concrete Strength

Since the concrete strut is expected to carry load at stresses

considerably less than the crushing strength of the concrete, the compressive strength has no direct influence on the amount of joint shear strength which can be allocated to this mechanism. The viability of the concrete strut mechanism depends on the availability of appropriate end conditions rather than on the material strength of the strut. The only significant effect of concrete strength on these end conditions lies in its influence on the bond strength of the flexural bars, which provide input shear to the joint. If the penetration of yield strain in beam bars into the joint can be reduced by greater bond strength, then a greater contribution to joint shear resistance may be expected from the direct strut mechanism. However greater concrete strength will also tend to reduce the neutral axis depths in the flexural members adjacent to the joint, and this may counteract any enhancement of the strength of the strut mechanism caused by greater bond strength and reduced yield penetration.

1.3.3 Column Axial Load

Clearly the level of column axial load may be expected to have a significant effect on the effectiveness of the direct strut mechanism. As the compressed area of concrete in the column section above or below a joint increases due to increasing axial load, so the amount of horizontal input shear transferred by bond within the compression zone will increase. This means that horizontal shear is available to combine with the vertical compression forces, so that the strut will be effective regardless of the presence or otherwise of concrete compression forces in the beam sections. The other expected benefit of axial compression lies in the probability that the bond environment for the beam bars should be improved in joints with heavier axial loads, so that yield penetration should be reduced. The minimum axial

compression load to be expected on a joint during seismic loading is likely to provide the critical load case for design.

1.3.4 Flexural Reinforcement

Although the quantity and strength of the beam flexural reinforcement provides the input shear forces for joint design, the composition of the beam reinforcement may also have some influence on the resistance of the joint to the applied shear. The size of the flexural bars relative to the column depth influences the bond stresses in the bars across the joint, and if yield penetration can be reduced by using smaller diameter bars, then the direct strut mechanism may be expected to carry more shear.

The distribution of applied joint shear between the two principal mechanisms of resistance may also be influenced by the ratio of the beam tension to compression reinforcement. If this ratio is greater than unity then some compression force must be carried by the beam concrete in the beam under negative moment, and this might improve the end conditions for concrete strut.

The distribution and amount of column flexural reinforcement will affect the concrete strut mechanism so far as the depth of compression in the column section is affected. It has already been noted in section 1.3.3 that vertical reinforcing is required through the joint to ensure that the truss mechanism functions properly.

1.3.5 Geometric Parameters

The aspect ratio of the joint h_c/h_b (see Fig.1.2), may have some influence on the joint performance, since if the column depth h_c is

made greater while the beam depth h_b remains constant, the depth of compression in the column is likely to increase, and hence more force can be acquired from the beam bars within the compressed area of the column. However the average compressive stress in the larger column is likely to be smaller and it is possible that the bond strength of the beam bars may thus be reduced sufficiently to negate the benefit gained by the larger depth of compression.

A second geometric parameter which may have some influence on the effectiveness of the joint direct strut mechanism is the ratio of the beam breadth b_b to the column breadth b_c. Joints for which the beam breadth is less than the column breadth should perform satisfactorily. However it seems likely that the efficient operation of the strut mechanism will be reduced in joints for which the column breadth is significantly less than the beam breadth.

The effective joint width, b_j, to be used in assessing nominal joint stresses as follows:

$$b_c \geq b_b$$

either $b_j = b_c$

or $b_j = b_b + 0.5\, h_c$ (1-11)

which ever is the smaller, and

$$b_c < b_b$$

either $b_j = b_b$

or $b_j = b_c + 0.5\, h_c$ (1-12)

which ever is the smaller

These equations imply limitations on the effectiveness of the joint for the case of narrow beam-wide column (Eq.1-11), and for the case of

narrow column-wide beam (Eq.1-12), whereas it could be postulated that the former situation may be more favourable to efficient joint response.

Further problems will arise in joints in which the beam and column centrelines do not intersect. Additional stresses due to torsional moments will be caused in joints of this type due to the eccentricity at which the horizontal shear is applied to the joint.

1.3.6 Location of Beam Plastic Hinges

Study of the postulated mechanisms of resistance to joint shear shows that two features are required to allow efficient joint shear transfer by the direct concrete strut mechanism. These are firstly the presence of significant concrete compression forces in all beams adjacent to the joint, and secondly limitation or elimination of the penetration of yield strain in the beam flexural bars into the joint core. It has been suggested [Paulay, Park and Priestley (1978)] that this might be achieved efficiently by reinforcing the beams so that the plastic hinges form at some distance away from the column faces, rather than immediately adjacent to the faces, as happens in conventionally reinforced beams. This relocation of the plastic hinges will result in the sections adjacent to the column faces remaining essentially elastic, so that beam compression forces can be sustained in this location, and penetration of yield strain into the joint core does not occur. Thus at some cost in reinforcing of the beam, the concrete strut mechanism can be made much more efficient than for conventionally reinforced beams, and the joint reinforcing can be significantly reduced.

1.4 REVIEW OF PREVIOUS RESEARCH

The behaviour of beam to column connections under seismic loading has been studied by many researchers over the last three decades. The factors investigated have included design procedure; connection details; analytical modelling; physical testing of beam-column sub-assemblies and frames. Since this study is in two parts, consisting of an experimental and an analytical investigation, the previous research in these areas is presented separately.

1.4.1 Experimental Research

1.4.1.1 Historical

The first experimental tests on beam-column connections were conducted in the United States by the Portland Cement Association and the University of Illinois in 1960 and were published by Hanson and Conner (1967). These experiments clearly demonstrated the benefits of confinement on the hysteresis response of beams. These tests, however, failed to simulate the complex behaviour of the beam-column joint region.

Since the 1960's, other investigators have provided some data applicable to the beam-column connection design problem. However, the real impetus to research into the behaviour of reinforced concrete beam-column joint regions under strong ground motion took off after the 1971 San Fernando Earthquake.

Since then, the problem has been studied by other searchers mainly in the U.S. [Lee et al. (1977) and Viwathanatepa et al. (1979)], as well as in Canada [Uzumeri and Seckin (1974)], Japan [Nakata (1980)], and New Zealand [Paulay et al. (1978) and Scarpas (1981)]. Although

the objectives have varied, the main emphasis of these studies has been to develop guide-lines which would ensure proper anchorage of beam bars in the joint and provide ductile behaviour under repeated cyclic loading.

1.4.1.2 Research Themes

The following literature review deals with reinforced concrete beam-column connections subjected to seismic loading, and it is organized into groupings of research under different themes.

a) *Effect of repeated cyclic loading*

Townsend and Hanson (1972), in their investigation of inelastic behaviour of connections observed that a large number of cycles of inelastic loading at relatively low amplitudes did not significantly reduce the strength of connections.

Higashi and Ohwada (1969) investigated the behaviour of beam to column connections subjected to lateral loads. They observed the appearance of cracks in the connection panel during the first loading cycle at a shear stress of 12% to 14% of the ultimate strength of the concrete. For specimens which experienced an early bond failure and slippage of bars, the specimens had less joint cracking. They also observed improved stiffness and strength of connections due to presence of transverse beams.

Other research related to the behaviour of beam to column joints, includes the investigation by Celebi and Penzien [Celebi and Penzien (1973)] of critical regions of reinforced concrete components, as influenced by moment and shear. They reported no significant influence

of dynamic loading on the stiffness degradation and energy absorption properties of specimens tested within a deflection ductility range of 1 to 4. However, the dynamic loading appeared to increase the yield strength by as much as 25%

In order to evaluate the effects of continuity and load redistribution on the response of connections, Hikmat and Durrani (1989) studied the response of beam-column joints in indeterminate (multiple) and single connections under earthquake-type loading, see Fig.1.5. Their first observation was that shear in both connections of the indeterminate subassembly was higher than in single-connection tests. They also observed that the exterior column in the indeterminate subassembly experienced higher moments, causing them to crack much earlier than expected. They also noticed that the energy dissipation was not affected by the continuity of the subassembly.

Uzumeri (1977) and Uzumeri and Seckin (1974) found that the loading history did not affect the strength, but seriously affected the stiffness of the beam to column subassemblies. They also considered that the use of joint reinforcement with flat yield plateau was undesirable for confinement. In their opinion, the joint shear reinforcement contributed to the shear strength in some proportion other than the one established for flexural members and recommended that the joint stirrups be extended above and below the beam reinforcement at the same spacing as in the joint.

Lee, Wight and Hanson (1977) observed that strength and energy dissipation capacity of beam to column connections degraded after every cycle of loading at the same displacement, and degradation was

found to be less for specimens containing more transverse reinforcement.

Abrams (1987) carried out a series of tests on small, medium, and large scale beam-column connections. The objective of his research programme was to determine and to study correlations in behaviour of reinforced concrete beam-column joints constructed at different scales. From the results obtained, the author noticed that the same resistance mechanisms were observed for all specimens, although there were quantitative differences in behaviour for specimens of different scale. Yield of reinforcement occurred in the beams within a hinging zone of width equal to the effective depth of the member. Crushing of concrete occurred within this zone, which limited flexural strengths. The investigator pointed out that bond stress was more relevant than scale factor. The author concluded that scale relations can be improved at the small (approximately one-twelfth scale) if bond strength of model reinforcement is enhanced. However, bond deterioration under repeated and reversed loadings may still not be modeled precisely.

b) *Anchorage of beam bars*

Magget (1971) studied the anchorage of beam reinforcement in seismic resistance of reinforced concrete frames and recommended that the joint reinforcement be designed to resist the shear entirely within its elastic limit.

Hawkins and Lin (1979) studied the reversed cyclic loading bond characteristics of reinforcing bars anchored in joints. They concluded that the deformations in joint must be considered and that the bond

slip can be modelled by a rigid body rotation of the beam at the column face. They concluded that the bond-slip characteristics for bars are as important as their stress-strain characteristics in modelling member response.

Patton (1972) investigated the use of anchorage blocks welded to the beam reinforcement to prevent their slippage through the joint core. The author also suggested the use of sufficient joint hoop reinforcement to compensate for any loss of confinement due to outward bowing of hoops.

Marques and Jirsa (1975), and Minor and Jirsa (1975) investigated the behaviour of 90° hooks anchored in concrete blocks simulating conditions in an exterior beam-column joint under seismic loading. Their results indicated the capacity of the hooked anchorage could be increased if both the confinement of the hook in the form of cover or ties, and the straight embedment length before the bar begins to bend, were increased.

Scott (1992) in his experimental investigation about detail of anchoring the beam longitudinal bars into column, studied the practice of bending beam tension steel up, down or 'U' fashion within the joint. The investigator concluded that the bars bent down and U-bar anchorage details performed significantly better than the bars bent up detail, and pointed out the use of bars bent up is undesirable in practical connection design.

Park and Paulay (1974) investigated the effect of the amount and arrangement of transverse steel in the joint region and the method of

anchoring the beam steel. They noticed that the use of U-bar anchorage detail for top and bottom bars led to rapid anchorage failure and proved to be considerably inferior to the separate anchorage of top and bottom bars. They disagree with Scott about the U-bar anchorage detail, unless the column has considerable depth. They also suggested that the anchorage length of the beam reinforcement should be calculated from the beginning of the 90^0 bend. For narrow columns, they advised the use of beam stubs for the anchorage region may be necessary.

Ha, Kim and Chung (1992) investigated the behaviour of reinforced high-strength concrete beam-column joints subjected to cyclic loading. They studied the structural performance of the joints designed with the conventional method, the response of the joints with the diagonal anchorage within the joint, and finally the efficiency of the joint using intermediate reinforcement with or without stirrups. From their results, they concluded that high strength concrete structures are more dangerous if they have high displacement ductilities, because under cyclic loading, the higher the concrete strength, the greater the stiffness and strength degradation for displacement ductilities. They also observed that the intermediate longitudinal reinforcement with closed stirrups helped to move away the location of plastic hinge from the column face, and that specimens behaved satisfactorily and dissipated more energy. They noticed that specimens with diagonal anchorage showed pinching in the hysteresis cycles due to sliding shear failure near the connection. They suggested the correction of this kind of anchorage for a better performance of the joint.

Soleimani, Popov and Bertero (1979) carried out an experimental

investigation into the behaviour of reinforced concrete cruciform beam-column sub-assemblies under cyclic loading. The hysteretic behaviour of the sub-assembly was studied with particular reference to the influence of fixed-end rotation of beams caused by bar pull-out from an interior joint. The inelastic behaviour of beams along their lengths was also carefully monitored. Based on the experimental results, some conclusions can be reached:

- After a loss of bond of the main beam bars in a joint, the inelastic deformations are concentrated at the beam fixed-ends.

- Bar pull-outs without a total loss of bond can contribute between 20 to 35% to the total lateral displacement of a sub-assembly. Therefore the beam fixed-end rotations should be included in accurate analyses. The development of these concentrated fixed-end rotations also leads to the deterioration of beam shear resistance.

Popov and Bertero (1973) carried out a series of test on half-scale reinforced concrete beam-column sub-assemblies under simulated severe seismic loading. In their experiments, both the material and the geometric non-linearities were prominent. Bond deterioration of the main reinforcement was brought out. Based on their results, together with other work of the authors they suggested that bond degradation of the beam's main bars within the core of a column at interior joints may be delayed or entirely prevented by forcing plastic hinges to occur in the beams away from the column faces. Either a reduced amount of reinforcement at the plastic hinge or a beam haunch can be used to obtain the desired result. The use of inclined bars at the plastic hinges has also been found to be very

effective in resisting the repeated application of shear reversals. Most of the work on the cyclic behaviour of reinforced concrete beams was done with members having rectangular cross sections, additional tests should be performed using T-sections.

Ha, Kim and Chung (1992) carried out a laboratory investigation on eight exterior reinforced high-strength concrete beam-column joints to study the response of the joints with the diagonal anchorage method. Based on their test results, they concluded that the diagonal anchorage method in the joint region appears to have a negative effect on the hysteresis behaviour (pinching of the loop), therefore this method of anchorage needs correction and improvement.

c) *Effect of axial load*

An investigation by Jirsa, Meinheit, and Woollen (1975) indicated that large variations in axial load and increases in transverse reinforcement above certain amounts had very little effect on the ultimate strength of the joint.

Beckingsale (1980) found that the joint core of beam column sub-assemblies carrying heavy column axial loads performed much better than those sub-assemblies which had low axial load. The heavy column load was shown to be beneficial to joint performance by providing good bond conditions for the beam flexural reinforcing bars, and by reducing the bond demand on the column flexural reinforcement. The author also observed that the test specimens with small axial load displayed slippage of reinforcing bars through the joint core.

Georgoussis and Phipps(1981)summarized the results obtained from

the work carried out on beam-column connections at the University of Manchester (UMIST). The authors examined the effect of low-strength concrete beams on the axial load capacity of high-strength concrete columns.

Their results showed that the axial load capacity of a column can be considerably reduced by the presence of weak concrete in the connection area (where the joint concrete is basically divided into two blocks, upper and lower which are separated by the beam neutral axis).According to these investigators, this reduction is particularly more pronounced in exterior joints and it can be as high as 50%. As a results of this research, the authors made some design recommendations and proposed equations for calculation of beam-column sub-assemblies.

Yunfei, Chingchang and Yufeng (1984) studied the effect of cyclic loading on thirty-six beam-column joints. In their experiments, they investigated the behaviour of the joint core and the main factors influencing the shear strength of the joint core, those include the confinement effect of intersecting beams, the shear and compression stress ratio, the anchorage slip of longitudinal beam bars in the core, and the relocation of plastic hinges on the beams. From the results obtained, they suggested that "fracture without collapse", the fracture stage should be taken as ultimate state in designing beam-column joint for ordinary frame structures, and the diagonal crack stage as ultimate state for special structures. The average shear stress in the joint core should be limited to a certain value; restrictions on beam and column width. In addition they suggested that yielding stress of hoop steel may be used to calculate the shear force taken by hoops.

Hawkins and Lin (1979) studied the bond deterioration in external beam-to-column connections under cyclic loading. They observed that under cyclic loading, bond failed at a much lower slip level than for monotonic loading. They also concluded that the compressive strength of concrete and the bar loading history significantly affected the bond failure and slip.

d) *Reinforcement configurations in connecting members*

Hanson (1971) from the results obtained on beam-column connections, observed that Grade 60 reinforcement can be used in sub-assemblies that are designed to develop ductile behaviour.

Scribner and Wight (1978) observed that intermediate longitudinal reinforcement in beams with maximum shear stress level greater than $3\sqrt{f_c'}$,N/mm^2, significantly increased both the total energy dissipation and stability of hysteretic response of beam-column subassemblies.

Lee (1976) has carried out a series of six tests on plane frame exterior joints which behaved well under cyclic loading, largely because the sum of the column flexural strengths above and below the joint was up to 4.3 times greater than the beam flexural capacity. The bond requirement for the column reinforcement down the joint was therefore moderate, which the elastic state of the column above and below allowed the joint concrete to develop a satisfactory strut mechanism for shear transfer, and thus reduced the demand on the joint reinforcement.

Ehsani and Wight (1985) carried out tests on exterior beam-column

subassemblies under cyclic loading to investigate the effects of the flexural strength ratio, the percentage of transverse reinforcement used within the joint, and the shear stress in it. In their conclusion, they suggested that a flexural strength ratio should be no less than 1.4 to avoid formation of plastic hinges in the joints and to improve the behaviour of the connections considerably. They also suggested that the maximum joint shear stress level in exterior connections should be limited to ($1.0\sqrt{f'_c}$,N/mm^2) in order to reduce excessive joint damage, column bar slippage, and beam bar pullout.

Bahjat and Wight (1987) investigated a technique for moving the plastic hinging zone away from the column face, by adding supplemental intermediate longitudinal reinforcement over a specific length of the beam adjacent to the joint. The strong column-weak beam philosophy was maintained. Based on the results of the specimens tested, they concluded that intermediate layers of longitudinal reinforcement and extra top and bottom steel in the beam over a certain length can be used to move the beam plastic hinging zone away from the column face. As a result, the beam sections adjacent to the column faces remained essentially elastic, and its reinforcement yielding did not penetrate into the joint core and, thus, a good environment was available for developing the required bond stresses inside the joint.

Ha, Kim and Chung (1992) carried out a laboratory investigation on eight exterior reinforced high-strength concrete beam-column joints. They studied the effects of the following variables on the performance of the connections:

a) the structural performance of the joints designed with the

conventional method.

b) the efficiency of the joint using intermediate reinforcement. Based on their test results, they made the following conclusions:

- High strength concrete structures are more dangerous if the they have high displacement ductilities.

- The supplemental intermediate longitudinal reinforcement over a specific length was successfully capable of moving the plastic hinge away from the column face, in addition, the structural performance of the joint improved in comparison with the conventional design method. Furthermore, this supplemental intermediate longitudinal reinforcement increased the load carrying capacity, and therefore the energy dissipation of the connection.

Zhu and Jirsa (1983) studied the bond deterioration in beam-column joints and recommended that the beam bars diameter should be not more than 1/20 of the column dimension and that the column bars diameter should not exceed 1/22 of the beam depth.

e) *Joint shear resistance*

In one of the earlier investigations of beam to column connections, Hanson and Conner (1967) observed that the presence of transverse beams (perpendicular to the plane of the loaded beams) considerably improves joint behaviour, and stressed the importance of proper detailing of the joint. The reasons for such behaviour is that, the transverse beams provide an additional shear area and resist some unknown portion of the total joint shear. In addition providing some

degree of confinement to the joint. The authors also pointed out that the requirement for shear reinforcement and confinement hoops within the joint were not directly related, being provided for independent purposes.

Magget and Park (1971) tested reinforced concrete beam-column sub-assemblies to determine the effect of transverse beams on the joint. Their results indicated specimens with the transverse beams behaved better than those without the transverse beams. This improved behaviour was attributed to the fact that the primary damage occurred in the main beam for specimens with transverse beams rather than in the joint.

Paulay, Park and Priestly (1978) discussed the contribution of joint shear reinforcement and inclined concrete compressive struts on the joint shear resistance. Due to the yield penetration into the joint under cyclic loading, it was suggested that the contribution of the concrete to the shear resistance of the joint should be neglected.

Meinheit and Jirsa (1977) studied the shear strength of reinforced concrete beam to column connections. They concluded that an increase in the percentage of transverse joint hoops increased the shear strength, but the increase was not proportional to the yield strength of the hoops. Fenwick and Irvine (1977) recommended the use of diagonal strut action instead of panel truss action for joint design. Their tests indicated a higher sustained strength and better ductile performance for joints with welded bond plates than the more conventional details. However, the welded bond plate detail would appear to be expensive for actual construction.

Birss (1978) in his investigation of the elastic behaviour of joints, indicated the importance of vertical as well as horizontal shear and stressed the need for using vertical shear reinforcement. Paulay et al (1977) proposed that the total joint shear force applied to a joint core be apportioned between that carried by the concrete diagonal strut and that carried by a truss mechanism consisting of horizontal stirrups, vertical stirrups and intermediate column bars.They also suggested a limit on the beam bar diameter to avoid bond failure and excessive slippage.

Zhang and Jirsa (1981) analysed the data of beam-to-column connections tested by various researchers and recommended the use of the compression strut mechanism to calculate joint shear strength. They found the use of welded and closely meshed reinforcement in both directions within the joint to be most effective.

Kaar, Fiorato et al (1978) investigated the limiting strain of concrete confined by rectangular hoops. They observed the limiting concrete strain for confined concrete to be of the order of four to five times the assumed ultimate strain. They recommended the use of smaller size hoops at smaller spacing to improving energy dissipation through higher ductilities.

Tsanos et al (1992) investigated the behaviour of external beam-column joints with inclined reinforcing bars under seismic conditions and other parameters. In their point of view, external beam-column joints with crossed inclined reinforcing bars showed high strength, reached their maximum capacity without any appreciable deterioration, and performed better than those with conventional

reinforcement.

Durrani and Wight (1985) have carried out a series of tests on reinforced concrete interior joints under reversed cyclic loading. The main objective of their study was to evaluate the performance of interior joints which have less transverse reinforcement than required by the draft recommendations of committee 352, and to investigate the effect of the level of joint shear stress on strength, stiffness, and energy-dissipation of beam-column sub-assemblies and to examine the slippage of beam and column bars through the joint. Based on their test results, they made the following suggestions :

a) The same grade reinforcing steel should be used in beams and columns in order to avoid the reduction of the column-to-beam flexural strength ratio.

b) The joint shear stress should be kept as low as possible without compromising the economy of member design.

Meinheit and Jirsa (1981) in their experimental investigation reported herein, studied the factors influencing the shear capacity of reinforced concrete beam-column connection. It appeared from the test results that, the transverse reinforcement in the connection improved the shear capacity but not in the same ratio as indicated by Beckingsale (1980) using the addition rule, $V_{concrete} + V_{steel}$, for shear. The column axial load had no influence on ultimate shear capacity of the connection. They also noticed that the connection geometry had no effect on shear strength of the joint, as long as the shear area, bd, of the connection remained constant.

Sarsam (1983), and Sarsam and Phipps (1985) analysed the results obtained from a series of five reinforced beam-column connections subjected to monotonic loading. They pointed out that, whatever the type of loading, joints sometimes have to sustain large shear forces transmitted from the connecting members, especially beams, and also due to disagreements on the contribution of concrete.

As a result of their investigation, they proposed a method for the design of ultimate shear strength for joints loaded statically and also made some suggestions for the serviceability design of joints.

Gefken and Ramey (1989) investigated experimentally whether the increase in joint hoops spacing in seismic joints could be achieved using steel fiber concrete in place of conventional concrete in the joint region. The tests showed that the fiber concrete specimens experienced very little or no spalling of the concrete, whereas the conventional concrete specimens exhibited extensive spalling of the concrete. Their results also indicated that the spacing of the joint hoops recommended by the ACI-ASCE committee 352 (1976) for a Type 2 joint could possibly be increased by a certain factor if steel fiber concrete is substituted for normal concrete in the joint region.

Renton (1972) from his tests of beam to column joints under cyclic loading, concluded that the unsupported length of ties could effect the confinement of the joint core and suggested the use of crossties.

Smith (1972) noted that the hoops placed close to the top and bottom reinforcement of beams were not effective joint shear

reinforcement. The investigator also concluded that the yielding of joint hoops caused disintegration of core concrete and resulted in the formation of a hinge within the joint. This, according to Smith, prevented the formation of a compression strut and severely reduced the load carrying capacity.

f) *Comments*

Cheung, Paulay and Park (1993) discussed the beam-column behaviour in the context of current design procedures for reinforced concrete ductile frames subjected to severe earthquake motions. They pointed out the significant differences in detailing requirements of beam-column joints that exist between various concrete design codes which led to an international collaborative research project involving the testing of full-scale beam-column-slab joint subassemblies under quasi-static cyclic loading. In the light of the test results, they concluded that good detailing of beam-column joint core regions is essential if reinforced concrete frames subjected to severe seismic motions are to respond in a satisfactory manner. The very large shear forces acting on joint cores need to be resisted, primarily through the use of horizontal and vertical shear reinforcement. The diameter of longitudinal column and beam reinforcing bars passing through joint cores must not be excessive to ensure adequate anchorage and to avoid premature bond failure.

g) *Conclusion*

Park (1992), in a recent paper described the capacity design of reinforced concrete building structures for earthquake resistance. The aim of this capacity design procedure is to ensure that the members and joints of structures have appropriate levels of strength in

flexure, shear and bond, so that appropriate detailing will lead to structures with sufficient ductility to survive severe earthquakes. The author summarized the "capacity design approach" as follows:

- The emphasis in the seismic design of reinforced concrete structures should be on good structural concepts and detailing. Poor structural concepts can lead to major damage or collapse due to column sidesway mechanisms or excessive twisting as a result of soft storeys or lack of structural symmetry or regularity. Poor detailing of reinforcement can lead to brittle and catastrophic failure.

- Structures in seismic regions can be designed for levels of design seismic force which are significantly lower than the inertia forces induced if the structure responded in the elastic range to severe earthquake, providing that the structure has adequate ductility.

- The ductility of reinforced concrete structures required for earthquake resistance is best achieved by ensuring in design that it occurs by flexural yielding of plastic hinges. The most important design considerations for flexural ductility of members is the provision of adequate longitudinal compression reinforcement as well as tension reinforcement, and the provision of adequate transverse reinforcement. The transverse reinforcement is required to act as shear reinforcement, to confine and hence enhance the ductility of the compressed concrete, and to prevent premature buckling of the compressed longitudinal reinforcement.

- It is recognized that uncertainty exists regarding the selection

of both the mathematical model representing the behaviour of the structure and in the characteristics of the imposed earthquake ground shaking. Hence the aim in seismic design should be to impart to the structure features which will result in the most desirable behaviour in the event of a severe earthquake. This philosophy can be achieved by the capacity design approach.

1.4.1.3 Summary of Experimental Research

A summary of major experimental tests carried out by many investigators worldwide is illustrated in Table 1.1.

Experimental studies of the behaviour of structural elements under earthquake-type loading have been concerned mainly with identifying the effects of variables that influence the ability of critically stressed regions in such specimens to perform properly. In terms of the quasi-static test that has been the most widely used for this purpose, proper performance would logically require that these critical regions be capable of sustaining a minimum number of cycles of specified amplitude without significant loss of strength.

Tests of beam-column joints subjected to large inelastic displacement cycles have indicated that the presence of transverse beams framing into the joint improved its behaviour. However, the same tests indicated that slippage of column reinforcement through the joint occurred with or without transverse beams. The use of smaller-diameter longitudinal bars has been suggested as a means of minimizing bar slippage. Whereas, to limit slippage of beam bars (pull-out from the joint) is, to impose some restrictions on the column dimensions for an interior joint, and for an exterior joint to

limit the beam bars size which terminate into it. Some investigators are stressing the use of the same grade of reinforcing steel in beams and columns, because a larger difference in yield strength of the steel could reduce the flexural ratio and may result in column hinging. The same investigators pointed out that the joint shear stress level should be kept as low as possible (without compromising the economy of member design). A lower joint shear stress level will help to minimize joint degradation under cyclic load. Another suggestion has been made to force the plastic hinge in the beam to form away from the column face. This can be accomplished by strengthening the segment of beam close to the column. To reduce the stiffness degradation of the joint and to avoid anchorage failure in exterior connection, some investigators are calling for the beam bar hooks to be embedded outside the heavily stressed joint region.

TABLE 1.1 Test on R/C Beam-Column Connections

Date	Authors	Parameters Studied	Joint Type
1967	Hanson & Conner	Column size, axial load and degree of confinement in the joint	Exterior
1969	Higashi & Ohwada	Effect of cyclic loading on cracking and ultimate concrete strength	Interior
1971	Hanson	Effect of grade 60 reinforcement on ductility	Interior & Exterior
1971	Magget & Park	Effect of transverse reinforcement ratio, and percentage of transvese reinforcement on the joint	Exterior
1971	ACI Committee 318 Cohen	Shear capacity of reinforced and unreinforced beam-column joints	Interior & Exterior
1971	Gulkan & Sozen	Response and energy dissipation of R/C B-C subjected to strong motios	Interior
1972	Townsend & Hanson	Effect of low amplitude in cyclic loading on the strength of beam bars	Exterior
1972	Patton	Benefit of welded anchorage on the slippage of beam bars connections	Exterior
1972	Renton	Effect of unsupported ties on confinement in the joint region	Exterior
1972	Smith	Effect of hoops on the joint shear reinforcement	Interior & Exterior
1973	Celebi & Penzien	Seismic behaviour of critical region of R/C components as influenced by moment and shear	Interior & Exterior

1973	Popov & Berter	Effect of scale on reinforced concrete beam-column connections	Interior & Exterior
1974	Park & Paulay	Amount and arrangement of transverse in the joint. Method of anchoring beam bars	Interior
1974	Uzumeri & Seckin	Behaviour of reinforced and unreinforced B-C joints. Concrete shear capacity	Exterior
1975	Park & Paulay	Summary of the behavioural aspects of beam-column joints	Interior
1975	Jirsa, Meinheit & . Woolen	Factors influencing shear strengths of joints	Interior
1975	Marques & Jirsa	A Study of hooked bars anchorage in beam-column joints	Exterior
1975	Minor & Jirsa	Behaviour of bent bars anchorage	Exterior
1976	Lee	Original and repaired beam-column sub-assemblies subjected to earthquake type loading	Exterior
1977	Fenwick & Irvine	Joints welded with bond plates and the strut action mechanism	Interior
1977	Lee, Wight & Hanson	Amount of transverse reinforcement, magnitude of axial load and severity of loading	Exterior
1977	Meinheit & Jirsa	Column reinforcement ratio, size spacing of hoops in the joint and beam-column ratio	Interior

1977	Townsend & Hanson	Effect of low amplitude in cyclic loading on the strength of the joint	Exterior
1977	Uzumeri	Effect of the joint behaviour on the response of the sub-assemblies	Exterior
1977	Paulay et al.	Capacity design of reinforced concrete ductile frames	Interior & Exterior
1978	Paulay, Park & Priestly	Contribution of joint shear reinf. and inclined concrete compressive struts on the joint shear resistance	Interior
1978	Birss	Elastic behaviour of joints	Interior
1978	Kaar et al.	Limiting strains of cincrete confined by rectangular hoops	Interior
1978	Scribner & Wight	Effect of intermediate longitudinal reinforcement	Interior & Exterior
1979	Hawkins & Lin	Anchorage of beam main bars in the joint region	Exterior
1979	Soleimani, Popov & Bertero	Studied the hysteresis cycle and the influence of fixed end rotation of beams	Interior
1980	Bertero, Popov & Forzani	Details of joint under cyclic loading and Ductility	Interior
1980	Beckingsale	Beam reinforcement configuration and column axial load	Interior
1981	Zhang & Jirsa	Verification of strut mechanism using data tested by other researchers	Interior & Exterior

1981	Meinheit & Jirsa	Factors influencing the shear capacity of the connections	Interior
1981	Georgoussi & Phipps	The influence of low-strength concrete beams on the axial load capacity of concrete columns	Interior & Exterior
1983	Zhu & Jirs	A study of bond deterioration in reinforced concrete B/C joints	Interior & Exterior
1983	Sarsam	Strength and deformation of structural concrete joints	Interior & Exterior
1984	Yunfei, Yufeng & Chingchang	Shear and compression ratio, slip of beam bars and relocation of plastic hinges	Interior & Exterior
1985	Ehsani & Wight	Effect of the flexural strength ratio and percentage of hoops on the joints	Exterior
1985	Ahmad & Wight	Joint with less hoops and level of joint shear stress	Interior
1985	Sarsam & Phipps	The shear design of in situ R/C B-C joints under monotonic loading	Interior & Exterior
1987	Abrams	Scale relations for reinforced concrete beam-column connections	Interior
1987	Bahjat & Wight	Moving plastic hinge away from the column face	Interior
1989	Hikma & Ahmad	Effect of continuity and load redis-tribution on the response of joints	Interior & Exterior
1989	Gefken & Ramey	Potential increases in joint hoop spacing using fibre concrete	Exterior
1992	Park	Capacity design of R/C ductile structures for seismic resistance	General
1992	Tsanos, Tegos & Penelis	Efficiency of inclined bars in the joint region	Exterior

1992	Ha, Kim & Chung	Structural performance of the joint design with conventional method and its response with diagonal anchorage	Exterior
1992	Scott	Effect of detailing on R/C beam-column joint and anchorage bent up and down	Exterior
1993	Cheung, Paulay & Park	Design criteria & Joint shear resistance	Interior & Exterior

1.4.2 Analytical Research

Hemmaty, DeRoeck and Vandewalle (1992) examined the behaviour of reinforced concrete corner joints subjected to positive bending, using a finite element modelling program called 'ANSYS'. In their parametric study, they studied the influence of detailing of main reinforcement, the percentage of steel, and concrete quality on the strength of the joint; they also examined the influence of shear retention factor β on the quality of the results. They observed that, detailing of main reinforcement, concrete quality and reinforcement ratio show that same tendency that has been observed by experimental evidence, and the efficiency of the joint increases with increasing the concrete quality and decreases with augmenting the steel ratio in the connecting members.

According to their results, they concluded that shear retention factor plays an important role in the accuracy of the finite element results, and consequently the choice of its value should be chosen carefully. They suggested that, for structures loaded to collapse, a small β value (between *0.0* and *0.05*) should be applied, because large

cracks can be expected.

In one of its projects, the Netherlands Concrete Mechanics Institute, conducted by Van Mier (1987), modelled a single-bay portal frame using a finite element program 'DIANA', in order to investigate the behaviour of the beam-to-column corner connection subjected to negative moment. The aim of this parametric study was to check the validity of this model by comparing the analytical and experimental results together. They studied the influence of the quality of concrete, the lay-out of the main reinforcement and the thickness of the cover on the strength of the joint. They observed that plasticity occurred at an early stage of loading, which seems unrealistic, and the Mohr-Coulomb failure criterion considerably under-estimates the strength of concrete under three-dimensional states (compressive) stress. On the other hand, their numerical simulation gave a good idea of the structural mechanism in the joint.

In this kind of study, they recommended a coarse analysis mesh should be made before refining. After such analysis it might be possible only to refine the mesh of a detail, such as the influence of concrete quality or the curvature of the reinforcing bar in the joint. They also suggested that the use of three-dimensional analysis would be required for a comparative and realistic output.

Grootenboer (1981) analysed an external beam-to-column subjected to cyclic loading using finite element Program. The structure was in 2-D plane stress. The aim of the analysis was to investigate the influence of certain parameters such as, the magnitude of the load at which cracks are formed, the crack spacing and their widths, the slip

of the reinforcement, and finally the stresses in the concrete and in the reinforcing steel.

They concluded that the slip of the reinforcement is of major influence upon the internal stress distribution. The scatter of tensile strength of the concrete in the structure, according to them, is found to be of major influence on the scatter in the crack widths and crack spacings. They suggested that one should take into account this scatter in analyses. For a better simulation, they recommended a 3-D analysis of the problem is necessary to minimize the errors. Furthermore, they stressed, for an objective analysis, to take into account the dowel action, the aggregate interlock and bond into consideration.

Pantazopoulou and Bonacci (1992) explored the mechanics of connections for the sake of improved understanding. They built their discussion of mechanics around : 1) unsettled questions result from selection of mechanically inconvenient coordinate systems for viewing the problem, and 2) consideration of joint deformation characteristics on performance to structural response. A collection of algebraic expressions was recorded. They pointed out that these expressions manage to link recognized design variables of joint behaviour and design in a manner that is physically sensible.
They concluded that the shear strength of a joint depends on the usable compressive strength of concrete, the axial compression force on column tends to encourage shear distortion, and axial force on beam works against it. In their conclusions, they suggested that the strength of a connection can be evaluated from the compressive stress-strain behaviour of concrete (by determining principal stresses

and strain). By establishing a relationship between loads applied to the joint and the resulting deformations, it possible to consider the mode of joint failure in addition to the associated strength.

El-Metwally and Chen (1988) used the thermodynamics of irreversible processes to develop the moment-rotation relationship of reinforced concrete beam-column connection idealized as a concentrated rotational spring. This model is a function of three parameters; the joint's initial stiffness and the ultimate moment capacity, and an internal variable that effects the energy dissipation of the joint. This analytical model is formulated for ductile and stiff joints where a flexural hinge is expected to form in the beam or the column. From their comparative study of experimental and analytical results, they concluded that this model can handle both static and earthquake-type loads. The analytical results from the proposed model were in good agreement with experimental data in case of monotonic load.

Morita and Kaku (1984) carried out a theoretical analysis of beam-column joint subjected to monotonic and cyclic loading based on experimental evidence obtained by other investigators. The aim of their investigation was to formulate an additional rotation due to the slippage of beam bars from the joint region. They obtained a M-ϕ_s relationship as bi-linear type under monotonic loading, and hysteretic loop as hard spring type under cyclic loading. They observed a good agreement between analytical and experimental results.

Filippou, Popov and Bertero (1986) conducted a parametric study on the cyclic behaviour of interior joints using an analytical model. The model takes into account the bond deterioration along reinforcing bars

anchored in the joint as well as the hysteretic behaviour of cracked concrete at beam-column interfaces. The aim of this model is to study the effect of some parameters, such as, amount of top and bottom reinforcement, yield strength of reinforcing steel and diameters of reinforcing bars on hysteretic joint behaviour.

From the results obtained, they made the following conclusions:

- The bond strength along the reinforcing bars anchored in the joint significantly affects the hysteretic behaviour of joints. A small reduction in the values of the bond stress-slip envelope curve leads to a considerable reduction in energy dissipation capacity of the joint.

- Equal amount of top and bottom reinforcement should be used in the girders framing into the joint. This considerably improves the hysteretic behaviour of a beam-column joint.

- The lower the yield strength of reinforcing bars and the smaller the bar diameter the better the hysteretic behaviour of a joint.

Ichinose (1992) proposed a design equation to prevent shear failure in a ductile reinforced concrete members after flexural inelastic deformation. The equation is based on truss-strut model. The author proposed some equations to calculate shear strength and shear reinforcement in the member. The suggested shear design equation is confirmed on the basis of existing experimental data. Furthermore, this equation is adopted in the 1990 Japanese Design Guidelines.

Ekhande et al. (1989) analysed beam-column using stability

functions as an alternative to the stress stiffness matrix. They derived expressions for stability functions for three-dimensional beam-columns, in terms of member length, cross-sectional properties, axial force, and the end moments. The effect of flexure on axial stiffness and the effect of axial force on flexural stiffness and stiffness against translation are considered. In addition, they presented the non-linear stiffness matrix of a three-dimensional beam-column by modifying the linear elastic stiffness matrix available in the literature. They also presented a numerical example showing the calculation of stability functions for a given beam-column.

Panahshahi, White and Gergely (1992) studied experimentally and analytically the behaviour of compression lap splices in reinforced concrete members subjected to high-level repeated cyclic loads. The main objective of the analytical study was to gain a better understanding of the behaviour of a compression splice. To model the problem, the investigators used a general purpose finite element program "ANSYS" because of its capability to handle non-linear analysis through the use of a variety of elements. A one-dimensional non-linear finite element model was used to analyse compression lap splices in axially loaded columns.

Their results indicated that compression lap splices can be designed to sustain a minimum of a dozen cycles of high-intensity loads (axial or flexural) into the inelastic range, where the maximum bar strain reaches at least three times the yield strain. Based on the comparison of the experimental and analytical results, the authors proposed a tentative recommendations for the design of compression lap splices under seismic loading.

1.5 OBJECTIVE AND SCOPE OF THIS PROJECT

The aim of this investigation is to study analytically and experimentally the behaviour of beam-to-column connections under earthquake loading and deals specially with the exterior joints of reinforced concrete moment resisting frame buildings. The principal objectives of this study are as follows:

i) To investigate experimentally, the structural performance of the joints using conventional stirrups and to compare with the response of beam to column connections which used a new kind of stirrup (specimens UD1 and UD2, Fig.1.6). The new stirrups were formed from two mild steel bars in U-configuration, then assembled together to form a square or rectangular shape as desired, see Fig.1.6. Special attention is to be focused on the confinement of concrete in the joint region, and the influence of variation of the overlap length on the behaviour within the joint region.

In a recent discussion with Professor Thomas Paulay, which took place at the University of Bristol on May 27th, 1993 concerning this subject, the author exposed the problem mentioning the need for this type of stirrups in a reinforced concrete beam-column joints region especially when the beam cage is pre-fabricated. Professor Paulay was pleased and agreed with this kind of reinforcement as far as interior connections are concerned. As for exterior connections, he pointed out that at least one of the stirrups must be hooked around the column main bars in order to avoid the stirrups becoming detached after spalling of the concrete cover in the column.

ii) In this experimental study, the placement and the confinement

effect of these stirrups on satisfactory performance of the subassembly were to be investigated. The study is intended to evaluate and compare joints with different reinforcement on one hand, and the overall behaviour of specimens on the other hand, as well as to make some suggestions for the design of connections

iii) The aim of the analytical study is to investigate the effectiveness of a finite element model of a moment resisting reinforced concrete beam-column sub-assembly.

It was intended to study aspects of the behaviour that could not be observed so easily with experiments. For example, the distribution of stress or strain along bars within the joint region is important but is difficult to measure in detail experimentally. Distribution of potential cracking can be studied using finite elements with appropriate capabilities. Furthermore, the distribution of compressive stress has an important effect on bond and can be studied more easily with the graphical capability of a finite element model.

In this research, the effect of the beam-to-column flexural strength ratio on the location of the plastic hinges is examined. Another parameter which also affects the joint region, that is to say the column axial load, is taken into consideration in this investigation.

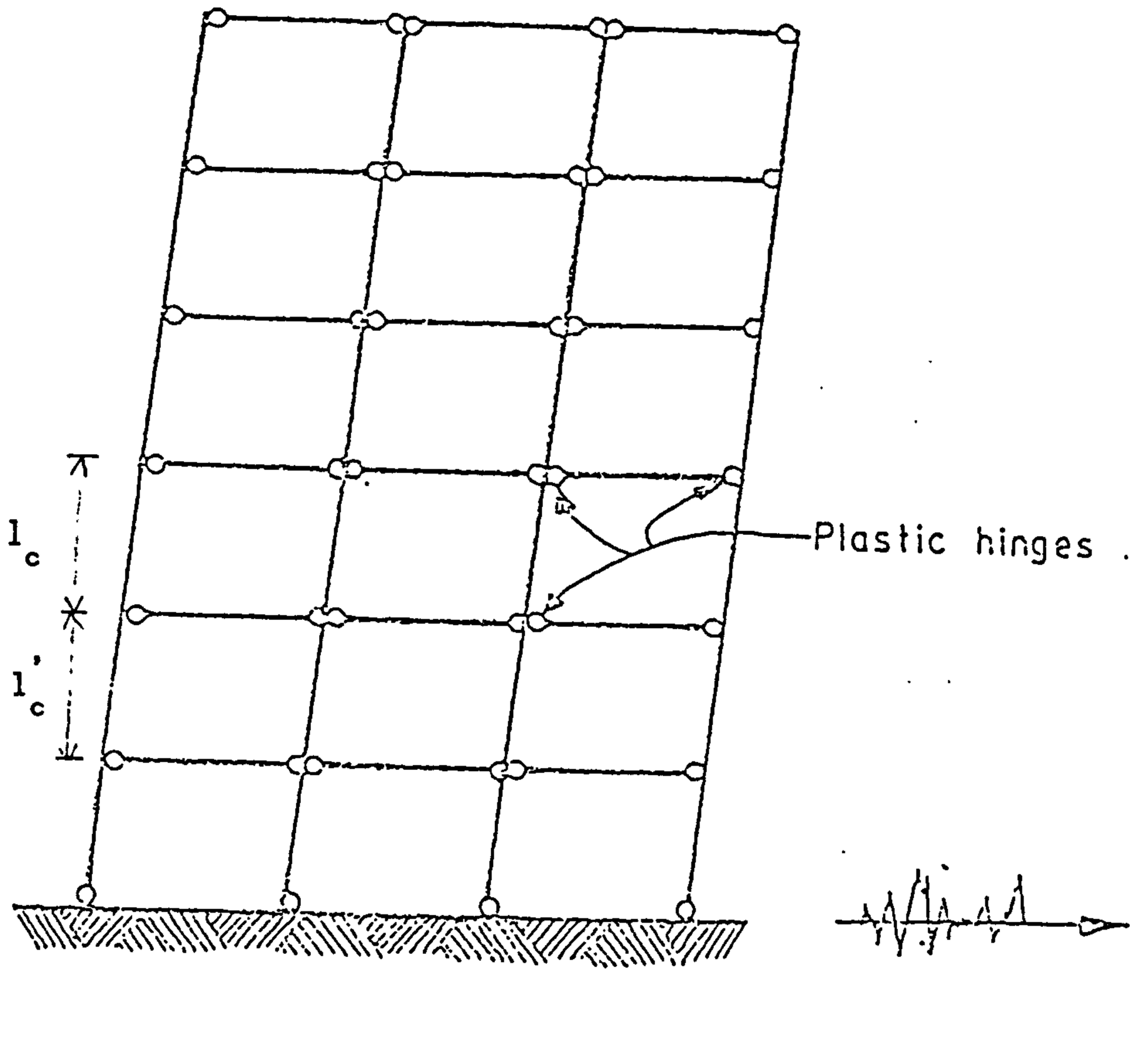

FIG. 1.1 BEAM SIDESWAY MECHANISM FOR FRAME UNDER SEISMIC LOADING

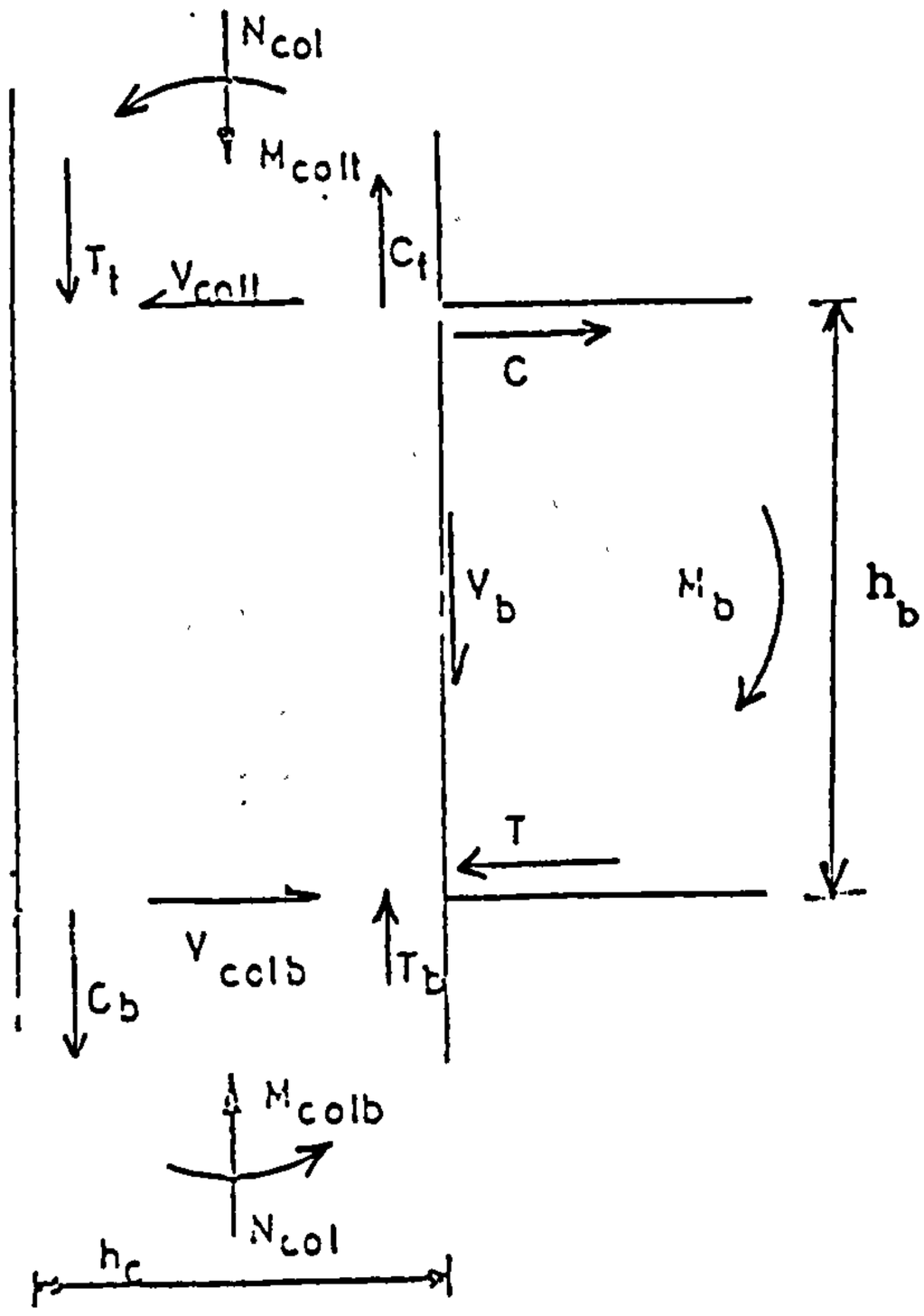

FIG. 1.2 ACTIONS ON JOINT

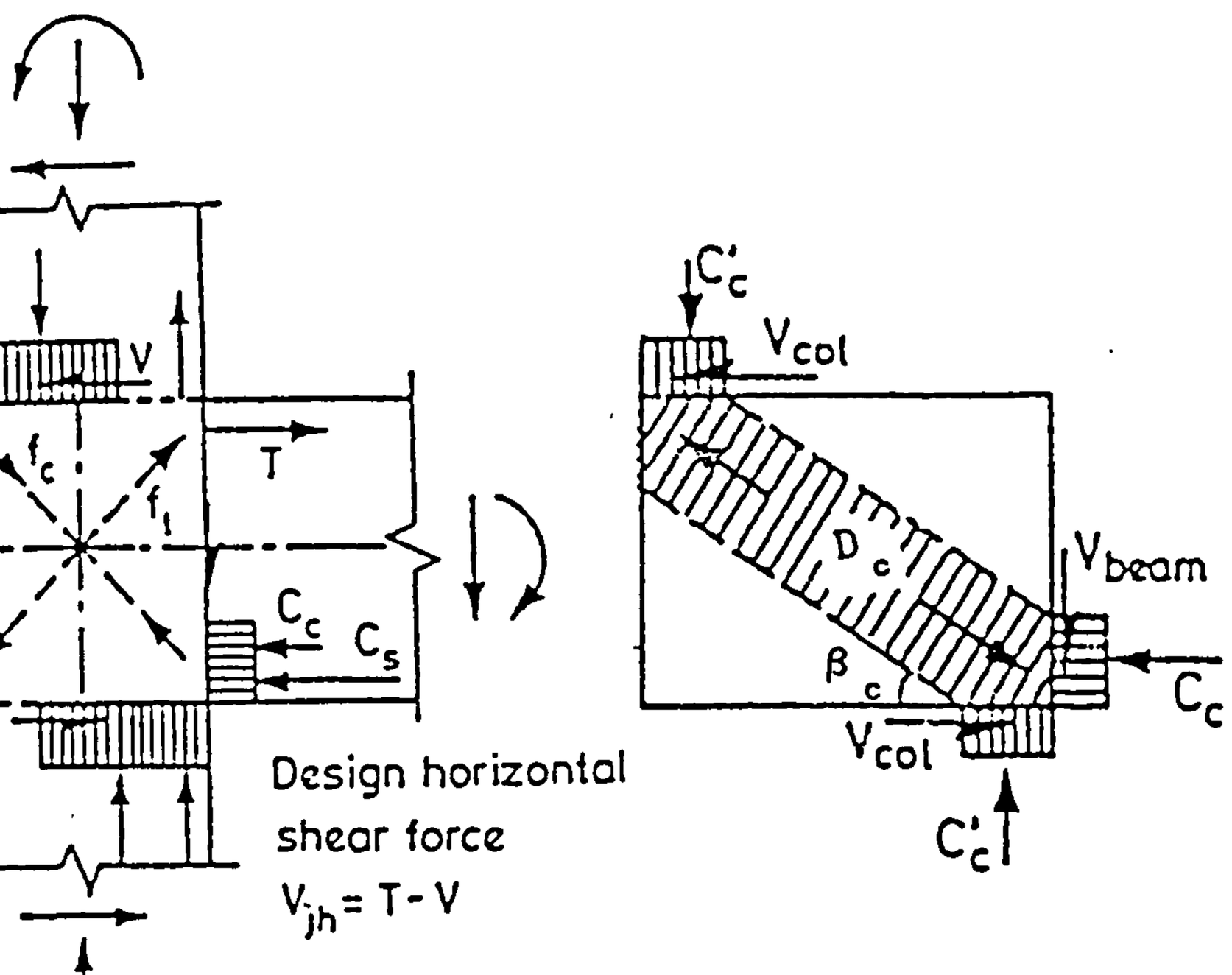

FIG. 1.3 CONCRETE DIRECT STRUT MECHANISM FOR JOINT SHEAR RESISTANCE

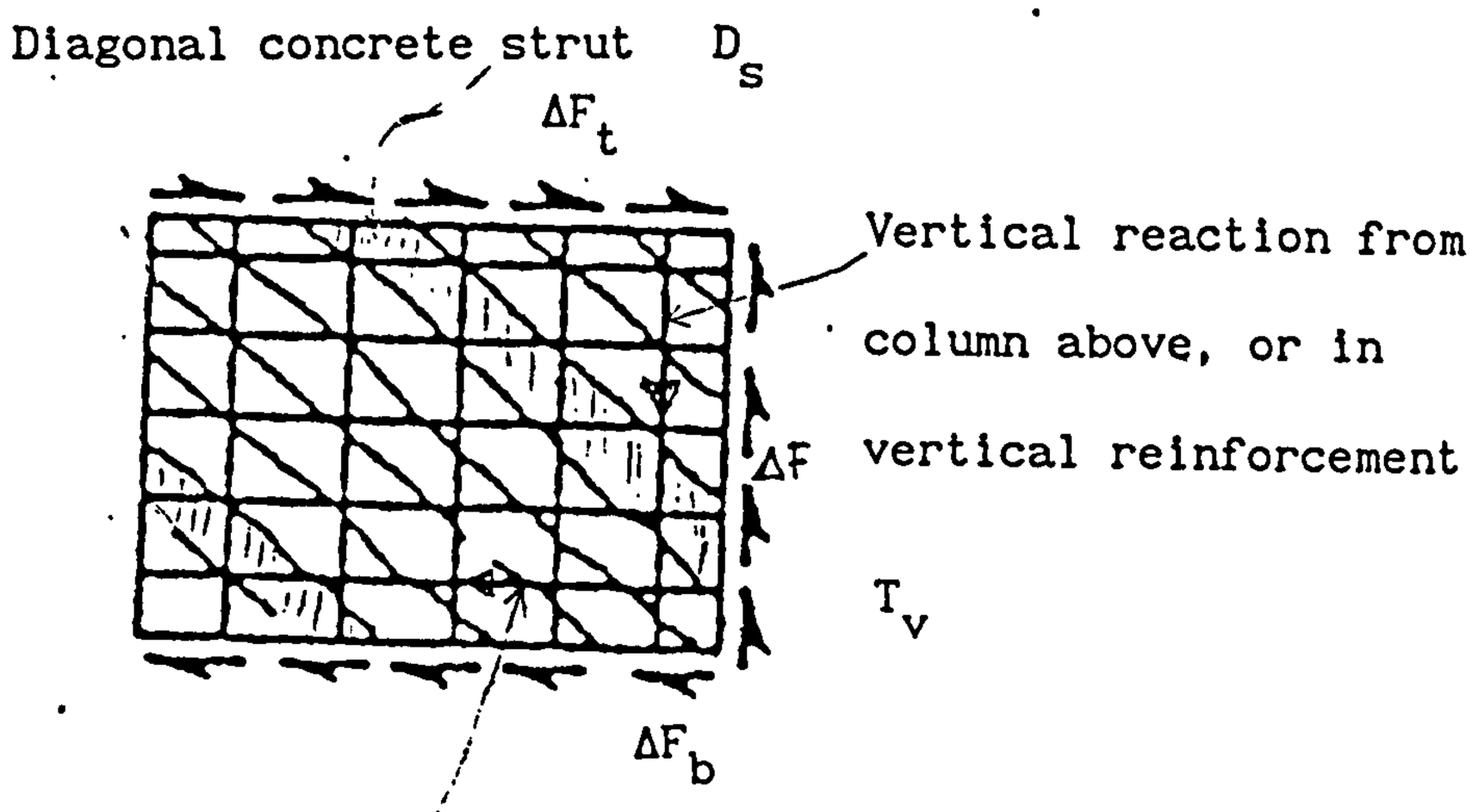

FIG. 1.4 TRUSS MECHANISM FOR JOINT SHEAR RESISTANCE

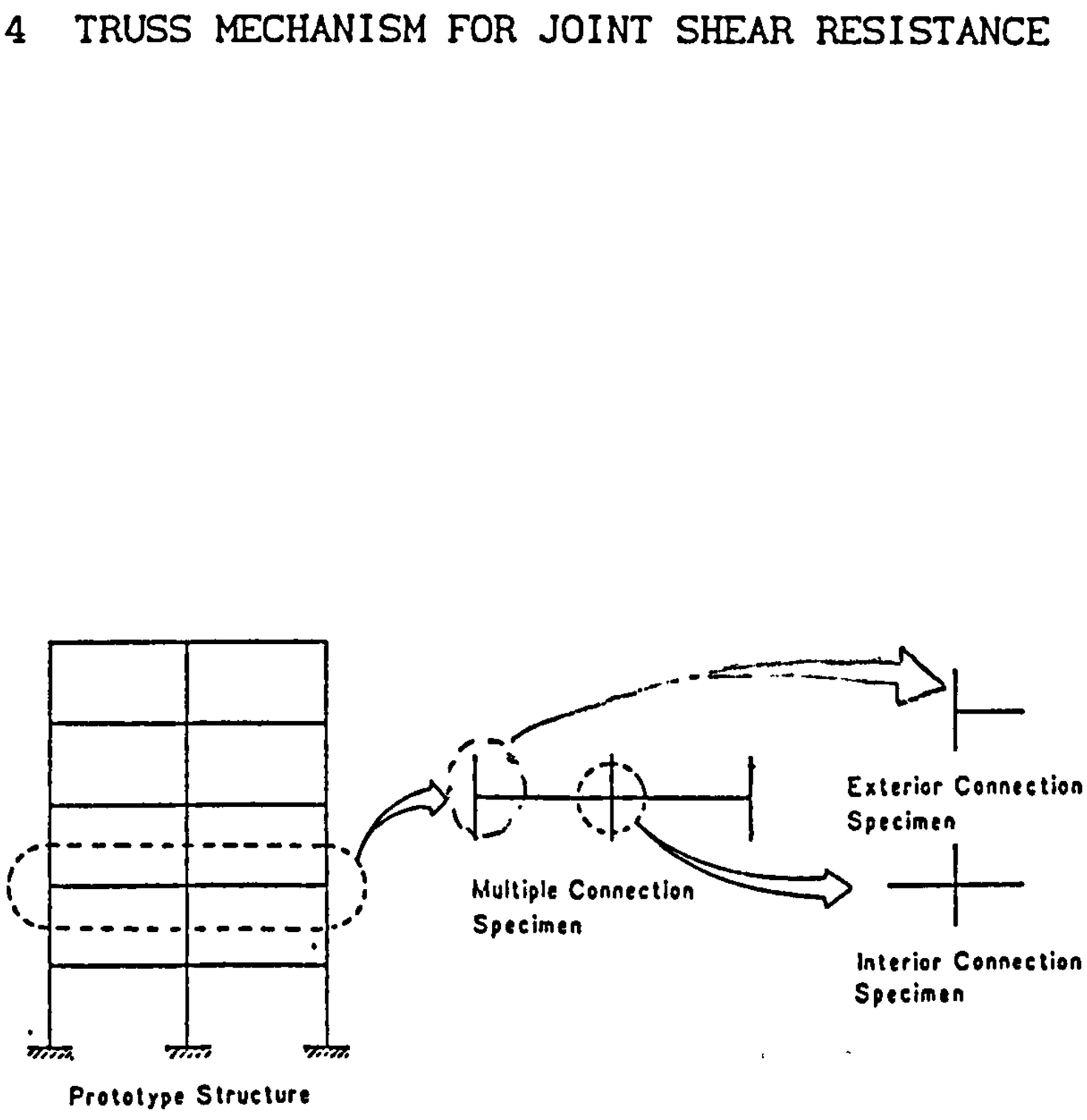

FIG. 1.5 CONFIGURATION OF TEST SPECIMENS

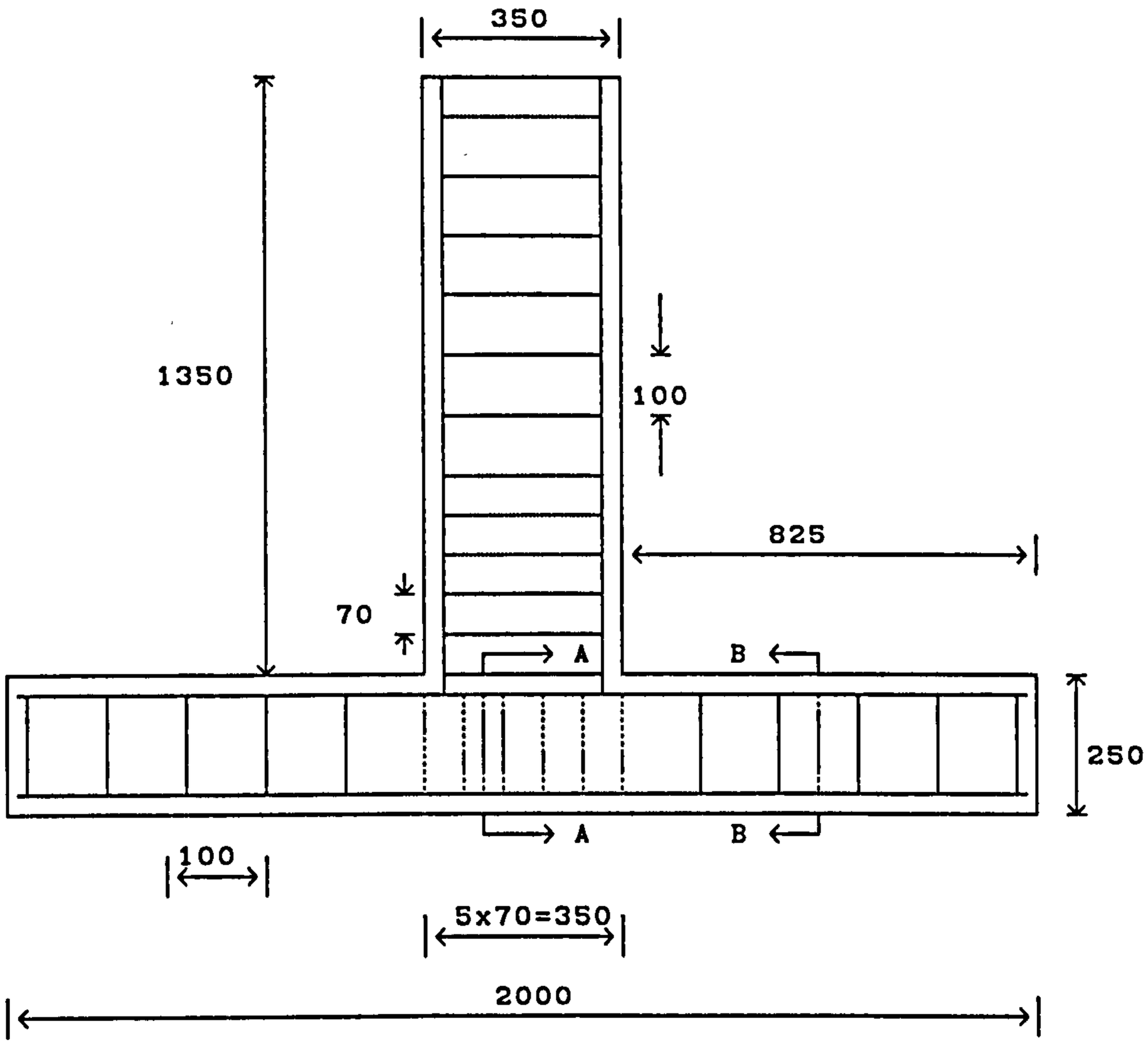

a) Specimen - UD1 -

FIG.1.6 BEAM-COLUMN SUB-ASSEMBLIES & JOINT STIRRUPS DETAILS

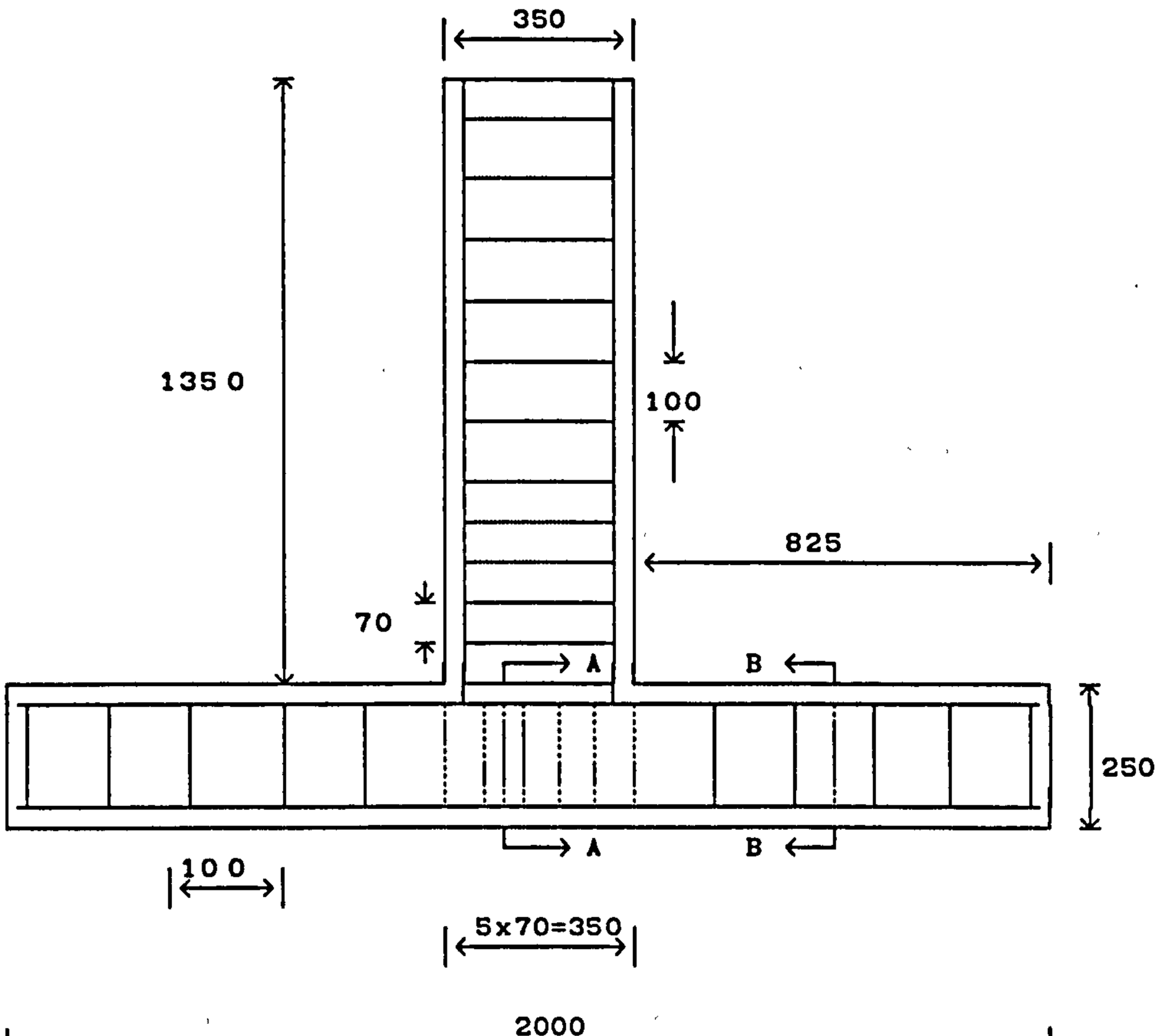

SECTION A-A

(within joint)

SECTION B-B

(outside joint)

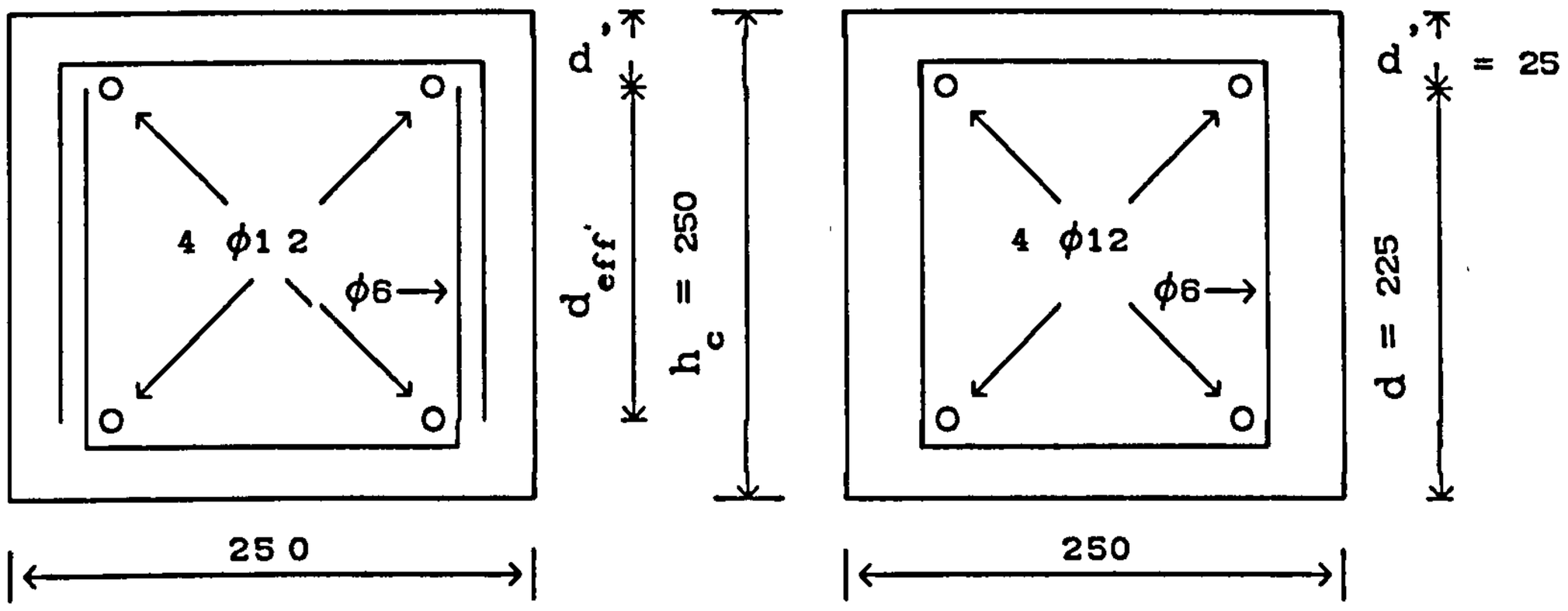

U-stirrups

Conventional stirrups

b) Specimen - UD2 -

* All dimensions are in mm

CHAPTER TWO EXPERIMENTAL INVESTIGATION

2.1 GENERAL

The primary purpose of the experimental part of this study was to investigate the performance that could be achieved using U-stirrups transverse reinforcement in the joint region for a reinforced concrete exterior beam-column joint (see Fig.1.6, chapter one). Confinement of concrete in the joint depends on the amount and the type of transverse hoop reinforcement and the configuration of framing members. The proposed role of U-stirrups is to simplify placement of stirrups in the congested joint region compared with using traditional stirrups, especially in interior sub-assemblies where at least four beams are running into it. It is much easier to construct and place around the column main bars once the beam cages are in-place, therefore it leads to gain of time and rapid construction.

2.2 DESIGN OF TEST SPECIMENS

In a reinforced concrete moment-resisting ductile frame, the lateral force moments due to a severe earthquake are generally much larger than the gravity load moments, particularly in the lower and intermediate stories.

Assuming a point of zero moment at the column mid-height and beam mid-span, a feasible testing arrangement for a beam-to-column connection is shown in Fig.2.1. Sub-assemblies of this type have been used before by many other researchers e.g. Hanson (1967), Park (1971), Paulay (1978), Wight (1985) etc. The deformed shape of the sub-assembly and the critical combination of forces acting on the

joint are shown in Fig.2.2 and Fig.2.3 respectively.

Consistent with the accepted design philosophy of strong columns-weak beams, the smallest ratio of the sum of the flexural strength of the column to that of the beam for this investigation was 2.04 which is higher than the ratio 1.4 required by the current design codes, ACI-ASCE Committee 352 (1976).

The primary variables of the testing program were :

- The placement and the arrangement of U-stirrups hoops in the joint region.

- The stirrups' overlap length necessary for a good confinement of the concrete core.

- The flexural strength ratio M_R, defined as the sum of the flexural capacities of the column to that of the beam.

- The influence of the column axial load on the performance of the joint.

2.3 DESCRIPTION OF TEST SPECIMENS

Four exterior beam-column sub-assemblies were tested during the experimental investigation. These specimens were divided into two groups of two specimens each. The group which had normal stirrups was designated as the EX-specimens and the other group which had U-stirrups links, was designated as UD-specimens. A numeral following the letter designation, represents the specimen number.

Figures 2.4 and 2.5 show the overall dimension and beam column

cross sections of a specimen. For comparison purpose, dimensions and major parameters for all specimens are illustrated in table 2.1.

All columns were reinforced with four 12 mm diameter longitudinal bars except for specimen EX1, where four 16 mm diameter longitudinal bars were used. Confinement reinforcement was provided in the form of 6 mm diameter closed links at 70 mm centre-to-centre spacing in the joint region, and at 100 mm elsewhere for all specimens.

In specimens EX1, beam was reinforced with two 12 mm diameter bars on each side, whereas beam reinforcement of specimen UD2 consisted of two 16 mm diameter bars on the tension side and two 12 mm diameter on the compression side. In the other two units, three 12 mm diameter bars were used on each side in each beam. This resulted in an under-reinforced beam with tension steel percentage under 1%.

The joint reinforcement consisted of six layers of a square hoop in the joint region for specimens EX1 and EX2, while the specimens UD1 and UD2 had six layers each, but consisting of double U-stirrups links. The overall specimen size, beam cross sections and the column cross sections were kept the same for all the specimens, and only the main reinforcement and the way of placing U-stirrups in the joint region was varied. The column axial load, the ultimate flexural capacities of beam and columns and the column to beam flexural strength ratios of all the sub-assemblies are given in table 2.2. The flexural capacities were evaluated using the ACI-code (1985). The flexural capacities of the specimens were found to vary from one specimen to another due to the longitudinal reinforcement used in the connecting members, and also because the concrete strength of the

specimens was different. More details of design and reinforcement of specimens can be found in Appendix A (Figs.A5(a) to A5(d)).

Table 2.1 Dimension and Major Parameters of Specimens

Specimen	Dimension (mm)		Reinforcement			
			Longitudinal		Transverse Stirrups	
	Beam	Column	Beam	Column	Beam	Column
EX1	250·350	250·250	Top 2 ϕ12 Bot 2 ϕ12	4 ϕ16	Rectan.	Square
EX2	250·350	250·250	Top 3 ϕ12 Bot 3 ϕ12	4 ϕ12	Rectan.	Square
UD1	250·350	250·250	Top 3 ϕ12 Bot 3 ϕ12	4 ϕ12	Rectan.	U-stirrups 50% overlap
UD2	250·350	250·250	Top 2 ϕ12 Bot 2 ϕ16	4 ϕ12	Rectan.	U-stirrups 100% overlap

Table 2.2 Flexural Strength of Beams and Columns -ACI-

Specimens	Column load applied in test (kN)	% Column load capacity	Flexural capacity of beam (kN.m)	Flexural capacity of column (kN.m)	$\frac{\Sigma\ Mcol}{\Sigma\ Mbeam}$
EX1	150 kN	18%	88	130.5	2.96
EX2	100 kN	12%	82	80	1.95
UD1	70 kN	8%	87.3	89.4	2.04
UD2	50 kN	6%	62.6	80.8	2.58

2.4 MATERIAL PROPERTIES

2.4.1 Concrete

The mix proportion by weight for all specimens were 1:2:4 (cement:fine sand:coarse aggregate) with a water cement ratio of 0.5.Crushed limestone aggregate with a maximum size of 14 mm, Bideford grit and Holm sand together with ordinary Portland cement were used throughout.

The concrete mix design was aimed at producing a target 28-days mean value of f_c' = 30 N/mm^2. Concrete compressive strength was determined from 150 mm cubes and tensile strength from 150 mm diameter and 300 mm long cylinders taken from each of the concrete batches. Table 2.3 shows the concrete strengths for all specimens, together with other characteristics including age of the control specimens. The mean f_c' values were all higher than 30 N/mm^2. Several factors may have contributed to this result, including:

1) Age of testing was much more than 28 days-up to 99 days for one specimen.
This is supported by the fact that the youngest specimen (80 days) was also the one nearest to the mean value of f_c'.

2) After the curing period, the control cubes and cylinders, just like the joint specimens they represent, were left to dry in the laboratory atmosphere.

3) Despite adjusting the water added to the concrete mixes to compensate for the sand water content, some unavoidable variation

occurred. The control specimens were tested using an Avery-Denison testing machine.

4) The high value of f_c' for specimen EX1 was due to low water-cement ratio. It was decided that this was unrepresentative and adjusted accordingly for remaining specimens.

Table 2.3 TEST RESULTS OF CONCRETE CONTROL SPECIMENS

Specimen	Mix	Slump (mm)	f_c' (N/mm^2)	f_{cu} (N/mm^2)	Age* (Days)	E_c (N/mm^2)	$f_{c(av)}'$ (N/mm^2)
EX1	A	10	80	4.0	96	36000	80
	B	20	80	4.4	96	36000	
EX2	A	90	35	5.5	82	24000	37
	B	124	39	5.3	83	24900	
UD1	A	80	39	4.4	99	26700	42
	B	65	45	6.0	98	30500	
UD2	A	100	41	6.4	95	29900	40
	B	110	39	5.7	95	28700	

*: Age indicated is that of the control specimens and the joint specimens.

where:

- f_c' concrete crushing strength.
- f_{cu} concrete tensile strength.

2.4.2 STEEL

All reinforcing steel was from a single supply batch, in order to minimize variations. Three different types of reinforcement were used. High yield bars of 16 mm and 12 mm diameter for the main reinforcement in columns and beams whereas the stirrups were from 6 mm diameter mild steel. The stress-strain characteristics of the reinforcing steel were obtained from tension tests of samples with approximately 460 mm length, performed on a 300 kN Avery testing machine with an attached load-extension plotter. The extension was measured by means of a 60 mm gauge length extensometer gripped to the reinforcing bar. Table 2.4 gives the results of testing two 460 mm long samples from each size of bar (6 mm, 12 mm and 16 mm).

Table 2.4 Test Results of Samples of Reinforcement

Bar Nominal Diameter(mm)	f_y(N/mm^2)	f_u(N/mm^2)	E_s(N/mm^2)	ε_y(10^{-3})
6	291	389	197000	1.47
12	471	565	198000	2.37
16	472	576	204500	2.30

Notes : - E_s and ε_y are based on an extensometer gauge length of 60 mm.
- Values in the table are based on the average of two results.

2.5 SPECIMEN MANUFACTURE

2.5.1 Cage and Placement

All reinforcement was fabricated into cages before being placed in the formwork. The beam cage and column cage were constructed separately for each specimen, then tied together to form an exterior beam-column connection. Spacer chairs were fixed on the bottom reinforcement of the assembly to provide the cover needed. Once the assembly was placed in the formwork, additional chairs were fixed on the side reinforcement. When the cage assembly was in place, two lifting bolts were anchored in the reinforcement cage at the top of the beam used later to lift the test unit by crane into the loading frame.

2.5.2 Formwork

The formwork was made from timber and consisted of :

i) Two bases for column and beam connected together to form the base of the specimen.

ii) Five side pieces, two for the beam and three for the column.

iii) Three end-plates completed the formwork.

Since the plywood used throughout for facing the formwork was not thick enough (18 mm) to resist the pressure of the wet concrete without distorting, it was stiffened throughout by means of 45 mm square-section timber. This provided an easier and stronger connection for the external sides to the base. The timber was fixed by means of screws at sufficient close centres to ensure water tightness during casting. Before placing the reinforcement cage and casting, the formwork was cleaned, varnished, oiled and sealed to prevent bleeding

of the concrete during vibration. Fig.2.6 shows the formwork with a cage reinforcement lowered inside it.

2.5.3 Casting and Curing

Two batches of concrete were used for casting each of the test units. The concrete was mixed in the laboratory pan mixer with a capacity of approximately 600 kgs per batch. A crew of three people performed the task. Two 150·150 mm cubes and two 150 mm diameter cylinders were cast from each batch. The control specimens and the test specimens they represented were vibrated externally with a vibrating table and internally by a vibrating poker respectively. Curing was at 100% humidity under damp hessian and polythene sheet covers. This applied equally to the joint specimens and the control cubes and cylinders. After 24 hours, the forms were removed and the specimens were re-covered with damp hessian under polythene to keep them moist. The test unit and their control specimens were checked frequently and kept damp for a week. Each joint specimen and its control cubes and cylinders were then left to air dry in the laboratory under the same conditions until they were tested. Before testing, the specimens were coated with white paint in the joint region to permit improved crack visibility during testing.

2.6 TEST RIG

The shape of the test specimen was such that it could not be tested in a conventional testing machine, and therefore a special reaction frame was required in order to apply the loading. An overall view of the test set-up is shown in Fig.2.7. The test frame was L-shaped braced diagonally with its base bolted to a strong floor. The specimen was tied down to the base near both ends of the column. To

represent the inflection point, a pair of rollers was placed on each side of the column near its ends. Thus the horizontal and vertical displacement of the column's ends were restrained while they could rotate freely. The axial load was applied to the column of the sub-assemblies by a hydraulic jack acting on one end of the column, and through two high tensile steel bars with a diameter of 20 mm horizontally one on each side of the column to provide a reaction force on the other end of the column, and hence simulate a compressive force on the column. This is shown in the Fig.2.7. To apply lateral reversed forces at the beam tip, a double acting actuator was fixed to the upper part of the frame by means of bolts, as shown in Fig.2.8.

2.7 INSTRUMENTATION

2.7.1 Steel Strain Measurement

Strains in the reinforcement were obtained by means of electrical resistance strain gauges, as illustrated in Fig.2.9. The number and distribution of these varied somewhat between the different specimens as shown in Fig.2.10 and 2.11. The strain gauges used were Showa 120 ohm foil gauges of 2 mm gauge length with a gauge factor of 2.14. The surface of each reinforcing bar (12 mm and 16 mm) was prepared for gauging by grinding down the ribs of the deformed bars at the desired locations. Silicon carbide grit paper was used to smooth the surfaces of the reinforcing bars (including stirrups) and to provide a strong connection of the gauges to the bars. Various precautions were taken to protect the gauges against the impact of aggregate during placing of the concrete, and to provide sufficient resistance to earth in the concrete environment. The primary protection was an application of silicone rubber protective sealant on the strain gauges and its regions, then covered with an adhesive heat shrink sleeving.

2.7.2 Concrete Strain Measurement

Concrete strains were measured by Demec points. These were placed on one side of the column and beam in the joint region of the specimens where the cracks were expected. With these it was possible to measure the concrete strain, the crack widths in the concrete, as shown in Fig.2.12.

2.8 TEST PROCEDURE

The strain, and deflection readings were recorded by a PC computer via an analogue/digital input board.

The column axial load was applied one day prior to the test to eliminate any immediate creep. Test specimens were subjected to reversed cyclic loads by means of a concentrated force P at the end of the beam member (Fig.2.8), so that the bending moments and shear forces would be the same as that of a beam-column subassembly in a laterally loaded moment-resisting frame. Maximum bending moments occur at the connection where the shear force is also maximum. To simulate seismic effects, shear force P was applied to the beam tip by a double acting jack so that the bending moments and shear forces could be reversed and cycled. The shear in the column was achieved by the two reactions at both ends of the column. Figure 2.13 shows a specimen in the test rig ready to be tested.

The load history consisted of two cycles at increments of 7 kN until yielding was reached. Afterward, multiples of 1.5, 2.0, 2.5, and 3.0 times that of the load at yield were applied until the specimen failed.

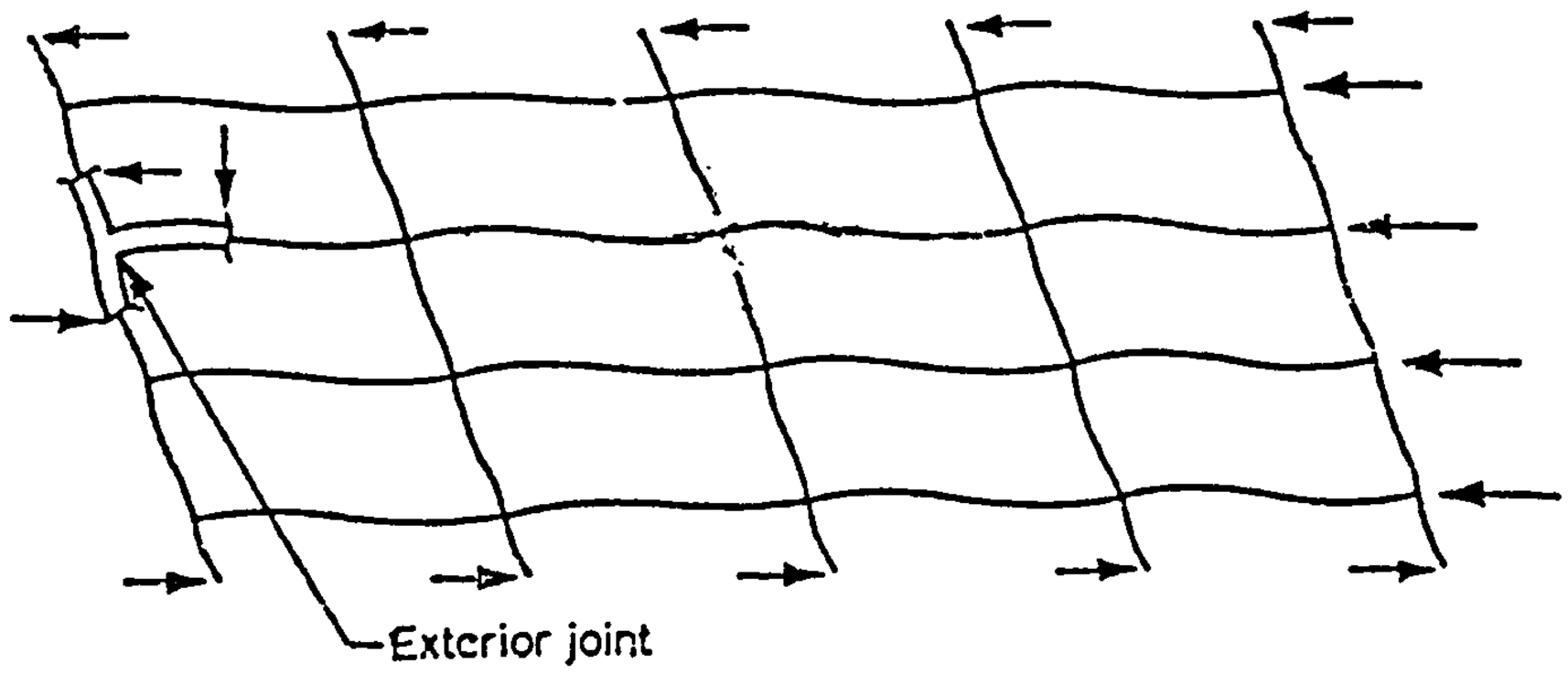

a) Exterior beam-column joint in a moment-resisting frame subjected to lateral loading

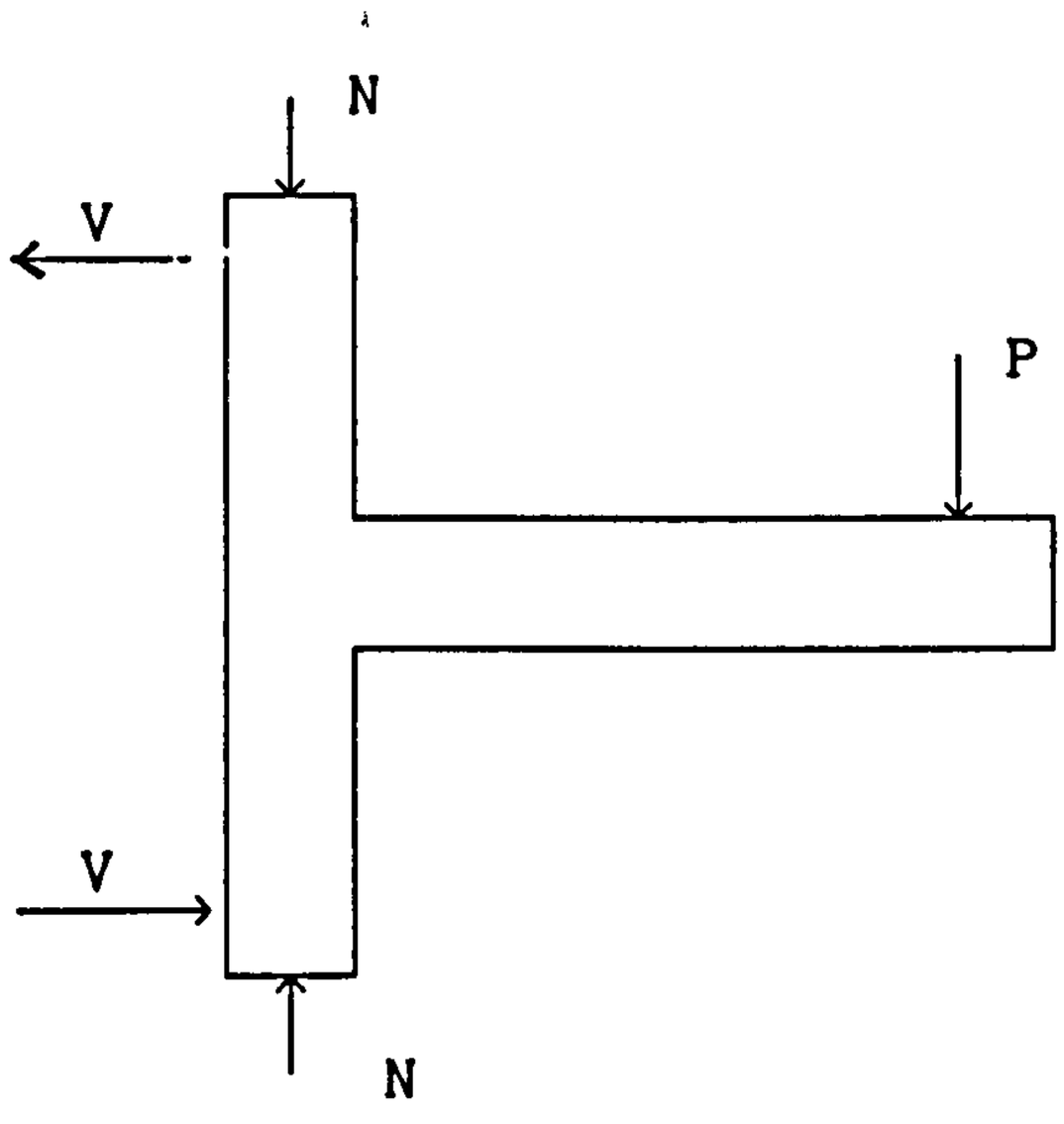

b) Detail of sub-assembly

FIG.2.1 ORIGIN OF TEST AND TESTING ARRANGEMENT

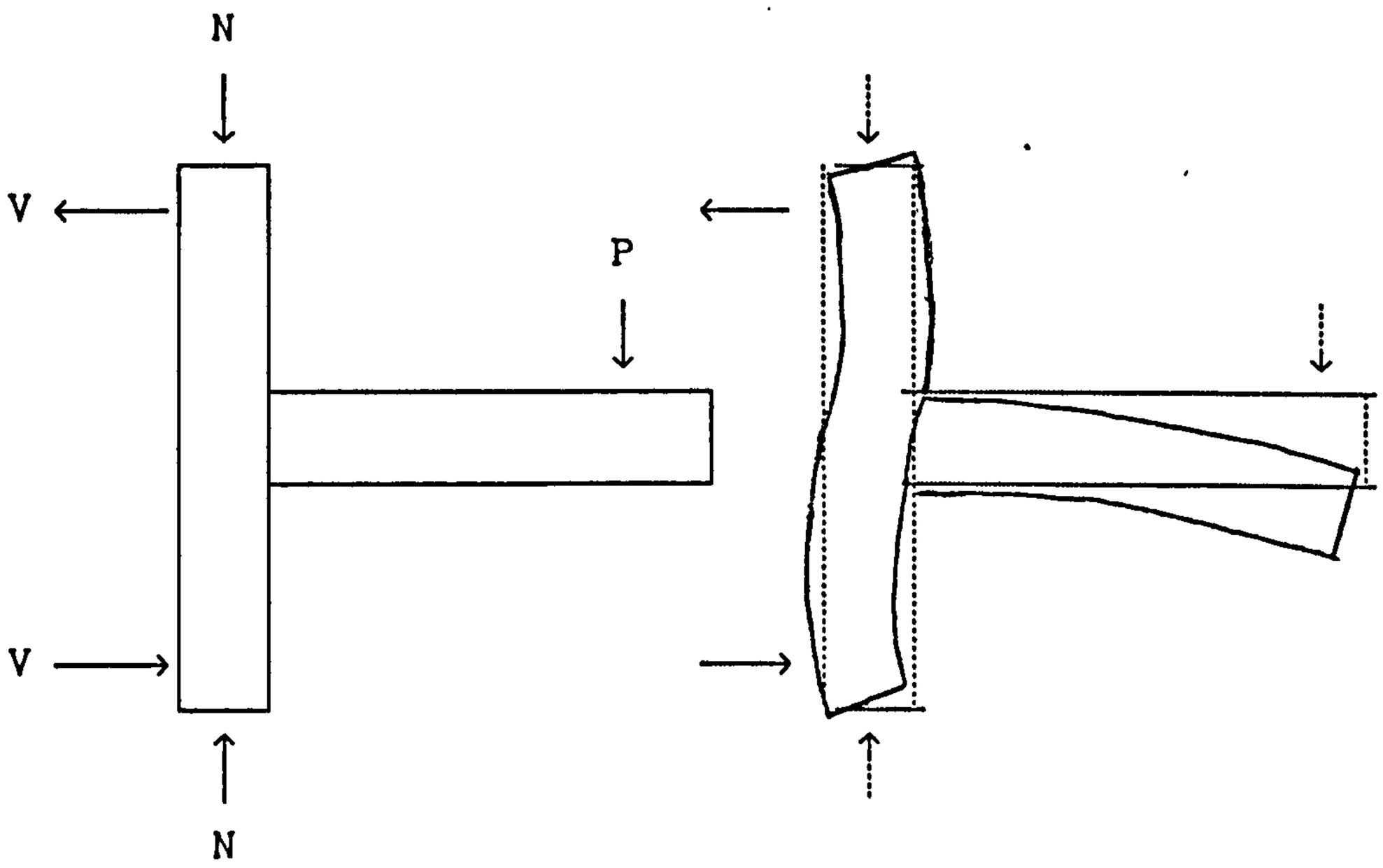

FIG.2.2 Deformed Shape of Beam-Column Sub-assembly

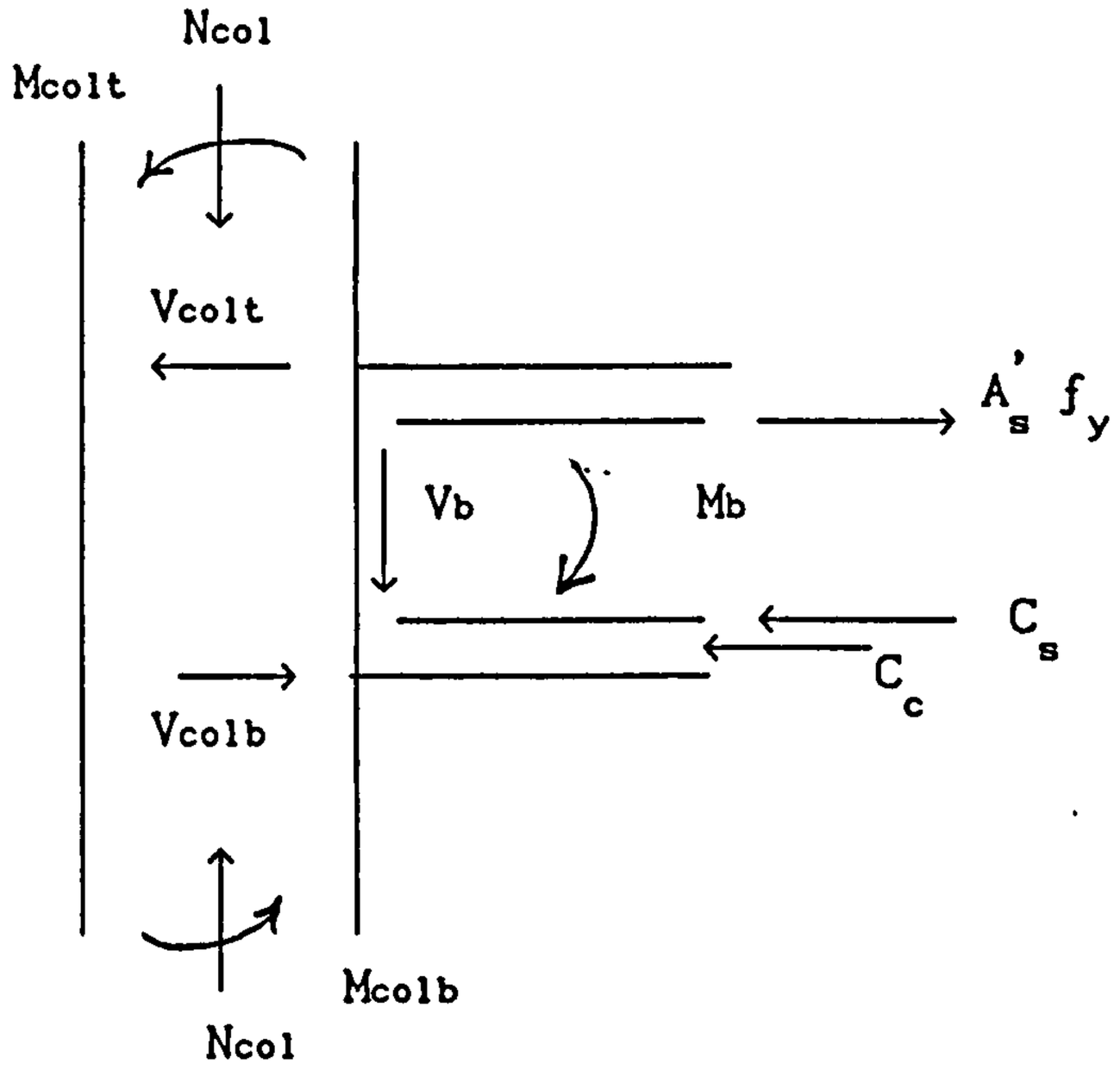

FIG.2.3 Critical Combination of Forces Acting on Joint

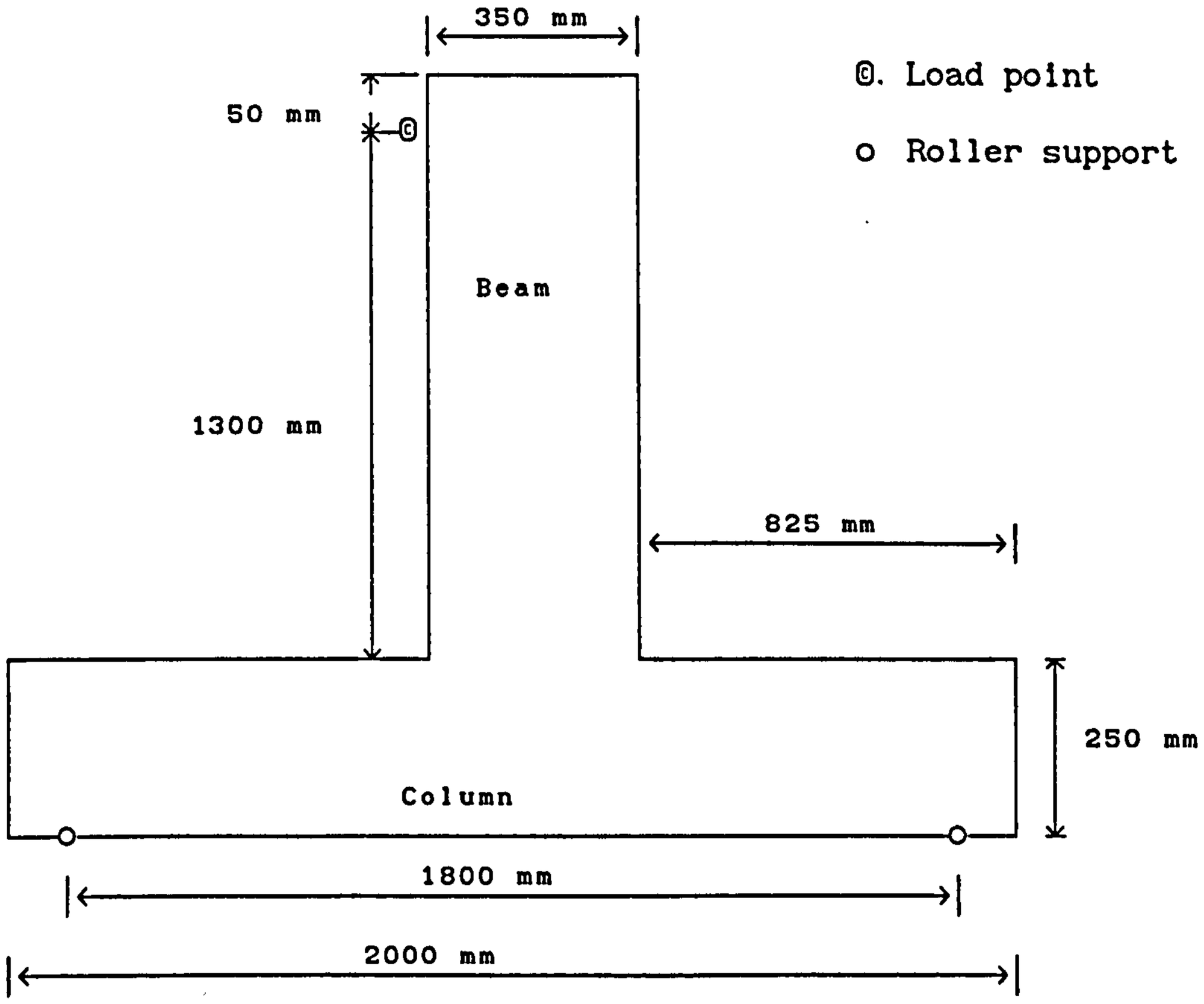

©. Load point

o Roller support

FIG.2 4 Overall Dimension of a Specimen

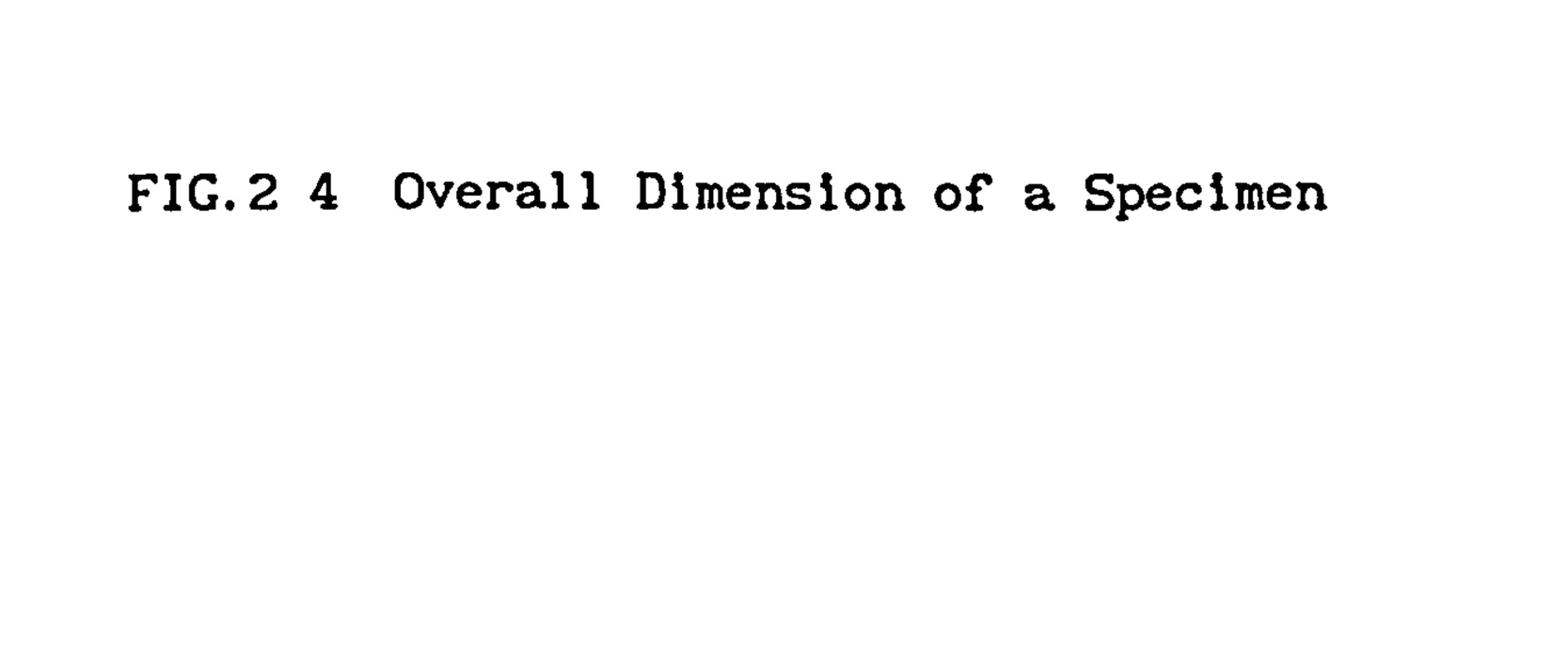

FIG.2.5 Beam and Column Cross Sections

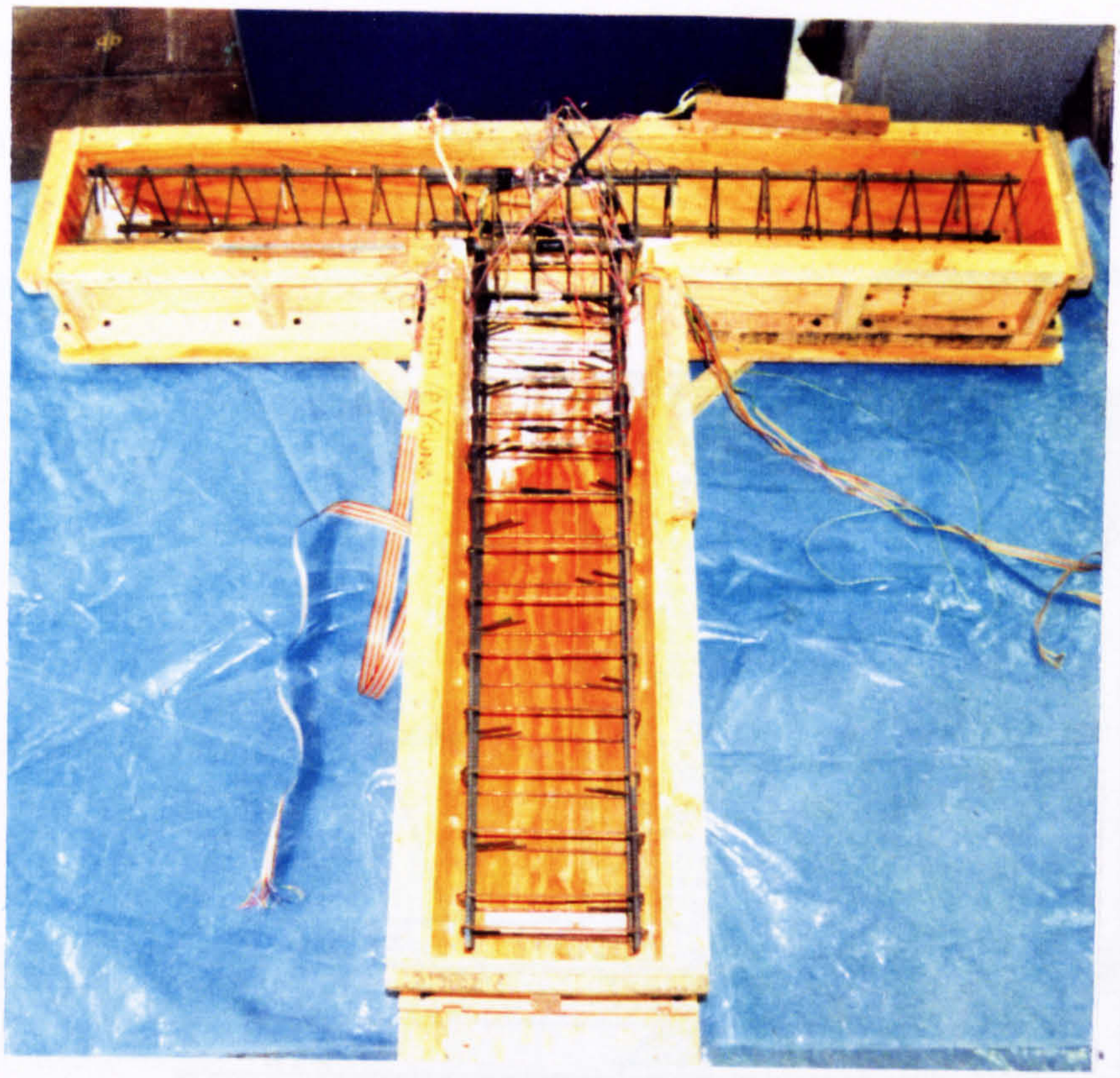

FIG.2.6 FORMWORK WITH STEEL REINFORCING CAGE

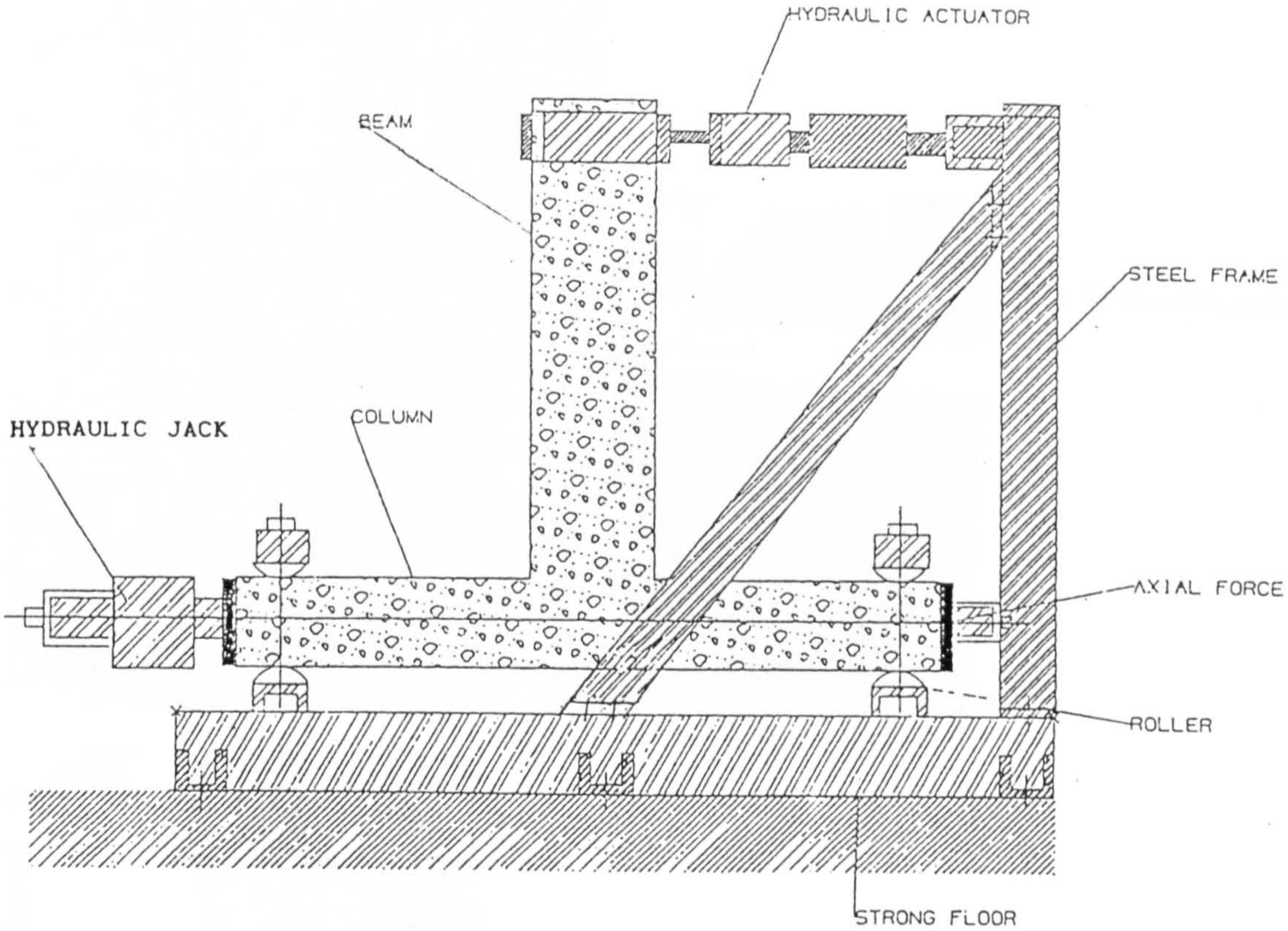

FIG.2.7 OVERALL VIEW OF THE TEST SET-UP

FIG.2.8 APPLIED LATERAL REVERSED FORCE AT THE BEAM TIP

FIG.2.9 TYPICAL STRAIN GAUGE DISTRIBUTION IN REINFORCING CAGE

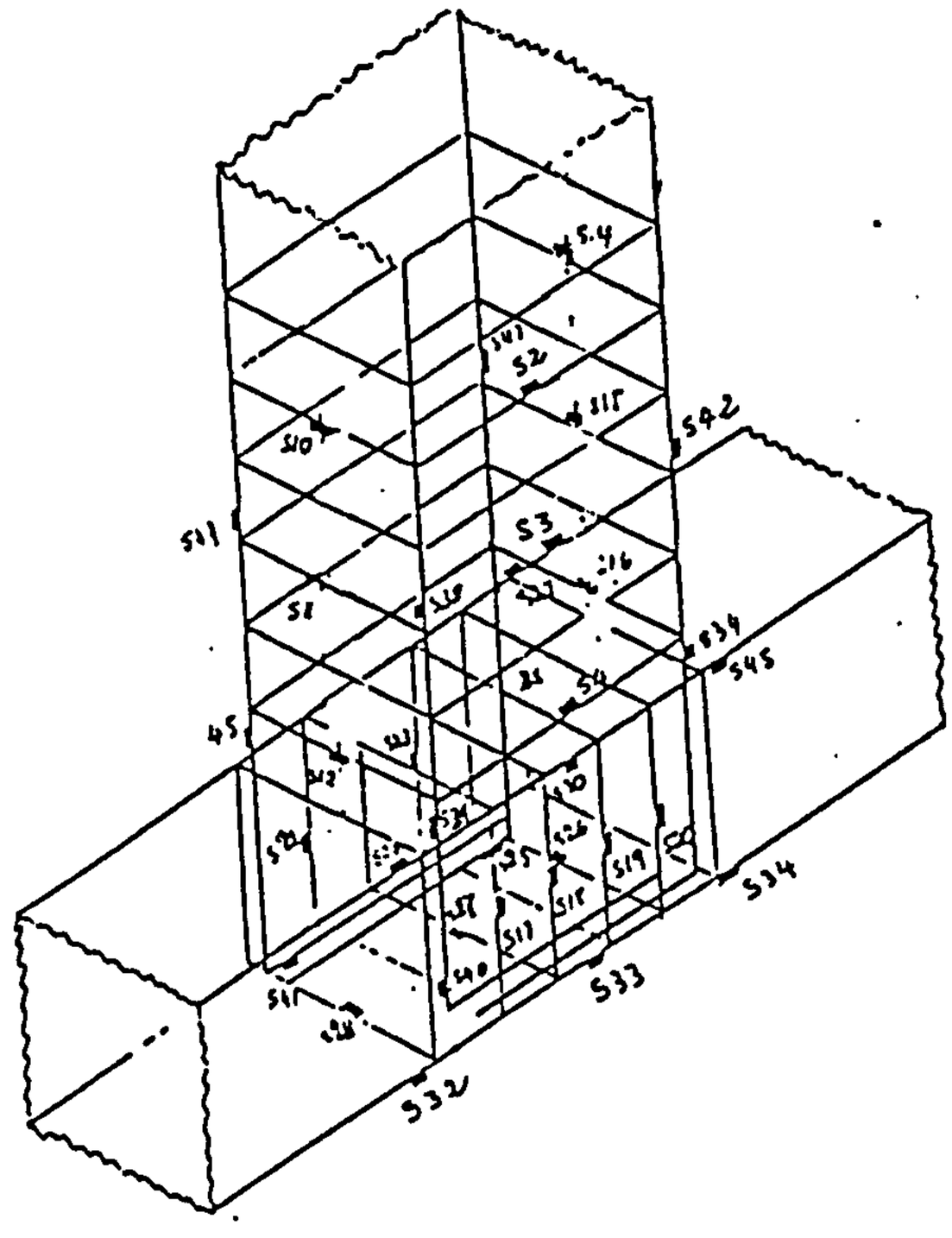

a) Specimen EX1

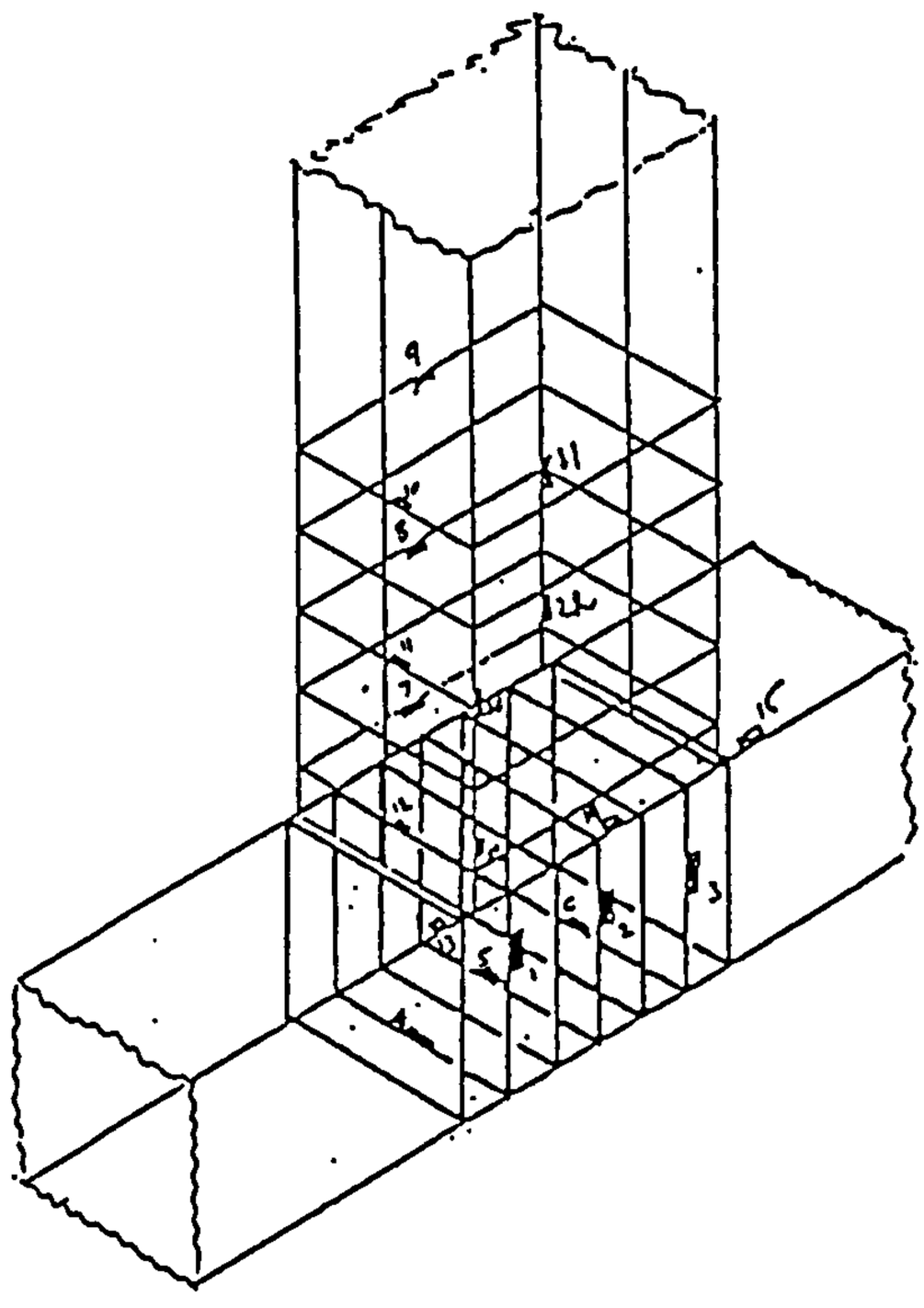

b) Specimen EX2

FIG.2.10 STRAIN GAUGE DISTRIBUTION IN EX-SERIES

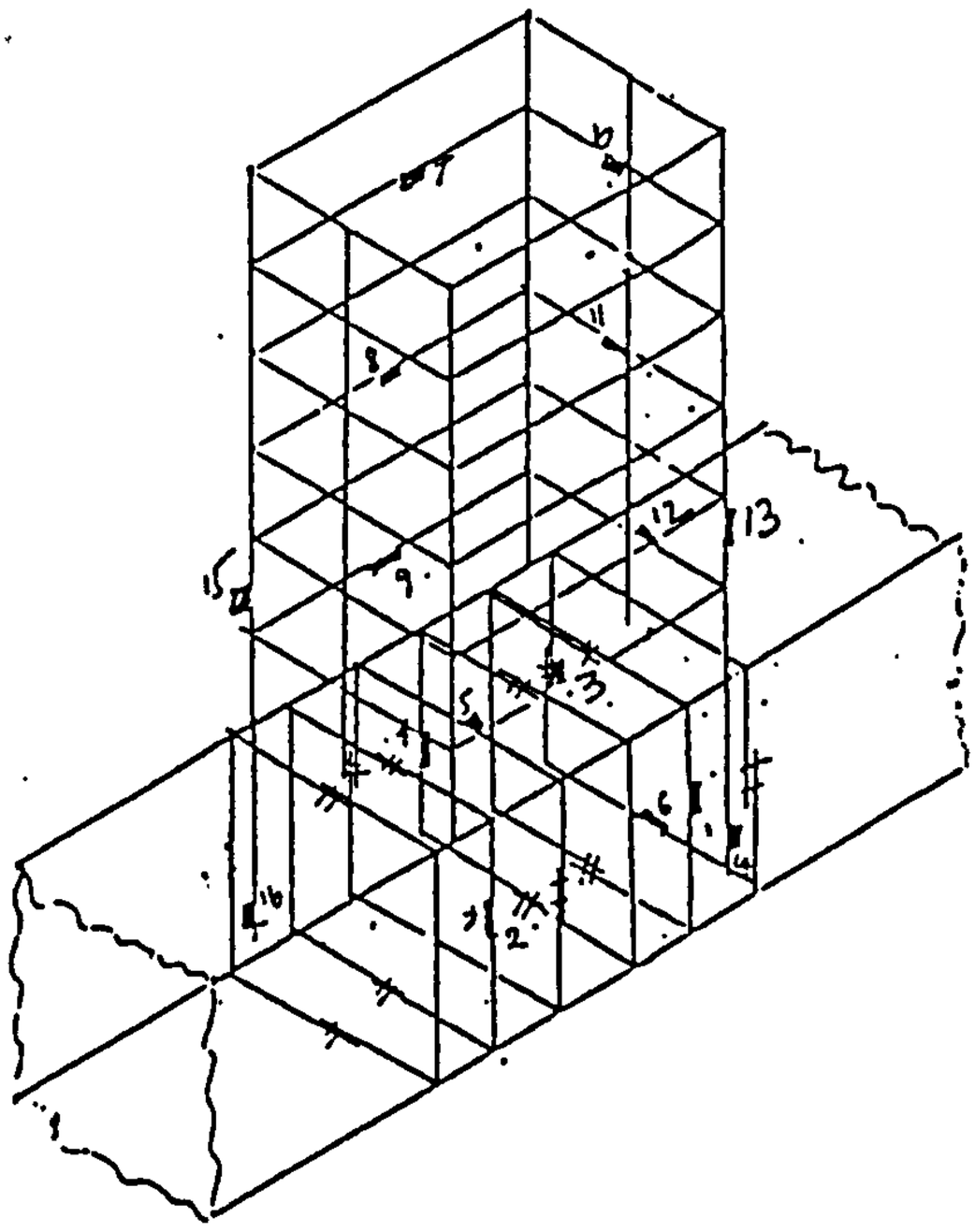

a) Specimen UD1

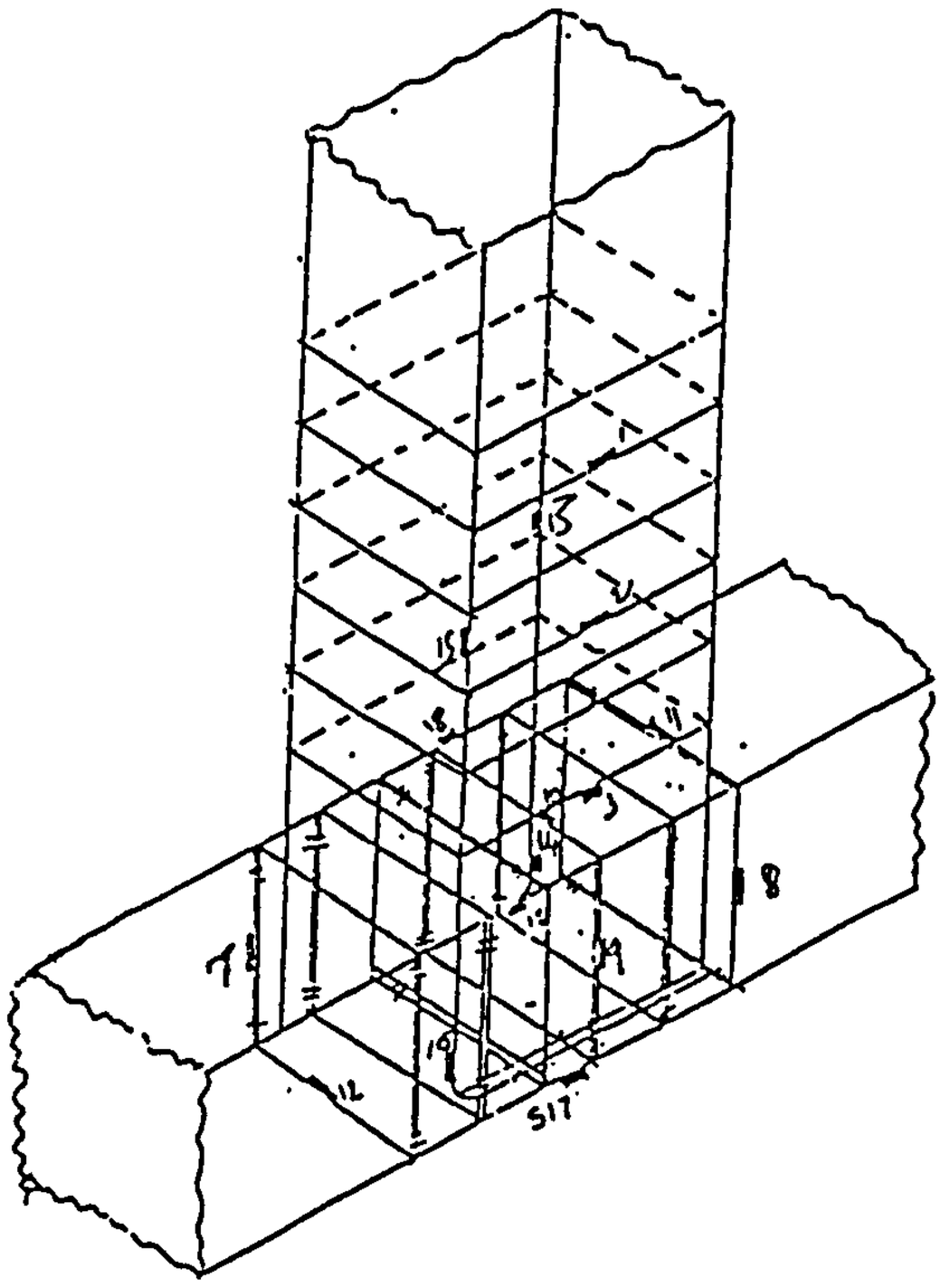

b) Specimen UD2

FIG.2.11 STRAIN GAUGE DISTRIBUTION IN UD-SERIES

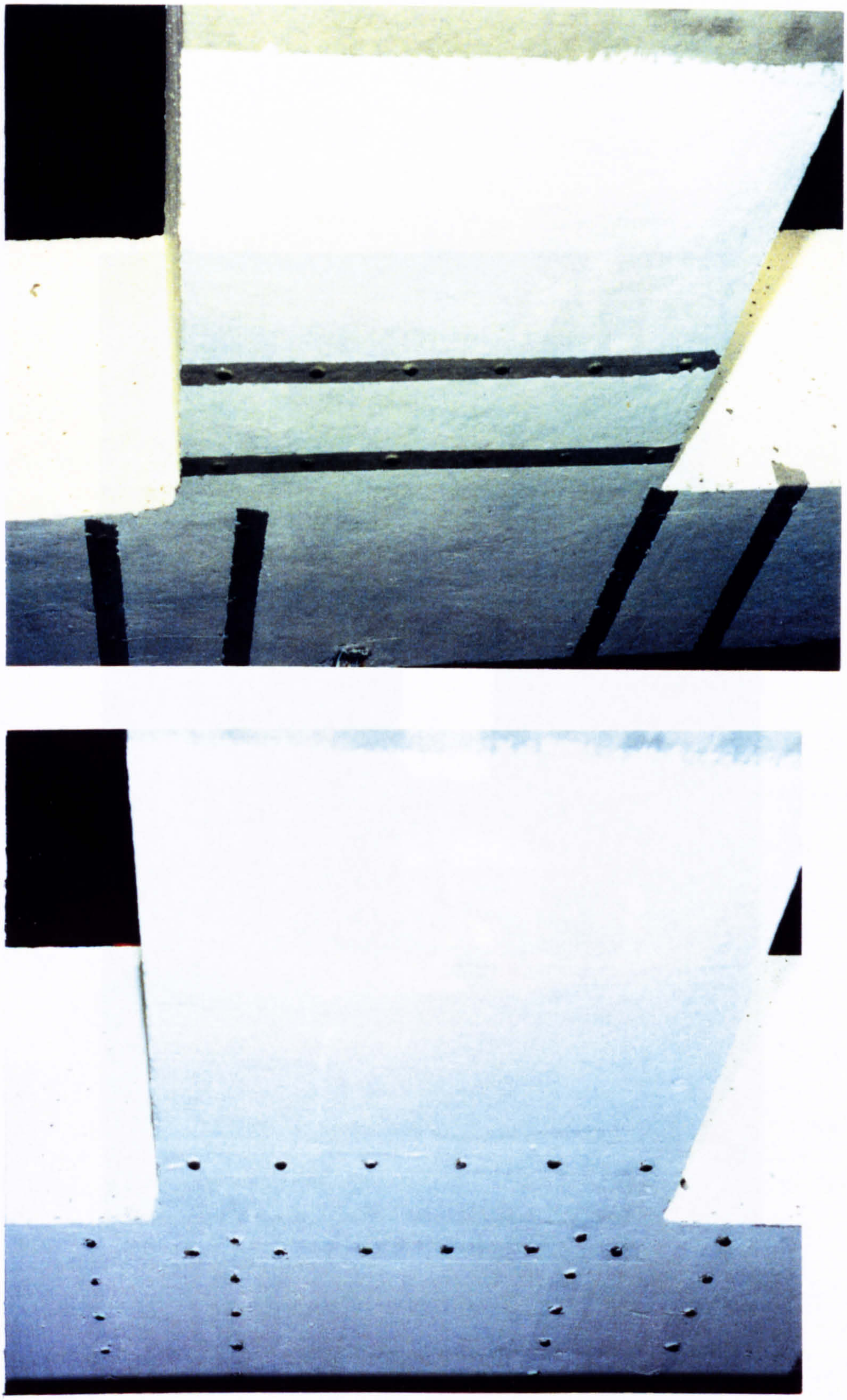

FIG.2.12 DEMEC POSITIONS IN SPECIMENS

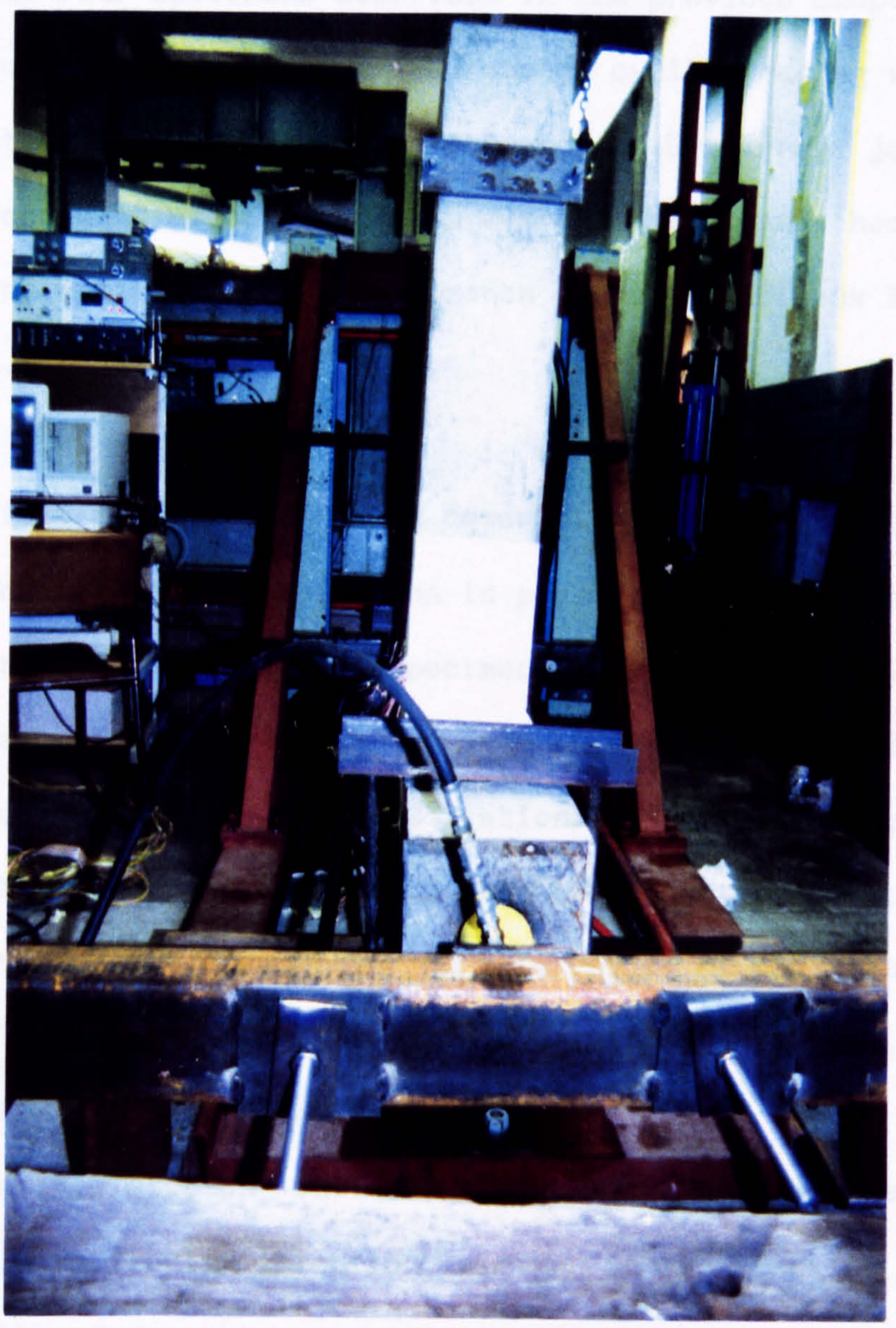

FIG. 2.13 A SPECIMEN IN THE TEST SET-UP READY TO BE TESTED

CHAPTER THREE EXPERIMENTAL RESULTS

3.1 INTRODUCTION

The four specimens described in the previous chapter were subjected to progressively increasing cyclic loading with the objective of studying the performance of U-stirrups joint reinforcement as compared with conventional square hoops. The load routine applied in the experiments for all specimens is illustrated in Fig.3.1.

First of all, a detailed description of the results of the tests on each of the four specimens is presented. This provides a full outline of the individual specimen behaviour. Secondly, the overall trends of performance are compared between the four specimens. These include indications from observations of crack development, strength and stiffness, and energy dissipation characteristics. Finally, conclusions are drawn based on this review of the results.

3.2 INDIVIDUAL SPECIMEN BEHAVIOUR

In this section, the behaviour of each specimen is examined in detail. Particular attention is given to the cracking history, severity of damage, energy dissipation, stiffness degradation, decay of strength, slippage of bars and other behaviour peculiar to the specimen. Certain aspects of behaviour were, however, common to all the specimens. Most of the cracking occurred in the beams at an early stage of loading in a region close to the joint, because the columns were flexurally stronger than the beams. The columns had a few hair line flexural cracks in two of the specimens and remained essentially

in the cracked-elastic range. In specimens EX2 and UD1 these cracks were more severe. The hysteresis loops for all the specimens showed a small varying degree of pinching, but in general, were of similar shape, except for specimen EX1.

The variables for each of the specimens were given in chapter two, Table 2.1 together with the pertinent parameters for the individual specimen to assist in behaviour identification.

Variables given for each specimen are; the beam and column moments, M_b and M_c ; the flexural strength ratio, M_R; the column axial load, N. The concrete compressive strength used, f'_c is given in Table 2.3, chapter two.

3.3 TEST ON UNIT EX1

3.3.1 Introduction

This test specimen EX1 had a much higher strength concrete than all the other specimens, and was the first specimen to be built and tested, and was designed according to the philosophy, weak-beam strong-column.

The intended column axial load was 17% of the ultimate load, causing a compressive stress of 0.03 $f'_c \cdot A_g$ over the column section. The ratio of top to bottom steel areas for the beam was 1.0. The specimen had six layers of hoops in the joint, each consisting of a square conventional stirrup. The hoops were at 70 mm centre-to-centre spacing and covering the width of the beam.

The specimen was loaded through eight cycles with a maximum

displacement ductility of 4.5. During the first cycle of loading to yield level, cracks of varying length appeared in the beam. The first crack (A1) was in the beam at a distance of 152 mm away from the column face, the second crack (A2) was much further from the first one at a distance of about 250 mm (1.21 times the effective depth of the beam), as can be seen in Figs.3.2. The third crack (A3) which was expected to occur first at the early stage of loading did not appear until the end of the cycle. This is explained by the fact that, the column axial load, which was 17% of ultimate load, induced compressive stress in the end of the beam, as well as in the column, thus delaying the flexural cracking in this region.

The other benefit of axial compression is that the bond environment for the beam bars should be improved in a joint with heavier axial load, so that yield penetration should be reduced.

Cracks on the other side of the beam are shown in Fig.3.2(b) when the direction of loading was reversed. The large crack (A3) at the junction of beam-column did not close up under reversed loading and, in fact, opened wider in each subsequent cycle of loading.

For the subsequent cycles, most of the inelastic action was concentrated at the end of the beam at the column face. Concrete in this area spalled off at the end of the fifth cycle and a wide crack occurred over the depth of the beam. It is worth noting that the column joint region was intact at the end of the test.

The load carrying capacity of the specimen began to reduce slowly after the third cycle and the hysteresis loops did not show any

pinching even with additional cycles as shown in Fig.3.3. The energy dissipation did not really decrease with additional displacement, this is probably because the jack stroke was not long enough, neither to reach the intended displacement ductility, nor to cause any significant damage in the joint region. Furthermore, the column was much stronger than the beam, with a flexural strength ratio of M_R = 2.96.

3.3.2 Beam Behaviour

As the end of the beam began to crack, the main beam bars tended to slip through the joint core. As the load was reversed, the tensile strain in the bar at location S41 decreased from point (A) to point (B) indicating a pull-out of beam main reinforcement from the joint, as shown in Fig.3.4(a). The reason for slip and the accompanying increasing tensile strain during the negative half of loading cycle will be explained later in the behaviour of specimen EX2, section 3.4.2. The main beam bar yielded in tension at the gauge location S41 during the positive half of the third loading cycle.

At a distance $d_{eff}/2$ (d_{eff}= effective depth of beam) from the face of the column, the main bars experienced both tensile and compressive strains, indicating very little slip. The plot of strain variation at this location (gauge S42) is shown in Fig.3.4(b). The strain in the bar varied over a narrow range between tension and compression during the first three cycles.

3.3.3 Column Behaviour

The load vs. strain of gauge S35 is shown in Fig.3.4(c). This column bar did not experience any yielding and remained elastic

throughout the test. As mentioned above, the compression load on the column section was quite significant and this helped the bars to stay under compression all through the test and with no sign of slippage at any locations in the bars, as illustrated in the above Figure.

3.3.4 Joint Behaviour

The transverse reinforcement hoops in the joint did not yield, at least the ones which had strain gauges attached to them.

Typical load vs. strain plots for stirrups at locations S17 and S18 are shown in Figs.3.5(a) and 3.5(b) respectively. The strain in gauge S18 which was located in the joint region near the loading point side, was much greater (twice the strain in S17) than in gauge S17 which was also located in the joint region, but near the compression side of the beam.

Both of these stirrups were under tension at the locations mentioned above whatever the direction of loading, as can be seen on those plots. The transverse reinforcement in this region kept the joint well confined and did not show any sign of reduction in the magnitude of cyclic strain or loss of confinement. At the end of the experiment, the joint area was intact as far as the column is concerned, as can be seen in Fig.3.6.

3.4 TEST ON UNIT EX2

3.4.1 Introduction

This specimen had the same amount, type and distribution of joint transverse hoop reinforcement placed at the same spacing as specimen EX1. The beam flexural steel consisted of six 12 mm diameter bars,

three on the tension side, and three on the compression side. The column was reinforced with four 12 mm diameter bars, one in each corner. In this test, a new jack with bigger stroke (260 mm) was provided to achieve the displacement ductility required. As in the first test EX1, the first cycle of loading to yield level caused flexural cracks in the beam. This time, the first crack appeared at the end of the beam (Fig.3.7(a)), the second crack took place at a distance equal to 1.16 times the effective depth of the beam (d_{eff}) away from the joint (not shown). In the third cycle, cracks appeared in the form of two hair lines at the face of the column in the joint region dividing the column in three segments, as shown in Fig.3.7(b). These hair-line cracks in the column on each side of the joint core are difficult to see (just visible). With an increasing number of cycles, more cracks appeared in the joint crossing the whole depth of the column, and the flexural crack at the end of the beam became more pronounced. During the fourth cycle, at a ductility level of 3.1, the concrete cover of the joint started to spall off. However, the joint core remained well confined by the hoops and the flexural hinge was forced to take place at the end of the beam near the joint. The condition of the specimen at the end of the test is shown in Fig.3.8(a) and 3.8(b).

The energy dissipated by the specimen increased with each additional cycle, especially after the second cycle reaching a maximum value of about 3 kN.m in the third cycle, as illustrated in Fig.3.9. The total energy dissipated during each cycle of loading throughout the experiment for all specimens is given in Table 3.1.

The load versus displacement history plot (Fig.3.10) indicated

that the load carrying capacity of the unit decreased after the third cycle, the strength and stiffness dropped, but not by much after this cycle.

TABLE 3.1 ENERGY DISSIPATION DURING EACH CYCLE (N.m)

SPECIMEN	1st cycle	2nd cycle	3rd cycle	4th cycle	5th cycle	6th cycle
EX1	1052	1121	1200	1098	986	880
EX2	56	322	2605	2278	-	-
UD1	33	106	1044	4756	3950	3123
UD2	19	87	106	723	2800	3556

3.4.2 Beam Behaviour

Main reinforcement in the beam yielded during the third cycle at a location S19, close to the face of the column. The locations and the Load vs. strain plots for this gauge is shown in Figs.3.11(a). During the first positive half of the fourth loading cycle, a reversal in the direction of strain occurs at point (A), as shown on the plot, Fig.3.11(a). As the load is reversed, the tensile strain in the bar decreased from point (A) to point (B) shown on the plot. While loading in the negative direction, it is expected that reinforcing bar would be subjected to compression at this location and tension at the corresponding location on the outer side of the joint. At point (B) on the plot, however, this expected trend changed and consequently, the strain in the bar, instead of continuously decreasing along (BC),

began to increase along (BD). It was assumed that this indicated the propagation of tensile stress through the core from the other side of joint and marked the beginning of slippage. The bar on the compression side, at location S22, slipped at the early stage of the second cycle at point (A), as shown in Fig.3.11(b). This means that, either a localized slip has occurred in this location, or the bar slipped. In the subsequent cycle, such a reversal of strain in the reinforcing bar was also observed at point (C), but only for the bar at location S22. So, the idea of localized slip is to be discarded, at least for this bar. Therefore, the beam bars at location S19 and S22 experienced some slippage.

3.4.3 Column Behaviour

The column bars remained elastic through all the loading cycles. Two distinctly different behaviours of the column bars are shown in Figs.3.12(a) and Fig.3.12(b) at locations S13 and S17 respectively. The column bar at location S13 indicates typical excursions into tension and compression without any slip. The bar at location S17 began to slip in the fourth cycle, as can be seen on the plot. The reasons for slip and the accompanying increasing tensile strain during the negative half of loading cycle have been explained previously in the behaviour of specimen EX1.

3.4.4 Joint Behaviour

The rectangular hoops in the joint did not reach the yielding point during the test. A typical behaviour of load vs. strain of stirrups at locations S1, S2, S4 and S6 are shown in Figs.3.13(a), 3.13(b), 3.13(c) and 3.13(d) respectively. The gauges were located at

the middle of the stirrups' legs. As can be seen from these plots, the strain in the longitudinal direction (parallel to the beam main bars) is higher than in the transverse direction because of the direction of loading.

The hoops kept the joint core well confined and no visible deterioration of the core was noticed through to the end of the test. In spite of the well confined core, there was some slippage in beam bars (pull-out) and consequently, an open crack at the beam-column interface was very noticeable, as it has been seen in section 3.4.1, Fig.3.9.

3.5 TEST ON UNIT UD1

3.5.1 Introduction

This specimen had six layers of stirrups in the joint as in the case of specimens EX1 and EX2, but unlike these units, the joint transverse reinforcement of this specimen was set up differently. Each one of these stirrups was constructed using U-stirrups bars with an overlap equal to one-half of the effective depth of the column, to form a complete stirrup, as shown in Fig.3.14(a). This design simplifies construction on site, and also reduces the congestion of the joint when placing the beam cage, whether in internal or external connection. The longitudinal reinforcement both in the beam and in the column was similar to that in specimen EX2. That is to say, six bars of 12 mm diameter (three on each side) for the beam and four bars of 12 mm diameter for the column. The transverse steel in the beam was kept constant in all specimens. Near the joint region, the transverse reinforcement consisted of seven layers of hoops spread over a distance equal to 1.5 times the depth of the beam. The first stirrup

was placed at 25 mm from the joint, and the remaining six were 70 mm centre-to-centre spacing. In the rest of the beam, the stirrups were at 100 mm from one another.

This unit was loaded through six cycles and reached a maximum displacement ductility of 6.40 at the last cycle. The propagation of cracks in the specimen is shown in Figs.3.14(b) to 3.14(e). During the first cycle of loading, the first crack (A) appeared on the tension side of the beam at a distance of 100 mm above the connection area and crossing half of its depth. In the following cycle, a second crack (B) occurred, this time at the beam-column connection. While loading in the other direction, the crack (A) closed up and was almost invisible. In the third cycle of loading to yielding level, cracks (C) appeared in the joint region and another tensile crack (D) appeared in the beam at a distance equal to the depth of the beam. In the subsequent cycles, more cracks occurred and were restricted to the column surfaces. Towards the end of the test the cover of the joint was observed to be separated from the core in some areas. This was determined by tapping the cover with a screwdriver handle, as can be seen in Fig.3.14(e) in which the rear face of the column is photographed in a mirror.

The beam suffered flexural cracks beginning in the first cycle. Most of the flexural cracking occurred at the end of the beam above the joint region and was confined within a distance equal to 1.20 times its effective depth from the column. A major crack at the beam-column junction opened to a width of 10 mm by the end of the test and extended through the depth of the beam. The column also exhibited severe flexural-shear cracking close to the joint. In this specimen,

the plastic hinge developed at the end of the beam. Damage occurred both in this region and in the beam-column joint. The condition of joint after test is shown in Fig.3.15(a) and 3.15(b). This shows a fully developed plastic hinge at the end of the beam, which has penetrated some way into the column face. Severe spalling also occurred where the column meets the joint core. Cracks may also be noted on the other side of the joint core.

Overlapping U-stirrups may be seen in Fig.3.15(c), together with buckling of beam bars under reversed loading. The overlaps appear to be intact despite loss of cover. However, at least one overlapping pair of U-stirrups did separate - but is not shown. A beam bar may be seen slipping in the anchorage zone, as shown in Fig.3.15(d).

3.5.2 Beam Behaviour

The beam bars on both sides experienced some slippage at an early stage of loading. Figures 3.16(a), 3.16(b), 3.16(c) and 3.16(d) show the strain history of these bars at locations S13, S14, S15 and S16 respectively. During the first two elastic cycles, the bars underwent both tensile and compressive strains. Bars at locations S16, S14 and S15 yielded during the third cycle. Bar at location S13 did not yield because of its location (far away from the joint region where high forces are expected). As can be seen from these plots, the strain in some locations in the bars was higher than the yield strain, causing wide flexural-shear cracks in the region adjacent to the column. Also the progressive opening of the crack at the plastic hinge at each cycle produced a ratcheting effect on the beam bar strain at location S14 (Fig.3.16(b)).

3.5.3 Column Behaviour

The column behaviour was almost similar to that of specimen EX2, except in the joint region where the column experienced more damage, as can be seen in the following section.

3.5.4 Joint Behaviour

Figures 3.17(a) to 3.17(e) illustrate the behaviour of joint stirrups at locations S1, S2, S3, S4 and S6 respectively. S1 and S2 behaved very well (Figs.3.17(a) and 3.17(b)). S3 and S4 reveal the tendency of stirrups to go progressively into tension as the cracks develop. Large strains (up to yield) occurred in S6, Fig.3.17(e) although it was not in the severely cracked region. In the fourth cycle, and after the concrete had crushed, the U-stirrups in the column within the junction started to separate from one another, leaving this area vulnerable to any tensile forces. This could be explain by the fact that, after yielding, and under reversed loading, the tensile strain in the U-stirrups increased whatever the direction of the load, and continue to increase in the subsequent cycles.

The reacting forces exerted by shear acting on the U-stirrups corners became significant, generating high stresses along the U-legs. These forces which needed support to be carried all over the bar length, have to be transferred through the overlap of these U-stirrups. In some instance this overlap was not enough to provide the transfer required. Consequently, at least one failed under these high forces and the joint became vulnerable to bar slippage especially under the tensile stress. The damage caused to this specimen and above all to the joint region at the end of the test, has been seen in section 3.5.1, Fig.3.15.

3.6 TEST ON UNIT UD2

3.6.1 Introduction

This specimen was the last one in the series to be built and tested, and was almost identical to unit UD1. The only differences between the two units were; the number of bars in the beam main reinforcement, and the overlap length in the U-stirrups in the joint area.

In this unit UD2, the main reinforcement in the beam consisted of four bars, two (ϕ16) on the tension side and two (ϕ12) on the compression side, and the overlap length in the stirrups, was equal to the whole column's effective depth (d_{eff}), as illustrated in Fig.3.18(a).

The column axial load was 5% of its ultimate load (less than in the case of specimen UD1, which had a column axial load of 7%),causing a compressive stress of $0.01 \cdot f'_c \, A_g$ over the column section.

The unit was loaded through six cycles with a maximum displacement ductility of 4.2. During the second cycle of loading to yield level, cracks appeared in the beam. The first flexural crack (A), shown in Fig.3.18(b), occurred at the beam-column junction, and not in the beam distant from the joint. In this unit, the axial load on the column was smaller than in unit UD1, and the concrete strength was less than in the preceding test. The second and the third cracks (B) and (C) occurred in the third cycle. (B) took place at the column-joint core junction and a further crack (D) occurred at distance equal to 1.24 times the beam effective depth, away from the column face. The first crack (B) in the joint area, occurred in the third cycle. In the subsequent cycles, the crack at the beam-column junction became wider

and wider, and there was again formation of a plastic hinge in the beam near the column face and more damage concentration in this region, but there was little damage in the joint, with partial loss of joint cover, as shown in Fig.3.19(b). The well confined nature of the joint core may be seen in Fig.3.19(c).

The load carrying capacity of the specimen was almost constant after the yielding cycle of loading, and the hysteresis loops did not show any pinching with additional cycles as shown in Fig.3.20. The energy dissipation reduced after the fifth cycle, and the displacement ductility factor was 4.2 in the sixth cycle, which was the last one.

3.6.2 Beam Behaviour

In this specimen, four strain gauges were attached to main beam bars, as illustrated in Fig.3.21. The beam at location S15 and S16 yielded in tension (yield strain about 2100 $\mu\varepsilon$) at a very late stage (cycle four), and did not show any sign of slippage, as can be seen in Fig.3.21(a) and 3.21(b). Figures 3.21(c) and 3.21(d) show the strain history of the bar at gauges S13 and S14 respectively. The slope of the load vs strain loops during the elastic cycles at location S14 (Fig.3.21(d)) is much steeper than at location S13 (Fig.3.21(c)). This is because it is at the start of the anchorage which is embedded well in the joint core. However, as the core deteriorates through cracking, it can be seen that it experiences strains similar to those on the same bar but outside the joint region (S13).

During the first two cycles, the bar at location S13 underwent both tensile and compressive strain. In the third cycle, the behaviour of strain at location S14 began to change indicating the beginning of

the slippage. In the subsequent cycles, the same phenomenon occurred in S13 and continued to occur to S14, which led to the conclusion that that bar experienced some slippage. In addition, the same bar (on the compression side) at these two locations (S13 and S14) showed sign of yielding (2200 $\mu\varepsilon$) during the fifth cycle, as shown in Fig.3.21(a) and 3.21(b).

3.6.3 Column Behaviour

Figures 3.22(a) and 3.22(b) show typical column bars behaviour. The column bars did not experience any yielding and remained elastic throughout the test. In the first half of the second cycle, the alternation of strain in which the column bars were subjected stopped, indicating the beginning of slippage at locations S17 and S18. This phenomenon was more evident at S18 as shown on the plots. In the subsequent cycles, there was no further increase in strain, and the column bars remained elastic throughout the experiment.

3.6.4 Joint Behaviour

In this specimen, the amount, the shape and the arrangement of transverse steel used in the joint, was similar to those in specimen UD1. The only difference was; the overlap length, which in this unit covered the whole length of the column effective depth (d_{eff}). Figures 3.23(a).to 3.23(d) show the behaviour of the double U stirrups in the joint region at locations S7, S8, S11 and S12 respectively. Most of these stirrups did not reach the yielding point, although gauge S7, may have yielded with an extra cycle. The strain in stirrups was very small in the first three cycles, because at this stage, the moment applied to the adjoining members was still small and did not lead to any extensive diagonal cracking yet, and consequently, the diagonal

tension stress on the transverse steel was still low. From the fourth cycle, the strain increased gradually with the diagonal cracking until the end of the sixth cycle, which was the last loading cycle. During these last few cycles, there was a sudden increase in strain only at location S7, as indicated in Fig.3.23(a). It is worth noting that S7 was located in a double leg and may have affected the gauge output. In spite of some slippage in those locations, most of the U-stirrups remained elastic exhibiting better behaviour than the ones in UD1, which helped the joint to be kept well confined and remained elastic. This behaviour did not allow the plastic hinge to form in this area, and pushed it away to take place at the end of the beam. At the conclusion of the test, no visible deterioration of the joint core was noticeable, as shown in section 3.6.1 (Fig.3.19).

3.7 GENERAL TRENDS OF PERFORMANCE

The data recorded during each test can be grouped into three categories:

(1) a continuous plot of load vs. displacement that determined the load history during the test.

(2) a record of strain at each gauge location in the specimen corresponding to each load point.

(3) a record of the crack development in the joint region for all specimens except EX1, corresponding to each change in lateral load on the beam as well as the shear on the column.

Each type of data individually reflects on certain aspects of the behaviour of a test specimen and collectively determines the influence

of a particular variable on the overall behaviour of the sub-assembly. The significance of each type of data as related to the behaviour of the joint, along with some general observations, will be discussed separately.

3.7.1 Crack Development

During each test the cracking pattern, location and size of cracks, provide a first insight into the specimens' behaviour. The failure mode is also partially determined by the extent of cracking at the critical regions of the subassembly. Cracking was expected in the beam near the joint region rather than in the column, because all the specimens were designed with strong column-weak beam philosophy, except for few hair line flexural cracks in a region close to the joint. However, column cracking was observed in the specimens especially in specimen UD1. These column cracks occurred in the joint region for the reasons which will be discussed later.

Fine flexural cracks in the beams appeared as soon as the specimens were loaded. These cracks were confined within an average distance equal to 1.16 times the depth of the beam on either side of the joint. The beam-column interface in all specimens had a major flexural crack at the end of the beam by the end of the test. The cracking pattern in the beams of all specimens was similar and extended nearly the same distance away from the column face.

The cracks in the joint region of the specimen EX2, UD1 and UD2 appeared during the third cycle. During successive cycles, the number of cracks in the joint increased. Their severity depended on the type of confinement used in the core.

3.7.2 Strength and Stiffness of Joint

The degradation of load carrying capacity and stiffness is easily seen from the applied load vs. load point displacement hysteresis curves. The hysteresis loops represent a combined behaviour of joint, beam and column. Most of the inelastic action occurred in the beam. However, if the joint were to have deteriorated before any significant damage occurred in beam, the hysteresis could represent the behaviour of the joint.

Comparing the response of the UD-specimens (UD1 and UD2), as shown in Figs.3.24(a) and 3.24(b), it can be seen that the load carrying capacity of specimen UD1 began to deteriorate soon after the first four cycles while specimen UD2 had no decay in strength for the first four cycles. Specimen EX1 had almost a stable load carrying capacity through the first three load cycles. Neither of the EX-specimens exhibited any significant reduction in strength with increased displacement ductility, see Figs.3.24(c) and 3.24(d). However, the specimen EX1 carried lower load during a repeated cycle, because of the limited stroke of the jack. To achieve more ductility for the other tests, a new jack with a longer stroke was necessary.

All the specimens except EX1, experienced a loss of stiffness as indicated by the reduction of the slope of the load vs. displacement hysteresis loops. The reduction in slope in each specimen varied slightly, depending upon the values of the variables used, e.g., beam-column flexural ratio, joint shear stress, shape and placement of stirrups in the joint region, and the concrete strength.

Pinching of the hysteresis loop near zero load indicates reduced ability to absorb energy and is caused mainly by:

- Wide flexural cracks in the hinging zone of the beam.
- Slippage of the column bars through the joint and the pullout of the beam's longitudinal reinforcement from the joint.

A careful examination of the hysteresis loops indicates that specimen UD1 had more stiffness degradation and loss of strength than specimen UD2 after the fourth cycle as can be seen by the reduction in the slope of the hysteresis cycle. The specimen UD2 had larger yield displacement and therefore, fewer loading cycles could be accomplished.

After taking into account the variation in loading history, the beam load vs. displacement hysteresis curve for specimen EX2 indicates that this specimen had less loss in strength and stiffness than specimen UD1. An explanation is that with specimen UD1 which had U-stirrups with an overlap length equal to one-half of the column depth in the beam-column intersection, the joint region experienced more damage because of the type of confinement used in that region, and this led to a loss of stiffness and strength, and to a pullout of the beam main reinforcement from the joint. In spite of this behaviour, the pinching in the hysteresis cycle of specimen EX2 was more obvious than in specimen UD1, although, both units had the same amount of main reinforcement in their beams.

A well designed and detailed specimen is expected to maintain its strength as well as its stiffness under cyclic loading within a

reasonable limit of displacement ductilities. Comparing all the specimens in EX-specimens as well as the UD-specimens, with respect to the main variables used, the following conclusion may be drawn based on the results obtained from the specimens tested:

- Specimens (EX2, UD1) which had three longitudinal reinforcement bars on each face in the beam, showed better strength and stiffness characteristics than those with only two layers (EX1, UD2).

- The flexural strength ratio (M_R) had a major effect on the location of the flexural hinging. In all specimens tested in this study, the flexural strength ratio was greater than 1.5. Therefore, in none of the specimens flexural hinges formed in the column. For the specimen which had flexural strength ratio considerably greater than 1.5, the cracks were distributed more into the beam and away from the joint.

- Comparing the UD-specimens together, the specimen UD2, with an overlap length equal to the effective depth of the column in the joint region, behaved much better than the UD1 unit, which had an overlap length equal one-half of column effective depth. Furthermore, this new stirrup arrangement, in comparing specimens UD2 and EX2, seemed to have the same effect, maybe better than the conventional confinement formed by square or rectangular stirrups.

- Specimens which had a moderate column axial load (EX1, EX2) showed better behaviour and less cracking in the joint region, and kept this area under compression at least for the first two or three cycles.

3.7.3 Energy Dissipation

The beam load vs. displacement curves, referred to as hysteresis loops, are the single most important source of information for load and stiffness degradation and for the energy characteristics of a sub-assembly. The area within the loops for each cycle of loading is proportional to the energy dissipated during that cycle. Energy dissipated during each cycle for all specimens is given in Table 3.1. Since the yield load and yield displacements were not the same for all the specimens, a more realistic comparison of energy dissipated for each specimen could be made by considering the normalized energy dissipation with the corresponding displacement ductilities.

Table 3.2 gives the energy dissipated, normalized with respect to the yield cycle energy dissipation, for different levels of displacement ductilities. In this context, the yield cycle is defined as the point at which the overall load-displacement curve goes non-linear, and does not mean yield of the reinforcement. It is useful to identify the energy dissipated in this complete cycle and refer to it as the "Yield cycle" [Ehsani and Wight (1985), Durrani (1989), Govindan at al (1986), etc.]. A plot of cumulative energy dissipation vs. cumulative displacement ductilities is shown in Fig.3.25.

A sufficient amount of energy dissipation without substantial loss of strength and stiffness constitutes a desirable behaviour for a beam-column sub-assembly under cyclic loading. Excessive pinching and a drop in the slope of the hysteresis loops, due to the severe damage either in the joint or in the adjoining areas, indicates a reduced energy dissipation capacity. Any significant crack in the elements of the subassembly contributes to the softening of the reloading

stiffness. The energy dissipation, however, is also dependent upon the load carrying capacity of a specimen. The energy dissipated by each specimen during each loading cycles can be seen in section 3.4.1, Fig.3.9.

TABLE 3.2 NORMALIZED ENERGY DISSIPATION

	1st cycle		2nd cycle		3rd cycle		4th cycle		5th cycle		6th cycle	
SPECIMEN	μ	ϕ	μ	ϕ	μ	ϕ	μ	ϕ	μ	ϕ	μ	ϕ
EX1	1	1	2.09	1.06	2.68	1.14	2.71	1.04	2.77	0.93	2.86	0.83
EX2	0.38	0.17	1	1	3.05	8.09	3.72	7.07	-	-	-	-
UD1	0.29	0.03	0.47	0.10	1	1	4.15	4.55	4.48	3.78	6.10	2.99
UD2	0.16	0.02	0.40	0.12	0.86	0.14	1	1	3.46	3.87	4.20	4.91

- : Not available

where : δ_i = displacement at cycle i

δ_y = yield displacement

U_i = energy dissipation at cycle i

U_y = energy dissipation at yield cycle

and

$$\mu = \delta_i/\delta_y$$

$$\phi = U_i/U_y$$

3.7.4 Effect of Joint Shear Stress

A reduction in the joint shear stress had a distinct effect on the load-carrying capacity of the specimens. As shown in Fig.3.24, specimen EX1 (Fig.3.24(d)) which had a joint shear stress of ($0.52\sqrt{f_c'}$), maintained its maximum first load cycle almost throughout the experiment. Specimen UD2 which had a joint shear stress value of $1.02\sqrt{f_c'}$, also maintained its load-carrying capacity until the end of test (Fig.3.24(b)). However, specimen EX2 and UD1, which had a joint shear stress values of $1.6\sqrt{f_c'}$ and $1.1\sqrt{f_c'}$ respectively, the load-carrying capacity deteriorated after the third cycle for EX2, and after the fourth cycle for UD1, as illustrated in Figs.3.24(c) and 3.24(a).

Examination of the specimens during and at the conclusion of the tests indicated that the specimens that had lower joint shear stress suffered less damage (EX1 and UD1) than those with higher joint shear stress (EX2 and UD1). Deterioration of the concrete in the joint due to higher shear stress had an effect on the anchorage conditions of the beam longitudinal reinforcement in the joint. As a result, specimens with higher shear stresses, beam bar pull-out started during earlier cycles of loading.

In specimens that had low shear stresses in the joint, beam bar pull-out did not occur during the first few cycles of loading. For more detail, a sample calculation of joint shear stress for specimen EX2 is given in Appendix A section (A3), together with a table (Table A3) summarizing the joint shear stress magnitude for all specimens tested.

3.7.5 Failure Mode of Specimens

For members undergoing cyclic loading, several investigators [Hooshang et al.(1981) and Young Soo et al.(1989)] have defined failure as the point where the member strength (moment) at maximum displacement (curvature) has dropped below 75% of the initial yield strength.

The failure mode depends on a number of different variables such as concrete strength, confinement ratio, and axial force. A section may fail in flexure due to concrete crushing or fracture of tensile steel, or it may fail because the transverse shear steel buckles. Other failure modes are related to shear or bond failure.

In this study, three failure modes were observed:

i) The first is the failure mode of specimen EX1. This specimen developed flexural hinge at the end of the beam near the column. At the conclusion of the test, the joint and the critical column region (junction) were intact. The damage was concentrated at the end of the beam (plastic hinge region) and had two characteristic features; concrete rupture in the beam compression zones and buckling of beam main reinforcement.

ii) The second failure mode is that of specimen EX2 and UD2. There were again formations of plastic hinge in the beam near the column face and more damage was concentration in this region, but there was little damage in the joint, with partial loss of joint concrete cover.

iii) The third failure type is that of specimen UD1. This specimen

developed flexural hinge in the beam. Damage occurred both in this region and in the beam-column joint. At the end of the test, plastic hinge did spread to the column face, as shown in Fig.3.15.

3.8 CONCLUSION

At this stage, a brief overall review of the behaviour of all specimens tested is necessary. Based on the test results, the following conclusions are drawn.

The flexural strength ratio had a major effect on the location of the flexural hinging in the specimens. All specimens tested in this study had flexural strength ratios greater than 1.5. Therefore, in none of the specimens did plastic hinges form in the column face.

The level of joint shear stress had a significant effect on the behaviour of the joint and the sub-assembly. Specimens with a lower joint shear stress had better behaviour than the specimens with a higher joint shear stress.

In all specimens, cracking occurred in the beam within a hinging zone equal to 1.25 effective depth of the member. In specimen UD1 cracking of the joint led to slippage (pull-out) of the beam main reinforcement

Crushing of concrete for all specimens occurred at the end of the beams, this led to yielding of beam main bars within this zone.

Specimens EX2 and UD1, to which were added intermediate longitudinal reinforcement in the beams, were capable of achieving an

increase in strength and dissipate more energy in comparison with specimens without beam intermediate bars. This is considered to be an improvement in structural performance. On the other hand, unit UD1 which had U-stirrups with short legs in the joint region, suffered more damage in this zone towards the end of experiment in comparison with specimen UD2, because the U-stirrups covering only one-half of the column effective depth, failed at this stage of loading to resist high shear which led to deterioration of the joint.

U-stirrups with a length equal to the whole effective depth of the column helped specimen UD2 to maintain its strength and load-carrying capacity almost throughout the test, and to resist higher shear forces than in the case of unit UD1, in addition to the well provided confinement of the joint core.

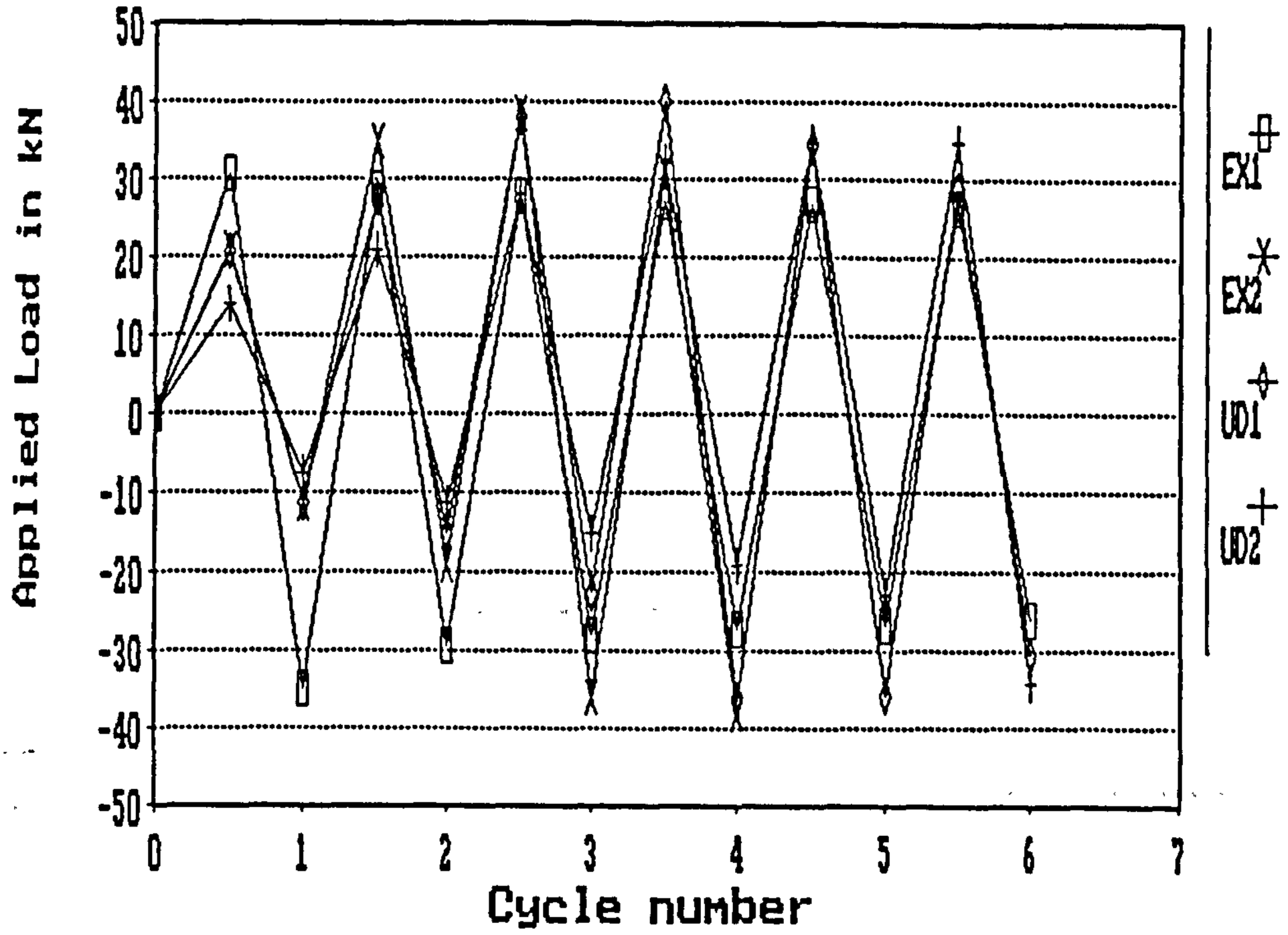

FIG.3.1 LOADING HISTORY

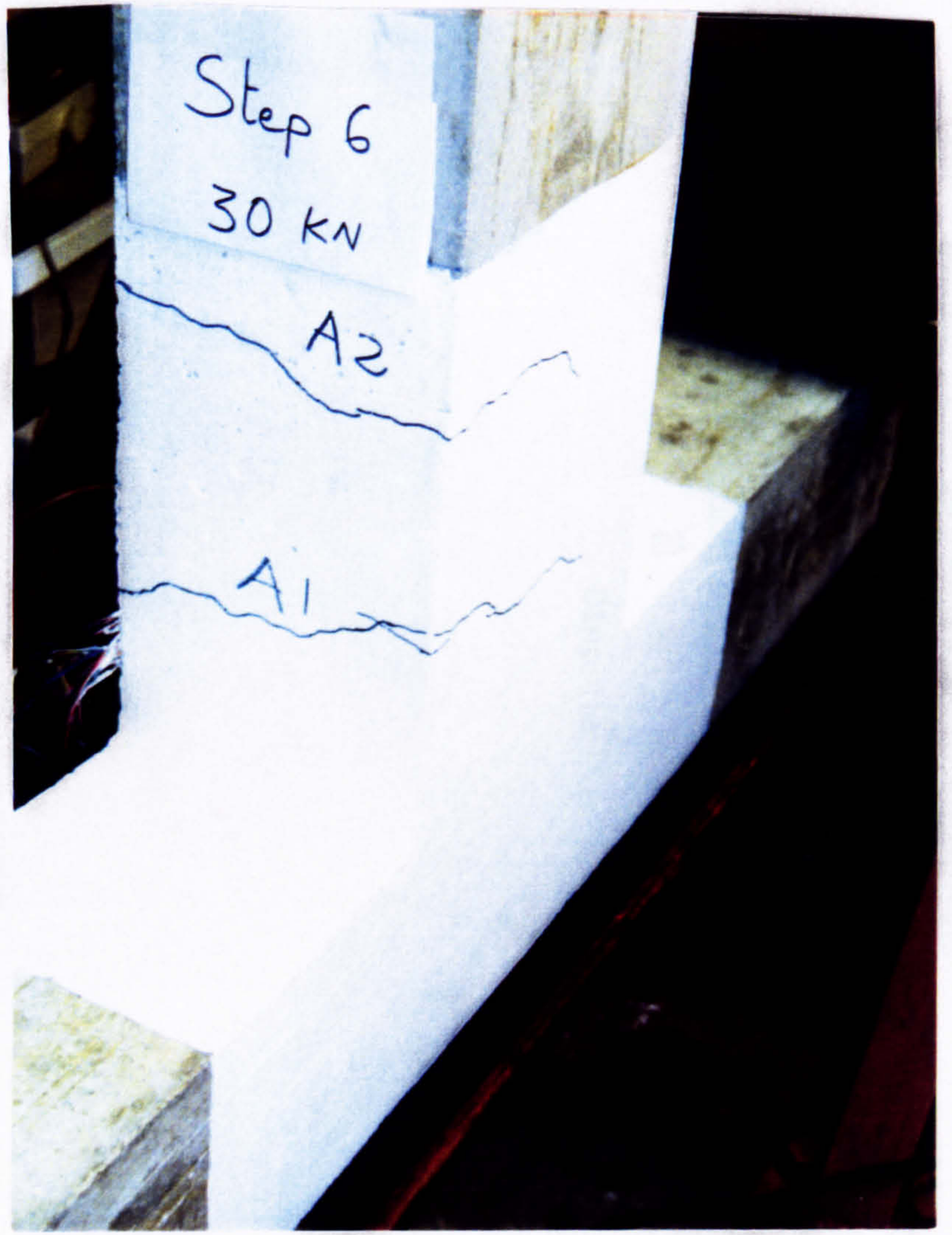

a)

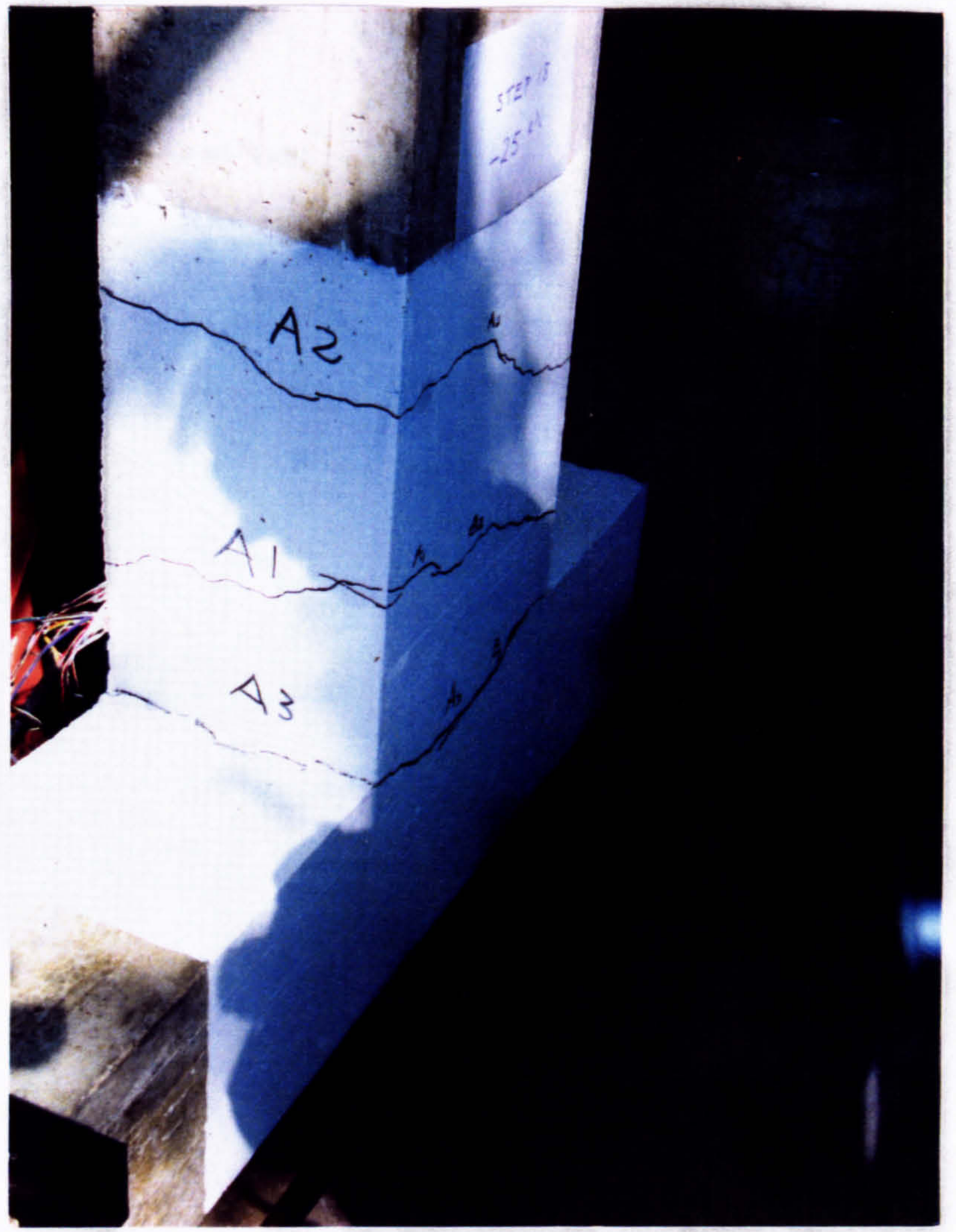

b)

FIG.3.2 FIRST CRACKS IN SPECIMEN -EX1-

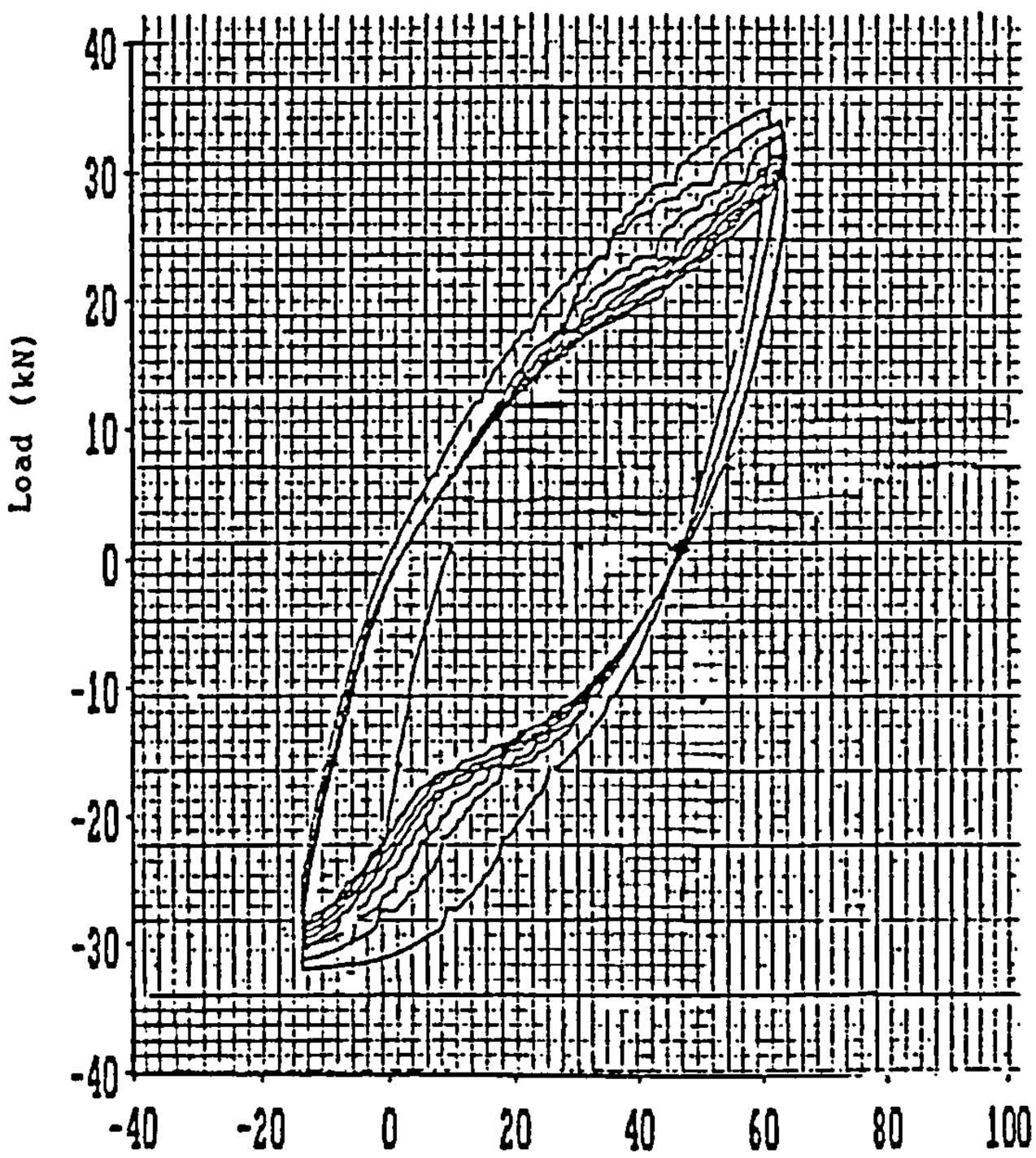

FIG.3.3 HYSTERESIS CYCLE OF SPECIMEN -EX1-

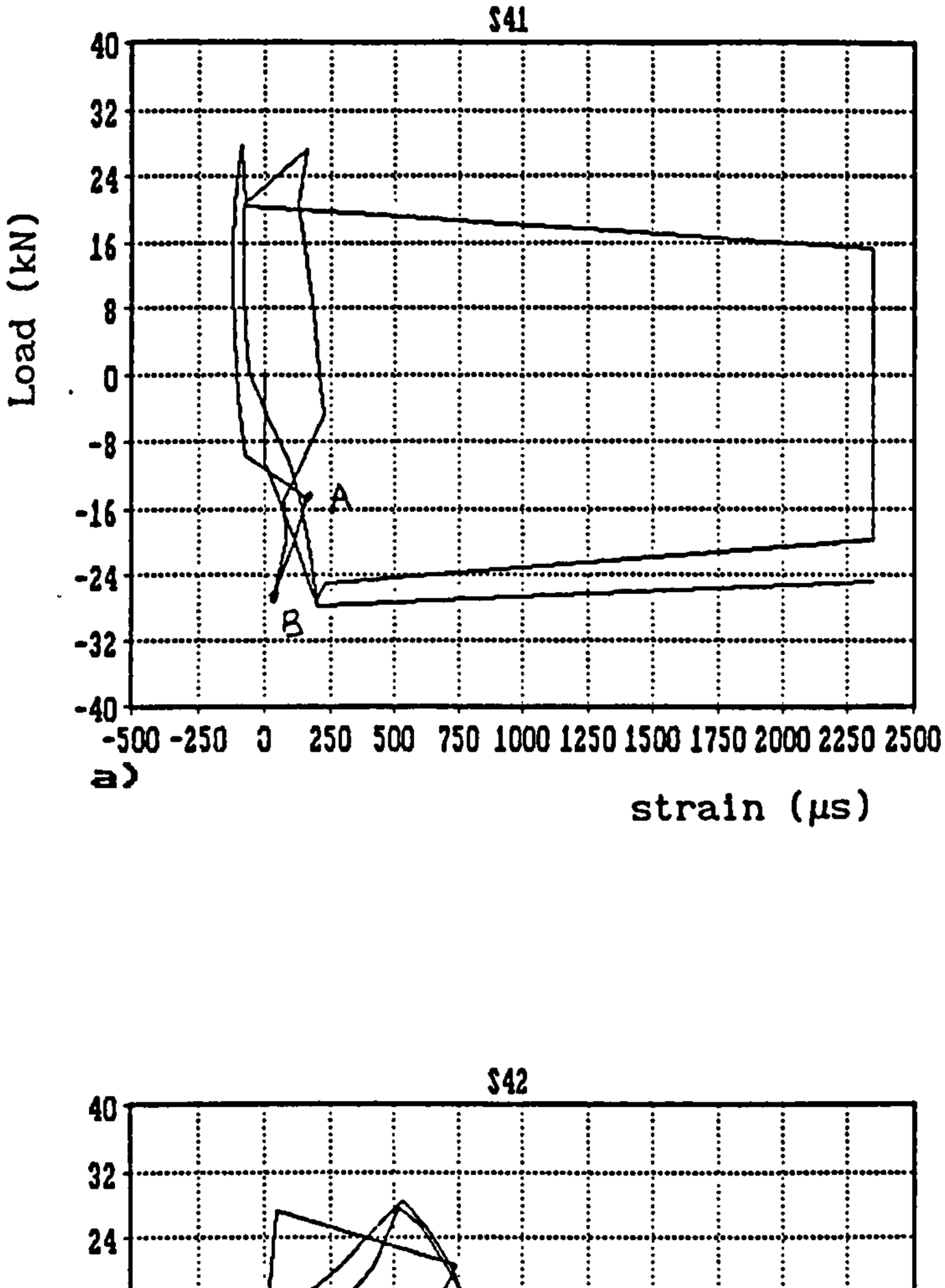

FIG.3.4 LOAD VS. STRAIN HISTORY

a) Gauge S41 b) Gauge S42 c) Gauge S35

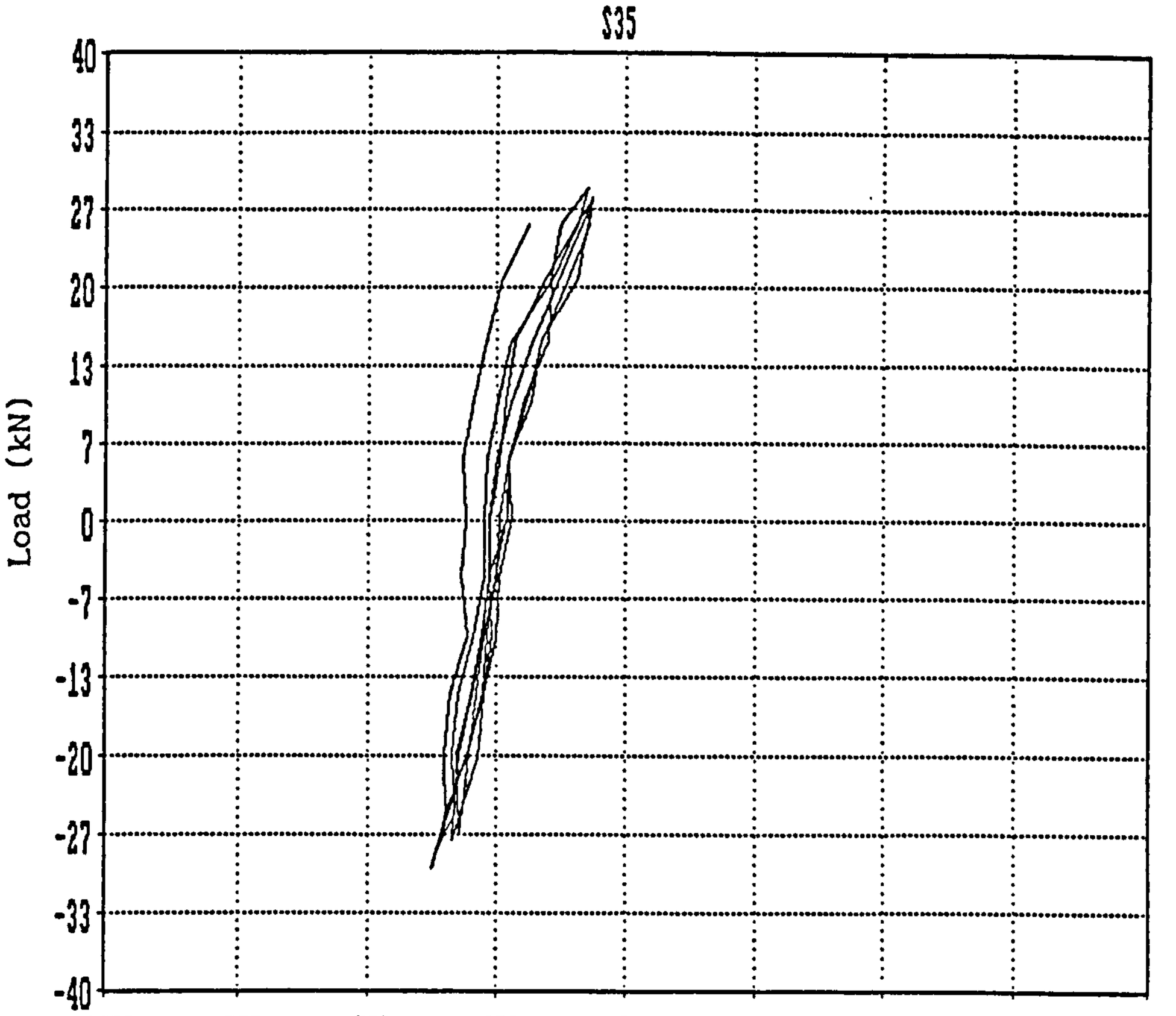
S35
40
33
27
20
13
7
0
-7
-13
-20
-27
-33
-40
Load (kN)
-1000
-750
-500
-250
0
250
500
750
1000
strain (μs)

c)

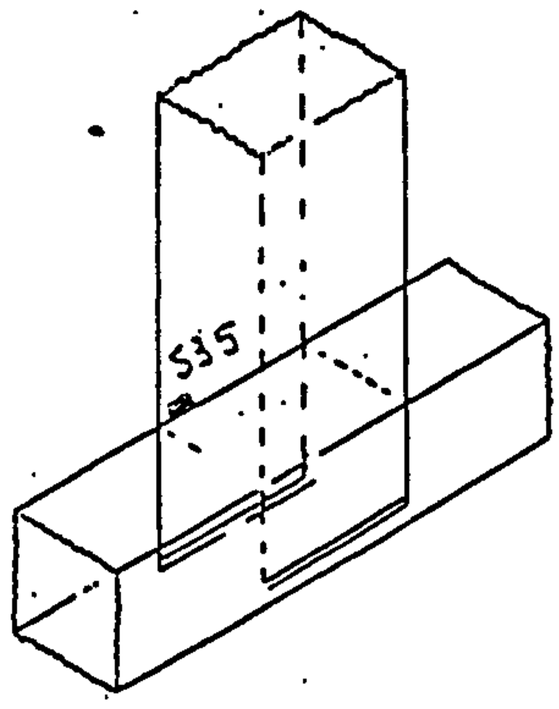
S35

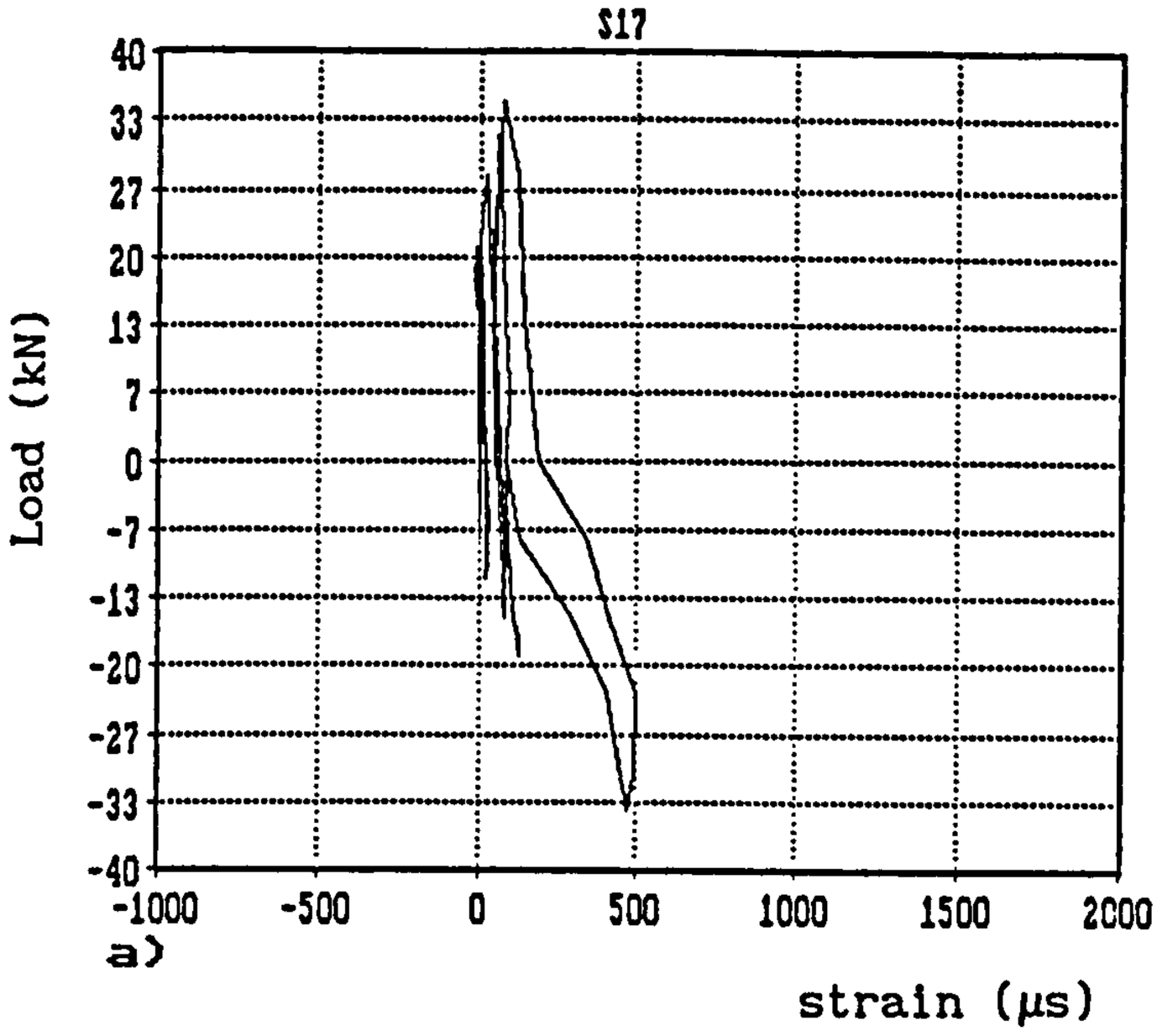

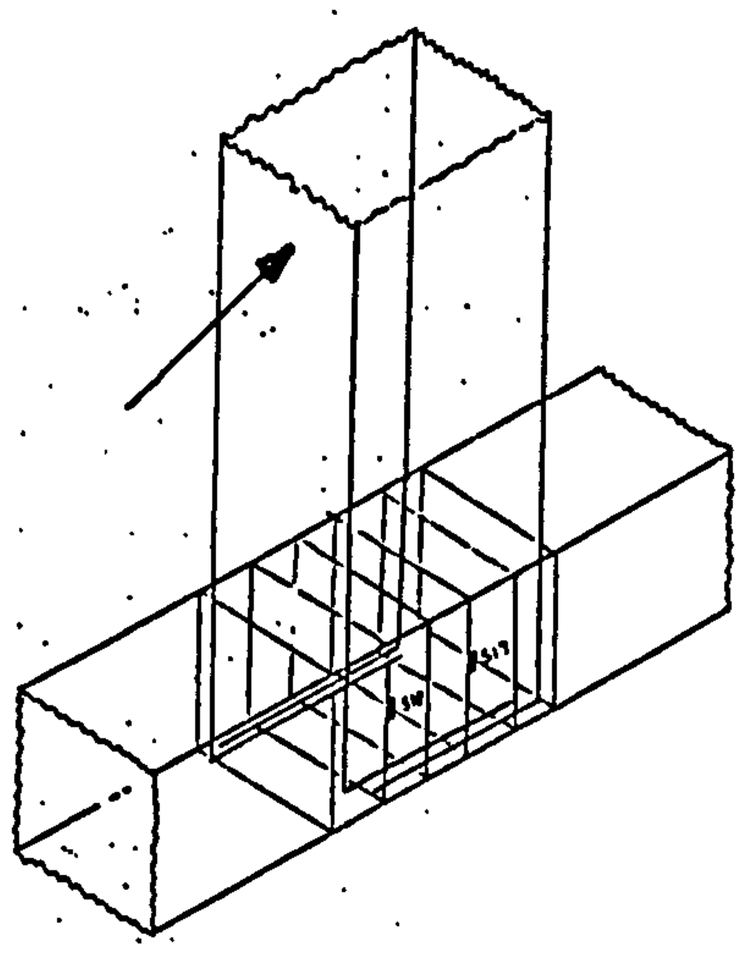

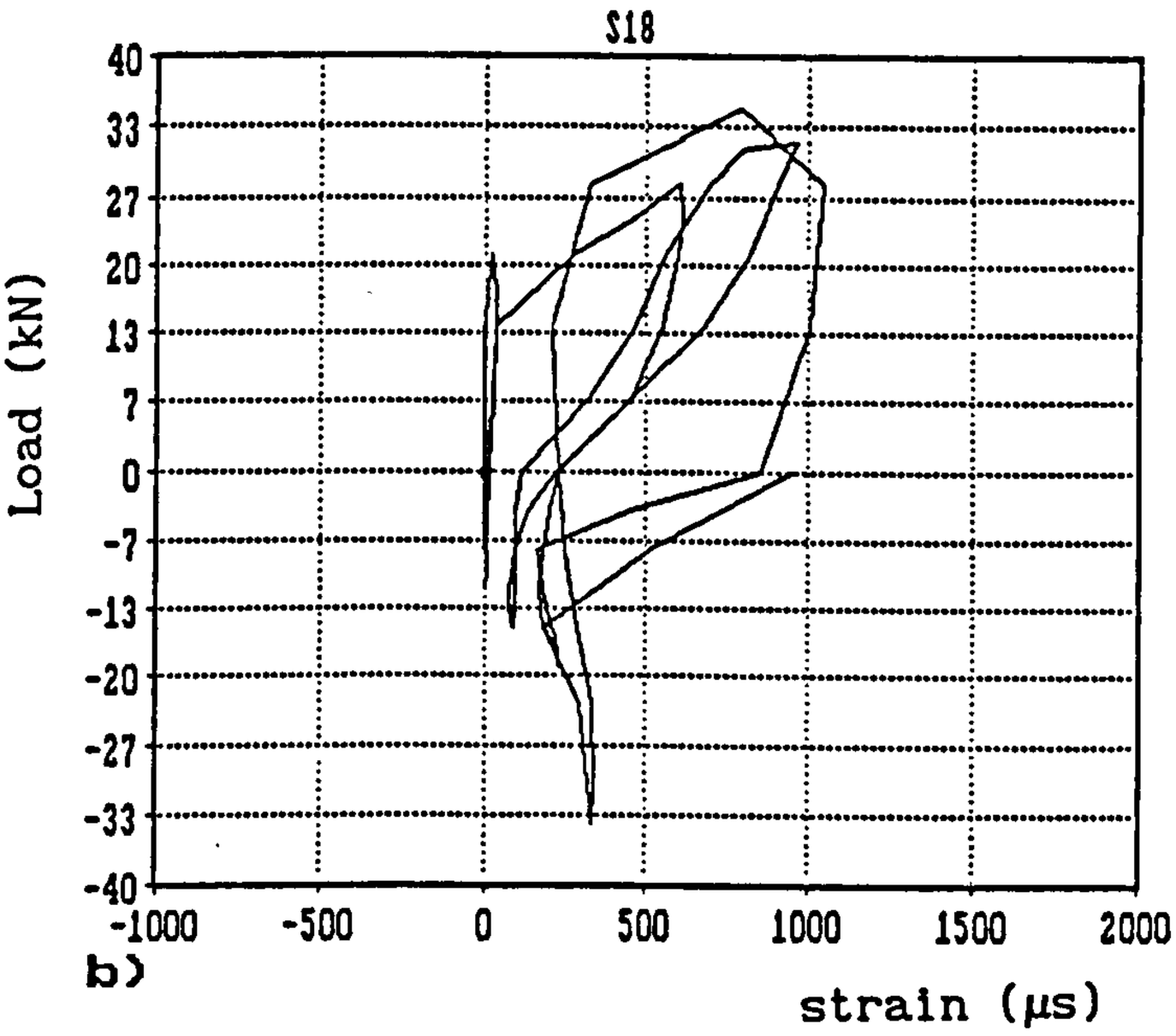

FIG.3.5 STRAIN HISTORY OF GAUGES:

a) S17

b) S18

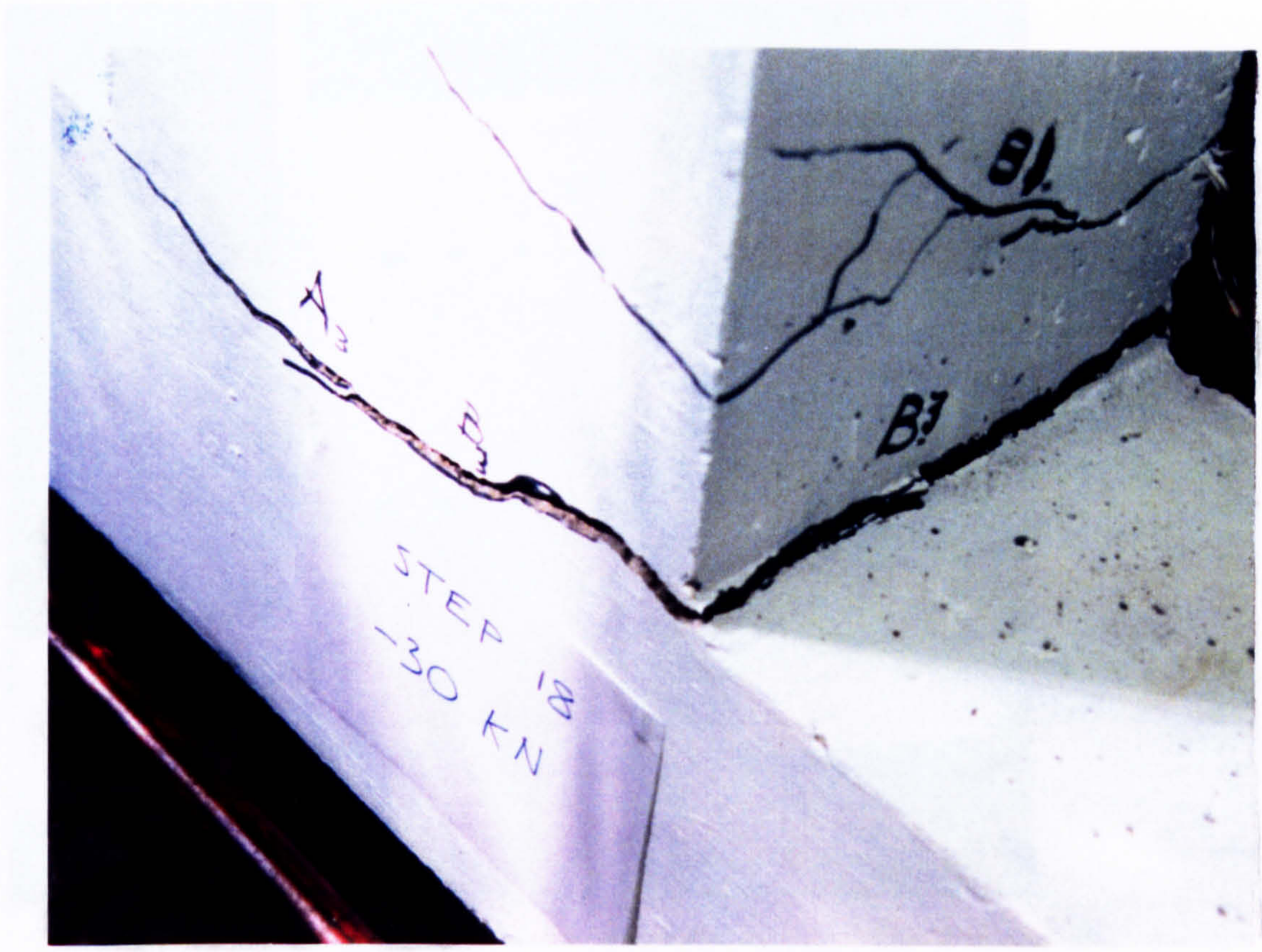

a)

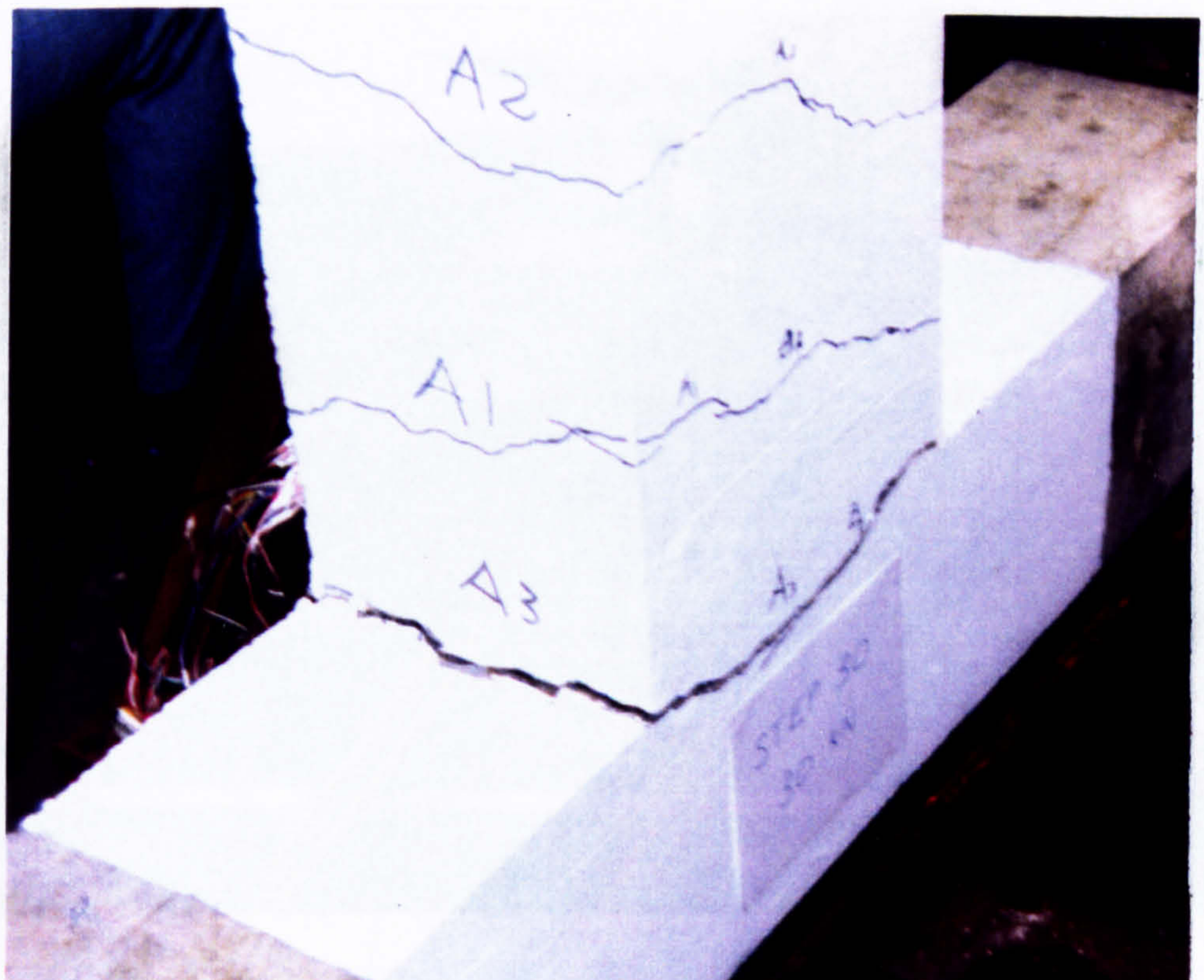

b)

FIG.3.6 STATE OF SPECIMEN -EX1- AT THE END OF THE TEST

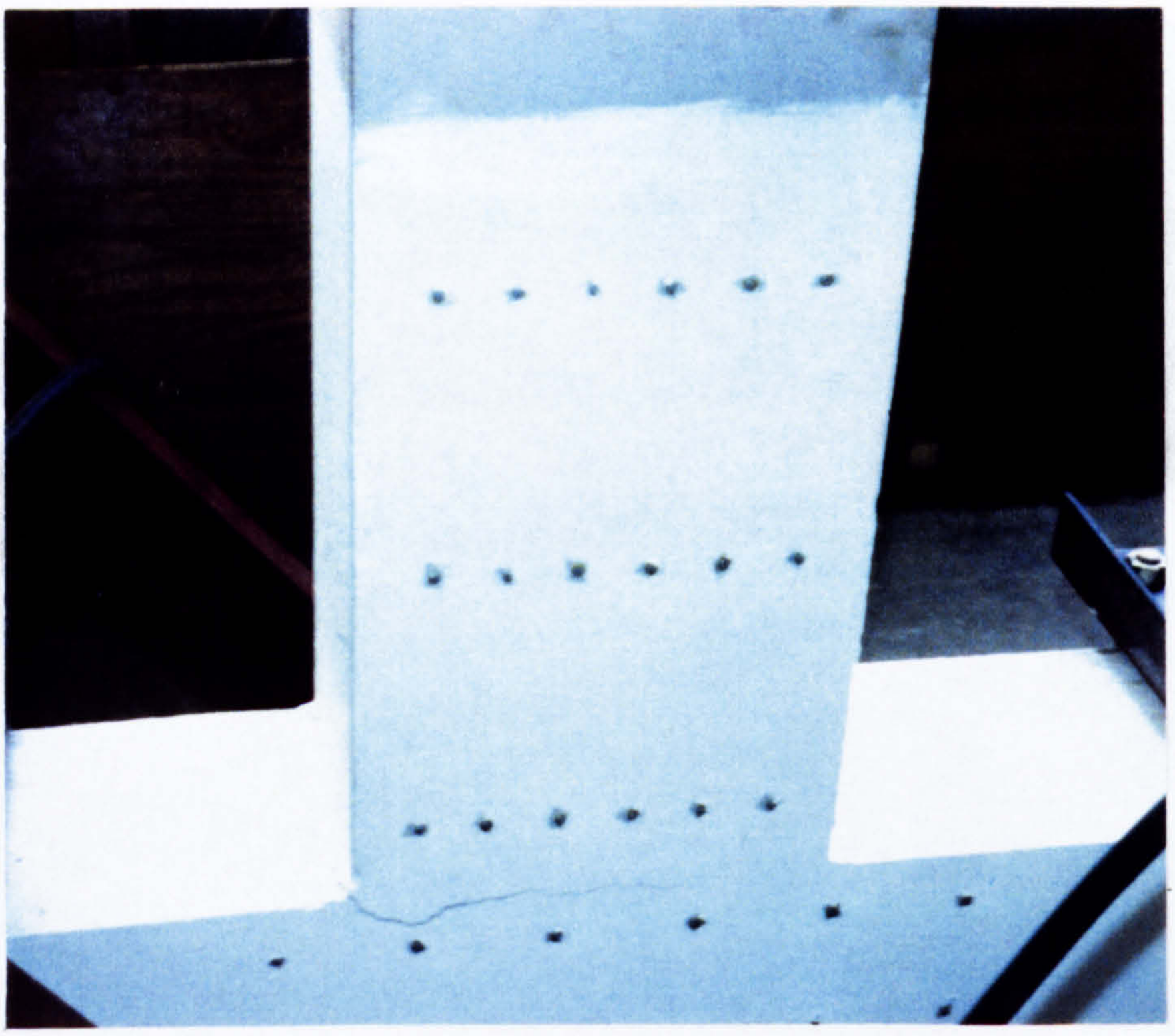

a)

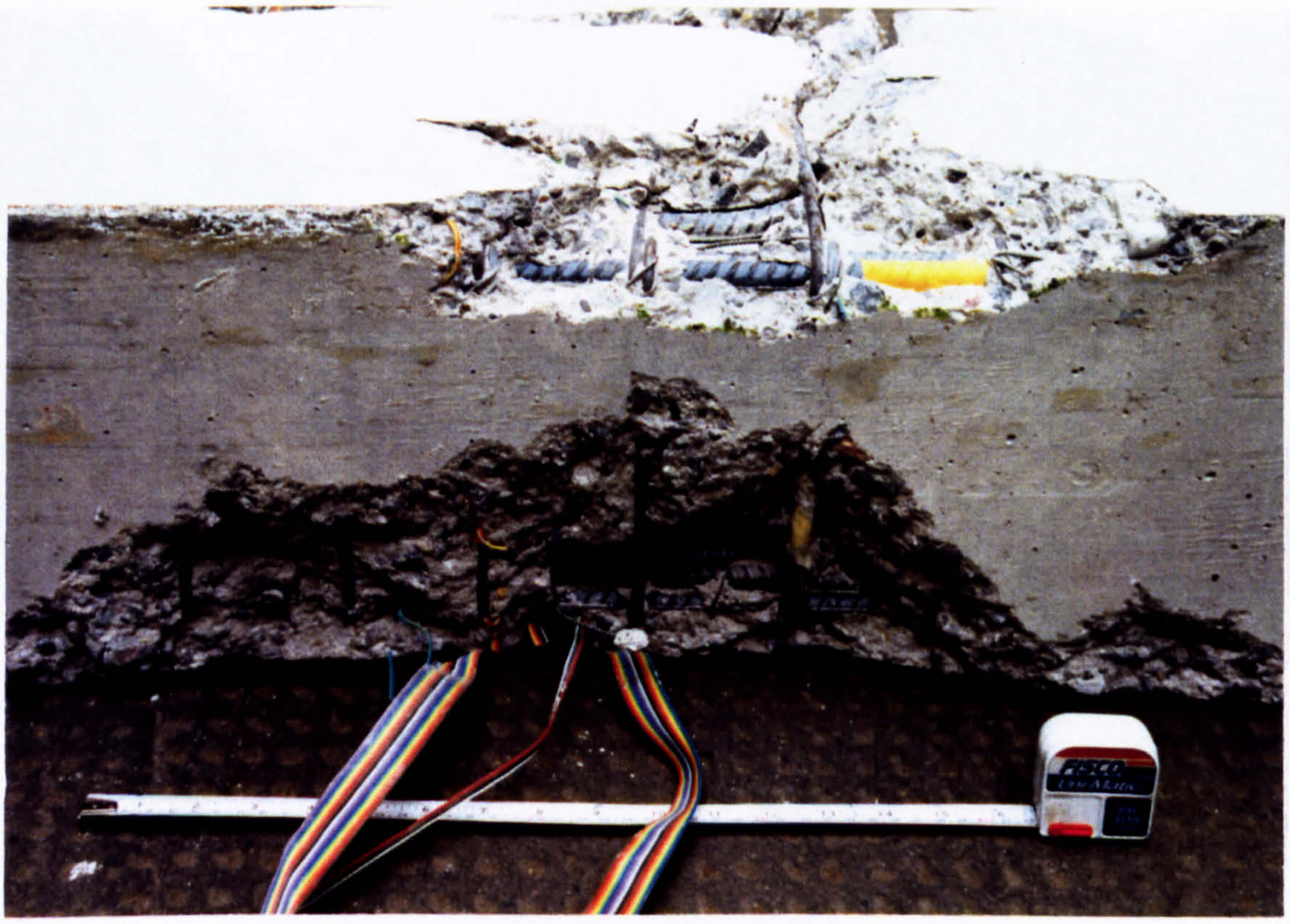

b)

FIG.3.7 CRACKING PATTERN IN SPECIMEN - EX2 -

a)

b)

FIG.3.8 STATE OF SPECIMEN - EX2 - AT THE END OF TESTING

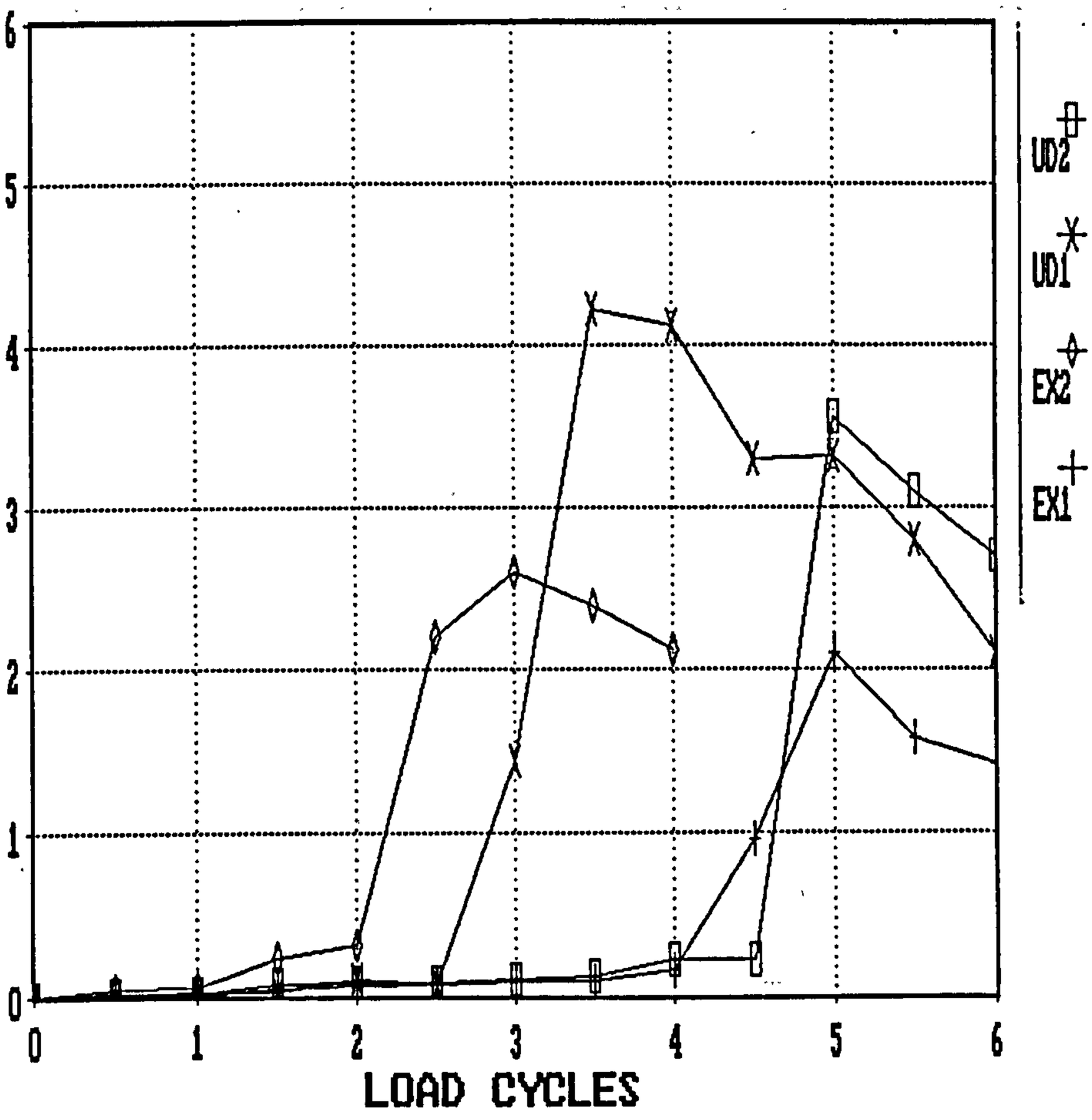

FIG.3.9 ENERGY DISSIPATION CAPACITY

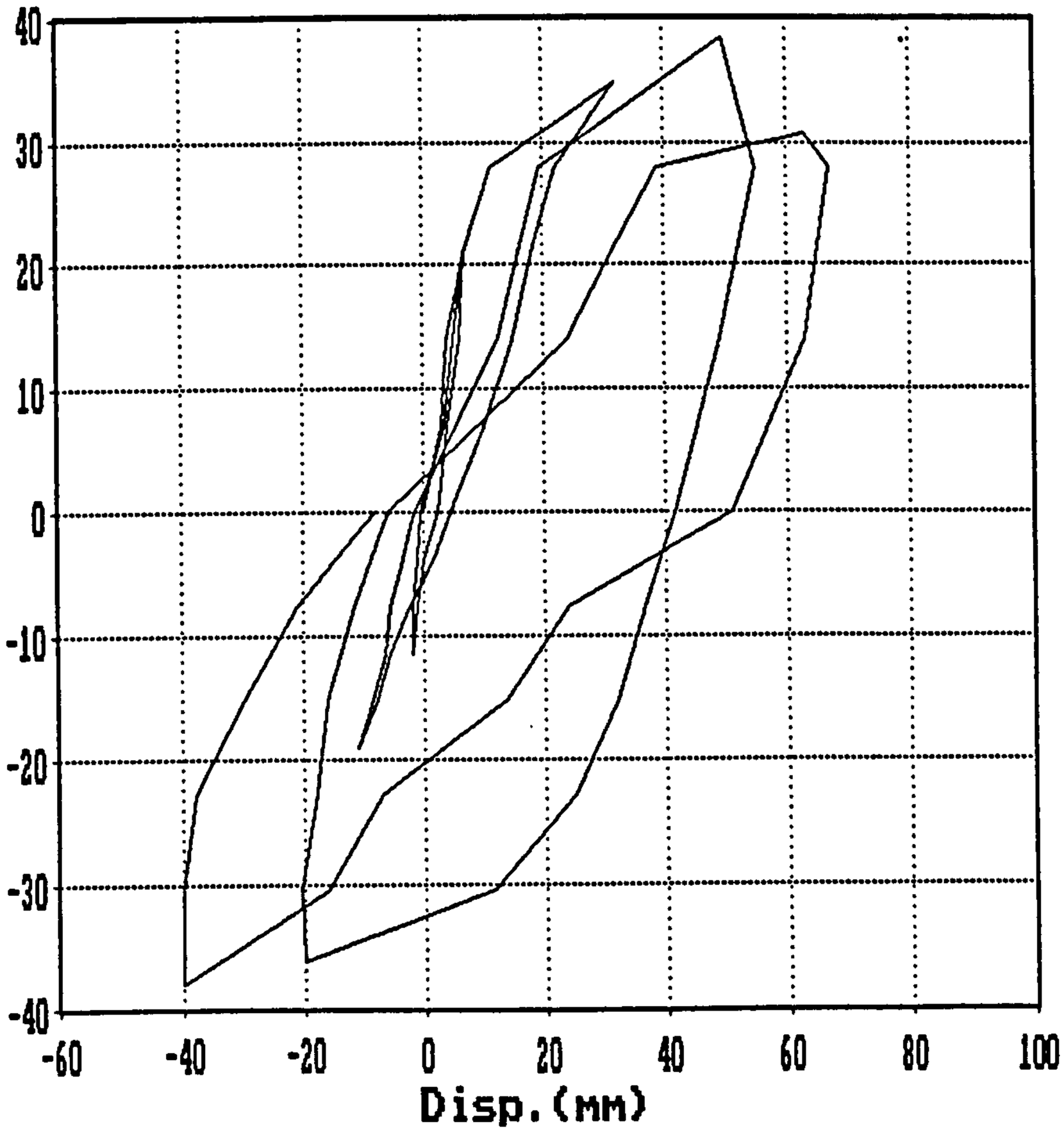

FIG.3.10 LOAD VS. DISPLACEMENT HYSTERESIS CYCLE - EX2 -

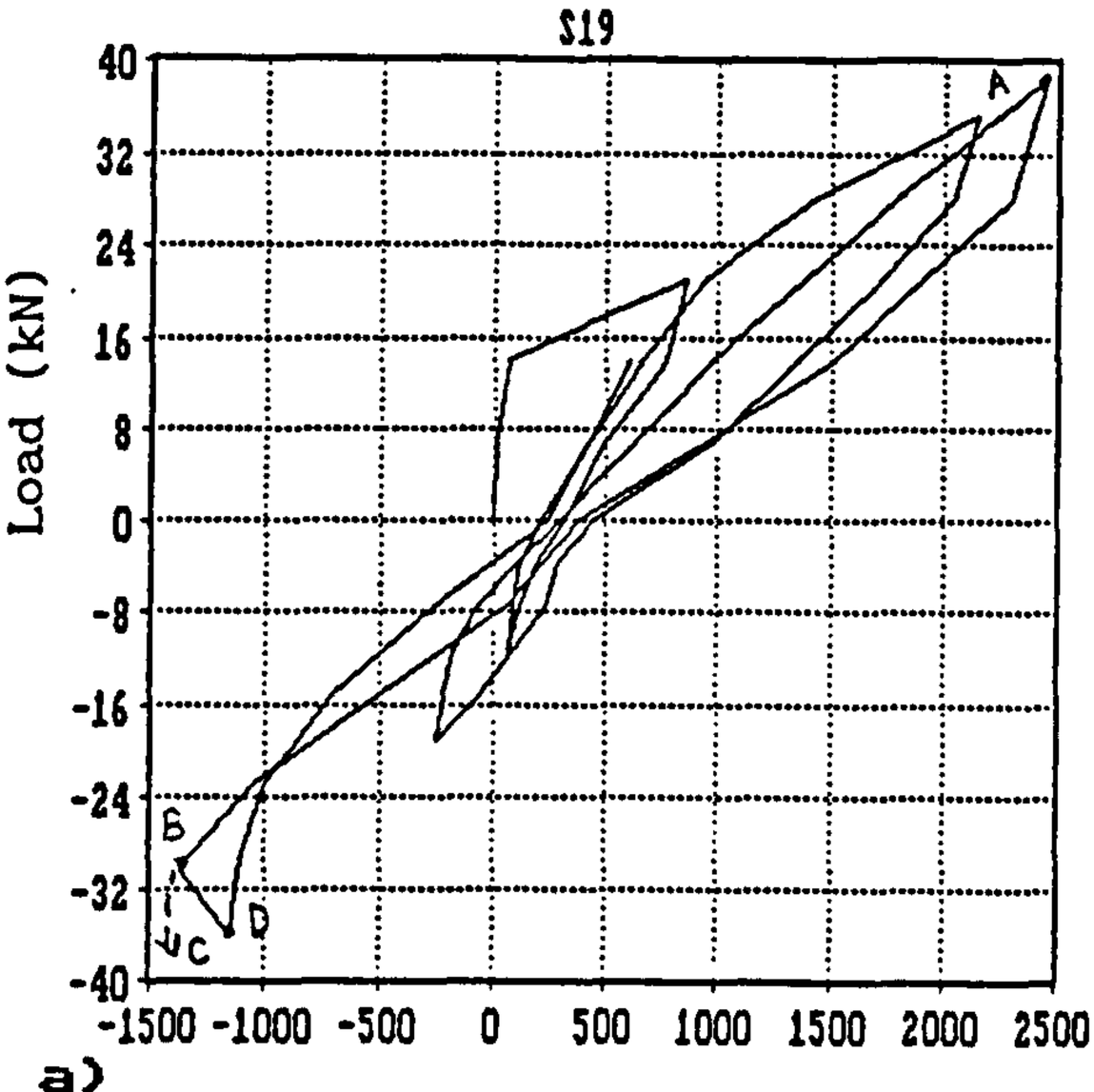

a)

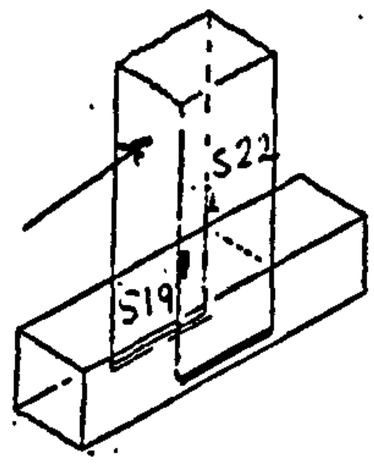

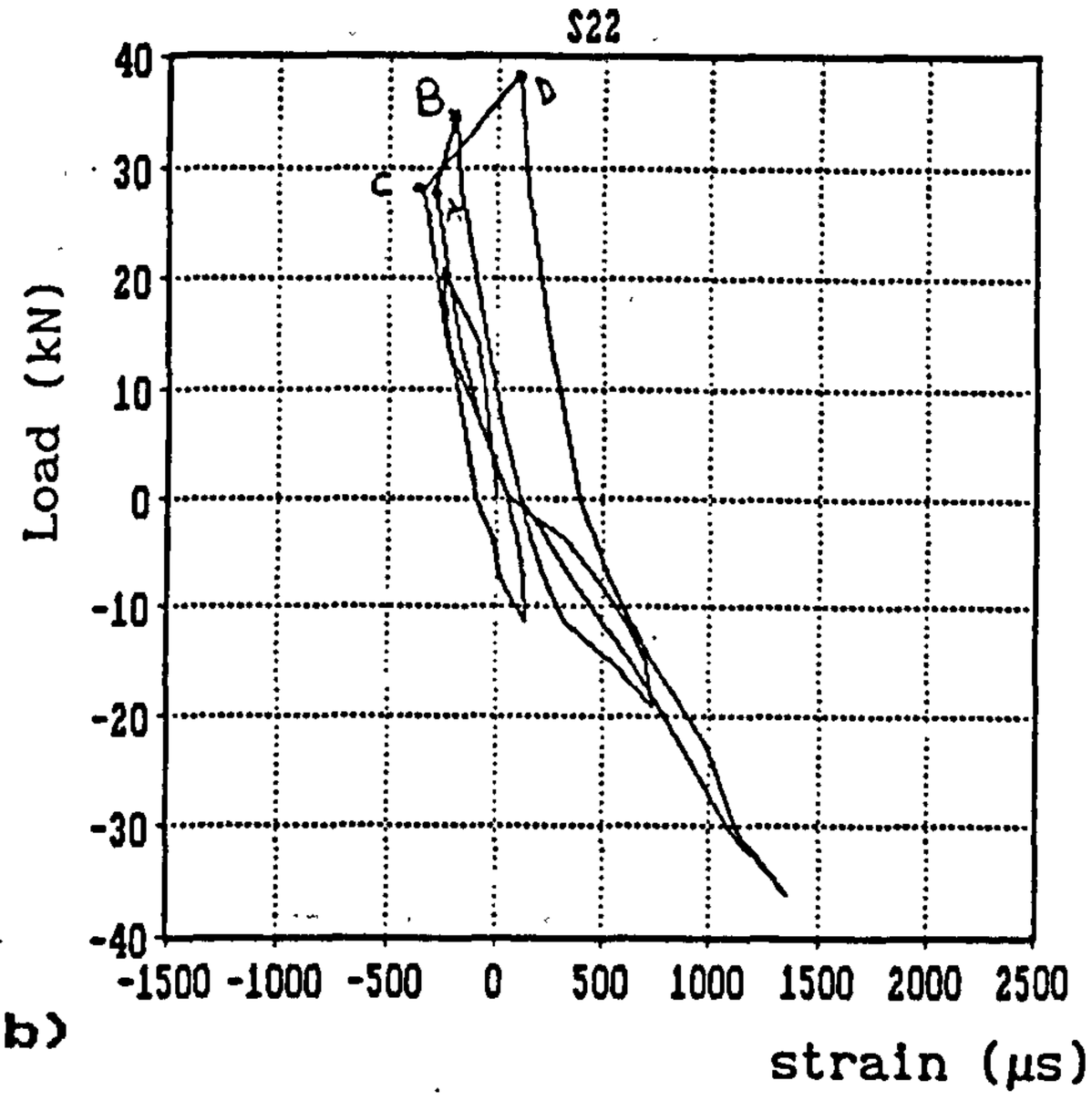

b)

FIG.3.11 LOAD VS. STRAIN HISTORY IN BEAM MAIN BARS

GAUGES S19 AND S22

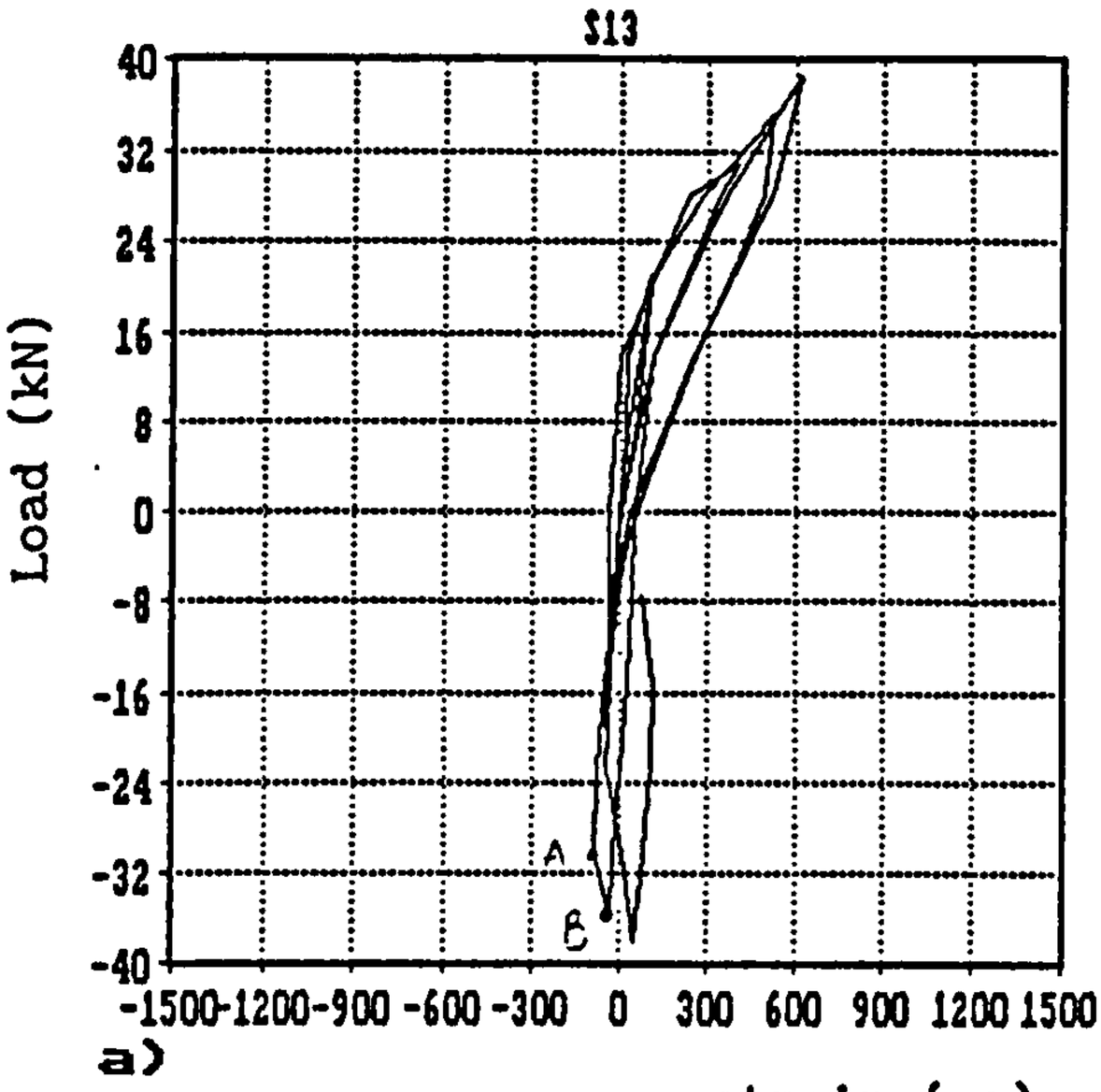

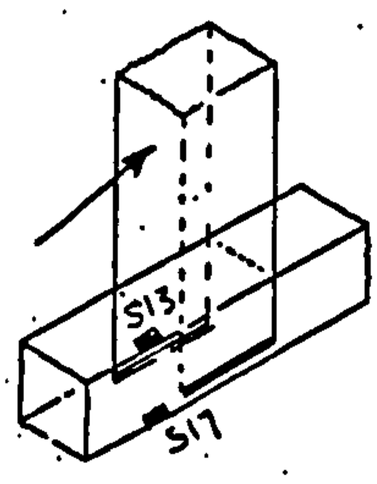

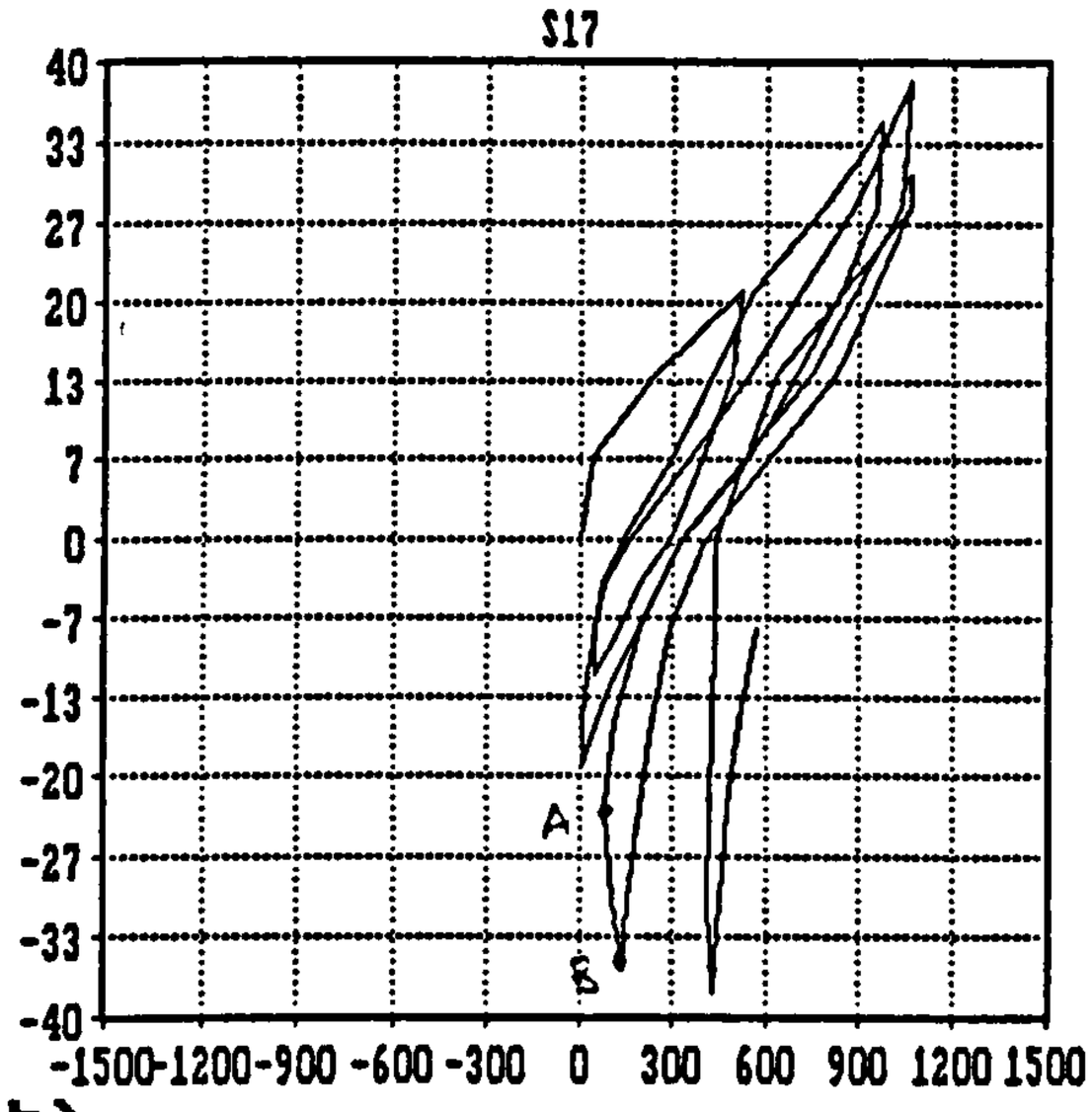

FIG.3.12 LOAD VS. STRAIN HISTORY IN COLUMN MAIN BARS

GAUGES S13 AND S17

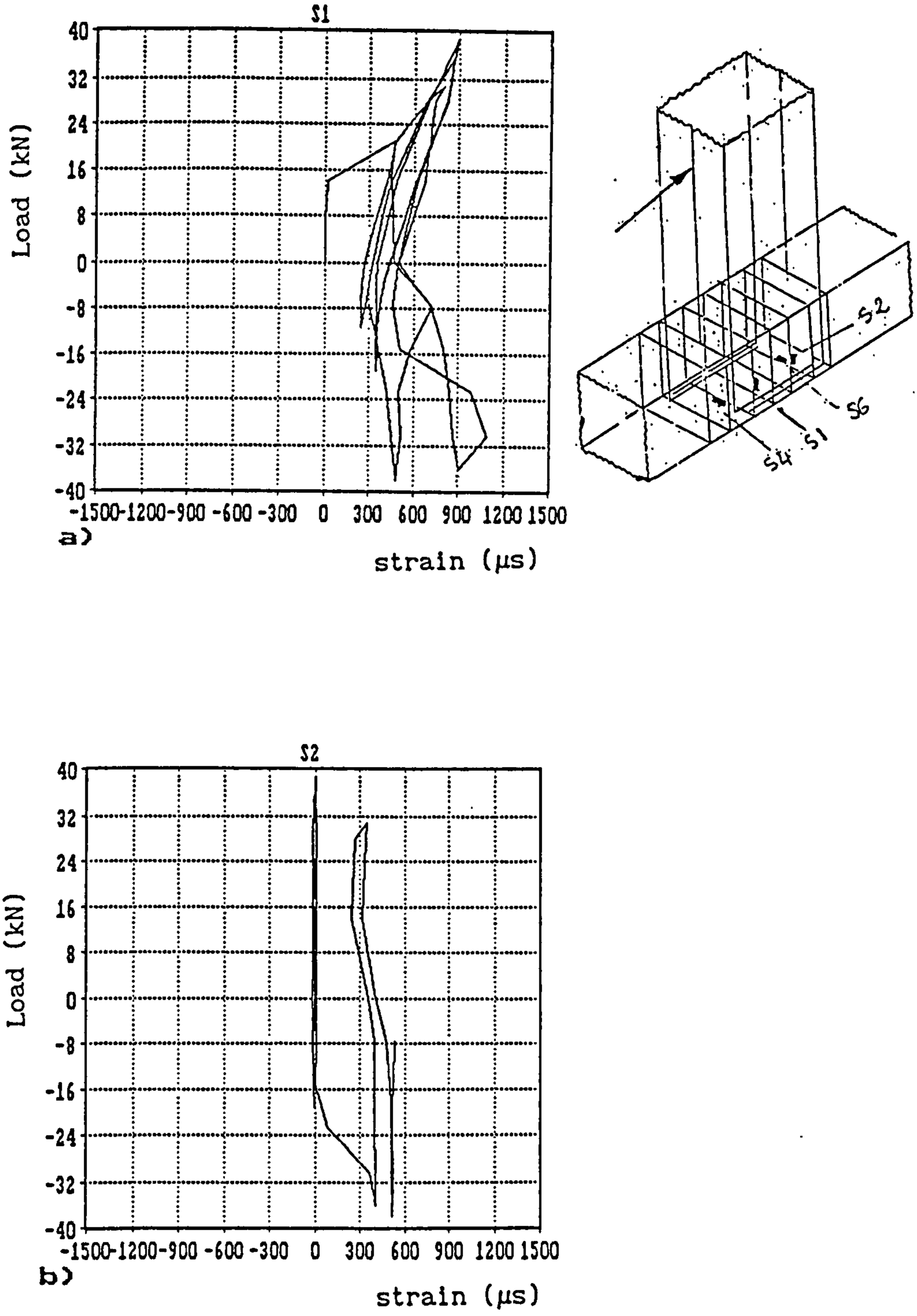

FIG.3.13 LOAD VS. STRAIN HISTORY IN STIRRUPS

GAUGES S1, S2, S3 AND S4

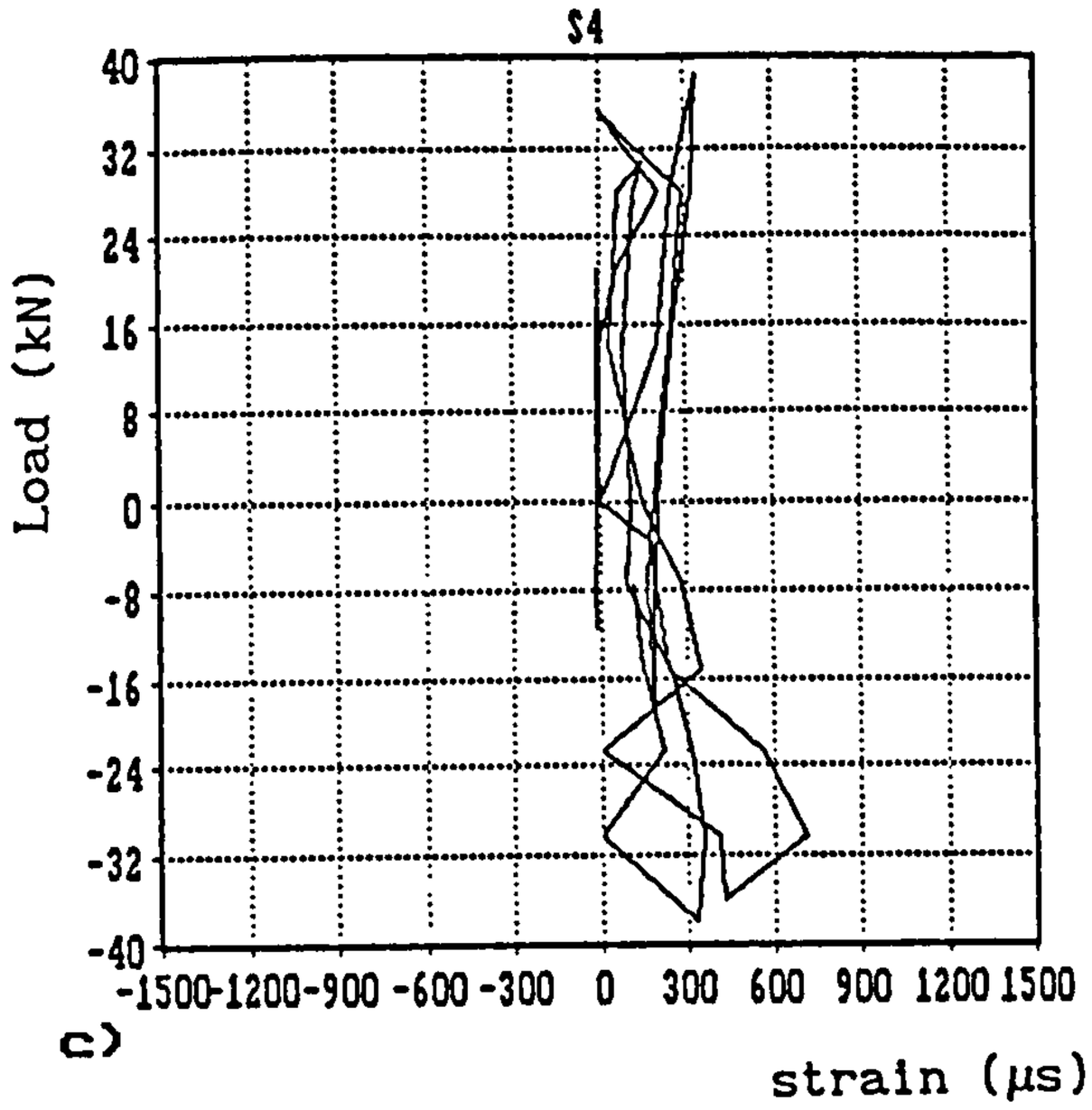
S4
40
32
24
16
8
0
-8
-16
-24
-32
-40
Load (kN)
-1500 -1200 -900 -600 -300 0 300 600 900 1200 1500
strain (μs)

c)

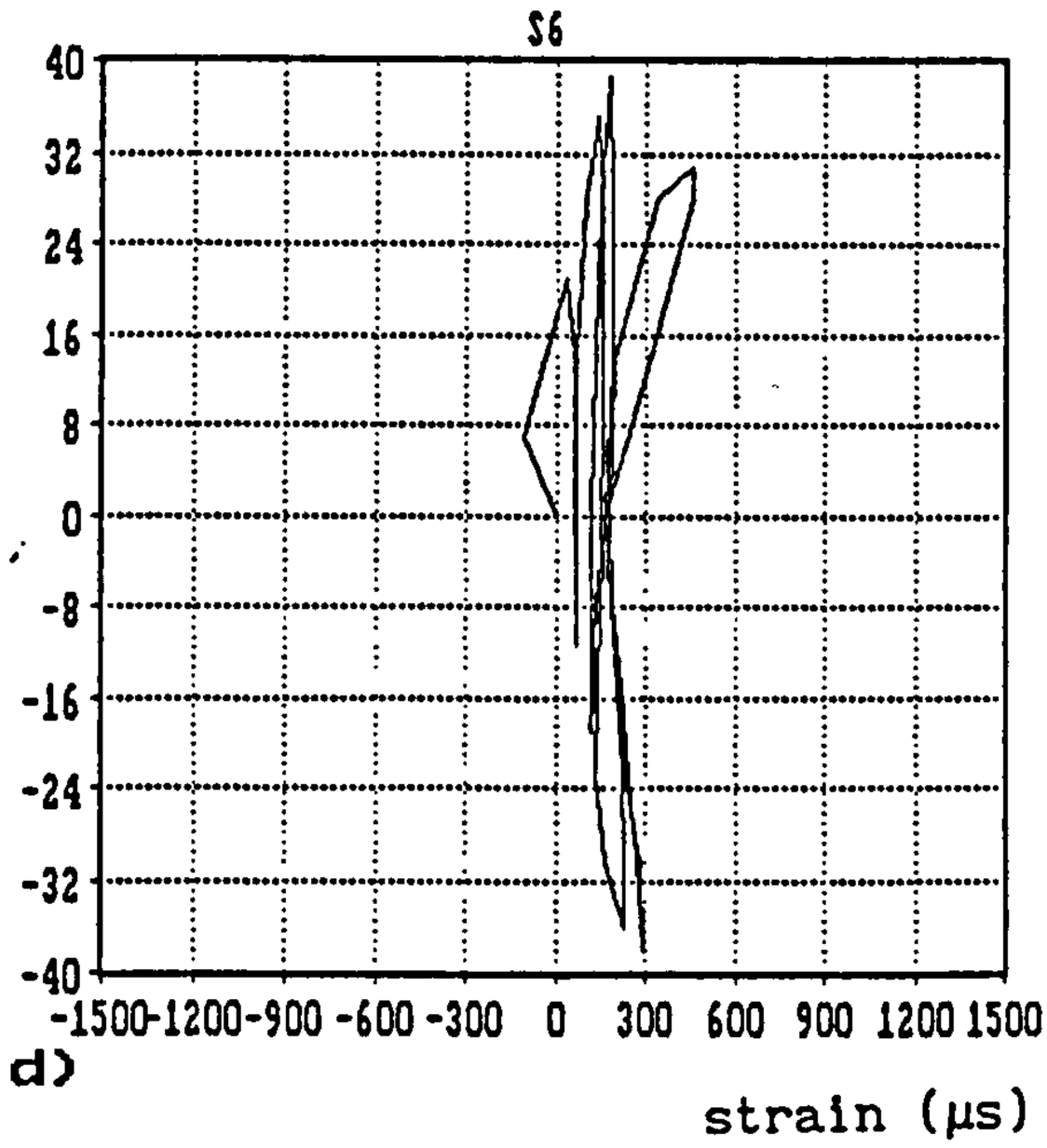
S6
40
32
24
16
8
0
-8
-16
-24
-32
-40
Load (kN)
-1500 -1200 -900 -600 -300 0 300 600 900 1200 1500
strain (μs)

d)

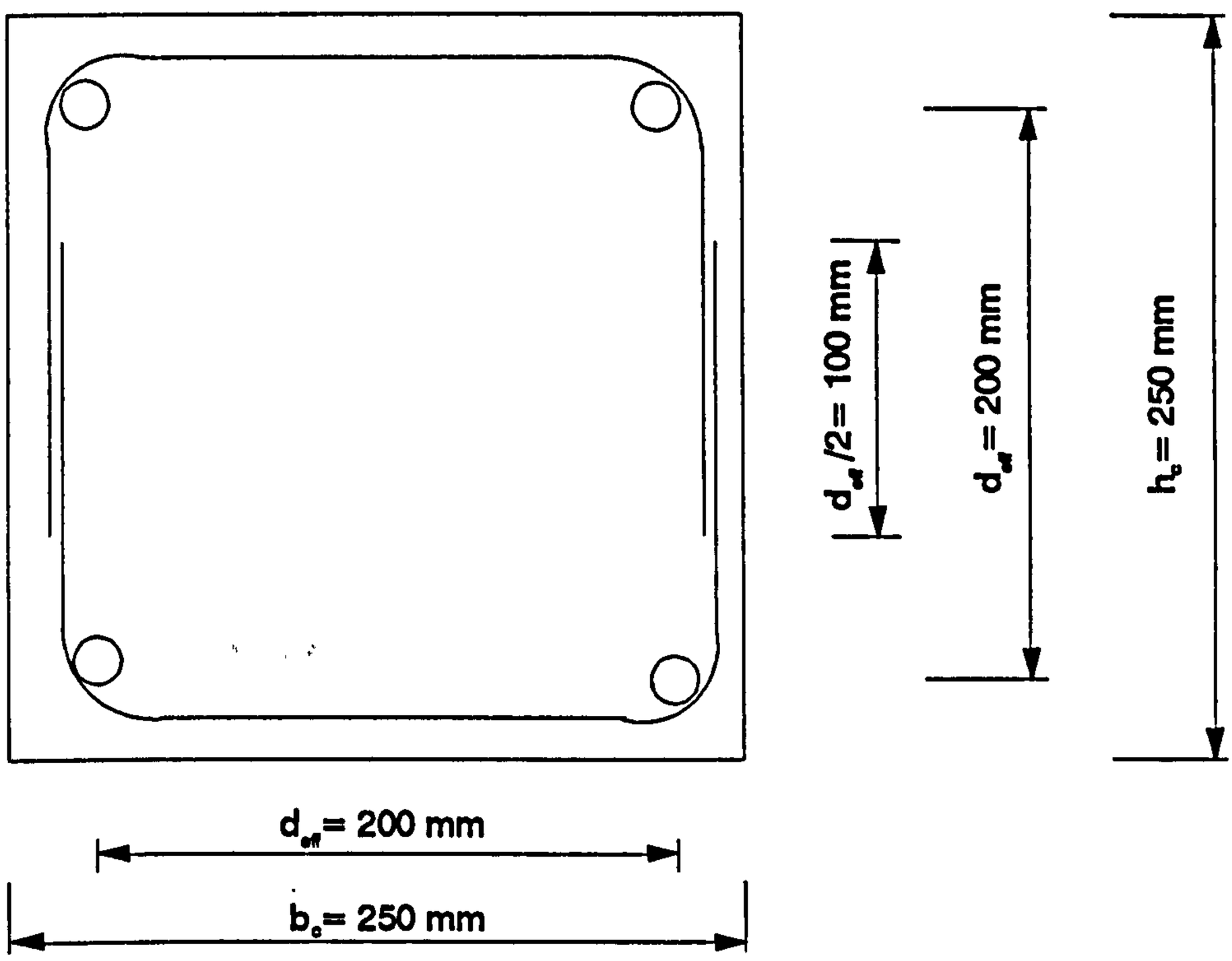

a) Detail of U-stirrups Overlapping - Specimen UD1 -

FIG.3.14 U-STIRRUPS OVERLAPPING & CRACKING PATTERN - UD1 -

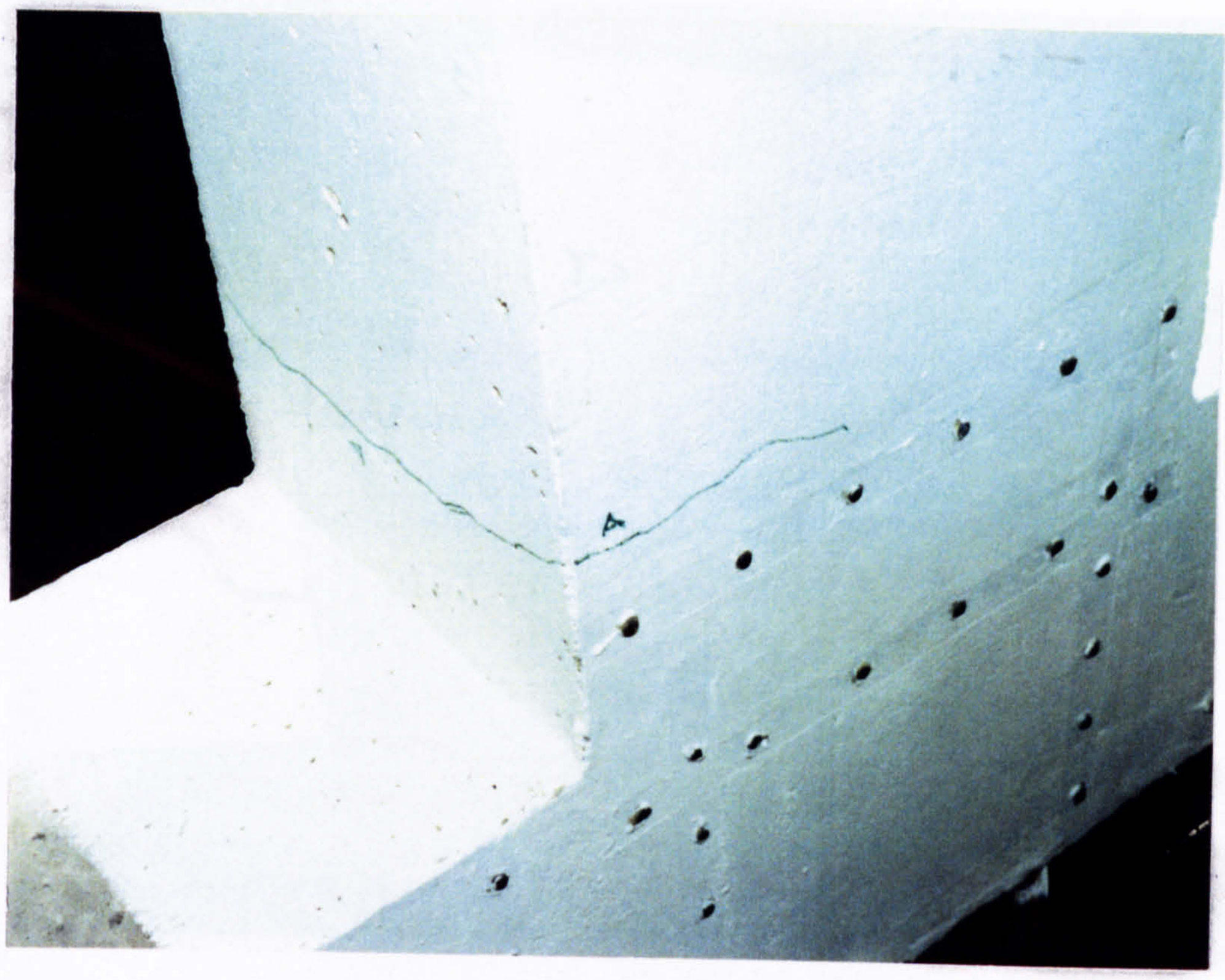

b)

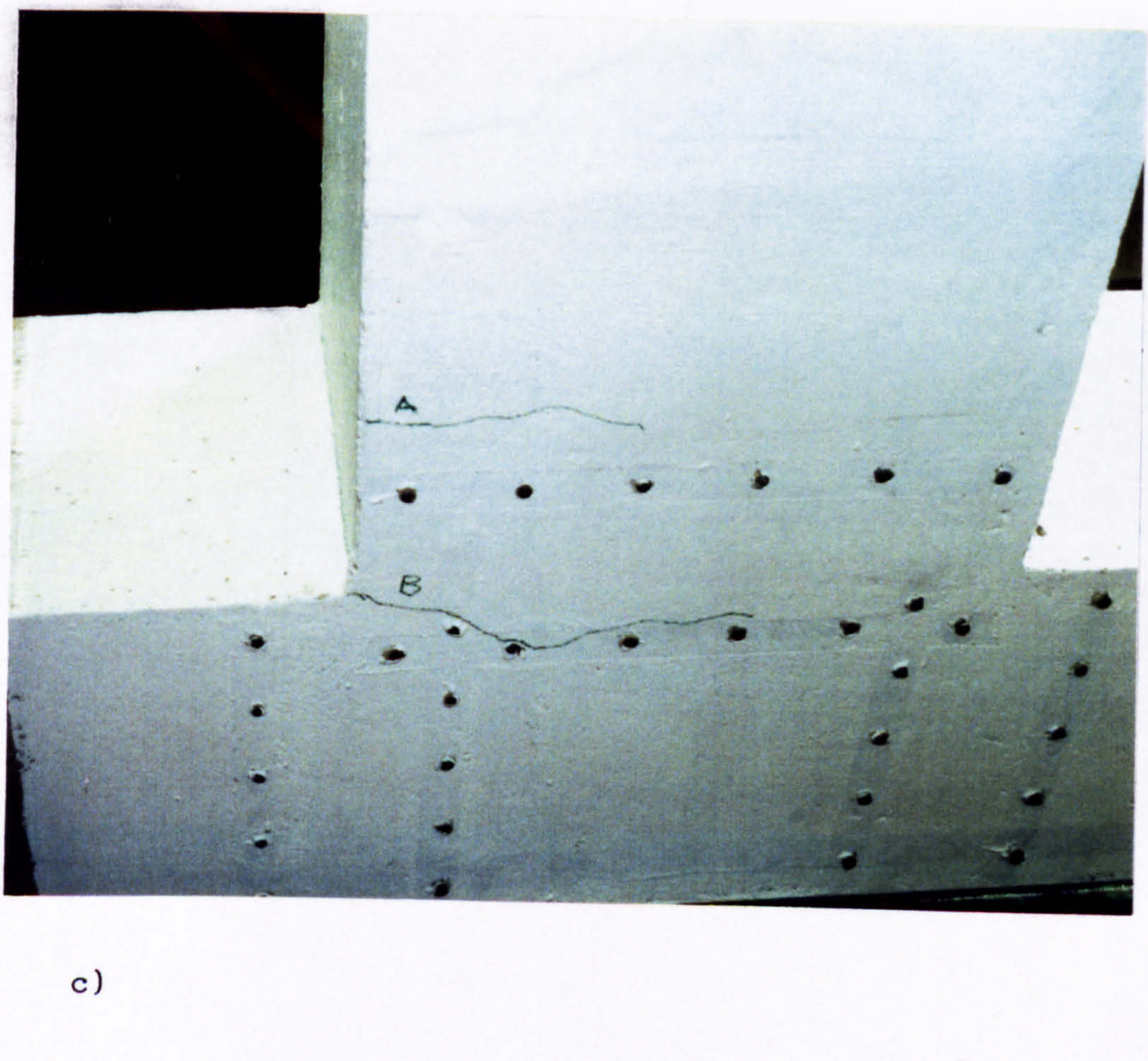

c)

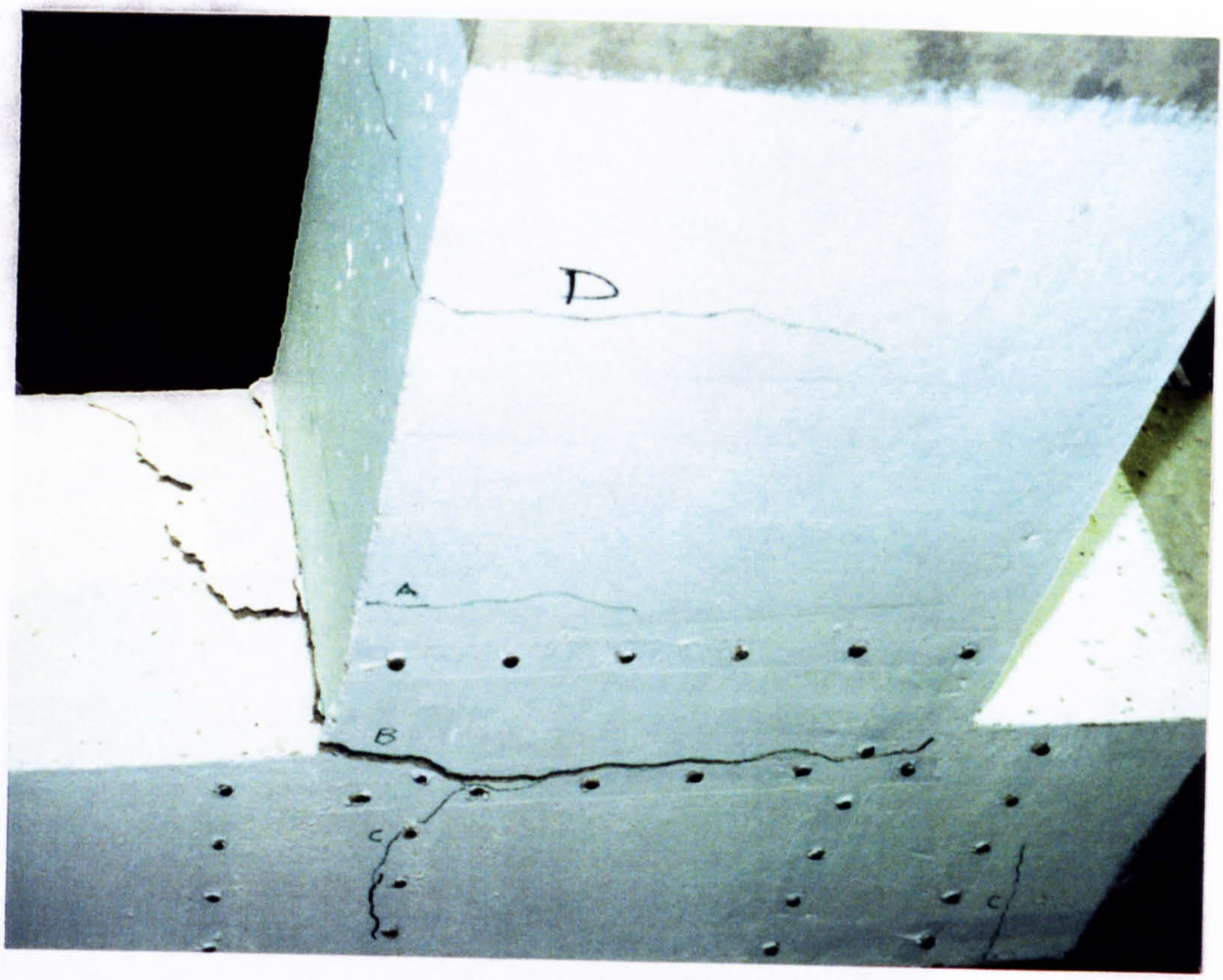

d)

e)

a)

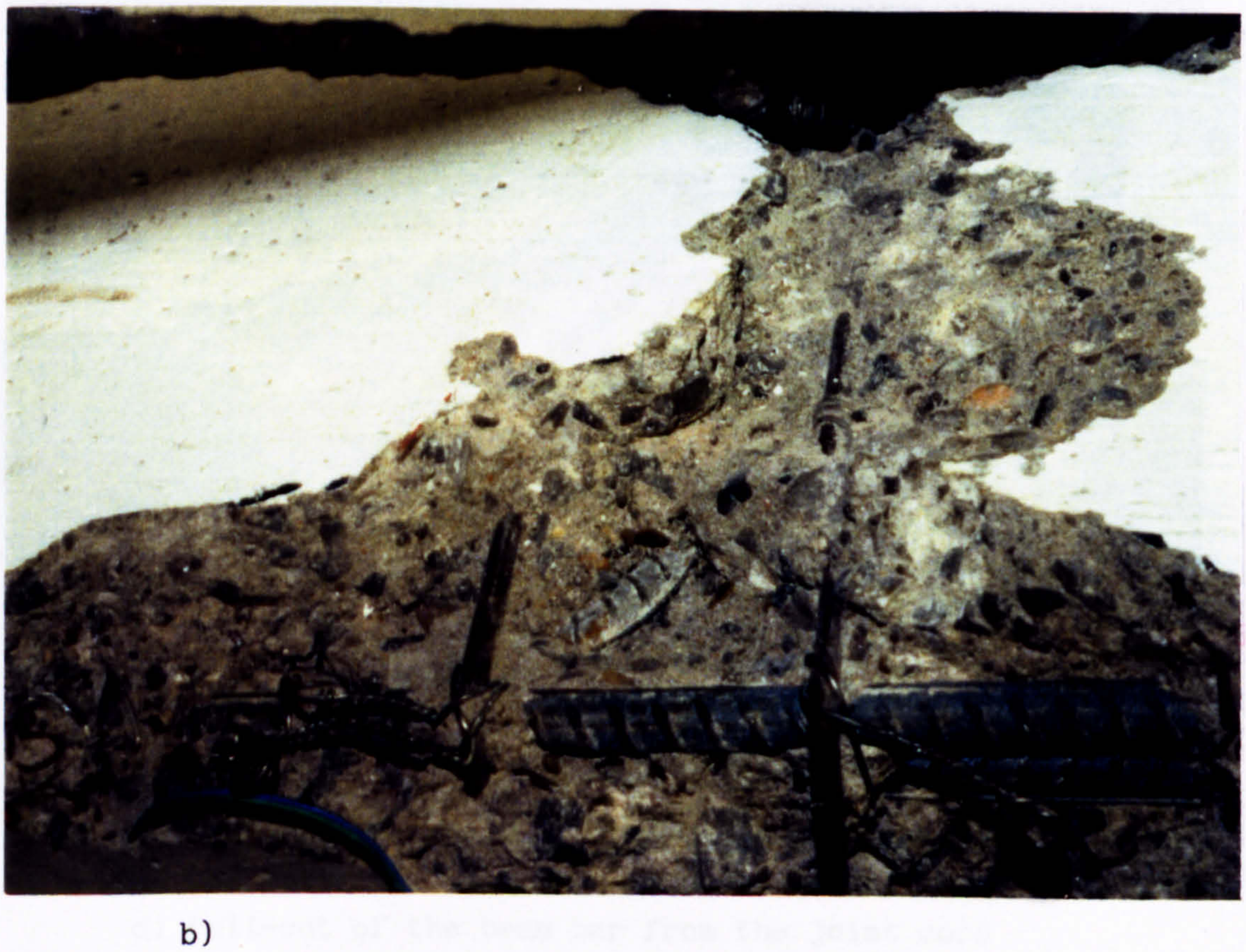

b)

FIG.3.15 STATE OF SPECIMEN - UD1 - AFTER EXPERIMENT

c) Buckling of beam bars & State of U-bars -final stage-

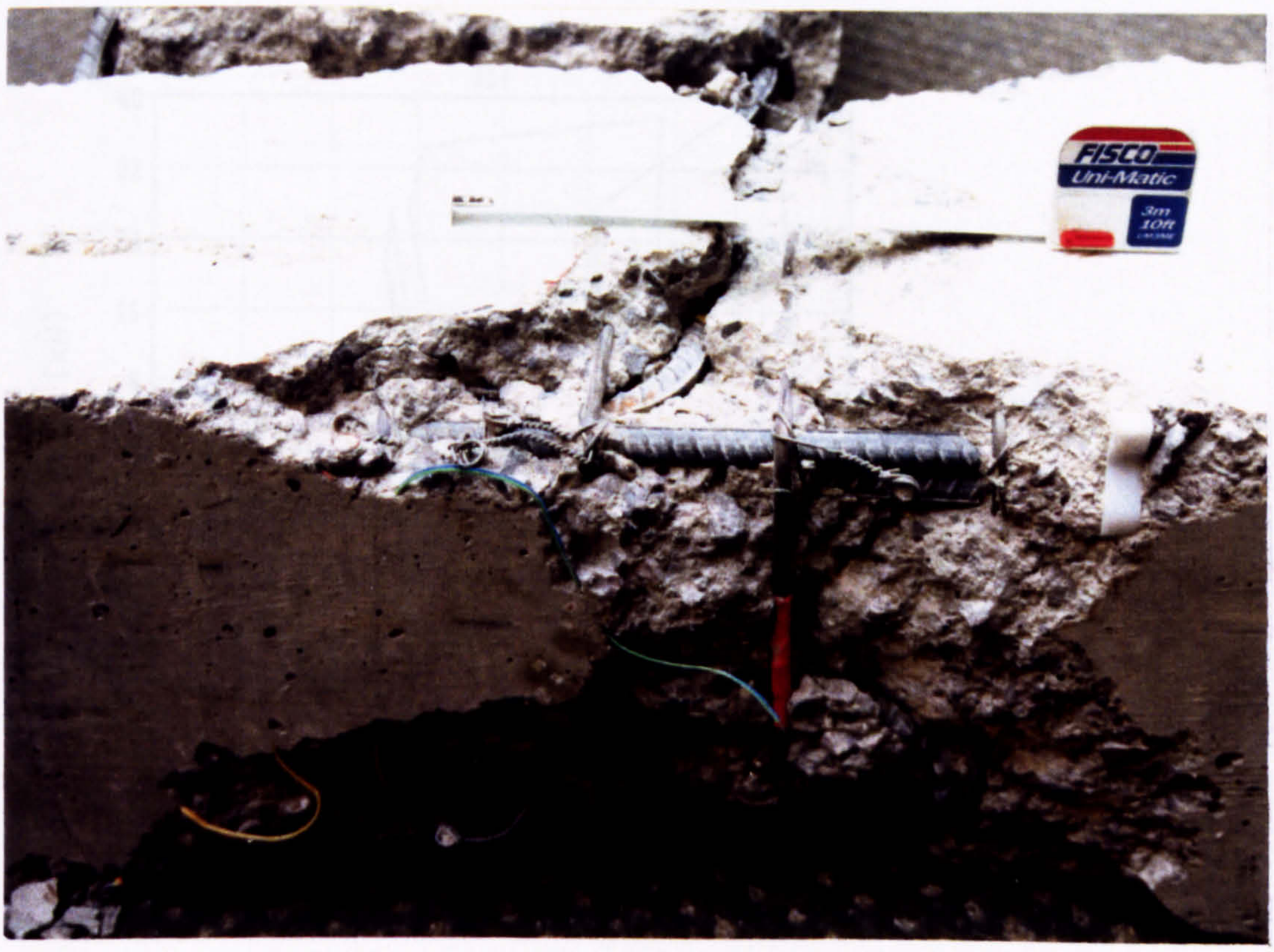

d) Pull-out of the beam bar from the joint core

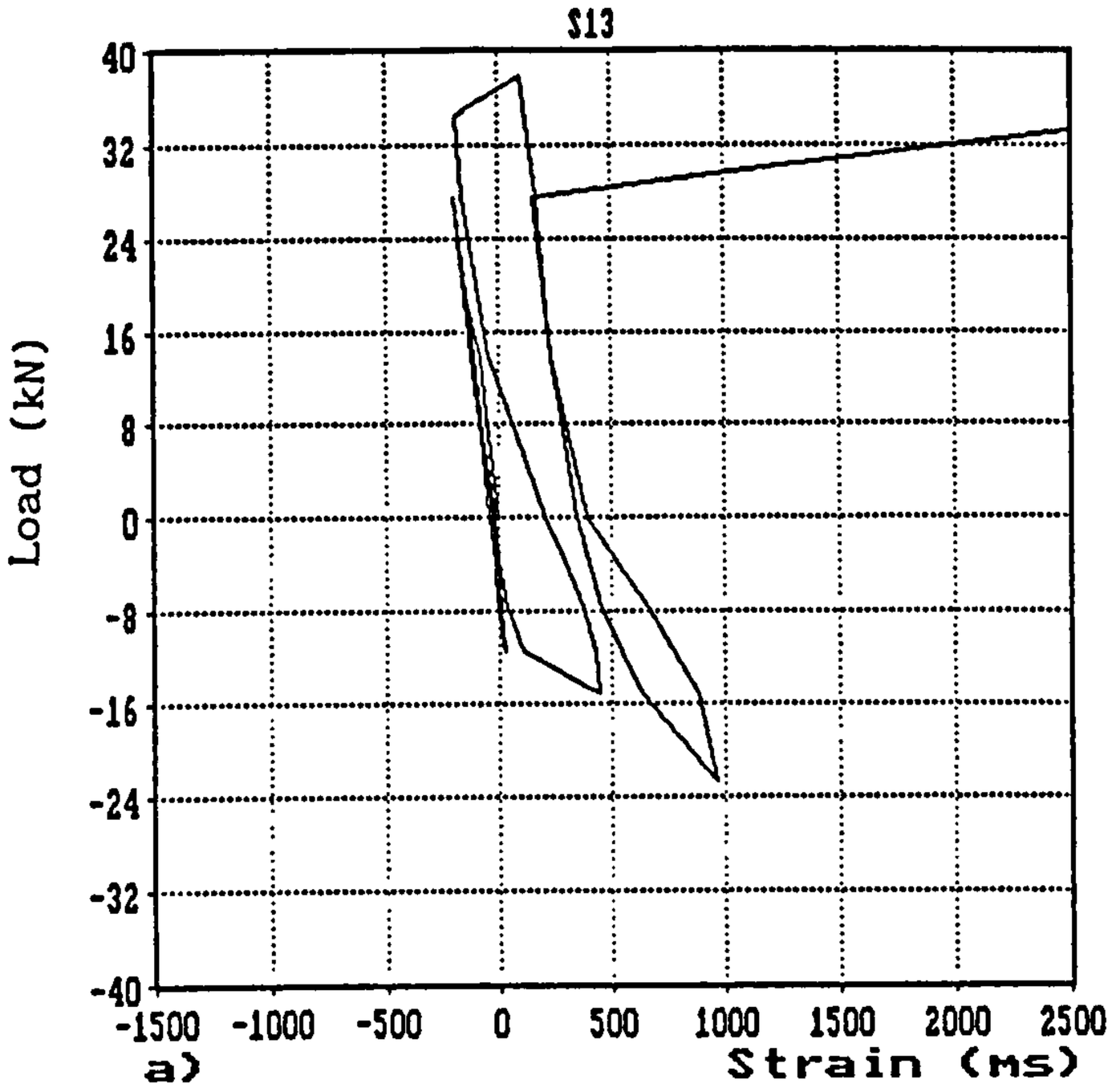

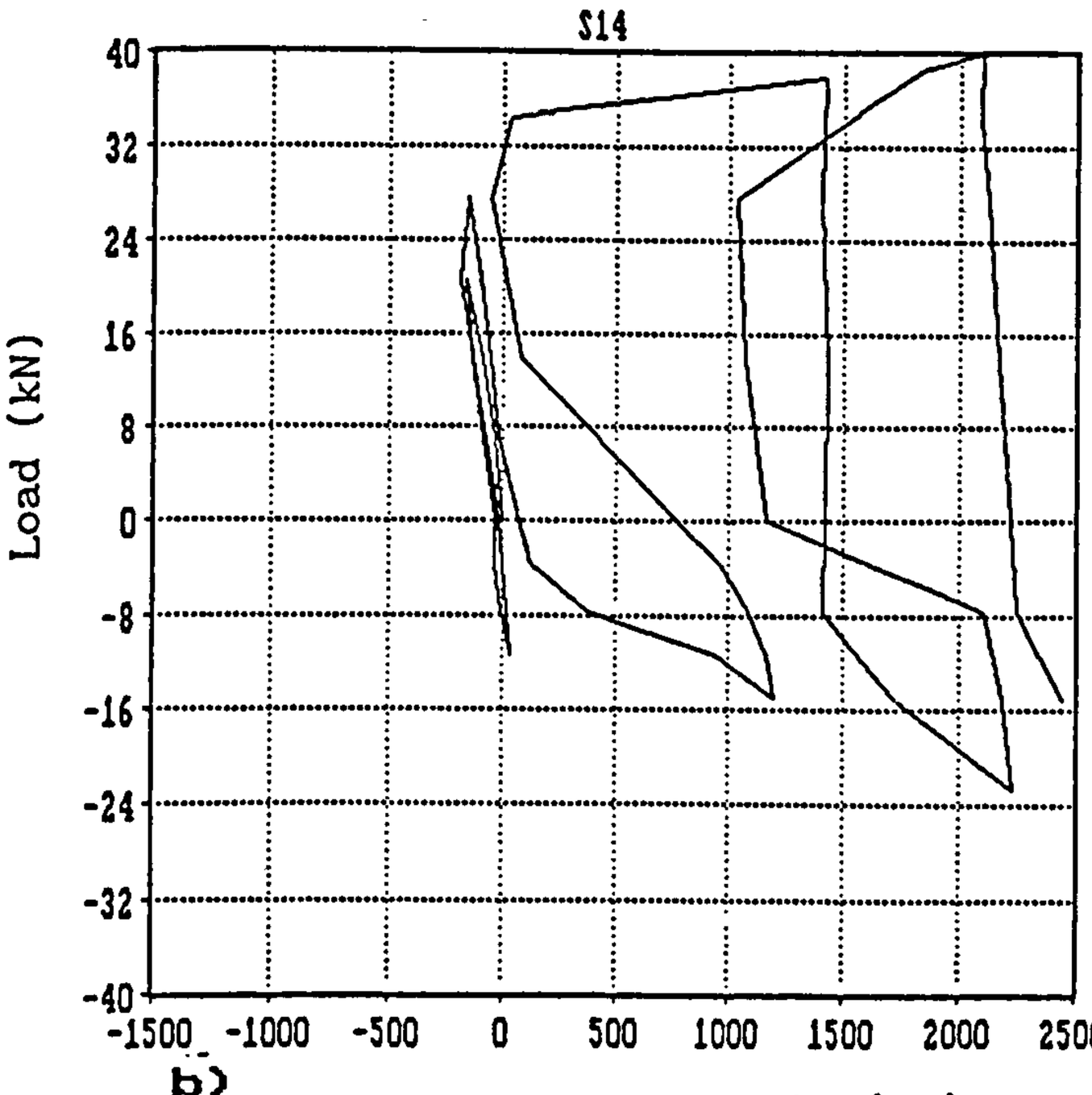

FIG.3.16 LOAD VS. STRAIN HISTORY OF BEAM MAIN REINFORCEMENT

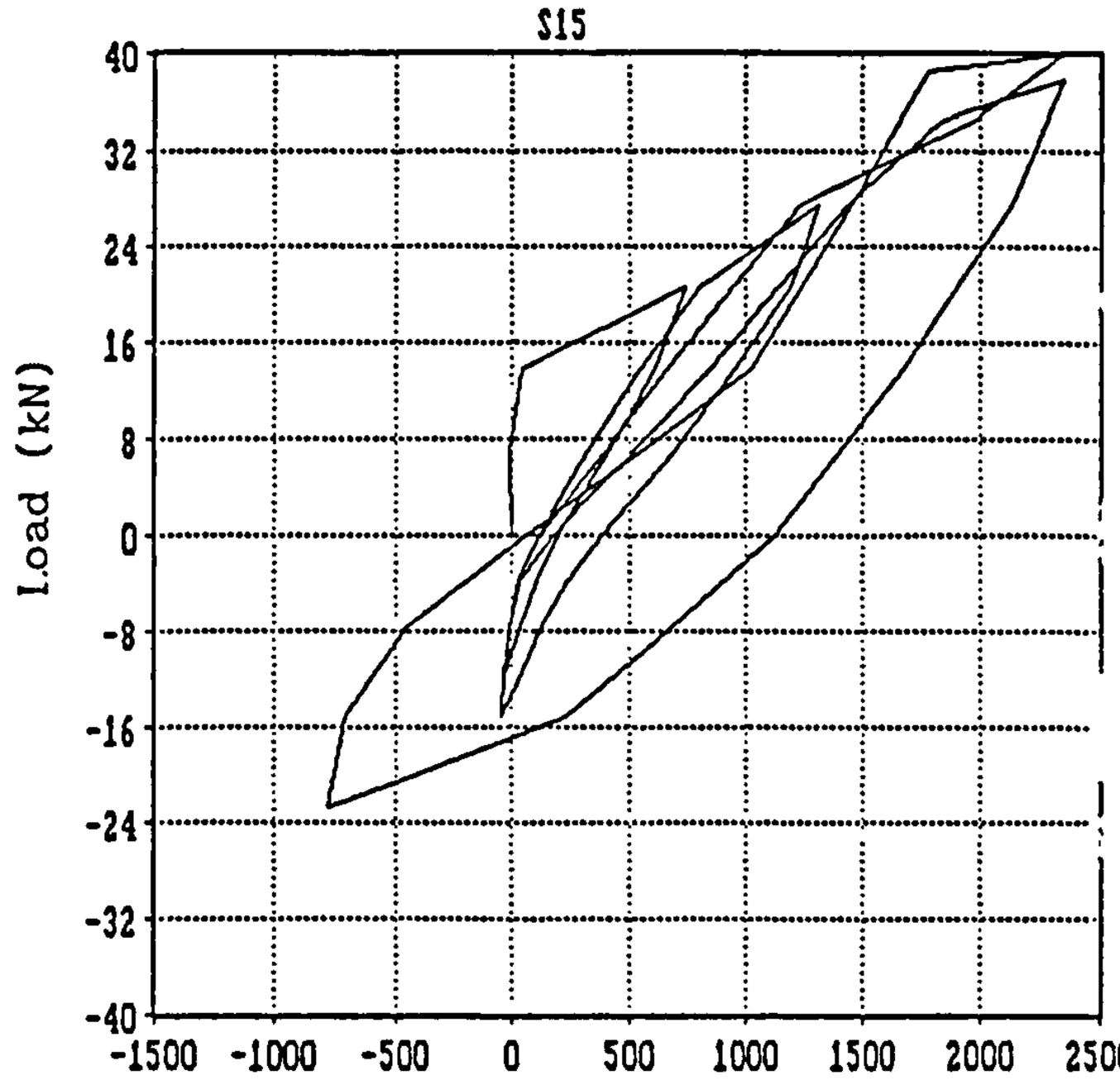
S15
40
32
24
16
8
0
-8
-16
-24
-32
-40
Load (kN)
-1500 -1000 -500 0 500 1000 1500 2000 2500
strain (μs)

c)

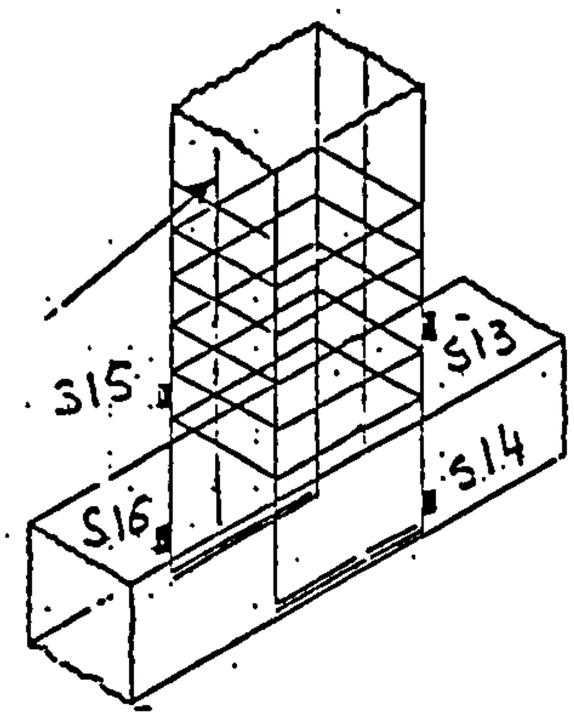
S15
S13
S14
S16

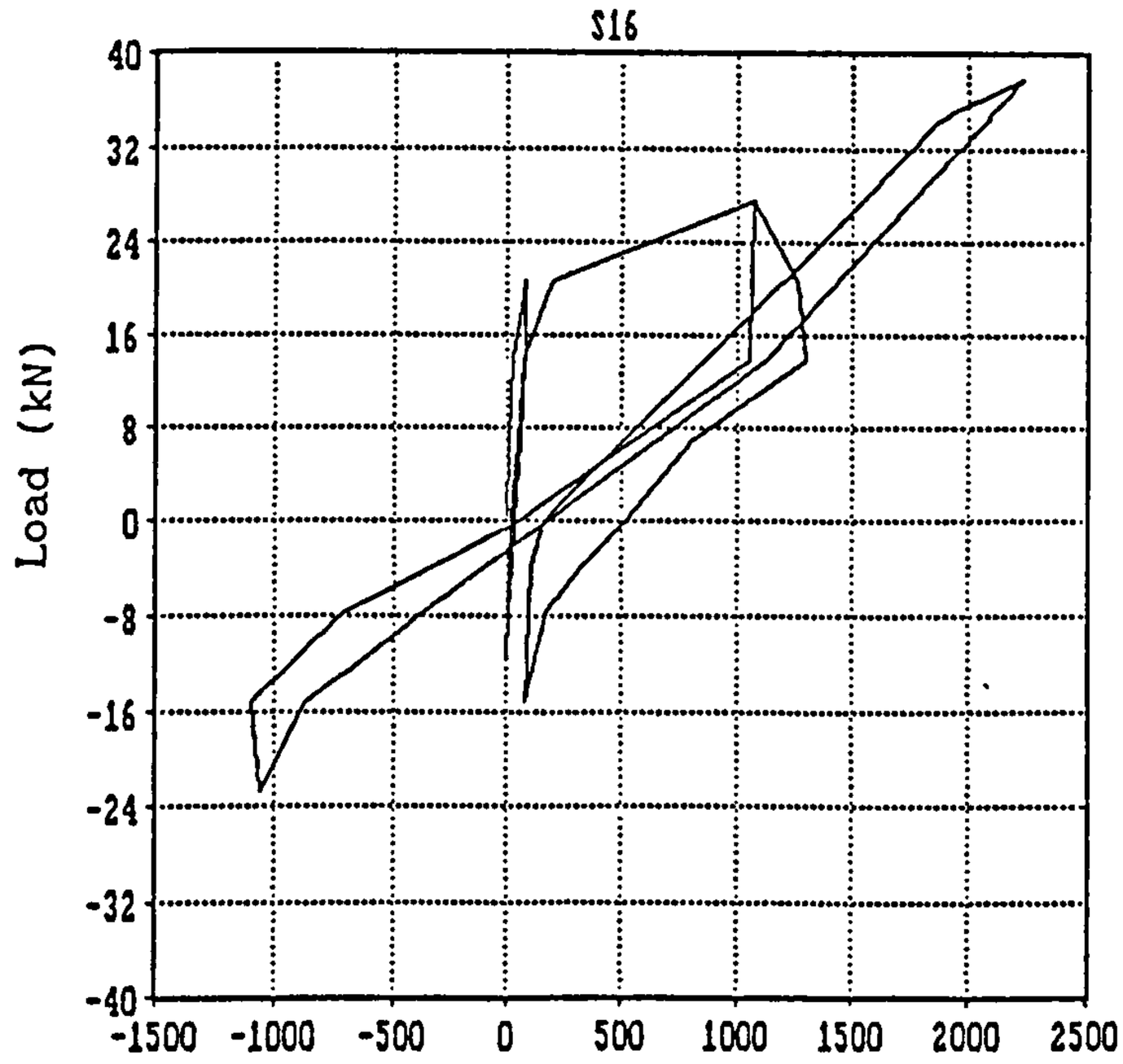
S16
40
32
24
16
8
0
-8
-16
-24
-32
-40
Load (kN)
-1500 -1000 -500 0 500 1000 1500 2000 2500
strain (μs)

d)

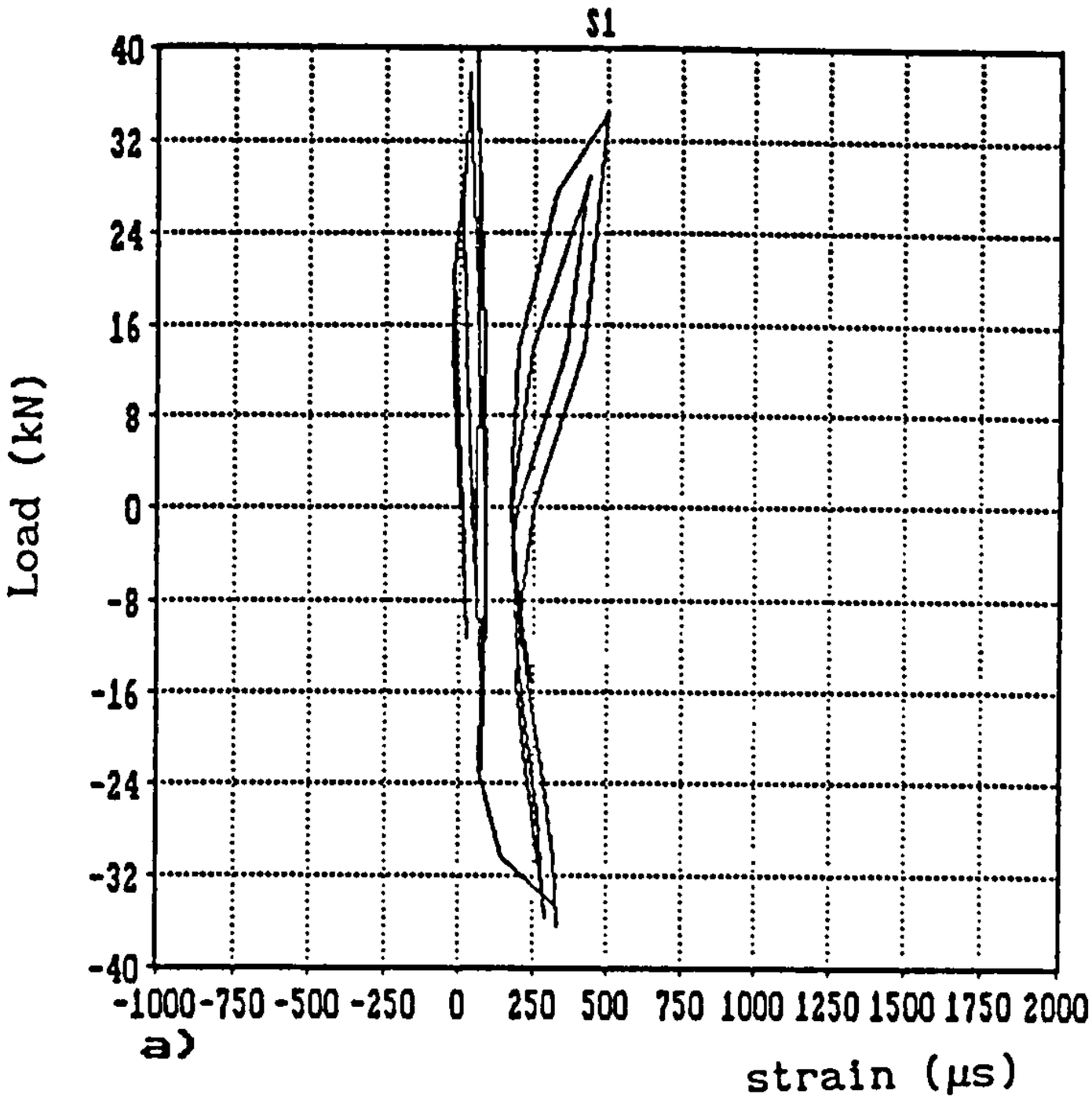

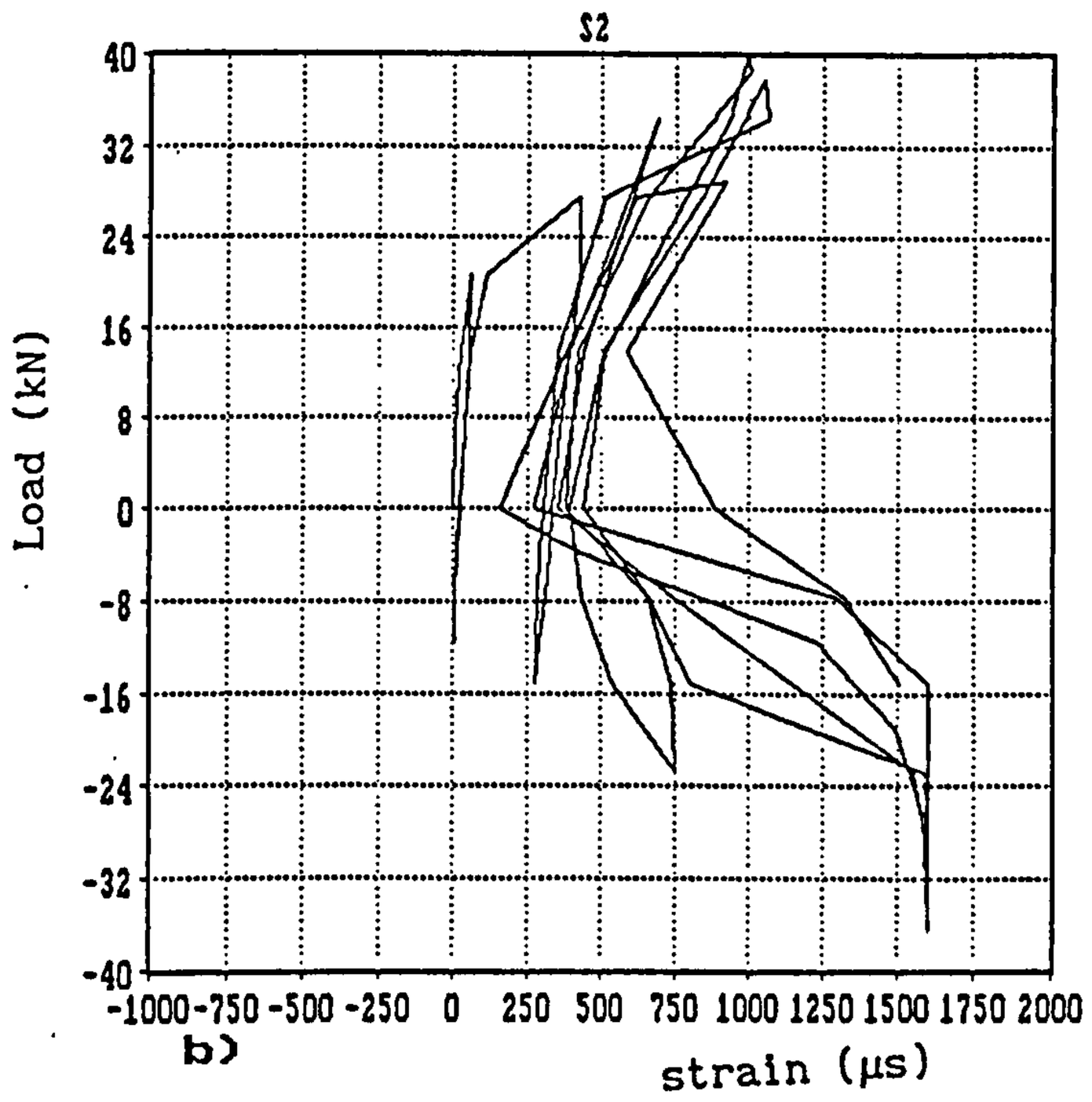

FIG.3.17 BEHAVIOUR OF STIRRUPS IN THE JOINT REGION

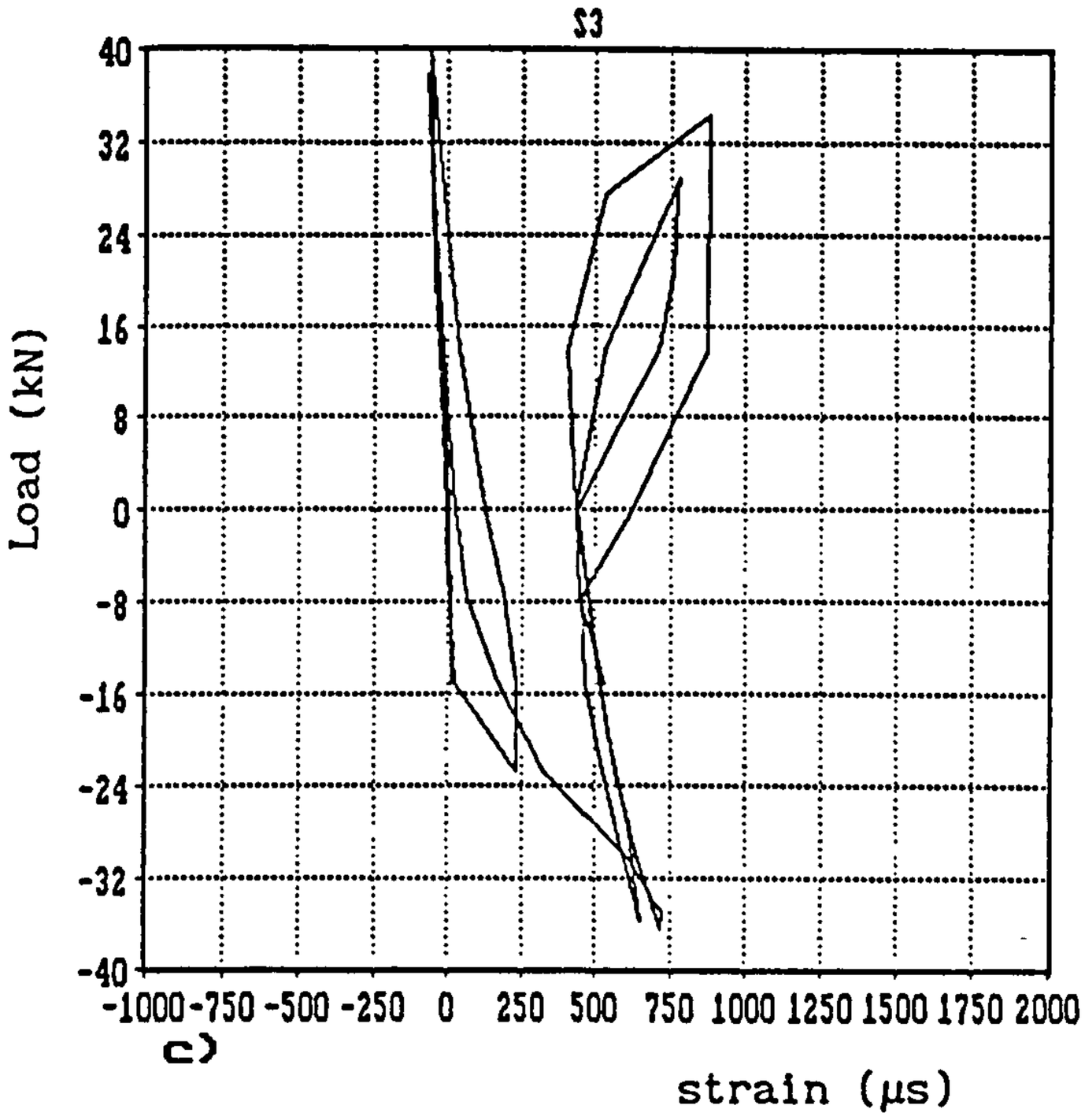
S3
Load (kN)
40
32
24
16
8
0
-8
-16
-24
-32
-40
-1000 -750 -500 -250 0 250 500 750 1000 1250 1500 1750 2000
strain (μs)

c)

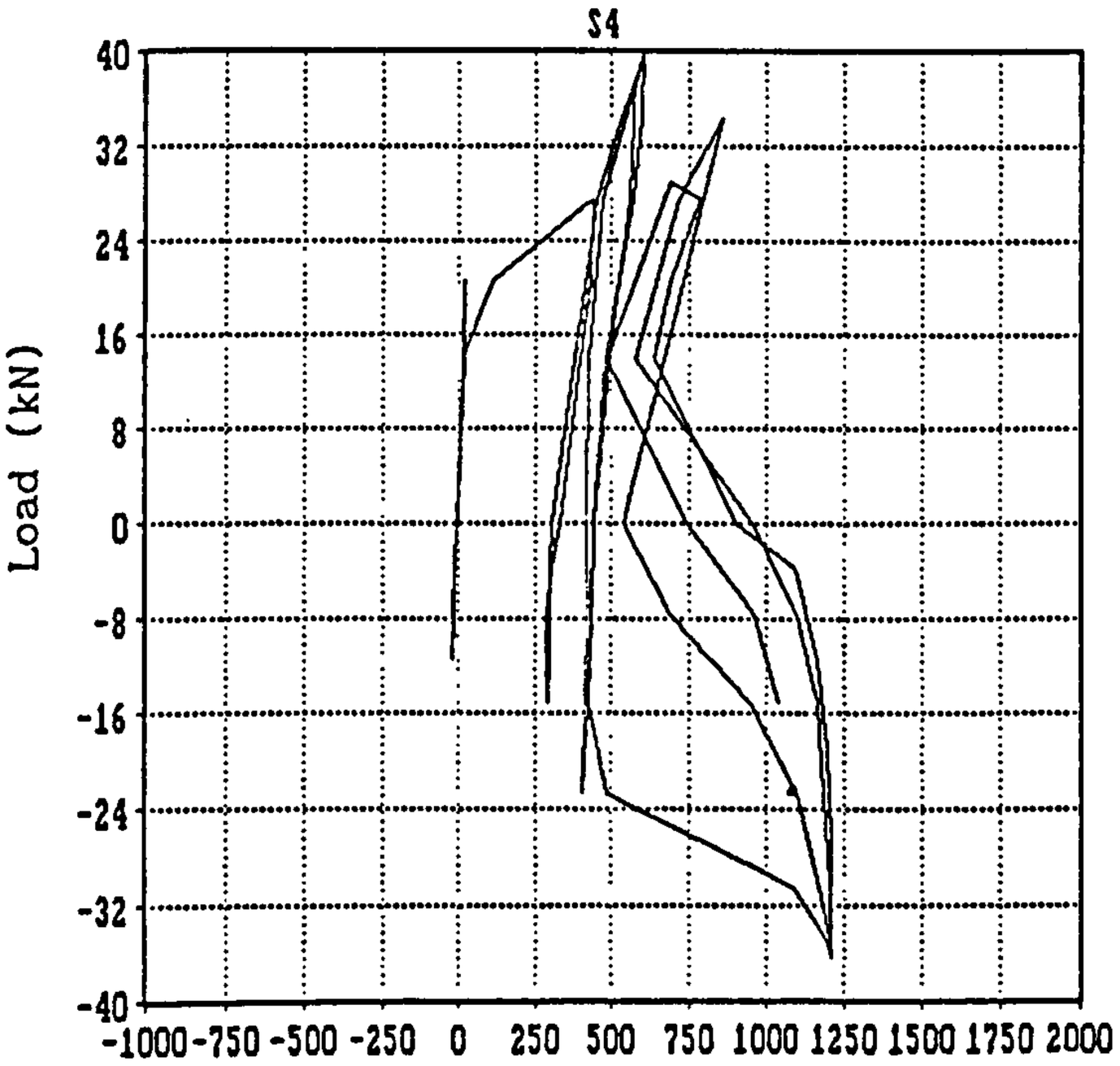
S4
Load (kN)
40
32
24
16
8
0
-8
-16
-24
-32
-40
-1000 -750 -500 -250 0 250 500 750 1000 1250 1500 1750 2000
strain (μs)

d)

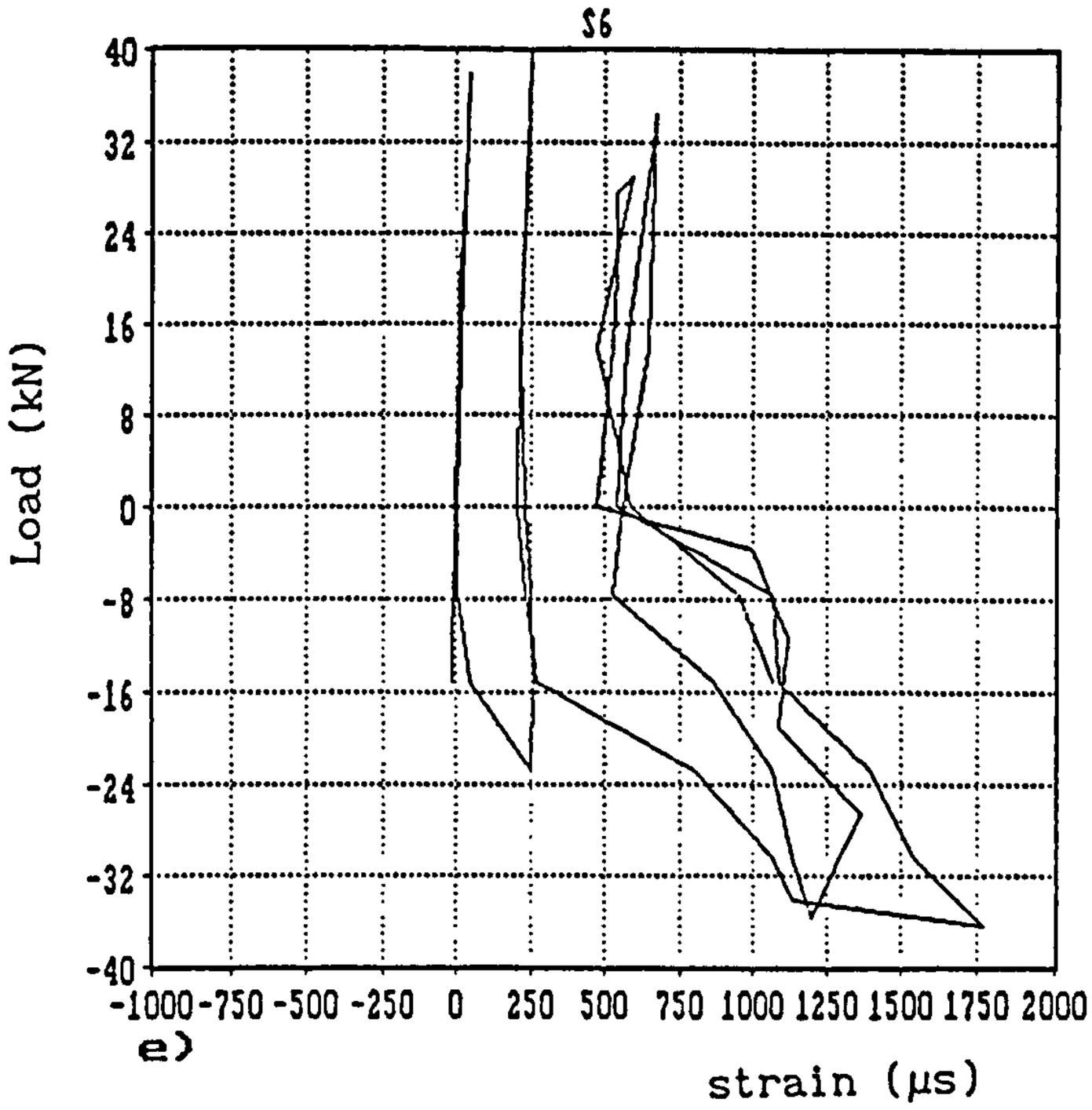
S6
40
32
24
16
8
0
-8
-16
-24
-32
-40
-1000 -750 -500 -250 0 250 500 750 1000 1250 1500 1750 2000
Load (kN)
strain (μs)
e)

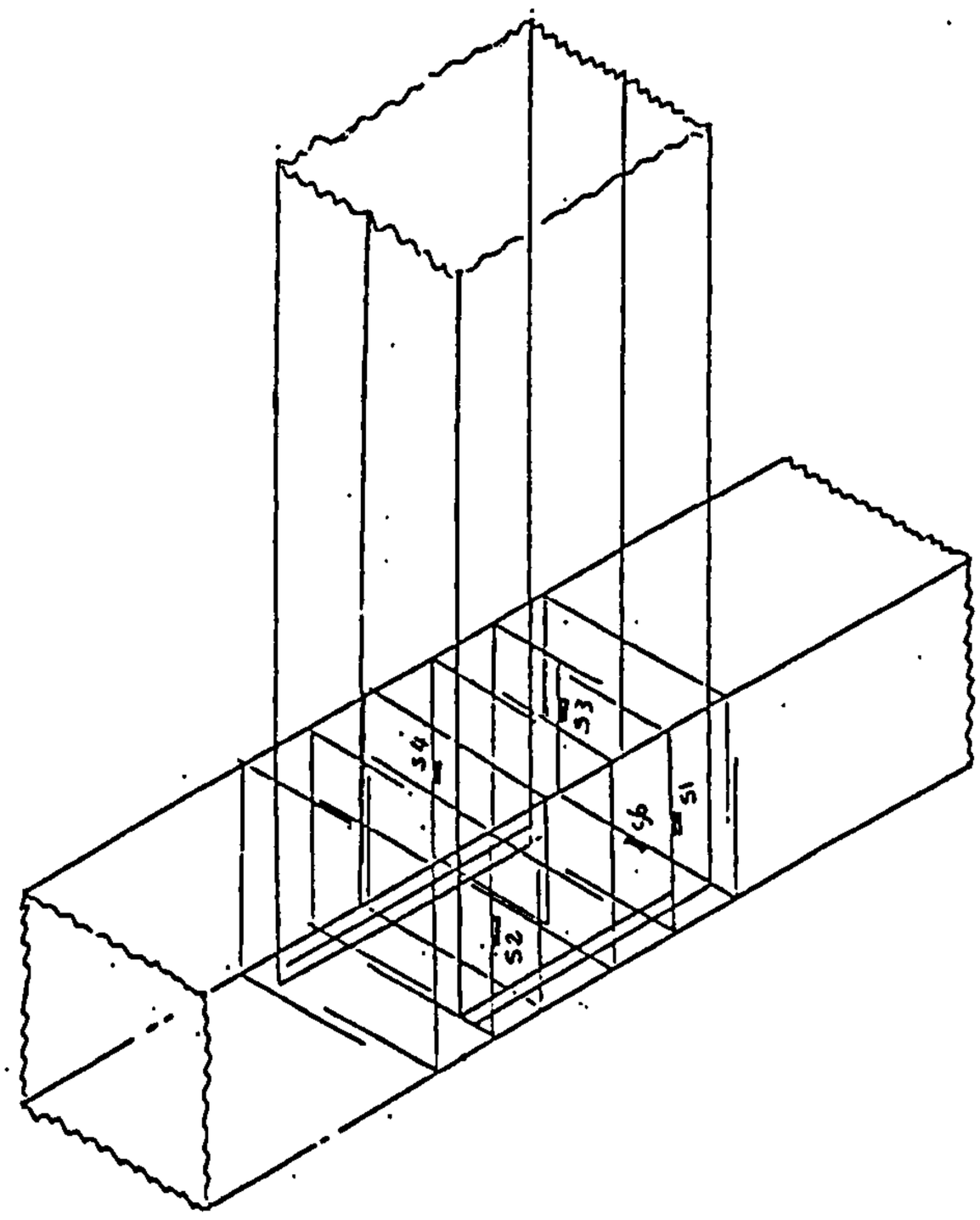
S4
S3
S1
S2

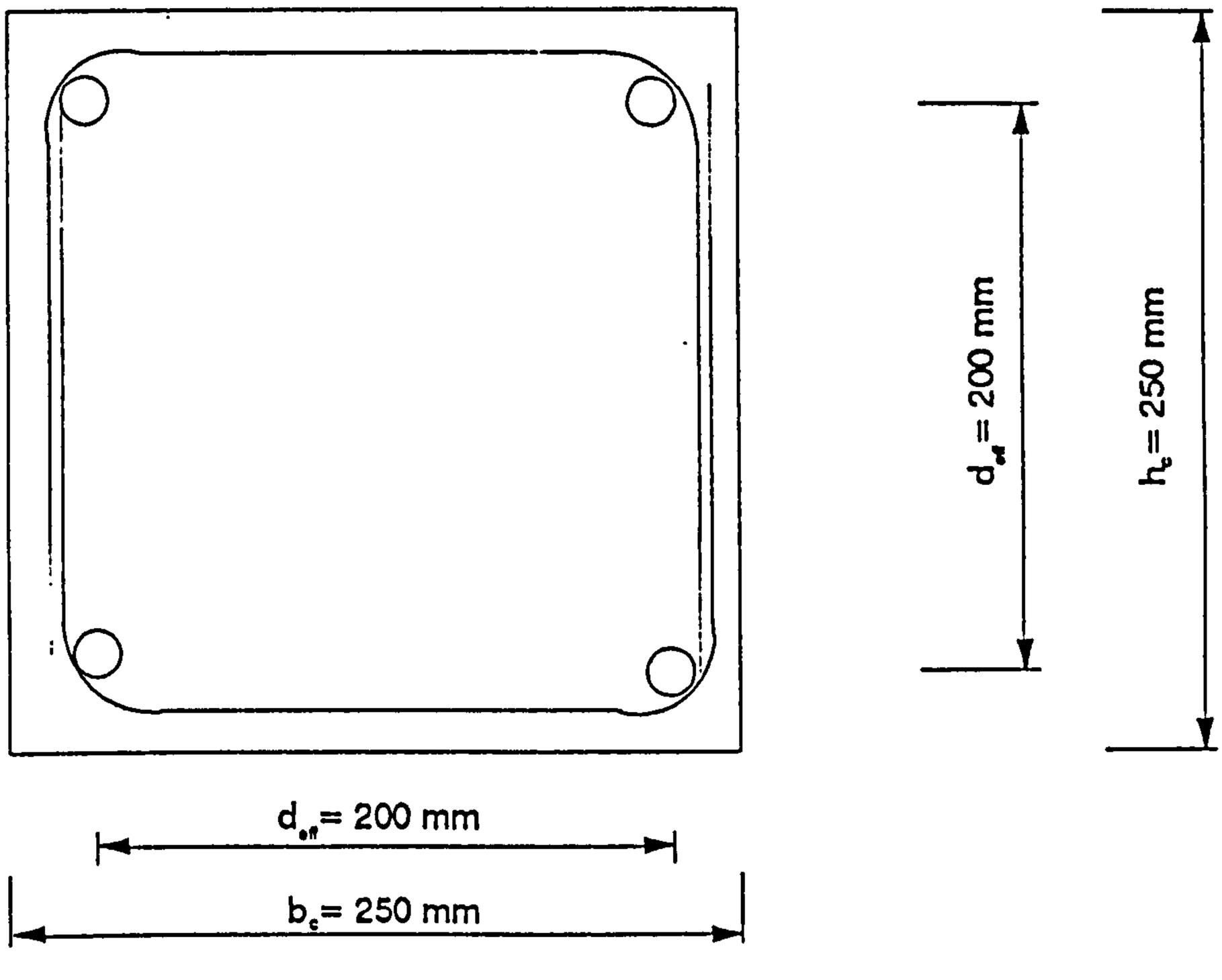

a) Detail of U-stirrups Overlapping - Specimen UD2

FIG.3.18 U-STIRRUPS OVERLAPPING & CRACKING PATTERN - UD2

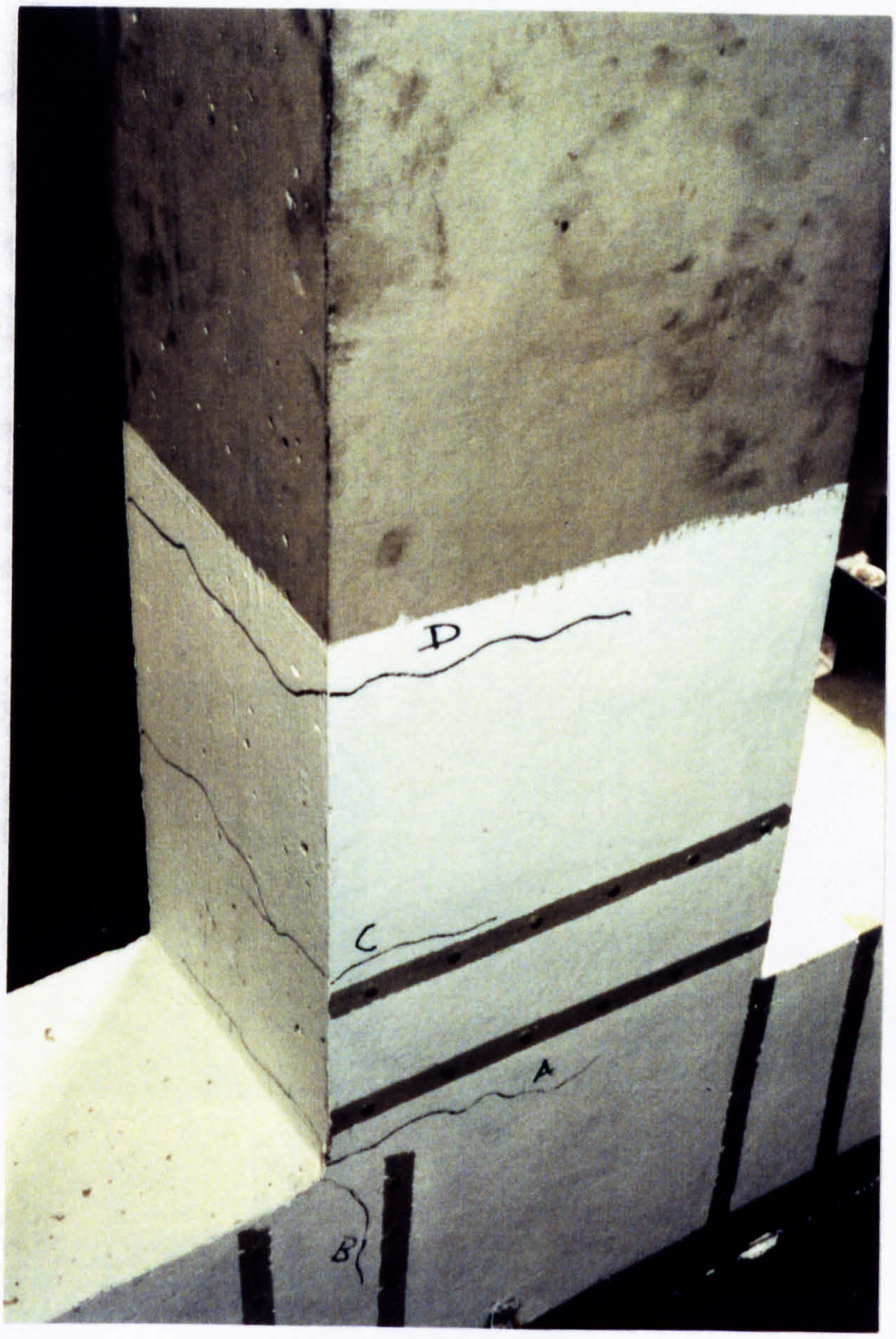

b) CRACKING PATTERN OF UNIT - UD2 -

a)

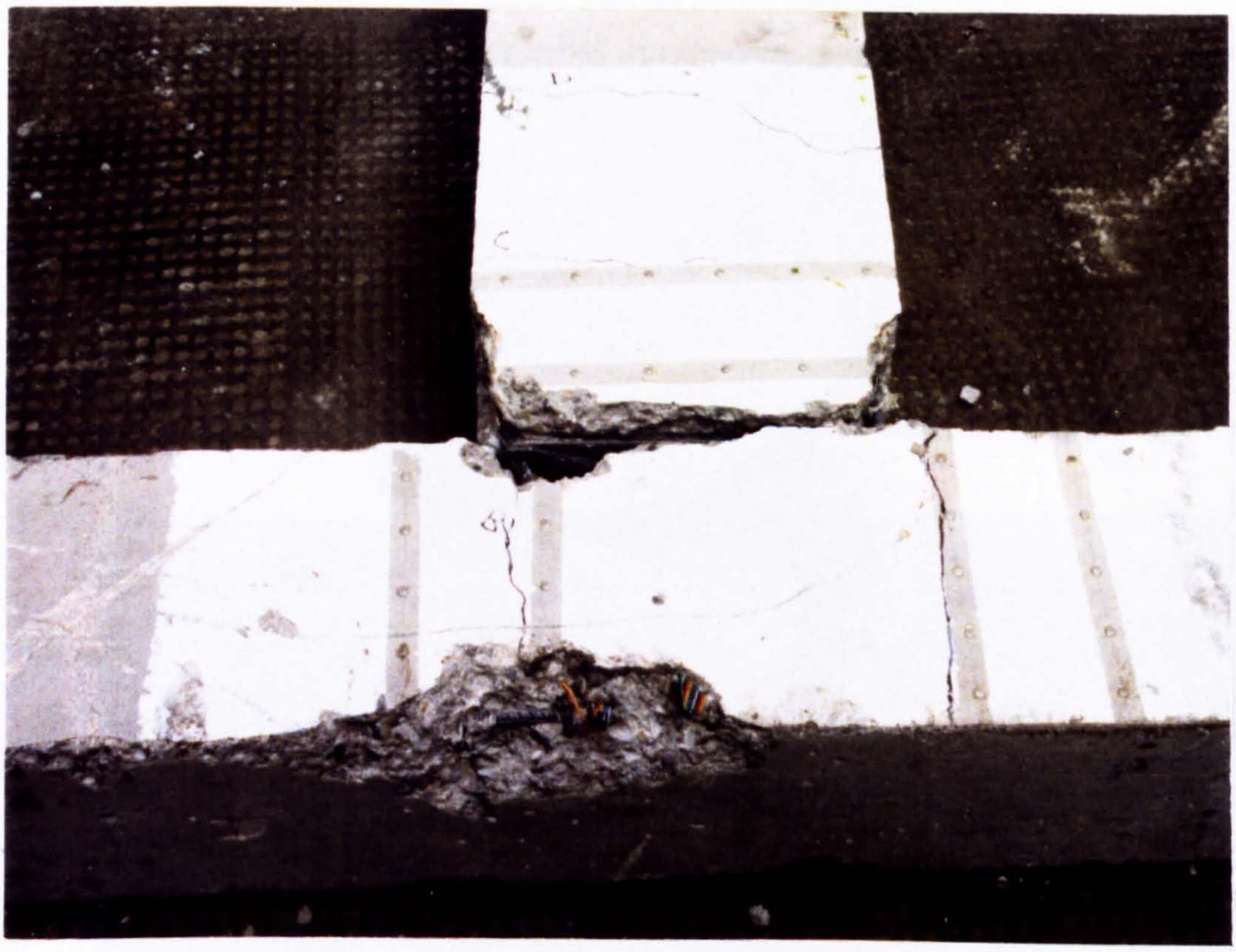

b)

FIG.3.19 STATE OF SPECIMEN - UD2 - AFTER EXPERIMENT

c)

d)

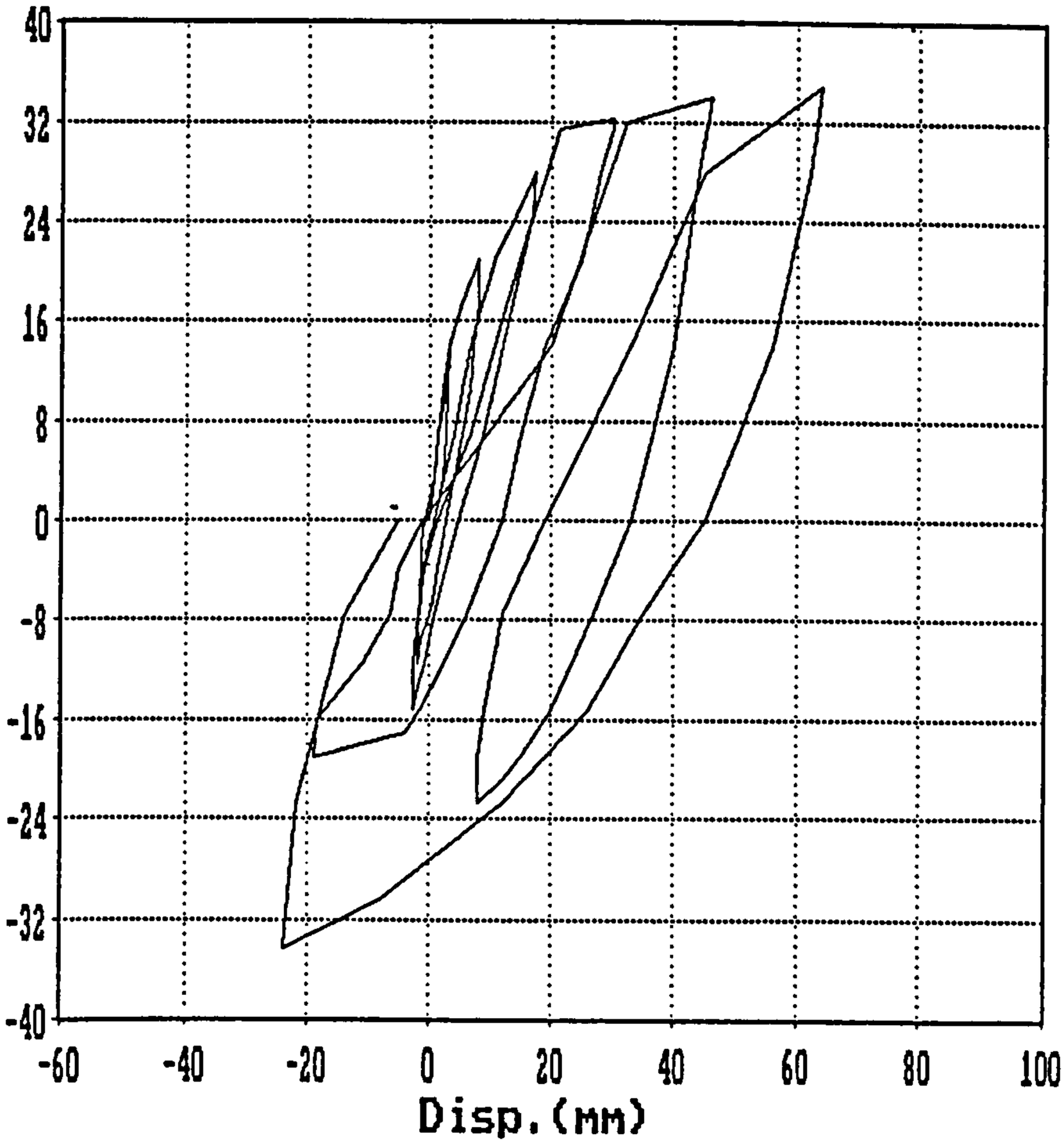

FIG.3.20 HYSTERESIS CYCLE OF SPECIMEN - UD2 -

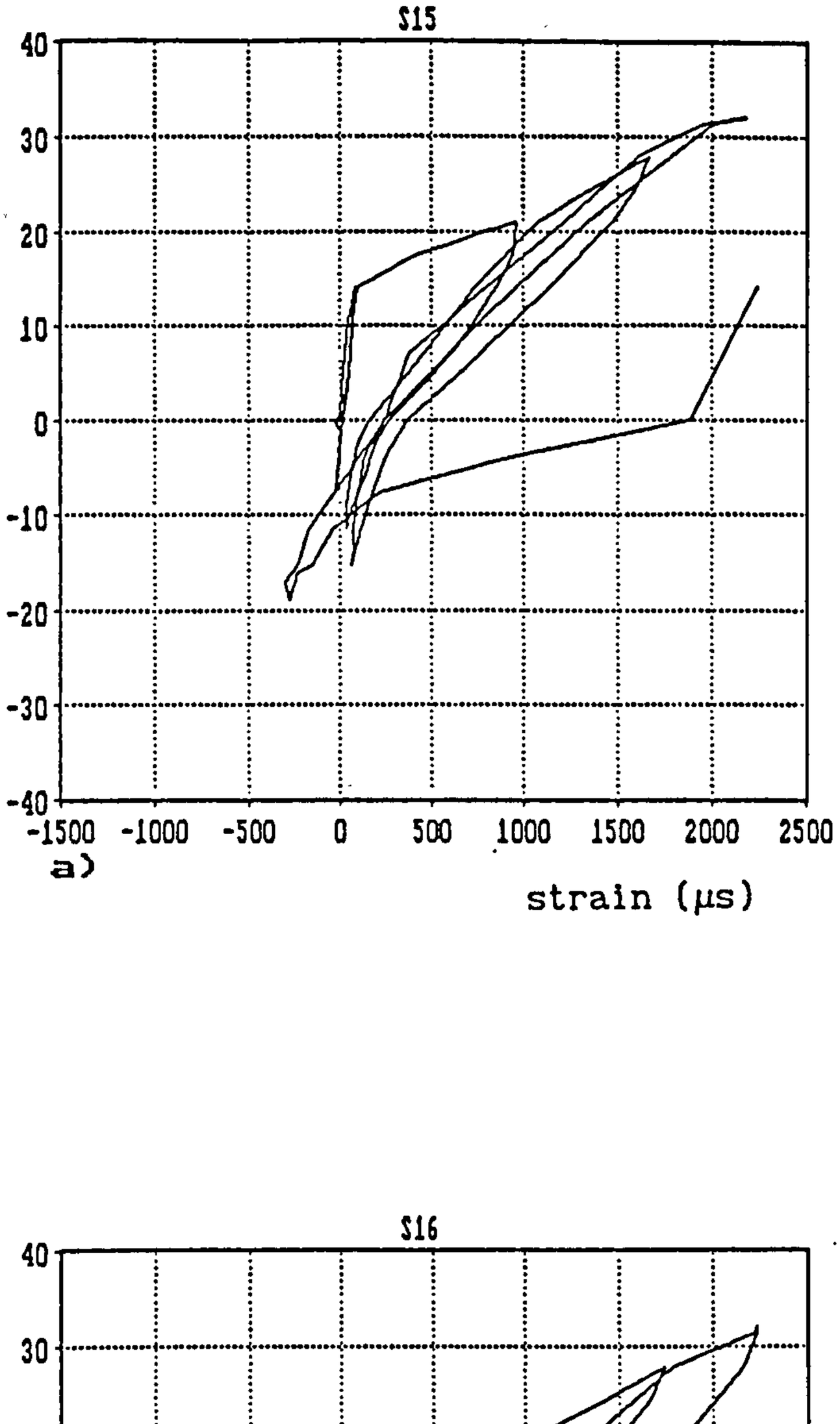

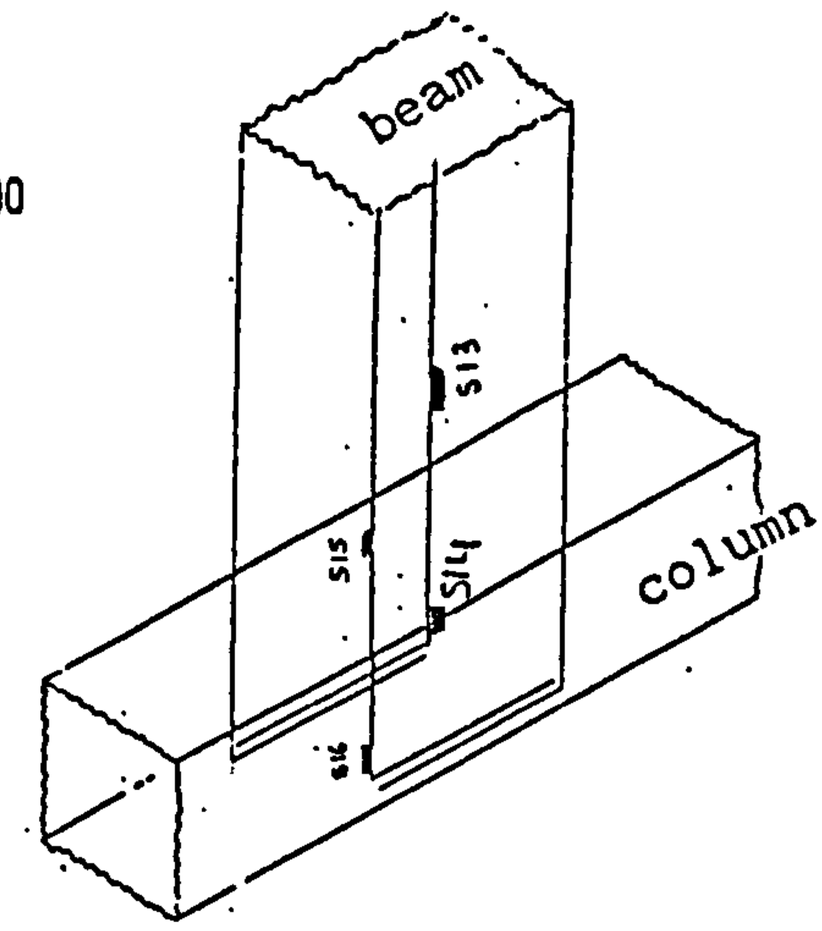

FIG.3.21 LOAD VS. STRAIN HISTORY OF BEAM BARS

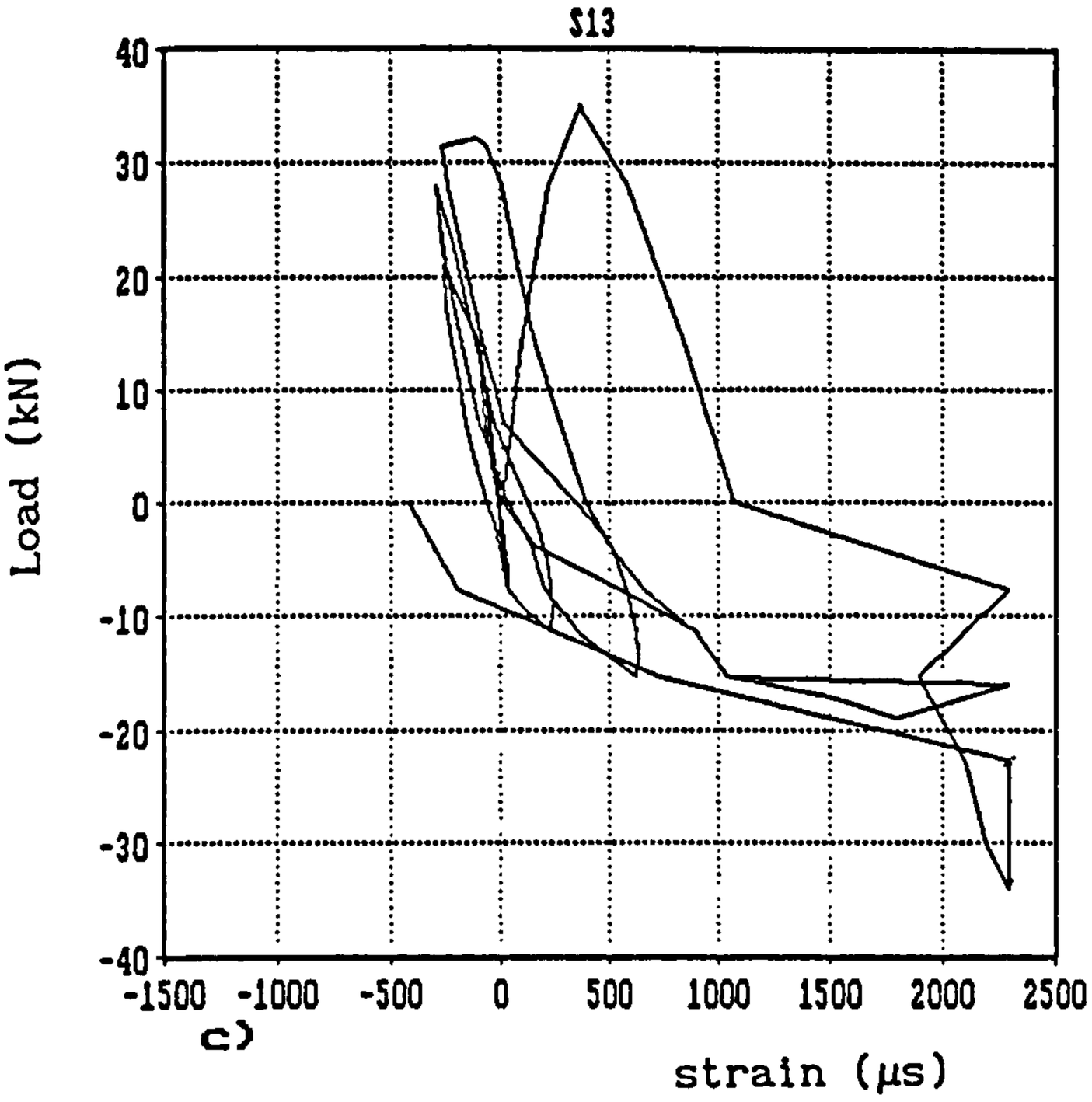
S13
40
30
20
10
0
-10
-20
-30
-40
Load (kN)
-1500
-1000
-500
0
500
1000
1500
2000
2500
strain (μs)

c)

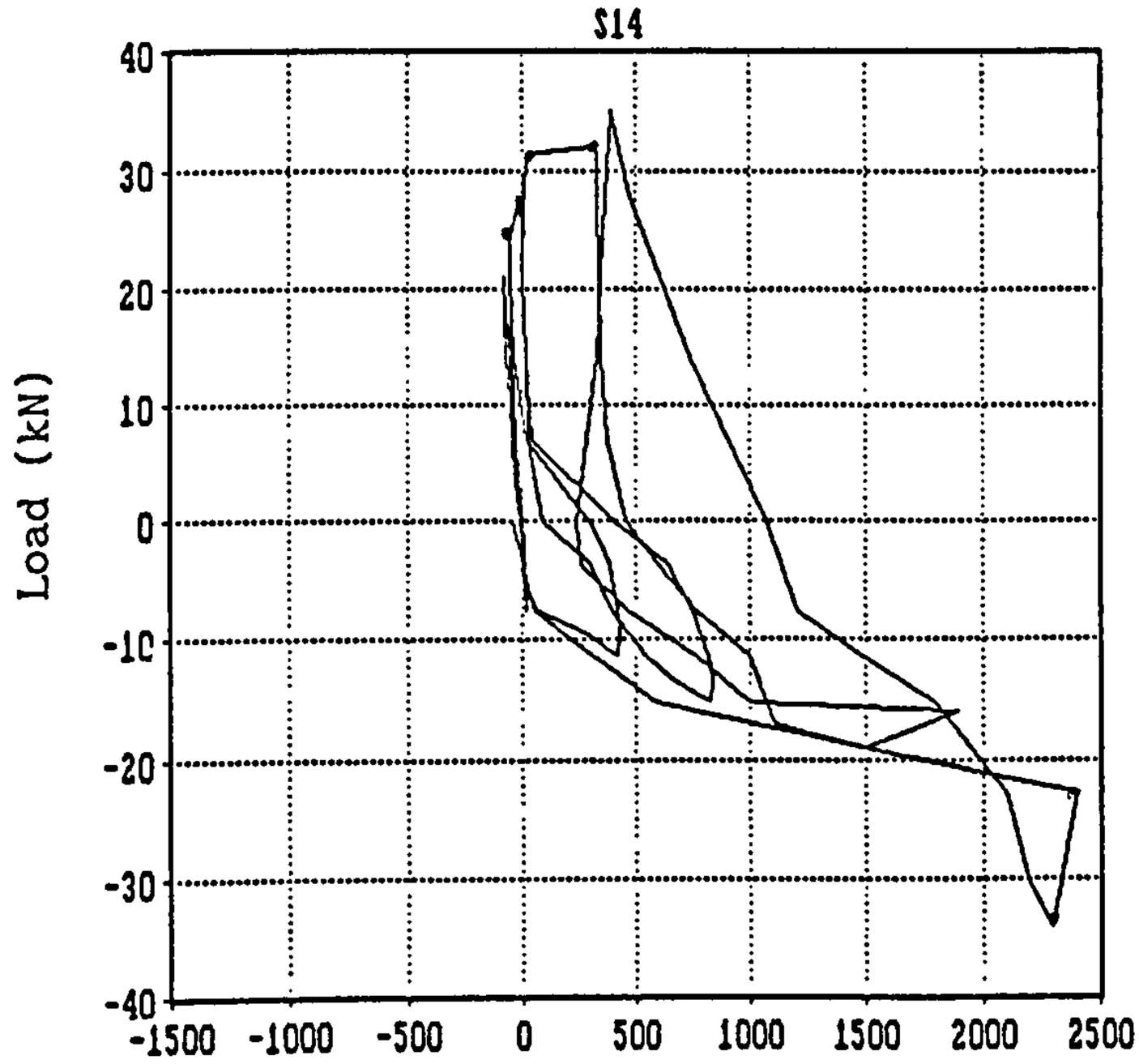
S14
40
30
20
10
0
-10
-20
-30
-40
Load (kN)
-1500
-1000
-500
0
500
1000
1500
2000
2500
strain (μs)

d)

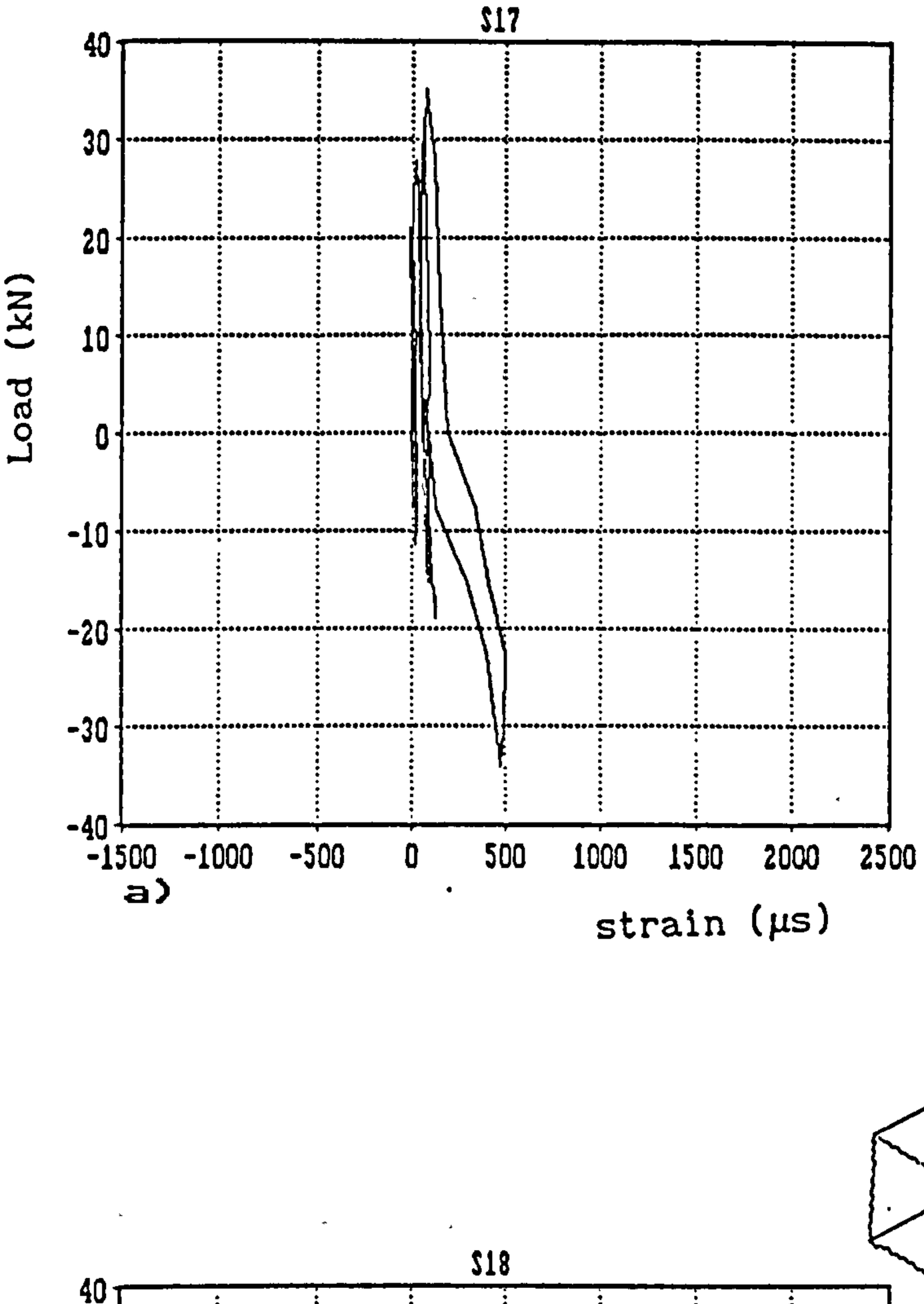

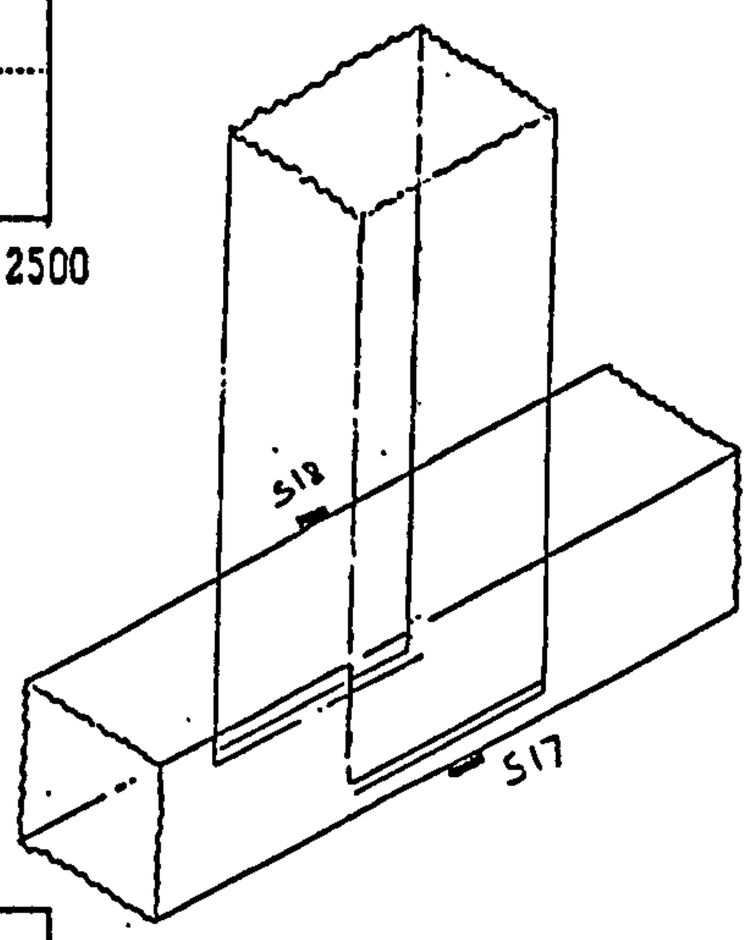

FIG.3.22 COLUMN BARS BEHAVIOUR UNDER REVERSED LOADS

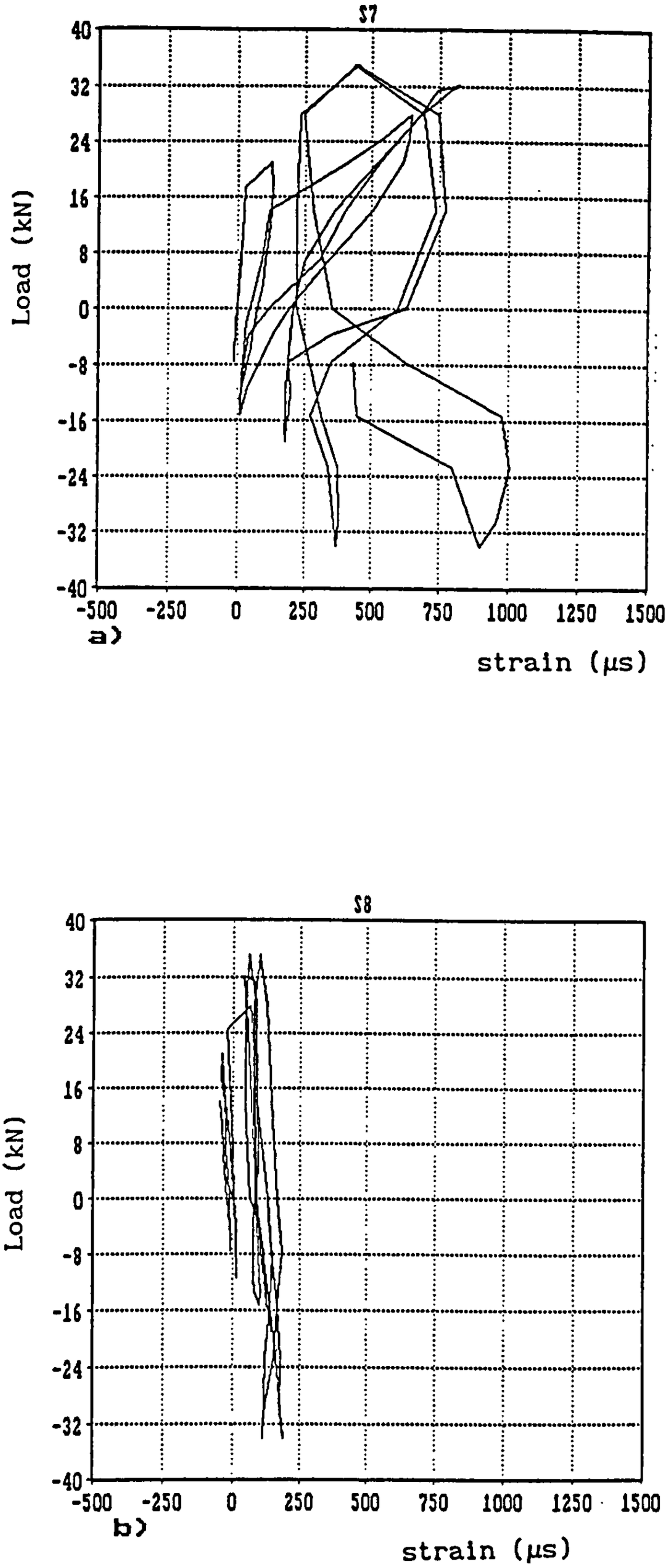

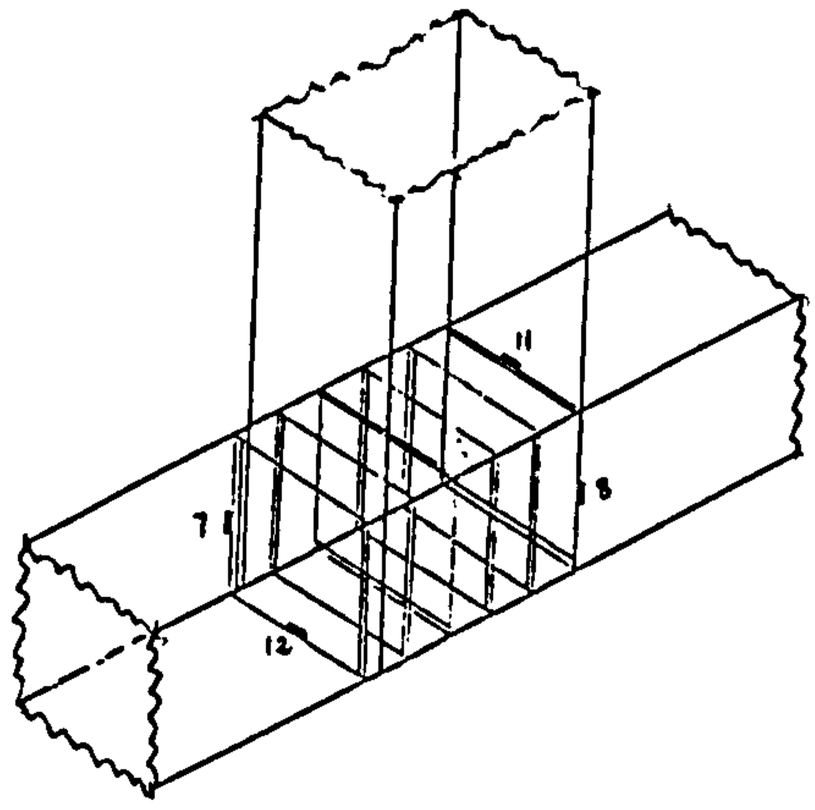

FIG.3.23 RESPONSE OF U-BARS TO CYCLIC LOADING - UD2 -

PAGE
NUMBERS
CUT OFF
IN
ORIGINAL

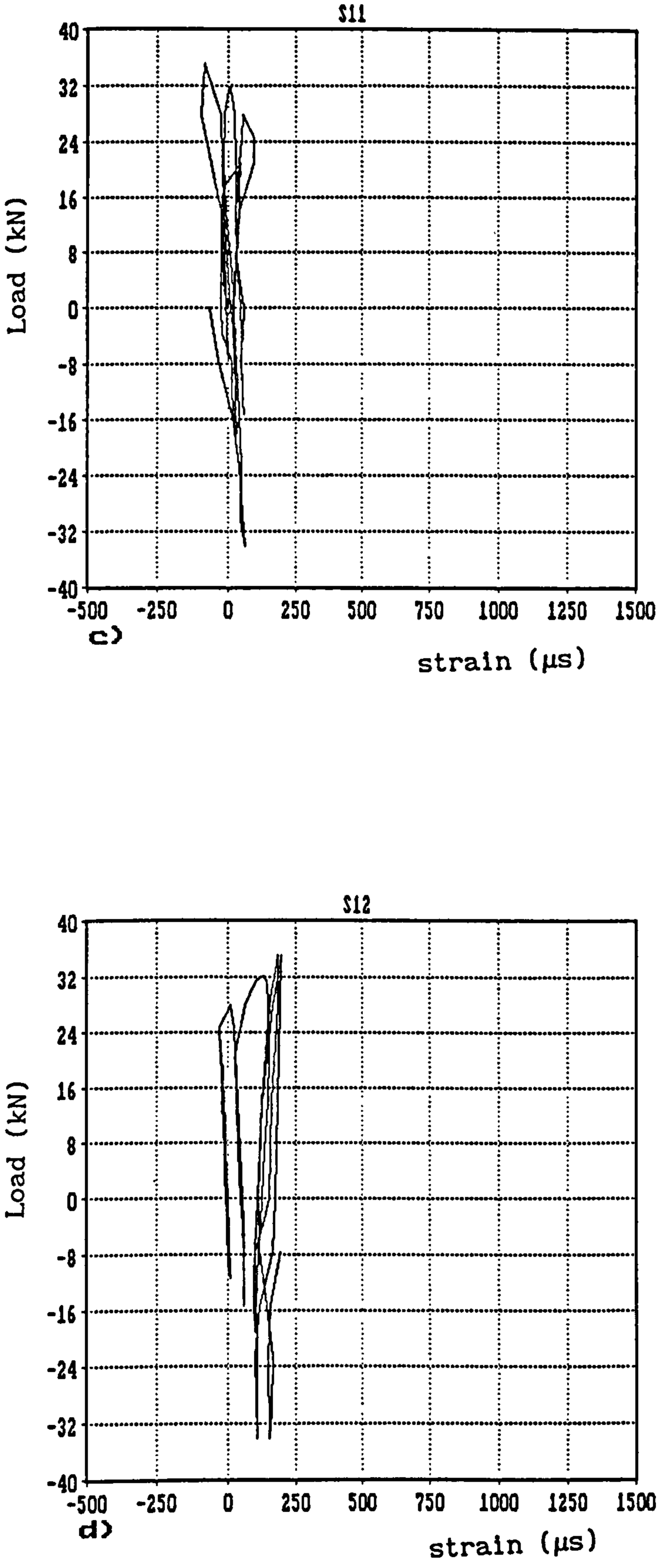
S11
40
32
24
16
8
0
-8
-16
-24
-32
-40
-500
-250
0
250
500
750
1000
1250
1500
Load (kN)
strain (μs)
S12
Load (kN)
strain (μs)

c)

d)

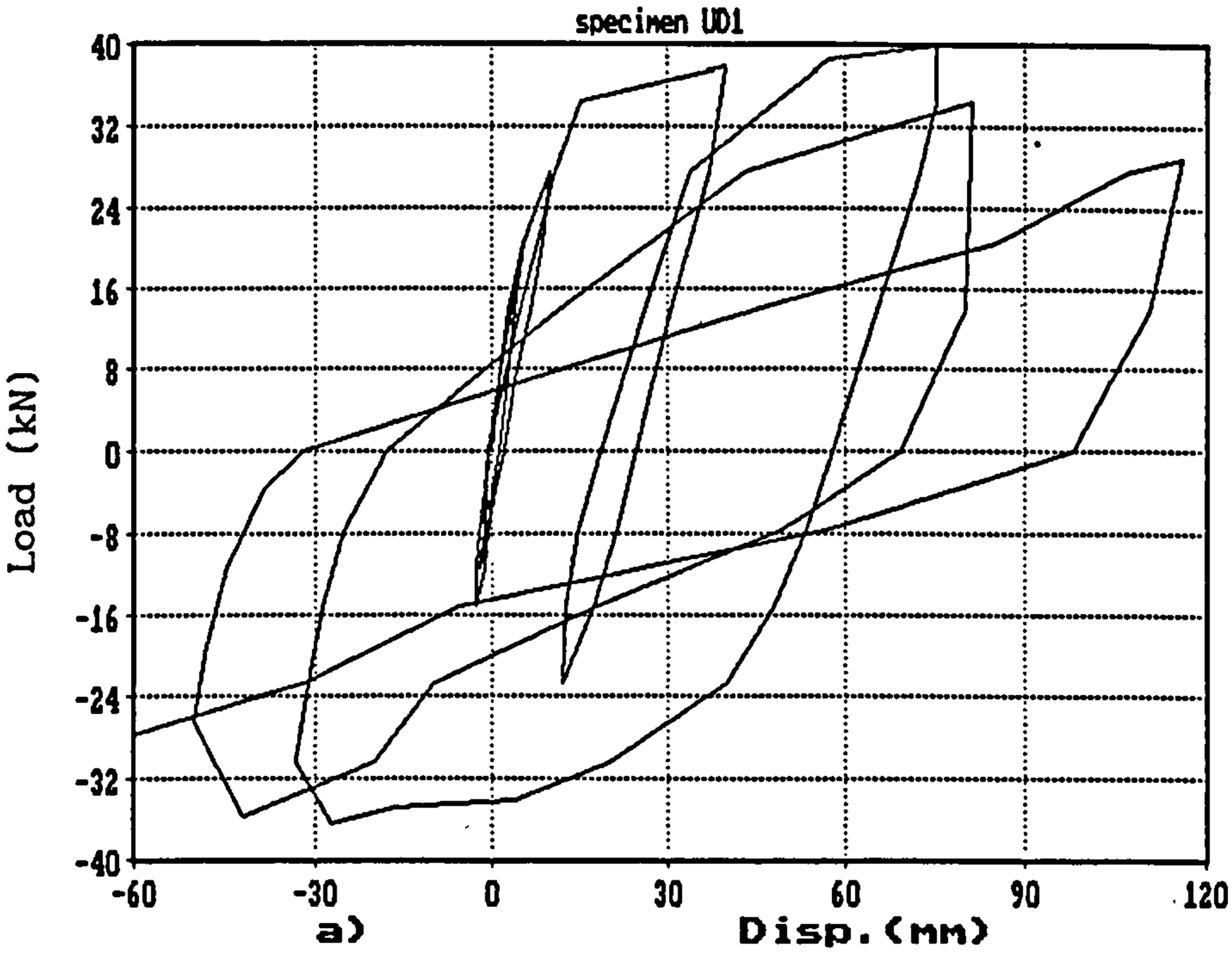

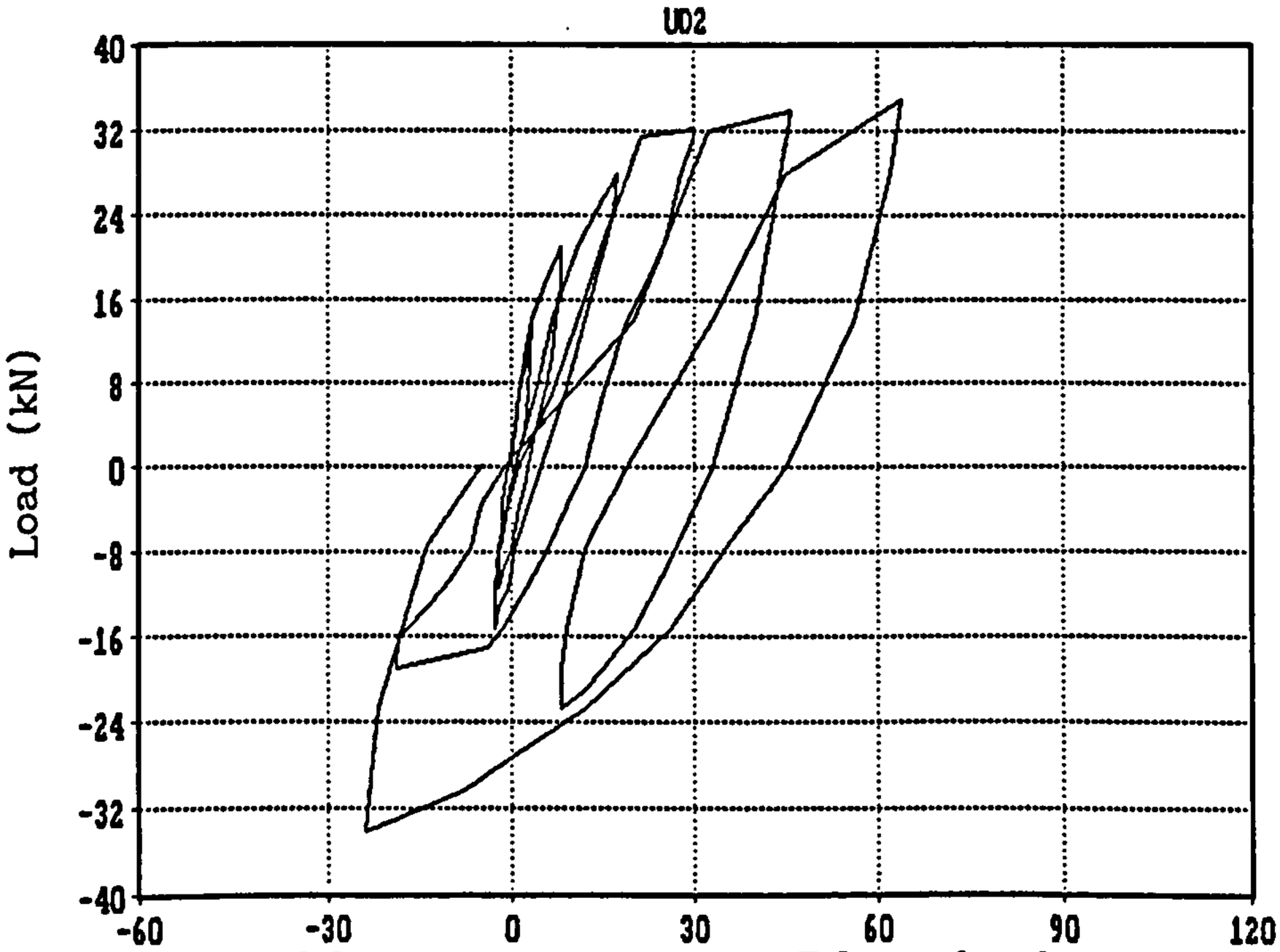

FIG.3.24 RESPONSE OF THE SUB-ASSEMBLY TO CYCLIC LOADING

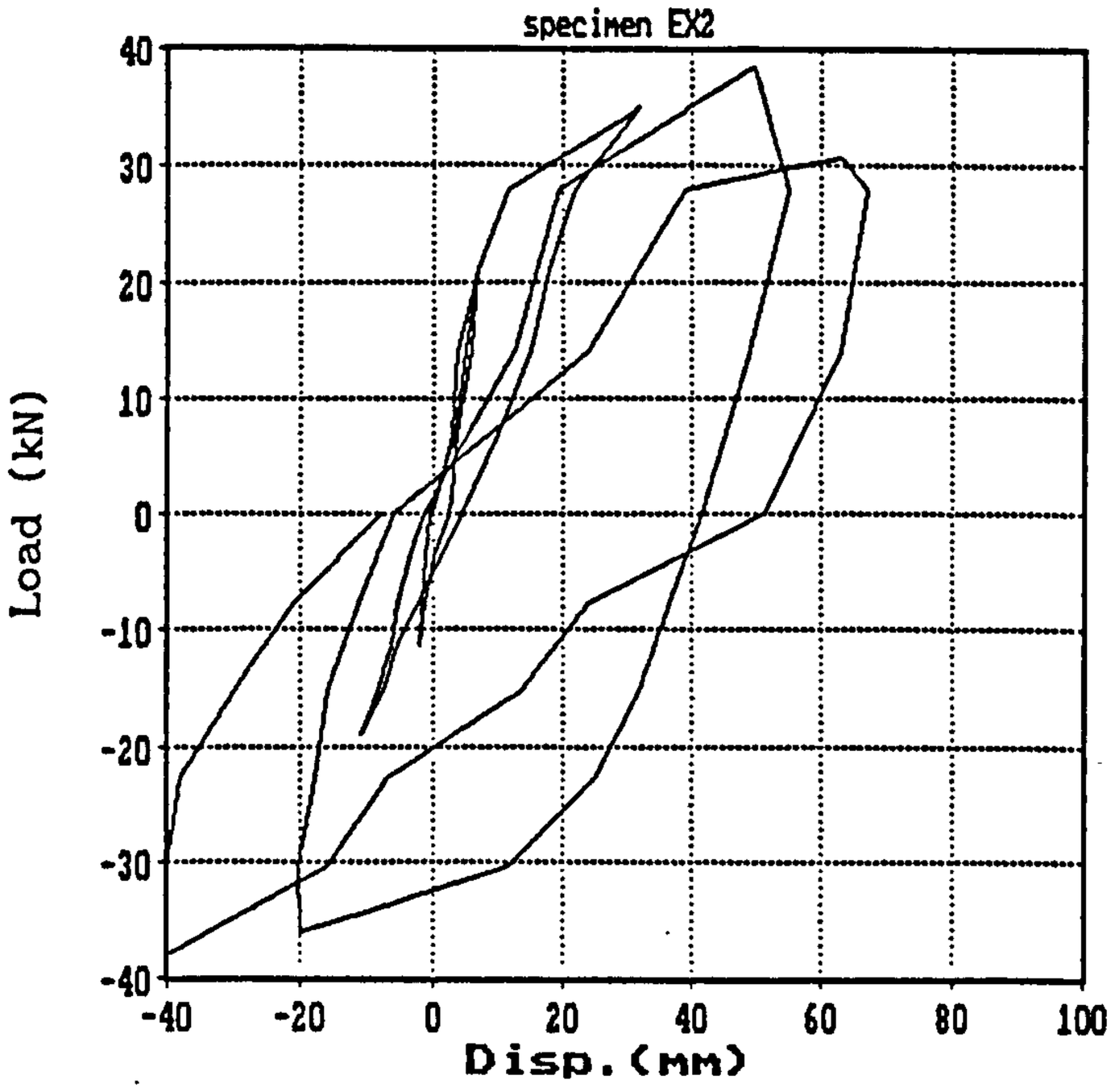
specimen EX2
Load (kN)
40
30
20
10
0
-10
-20
-30
-40
-40
-20
0
20
40
60
80
100
Disp.(mm)

c)

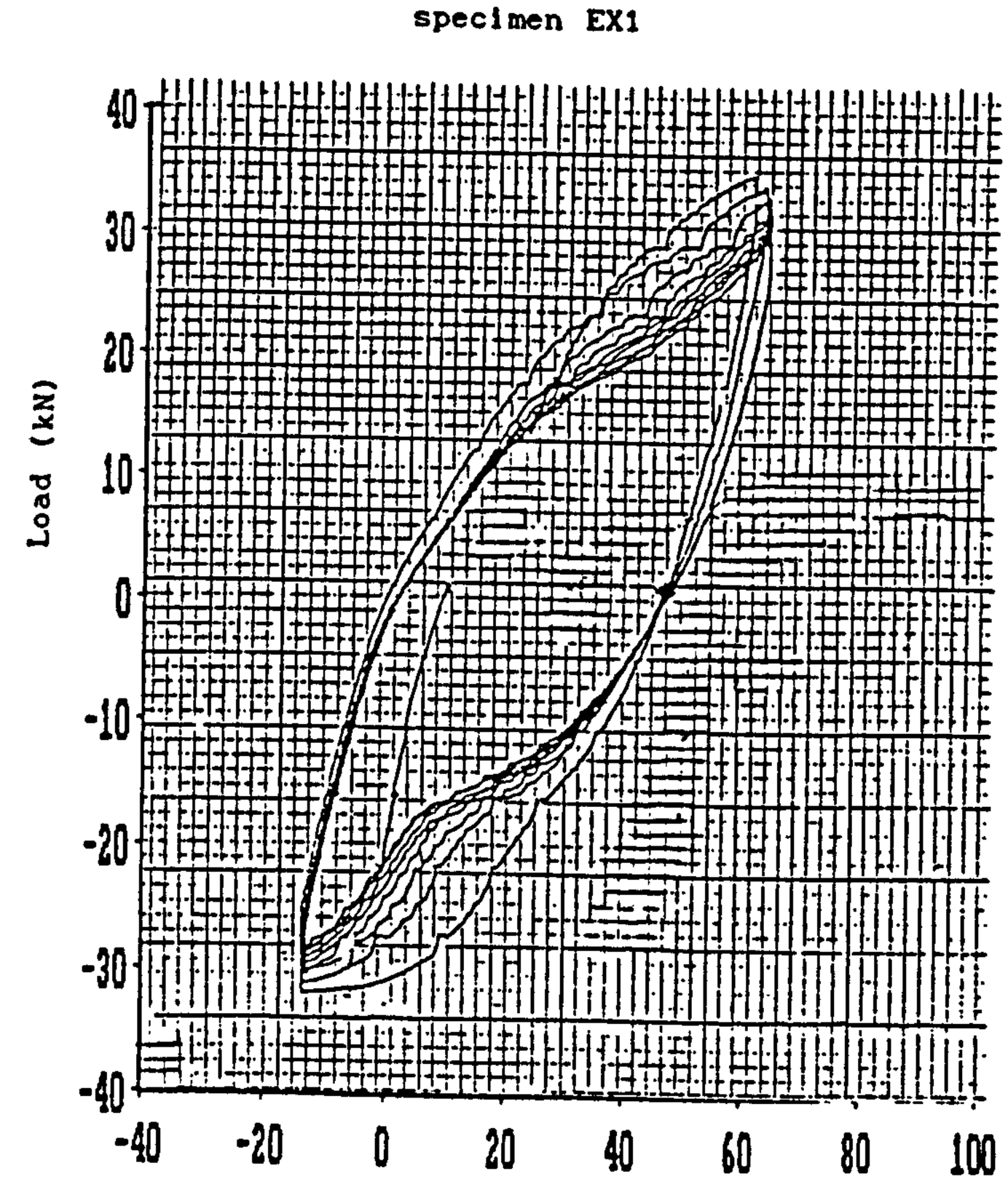
specimen EX1
Load (kN)
40
30
20
10
0
-10
-20
-30
-40
-40
-20
0
20
40
60
80
100
Disp. (mm)

d)

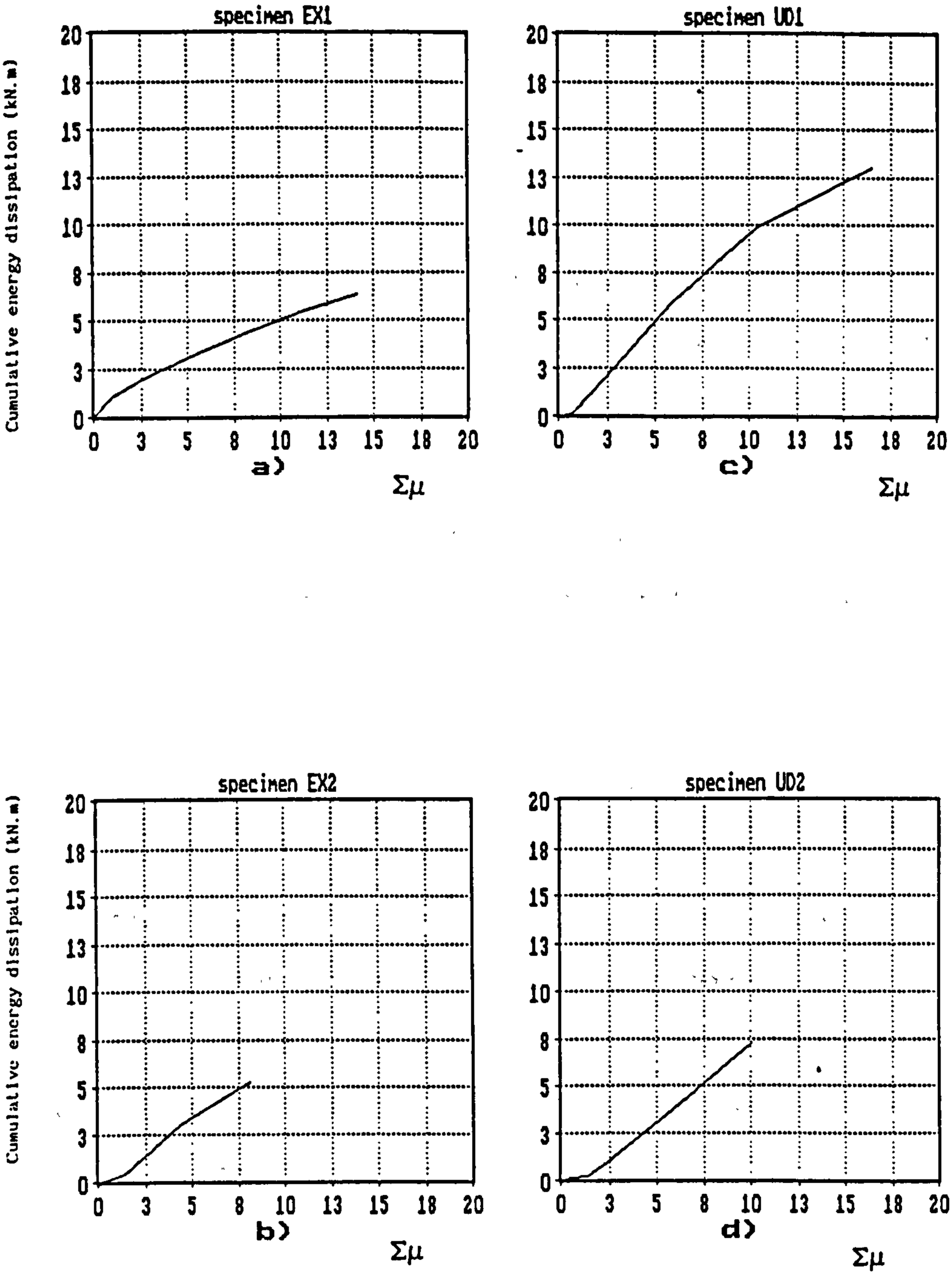

FIG.3.25 CUMULATIVE ENERGY DISSIPATION VS. CUMULATIVE DUCTILITY RATIO FOR SPECIMENS TESTED

CHAPTER FOUR ANALYTICAL STUDY USING FINITE ELEMENT ANALYSIS

4.1 GENERAL

Finite element modelling of reinforced concrete structures involves non-linear analysis using concrete elements with crushing and cracking capability, and reinforcement elements with post-yield strain behaviour [Ottosen (1980) and Kupfer et al.(1973)]. This is computationally very demanding and it is only in recent years that analysis of practical configurations has been feasible [DeSalvo (1987) and Van Mier (1987)].

In this study finite element modelling of reinforced concrete joints was carried out with the objective of learning more about the complex behaviour in the joint region than is possible with experimental observations. For example, it was hoped to study the distribution of strain along reinforcing bars, the distribution of cracking and crushing, and the apportionment of shear between the concrete and the transverse reinforcement. In this way it was hoped to provide a better insight into reinforced concrete joint behaviour in order to improve the design rules.

Taking the advantage of available computer finite element analysis, the analysis of reinforced concrete joints can be carried out to failure, with non-linearity caused by materials (steel and concrete), geometry and cracking taken fully into account.

The non-linear finite element program which is employed in this study is ANSYS 4.4, a general purpose finite element computer program,

available at Bristol University on a network system IBM 3090 mainframe. The capability of this program to include reinforced concrete properties will be outlined later on in this chapter (section 4.5).

4.2 FINITE ELEMENT METHOD

The finite element method is the most widely used numerical technique arising from the direct stiffness approach introduced into the analysis of structural continua, eg. Zienkiewicz (1977). A structure is idealized by an assemblage of discrete one-,two or three-dimensional finite elements having a certain number of degrees of freedom at each node. The finite elements are introduced at their nodal points in such a way that the nodal displacements approximate the continuity of deformation and maintain the equilibrium of the structure. Many elements of different shapes may be inserted into the computer model so that the method can be used to tackle complex problems incorporating geometrical as well as material non-linearities.

The convergence, and therefore the accuracy, of the solution depends largely on the deformation pattern chosen for the finite elements. That is, a close similarity between the displacement patterns of the original structure and the mathematical model must be obtained. This is possible only if the displacement patterns for the elements are chosen in such a manner as to satisfy compatibility of displacements and stresses within the elements and everywhere at the boundaries between the adjacent members. Such an idealization ensures that as the element sizes decrease, the displacement components and therefore stress components in the model converge to the actual values

at the representative points. The unknown nodal point displacements and forces are determined through a general stiffness analysis procedure. The internal forces and stresses for each element are derived accordingly.

Several numerical solution techniques are available in ANSYS, and have been treated extensively by De Salvo [De Salvo 1987)].

4.3 CONCRETE MATERIAL BEHAVIOUR

4.3.1 Behaviour of Concrete in Compression

Up to approximately one-third of its ultimate compression strength, no major microstructural changes take place in concrete which behaves essentially as a homogeneous, isotropic material obeying linear elastic rules. Above this linear elastic limit concrete begins to soften until it reaches its peak stress. This softening is believed to be caused by microcracks which appear at the interface between the aggregate particles and mortar or within the mortar itself [ASCE (1981)].

Upon further straining, these microcracks begin to grow in length, width and number and develop into macrocracks. At about 80% of the ultimate strength, a large number of cracks have already developed and the stress-strain curve starts flattening significantly. Damage continues to accumulate until the ultimate stress is attained after which further strain softening occurs and the stress-strain curve begins to descend.

Most finite element investigations reported in the literature consider concrete to behave linearly in compression up to a yield

surface. Beyond the yield surface concrete is either assumed to be perfectly plastic or to possess some non-zero degraded stiffness. The first stress-strain curve of concrete under biaxial compression incorporated into the finite element method was developed by Nilson (1968), who assumed that the tangent modulus of elasticity in one principal direction is affected by the stress in the other principal direction. Also Suidan and Schnobrich (1973) considered concrete in compression as an elastic perfectly plastic material which obeys the Von Mises failure criterion. Kupfer an Gerstle (1973) adopted the Von Mises yield criterion in conjunction with the associated flow rule to model the crushing behaviour of concrete in biaxial compression while Lin and Scordelis (1975) used a flow rule in which plastic strains were unconstrained and the stresses were fixed at the initial yield point values.

4.3.2 Behaviour of Concrete in Tension

Up to about two-thirds of its ultimate tensile strength, concrete behaves nearly linearly after which bond microcracks start forming. Since the propagation of the cracks is transverse to the stress direction, cracks will form and grow very quickly over a short interval. The descending branch of the curve is very difficult to follow since the stress drops off rapidly due to instability in crack propagation. The direct tensile strength of concrete is very difficult to measure and is often approximated by the modulus of rupture or the split cylinder test. The modulus of elasticity of concrete in tension is somewhat higher than its modulus of elasticity in compression. Under biaxial tension, concrete exhibits a constant [Kupfer et al. (1969)] or possibly a slightly increased tensile strength [Tasuji et al. (1978)], whereas under the combination of tension and compression

it exhibits reduced strength.

In most finite element analyses of reinforced concrete structures, concrete is considered to behave linearly up to a limiting tensile strength. Once this value is reached, the concrete is either assumed not to take any stress in the direction normal to the cracking plane, or else a softening with the stress decreasing strain is allowed, as illustrated in Fig.4.1.

4.3.3 Tension Stiffening of Cracked Concrete

When reinforced concrete cracks, concrete on either side of the crack can still resist tension. This phenomenon of tension stiffening is particularly significant for lightly reinforced concrete members where the tensile stresses in the concrete teeth between the cracks are not negligible, as reported by Cope et al. (1980). At a cracked zone the load is carried by the reinforcement only, whereas between the cracks the uncracked concrete contributes to the overall stiffness of the system. Therefore the concrete stress is zero at the cracks but the averaged stress over the cracked region is not zero. As cracks continue to form, the average concrete stress over the cracked region will progressively decrease.

Tension stiffening of concrete has been incorporated in many models. The tensile strength of concrete is assumed to be zero when the tensile strain exceeds a limiting value $\alpha\varepsilon_{cr}$, where α a factor which determines the length of the descending branch. This factor has been proved to have considerable effect on numerical results. Values for α ranging from *5* to *25* have been reported in the literature such as Lin (1973) and Hinton et al. (1976).

4.3.4 Shear Transfer in Cracked Concrete

Shear transfer in cracked concrete is caused mainly by two mechanisms: aggregate interlock; and dowel action.

(i) *Aggregate interlock*

Aggregate interlock is a mechanism where, due to an excess of tensile stress in the concrete, the opposite faces on either sides of the crack are subjected to a parallel differential movement as well as a normal displacement. If the normal displacement is prevented by reinforcing bars crossing the crack or by the adjacent uncracked concrete, vertical compressive stresses develop in the concrete. Since the texture of the cracked surfaces is usually rough and irregular, sliding of both surfaces is prevented by the frictional forces caused by the vertical compressive stresses. This phenomenon of shear transfer is particularly important for normal strength concrete rather than for high strength concrete since the latter tends to produce smoother cracked surfaces as a result of the high strength of the paste which approaches that of the aggregate.

The aggregate interlock effect is incorporated into finite element models by using an equivalent shear stiffness and shear strength for cracked concrete. Analyses which neglected this effect have resulted in some incoherence with observed crack patterns. Those retaining some shear stiffness in the cracking plane have given good correlation with test results as found by Suidan and Schnobrich (1973). The value of the shear coefficient β is chosen such that $0 \leq \beta \leq 1$ [Chen (1982)]. It has been found that results are not very sensitive to the value of β as long as $\beta > 0$. A crack may also close on further loading. Closing of the crack causes a compressive stress to be transmitted across the

crack and a similar effect of shear resistance develops resulting in a somewhat higher value for β. Many analyses have adopted a value of unity for β when a crack closes which is assumed to occur when the direct strain across the crack becomes compressive.

(ii) *Dowel action*

Dowel action of reinforcing steel develops when major shear deformation occurs after tension cracking has occurred in the concrete. The main longitudinal reinforcement acts as a dowel and significant shear forces are transmitted to it.

Dowel action may be incorporated into the finite element analysis in the same manner as for aggregate interlock. In an early model developed by Ngo and Scordelis (1967) dowel action resulted in a disconnection of the main reinforcement from the concrete over an effective dowel length representing the distance over which bond was assumed to have been destroyed.

4.3.5 Bond-Slip between Concrete and Steel

Bond between concrete and reinforcement is an important parameter since it affects the stress distribution in both materials as well as the width and the spacing of cracks. Such localized effects develop in structures subjected to high shear forces, such as at the beam-column connections, or at the anchorage zones. Under cyclic loading the reinforcement tends to slip through the surrounding concrete which remains undisturbed.

Some mathematical formulations to account for the bond-slip behaviour have been derived by Nilson (1968) and Houde (1973). Ngo and Scordelis (1967) modelled this effect by means of discrete or

distributed springs which simulate the contact forces along the faces of the bars.

4.3.6 Concrete Cracking and Crushing

Cracking is considered to be one of the most important effects of concrete together with the tensile yielding of steel. Crushing also contributes to this non-linearity but is less important; since even at, or near, the ultimate load only a small portion of a reinforced concrete structure is subjected to high compressive stresses.

4.3.7 Tensile Cracking

Concrete is assumed to crack when one of the principal stresses exceeds the tensile strength. A crack forms in the direction perpendicular to the offending stress and the tensile stress at the position of the crack drops to zero. The material does not offer any resistance against further deformations normal to the crack. However, the stress in the direction of the crack is non-zero and the material is assumed to carry stress according to uniaxial or biaxial conditions.

Two main approaches have been used to model cracking of reinforced concrete: the smeared model and the discrete model. The choice of either crack representation depends on the purpose of the analysis. The smeared crack model is best for predicting overall load-deflection behaviour of reinforced concrete structures up to failure without regard to completely realistic crack patterns and local stresses. The discrete crack representation, however, is more appropriate if detailed behaviour at all stages up to failure is of interest, particularly in relation to the size of the elements. Where the

behaviour of a structure is dominated by a few major cracks a discrete crack model may be desirable. However, the smeared crack model can still be very effective if the size of elements is appropriately reduced.

4.3.8 Compressive Crushing

Concrete under uniaxial compression is assumed to crush when the compressive strain exceeds a limiting value, ε_{cr}, usually taken in the range 0.003 to 0.005. When this limiting value is reached, the concrete loses all its stiffness and the stresses are reduced to zero. In multiaxial cases the concrete is assumed to crush when the largest compressive strain exceeds the limiting strain value of concrete at ultimate load, ε_{cu}.

4.4 REINFORCEMENT MATERIAL BEHAVIOUR

In contrast with concrete, the mechanical properties of steel reinforcement are well known. The reinforcement stress-strain relationship is generally idealised by a bi- or tri-linear curve, Fig.4.2. The reinforcement is assumed to be either elastic or perfectly plastic or else an elastic strain hardening constitutive relationship is assumed. The stress-strain curve of steel in compression is assumed to be similar to that in tension.

4.5 ANSYS FINITE ELEMENT PROGRAM

4.5.1 General

The ANSYS finite element package is a general purpose program which offers a wide range of elements and analysis types (linear and non-linear). The program possesses two powerful pre- and post-processing routines which may be used to analyse any kind of

structure. ANSYS uses a wave-front solution method to solve the system of equations [Irons (1970), Melosh and Bamford (1971)]. This is a powerful method in which solutions are evaluated on an element by element basis rather than node by node basis as is done with the alternative approach employing band solvers. The elimination process is characterised by a wave which sweeps over the structure in the specified element numbering sequence. The nodes belonging to the element under consideration are designated as "active". The stiffness coefficients associated with these nodes are summed and may be eliminated. The reduced stiffness of the element is then combined with the original stiffness of the adjacent element and the process is repeated until the formation of the structure stiffness matrix is complete.

The number of active nodes at a given time is known as the wave-front size. In order to minimize the size of the wave-front, the elements should be properly numbered. ANSYS is provided with a renumbering algorithm which is used in conjunction with the frontal solver. The user is only required to specify a suitable starting node and the renumbering is done automatically. This technique is extremely powerful for long and complicated geometries.

4.5.2 ANSYS Material Model

4.5.2.1 Concrete element

The ANSYS concrete element used in this investigation is an eight-noded solid with three degrees of freedom at each node, as shown in Fig.4.3(a). The element uses a 2·2·2 lattice of integration points together with a Gaussian integration procedure, as shown in Fig.4.3(b). Cracking at the integration point is allowed in three

orthogonal directions. When a crack occurs at an integration point, it is modelled through an adjustment of the material properties. Cracks are thus assumed to be smeared over the element. The solid is also capable of crushing in compression. Whenever the material at an integration point fails in uniaxial, biaxial or triaxial compression, it is assumed to crush at that point. Suidan and Schnobrich (1973) believe that this approach of cracking and crushing at integration points is better than assuming a complete element to crack or crush. Cracking or crushing involves only modifications of the contribution of that particular integration point to the element stiffness, the rest of the element stiffness remaining intact.

The ANSYS concrete element is assumed to be isotropic. It also has an optional rebar capability which may by used to model the reinforcement. Up to three rebar materials can be defined. The rebar is assumed to be smeared throughout the concrete element. Each of the rebars, which has uniaxial stiffness only, is defined by a volume ratio, i.e. the volume it occupies in the solid element, and its orientation defined by two angles measured from the global cartesian system as shown in Fig.4.3(c). The rebar capability was not used in this study, the reinforcing bars being modelled by separate elements.

Beside cracking and crushing, the element is capable of modelling non-linear material properties such as creep, swelling and plastic deformations. The rebars are capable of modelling creep and plastic deformations.

4.5.2.1.1 *Linear Behaviour*

Prior to cracking or yielding, concrete is assumed to be an

isotropic material. The stress-strain relationship for an infinitesimal material element can be written in matrix form as

$$\{\sigma\} = [D_c]\{\varepsilon\} \tag{4-1}$$

where $\{\sigma\}$ is the stress vector and $\{\varepsilon\}$ the strain vector, given by

$$\{\sigma\} = \{\sigma_x, \sigma_y, \sigma_z, \tau_{xy}, \tau_{yz}, \tau_{zx}\}^T \tag{4-2}$$

$$\{\varepsilon\} = \{\varepsilon_x, \varepsilon_y, \varepsilon_z, \gamma_{xy}, \gamma_{yz}, \gamma_{zx}\}^T \tag{4-3}$$

and $[D_c]$ is the elastic material stiffness matrix given by

$$[D_c] = \frac{E_c}{(1-\nu)(1-2\nu)} \begin{bmatrix} 1-\nu & \nu & \nu & 0 & 0 & 0 \\ & 1-\nu & \nu & 0 & 0 & 0 \\ & & 1-\nu & 0 & 0 & 0 \\ & & & \frac{1-2\nu}{2} & 0 & 0 \\ & & \text{symmetric} & & \frac{1-2\nu}{2} & 0 \\ & & & & & \frac{1-2\nu}{2} \end{bmatrix} \tag{4-4}$$

The matrix $[D_c]$ may be modified to allow for the presence of orthotropic reinforcement by introducing the following steel material matrix:

$$[D_s]_i = \begin{bmatrix} E_{si} & 0 & 0 & 0 & 0 & 0 \\ 0 & 0 & 0 & 0 & 0 & 0 \\ 0 & 0 & 0 & 0 & 0 & 0 \\ 0 & 0 & 0 & 0 & 0 & 0 \\ 0 & 0 & 0 & 0 & 0 & 0 \\ 0 & 0 & 0 & 0 & 0 & 0 \end{bmatrix} \tag{4-5}$$

in which E_{si} is the steel modulus of elasticity for reinforcement bar i. The matrix $[D_s]_i$ is defined in the reference coordinate system aligned in the direction of the orientation reinforcement bar *i*. The material behaviour of the reinforcement is transformed into the global coordinate system by the following equation

$$[D_s]_i = [T]^T [D_s]_i [T] \qquad (4\text{-}6)$$

where *[T]* is a transformation matrix relating the local coordinates to the global coordinates defined by Suidan and Schnobrich (1973) as

$$[T]=\begin{bmatrix} a_{11}^2 & a_{12}^2 & a_{13}^2 & a_{11}a_{12} & a_{12}a_{13} & a_{11}a_{13} \\ a_{21}^2 & a_{22}^2 & a_{23}^2 & a_{21}a_{23} & a_{22}a_{23} & a_{21}a_{23} \\ a_{31}^2 & a_{32}^2 & a_{33}^2 & a_{31}a_{32} & a_{32}a_{33} & a_{31}a_{33} \\ 2a_{11}a_{21} & 2a_{12}a_{22} & 2a_{13}a_{23} & a_{11}a_{22}+a_{12}a_{21} & a_{12}a_{23}+a_{13}a_{2} & a_{11}a_{23}+a_{12}a_{22} \\ 2a_{21}a_{31} & 2a_{22}a_{32} & 2a_{23}a_{33} & a_{21}a_{32}+a_{22}a_{31} & a_{22}a_{33}+a_{23}a_{2} & a_{21}a_{33}+a_{13}a_{21} \\ 2a_{11}a_{31} & 2a_{12}a_{32} & 2a_{13}a_{33} & a_{11}a_{32}+a_{12}a_{31} & a_{12}a_{33}+a_{13}a_{2} & a_{11}a_{33}+a_{31}a_{13} \end{bmatrix} \qquad (4\text{-}7)$$

The terms a_{ij} are obtained from the matrix

$$[\,A\,] = \begin{bmatrix} l_1 & l_2 & l_3 \\ m_1 & m_2 & m_3 \\ n_1 & n_2 & n_3 \end{bmatrix} \qquad (4\text{-}8)$$

where the vector $\{l_i\}$ contains the direction cosines between the local reinforcement x-axis and the global coordinate system, while the

vectors $\{m_1\}$ and $\{n_1\}$ are unit vectors mutually orthogonal to the vector $\{l_1\}$.

Combination of Eqs.(4-5), (4-6) and (4-7) yields the following expression :

$$[D_s]_1 = [E_s]_1 \begin{bmatrix} a_{11}^2 \\ a_{12}^2 \\ a_{13}^2 \\ a_{11}\ a_{12} \\ a_{12}\ a_{13} \\ a_{11}\ a_{13} \end{bmatrix} \begin{bmatrix} a_{11}^2 \\ a_{12}^2 \\ a_{13}^2 \\ a_{11}\ a_{12} \\ a_{12}\ a_{13} \\ a_{11}\ a_{13} \end{bmatrix} \tag{4-9}$$

which shows that the only stress component involved is the axial stress in the x-direction.

The global reinforced concrete matrix for the element is then defined by

$$[D] = (1-\sum_{i=1}^{3} v_{ri})[D_c] + \sum_{i=1}^{3} v_{ri}[D_s]_i \tag{4-10}$$

where it can be seen that a volume ratio of zero ($v_r = 0$) would eliminate completely the rebar capability.

4.5.2.1.2 *Nonlinear Behaviour*

The idealized stress-strain relationship of concrete under uniaxial compression is shown in Fig.4.1 in which concrete is considered to be an elastic-plastic material. Crushing of concrete is assumed to occur when the compressive strain at any integration point exceeds the limiting crushing strain, at which point concrete loses all its strength. In the present model, concrete in tension is

modelled as a linear elastic-brittle material and the maximum tensile stress criterion is employed to distinguish elastic behaviour from brittle fracture.

The behaviour of concrete under multiaxial stress conditions is described by the 3-D failure surface of William and Warnke (1975) shown in Fig.4.4, in which; (r_1, r_2) are functions representing the failure surface, and (η) is the angle of similarity of principal stresses. If a point representing the concrete stress state is inside the envelope, then the material is considered to be elastic, otherwise failure of the material is assumed. The failure surface is expressed individually for regions of triaxial compression, uniaxial tension-biaxial compression, biaxial tension-uniaxial compression and triaxial tension.

In the triaxial compression regime (σ_1, σ_2, $\sigma_3 < 0$), concrete stressed beyond the elastic limit is assumed to yield and a plasticity formulation is used to establish the plastic stress-strain relationship. The ANSYS program provides plasticity formulation options based on Von Mises yield criterion or its variants together with associative or non-associative flow rules. After a certain degree of plastic flow, concrete reaches its ultimate strain and crushes.

Under triaxial tension (σ_1, σ_2, $\sigma_3 > 0$), concrete is assumed to crack in a direction normal to the maximum principal stress direction once this stress exceeds the tensile strength of concrete. Cracking of concrete occurs also under biaxial tension - uniaxial compression regime or uniaxial tension - biaxial compression regime. For such cases the cracks develop in a direction normal to the direction of the

principal tensile stress. However cracking takes place at much lower values of tensile stress.

4.5.2.1.3 *Cracked Concrete*

Before any crack forms, concrete is assumed to be isotropic and the concrete material matrix is independent of the orientation of the coordinate system. Therefore the uncracked material matrix $[D_c]$ is applicable in the principal stress coordinate system. Once the maximum principal tension stress exceeds the tensile capacity of the concrete, a crack will form in a plane normal to the principal stress direction. The stress-strain relationship defined in the coordinate system parallel to the principal stress directions with the X-axis perpendicular to the crack face are given by

$$[D_c'] = \frac{E_c}{(1+\nu)(1-2\nu)} \begin{bmatrix} 0 & 0 & 0 & 0 & 0 & 0 \\ & \frac{1-2\nu}{1-\nu} & \frac{\nu(1-2\nu)}{1-\nu} & 0 & 0 & 0 \\ & & \frac{1-2\nu}{1-\nu} & 0 & 0 & 0 \\ & \text{symmetric} & & \beta_t\frac{1-2\nu}{2} & 0 & 0 \\ & & & & \frac{1-2\nu}{2} & 0 \\ & & & & & \beta_t\frac{1-2\nu}{2} \end{bmatrix} \quad (4\text{-}11)$$

where β_t is a reduction factor for open cracks representing the remaining shear stiffness in the cracked plane due to aggregate interlock and dowel action.

If the crack strain across the crack becomes compressive, the crack closes and all the compressive stresses normal to the crack plane are transmitted across the crack. However, a plane of weakness along the closed crack of the compressive concrete exists and only a

small shear resistance remains. This reduction in shear strength is accounted for by the factor β_c which is for closed cracks. The cracked concrete matrix becomes:

$$[D_c'] = \frac{E_c}{(1+\nu)(1-2\nu)} \begin{bmatrix} 1-\nu & \nu & \nu & 0 & 0 & 0 \\ & 1-\nu & \nu & 0 & 0 & 0 \\ & & 1-\nu & 0 & 0 & 0 \\ & & & \beta_c\frac{1-2\nu}{2} & 0 & 0 \\ & & & & \frac{1-2\nu}{2} & 0 \\ & & & & & \beta_c\frac{1-2\nu}{2} \end{bmatrix} \quad (4\text{-}12)$$

The cracked concrete matrix $[D_c']$ is then transformed back to the global coordinate system by a transformation similar to the one given by Eq.(4-6). The open or closed status of an integration point is based on a so-called "crack strain" given by

$$\varepsilon^{ck} = \varepsilon_x^{ck} + \frac{\nu}{1-\nu}(\varepsilon_y^{ck} + \varepsilon_z^{ck}) \quad (4\text{-}13)$$

The terms $\varepsilon_x^{ck}, \varepsilon_y^{ck}$ and ε_z^{ck} are the normal component strains in any particular crack orientation. If ε^{ck} is negative, the associated crack is assumed to be closed; if ε^{ck} is positive, the associated crack is open.

4.5.2.1.4 *Crushed Concrete*

Concrete can still resist some compressive stress when subjected to a compressive strain after reaching a limiting strain, ε_{cu}. In most finite element analyses, when the strain in an element reaches the crushing surface, that element is assumed to lose all its stress

bearing capacity and stiffness. In the present model, if the material at an integration point fails in uniaxial, biaxial or triaxial compression, the material is assumed to crush at that particular point. The remainder of the element stiffness remains intact. Concrete is assumed to lose all its integrity only when the number of integration points exceeds a predetermined level per element.

4.5.2.1.5 *Shear Retention*

Concrete cracks are capable of transmitting shear forces because of their rough surface. These forces, which have a frictional nature, will induce normal stresses which tend to stiffen the cracked concrete. In order to take the shear stiffness into account, a reduced shear is retained in the stress-strain matrix, as illustrated in Eqs.(4-11) and (4-12), through a reduced shear coefficient β. This is equivalent to introducing a number of springs parallel to the crack to represent the effect of aggregate interlock and, to some extent, dowel action. It has been demonstrated that, in most cases, when shear is not dominant, the numerical solution is not very sensitive to the non-zero value of β adopted. A value of *0.5* has often been used for β [eg Suidan and Schnobrich (1973); Grayson and Stevens (1979)] and is used in this analysis.

4.5.3.1 **Reinforcement Element**

The steel reinforcement (rebar) is assumed to be perfectly bonded to the surrounding concrete.

In this present analytical study, the rebar capability of the concrete element was not used. The reinforcing steel bars (longitudinal and transverse) have been modelled as separate spar

elements. The 3-D spar element is an uniaxial tension-compression element with three degrees of freedom at each node namely translations in the x,y and z directions, as illustrated in Fig.4.5. No bending of the element is considered. Plasticity and stress stiffening capabilities are included. The linear and non-linear behaviour of these elements is exactly the same as for the concrete rebar elements.

The reinforcing bars, as described previously, are capable of plasticity. In the present model, since steel reinforcement is assumed to have uniaxial properties in the direction of the bar, an elasto-plastic model was adopted. More information can be found in the theoretical manual of ANSYS, description of element STIF8 [Denn (1969)].

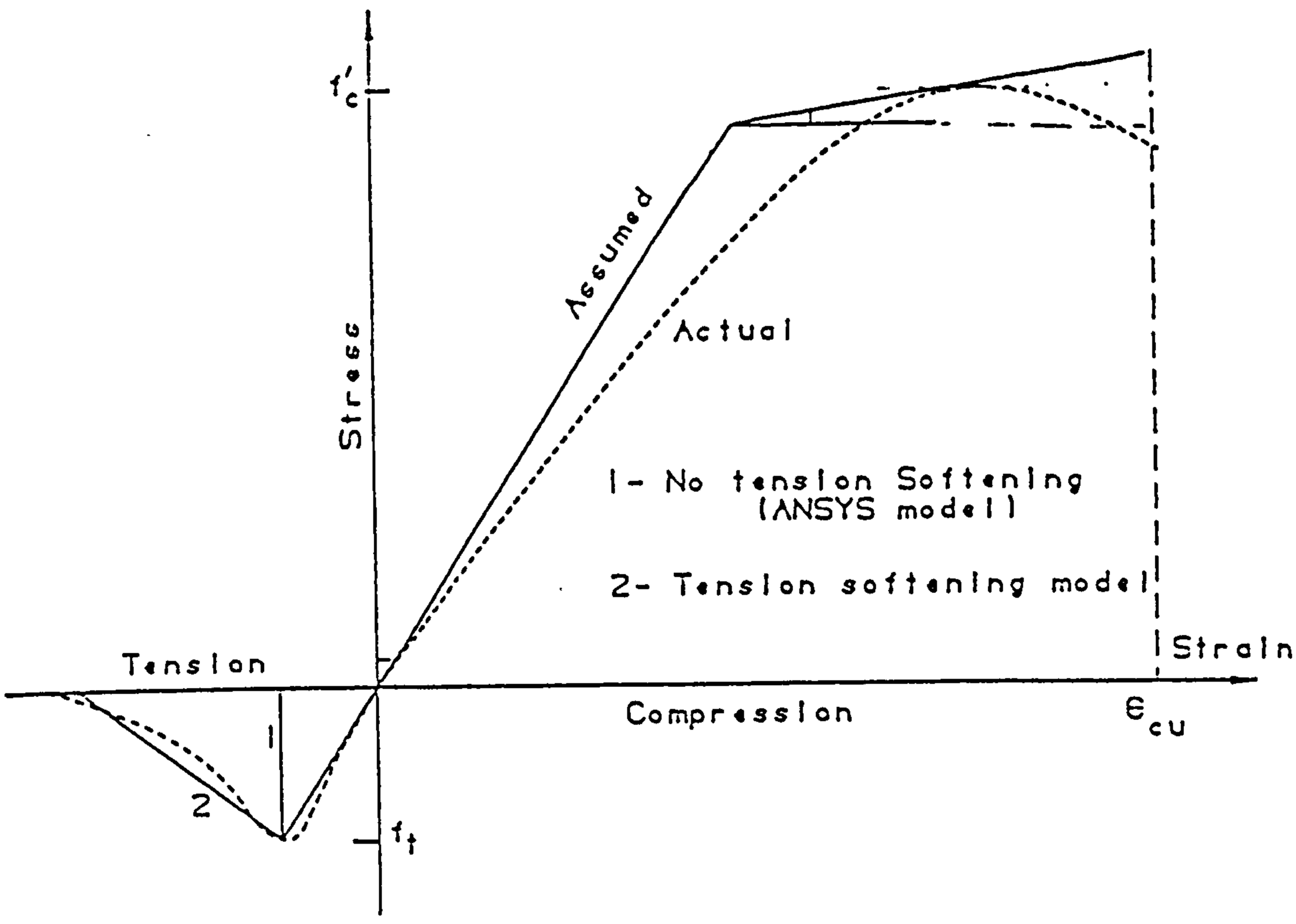

FIG. 4.1 IDEALISED STRESS-STRAIN CURVE FOR CONCRETE

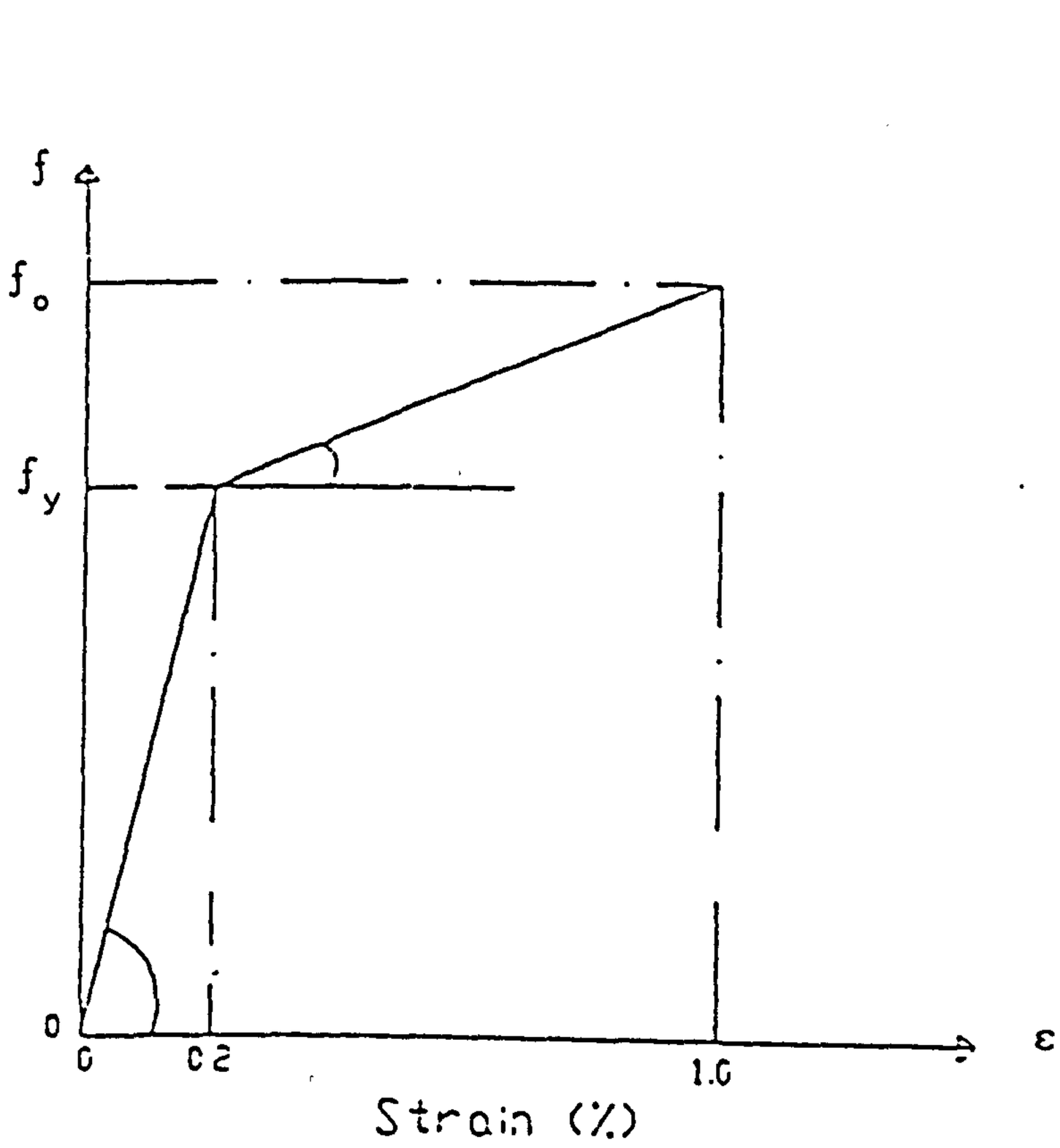

FIG.4.2 STRESS-STRAIN CURVE FOR STEEL

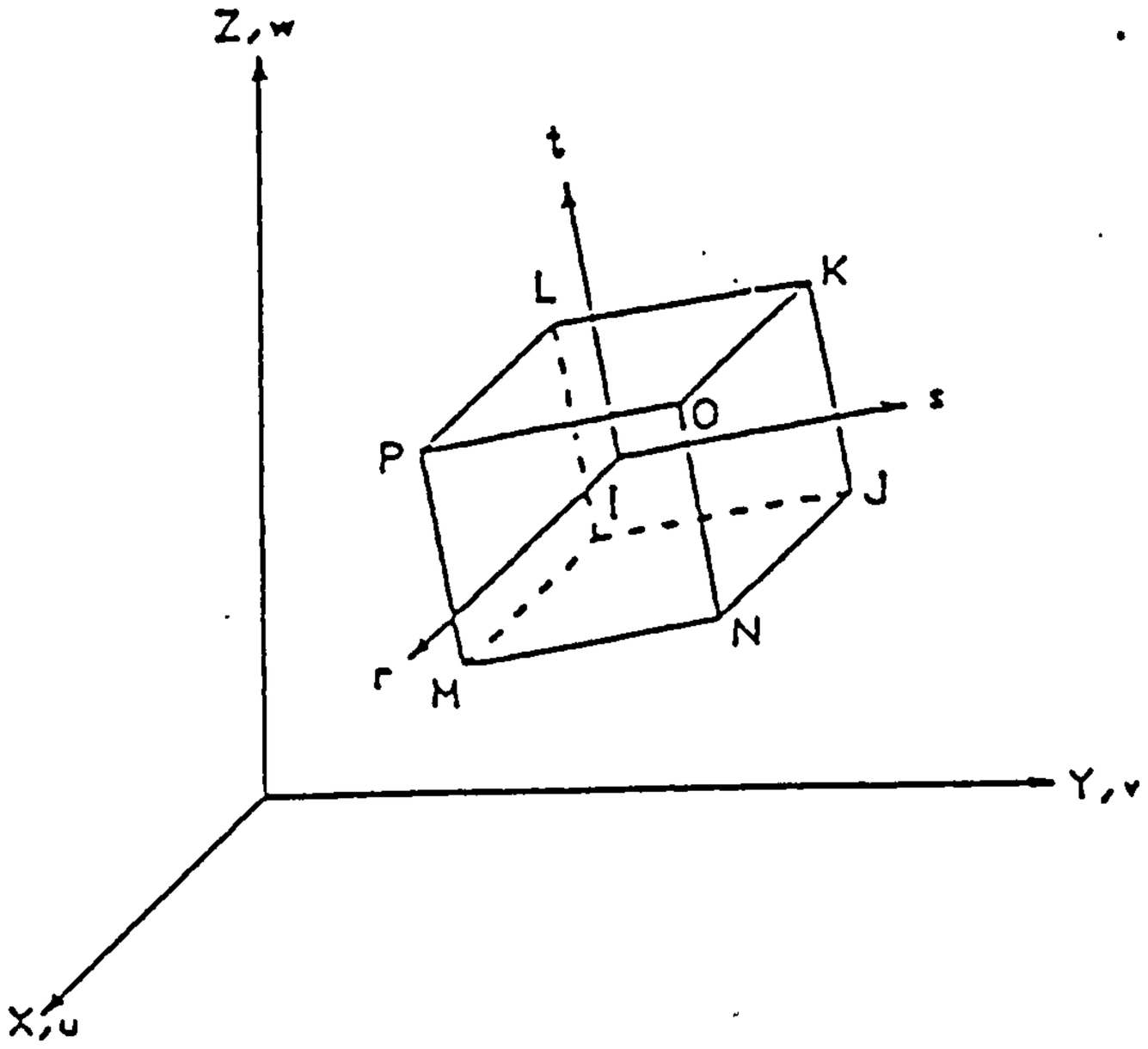

a) 3-D Reinforced Concrete Solid

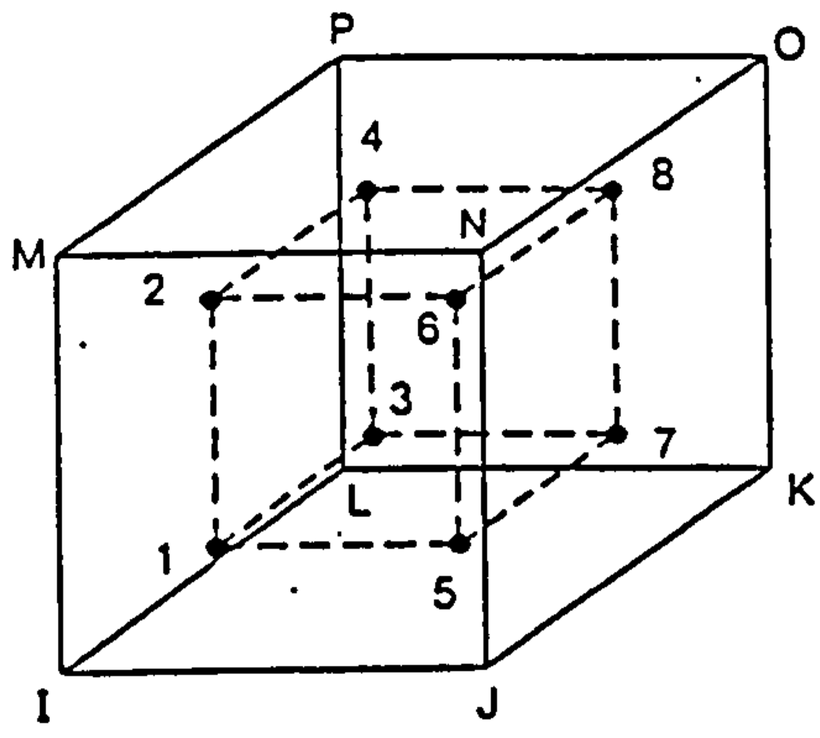

b) Integration point schemes

FIG.4.3 3-D REINFORCED CONCRETE SOLID ELEMENT

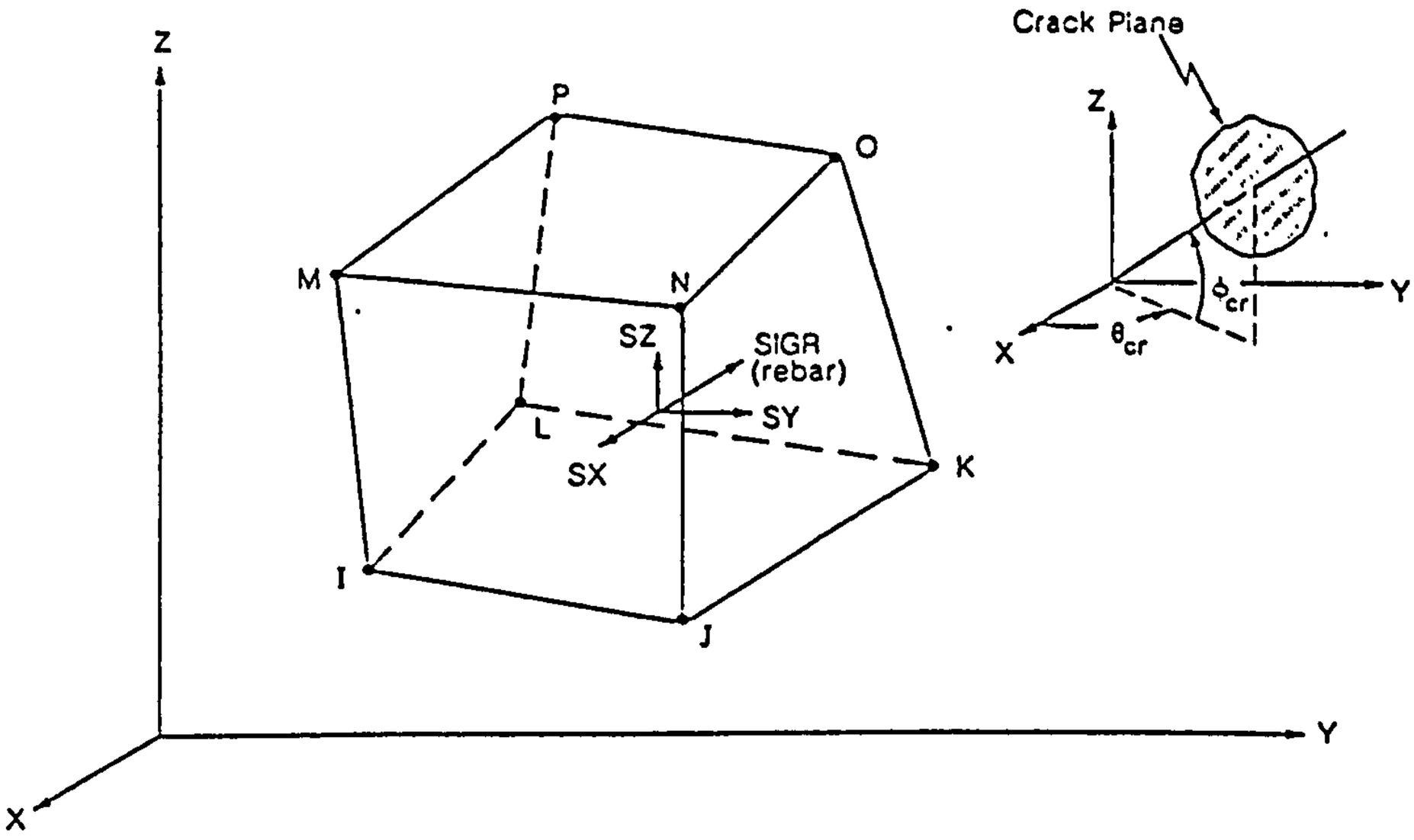

c) 3-D Reinforced Concrete Solid Output

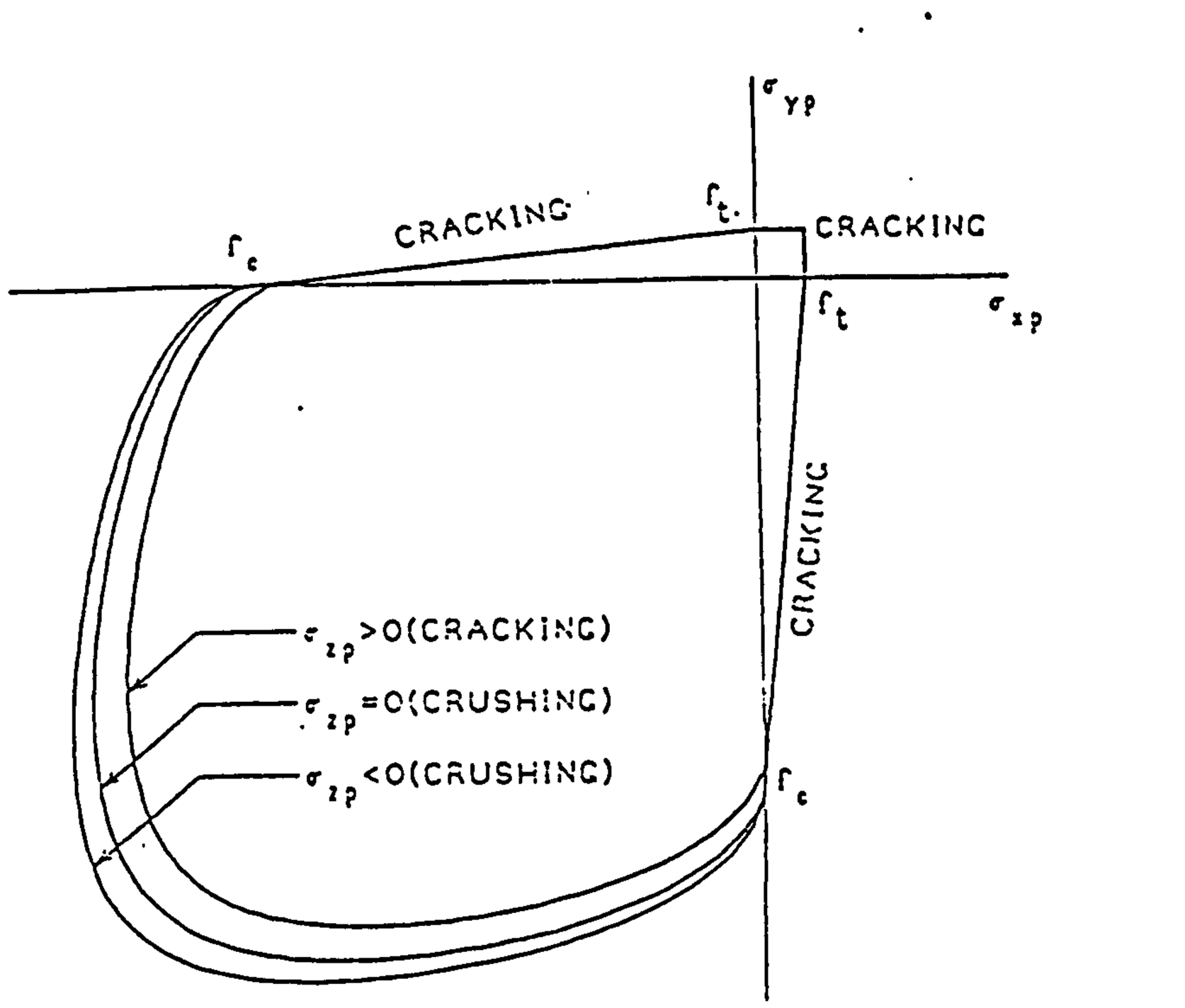

a)

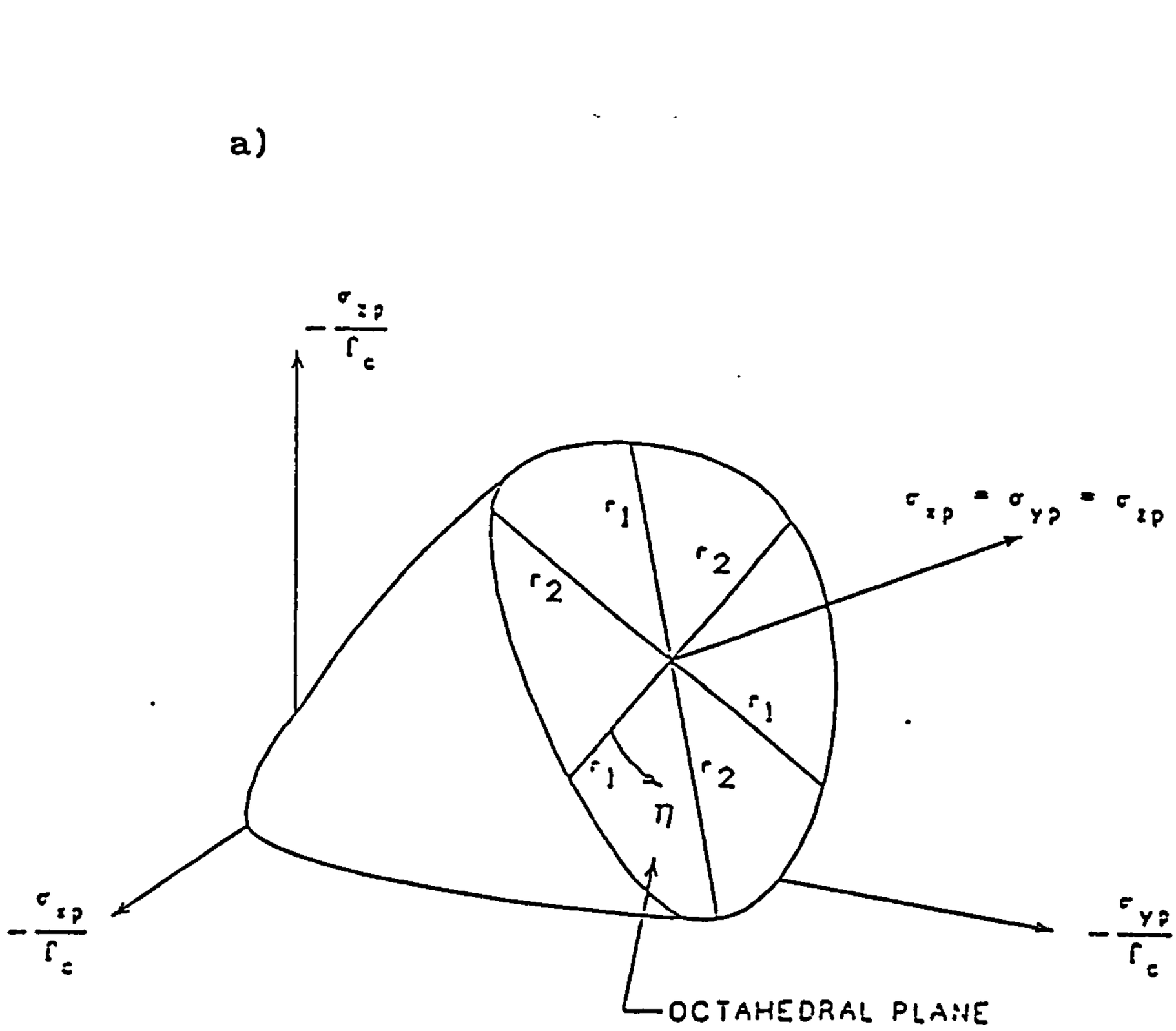

b)

FIG.4.4 3-D FAILURE SURFACE OF WILLIAM AND WARNKE

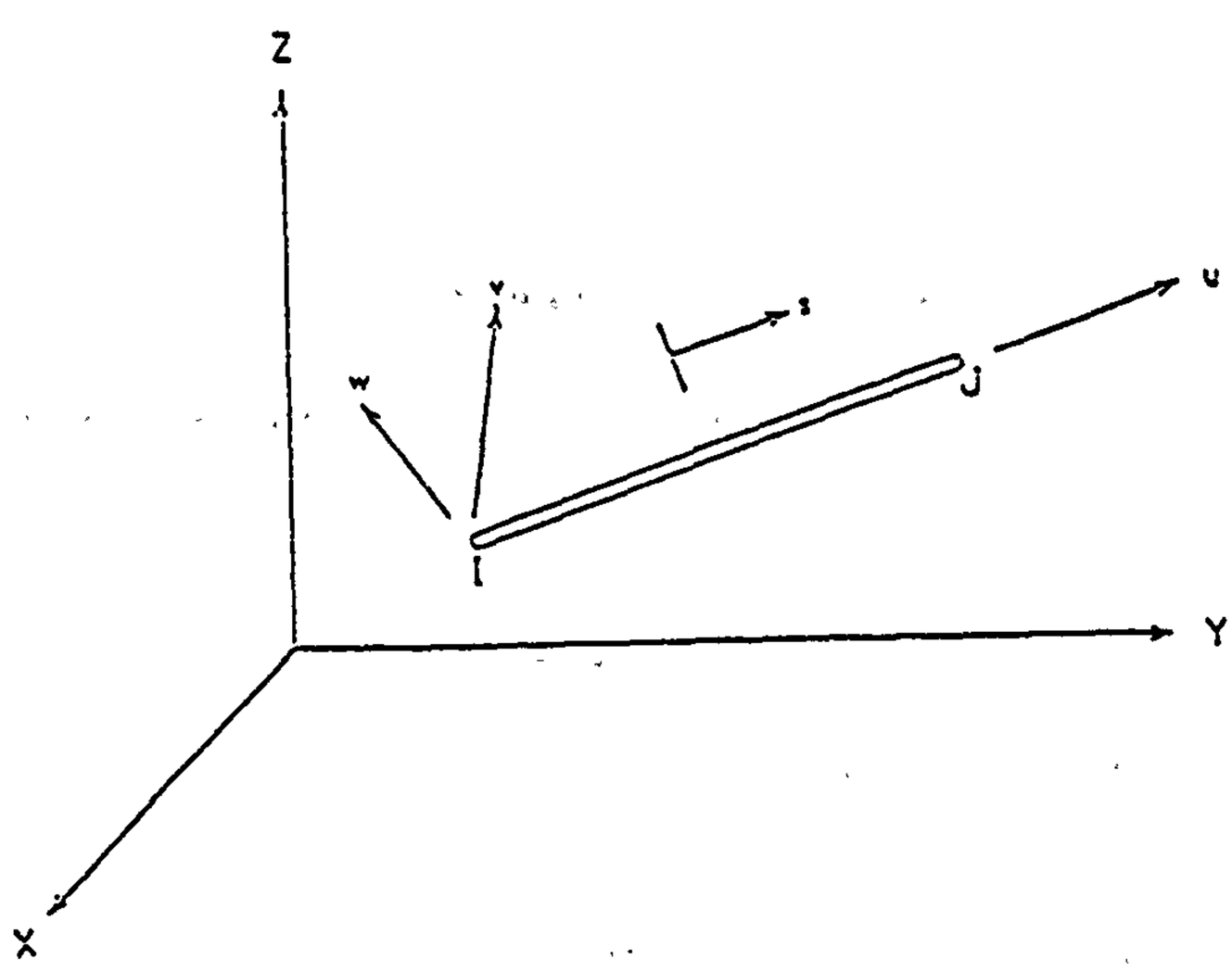

a) Three-dimentional Spar

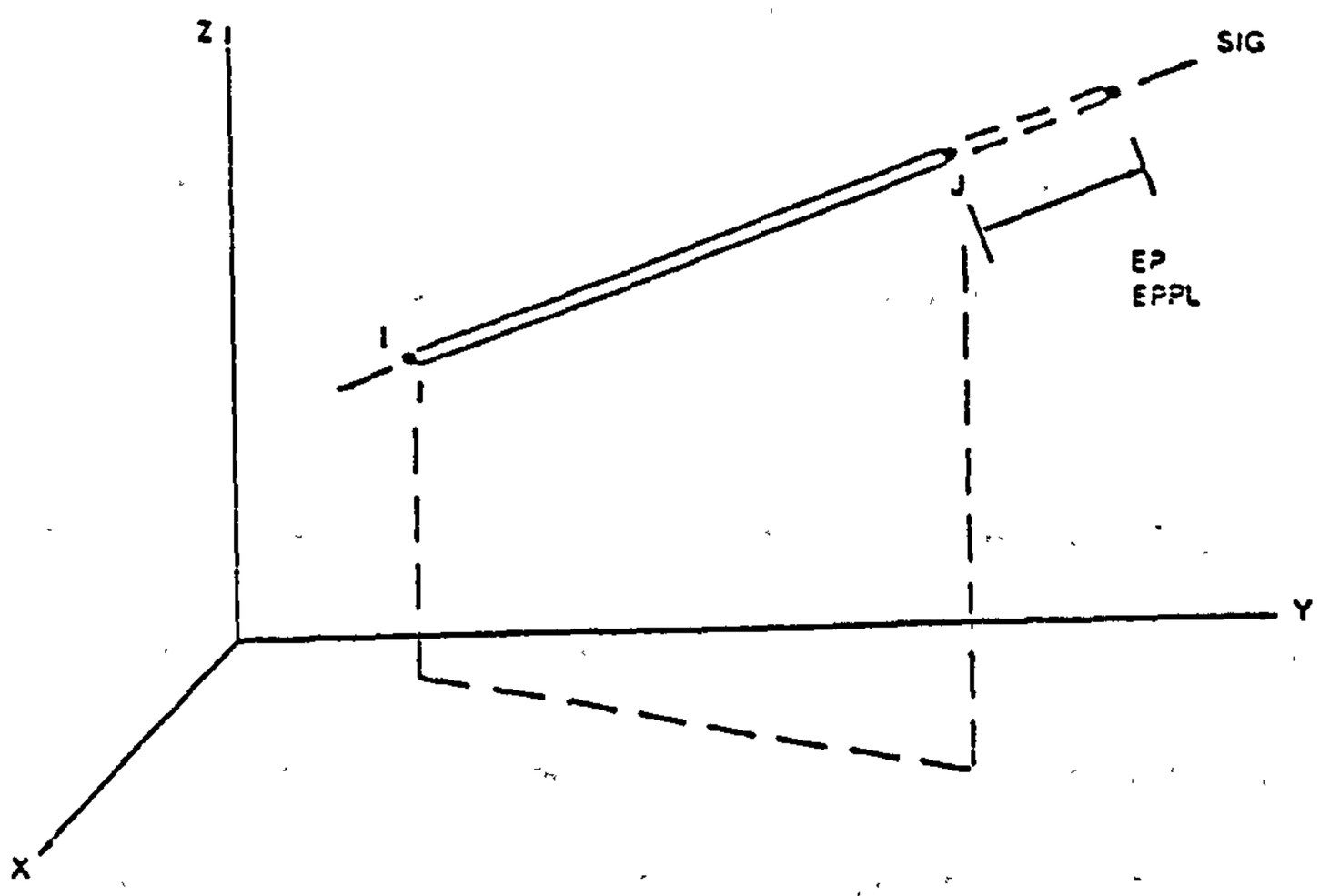

b) Three-dimentional Spar output

FIG.4.5 3-D SPAR ELEMENT

CHAPTER FIVE ANALYTICAL STUDY BY NON-LINEAR FINITE ELEMENT MODEL - COMPARISON OF EXPERIMENTAL AND ANALYTICAL RESULTS -

5.1 INTRODUCTION

5.1.2 Objectives

The objectives of the non-linear finite element study of reinforced concrete beam-column joints were as follows:

i) To investigate the effectiveness of numerical modelling of beam-column joints subjected to cyclic loading up to failure.

ii) To identify characteristics of structural performance that were not measured in the experimental study, such as stress and (or) strain profile along reinforcing steel (main bars and stirrups), stress distribution in concrete, etc.

iii) To use the numerical model to study the behaviour of joints whose design parameters were not included in the study.

As outlined in Chapter one, there have been a number of non-linear finite element studies of reinforced concrete elements before. These have included studies of beams or columns [Panahshahi et al.(1992)], corner joints [Grootenboer (1981), Van Mier (1987) and Hemmaty et al. (1992)], etc. However, in all cases these have been under static load increasing monotonically up to failure. Studies of cyclic loading have only been applied to single finite elements.

In the experimental tests attention was focussed on overall cyclic hysteresis behaviour and on strain behaviour of certain bars at

critical locations. With the use of a verified numerical model it should be possible to study factors such as the distribution of strain along certain bars, the distribution of stress in the concrete, the internal forces acting in the reinforcement, and the exact location of yielding in the reinforcing bars, etc.

In this respect, four analyses were carried out initially and these were direct simulations of the four specimens tested experimentally. The analysis of one of these (specimen UD2) is presented in full detail in order to achieve objective (i). Next, data is presented showing features of the behaviour of the joints which were not measured in the tests as mentioned above. Finally, the analytical model can then also be employed to study the behaviour of joints with different design parameters from those adopted in the tests, e.g. flexural strength ratio of column to beam, axial load, transverse reinforcement, strain profile along U-stirrups, etc.

Taking advantage of available computer finite element analysis, the performance of a reinforced concrete joint can be evaluated up to failure and non-linearity caused by materials (steel and concrete), geometry and cracking can be taken into account.

The non-linear finite element program which is employed in this study is ANSYS 4.4, a general purpose finite element computer program, available at Bristol University on a network system IBM 3090 mainframe.

5.1.3 Modelling with ANSYS

In a numerical analysis based on finite elements, a structure is divided into a large number of "elements", which are interconnected by nodes. The nodes are generally situated in the corners, but also may appear along the edges. Loads and supports are specified, and for the system a set of equilibrium and compatibility equations is set up, which can be solved numerically. Several numerical solution techniques are available in ANSYS.

Results are given at so-called integration points, which do not coincide with the nodes. The element is an eight-noded quadratic iso-parametric element with nine-points (Gaussian) numerical integration.

Material properties are defined for these "concrete" elements, and in contrast to a linear analysis, where only the Young's modulus E and the Poisson's ratio ν have to be specified, a non-linear analysis will require knowledge of several more parameters. These parameters and the related material models are presented and discussed in section 5.2.

Reinforcement is modelled as spar elements and the stiffness of the reinforcement is simply added to the stiffness of the elements in which the bar is "embedded", as it has been seen in chapter four.

The elements which have been used in this study to model the beam-column sub-assembly are as follows:

- A 3-D eight noded solid reinforced concrete element for

modelling the concrete without reinforcement.

- A 3-D spar, is used for modelling both longitudinal and transverse reinforcement.

Concrete is modelled using STIF65 solid element available in the ANSYS program [Denn (1969)]. The most important feature of this element is its capability of treating non-linearity. The concrete can undergo cracking, crushing and plastic deformation. A shear retention factor ($0 \leq \beta \leq 1$) can be used to take into account the aggregate interlock contribution to the shear-flexural capacity of the element, the value 0.0 representing a smooth crack (that is to say a complete loss of shear transfer) and 1.0 no loss of shear transfer (rough crack).

More information about this element can be found in the theoretical manual of ANSYS, description of element STIF65 [Ahmad et al (1970), Bathe (1982), and Biot (1965)].

The reinforcing steel bars have been modeled as separate spar elements. The 3-D spar element is a uniaxial tension-compression element with three degrees of freedom at each node: translations in the nodal x, y, and z directions. No bending of the element is considered, as in a pin-jointed structure. Plasticity, creep, swelling, and stress stiffening capabilities are included. More information about this element can be found in the ANSYS theoretical manual, description of element STIF8 [Ahmad et al.(1970)].

5.1.4 Presentation of Results

5.1.4.1 Graphical representation

The graphical facilities of ANSYS are used. In general, load-displacement, load-strain diagrams, strain distribution in the reinforcement especially in the stirrups in the joint region, and the crack patterns are shown and compared with the experimental results. As mentioned before, strains, stresses, cracks, etc. are represented at the integration points.

When stresses are shown, the tensile stresses are positive, whereas the negative sign refers to compression stresses. Cracks are shown in different colours depending on their directions and intensity (i.e. open, closed, cracked and crushed), see Table 5.1 section 5.3.2. Plasticity in the reinforcing steel elements when plotted, is displayed by means of colour plots, each colour showing the state of plastic stress and strain level reached by a particular element. It is worth noting that the intensity of stress and (or) strain and the cracking state is displayed in multitude of colour; ranging from the blue colour which is the lowest value to the red colour which is the highest value.

In order to have clear insight of the effectiveness of the modelling, an experimental and analytical comparative study is presented here. The results obtained analytically are discussed and compared with the experiments later on in this chapter. Because of the huge data obtained from this analysis, only the results of specimen UD2 are discussed in full detail.

The presentation of these results is as follows:

a) Load-displacement curves of specimens EX2 and UD2 are presented, special attention being paid to the hysteresis cycle of specimen UD2.

b) Plots of the strain variations along beam and column main bars, as well as in stirrups are shown. The load vs. strain curves of certain reinforcing bars in some locations (which coincide with strain gauge locations in experiment) are plotted.

c) As an indication of the behaviour of the specimens in the linear and non-linear stage, the analytical crack patterns are shown and compared with the experimental.

d) Finally, all specimens are compared together in terms of hysteresis loops, cracking patterns, and strain profiles. In addition, the strength of these specimens will be looked at it in term of loss of stiffness (or strength degradation) during loading cycles.

5.2 ANALYSIS OF SPECIMEN UD2

5.2.1 Design of Specimen

For a realistic analysis of the joint, a three dimensional model would be required. The behaviour of the connection is described in three dimensions. The element mesh, reinforcement, loading and supports are shown in Figs.5.1(a) and 5.1(b). The mesh is refined where stress concentrations are expected, i.e. in the connection area. Perfect bond is assumed between the reinforcement and the concrete. The radius of the curved reinforcing beam bars (anchorage) in the

joint area was not taken into account because of the difficulties of modelling such curved elements. This may have considerable influence on the behaviour of the joint, as it has been seen in experiments (i.e. pull-out of the beam main reinforcement from the joint region).

5.2.1.1 Material properties

5.2.1.1.1 *Plasticity*

Several different types of behaviour are available in 'ANSYS' and any one may be selected. In this study, the Classical Bilinear Kinematic Hardening has been adopted because it is recommended for general use. In this option, non-linear materials are described by a single table per material. The table is defined as a series of real numbers such as stress-strain curves, creep, swelling, etc.

The above option assumes the total stress range is equal to twice the yield stress, so that the Bauschinger effect is included, as shown in Fig.5.2(a). The material behaviour is described by a bi-linear stress-strain curve starting at the origin. The initial slope of the curve is taken as the elastic modulus of the material. At the specified yield stress, the curve continues along the second slope defined by the tangent modulus (E_T), as shown in Fig.5.2(b).

5.2.1.1.2 *Concrete*

The material model (elastic-plastic) is used to define both the linear and non-linear material property data. The stress-strain curve for concrete used in this analysis is shown in Fig.5.3(a).

In the linear stage, the input parameters required by the analysis for concrete element are the elastic modulus E_c and the Poisson's

ratio ν (ν = 0.15). The Young's modulus for all specimens varied between 24000 and 36000 N/mm^2. For more detail, see chapter two.

The non-linear material input required by a non-linear analysis of this type is listed below. For a better understanding of parameter values chosen for plasticity, more information is available in ANSYS theoretical manual.

i) Young's modulus of concrete E_c.

ii) shear transfer coefficients β (for open crack) = 0.01. This (small) value is universally used [Ottosen (1980) and Hemmaty et al. (1992)] in the case of structures loaded close to collapse, where large crack widths can be expected.

iii) shear transfer coefficients β (for closed crack) = 0.5 (medium value).

iv) ultimate uniaxial tensile (cracking) stress = f_{cu}.

v) ultimate uniaxial compressive (crushing) stress = f_c'

vi) tangent modulus E_T taken as one-tenth (1/10) of Young's modulus E_c after yielding.

5.2.1.1.3 *Steel*

The elastic-plastic model for steel is the same as for concrete (Fig.5.2(b)). The material linear input consists of Young's modulus (E_s) and poisson's ratio ν (0.3).The stress-strain curve for steel used in the analysis can be seen in Fig.5.3(b).

In the case of non-linearity, the input parameters are as follows:

i) Young's modulus of steel E_s.

ii) yield stress f_y.

iii) tangent modulus $E_T=(1/10)\cdot E_s$ after yielding.

5.2.1.2 Loading sequence

To establish the entire deformational response of the beam-column sub-assembly up to collapse load, an incremental procedure was employed, as shown in Fig.5.4. In the general non-linear analysis of reinforced concrete structures a number of load increments must be used as these structures are path dependent.

Since both cracking and crushing together with plasticity were modelled, the load increments had to be chosen to be sufficiently small to prevent spurious cracking or crushing before a convergent solution in the plastic stage. Unfortunately, this task is very difficult to achieve, indeed almost impossible for a good simulation of experiment. In addition, it is time consuming. Therefore, the size of the load increments employed in the present analysis were kept similar to those in the experiment. In this present analysis, the specimen UD2 was subjected to load control. The load increment used was about 7 kN. ANSYS cannot perform a cyclic loading analysis, but nevertheless possesses a restart facility which is difficult to use and time consuming. The restart option consists of breaking the analysis into manageable parts.

A typical input data listing for the analysis of a beam-column

sub-assembly used in this study is presented in Appendix B.

5.2.2 Load-Displacement Response

An indication of the behaviour of the sub-assembly is obtained from the load-displacement plot. The predicted and experimental load vs. displacement relationships of specimen UD2 are presented in Figs.5.5(a) and 5.5(b).

During the second cycle the theory predicted cracking and consequently considerable displacement and hysteresis. This pattern is repeated in the third and fourth cycles with increasing displacement.

However, in the experiment there was little displacement in the first three cycles. Significant cracking was not evident until the fourth cycle with cracks developing and displacement increasing in the fifth and sixth cycles.

In the theoretical model complete failure occurs in the fifth cycle due to crushing and cracking in certain concrete elements. The numerical solution becomes unstable as soon as the number of crushed integration points exceeds a certain limit, and computation is forced to cease.

Although the area of the hysteresis loops are considerably different in the theory when compared with the experiment, there are certain features that are modelled reasonably well. These include the stiffness softening, as well as the qualitative prediction of stress softening development.

5.2.3 Beam Strains Profile

The strain (plastic) distribution in the reinforcing steel cage (longitudinal and transversal) at a load level of 35 kN is shown in Figs.5.6(a) and 5.6(b).

As can be seen in Fig.5.6(a), the beam bar on the tension side at the end of the beam reached a value of strain about 26996 μs (red colour). The other bar On the compression side did yield at the same location (dark blue colour) reaching a compression strain of -7824 μs. It is worth noting that the plastic length in the bar under tension is more noticeable (as indicated by the green, yellow and red colour) than in the compressed bar.

The beam stirrups did not show any sign of yielding as was expected, and reached a strain value of 1028 μs near the junction, as shown in Fig.5.6(b).

This behaviour of the beam reinforcement in the linear stage is in good agreement with experiments. In the non-linear stage, the level of strains in the reinforcing steel recorded analytically (about 27000 μs) was not possible experimentally because of the limitation of the equipment used in laboratory (the maximum recording by amplifiers was about equivalent to 4600 μs).

The load versus strain history for some critical locations in the beam main reinforcement were recorded throughout the analysis. Figures 5.7(a) to 5.7(d) show the gauges locations and strain variations during loading according to the analysis. For a consistent comparison,

the strains were recorded at some locations analytically and experimentally and the behaviour of these gauges will be discussed later in this section.

It will be noted that larger strain variations occurred in the beam bars well away from the column junction (S13, S15), than within the joint core region (S14, S16).

The strain distributions along main beam bars on both tension and compression sides including the anchorage zone at different levels of loading 21 kN, 28 kN, 31.5 kN, 35 kN and -21 kN, are plotted in Figs.5.8(a) to 5.8(j). Tensile strains are plotted on the outside of the bars, compressive strains on the inside; peak tensile and compressive strains, beam load and its direction (forward or backward) are indicated for each load case.(This presentation of the strains variations will also be used in Fig.5.24). Note that there is a full load cycle between each diagram, since the maximum load at successive cycles is shown (except for the last step of one-half cycle).

First, loading the beam (forward) brought the whole beam bar (tension side) into tension, and the tensile strains then steadily increased with each load increment, as well as the crack width. At a load of 35 kN, (it is assumed that concrete has already crushed at the end of the beam) the bar reached the value of 2300 μs, which is beyond the yielding point (2100 μs), as shown in Fig.5.8(g). At the earlier stage of loading, a significant proportion of the anchorage leg was in compression. Tension then steadily progressed down the leg with each further load increment until, when the cracks became more apparent, the whole leg was tensile.

The beam bar on the compression side followed the same pattern as the bar on the 'tension side', but in compression. The compressive strains are expected to increase with increasing the load level (as in the case of tensile strains). After three successive load levels (28 kN, 31.5 kN and 35 kN), it was observed that the compressive strains remained the same (-1000 μs). Therefore, it was concluded that slippage (pull-out) of the beam bars had taken place. This phenomenon was also observed in other bars on the 'tension side', but to a less degree; probably just a local slippage. In the anchorage zone, the whole straight leg was already in tension after the first crack appeared in the column at about a load level of 28 kN.

Loading in the other direction, the beam tension side became compression side and vice versa, as shown in Figs.5.8(i) and 5.8(j). The behaviour of these bars confirmed what has been said earlier above, and showed the vicinity where the concentration of strains is likely to be. Once again, the strains in the anchorage legs at this stage of loading, are nearly half in compression and half in tension. With further loading, the number and the size of cracks increase in the joint region, and consequently the compressive strains area in the anchorage legs become more and more tensile until the whole legs are under tension, which means the concrete in that region has crushed and the joint area is deteriorating. For the sake of comparison, and as a confirmation to what have been mentioned above, load vs. strains recorded analytically and experimentally from three gauges (S16, S15 and S13) attached to the beam bars are shown in Figs.5.9 and 5.10 respectively.

The beam transverse reinforcement did not experience any yielding and stayed in linear stage throughout the analysis which is a good reflection and agreement with experiment. The analytical and experimental load versus strain history of gauges S2 and S3 in the beam's stirrups are shown in Figs.5.11(a) to 5.11(d).

5.2.4 Column Behaviour

The strains profile curves measured along inner and outer column main bars of specimen UD2 at load levels of 10.5 kN, 21 kN, 24.5 kN and 35 kN are plotted in Figs.5.12(a) to 5.12(h).

From these plots, one can see that the stress concentrations in the column main reinforcement were more pronounced within the connection area than outside.

In the joint area, the results obtained are being typical of specimen with low axial load, because bars in high column load are expected to remain in compression throughout the test, though the shape of the strain distributions may change in response to beam loading.

In this specimen UD2, where the axial load is low (about 5% of the ultimate column load), tensile strains occurred, with flexural cracks being observed especially above the connection. These bars alternated between tension and compression depending upon the direction of the load. It is interesting to note that, in the earlier stage of loading, and before any cracks were detected in the joint region, column outer bars in compression were on the tensile side of the beam main bars, as shown in Figs.5.12(a). After cracking occurred in the connection area,

the same column bars (adjacent to the beam bars in tension) went gradually into tension (see Fig.5.12(c)). In the subsequent cycles, and with further propagation of cracks, the tensile strain in these outer bars continued to increase reaching a strain value of about 1600 μs at the end of analysis (Fig.5.12(e) and 5.12(g)). On the other hand, the inner column bars situated beneath the beam compression side were in compression at the beginning of loading (Fig.5.12(b)). With the increase of load levels, the compressive strain increased in these bars (Fig.5.12(d)). With further cycles, the inner bars became more and more tensile reaching a strain value of 2200 μs, as shown in Fig.5.12(f) and 5.12(h).

Outside the joint region, the column bars remained almost unstressed throughout the analysis, as can bee seen in Figs.5.12.

5.2.5 Joint Behaviour

In this specimen, as described in chapter two, the transverse reinforcement in the joint region consisted of U-stirrups linked together forming conventional stirrups.

An analytical presentation of detail of the U-stirrups is shown in Figure 5.13. In the same Figure, strain distributions and the internal forces (red arrows) acting on the U-stirrups legs in the joint region can be seen. It is interesting to note that, the sides of stirrups formed by one leg are more stressed (size of arrows for internal forces, and yellow and red colour for strains) than those formed by two legs. Therefore, the use of this type of stirrups in a well detailed manner could improve the confinement of the joint core.

The variation in strain in the column stirrups is shown in Fig.5.14(a) to 5.14(d). The locations of points at which the strains are recorded are shown in Fig.5.14(e). In this way the relative behaviour of the stirrups distributed along the column may be illustrated. The variations are shown for stirrup legs on the inner column face (adjacent to beam), and the outer column face. As it was expected, the amount of strain outside the joint region is negligible compared with the amount of strain within the joint region. This is evident because of high forces acting in that zone coming from the connecting members, especially the beam.

At an earlier stage of loading, the strains of the top legs of stirrups in the joint region, adjacent to the beam bars in tension, were tensile. These strains decreased reaching zero value at the middle of the beam, and continue to decrease until becoming compressive strains near the other side of the beam, as shown in Fig.5.14(a). The strains in bottom side were very low and increased (following direction of loading) reaching a tensile strain value of 100 μs near the compressed beam side, and then dropped to the vicinity of zero.

In the subsequent cycles and at a load level of 35 kN (loading forward), the strains profile followed the same path as above, but with higher values of tensile and compressive strains, 1600 μs for stirrups legs (top) on the tension side of the beam and 1700 μs for those (bottom legs) on the compression side, see Fig.5.14(c).

Another representation of strain envelope is given in Fig.5.14(f). This increase in strains is due the increase of joint shear stress

which is directly proportional to the beam tip load, and also because of propagation of cracks in the joint region and the irreversible state of the concrete (crushing) at this late stage of loading. Loading backward, a mirror image of Fig.5.14(a) is produced, as can be seen in Fig.5.14(b). These two Figures represent strain envelopes at the same locations and load levels. Loading in this direction, the strain distributions would have the same envelopes as in the case of loading forward, but inverted.

In the stirrups legs parallel to the beam main reinforcement (on both sides; left and right), the strain variations are shown in Fig.5.14(d). These legs on both sides yielded in tension. On the other hand, the compressive strains are still very low, indeed negligible, in the same region. This means that concrete at these two locations has already cracked, but there was no crushing yet and concrete can take further compressive forces.

5.2.6 Cracking Behaviour

In the ANSYS concrete element STIF65, cracking is permitted in three orthogonal directions at each integration point, as shown in Fig.5.15(a). If cracking occurs at an integration point the cracking is modelled through an adjustment of material properties which effectively treat the cracking as a "smeared band" of cracks, rather than discrete cracks. For a 3-D reinforced concrete element, the crack directions (1, 2 and 3) are parallel to the global Cartesian coordinate system (X, Y and Z) respectively. The crack directions and plane are illustrated in Fig.5.15(b). Cracks are plotted according to the integration point directions (1,2,3) as crushed, cracked (open or closed), or neither, as shown in Table 5.1. In addition, cracks can

also be shown as representative curves.

Table 5.1 Intensity and Direction of Cracks

Keys	Crack Directions		
	1	2	3
1	crushed	crushed	crushed
2	open	-	-
3	closed	-	-
4	open	open	-
5	open	open	open
6	closed	open	open
7	closed	open	-
8	open	closed	open
9	closed	closed	open
10	open	closed	-
11	open	open	closed
12	closed	open	closed
13	closed	closed	-
14	open	closed	closed
15	closed	closed	closed
16	-	-	-

(-) Directions not mentioned are assumed to be neither cracked nor crushed.

The cracking behaviour of all specimens was well predicted especially in the linear stage, even though the loads causing these cracks were higher in the analyses than in the experiments.

After yielding of specimens and propagation of cracks in the connecting members, it was rather difficult to follow precisely the spreading of the analytical cracking patterns and to make comparisons

with experiments. This is probably due to the concrete parameters input, and also the smeared crack approach which makes a decent comparison rather difficult. Nevertheless, the impression is that the locations and directions of cracks are rather well predicted. The two ways of representing cracks can be seen in Figs.5.15(c) to 5.15(h). In Fig.5.15(c), the first cracks appeared in the beam on the tension side, and then in column. These cracks remained open in the positive direction of loading as suggested by the value 2 of the curve in Fig.5.15(d).In the following cycles, more elements in the column (joint region) have cracked and no further cracks appeared to happen in the beam, as shown in Fig.5.15(e) and 5.15(f). In the subsequent cycles, cracks spread all over the joint region, as indicated in Fig.5.15(g). Figure 5.15(h) revealed that some change in directions and intensity of these cracks has occurred (dark blue: open cracks in direction 1, which coincide with direction of positive loading; light blue: closed cracks in direction 1, 2 and remained open 3; Yellow: open in 2 and closed in 3, etc.).

5.2.7 Crack Patterns

Cracking pattern computed at the end of both analysis and experiment is shown in Figs.5.16(a) and 5.16(b).

In the analysis, the first crack appeared in the specimen at a load of 14 kN (see Fig.5.17(a)) and was located at the beam-column connection; in the experiment the same phenomenon happened at the same location (first crack A), but at a load about 20 kN, see Fig.5.17(b). Such difference in load level could be explained analytically by the fact that any number of sampling points are allowed to crack simultaneously. In reality, cracks tend to open relatively slowly at a

few positions, and with stress relieved in concrete between growing cracks. In the subsequent cycles (21 kN, 28 kN and 35 kN), the cracks computed from the analysis predicted rather well the experiment, as shown in Figs.5.18(a) to 5.18(d). The figures 5.18(a) and 5.18(c) obtained analytically are mirror images of those from experiment.

As a recapitulation, the analytical cracking patterns of specimen UD2 computed throughout the analysis are given in Fig.5.19. Therefore, the strong column-weak beam design approach with a good detailing of the joint has allowed the plastic hinge not to happen in the column face.

In this model, the concrete is assumed to lose all its strength when a limiting tensile strength is reached. In practice, concrete stress does not drop abruptly to zero when the limiting value is exceeded but reduces gradually. This sudden change may have affected the element stiffnesses especially at large load increments when a significant number of sampling points may crack as the ultimate load is approached.

Another factor which may have affected the results is the assumption of an elastic-perfectly plastic model for both the concrete and the steel material properties assumed in the analysis. This latter model is more severe for concrete since its properties are not well defined. However, the parameter which has the most significant effect on the sensitivity of this present analysis is the assumed concrete tensile strength. The assumption of a constant crack shear coefficient $\beta = 0.5$, may influence the results. It would be expected that, as the width of a crack increases, the shear carried across the crack by

aggregate interlock would be reduced and a more flexible response would be obtained.

5.2.8 Overall Review

In order to have a clear insight how specimen UD2 behaved during the analysis and what observations can be made, an overall view is needed as follows:

i) As has been seen in the load-displacement hysteresis curve (Fig.5.5(a)), the overall response of specimen to reversed loads is less accurate. In the earlier stage of loading the loops simulated rather well the experiment, although after yielding the shape of the two hysteresis loops differed. The analytical hoop dissipated more energy and reached a ductility factor of 4, whereas the experimental curve showed less energy dissipation and less ductility 3.

ii) The load vs strain hoops of the main reinforcement in both beam and column predicted quite well the overall shape of experiment, even though in the last cycles the differences were noticeable. The slippage (pull-out) of the main bars from the joint took place during the analysis, as was mentioned in section 5.2.3. The strain in the main bars in beam as well as in column were in very good agreement with experiment at the gauge points where they were measured. The concentration of strains in bars in certain locations (e.g. end of the beam, above the anchorage zone, and column bars in the joint area) compared well with the experiment observations.

iii) The load vs strain and strain variation in U-stirrups legs were presented in section 5.2.5. From those plots and as mentioned

earlier, the most vulnerable U-legs to high shear are those located in the connection area. From Fig.5.13, one can see that the stirrups with one leg situated near the beam main bars were subjected to high forces and went far beyond the yielding point, whereas stirrups with double legs, some of them, did yield but were still in a state of taking further stresses. This is because forces acting in stirrups with two legs are shared out between these two legs, unlike the other stirrups formed by one leg. However, in practice there would be a gradual build up in stress from the free end of a U-bar, by bond. But this may happen more rapidly that expected.

So, the gain from this form of reinforcement is, first a better confinement of the core area, and second a high resistance to the high shear forces acting in the joint region.

iv) The cracking pattern was generally well predicted in terms of locations. In terms of loads the cracks occurred at a late load stage in comparison with experiment. This is thought to be the assumption of the concrete model used in this analysis as mentioned in section 5.2.6, and also the concrete material properties which are not well defined, especially the crack shear coefficient which may influence the results.

5.3 OTHER FEATURES OF PERFORMANCE

5.3.1 Distribution of strains along main bars

Taking advantage of the facilities offered by this finite element package, it is possible to plot curves representing strain and stress variations all along any reinforcing bars. It is quite difficult to achieve this objective experimentally in laboratory, although an

ingenious method was devised by Scott (1992).

The strain variations along most main bars in both beams and columns for all specimens were plotted for major cycles. Because of the huge number of plots computed, only those of importance are shown.

First, the strain distribution curves measured in the column main bars in the inner and outer faces for specimens EX2 and UD1 can be seen in Figs.5.20(a) to 5.20(d). As it was expected, the strain concentrations in column bars were located on both sides of the beam at the junction zone.

In specimen EX2, the strains in both inner and outer column bars alternated between tension and compression. At a load level of -14 kN, the outer bars reached a tensile strain of 100 μs (Fig.5.20(a)). The tensile strain in the inner bars was 600 μs (Fig.5.20(b)). The reason for these very low values of strain will be seen later in this section.

In specimen UD1 when loading forward at a load level of 14 kN, the outer bars stayed in tension and developed strain values of 900 μs, see Fig.5.20(c). The inner bars were tensile (1100 μs) over a rather important portion of the joint (450-1150 *mm*), but had a small excursion in compression (Fig.5.20(d)).

Even though the loading direction of these specimens is different, a sensible comparison still can be made in comparing column outer bars (situated beneath beam tension side when loading forward) of specimen EX2 to column outer bars of specimen UD1 (located on the beam tension

side when loading backward this time).

This difference in behaviour of the two specimens could be explained by comparing the axial forces on columns in both specimens. The axial load in EX2 was about 100 kN, which is quite high, kept the tensile forces in column bars transferred from the beam under bending, and also from the confinement of the radial bursting forces in the concrete arising from the high bond stresses, to stay low. In specimen UD1, the axial load was about 50 kN, and could not kept tensile forces low.

Second, most of the beams bars were under high strains at the junction of columns. This is obvious because of the effect of reversed load introduced at the end of beams under positive and negative bending moments, as it has been seen in Figs.5.8(a) to 5.8(j). As can be seen from these plots, the beams bars were subjected to tension and compression following the direction of the external force. This behaviour is a good prediction and matched reality very well. In the anchorage zone, (same plots above) the bars did not always follow the loads direction because of the complexity of forces acting in this area. To model analytically the curvature of the anchorage is very difficult and no attempt has been made so far to do so. However, the 90^{o} curvature simulation reflects the reality to some extent.

5.4 COMPARISON OF SPECIMENS

5.4.1 Performance of U-stirrups

5.4.1.1 Introduction

As mentioned in chapter two, the transverse reinforcement of specimens UD1 and UD2 in the joint region was in the form of

U-stirrups with a different overlap length. In UD1, the overlap length was one-half of the column effective depth, whereas the overlap length in UD2 was equal to the effective depth of the column. The other difference between these two specimens lay in the number of reinforcing bars in beams. The beam in UD1 had three bars on each side, while in UD2 the beam had only two bars on each side.

In order to have a clear insight of the overall behaviour of these two specimens, and the effect of the U-stirrups on the performance of the joint, a comparison of UD1 and UD2 is necessary.

5.4.1.2 Comparison of U-stirrups

In order to investigate the effectiveness of the U-stirrups, the displacement shapes of the reinforcing cages in both specimens UD1 and UD2 are plotted in Figs.5.21(a) and 5.21(b) respectively. From Fig.5.21(a), one can see the deformed shape and the tendency of these U-stirrups legs, which had an overlap length of one-half of the column effective depth (d_{eff}), to separate from one another under shear forces leaving the joint core vulnerable to tensile forces. This behaviour with further loading cycles, can lead to the formation of plastic hinge in the face of the column and therefore to the collapse of the subassembly. However, this tendency of separation was not observed in the U-stirrups legs, which had the overlap length similar to the column depth, in specimen UD2.

The strains variations along top and bottom legs of stirrups in both specimens UD2 and UD1 in the joint region at a load of 35 kN are plotted in Figs.5.22(a) and 5.22(b). From these curves which represent envelopes of strains in the connection area, one can see that the

U-stirrups legs of specimen UD2 (Fig.5.22(a)), when loading forward reached yielding point (about 1700 μs). When the load is reversed, the same phenomenon happened on the compression side of the beam with a strain value about 1700 μs. As it is shown on the plot, the most stressed stirrups legs are those adjacent to the beam main bars (inner and outer sides) and perpendicular to it. In the case of specimen UD1 (Fig.5.22(b)), the maximum tensile strain reached was about 1000 μs.

As it has been mentioned in section 5.2.5, these high strain values reached by stirrups legs of specimen UD2, is an indication of the good behaviour of this type of stirrups in sustaining high shear forces and confining the joint core. Whereas, the strains profile of specimen UD1 showed that the U-legs with a short overlap (one-half) did not take high values of strain. This is due probably to the overlap length which was not long enough to sustain forces acting in that region. This is to say the resistance of these stirrups to shear forces is doubtful, and therefore can lead to the deterioration of the joint core, penetration of plastic hinge in the column face and also to buckling of column main bars in that region.

5.4.1.3 Comparison of U-stirrups with conventional stirrups

The shear vs. strains variations in columns stirrups for specimens EX2, UD1 and UD2 in the joint region are given in Figs.5.23(a) to 5.23(c) respectively. The locations of these gauges are shown in Figs.5.24(a) to 5.24(c). Even though the strain gauge locations differ slightly from one specimen to another, an overall comparison of the behaviour of these gauges can be made.

Gauge S8 of specimen UD2, had the highest strain (about 1450 μs) in comparison with gauges S1 and S3 of specimens UD1 and EX2. Gauge S1 of specimen UD1 had the lowest tensile strain. These graphs show that the stirrup leg in UD2 developed some of its strength and probably with a higher lateral force it would experience yielding. In the case of gauge S3 of specimen EX2, the maximum strain reached at a load level of 28 kN is about 1200 μs. Therefore, one can suggest the stirrups with U-legs behaved like conventional stirrups, perhaps better.

For the other gauges, situated towards the compression side (when loading forward), the amount of compression strain reached by each one is more or less similar as shown in the above curves.

As a recapitulation, the effect of inner and outer legs of stirrups is not fully mobilized until the concrete undergoes sufficient lateral expansion under the action of compressive forces. At this stage, the outer shell of concrete (cover) has reached its useful load limit and starts to spall. The confining action of rectangular hoops mainly involves reactive forces at the corners, with only minor restraint provided along the straight unsupported sides. In the case of U-hoops, the straight legs tied together provided additional restraint to the unsupported sides.

Because of this, rectangular stirrups formed with double U-legs, if well detailed, are generally more effective than conventional (rectangular) stirrups in confining concrete core members subjected to compressive forces. Left and right legs of stirrups are mobilised due to shear by means of truss action. This tends to support the mechanisms proposed by Park and others (1973).

5.4.2 Main Reinforcement

As a reminder, beam of specimens EX1 had four bars (ϕ12 mm), two on each side, while beam of specimen UD2 had two ϕ16 mm on the tension side and two ϕ12 mm on the compression side. Column of specimen EX1 had four bars of ϕ16 mm, whereas column of specimen UD2 was reinforced with ϕ12 mm. Specimens EX2 and UD1 had the same configuration in term of main reinforcement, six bars of ϕ12 mm in each beam and four bars of ϕ12 mm in each column.

As it was mentioned earlier in this chapter, the strains concentration in beams main bars just at the junction of the sub-assembly was expected. As a confirmation of the reality, all the main beams bars showed increase in compressive and tensile strain (depending on the direction of the load) starting from the mid-span of the beams and reached maximum values at the beam-column junction, as can be seen in Figs.5.25(a) to 5.25(f). These curves which represent the strain variation of main bars for specimen EX2 were plotted at different rate of loading 21 kN, 35 kN and -14 kN. For specimen UD2, the variations of strain along main beam bars were presented earlier in this chapter, see Figs.5.8(a) to 5.8(j).

In specimens which had three bars in beams, the peak of strain was at the same location (beam-column junction), but the amount of strain was less. At a load level of 21 kN, the tensile and compressive strain reached by beams bars in both specimens are, 1300 μs and -650 μs for specimen UD2, and 1200 μs and -400 μs for specimen EX2. At a load level of 35 kN, the tension bar in UD2 yielded (2300 μs), whereas bar at the same location in EX2 did not experience any yielding (1900 μs).

In the compression sides of the two specimens, the compressive strain was more important in beam bars of UD2 than in EX2. This difference in behaviour of the two specimens is due to the amount of main reinforcement, as mentioned above. In the case of EX2, which had three bars on each side of the beam, the amount of strain was shared between bars and therefore, these bars were less stressed.

Strain and stress (plastic) measured in the column main bars in inner and outer faces of the columns at a given load level for specimens EX1 are plotted in Fig.5.26. The strain and stress pattern obtained were expected. The tensile strain reached by column inner bars in the joint region was 650 μs (Fig.5.26(c). In Figs.5.26(a) and 5.26(b), the amount of stress (437.5 N/mm^2) remained below yielding stress value. In spite of these strain and stress concentrations in column bars at the junction due mainly to bending transferred by the beam bars forces, the column bars did not experience any yielding and stayed in linear stage. This low stress and strain in column main bars is due to a relatively high compressive forces (about 1700 kN) acting on the column sections.

5.4.3 Concrete Strength

The response of reinforced concrete to cyclic loading is complicated by the complex interaction between steel and concrete. This is reflected by the numerous possible failure modes in flexure, shear, or bond.

As concrete is subjected to reversal loads of increasing intensity, it undergoes different phases of damage, from microcracking up to ultimate failure depending on its strength.

Specimen EX1 had the highest concrete strength about 80 N/mm^2 among the four tested specimens. Experimentally, the column of this specimen did not experience even a single crack, unless they were invisible to naked eye. The beam experienced few flexural cracks which were located within distance equal to its depth. The damage was concentrated at the beam-column junction.

Analytically, both beam and column of EX1 experienced cracks (dark blue: open in direction 1, which coincide with column neutral fiber; light blue: closed in the same direction) and the damage was located in the column at the connection area, as shown in Fig.5.27. This propagation of cracks in the joint core did not reflect the experiment as far as column is concerned. This anomaly is thought to be due to the difficulties found to model the concrete material parameters input.

As an example of concrete under tensile and compressive forces, Figure 5.28 shows the stressed (principal stress σ_3) state of specimen EX1 at the early stage of loading backward. From this plot, the stress distribution is well predicted. Colour blues (light and dark) represent the most compressed areas, whereas the red colour is an indication of the tensile stress.

The other three specimens (EX2, UD1 and UD2) had almost the same concrete strength ranging between 37 N/mm^2 and 42 N/mm^2. The cracking patterns of these specimens simulated rather well the experiments to some extent, specially in the linear stage.

column are represented graphically at two load levels, as shown in Figs.5.30(a) and 5.30(b).

5.4.5 Effect of Flexural Strength Ratio

Experimentally, the flexural strength ratio had a major effect on the location of the flexural hinging in specimens. All specimens tested (analysed) had flexural strength ratios greater than 1.5 as recommended by Design Codes. Therefore, in none of the specimens did flexural hinges form in the columns inside or outside the joint. In specimen EX1 which had the highest flexural strength ratio 2.96, the cracks were distributed into the beam and away from the column face. In the other specimens which had flexural strength ratios ranging from 2.04 to 2.58 had cracks in the joint region. The flexural strength ratio of specimen UD1 was 2.04. In this specimen flexural hinge formed in the beam, but spread into the joint at a late stage of loading because of the type of transverse reinforcement used in the joint region. This led to the pullout of the beam longitudinal bars, followed by a drop of the load-carrying capacity, and therefore to stiffness degradation of the specimen at the end of the fourth cycle, as shown in Fig.5.31.

5.5 REVIEW AND CONCLUSIONS

This three- dimensional analysis was carried out in order to obtain an idea of the overall behaviour of the beam-column connection and, especially, of the joint region.

In the numerical analysis, a coarse mesh of one and two elements over the width of the specimens were used for specimens EX1, EX2 and UD1 and UD2 respectively. The stiffness of the reinforcement is

UD1 and UD2 respectively. The stiffness of the reinforcement is superimposed on the stiffness of the concrete element. The results obtained from analyses were in reasonable agreement with experiment.

In comparing the results of analyses with those of experiments it appears that this finite element program can provide a good first insight into the behaviour of such structures. From the analysis of the beam-to-column connections, it emerges that the cracks are of major influence upon the internal stress distribution, the magnitude of the failure load and the deformation of the structure. The development of dominant cracks are well reproduced in the analyses. The models confirmed the results of the tests with regard to serviceability limits of cracking and deflection. Finite element calculations show that the efficiency of the beam-column connections increases with increasing the concrete quality (i.e. EX1) and decreases with augmenting the reinforcement percentage in the connecting members (i.e. EX2 and UD1) "beam" and "column".

The sensitivity of the model to some parameters such as shear retention factor may be significant for the accuracy of the finite element results. Still this factor should be defined by further experimental and numerical investigations.

In general, non-linear analytical procedures are very complicated and difficult to match with the actual non-linear behaviour of complex systems such as reinforced concrete structures. Errors can be introduced via many parameters such as material models, spacing of sampling stations, use of numerical integration processes and inadequacies in the non-linear equation solver.

Because all the tests series carried out on reinforced concrete beam-column joints world wide were subjected to cyclic loading (quasi-static) to simulate the effect of earthquake, and also because this type of experiment cannot be tested otherwise, it would be very helpful if incorporation of 'cyclic loading' option is considered in the ANSYS finite element program.

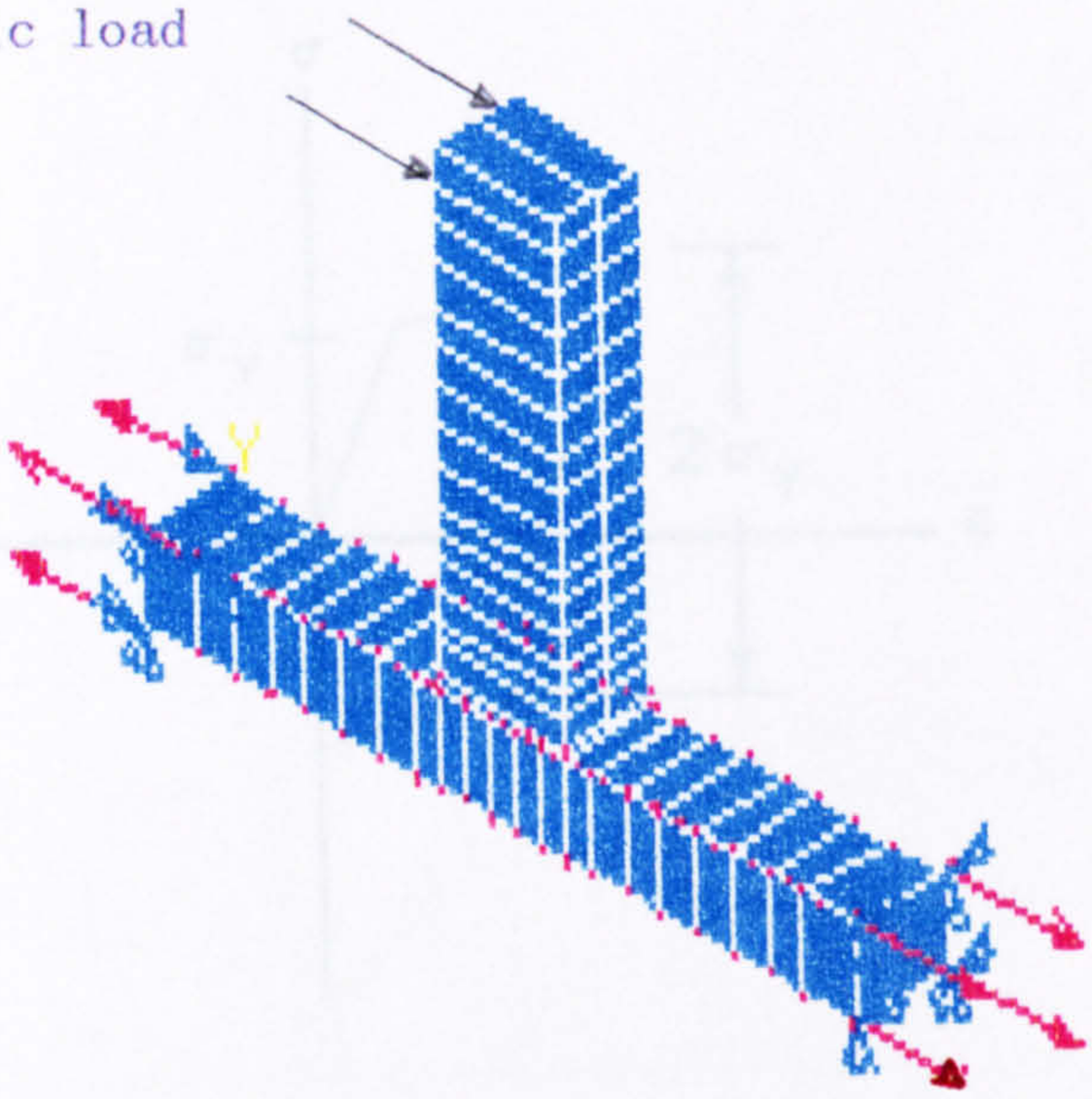

a) Concrete Mesh, Loading and Support - Specimen UD2 -

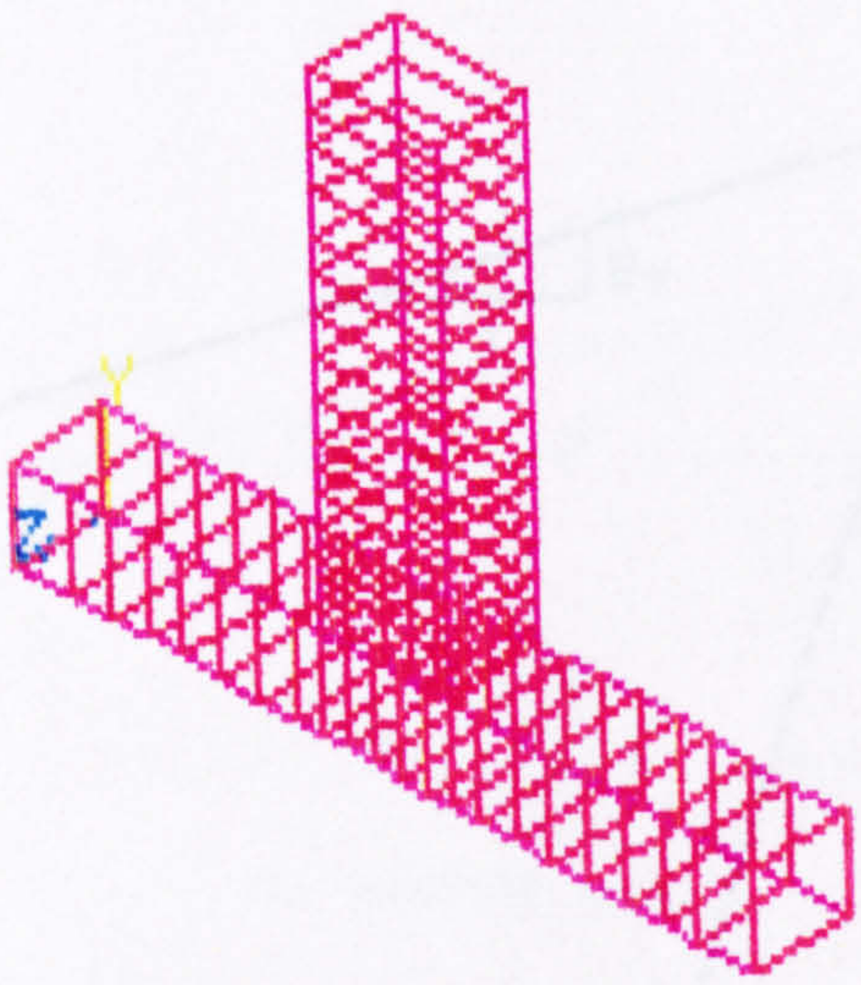

b) Reinforcing cage (main & transverse reinforcement)

FIG.5.1 BEAM-COLUMN SUB-ASSEMBLY

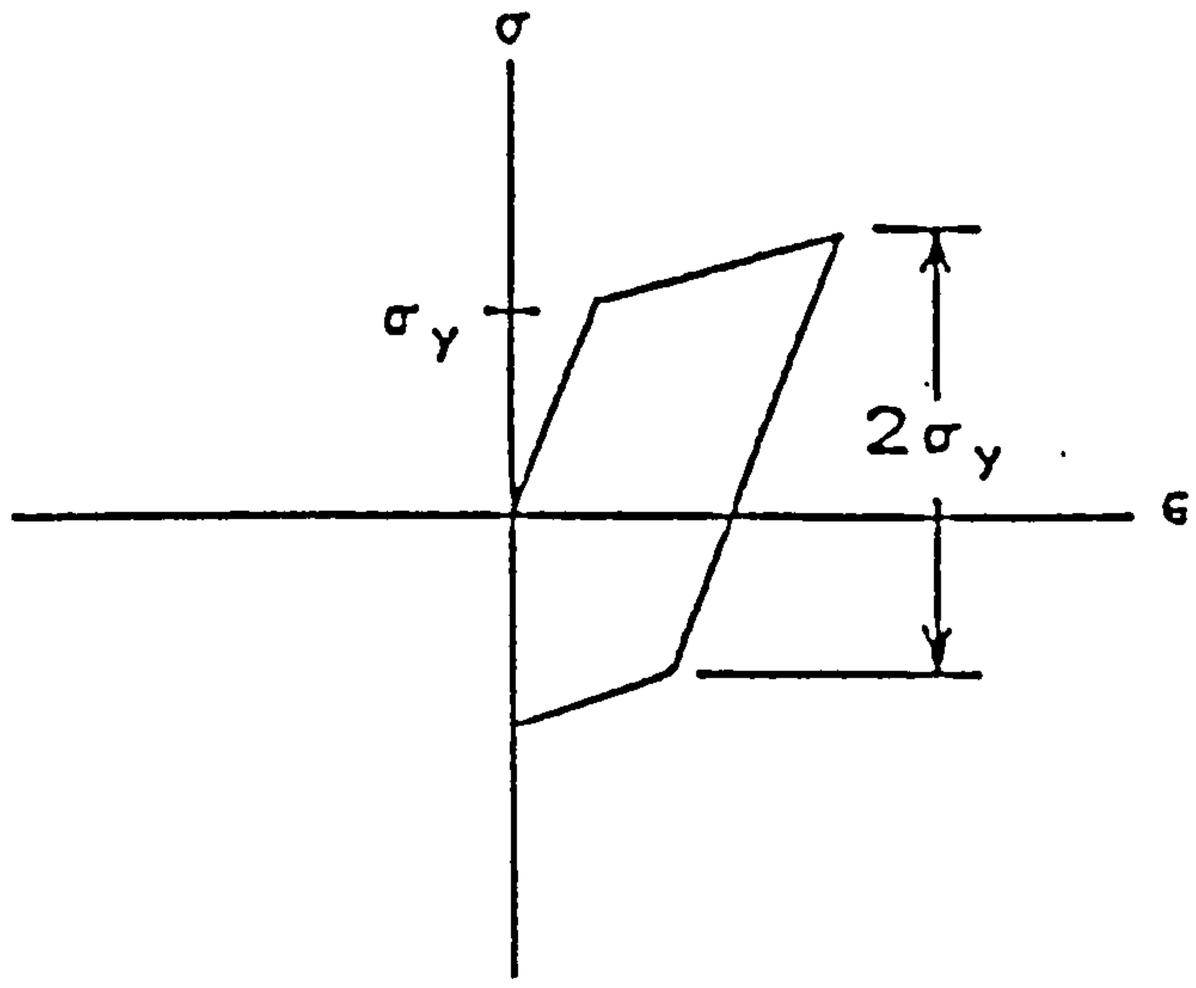

a) Bilinear Kinematic Hardening

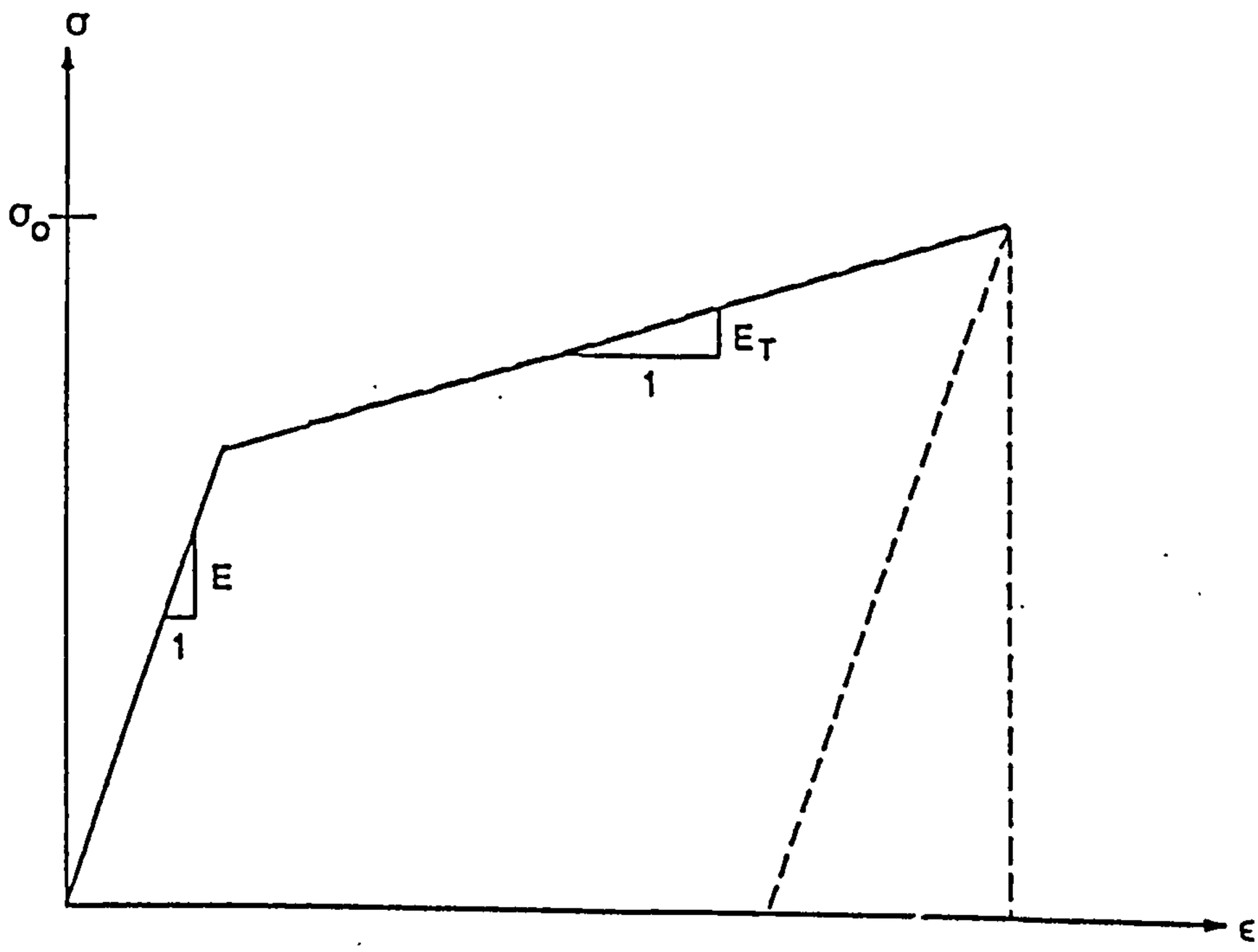

b) Bilinear Stress-Strain Curve

FIG.5.2 REPRESENTATION OF MATERIAL PROPERTIES - Plasticity -

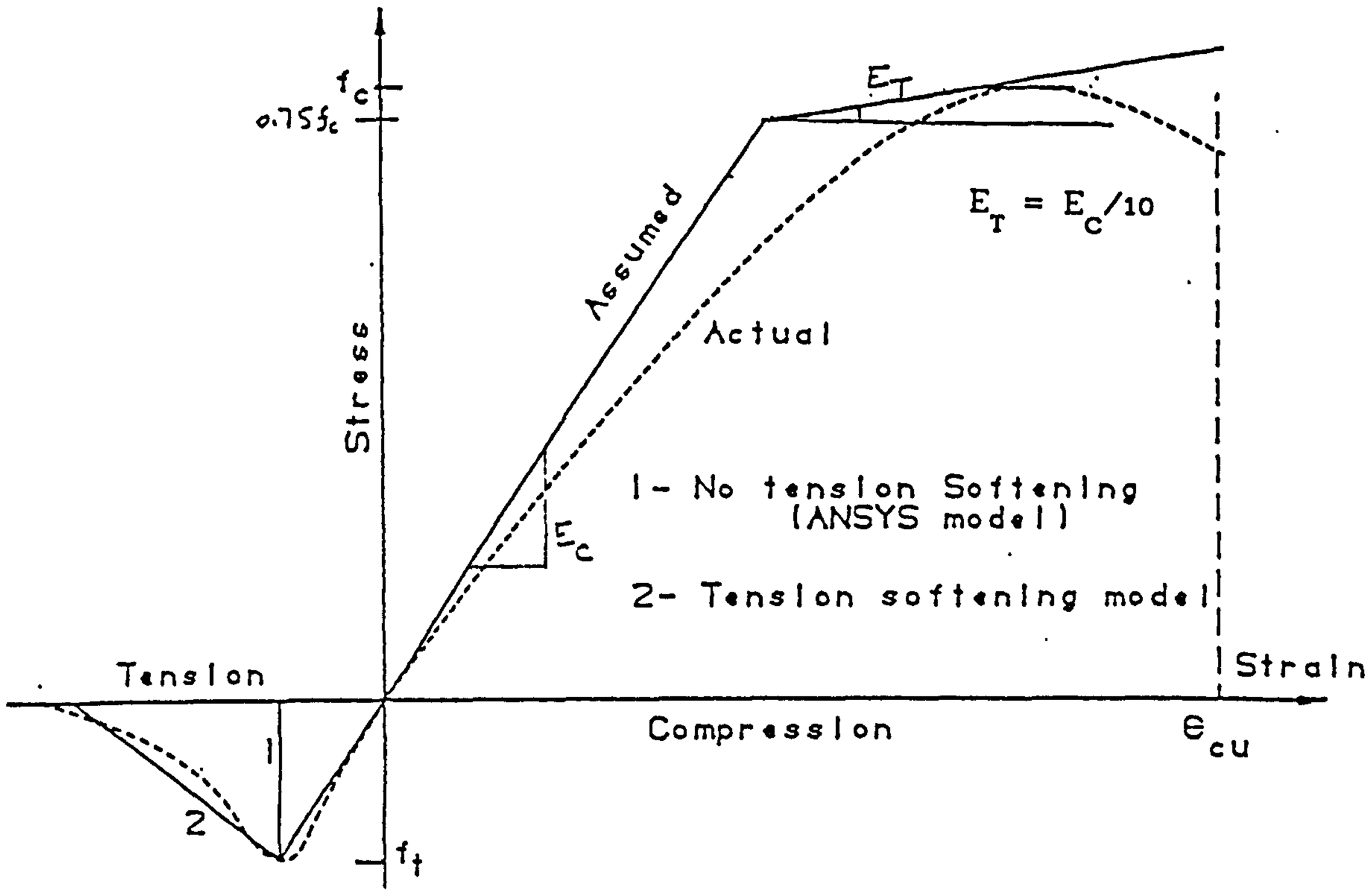

a) Stress-Strain Curve for Concrete

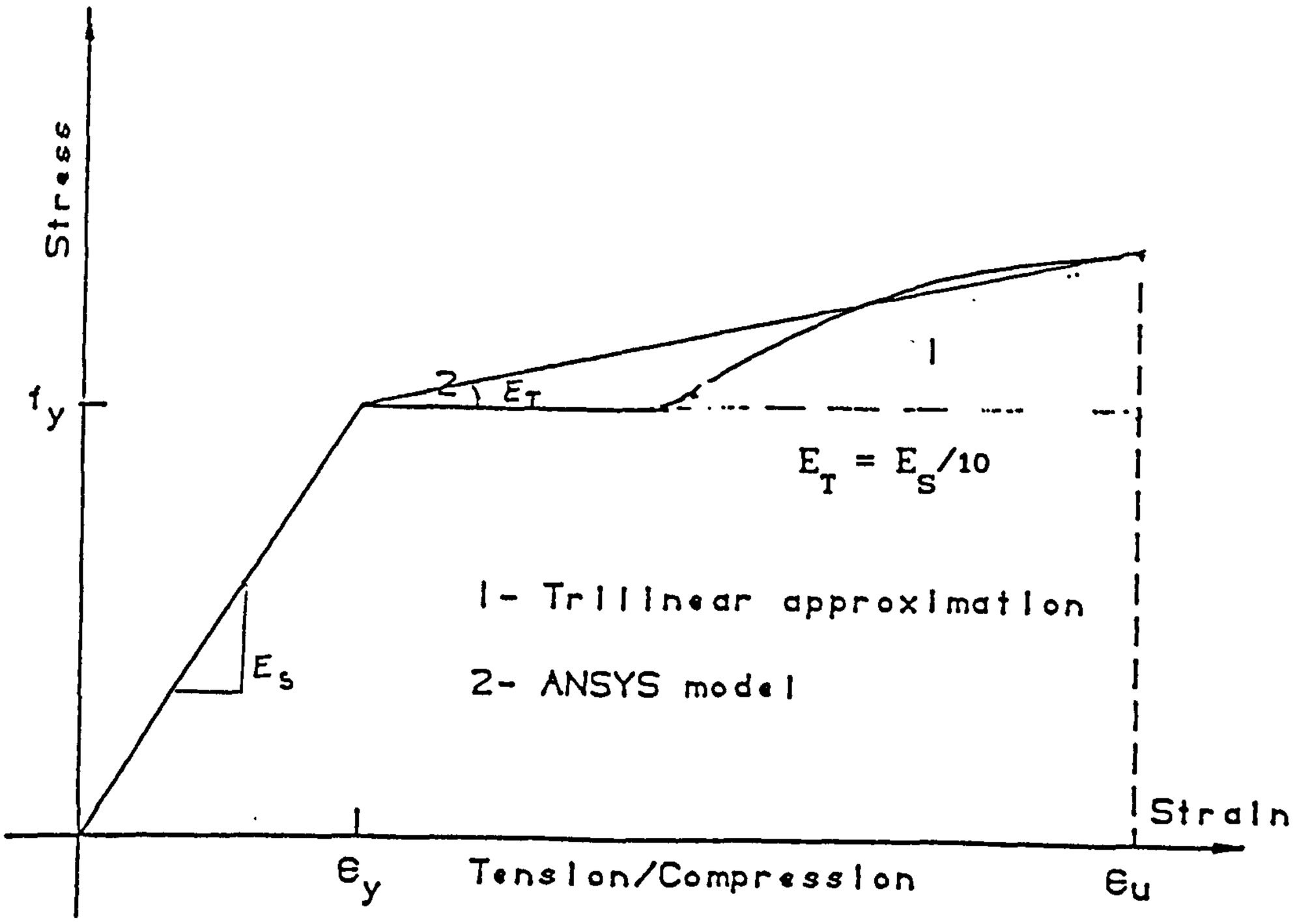

b) Stress-Strain Curve for Steel

FIG. 5.3 STRESS-STRAIN CURVES FOR STEEL AND CONCRETE

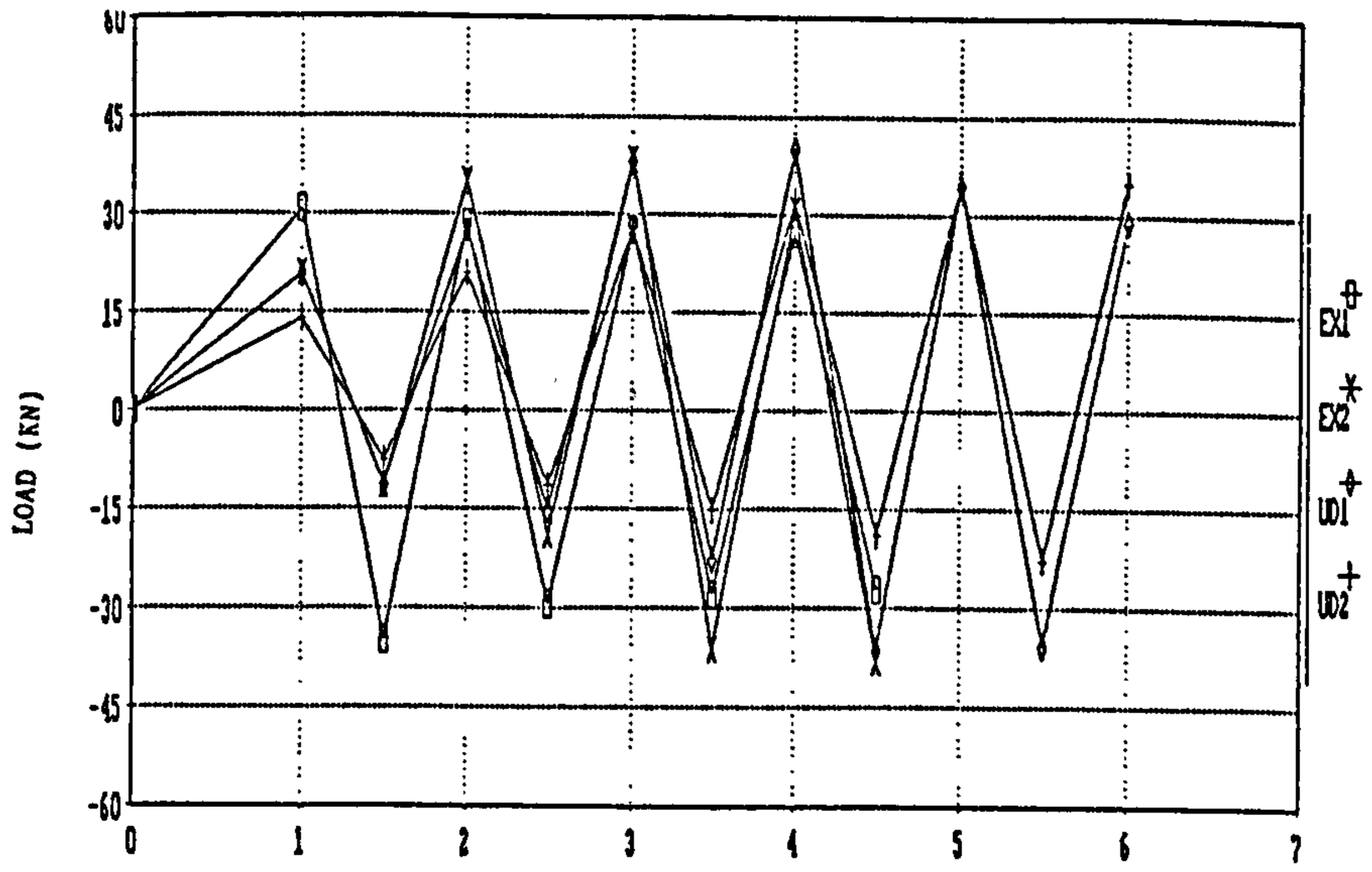

FIG.5.4 LOAD SEQUENCE DIAGRAM

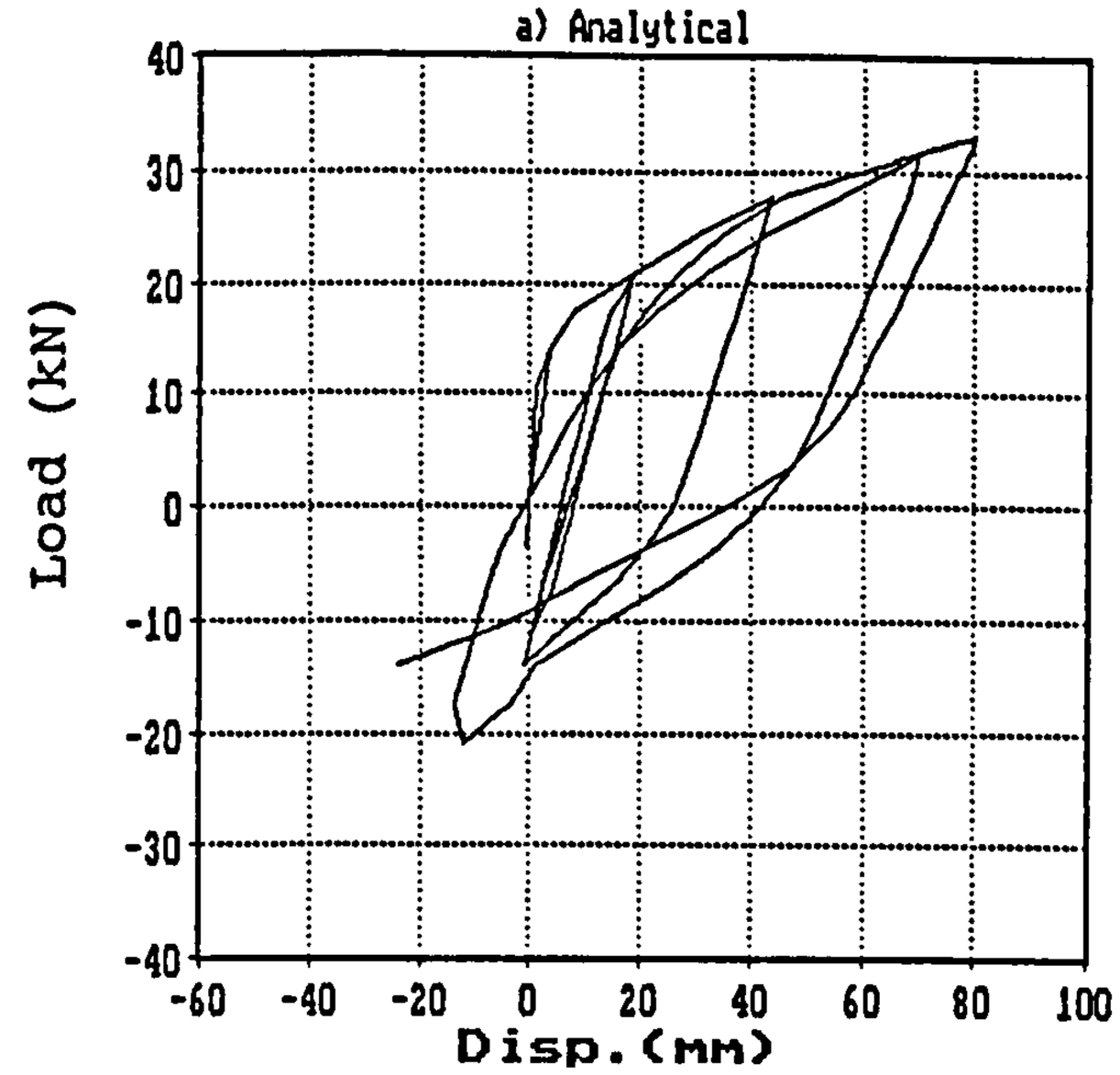

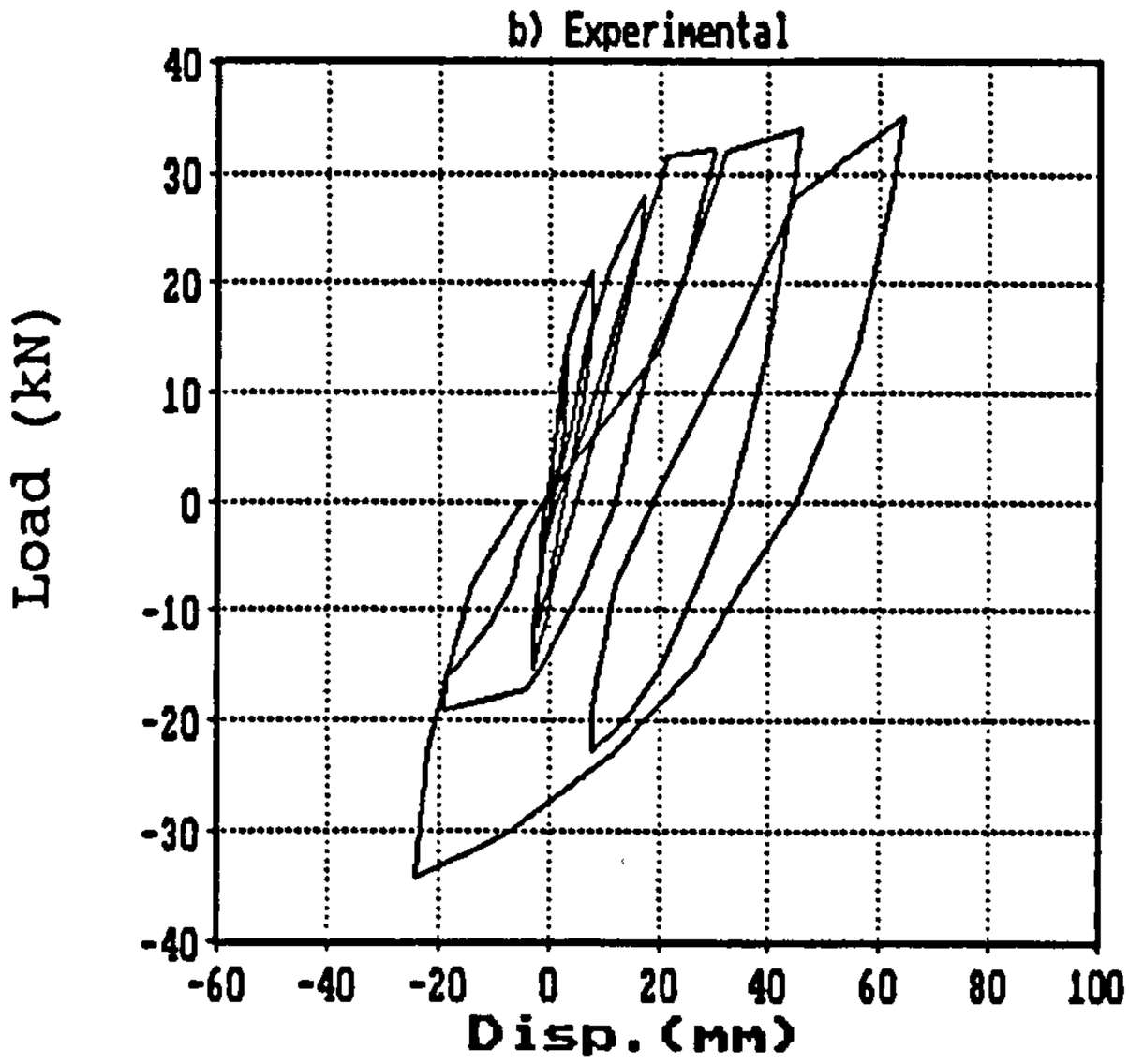

FIG.5.5 ANALYTICAL AND EXPERIMENTAL HYSTERESIS LOOPS FOR SPECIMEN UD2

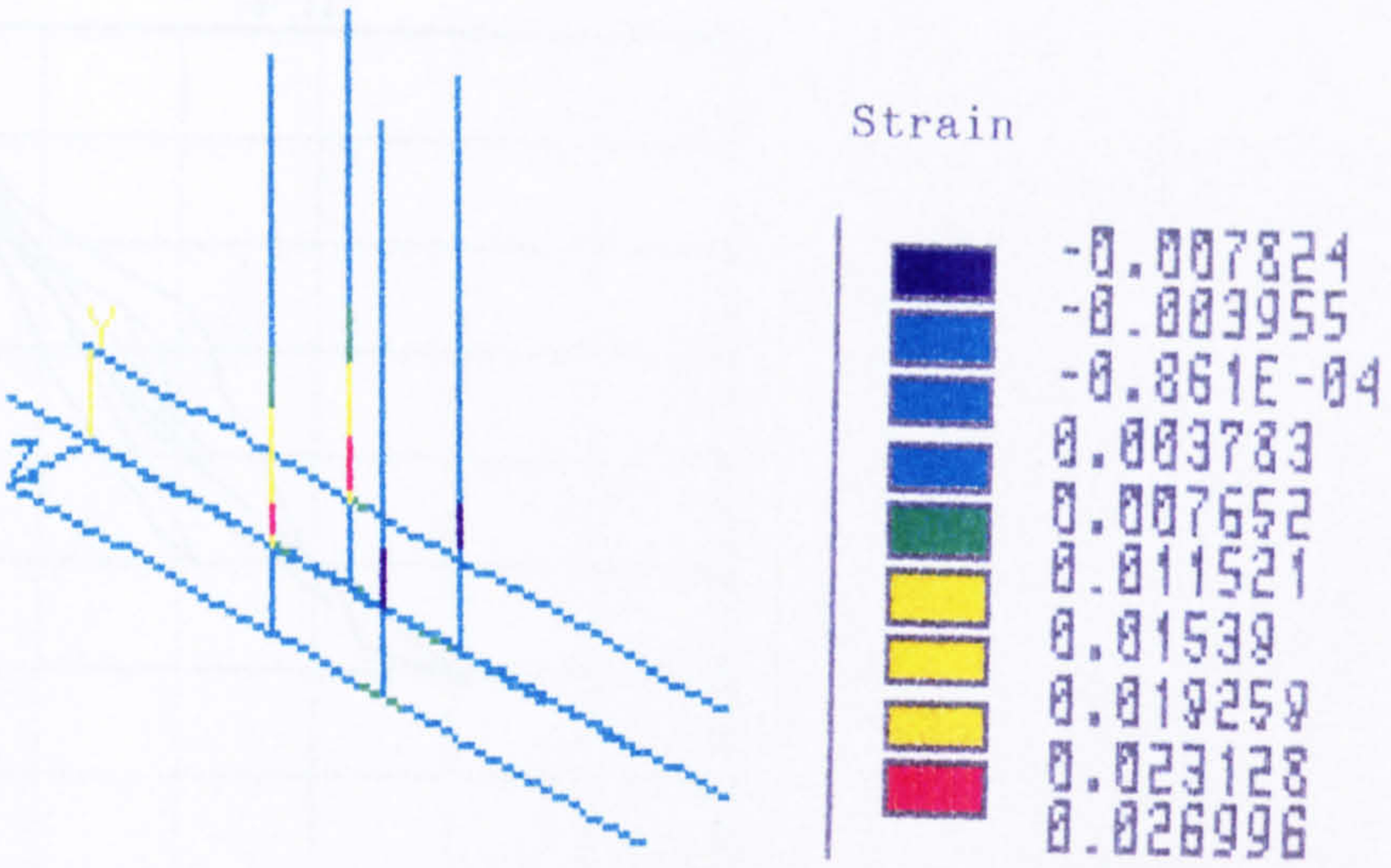

a) Main Reinforcement

F = 35 kN

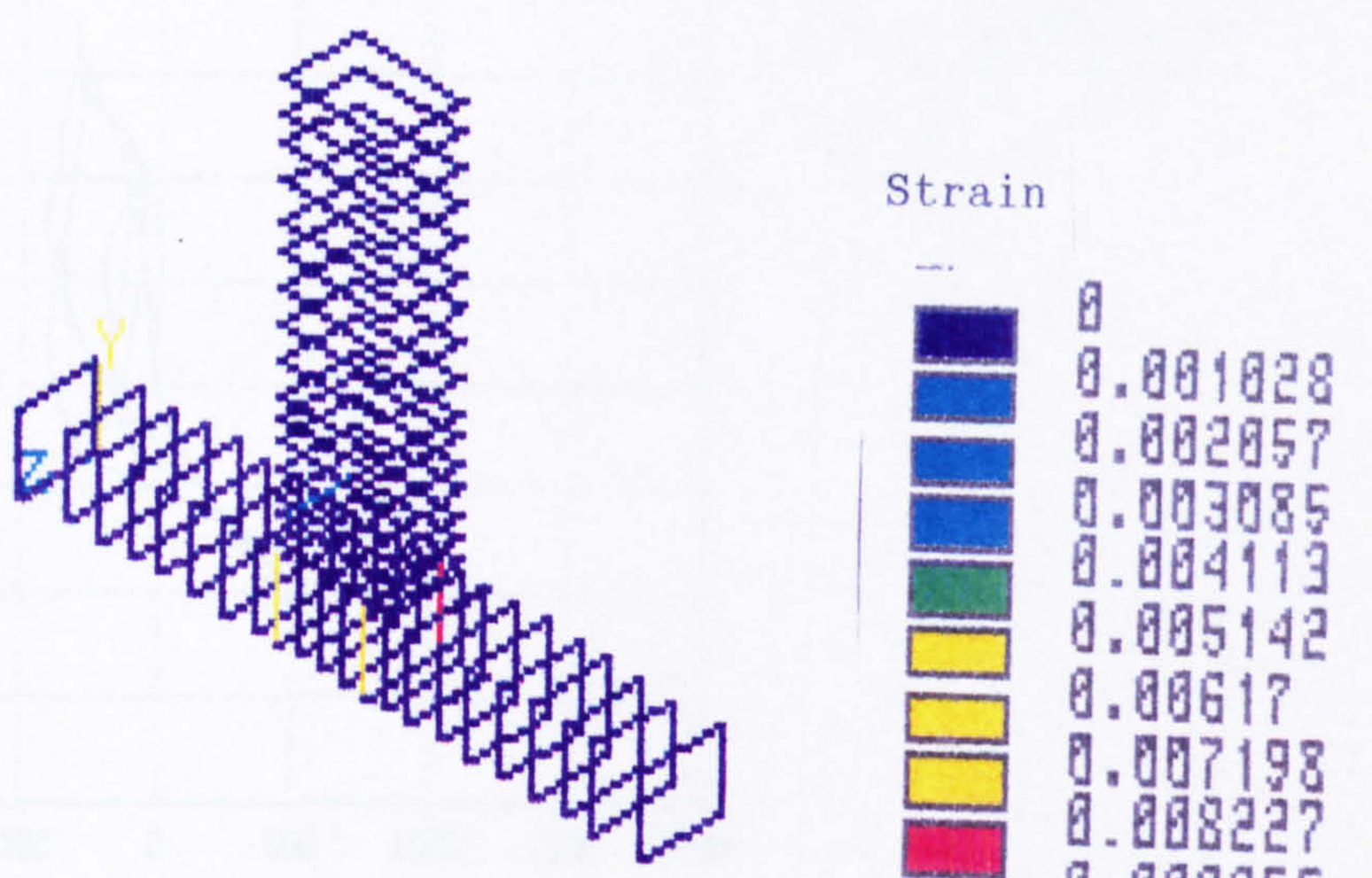

b) stirrups

FIG.5.6 STRAIN (PLASTIC) DISTRIBUTION IN REINFORCING STEEL

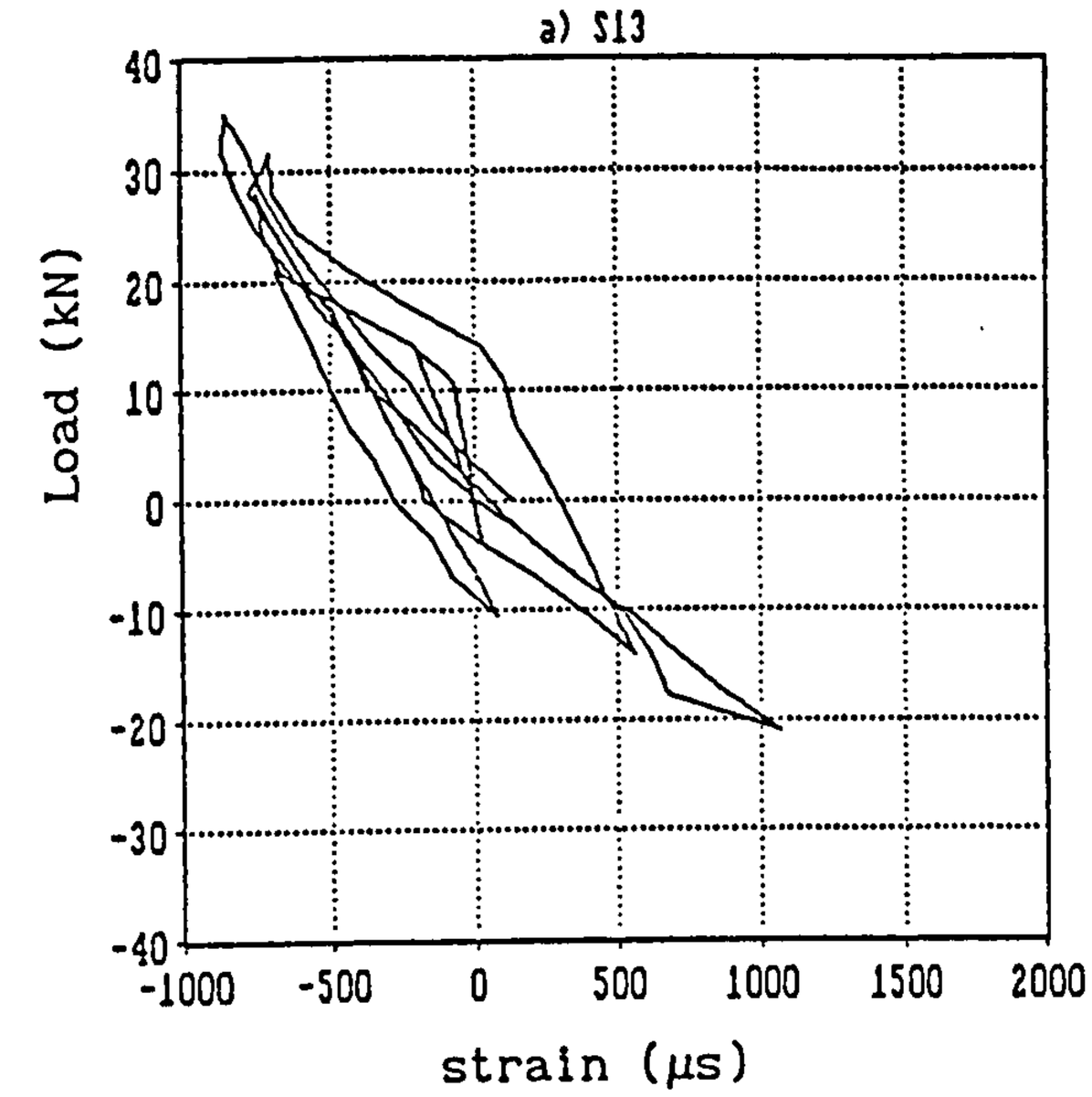

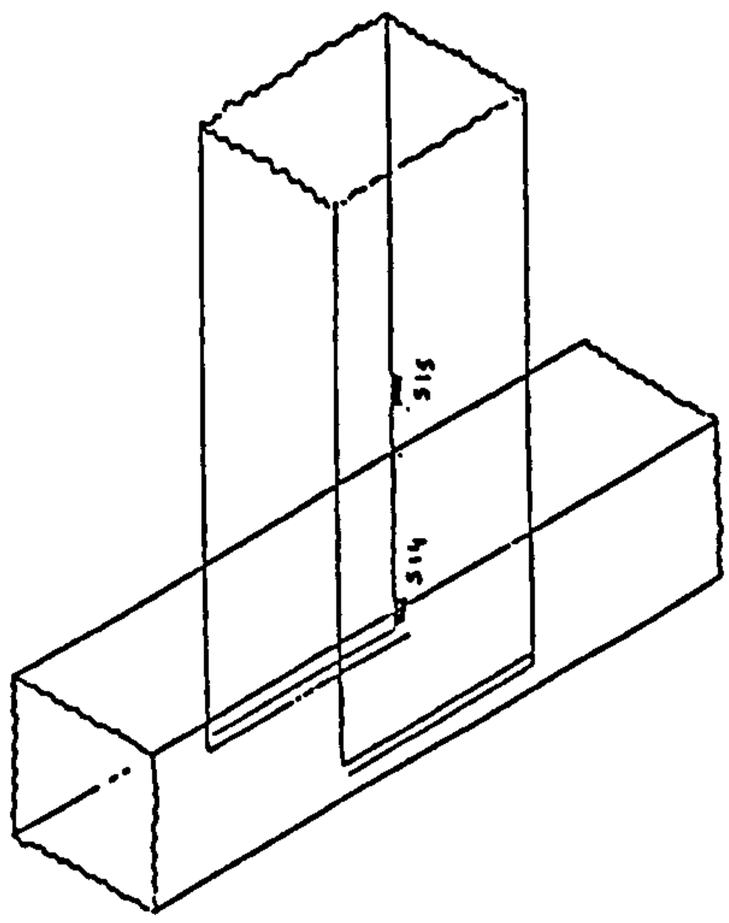

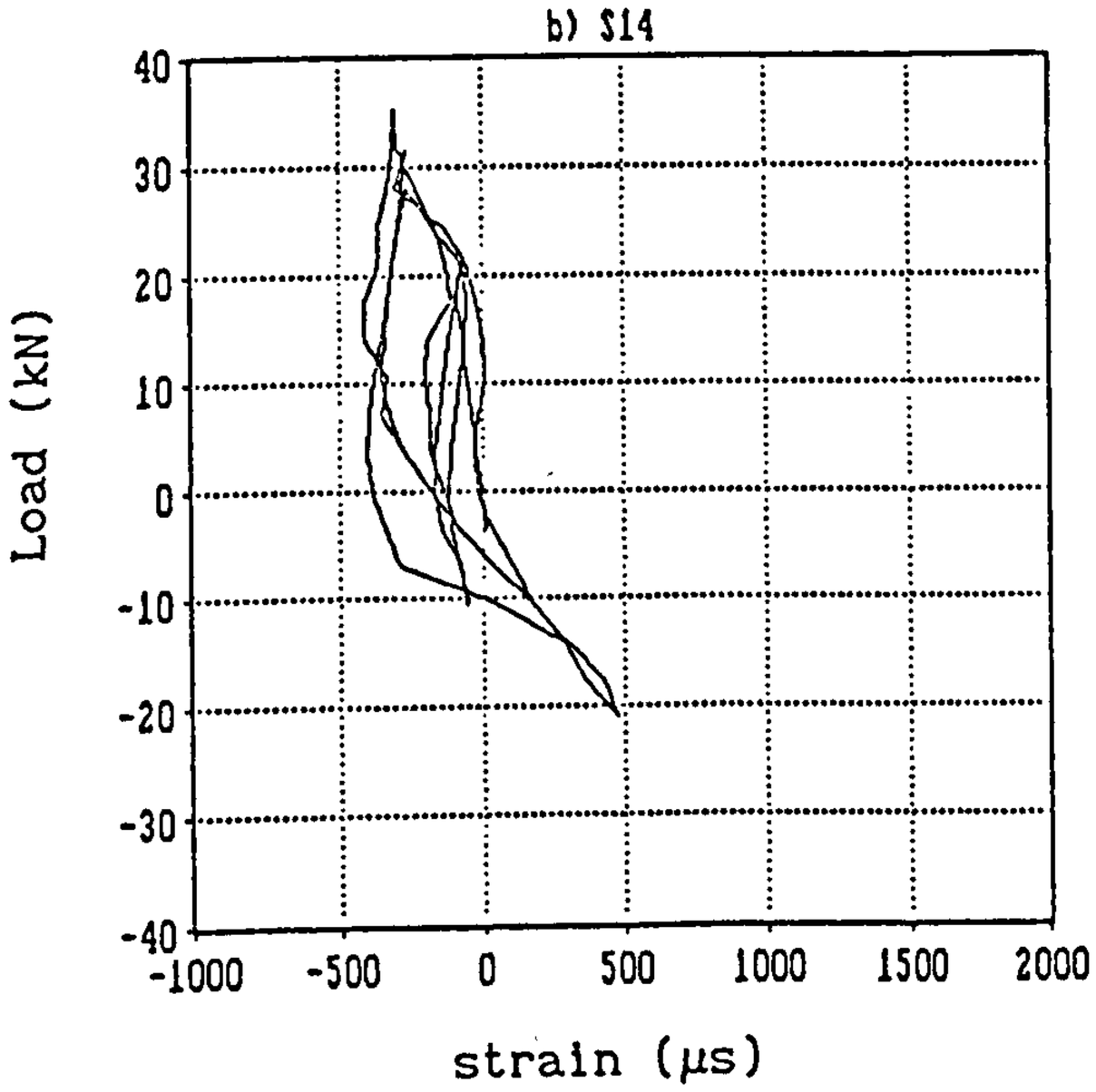

FIG.5.7 LOAD VS. STRAIN PROFILE IN BEAM MAIN REINFORCEMENT

c) S16

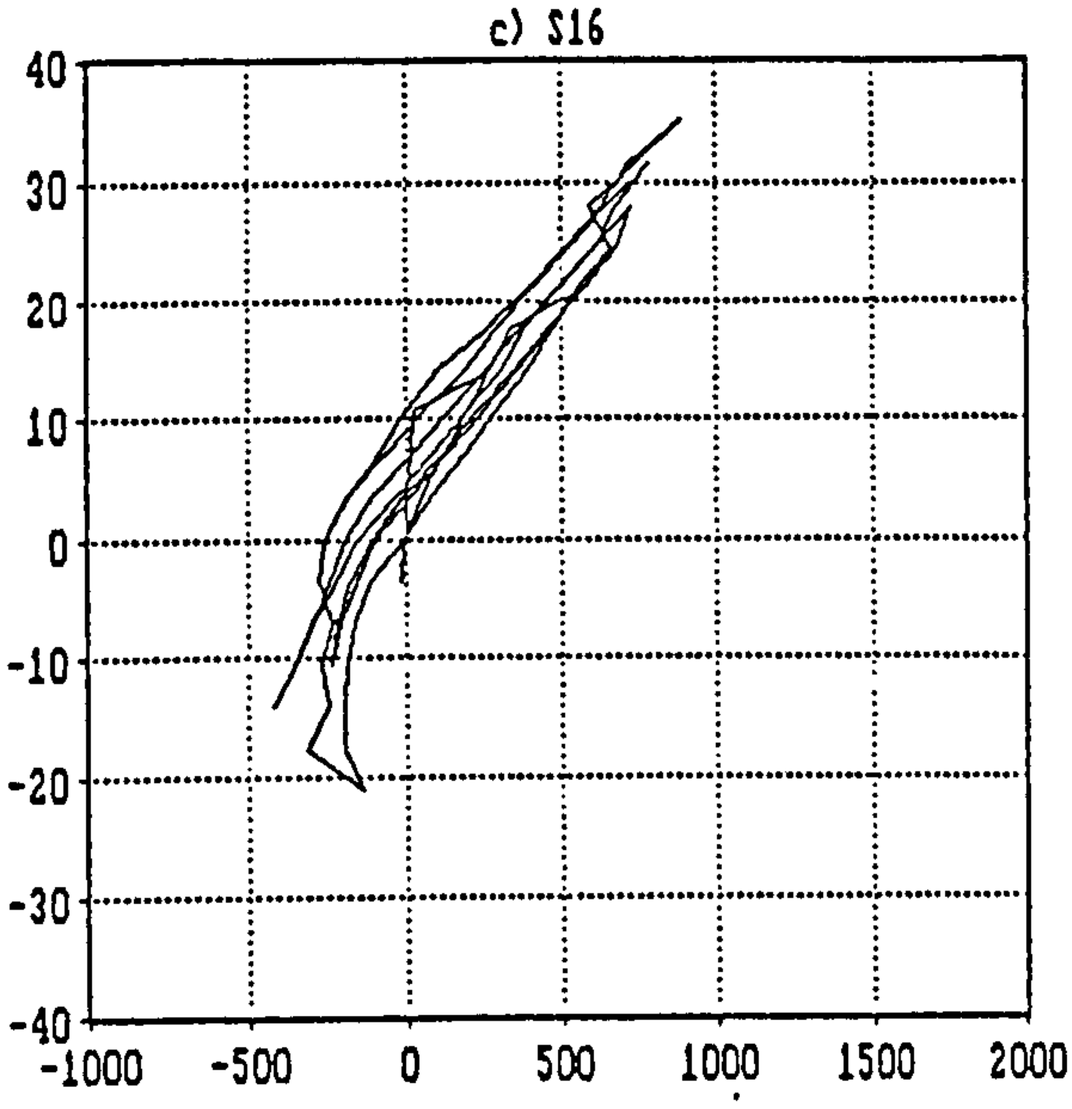
Load (kN)
40
30
20
10
0
-10
-20
-30
-40
-1000
-500
0
500
1000
1500
2000
strain (μs)

d) S15

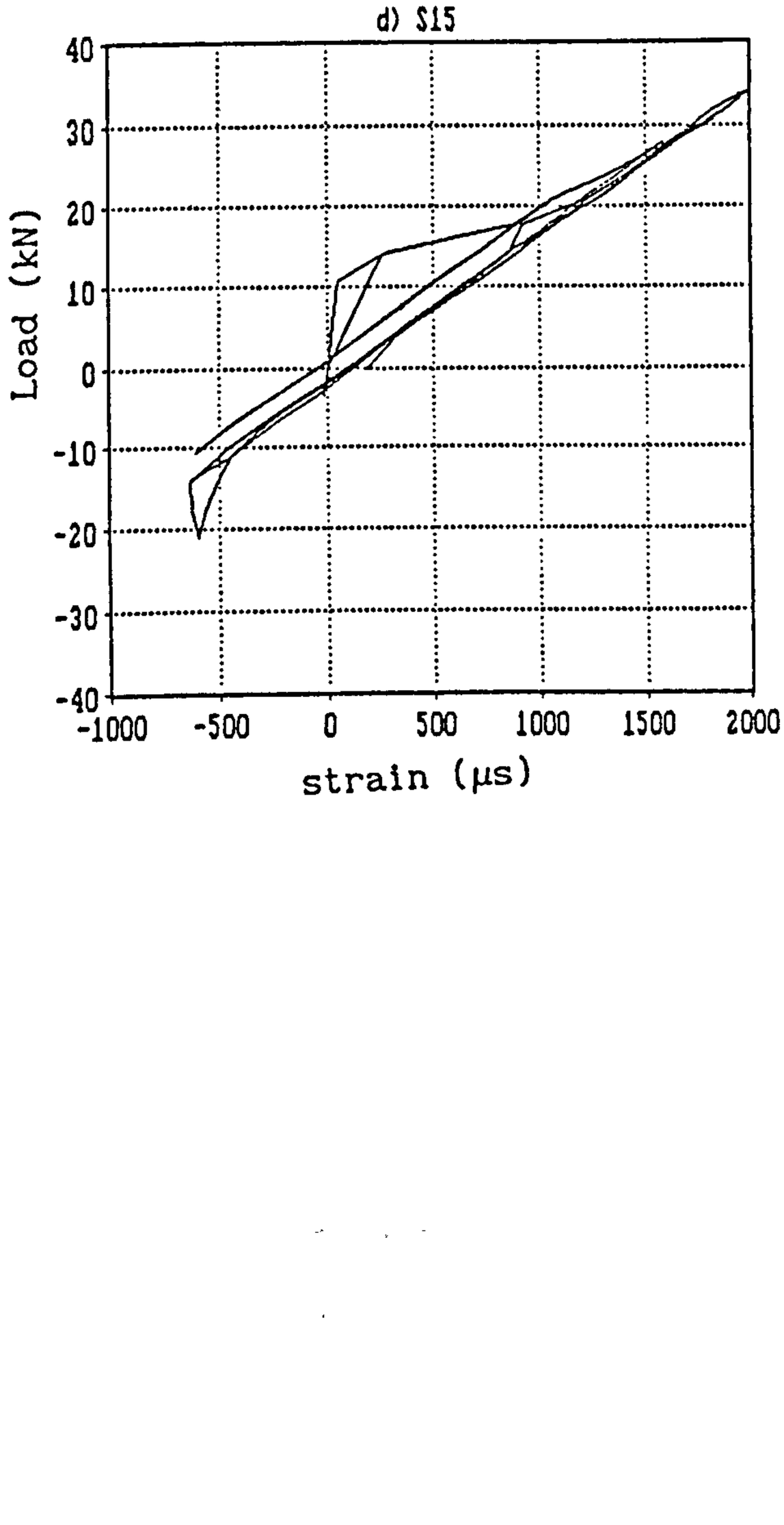
Load (kN)
40
30
20
10
0
-10
-20
-30
-40
-1000
-500
0
500
1000
1500
2000
strain (μs)

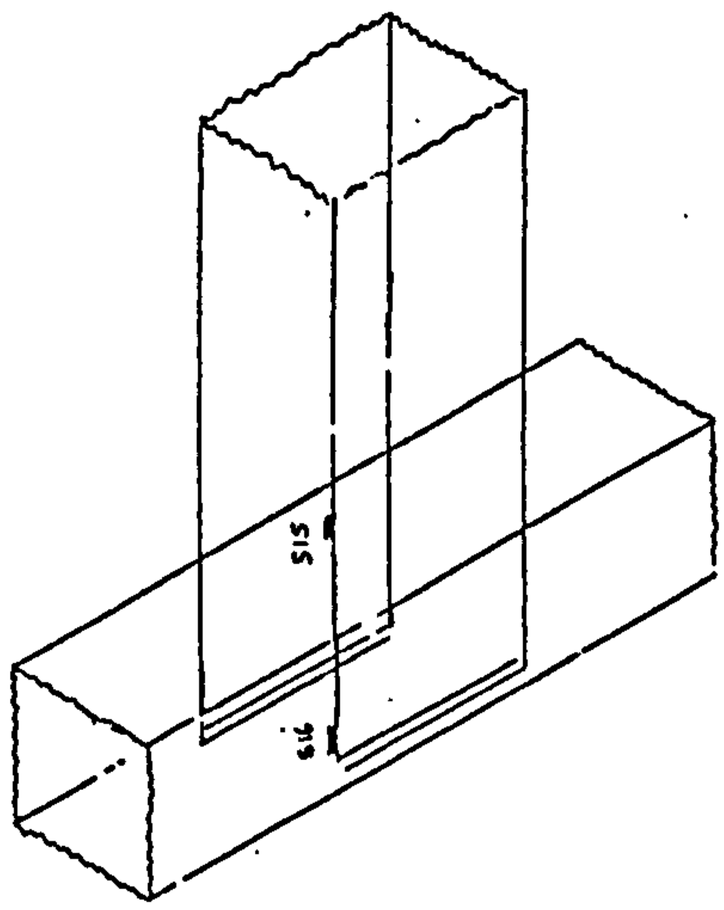
S15

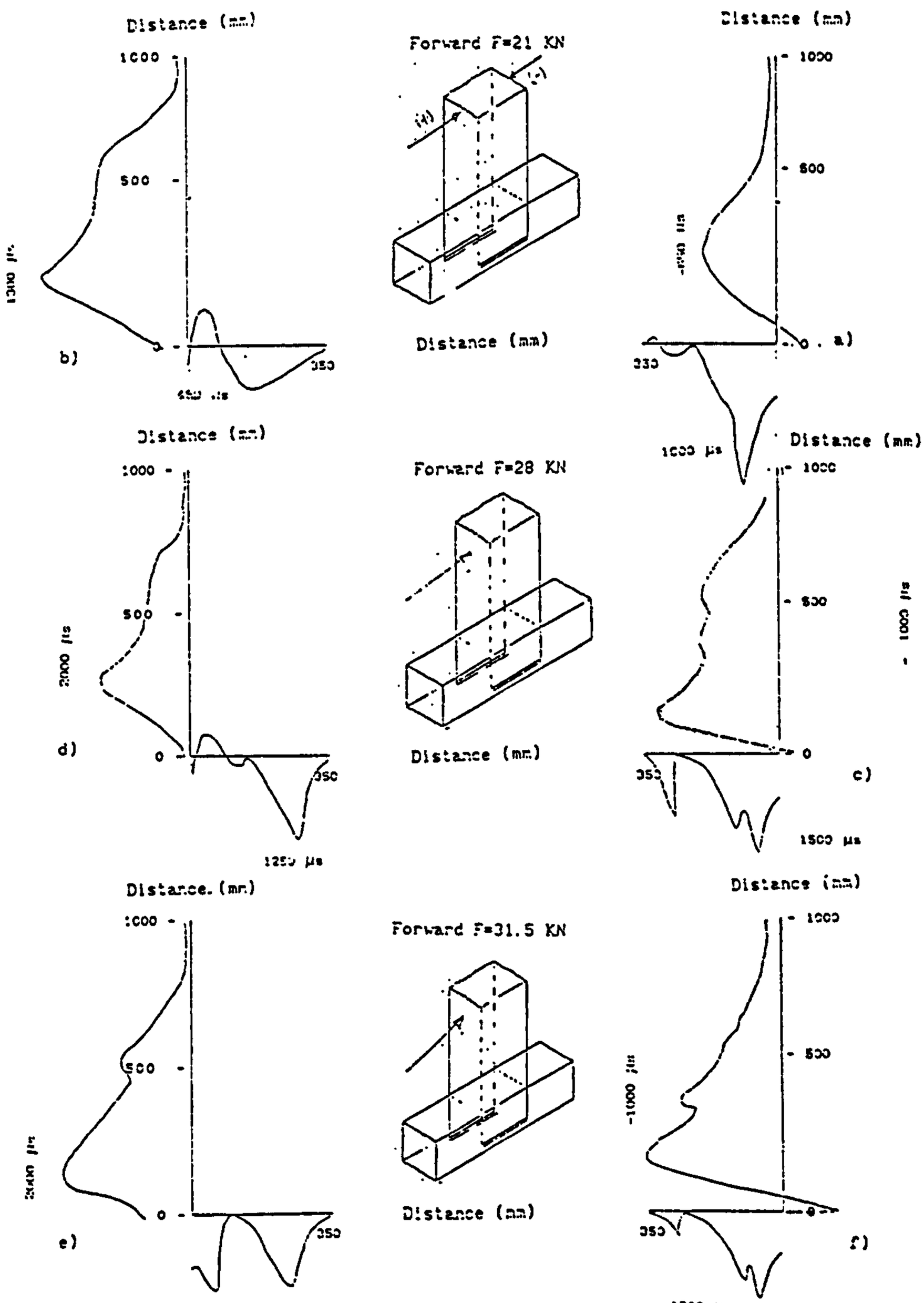

FIG.5.8 STRAIN DISTRIBUTION ALONG BEAM MAIN REINFORCEMENT (INCLUDING ANCHORAGE ZONE) - SPECIMEN UD2 -

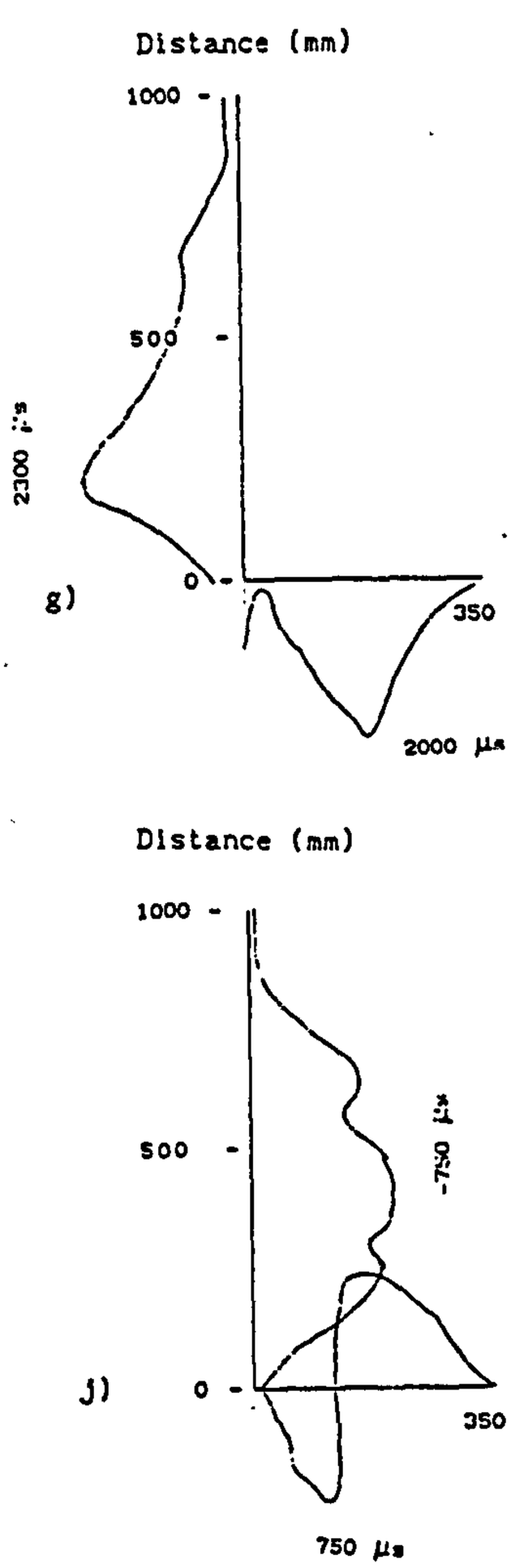
Distance (mm)
1000
500
0
2300 µs
350
2000 µs
g)

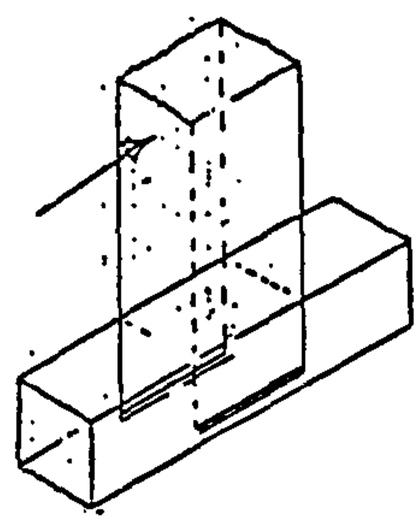
Forward F=35 KN
Distance (mm)

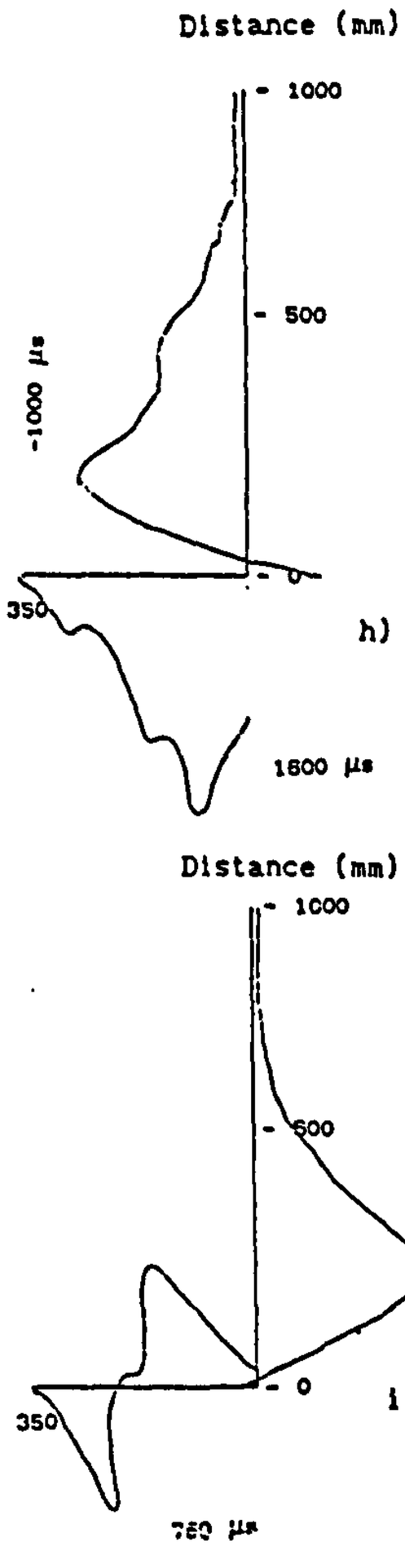
Distance (mm)
1000
500
0
-1000 µs
350
1600 µs
h)

Distance (mm)
1000
500
0
-750 µs
350
750 µs
j)

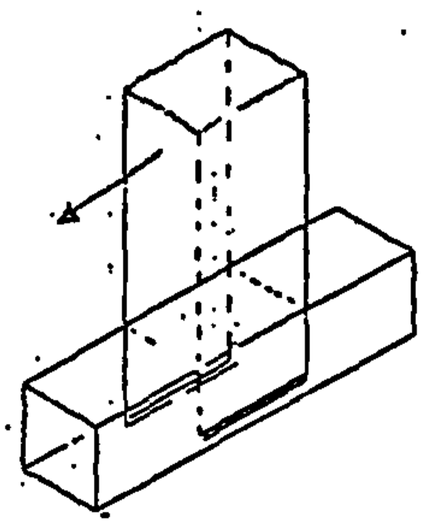
Backward F=-21 KN
Distance (mm)

Distance (mm)
1000
500
0
1300 µs
350
760 µs
i)

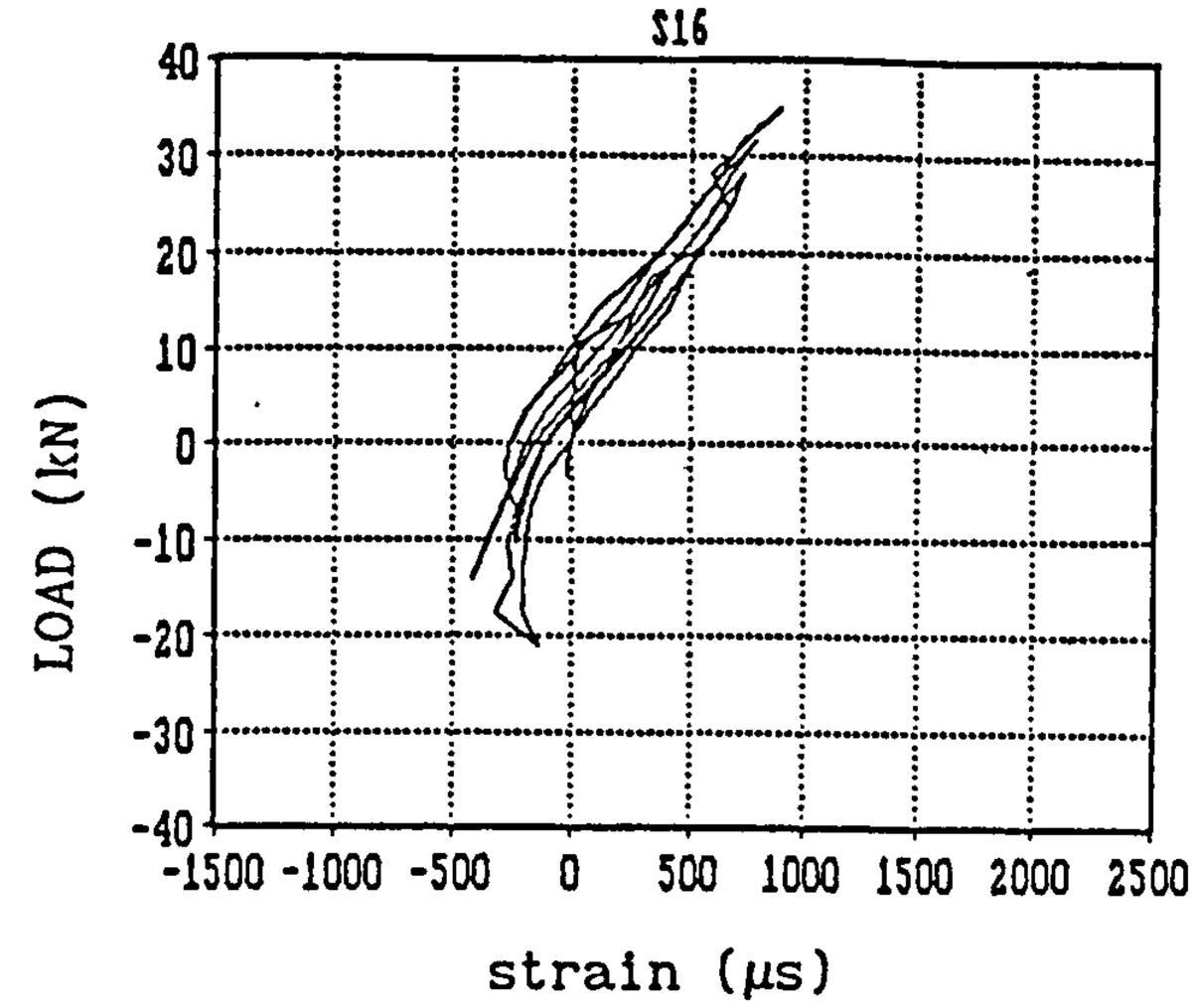

a)

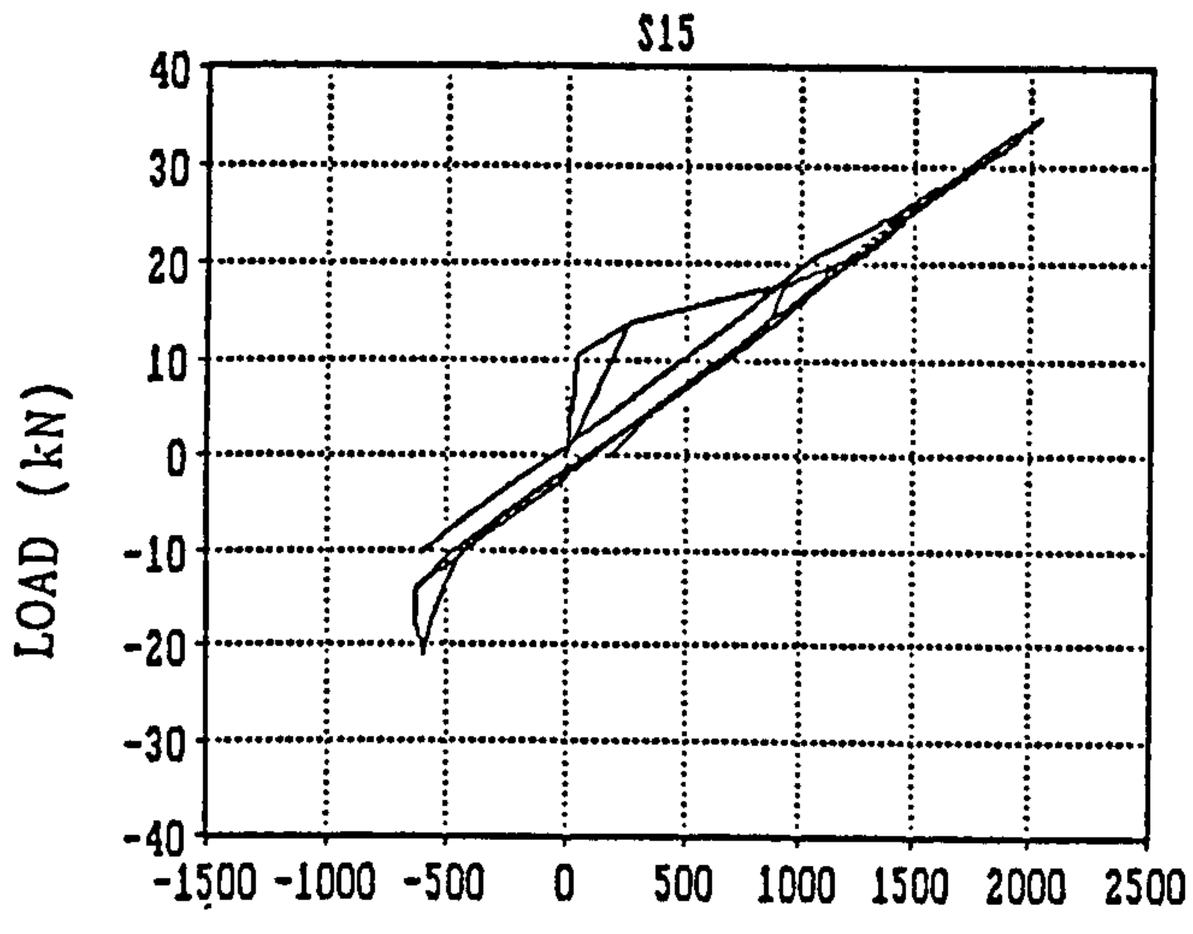

b)

c)

FIG.5.9 ANALYTICAL LOAD VS. STRAIN VARIATION

- BEAM MAIN REINFORCEMENT -

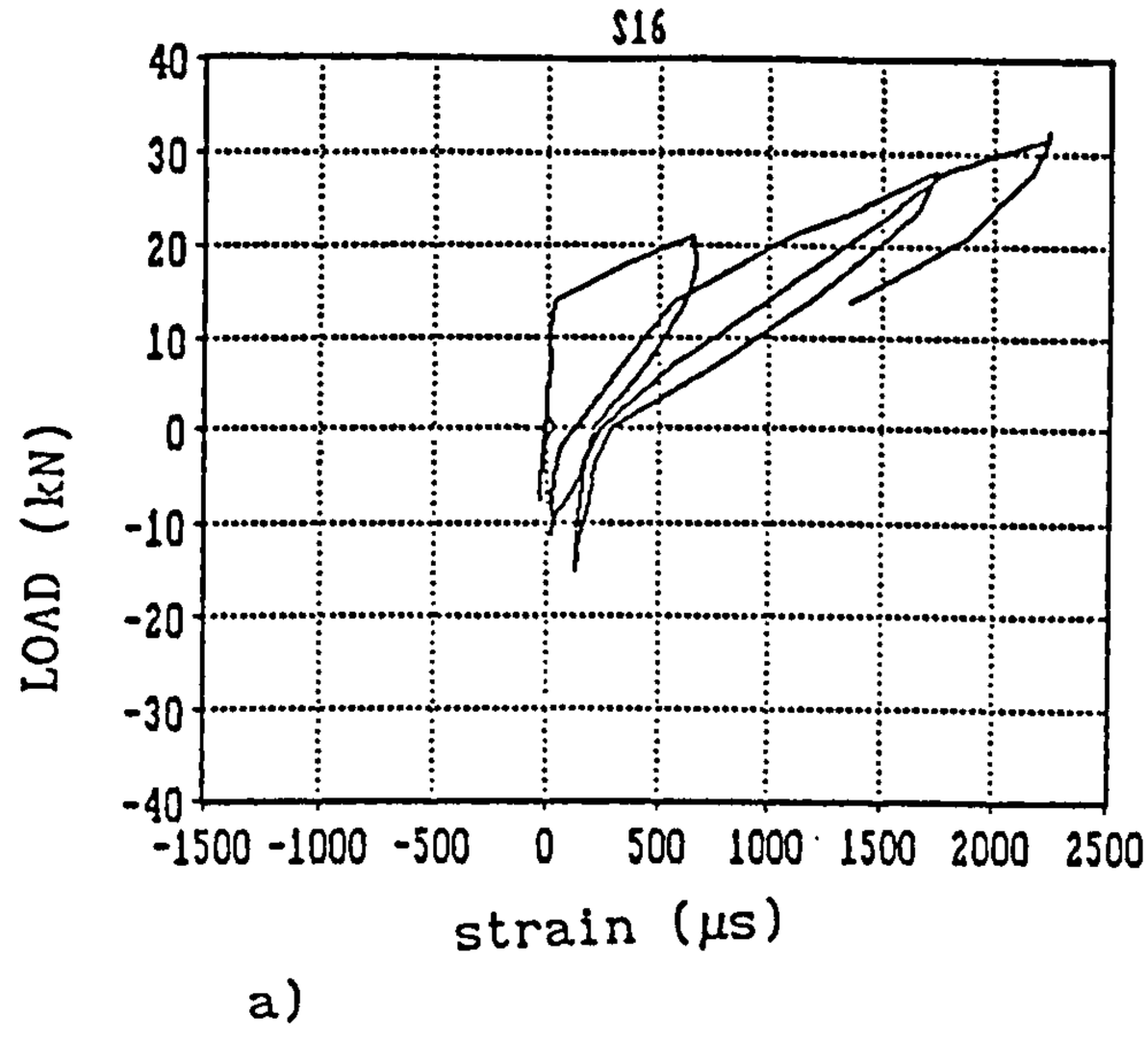

a)

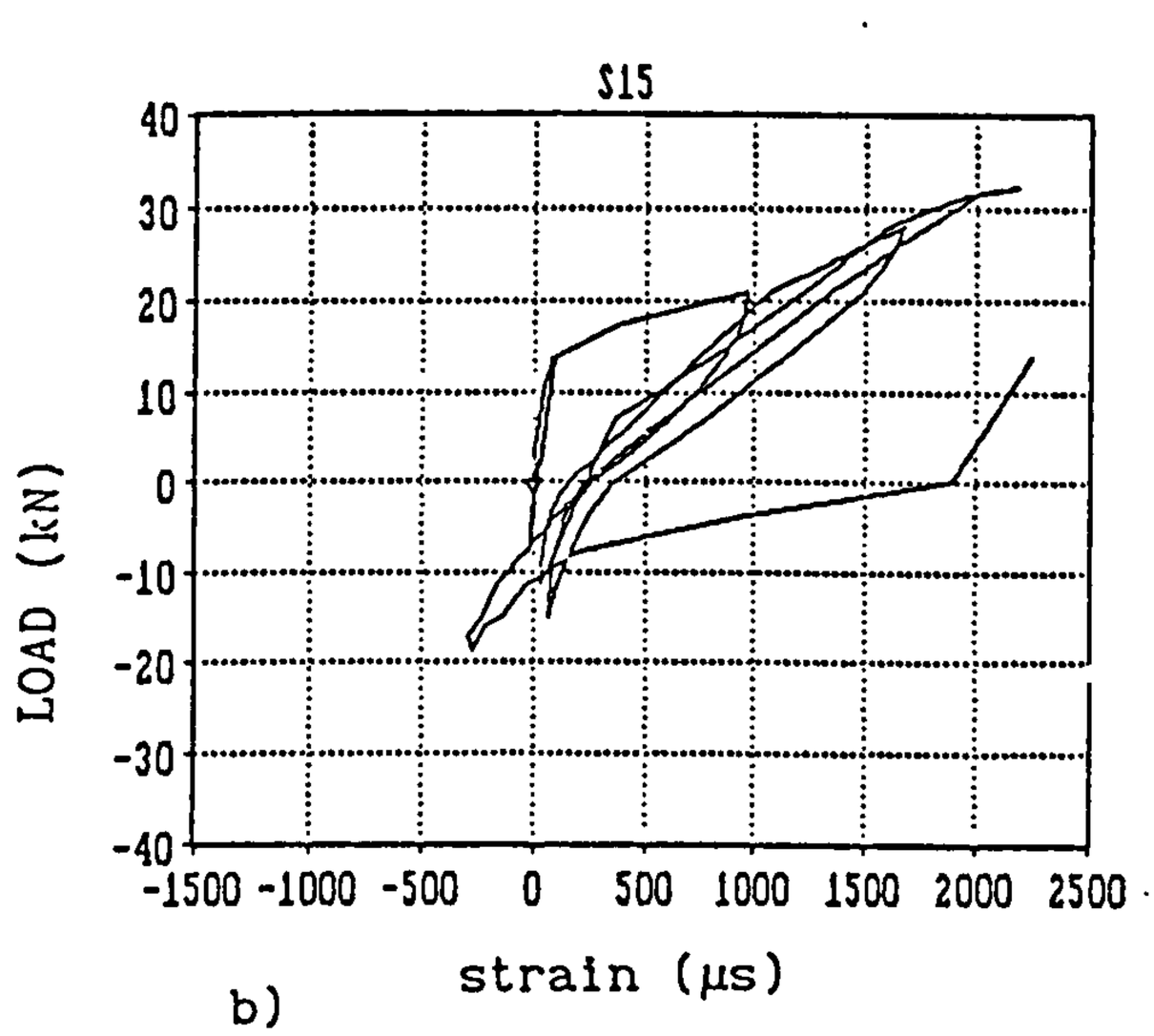

b)

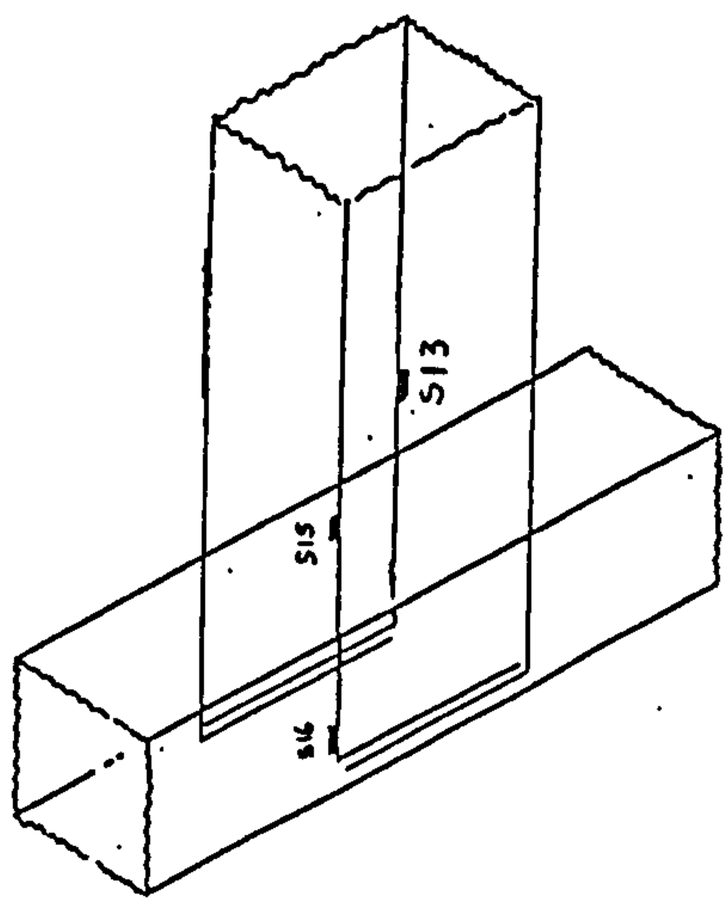

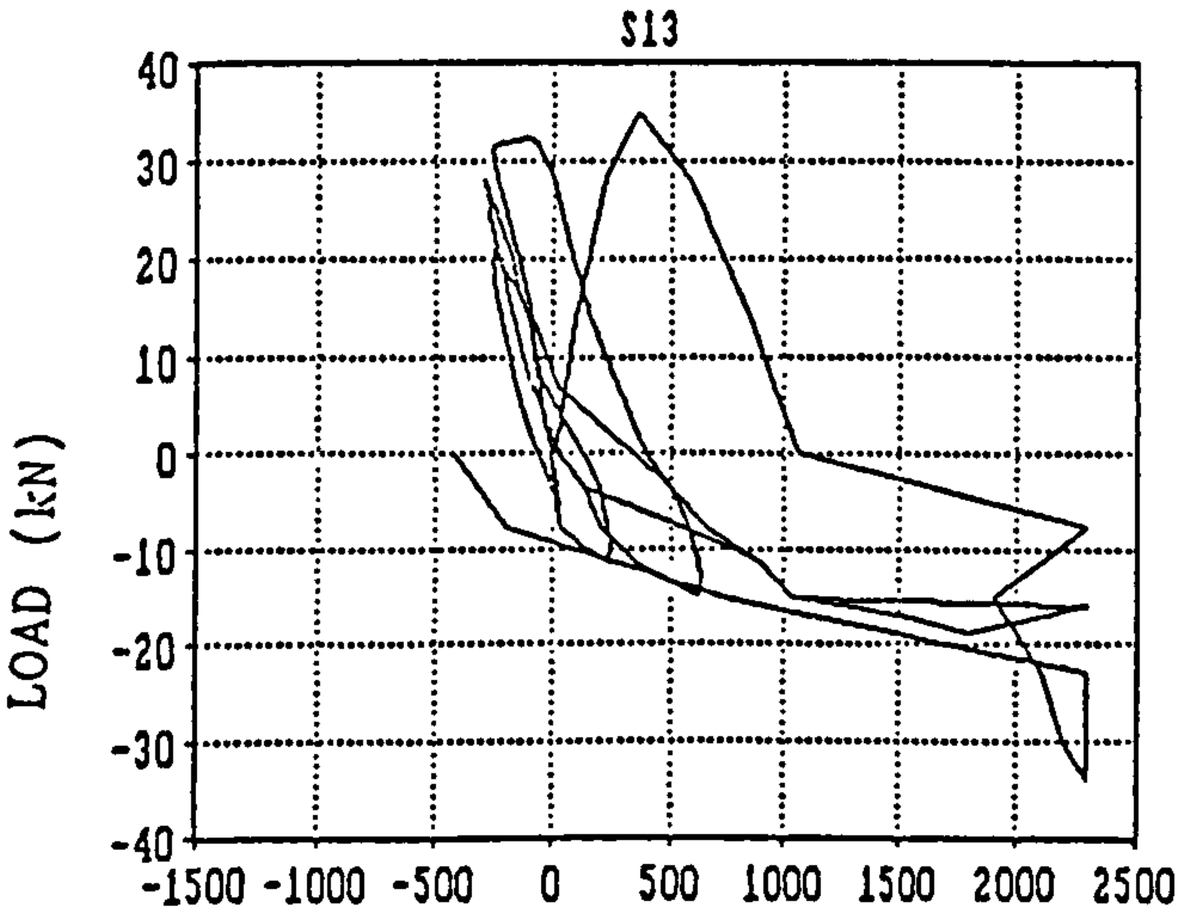

c)

FIG. 5.10 EXPERIMENTAL LOAD VS. STRAIN VARIATION

- BEAM MAIN REINFORCEMENT -

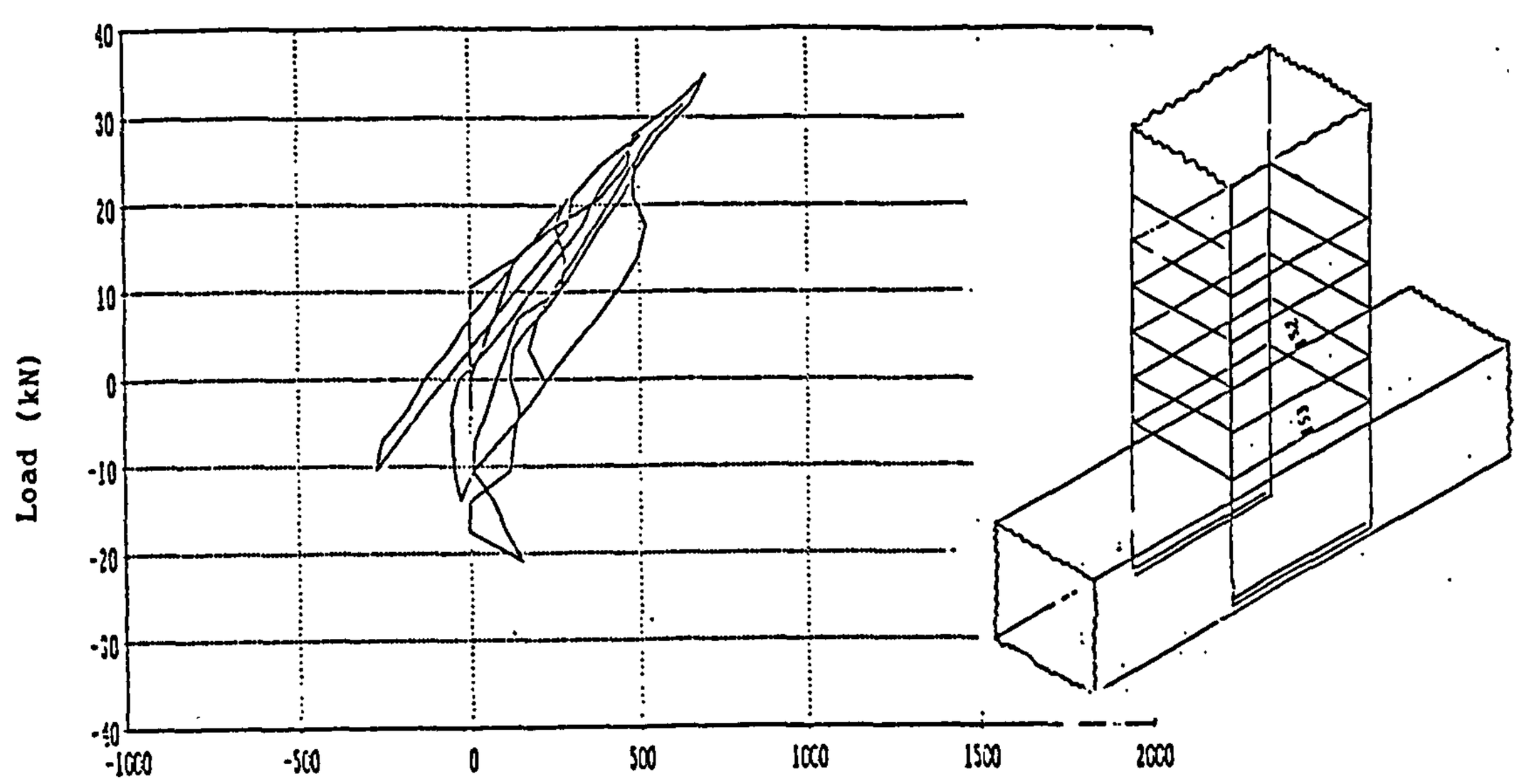

a) Analytical S2

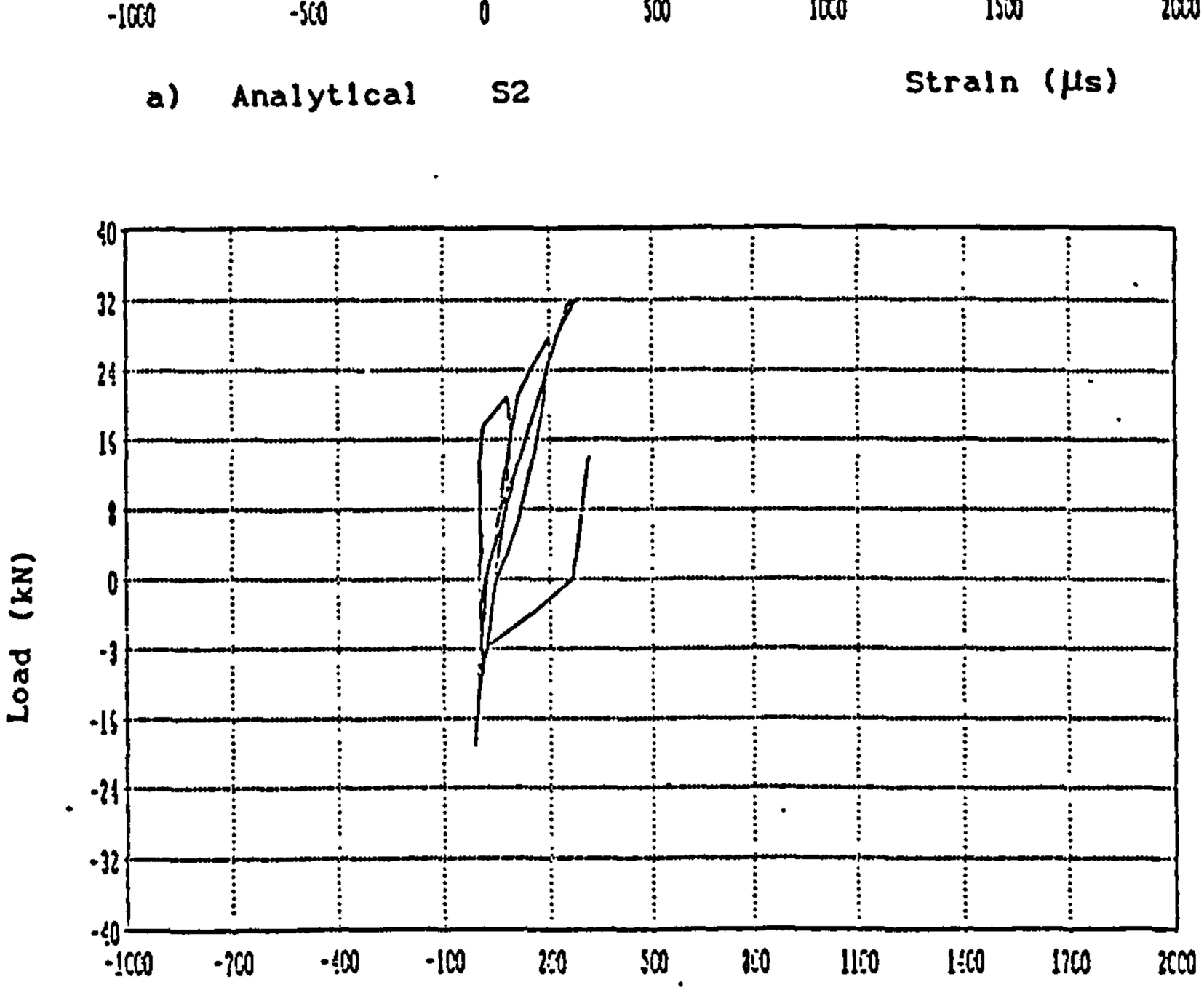

b) Experimental S2

Fig.5.11 ANALYTICAL AND EXPERIMENTAL LOAD VS. STRAIN

- BEAM STIRRUPS -

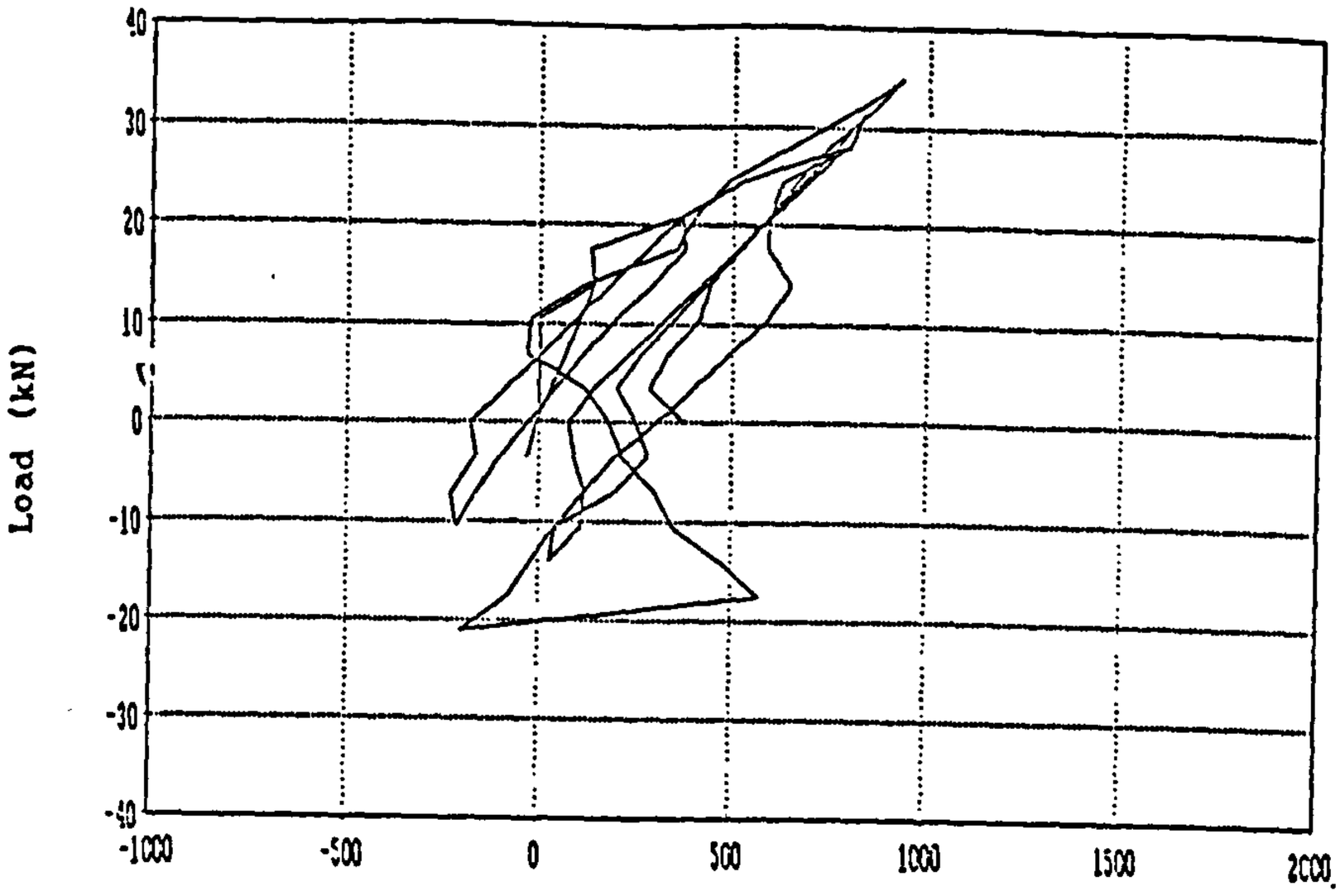

c) Analytical S3

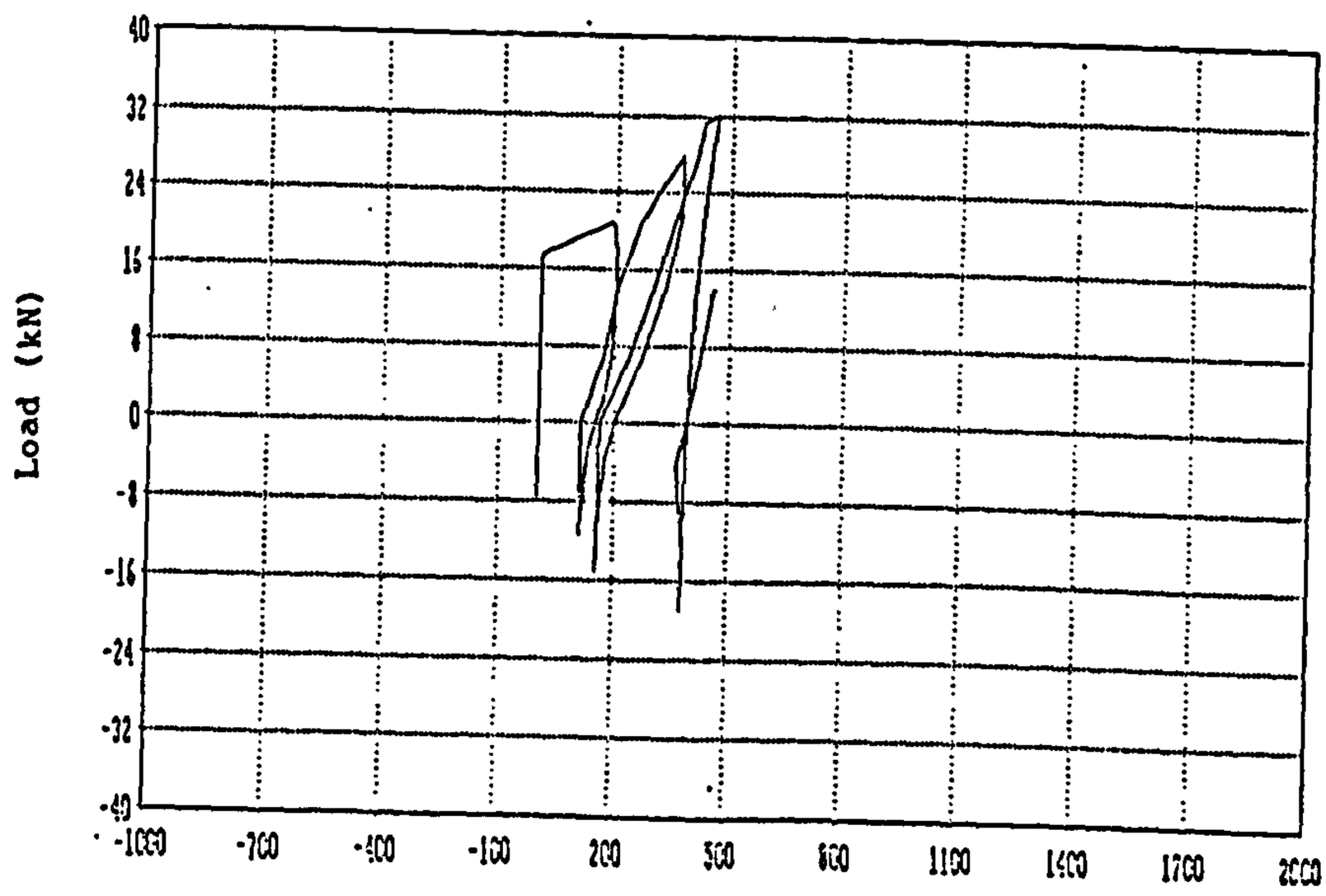

d) Experimental S3

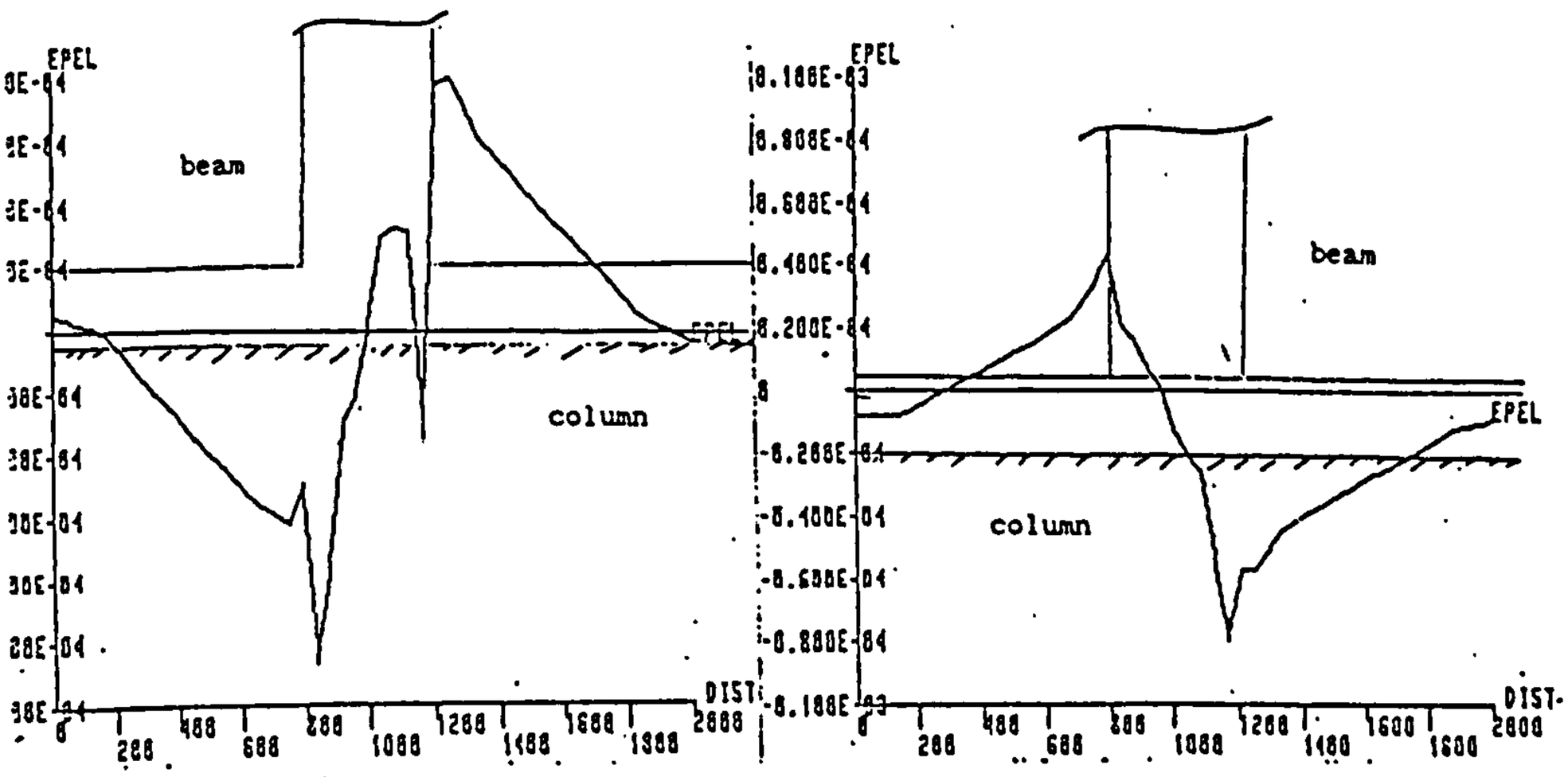

FIG.5.12 STRAIN VARIATION ALONG COLUMN MAIN BARS

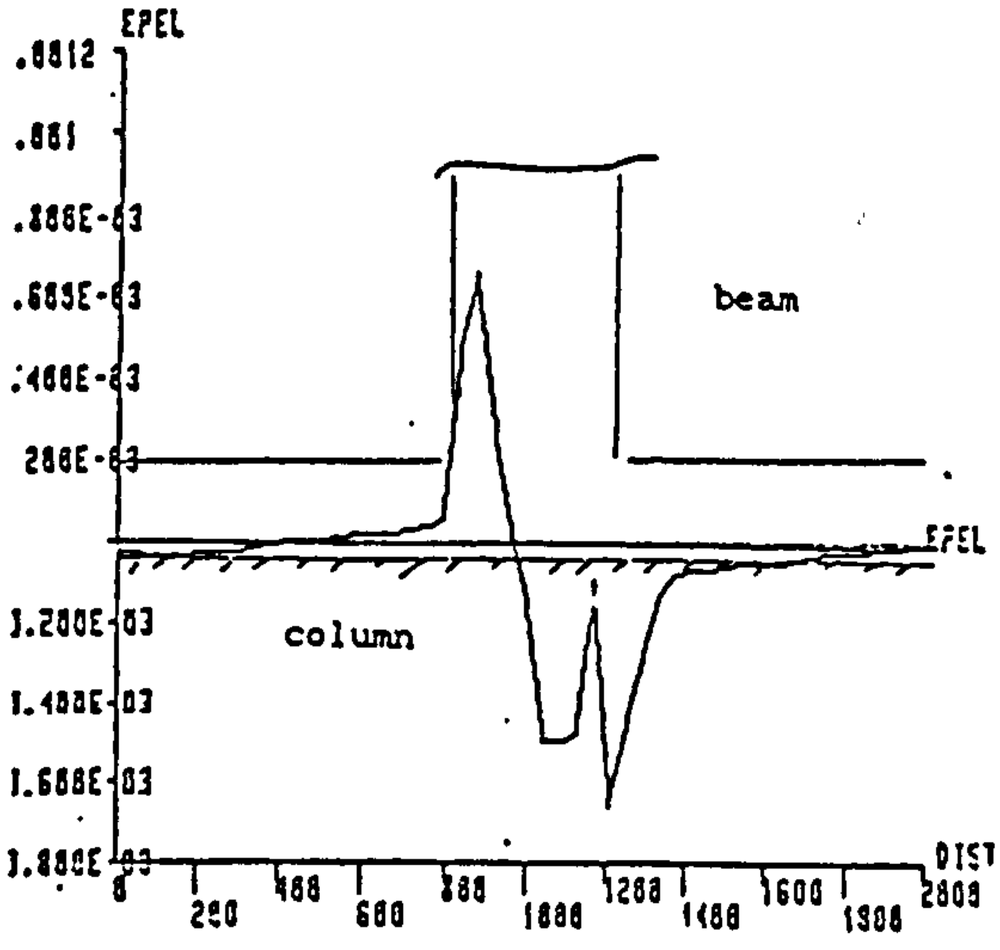

e)

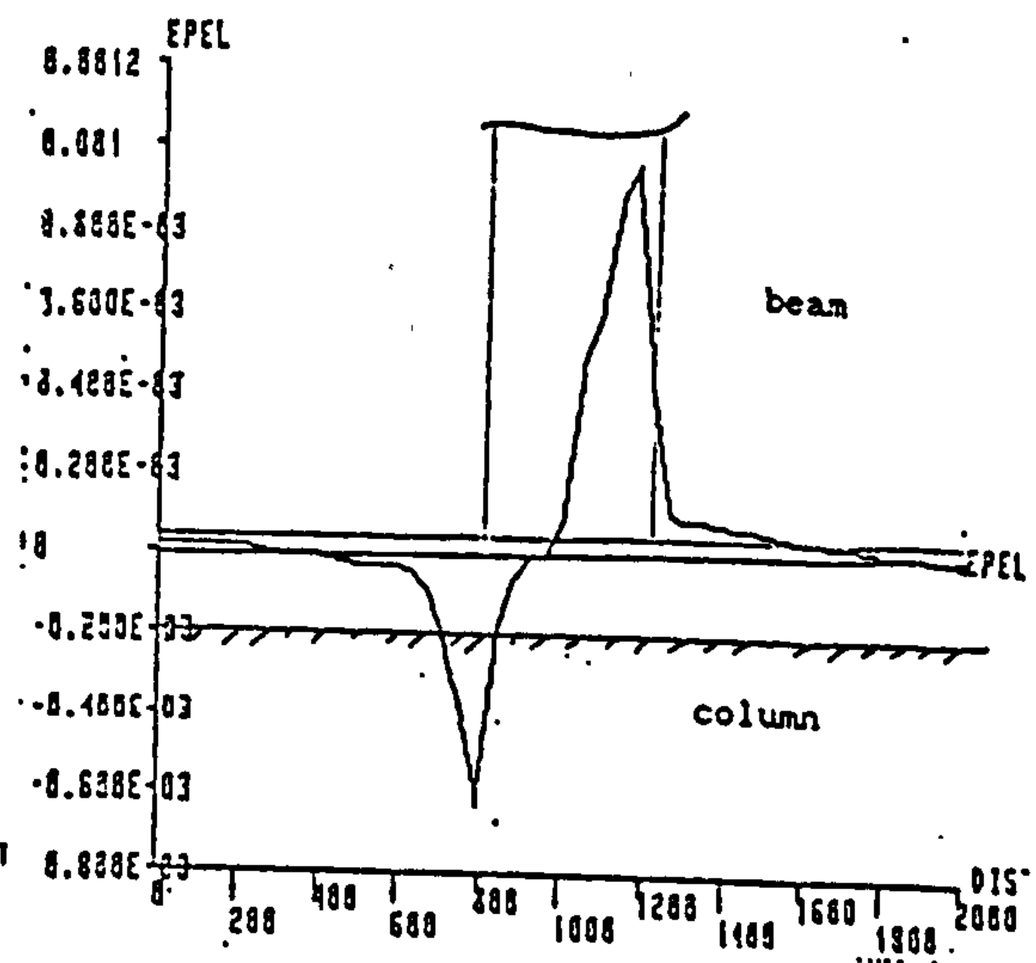

f)

F = 24.5 KN

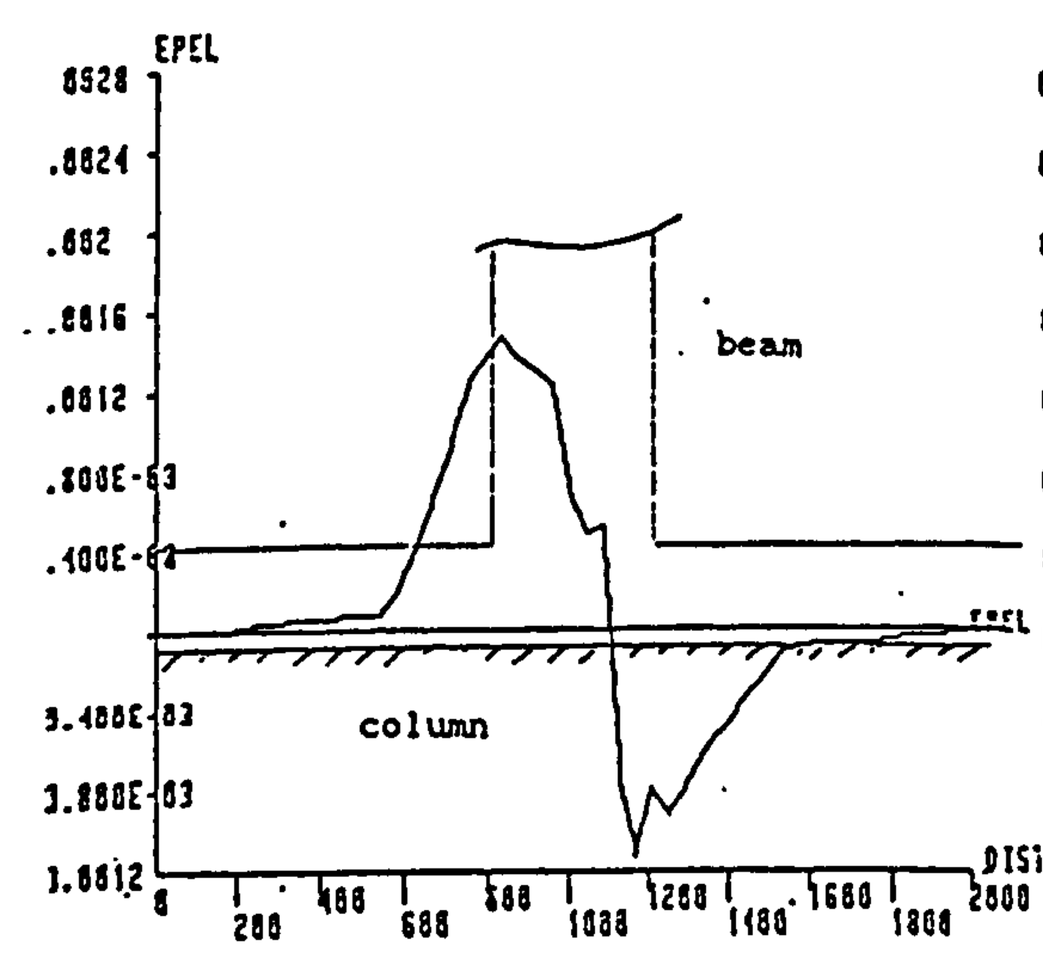

g)

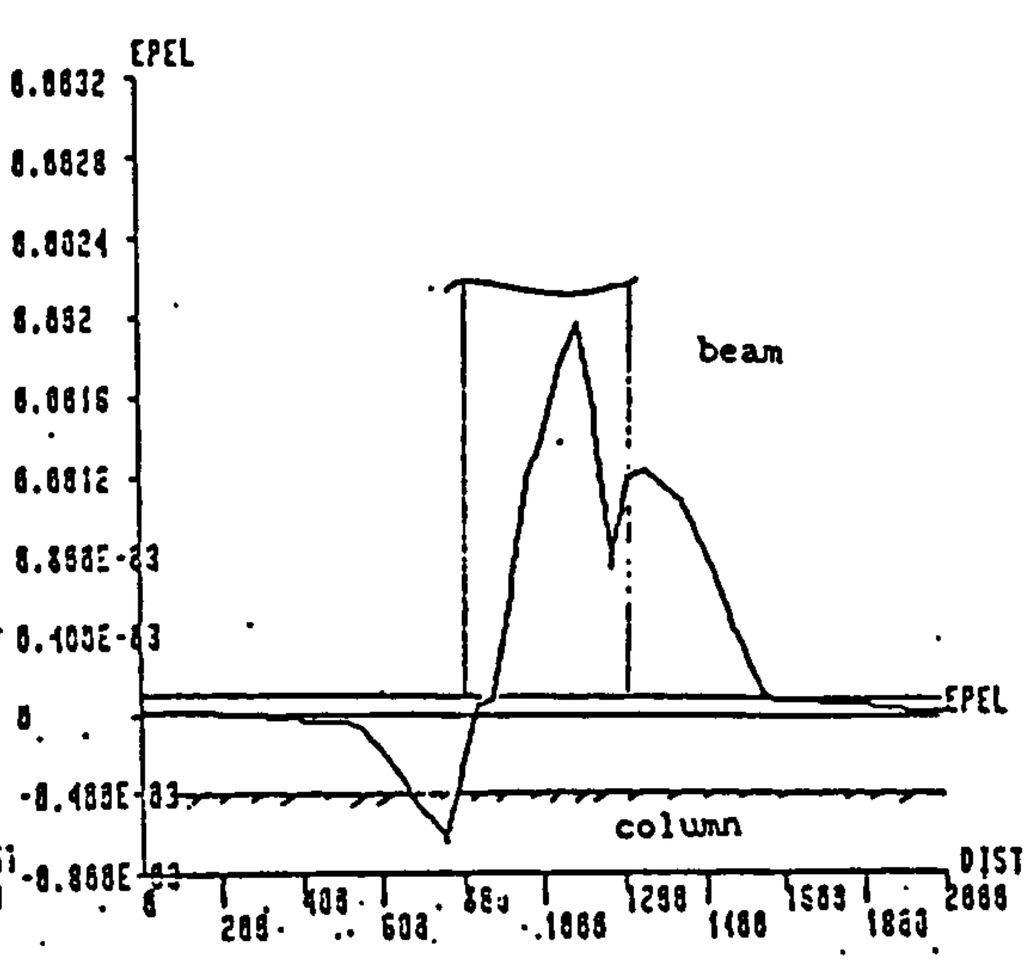

h)

F = 35 KN

a), c), e) and g) Outer bars

b), d), f) and h) Inner bars

* EPEL: Elastic strain

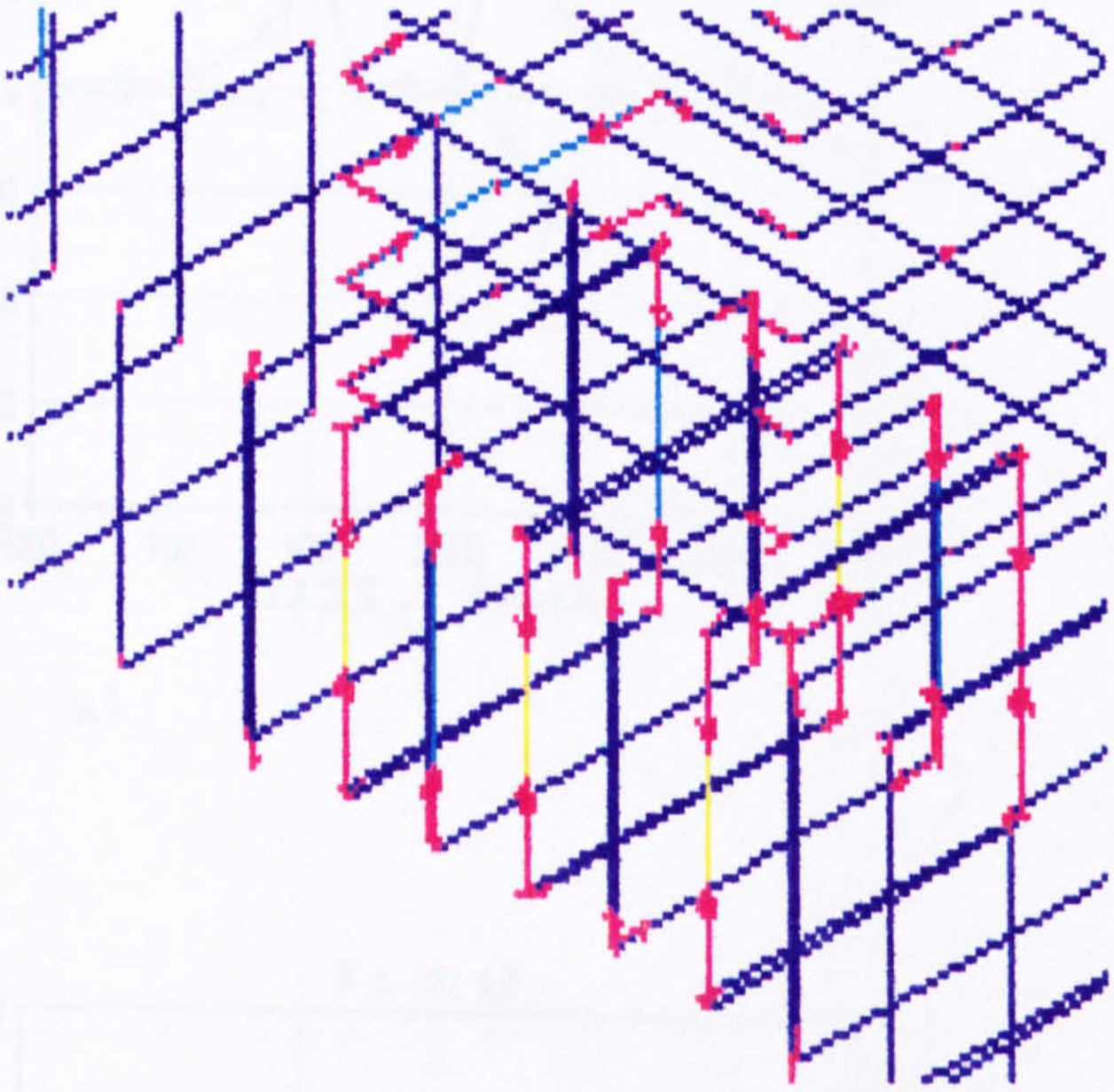

FIG.5.13 REACTION FORCES AND STRAIN DISTRIBUTION

IN U-STIRRUPS - JOINT AREA -

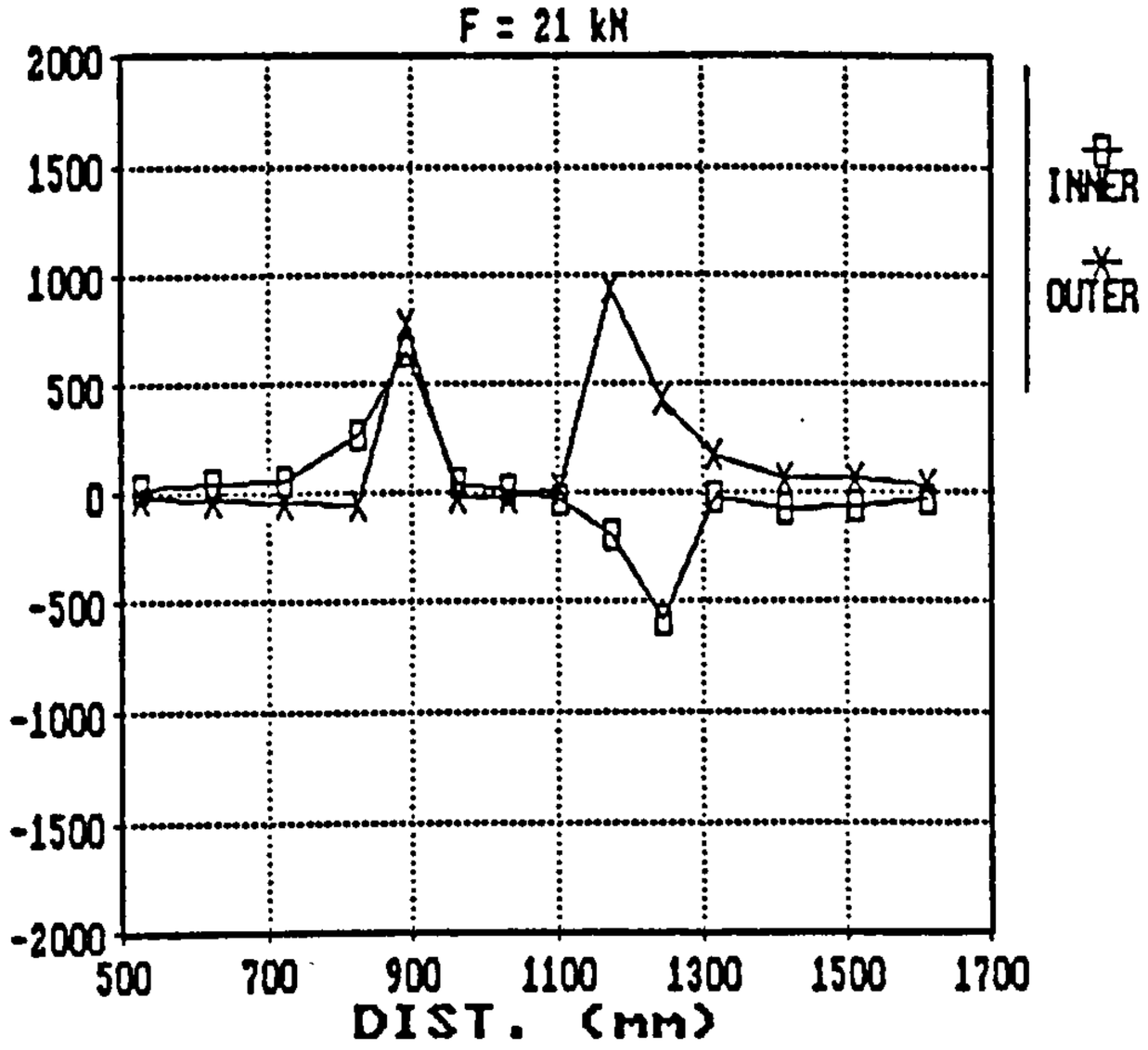

a)

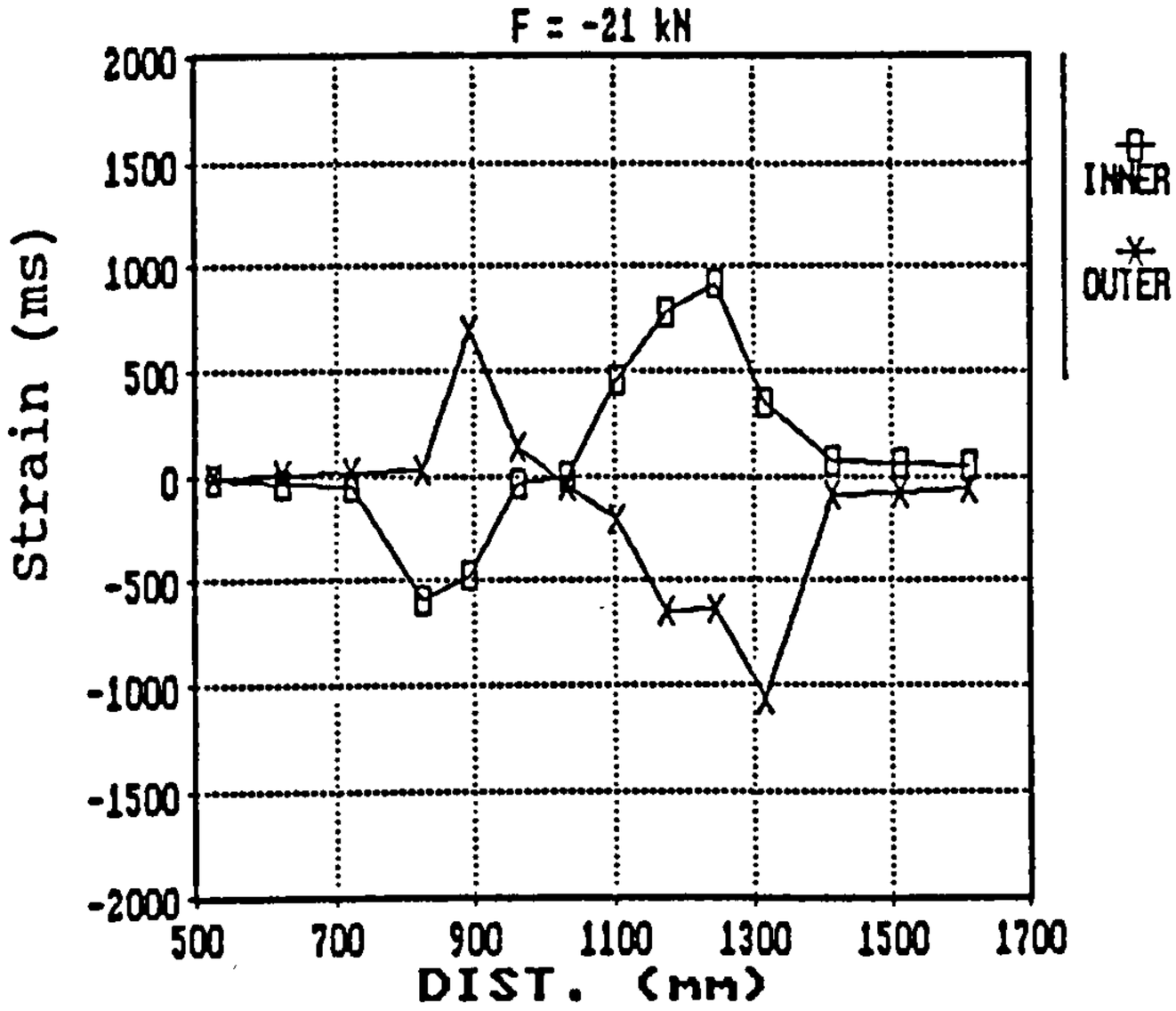

b)

FIG.5.14 STRAIN VARIATION IN U-STIRRUPS LEGS ALONG JOINT

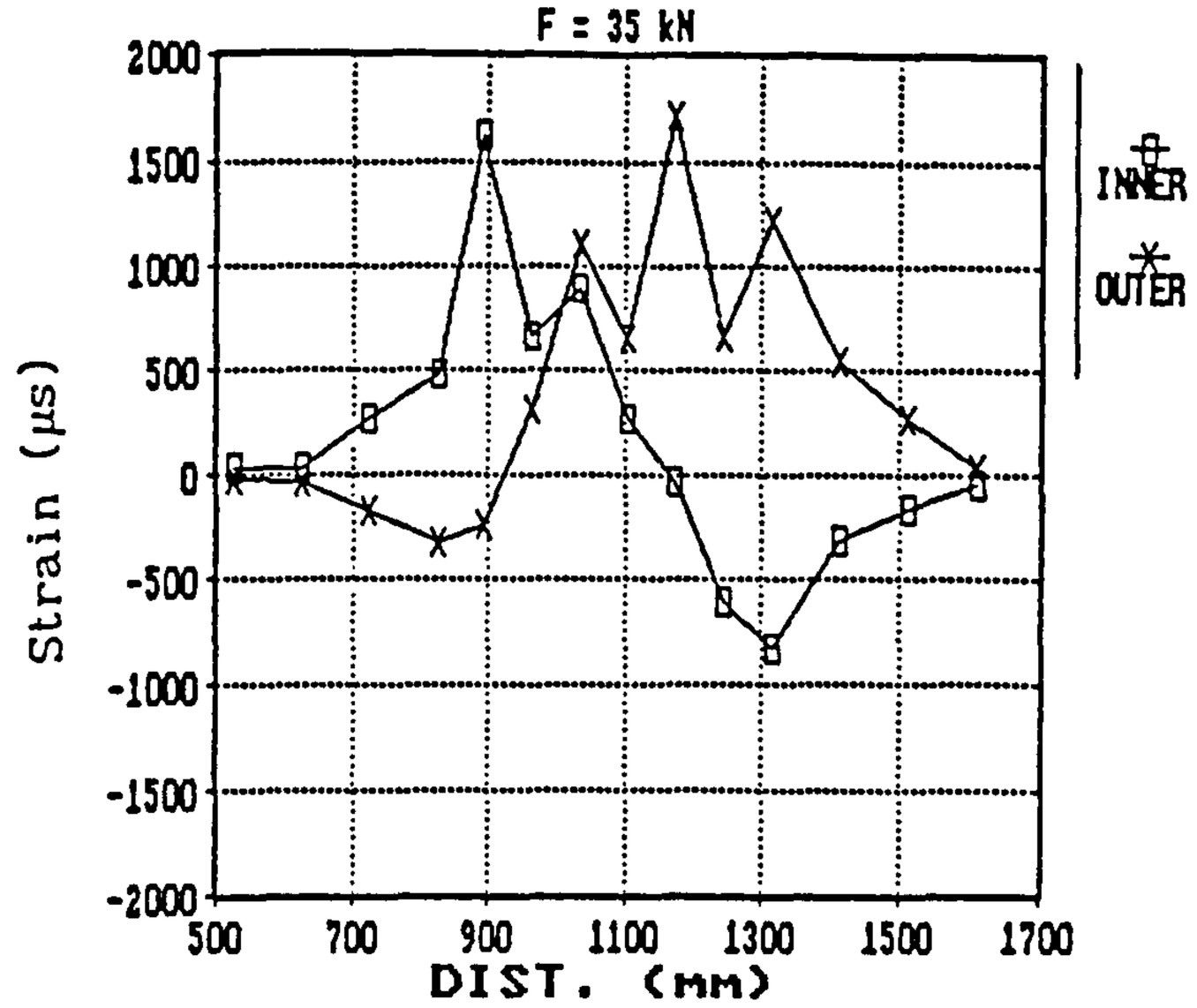
F = 35 kN
2000
1500
1000
500
0
-500
-1000
-1500
-2000
Strain (μs)
500
700
900
1100
1300
1500
1700
DIST. (mm)
INNER
OUTER

c)

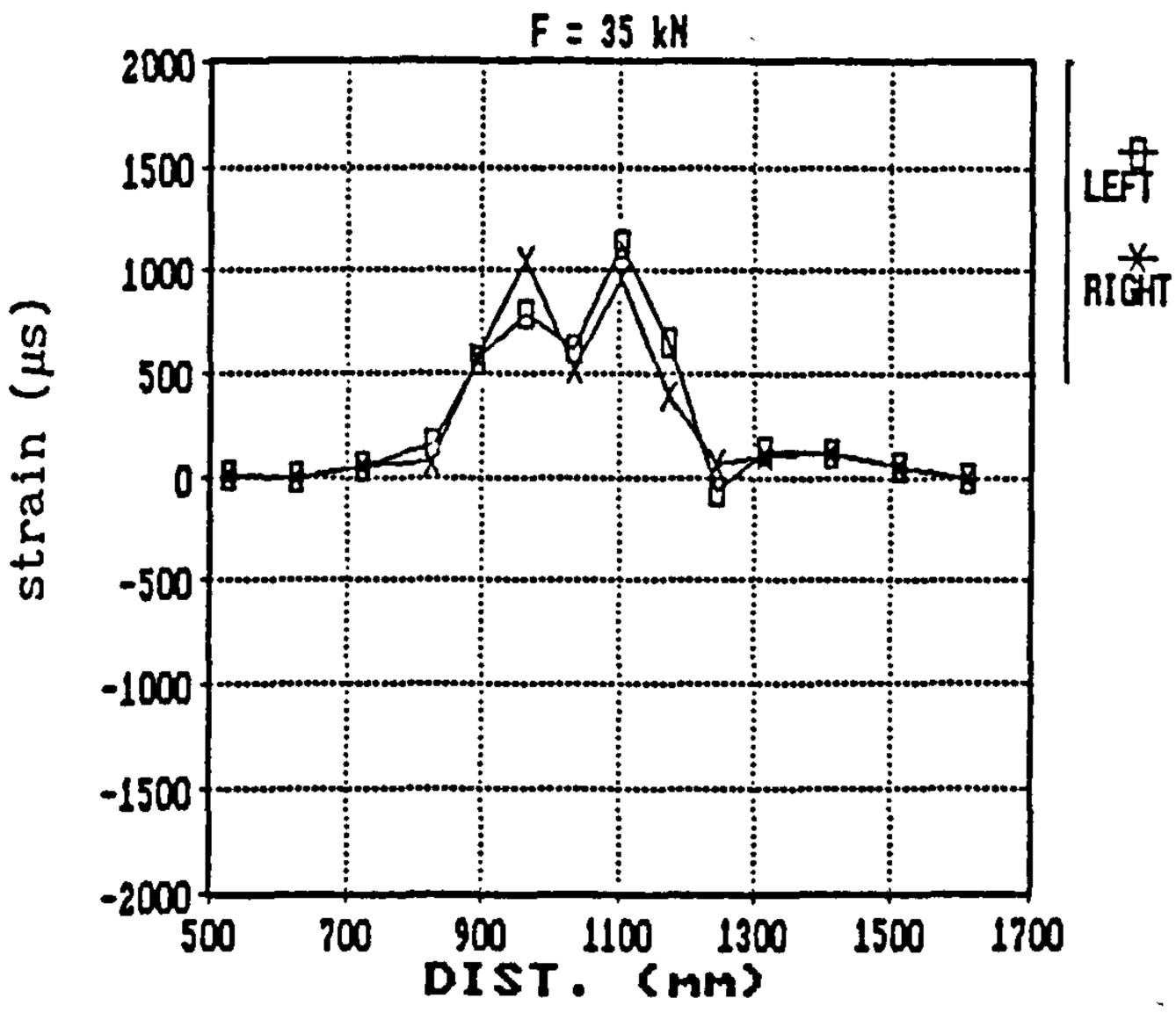
F = 35 kN
2000
1500
1000
500
0
-500
-1000
-1500
-2000
strain (μs)
500
700
900
1100
1300
1500
1700
DIST. (mm)
LEFT
RIGHT

d)

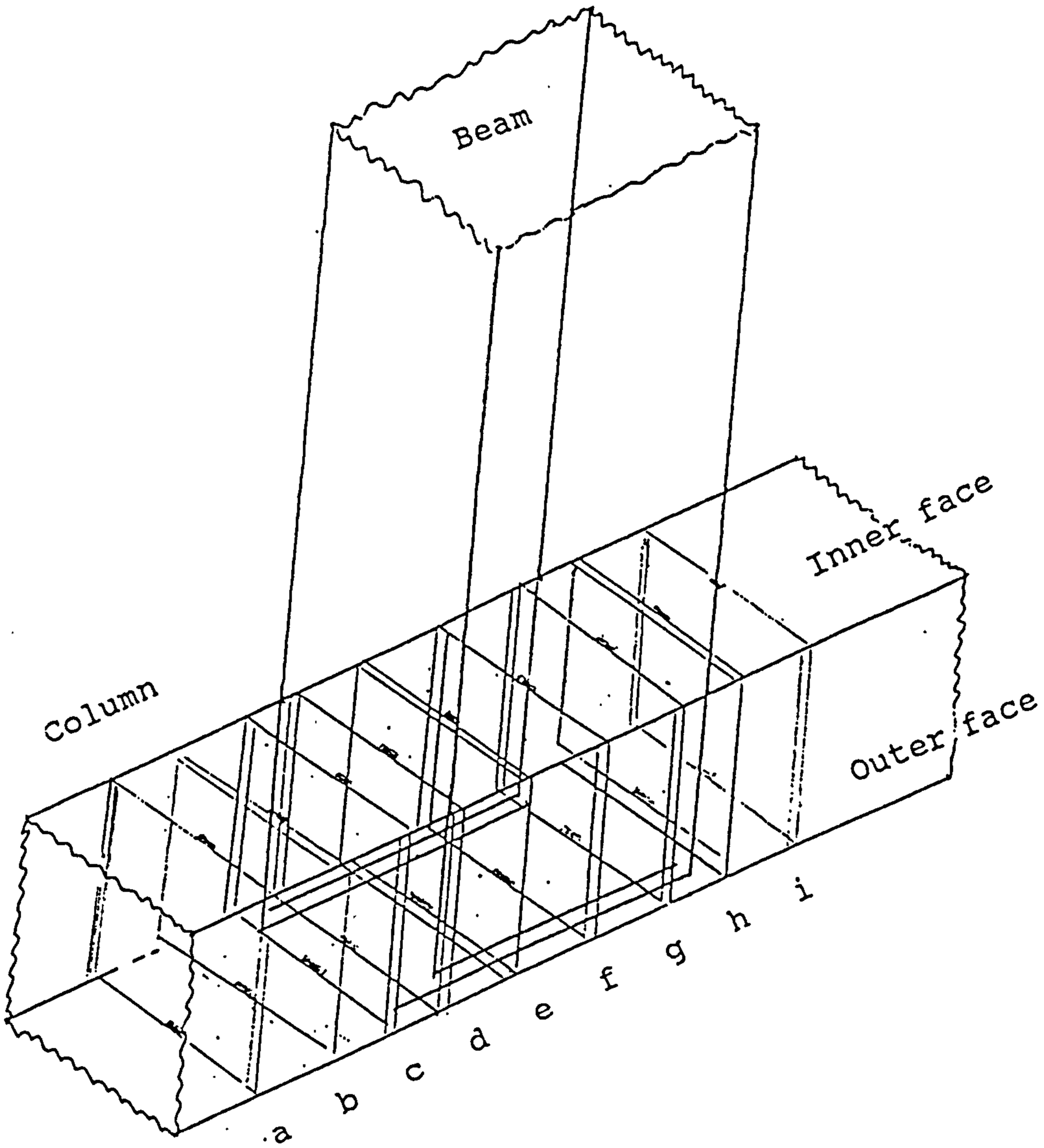

e) Locations of recorded strains

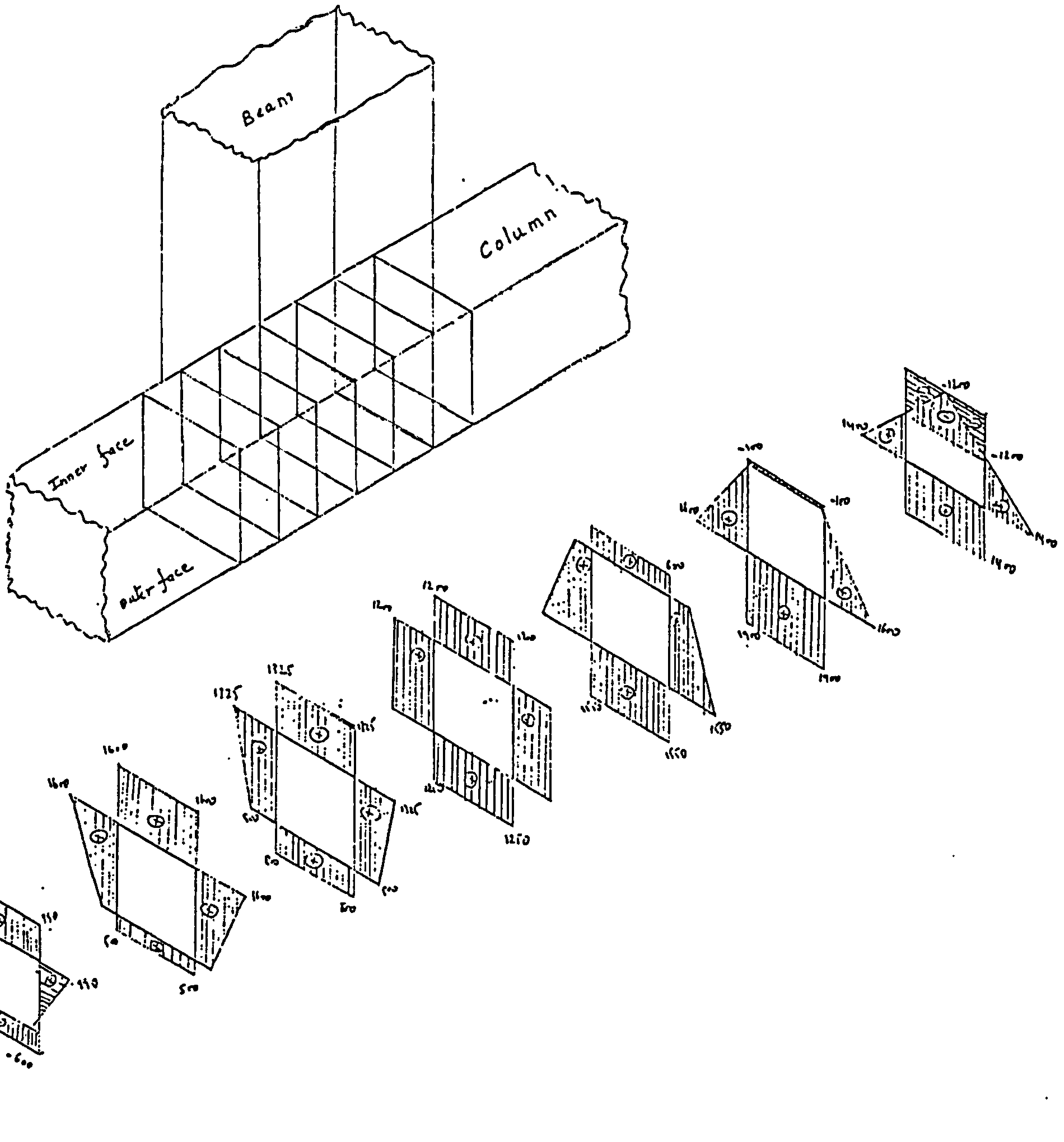

f) Strain variation in joint region in:

inner, outer, left and right stirrups legs

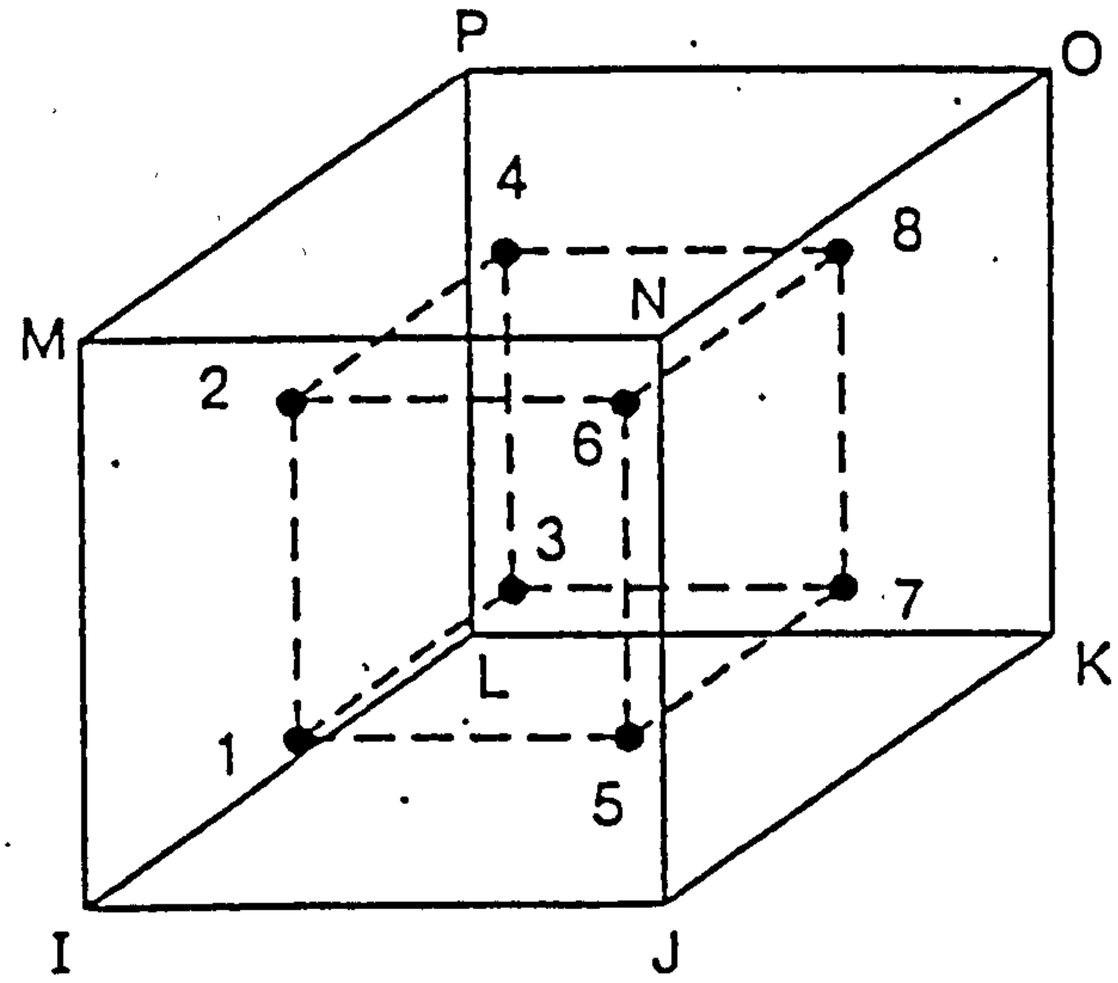

a) Integration point schemes

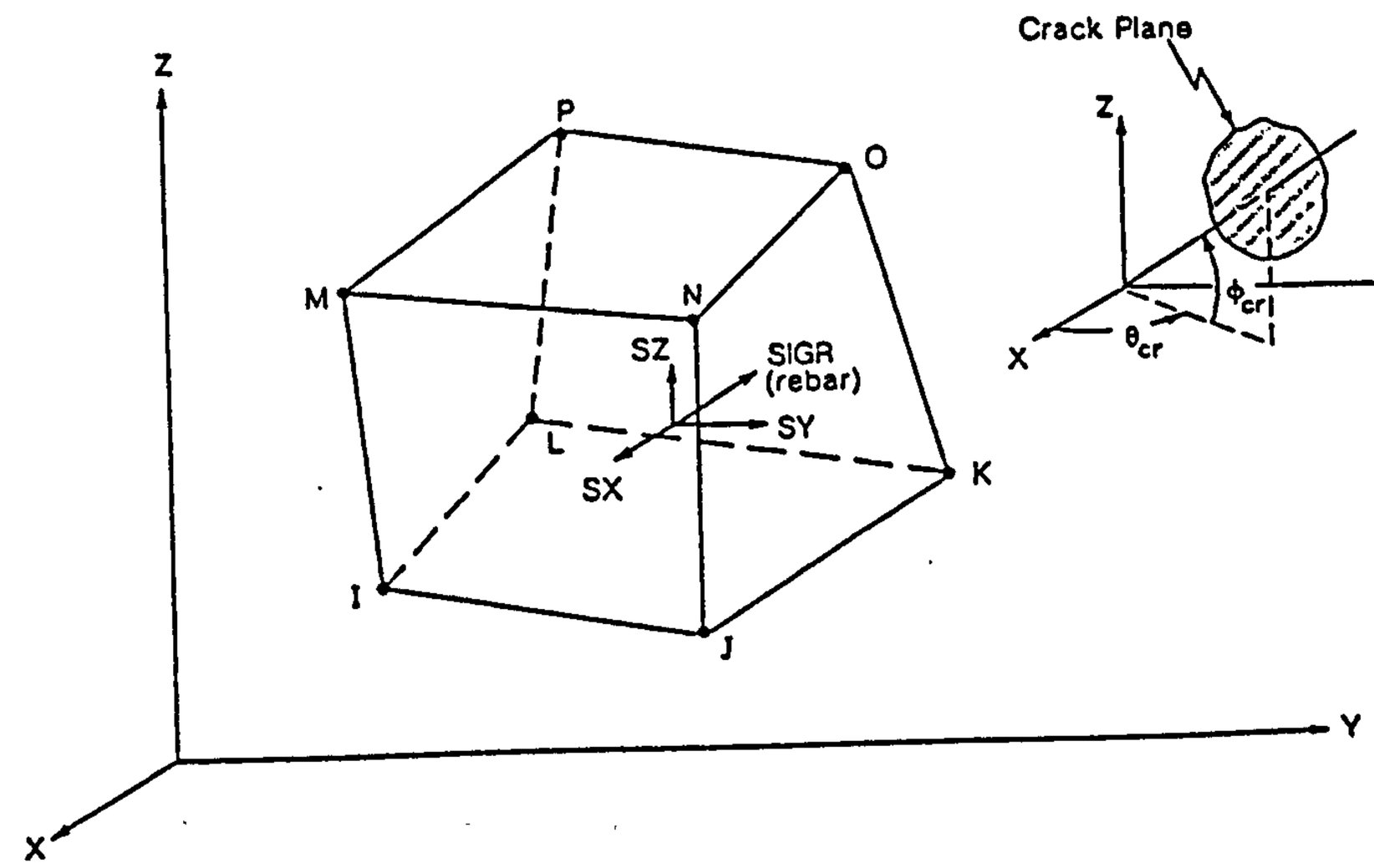

b) Crack directions

FIG.5.15 REPRESENTATION OF CRACKS

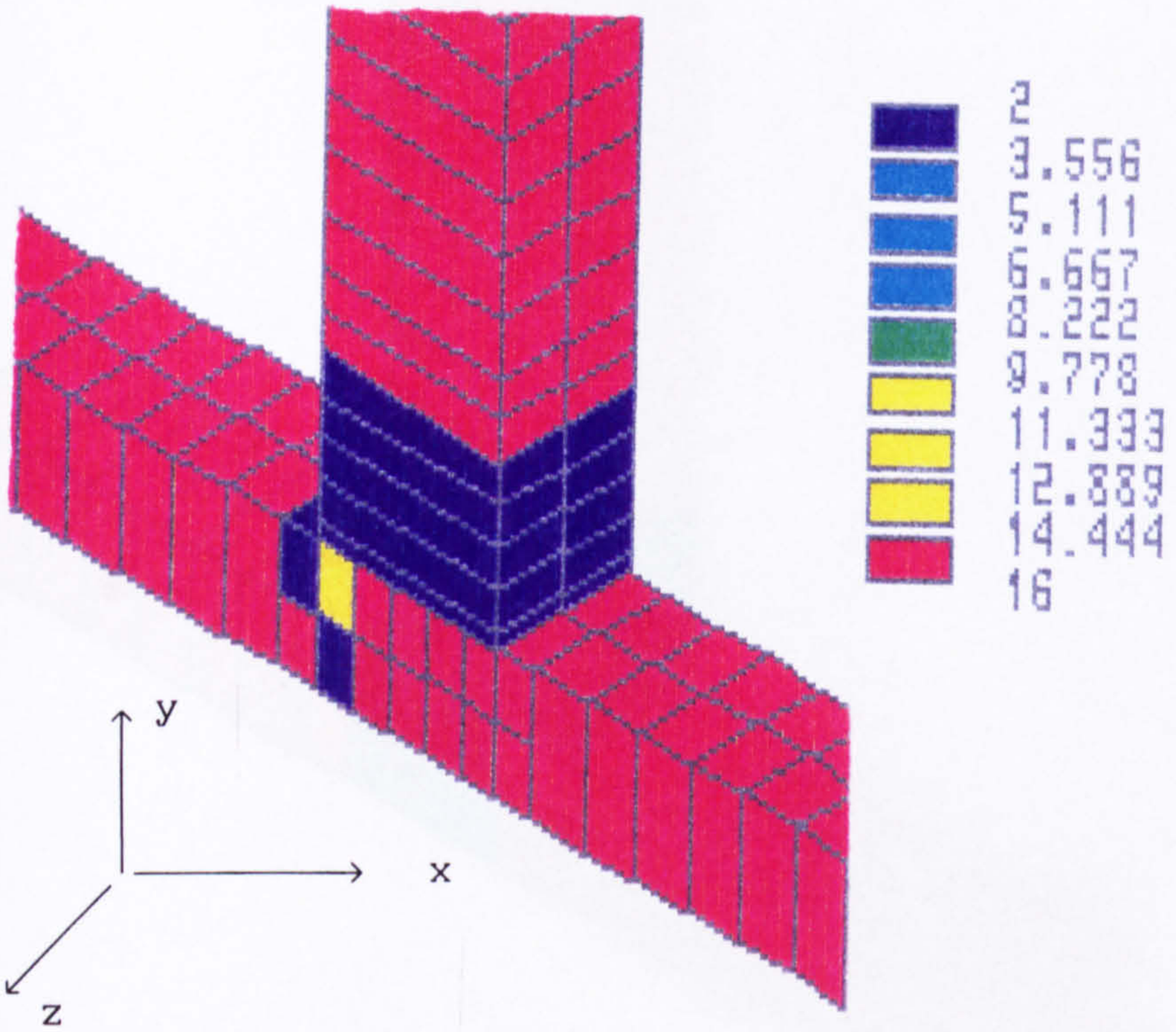

c)

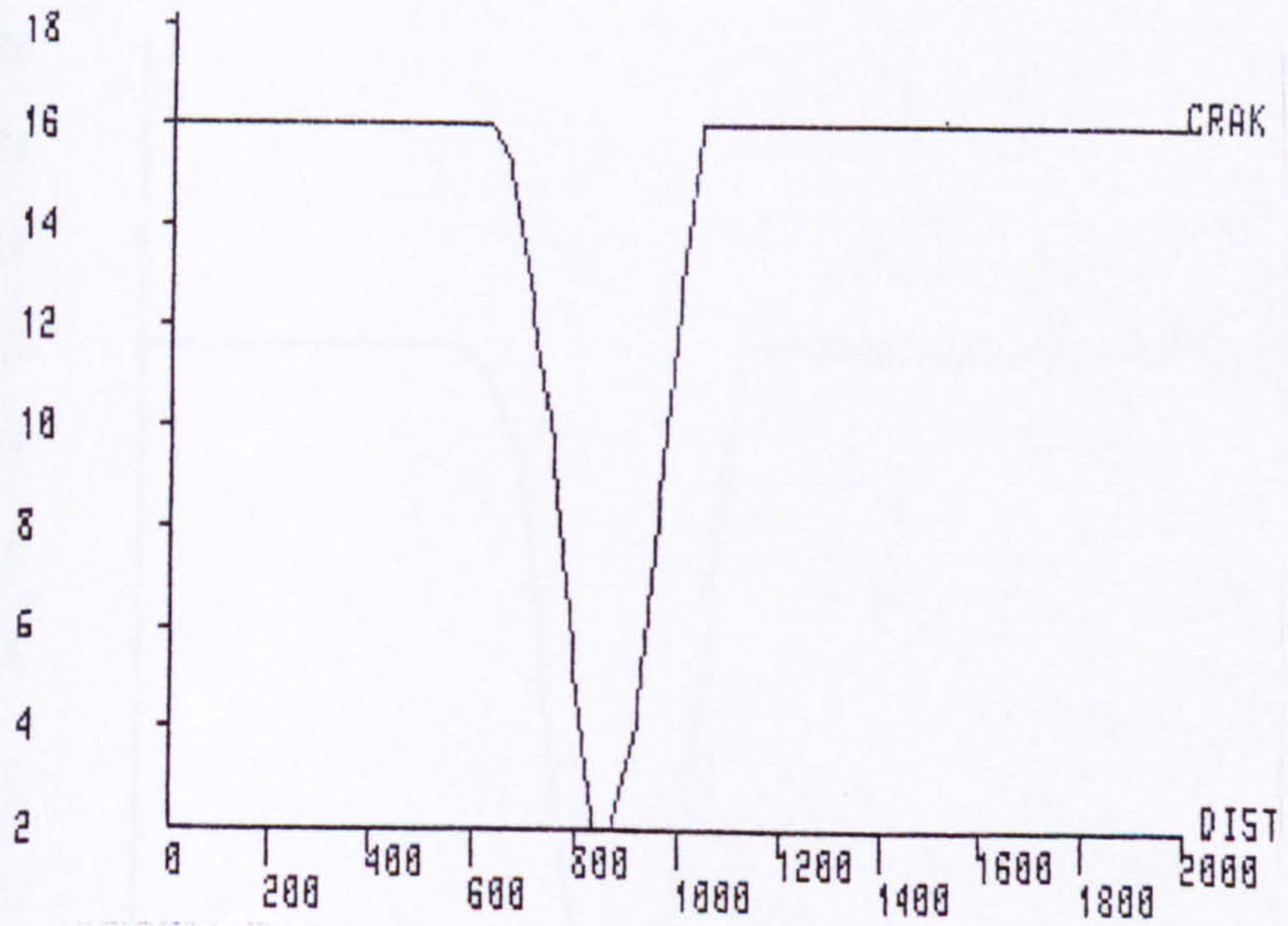

d) Column length

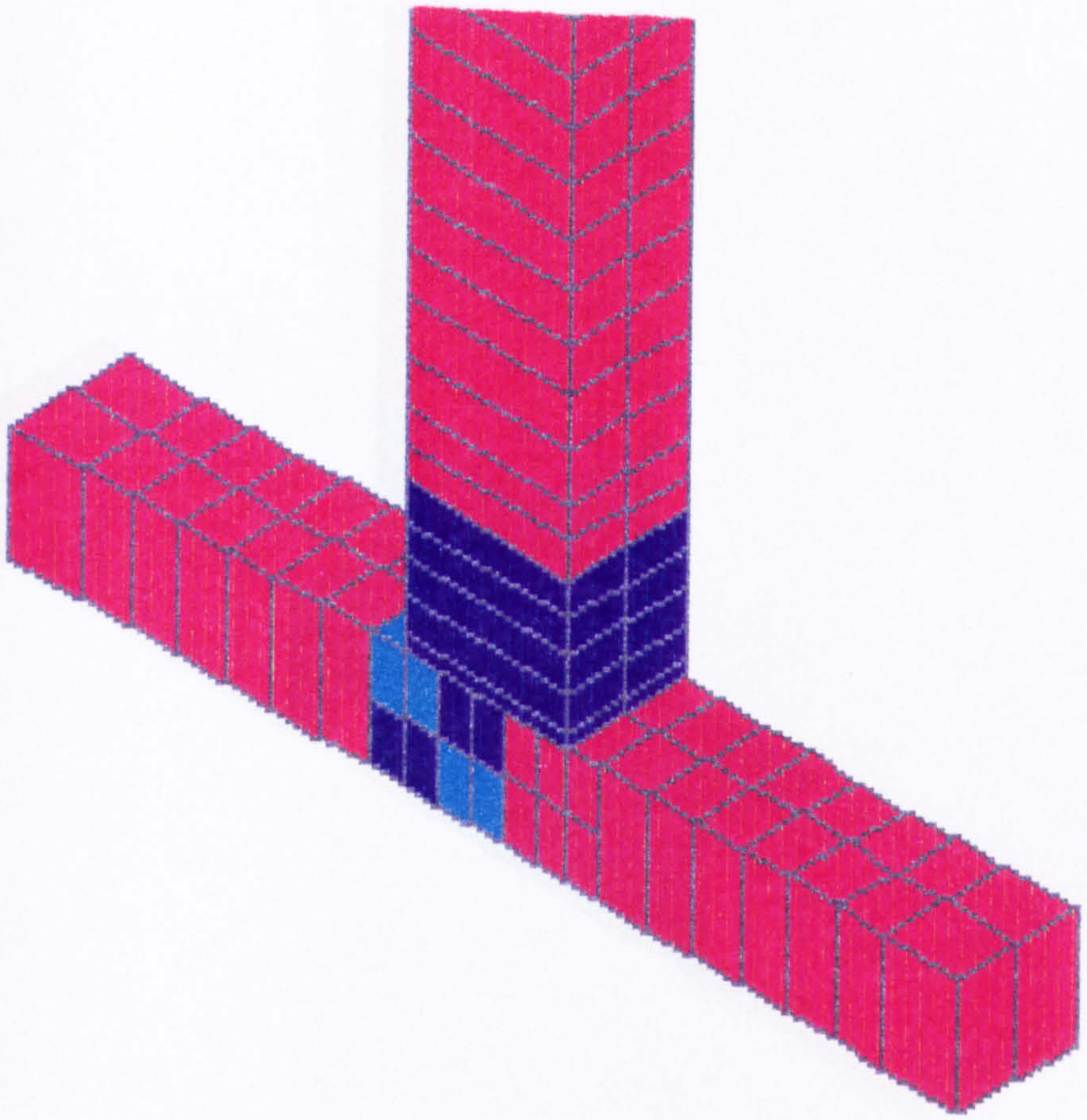

e)

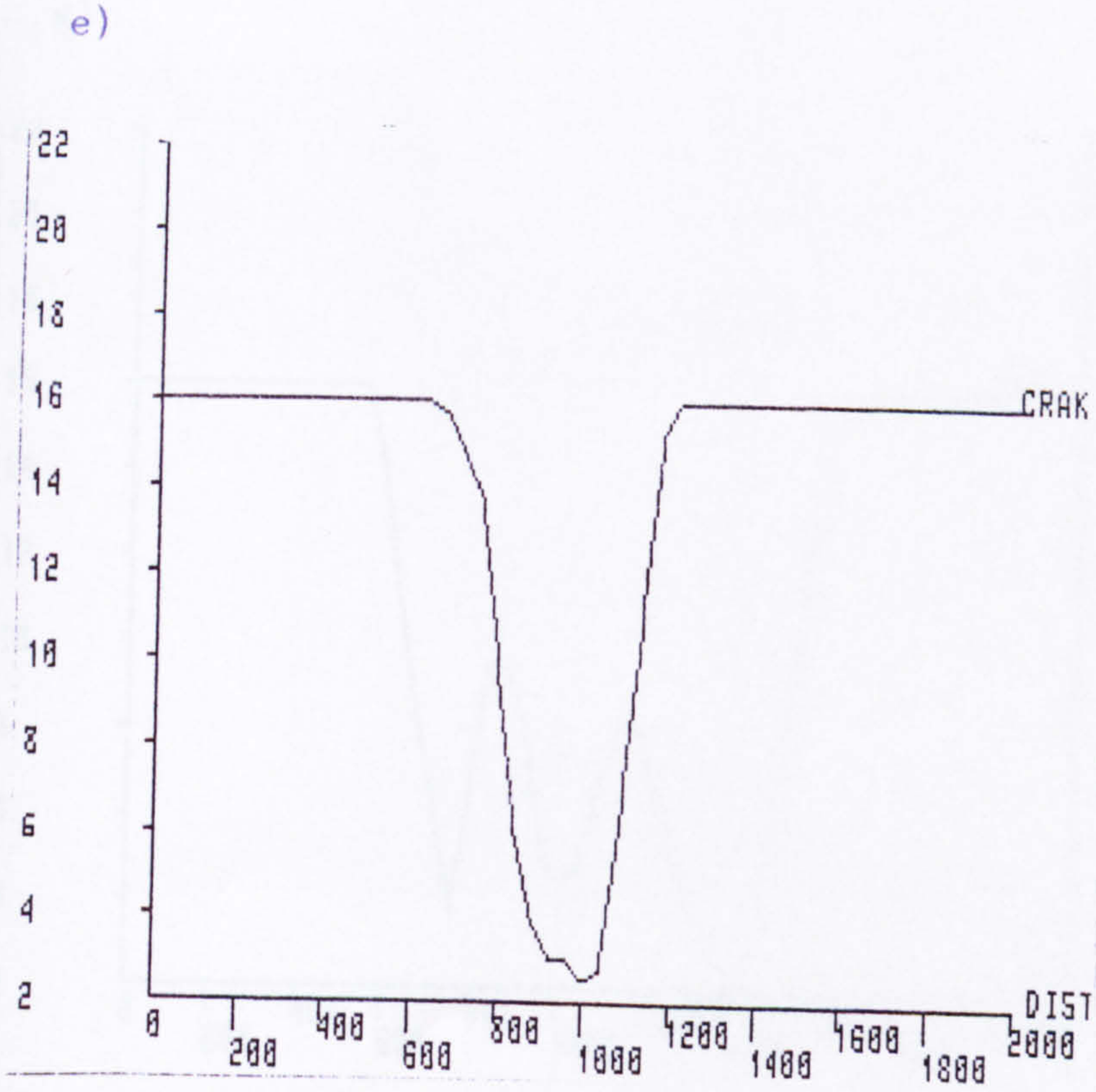
22
20
18
16
14
12
10
8
6
4
2
CRAK
0
200
400
600
800
1000
1200
1400
1600
1800
2000
DIST

f)

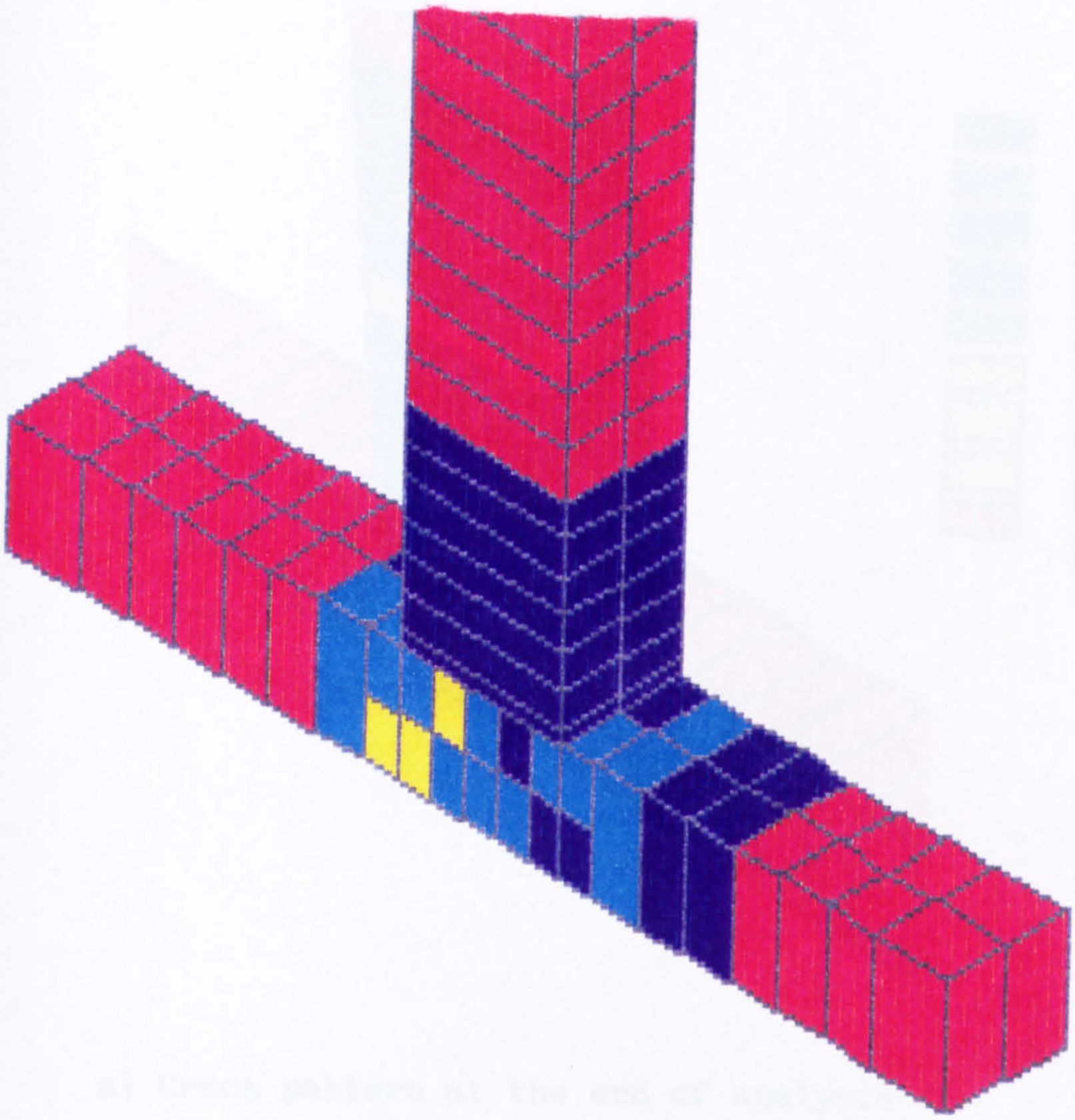

g)

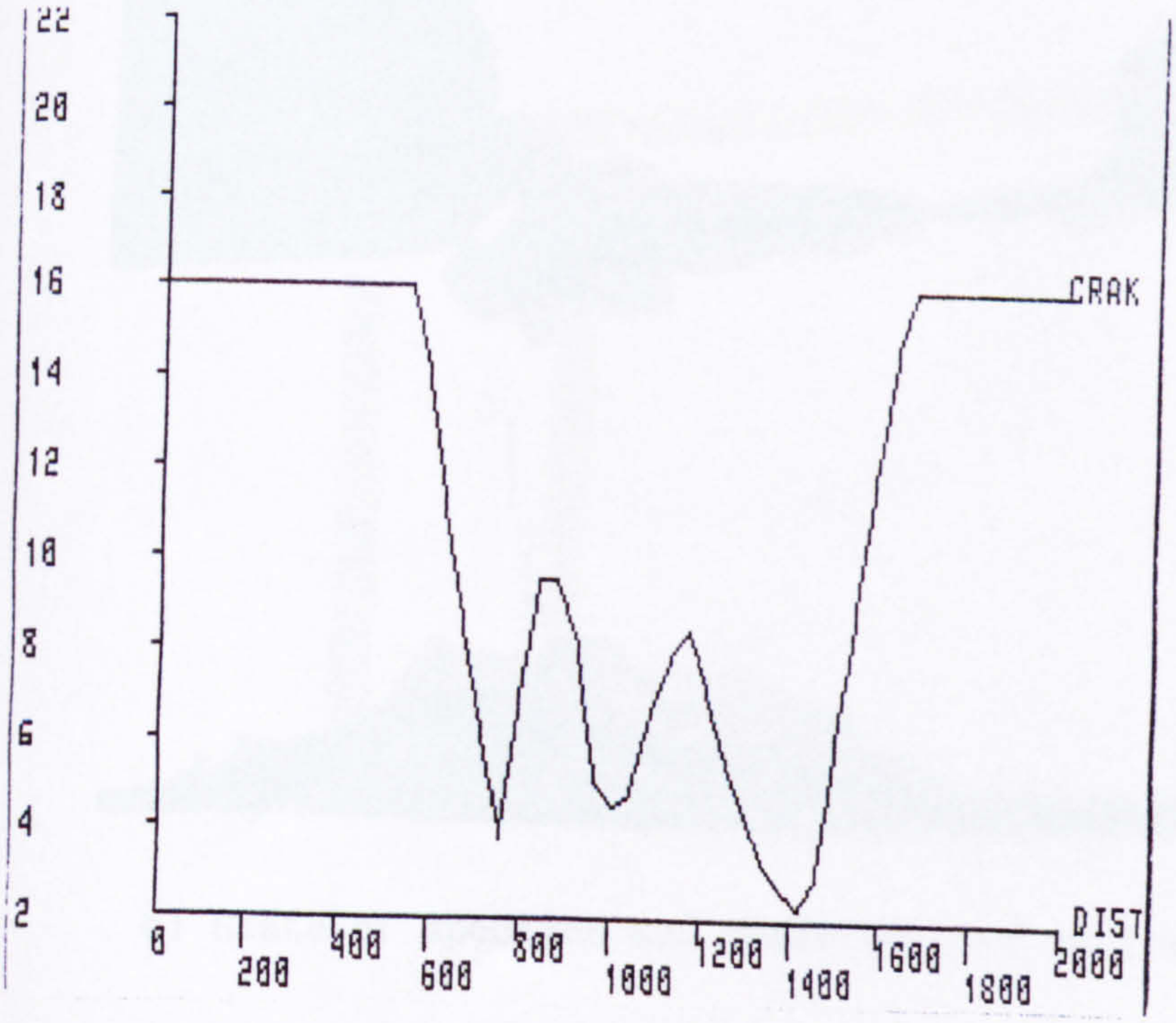
22
20
18
16
14
12
10
8
6
4
2
CRAK
0
200
400
600
800
1000
1200
1400
1600
1800
2000
DIST

h)

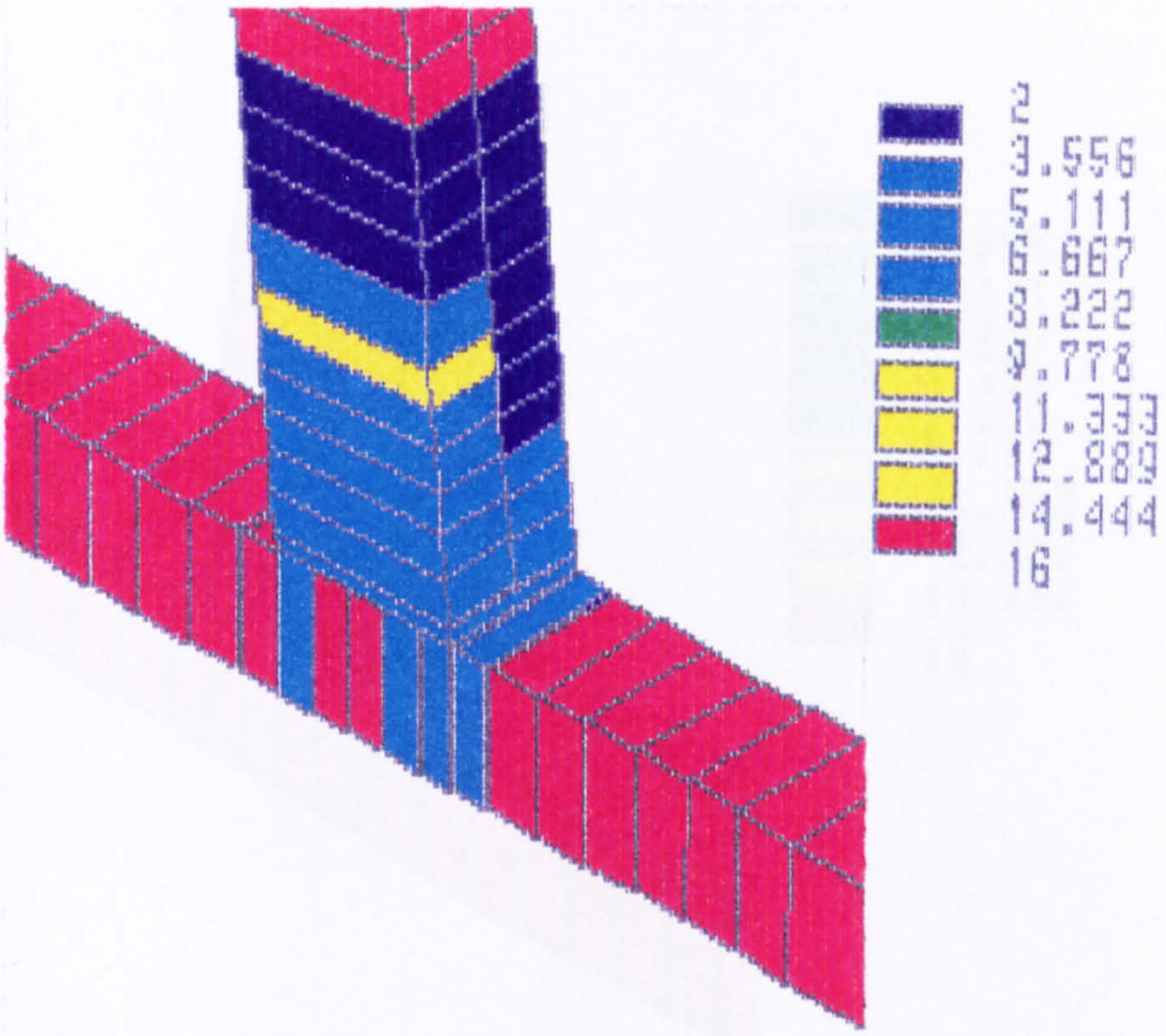
16
4
1
1
1

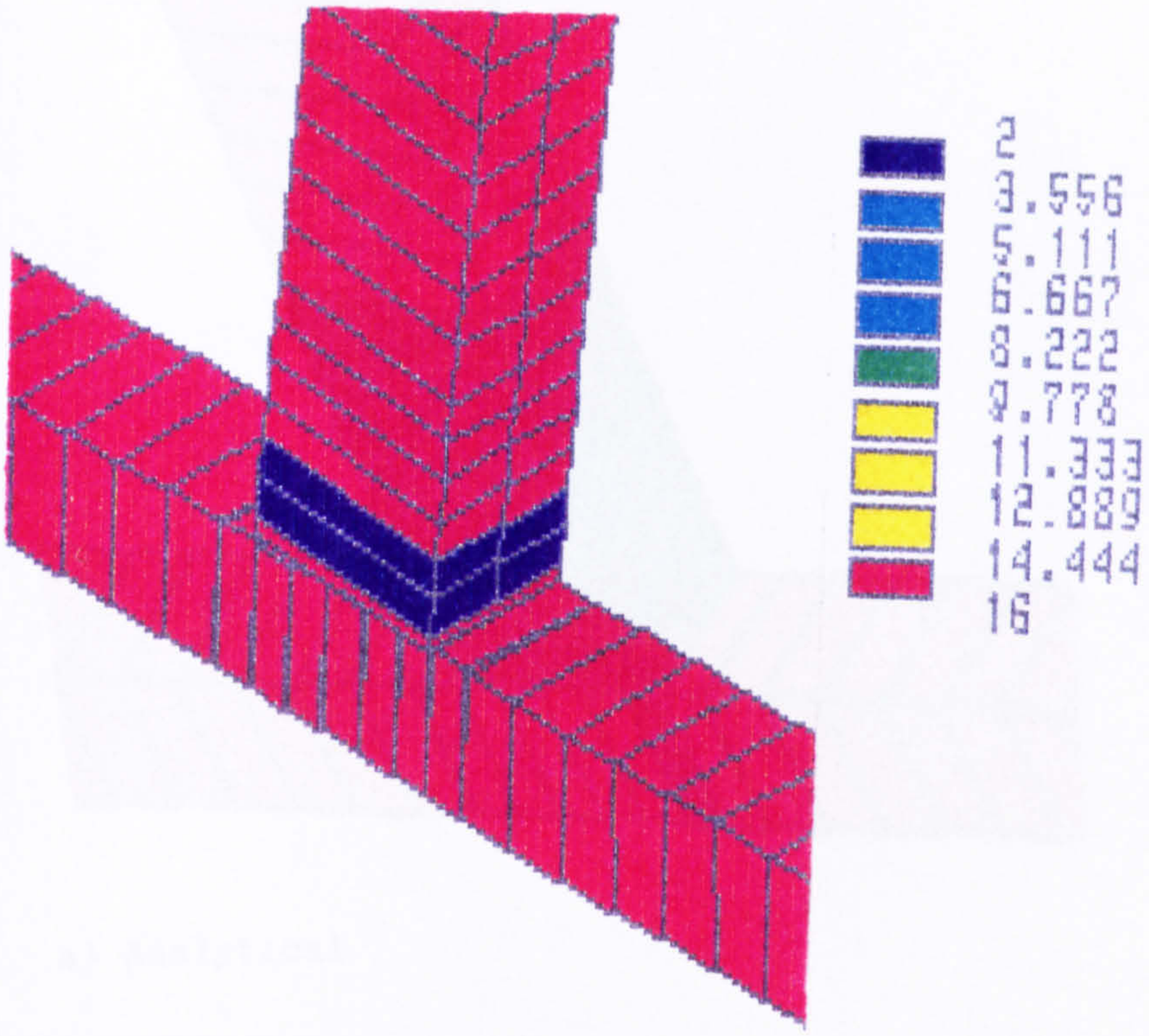

a) Analytical

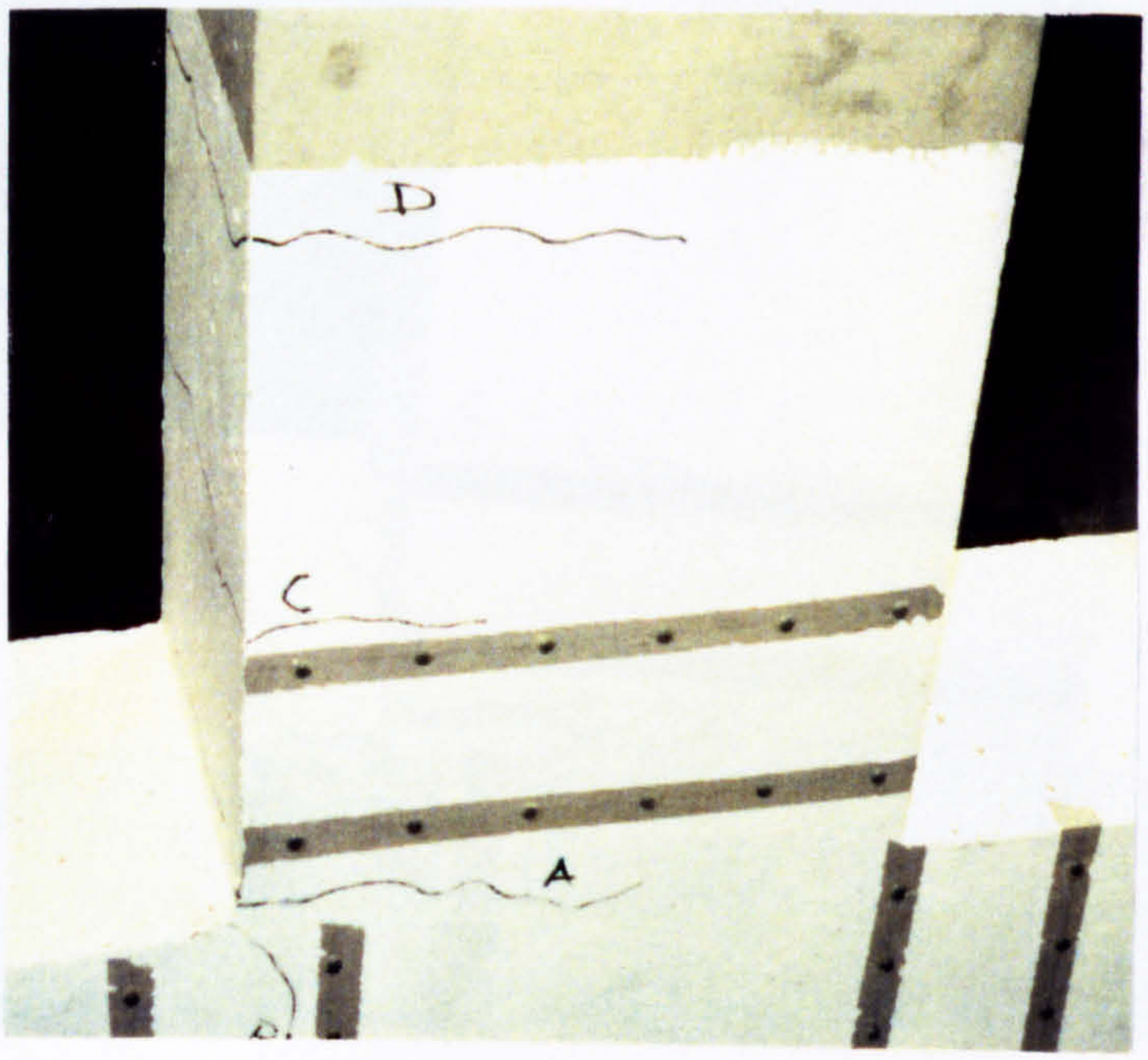

b) Experimental

FIG.5.17 FIRST CRACKS IN SPECIMEN UD2

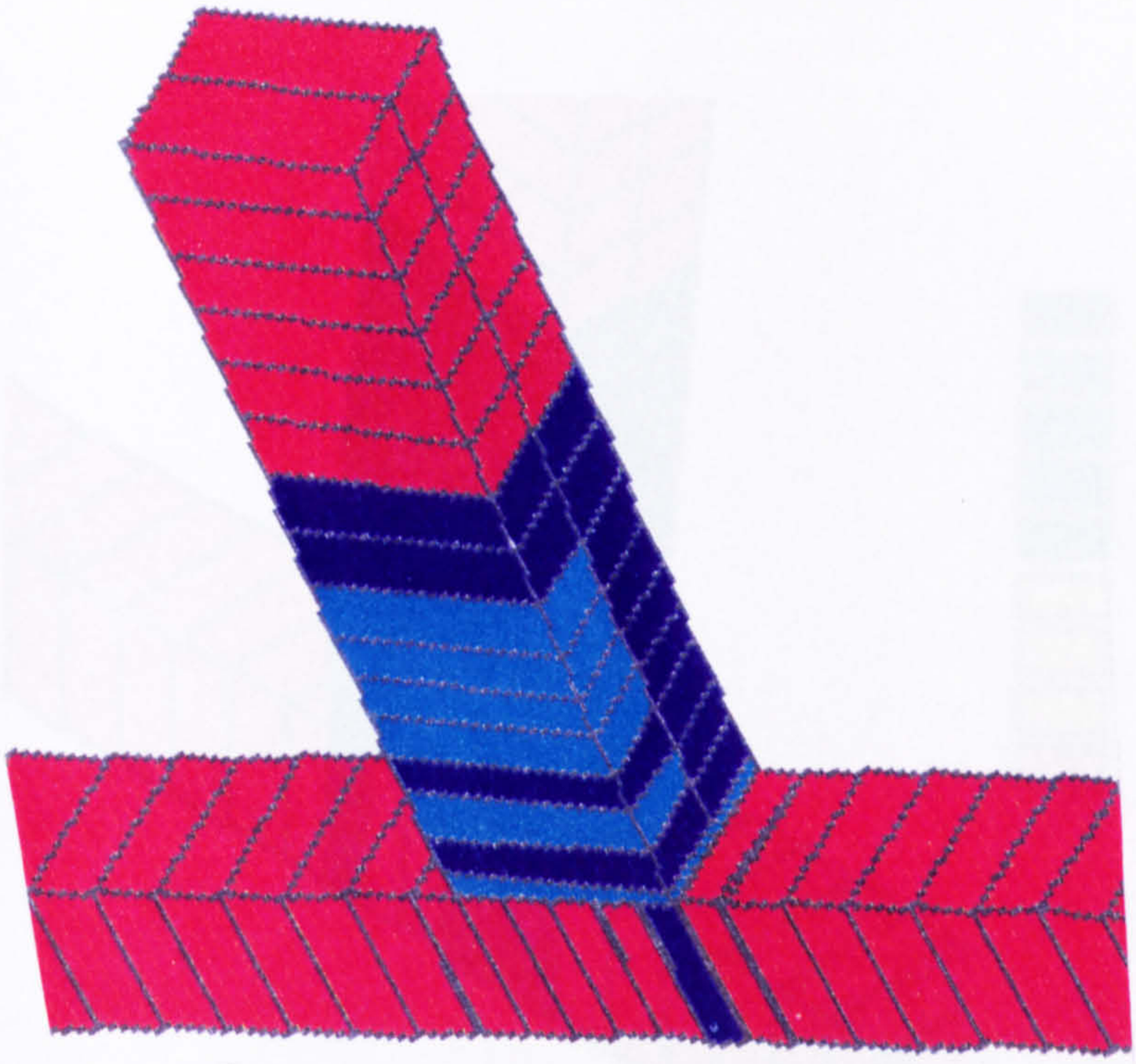

a) Analytical

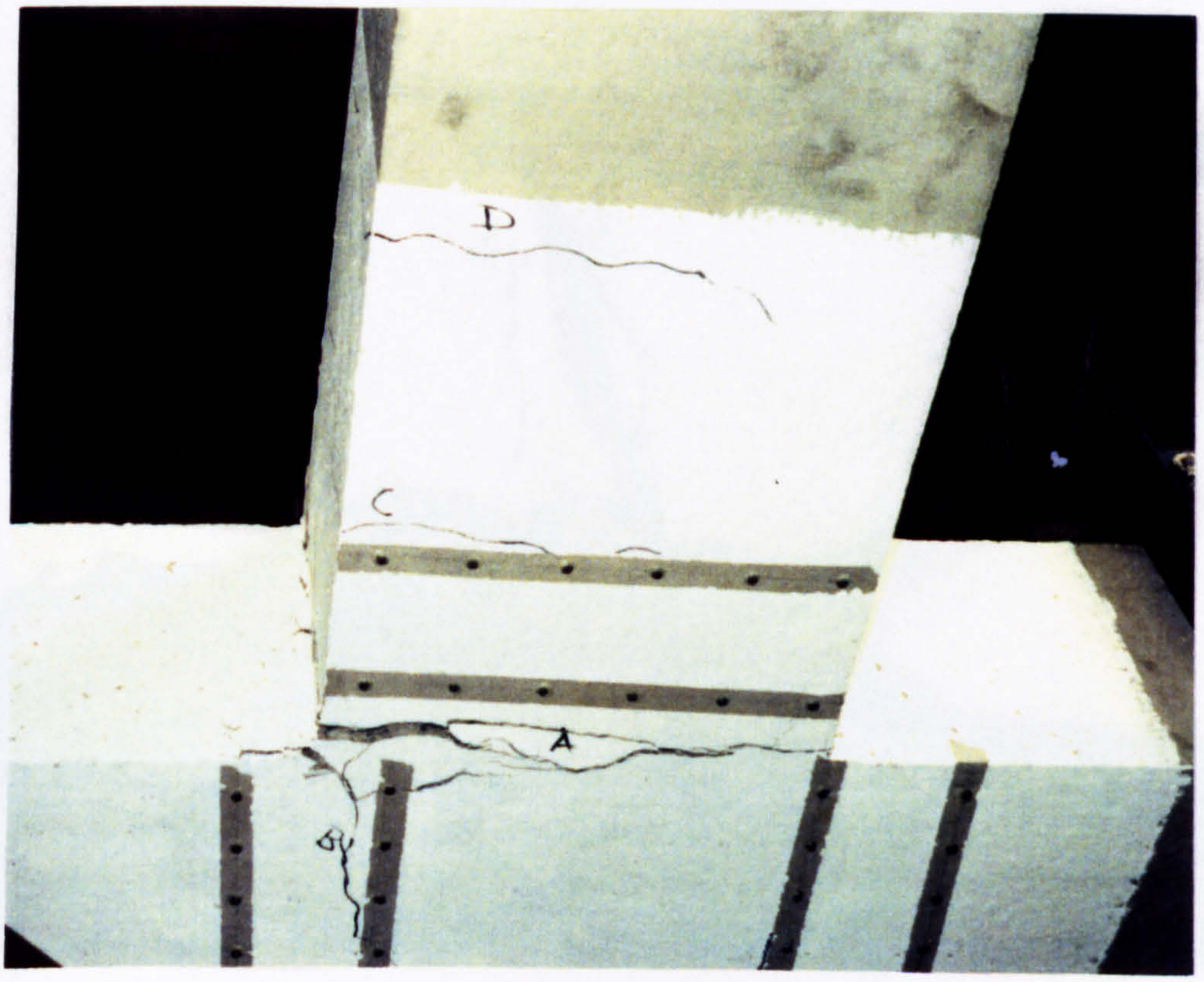

b) Experimental

FIG.5.18 ANALYTICAL AND EXPERIMENTAL CRACKING PATTERN

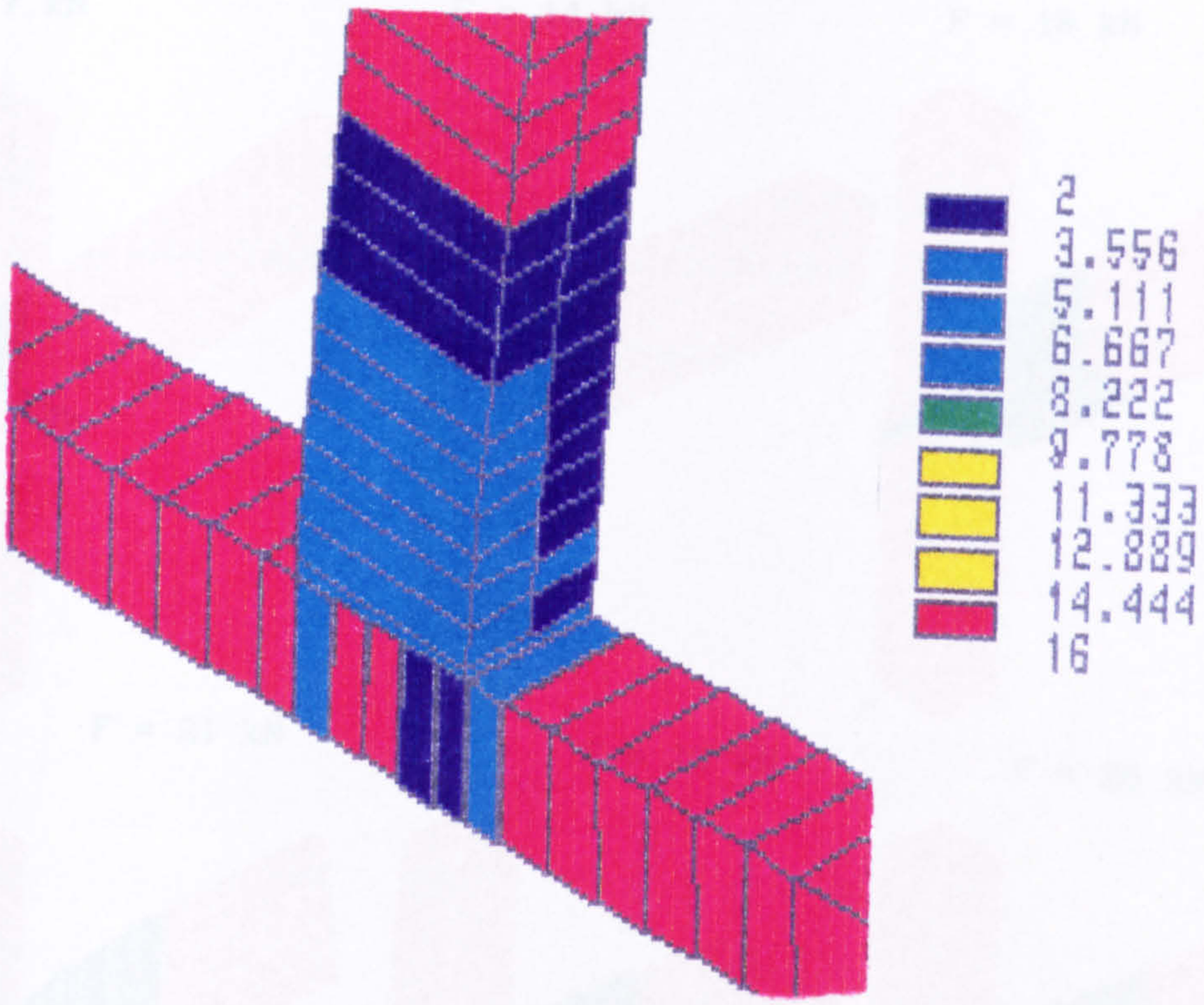

c) Analytical

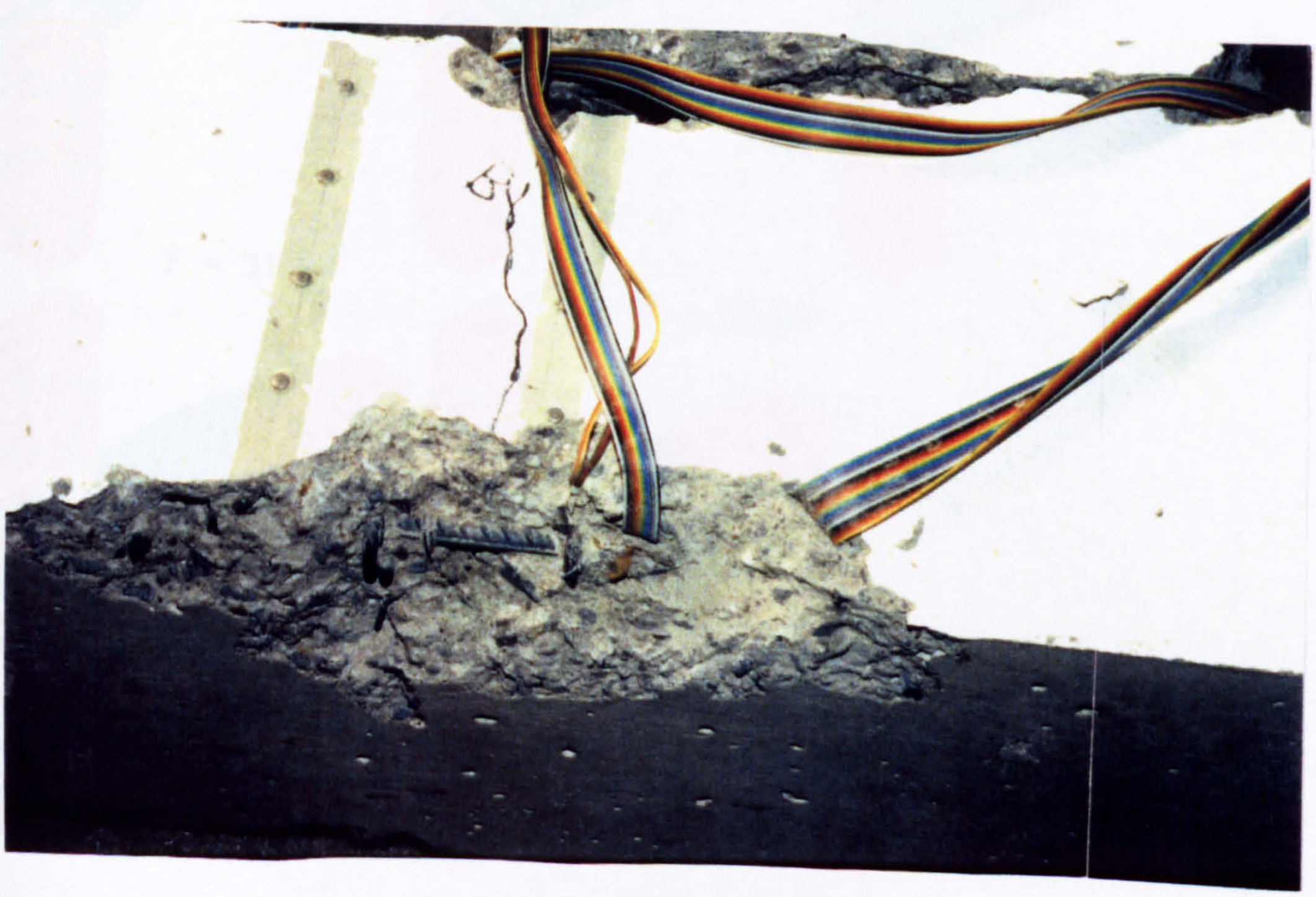

d) Experimental

F = 7 kN

F = 14 kN

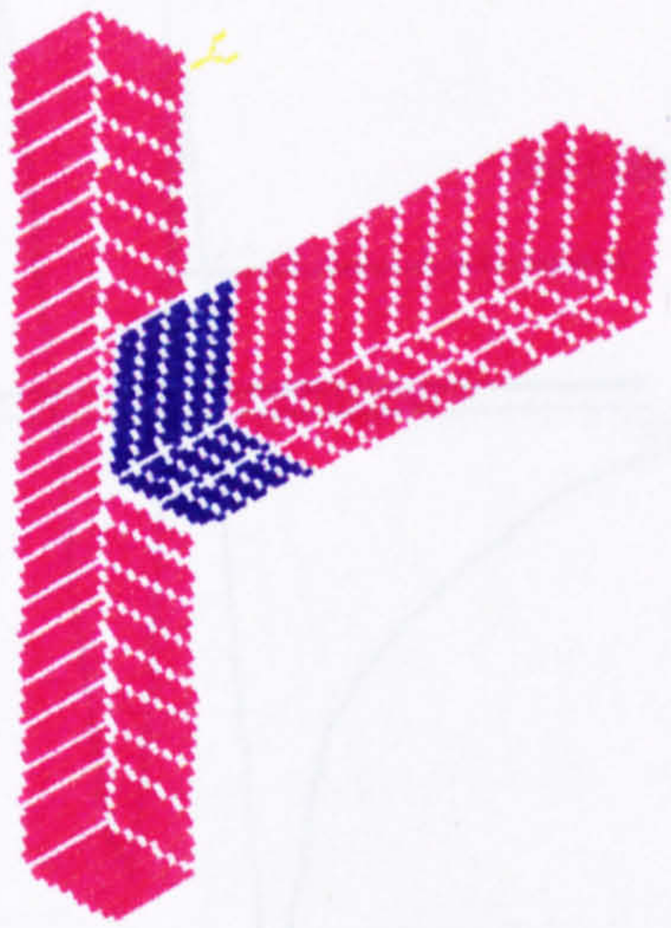

F = 18 kN

F = 21 kN

F = 25 kN

F = 28 kN

F = 31 kN

F = 35 kN

FIG.5.19 ANALYTICAL CRACKING PATTERNS

- SPECIMEN UD2 -

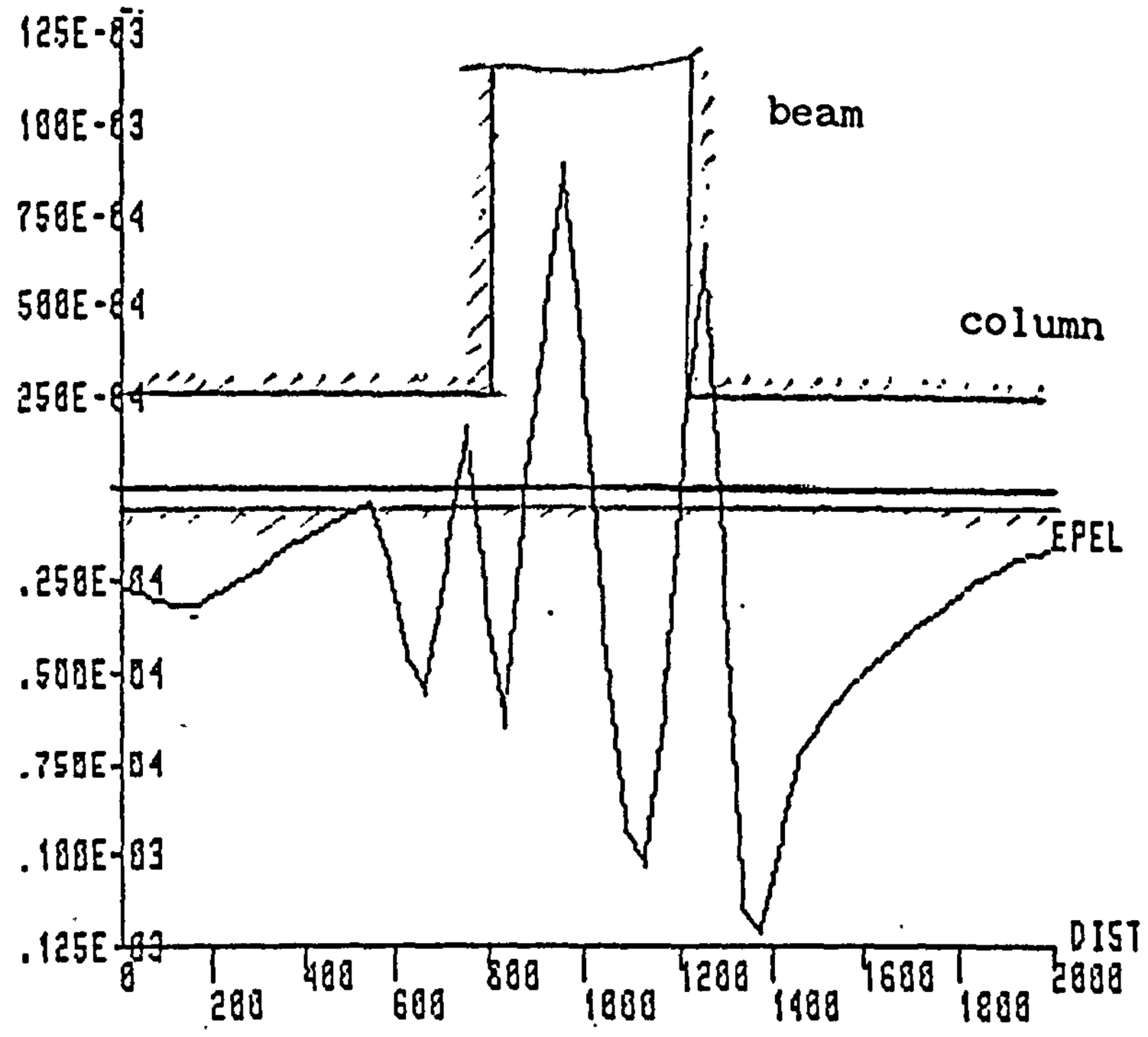

a) Specimen EX2 :outer bars F = -14 kN

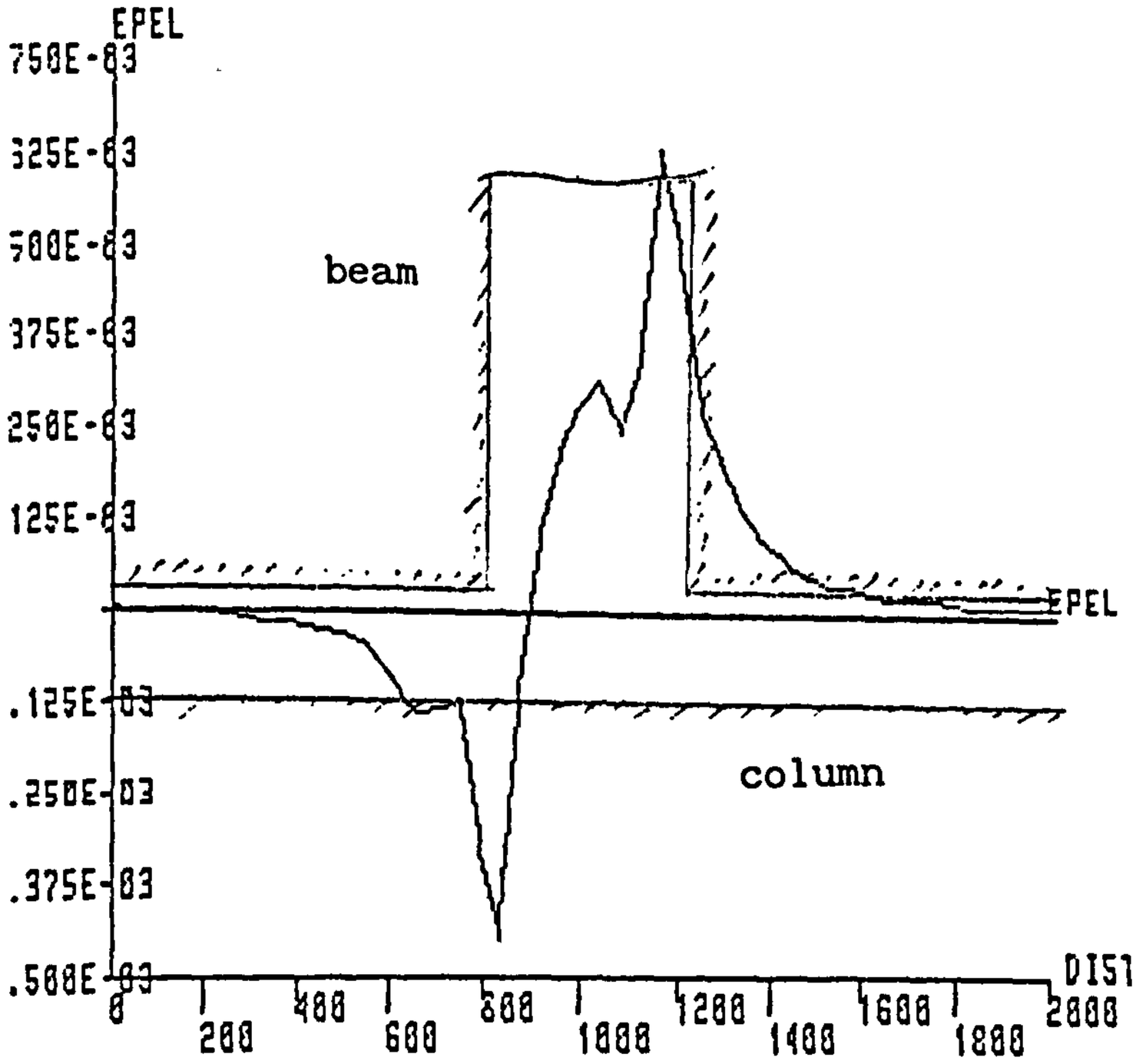

b) Specimen EX2 :inner bars F = -14 kN

* EPEL : ELASTIC STRAIN

FIG.5.20 STRAIN VARIATION ALONG COLUMN MAIN REINFORCEMENT (INNER AND OUTER BARS) SPECIMENS EX2 & UD1

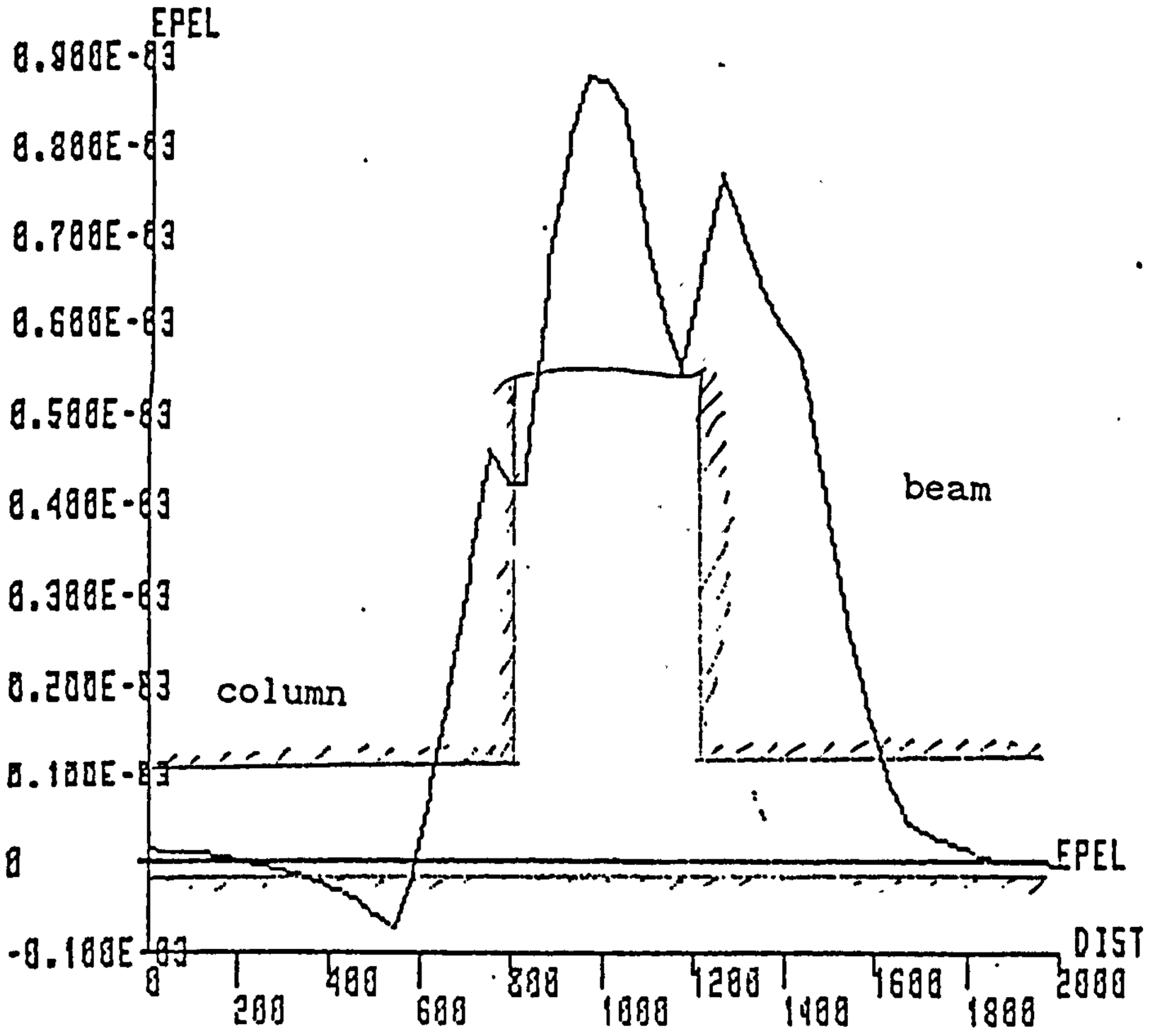

c) Specimen UD1 :outer bars F = 14 kN

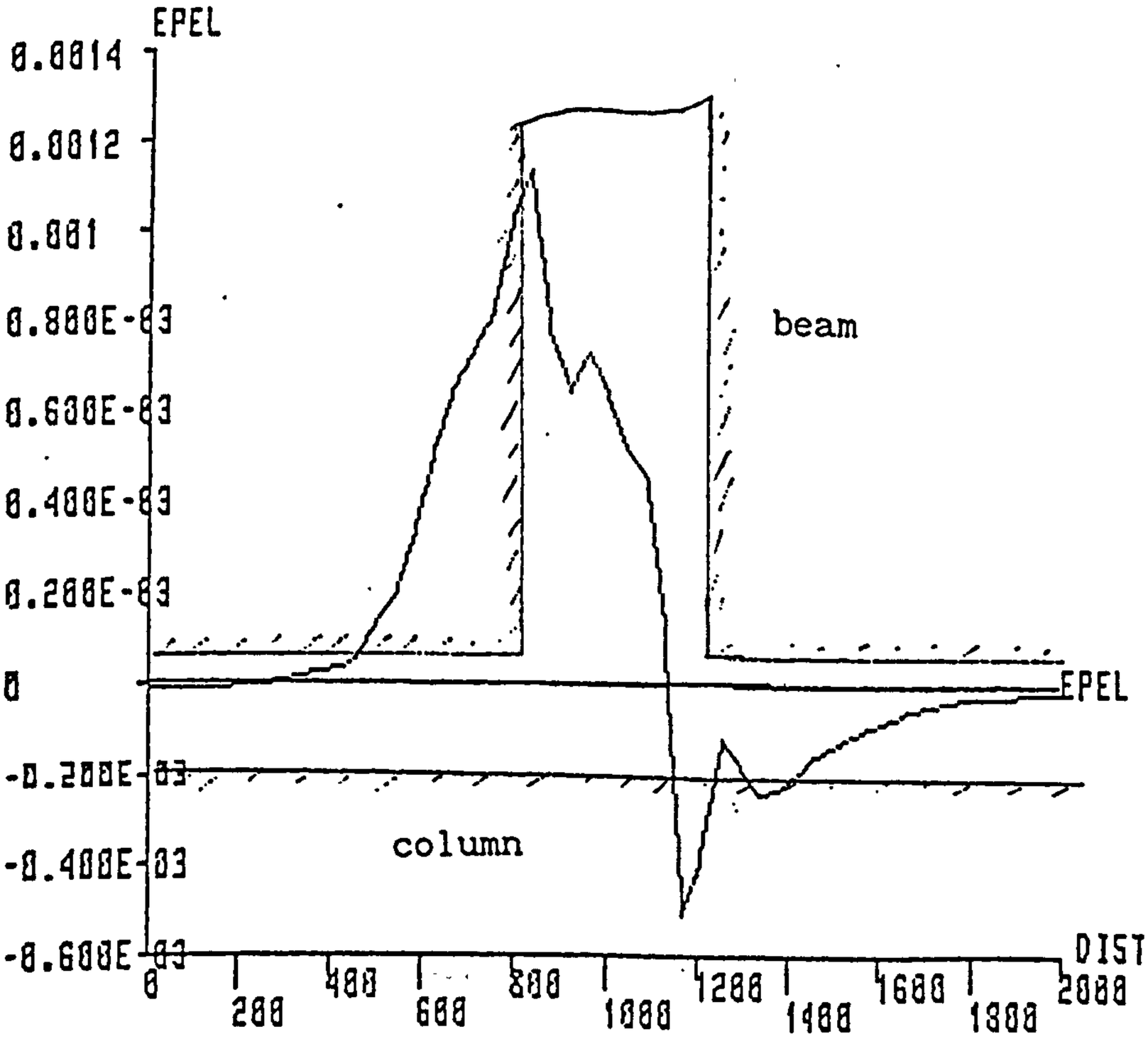

d) Specimen UD1 :inner bars F = 14 kN

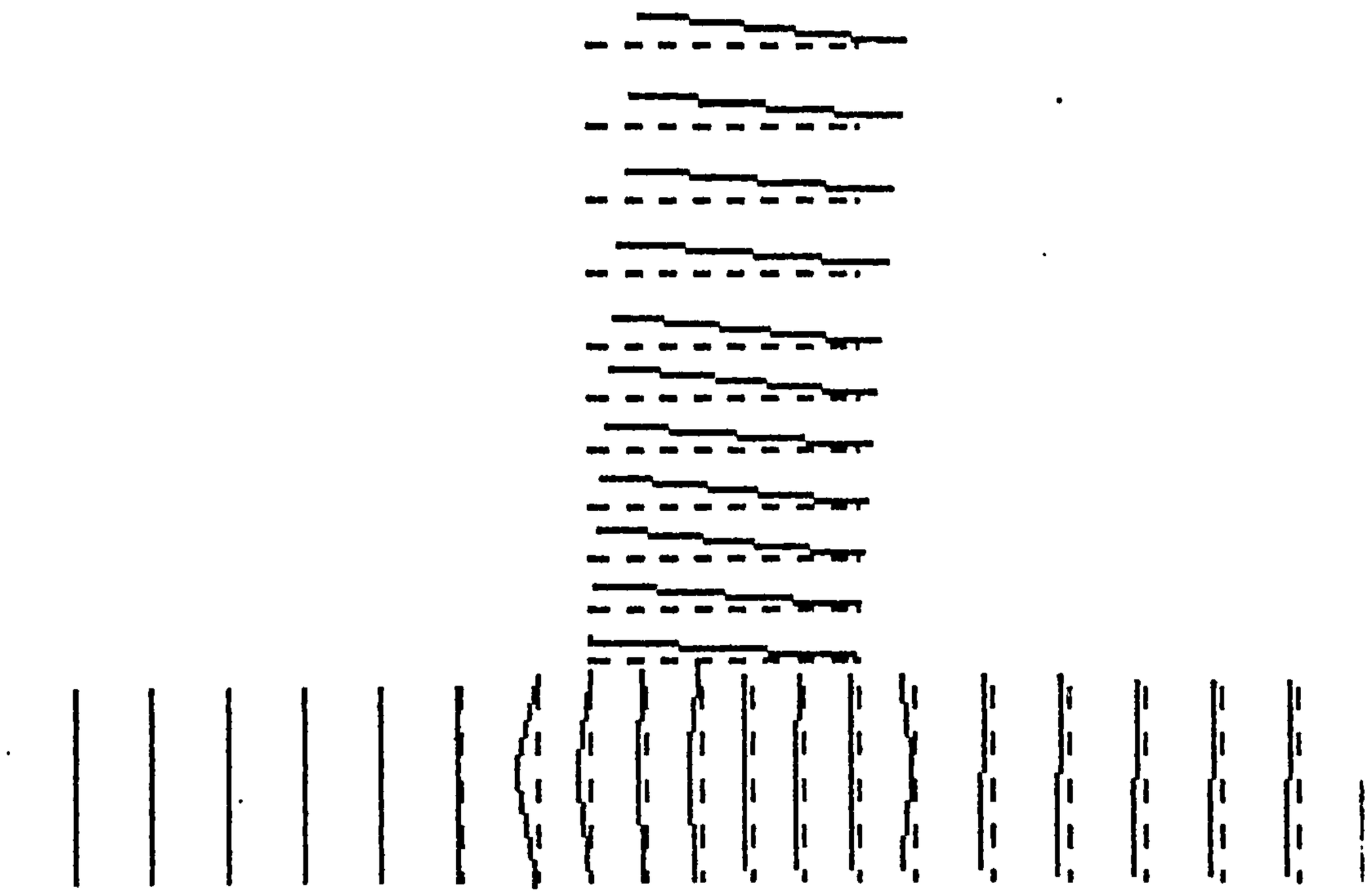

a) Specimen UD1

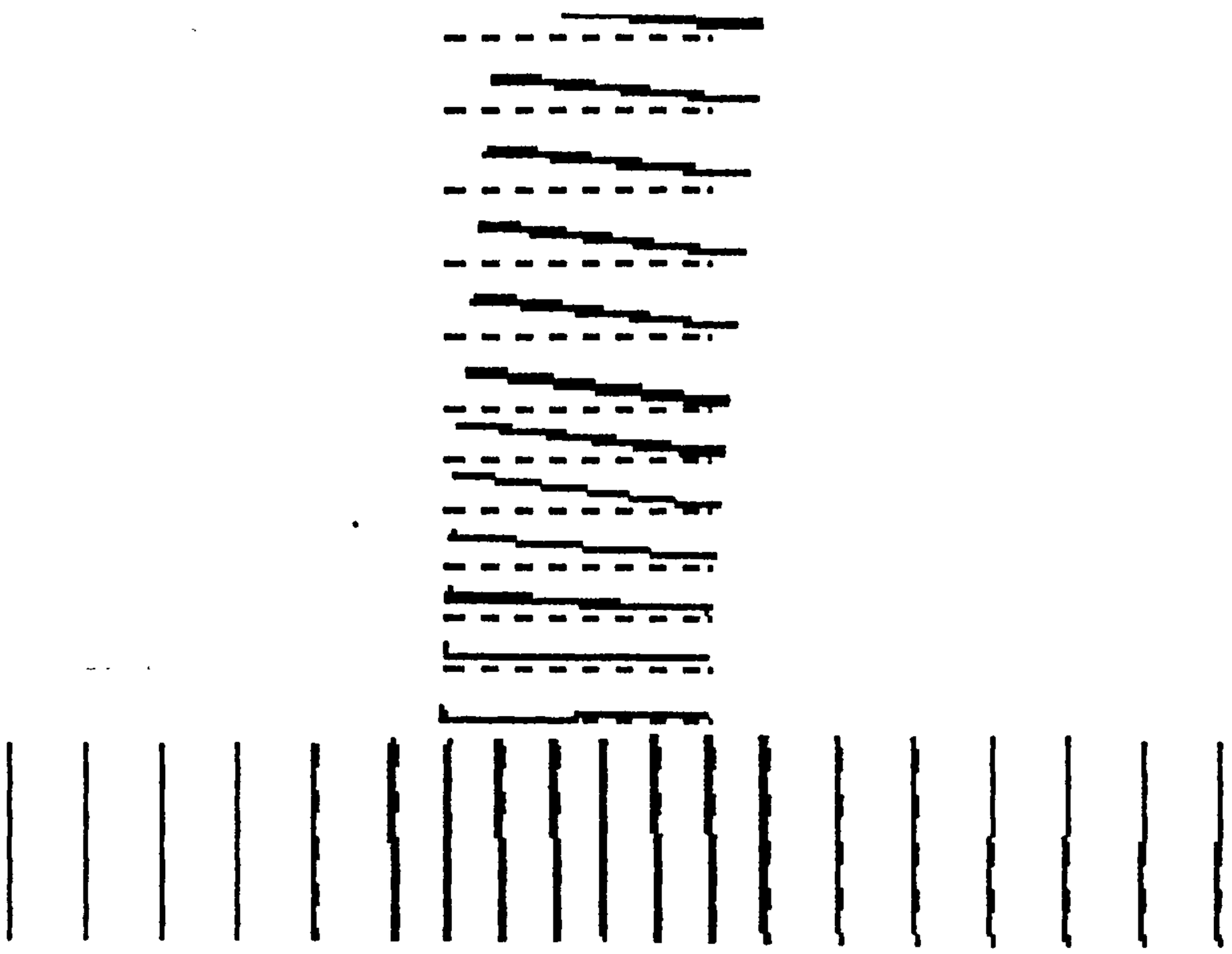

b) Specimen UD2

FIG.5.21 INITIAL AND DEFORMED SHAPE OF REINFORCING CAGE

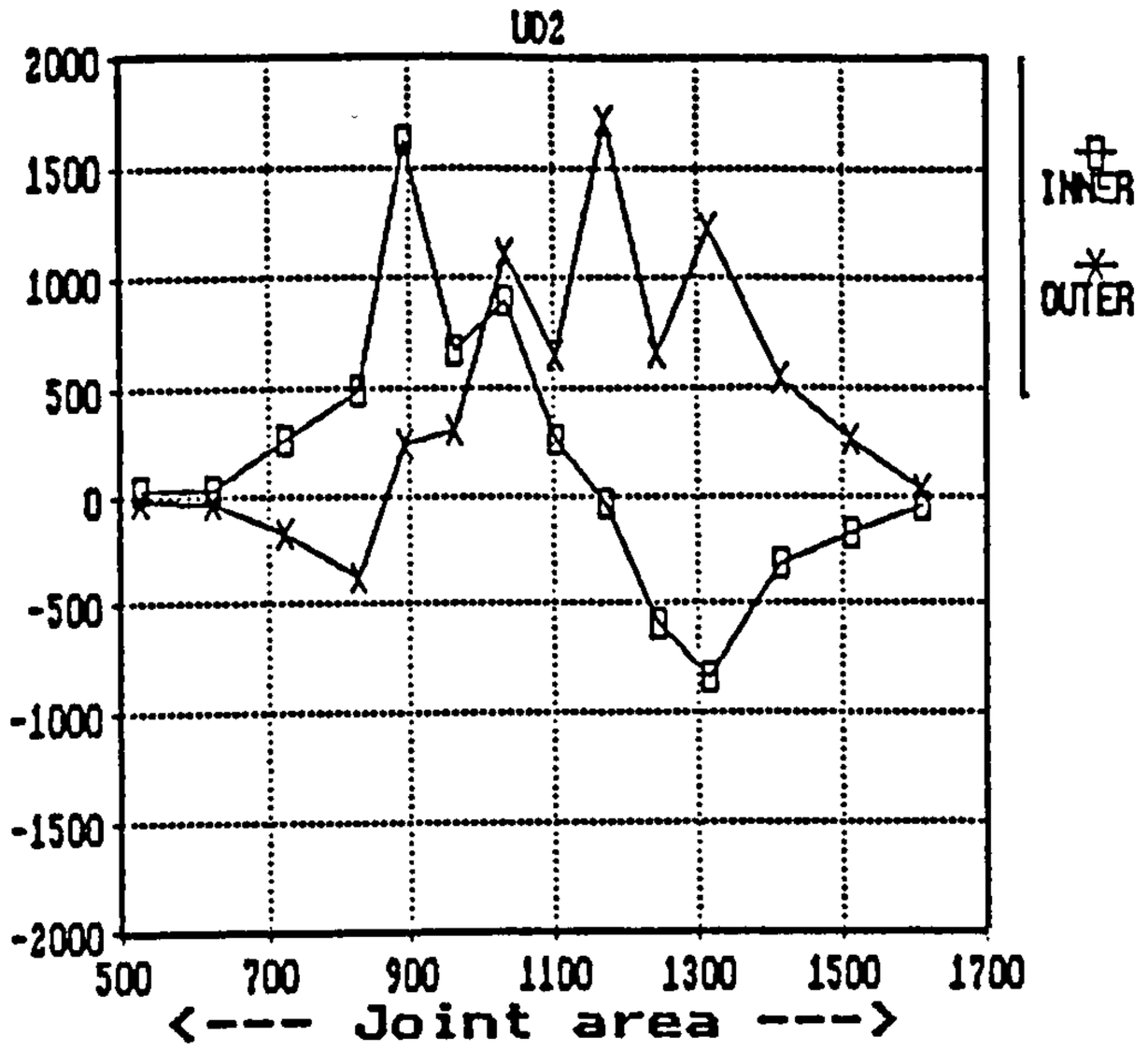

a)

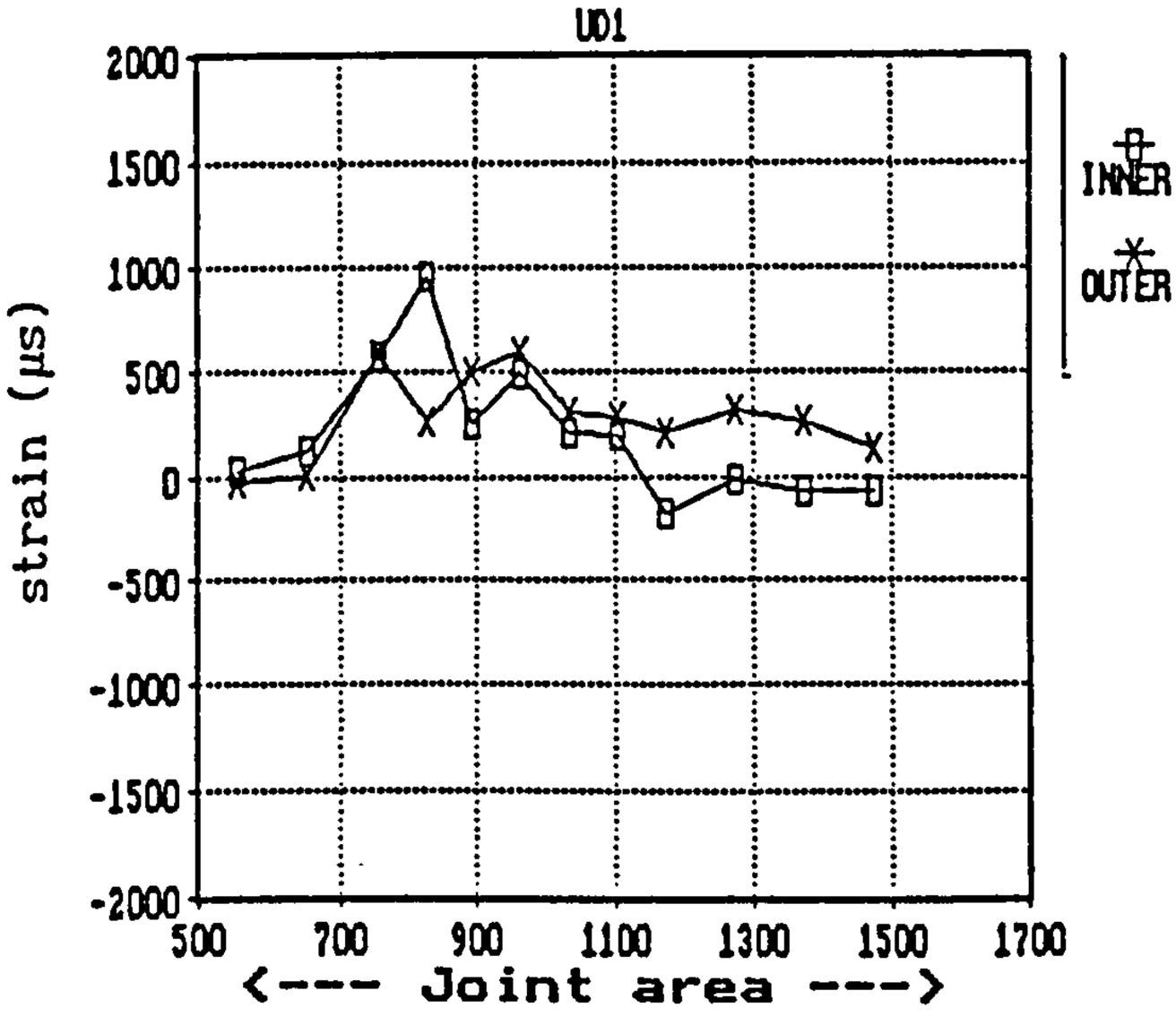

b)

FIG.5.22 STRAIN VARIATION ALONG INNER AND OUTER STIRRUPS LEGS IN THE JOINT REGION - UD2 & UD1 -

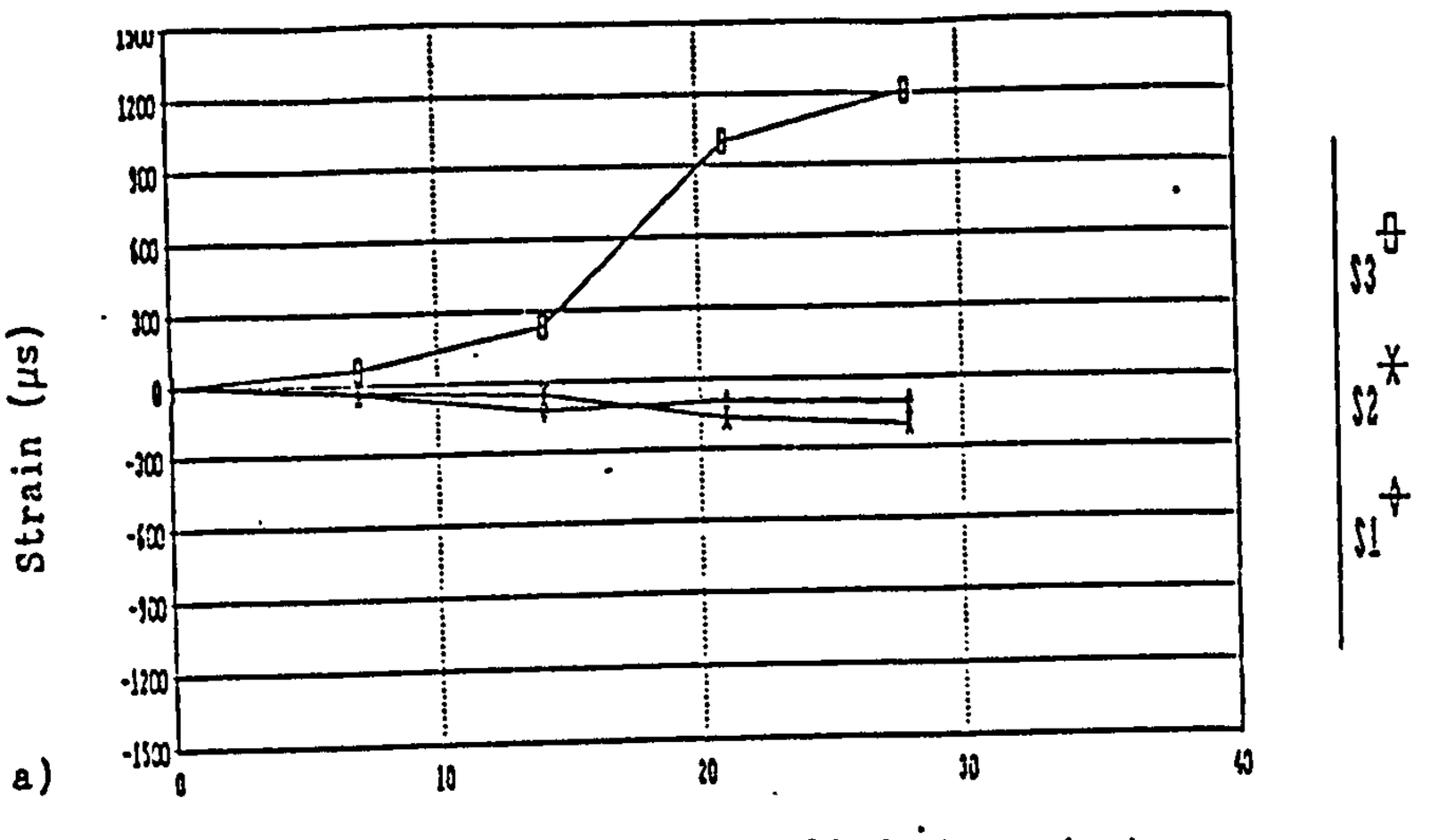

a)

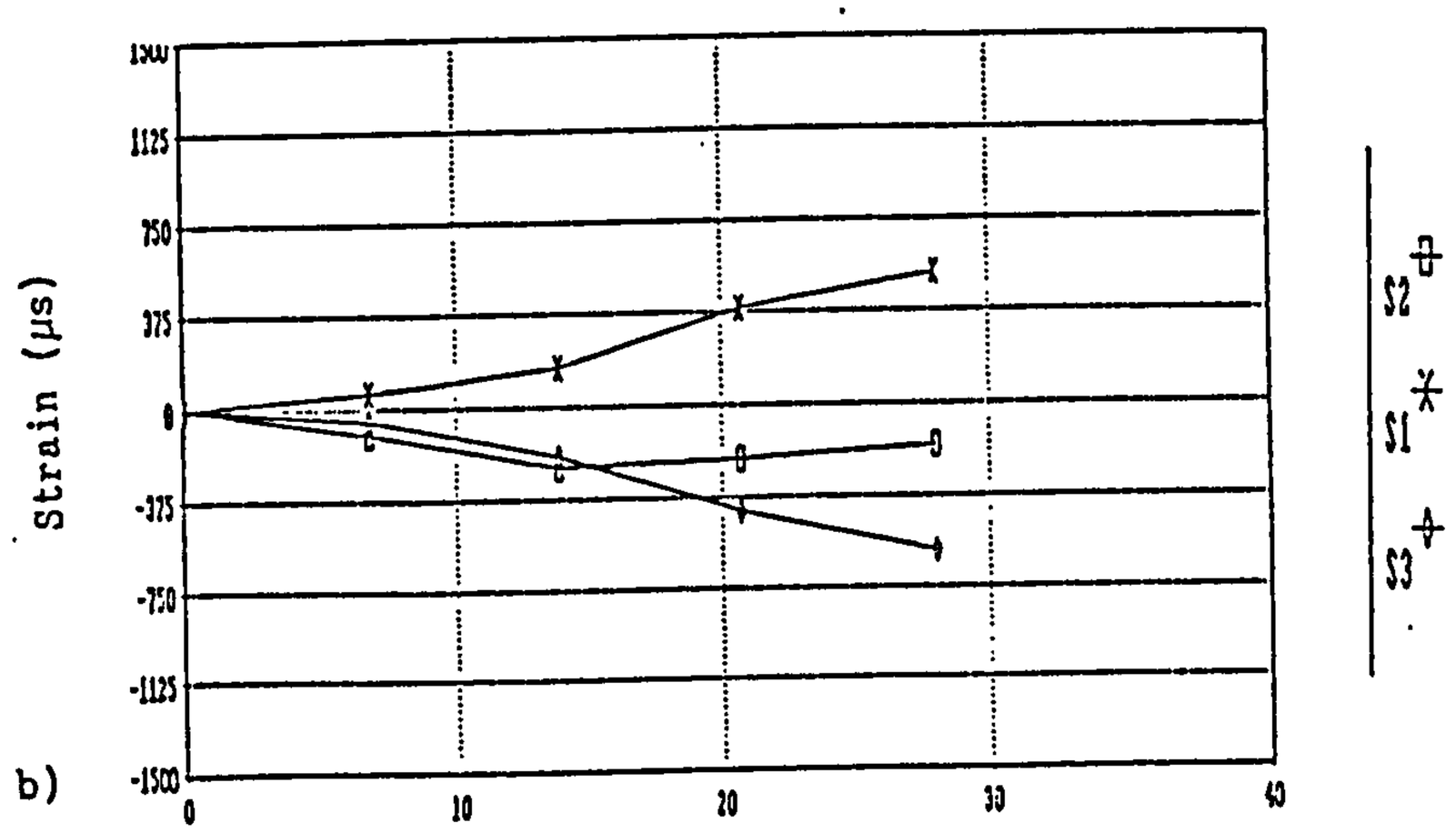

b)

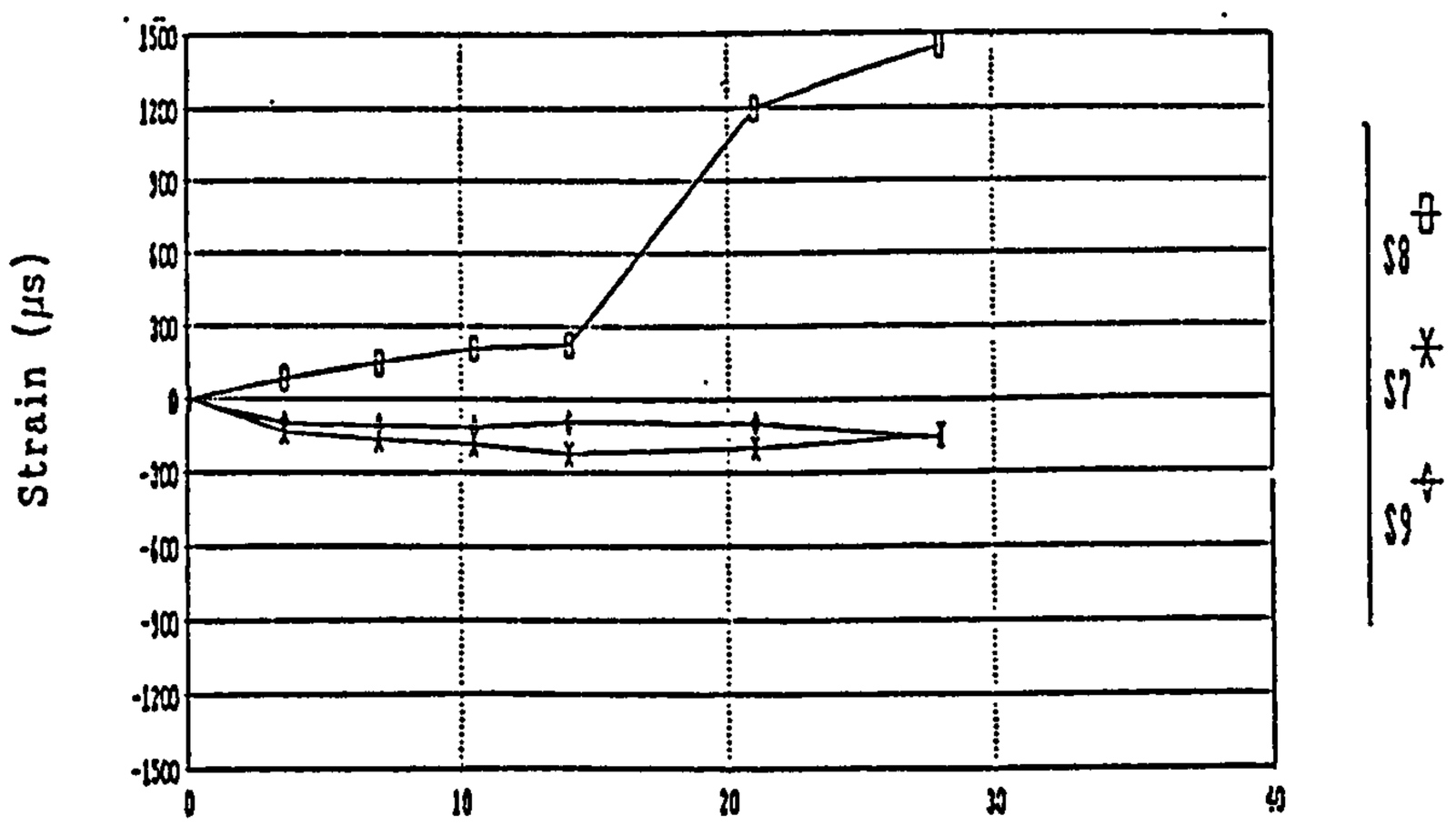

c)

FIG.5.23 APPLIED SHEAR VS. STRAIN (SPECIMEN EX2, UD1 AND UD2)

a) Specimen EX2, location :S3, S2 and S1

b) Specimen UD1, location :S2, S1 and S3

c) Specimen UD2, location :S8, S7 and S9

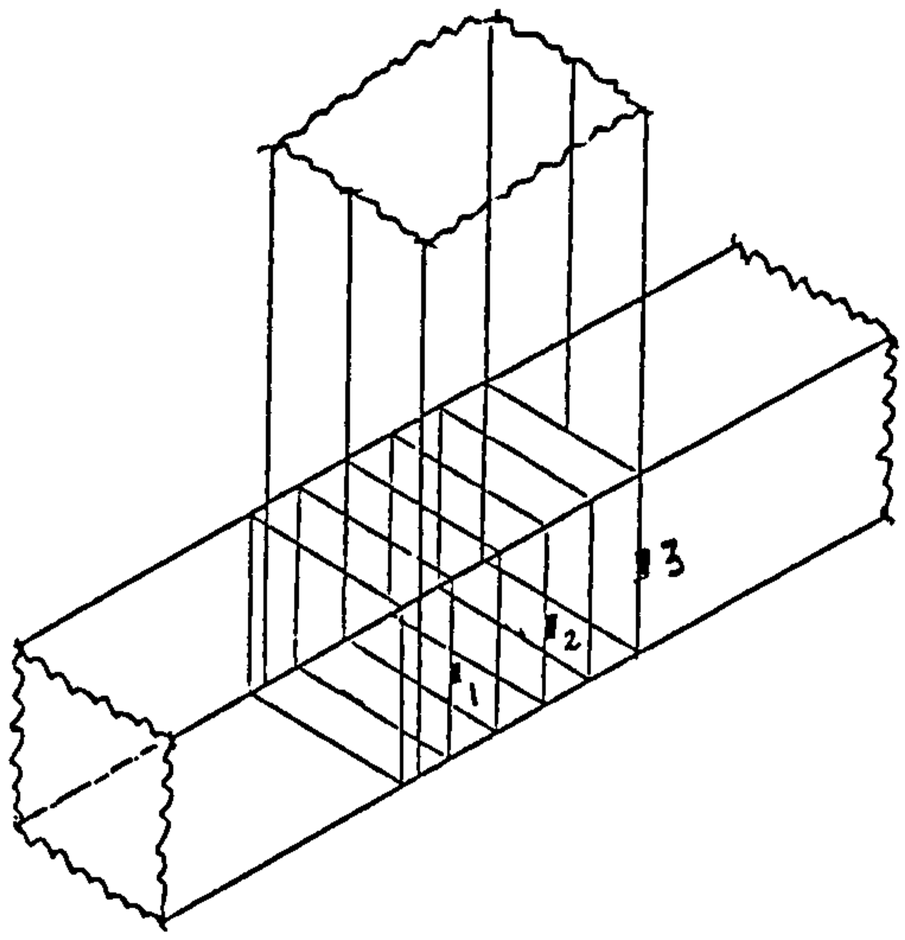

a)

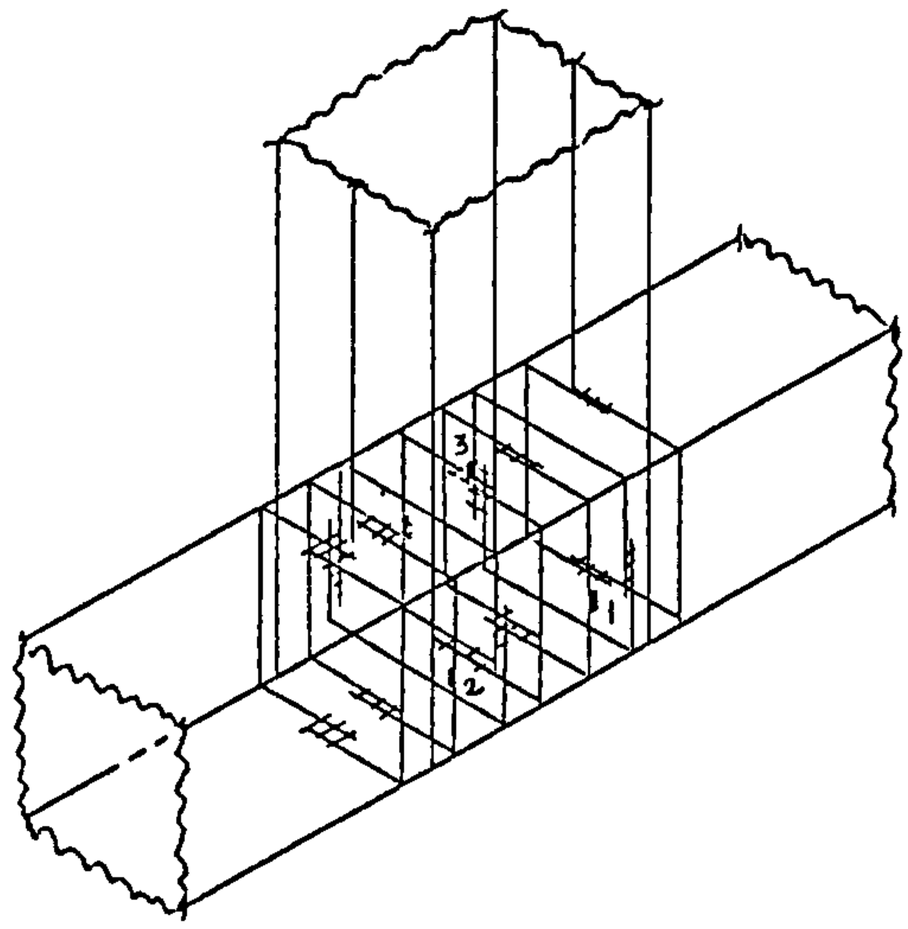

b)

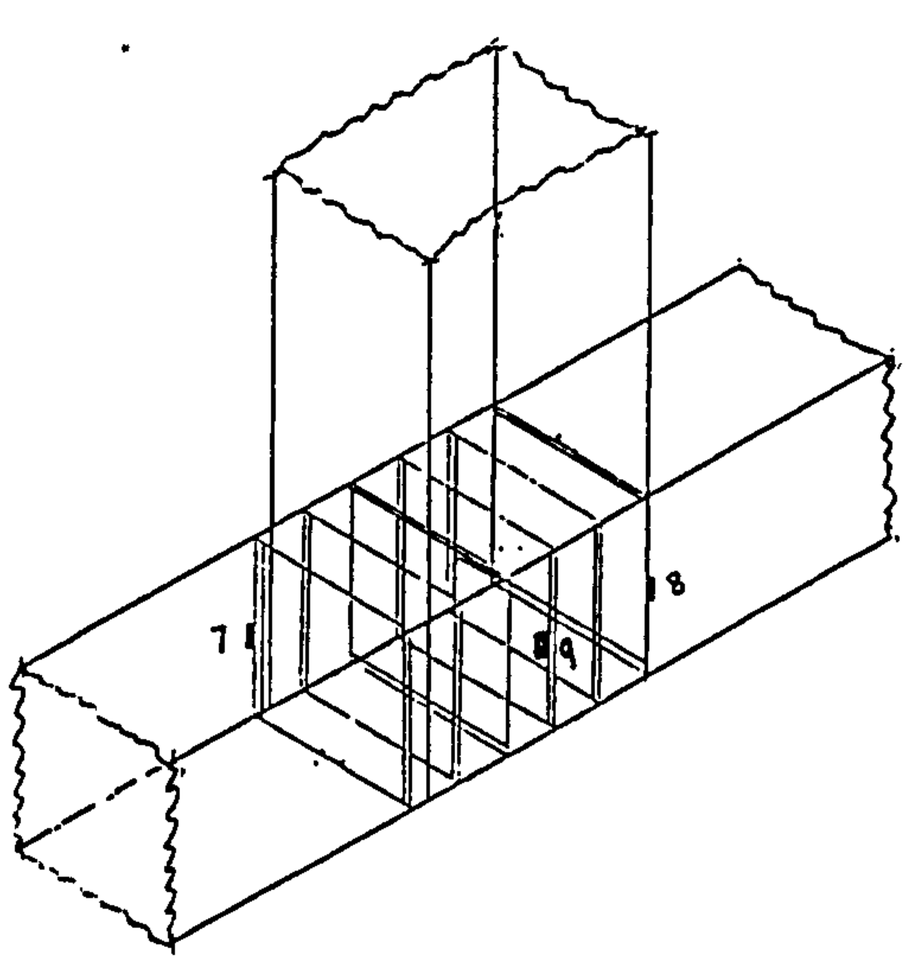

c)

FIG.5.24 STRAIN GAUGES LOCATION

a) Specimen EX2 - b) Specimen UD1 - c) Specimen UD2

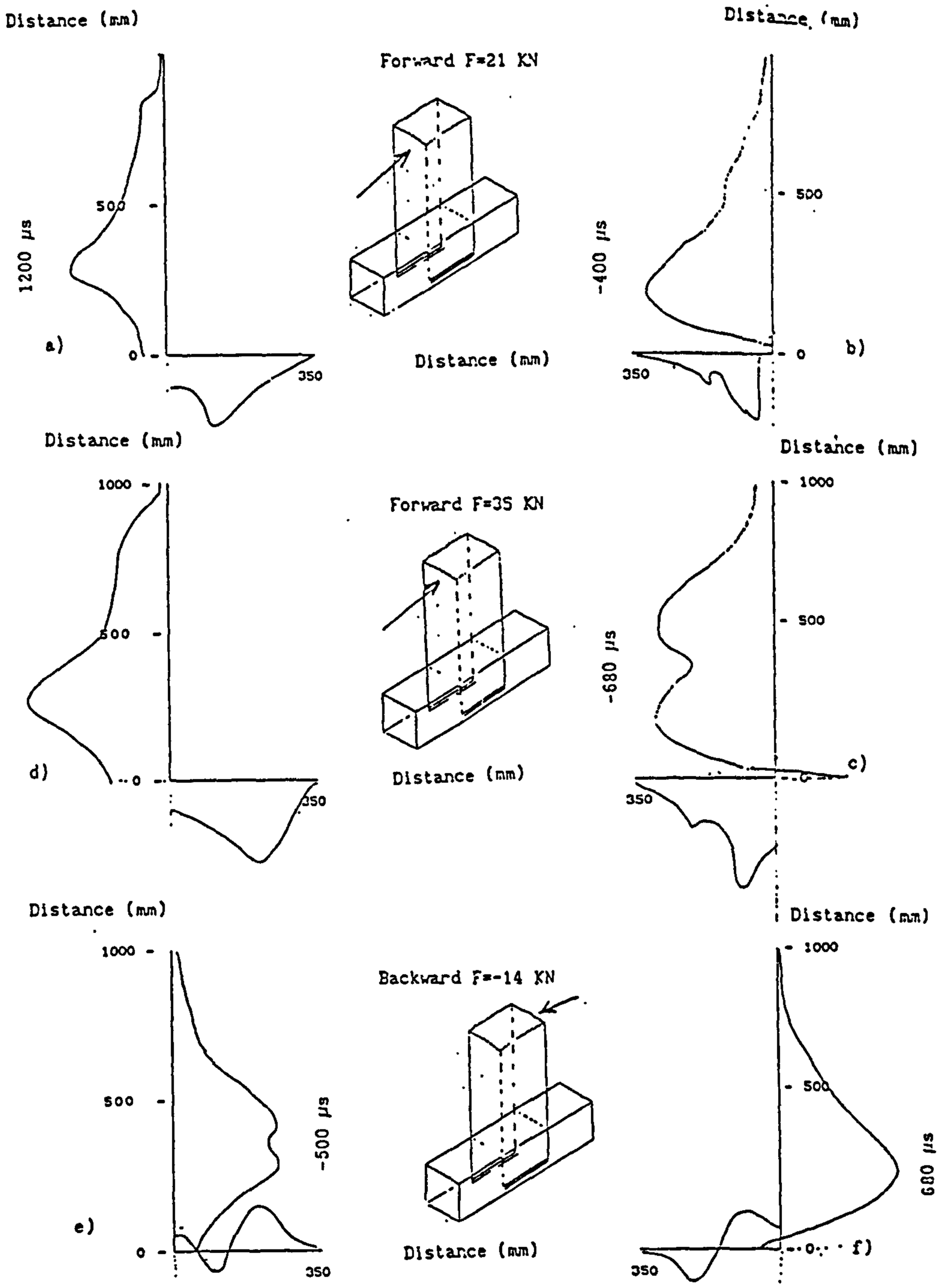

FIG.5.25 STRAIN DISTRIBUTION ALONG BEAM MAIN REINFORCEMENT (INCLUDING ANCHORAGE ZONE) - SPECIMEN UD2 -

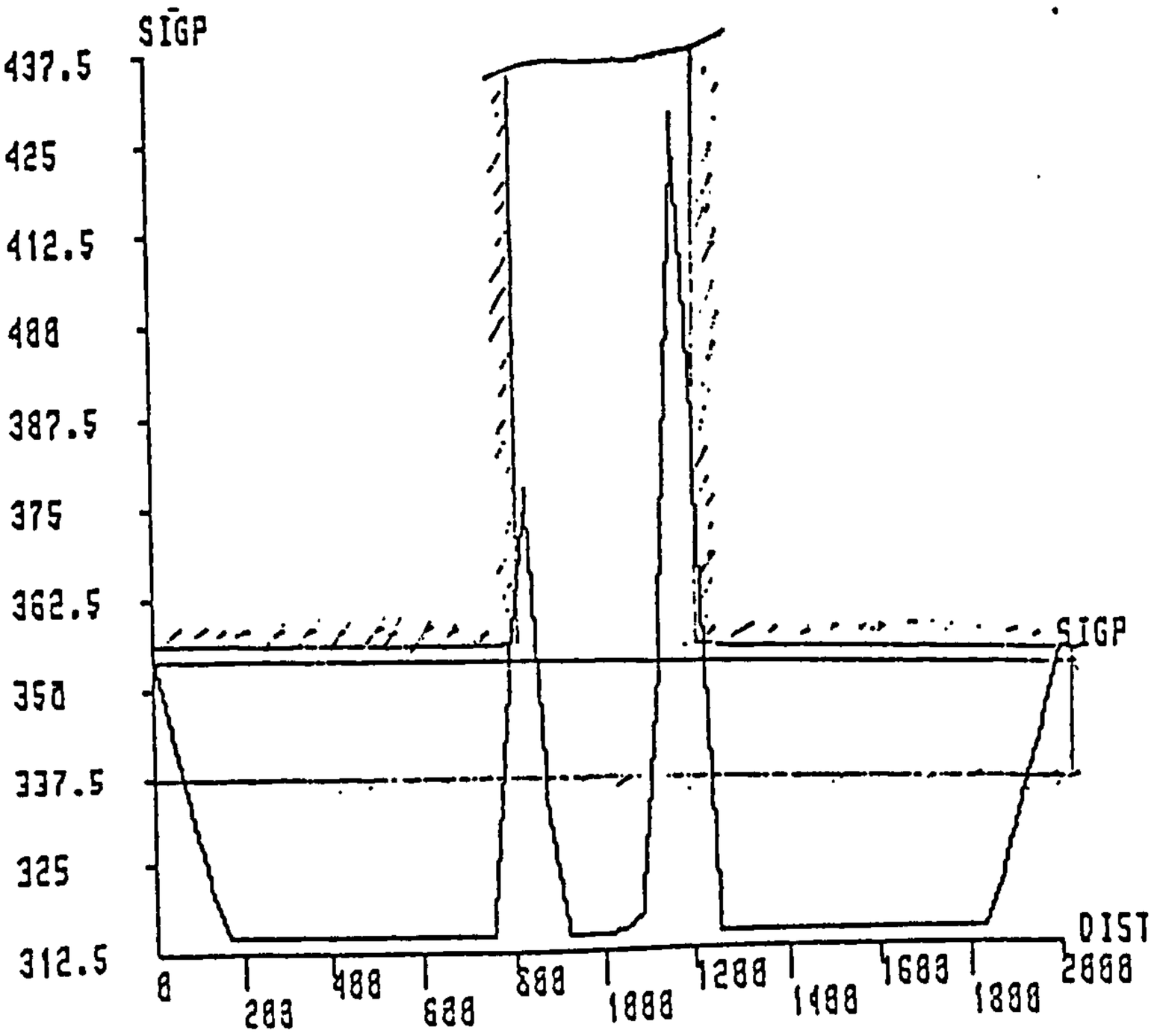

F = 35 kN

a)

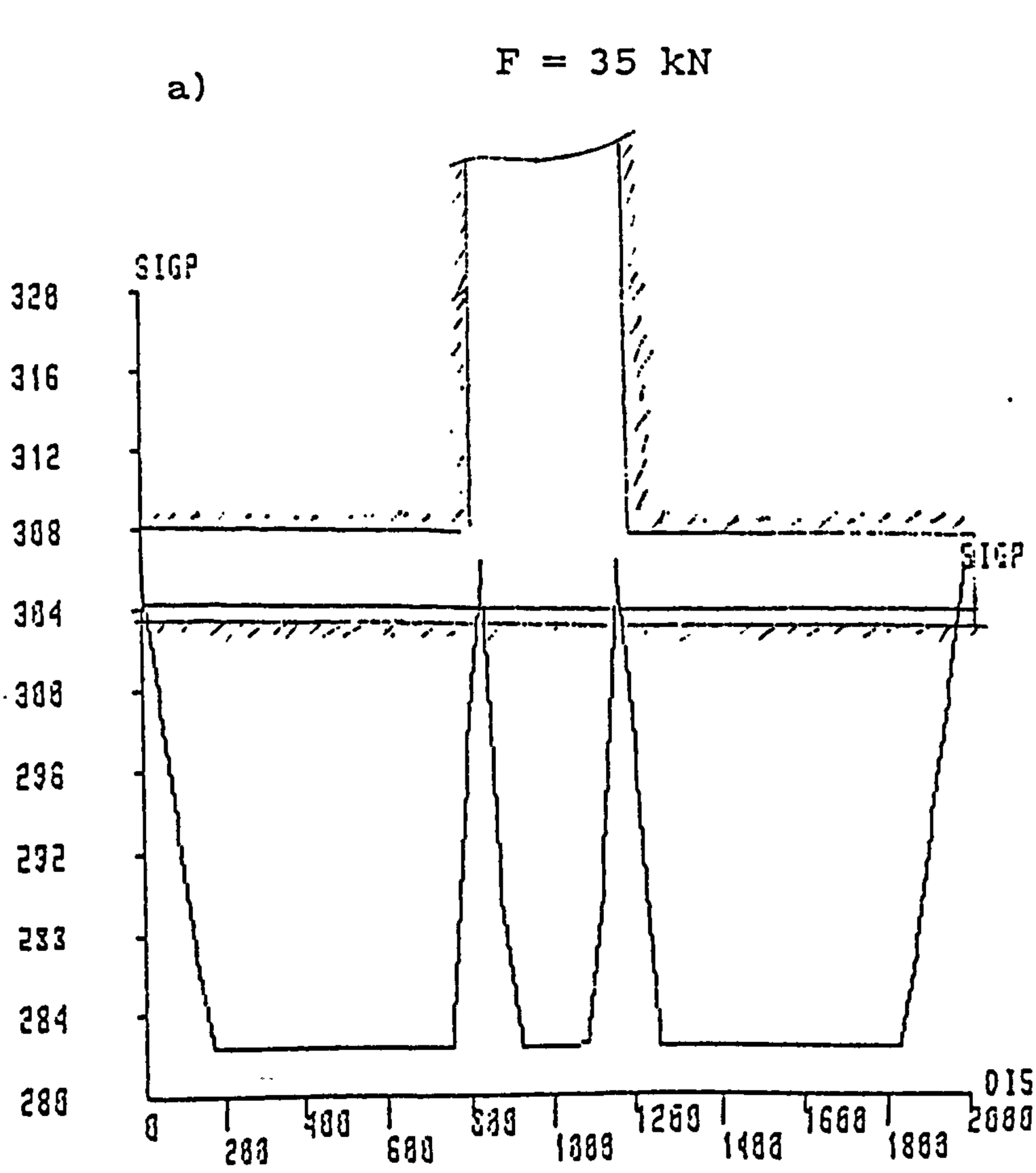

F = 35 kN

b)

FIG.5.26 STRESS AND STRAIN (PLASTIC) DISTRIBUTION IN COLUMN MAIN REINFORCEMENT

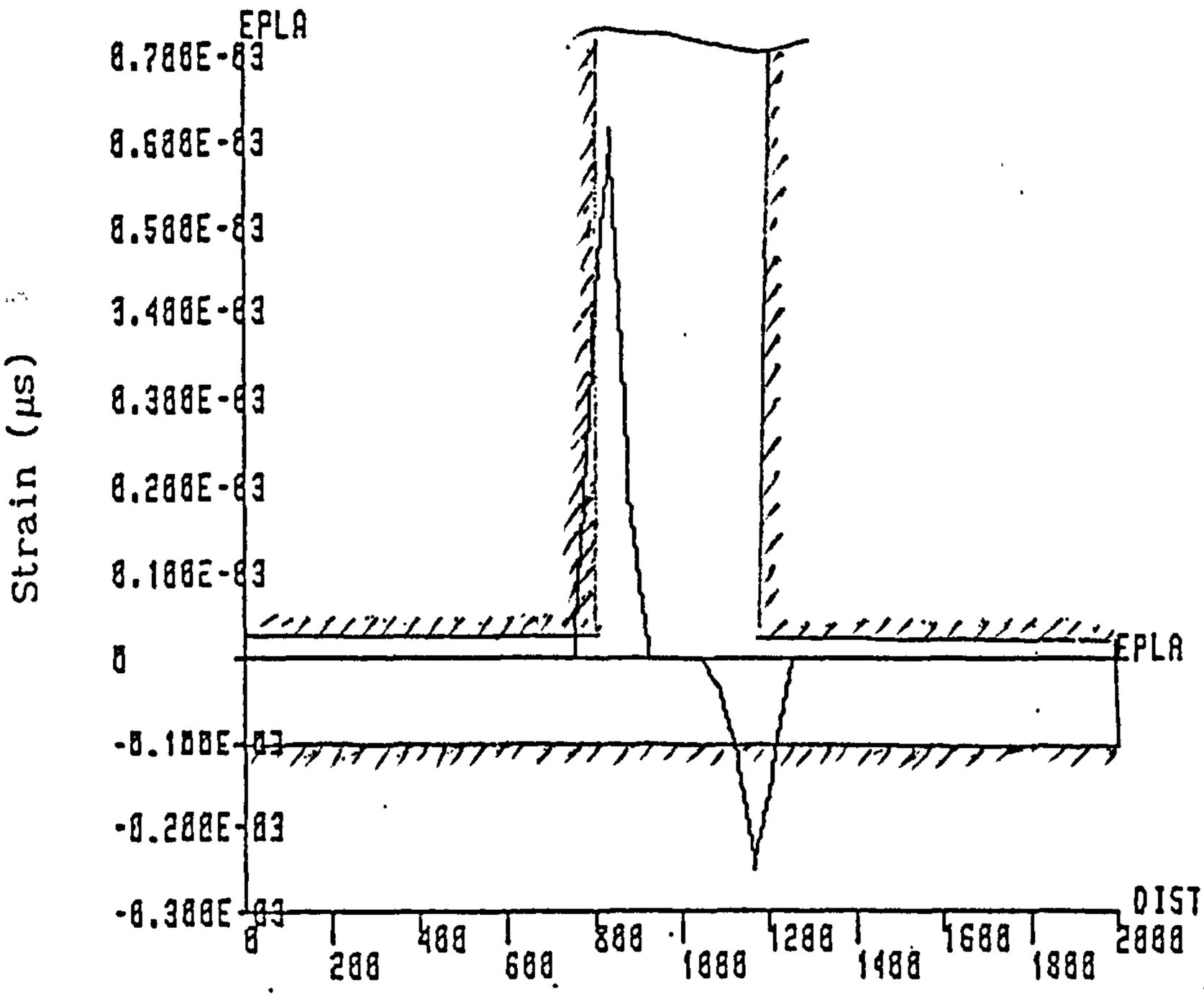

c)

F = 35 kN

* SIGP: Plastic Stress

* EPLA: Plastic Strain

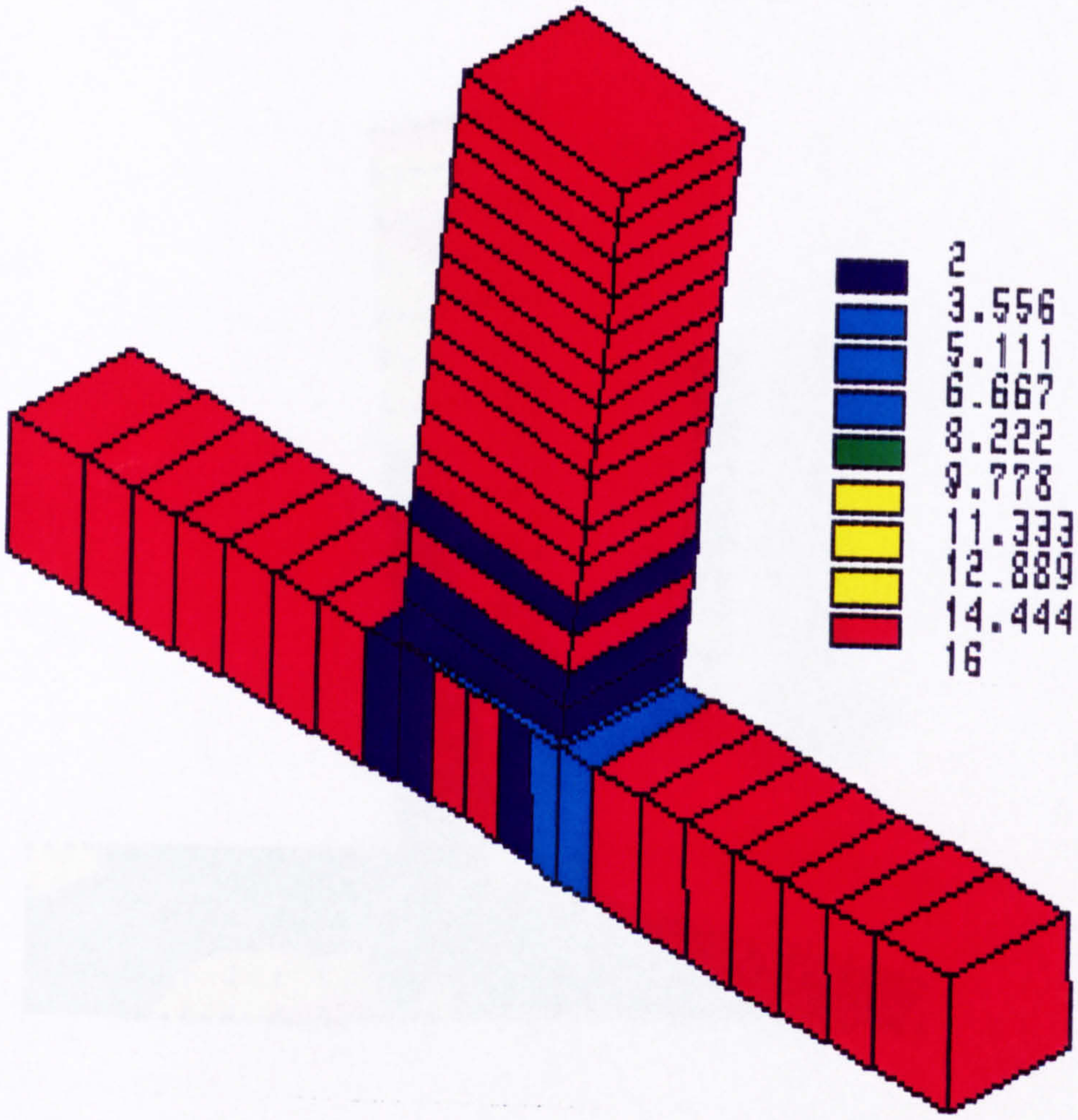

Crack intensity

FIG.5.27 CRACKING PATTERN - SPECIMEN EX1 -

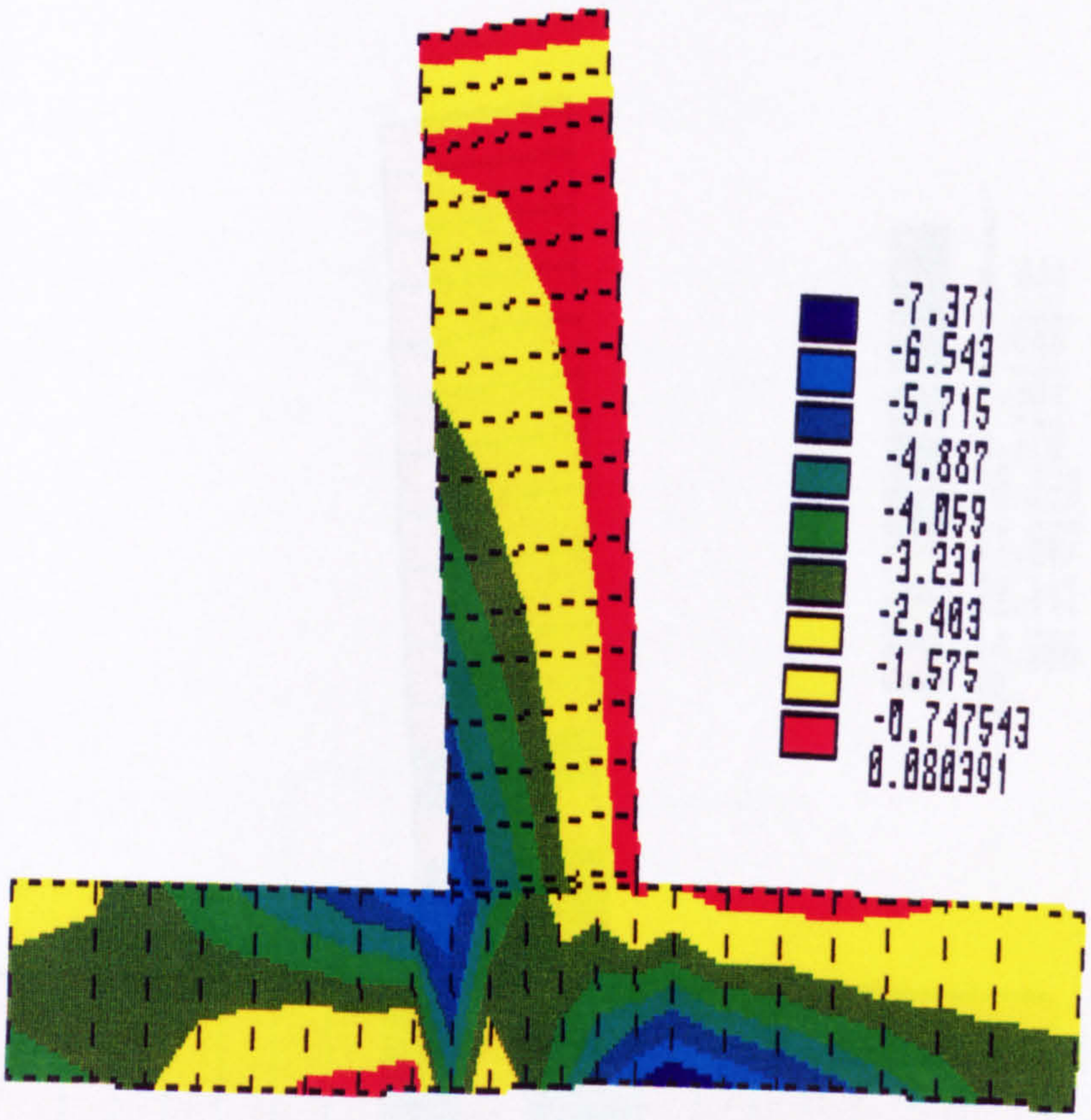

Stress intensity (N/mm^2)

FIG.5.28 STRESS DISTRIBUTION (σ_3) IN SPECIMEN EX1

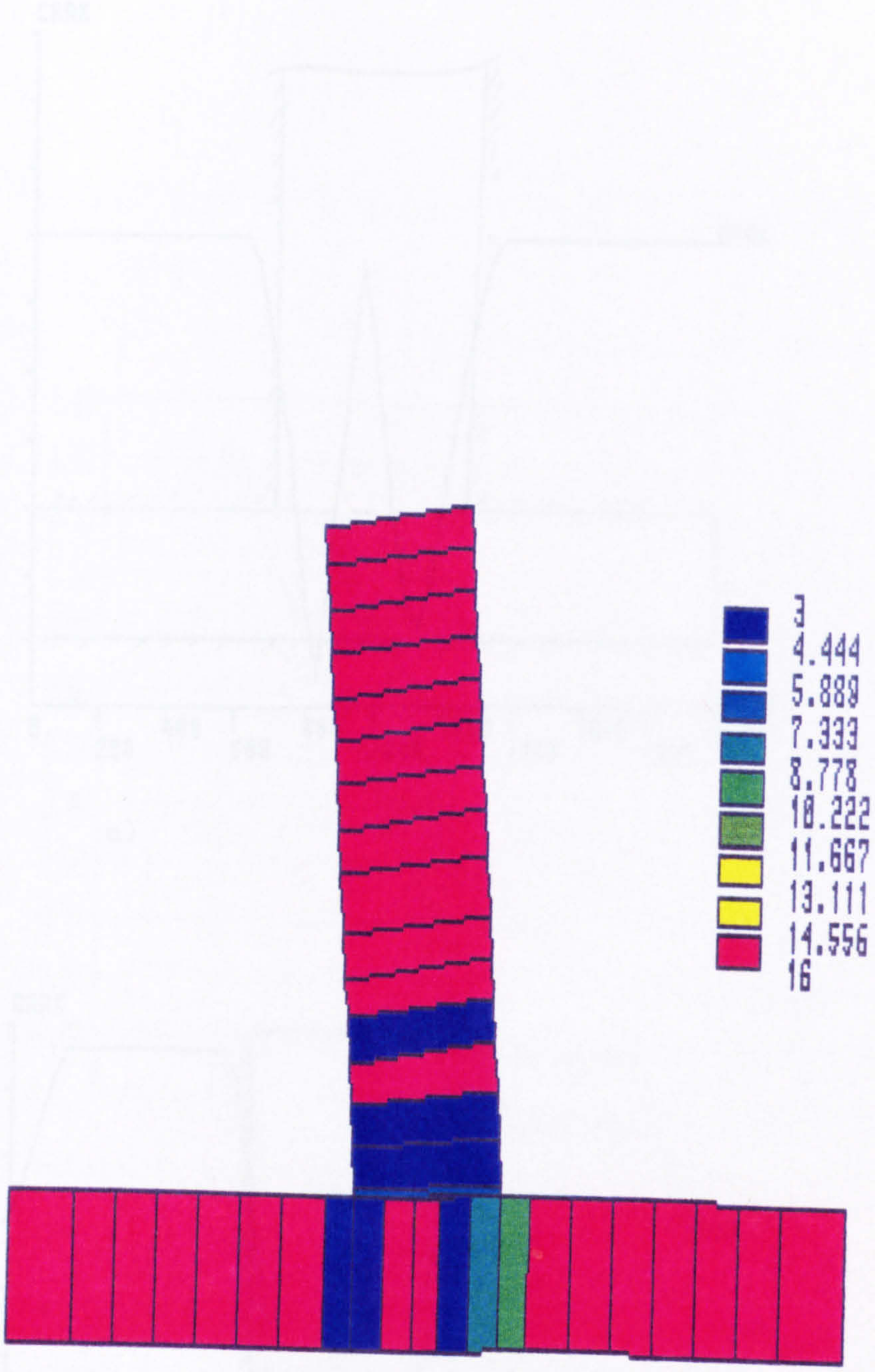

Crack intensity

FIG.5.29 CRACKING PATTERN SPECIMEN - EX1 -

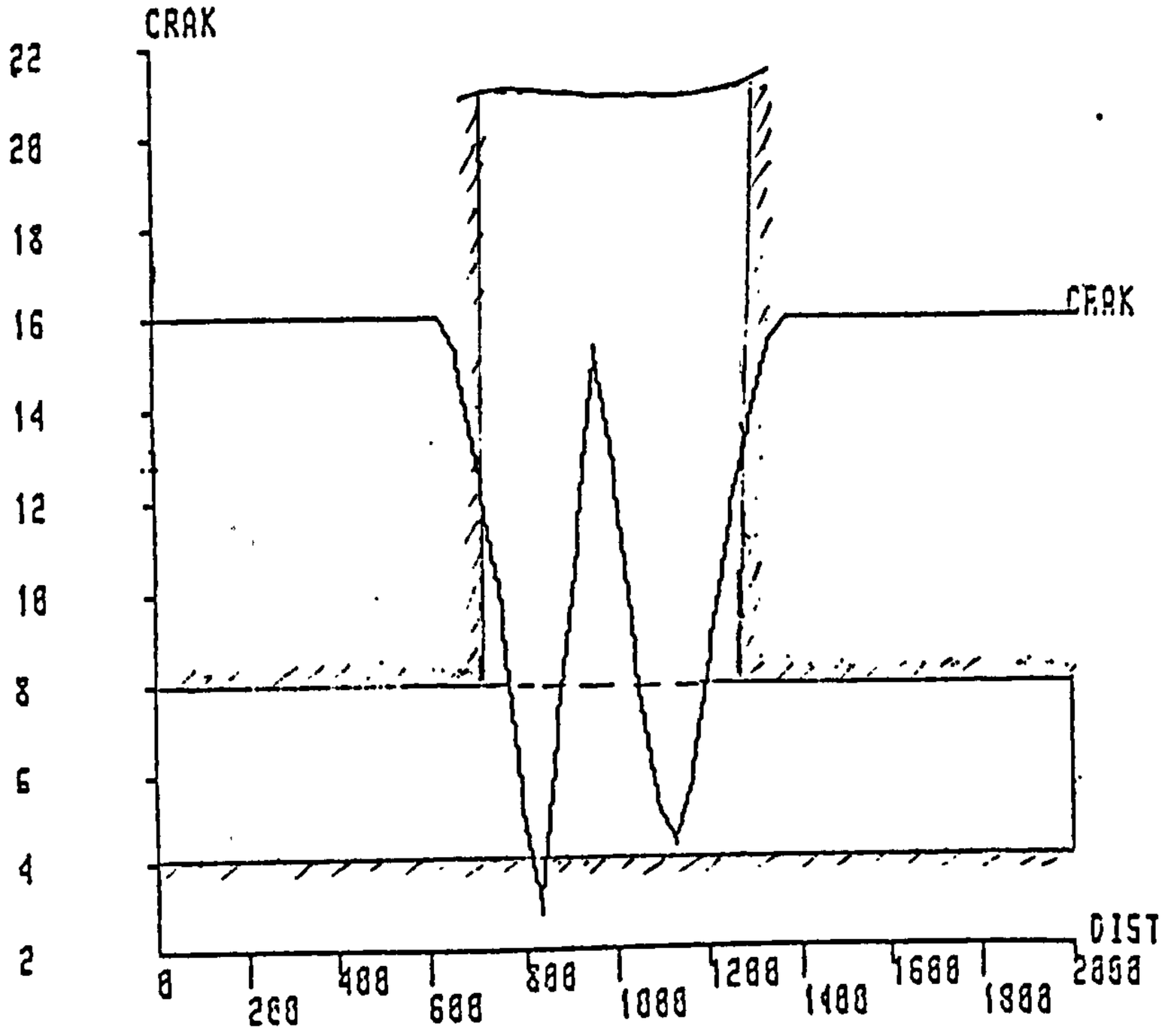

a)

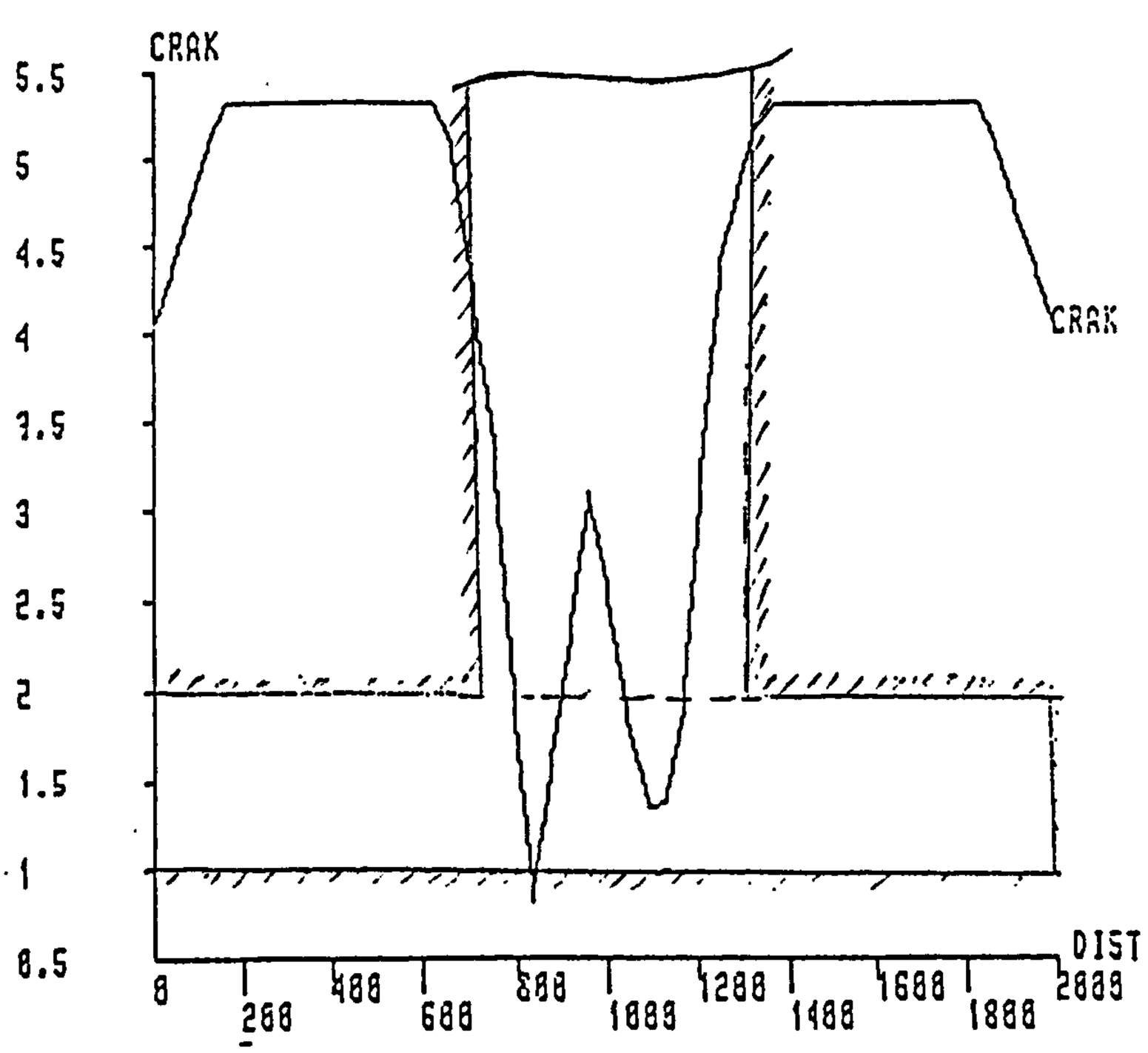

b)

FIG.5.30 CRACKS VARIATION ALONG COLUMN - EX1 -

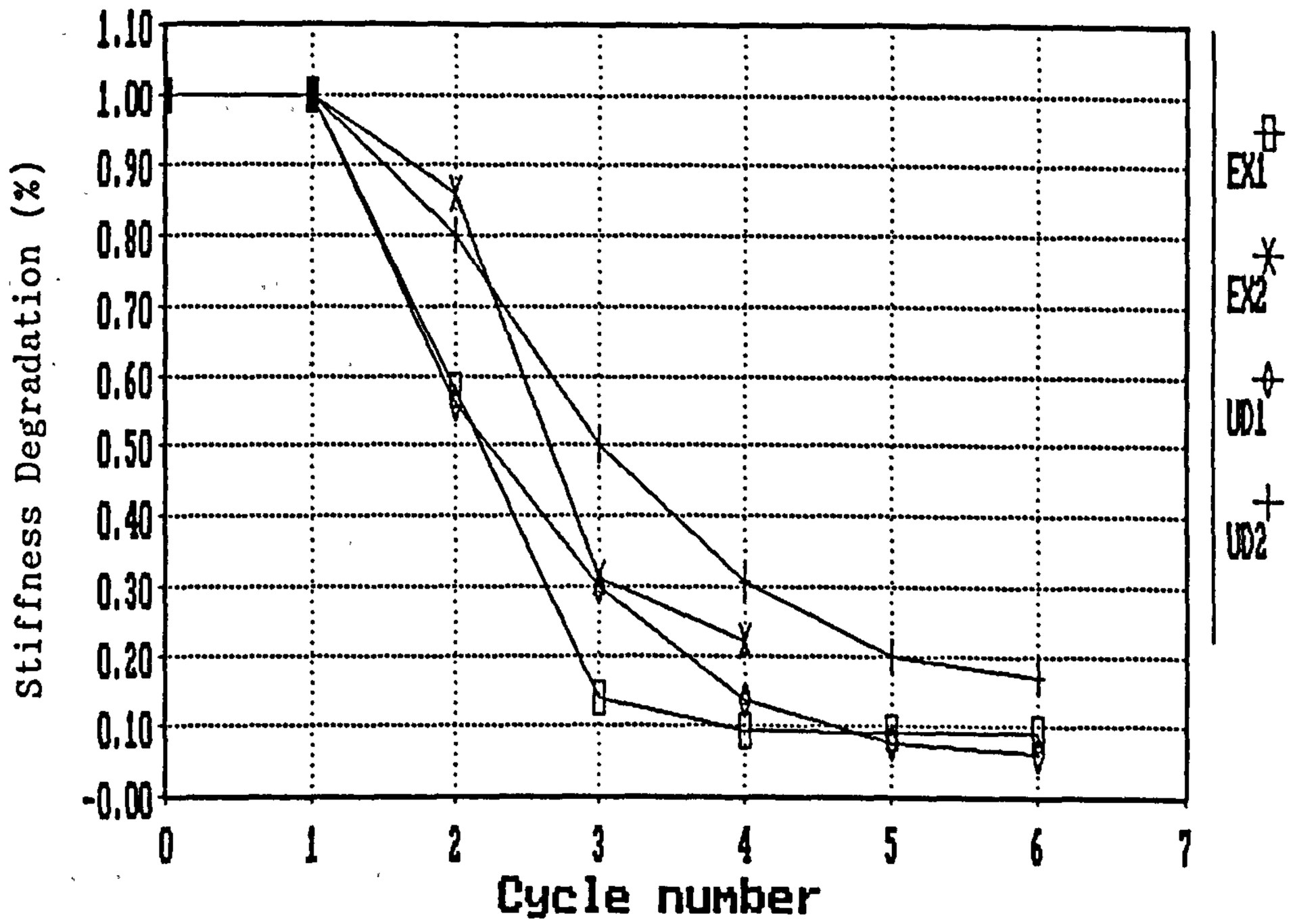

FIG.5.31 STIFFNESS DEGRADATION OF SPECIMENS

CHAPTER SIX DISCUSSION OF THE TEST RESULTS

6.1 COMPARISON OF TEST RESULTS WITH THEORY AND DESIGN RECOMMENDATIONS

6.1.1 Introduction

Four tests on exterior beam-column joint specimens were carried out experimentally and analytically as described in the previous chapters. Performance of all specimens was satisfactory in both experiment and analysis although slippage of beam bars through the joint compromised the response of unit UD1 in the last cycles due to the nature of confinement used in the connection area. Some yielding of the joint reinforcement was observed in specimens EX2 and UD2, but the overall response was not seriously affected. Most of the stirrups stayed linear.

The purpose of this chapter is to compare experimental results, which were not compared in the previous chapter, with the finite element analysis, and with the published procedures for joint design.

6.2 COMPARISON WITH ANALYSIS

6.2.1 Stiffness

Because a comparative study has already been carried out in chapter five, only stiffness of the sub-assemblies and strain in some stirrups from both experiment and analysis are compared in this chapter.

Stiffness is defined here as the load required to cause unit deflection at the point of application of load on a specimen.

A major cause for stiffness loss in the specimens is the pullout

of the beam's longitudinal reinforcement from the joint, especially when the joint yields earlier during the test and the cracked joint concrete loses its ability to resist the bond forces exerted by the beam main reinforcement which was anchored in the joint. The beam bars could then be partially pulled out of the joint as the bar yield stress was developed. Thus the less cracked the beam-column joint concrete is, or the later the beam-column joint yields during an earthquake, the less beam and column reinforcement slippage occur.

Fig.6.1(a) compares the experimental stiffness of all specimens during cyclic loading. At the initial stage of loading (before cracking), stiffness of specimen UD1 was found to vary from 6 kN/m during the first cycle of forward loading to 1 kN/m during the third cycle of forward loading. During the first cycle of reversed loading and after cracking has occurred, its value was found to be about 4 kN/m, which reduced to 1.5 kN/m in the third cycle of reversed loading. Stiffness of specimen UD2 dropped to about 1.6 kN/m in third cycle when loading forward. During reversed loading (second cycle), the stiffness dropped to 3.8 kN/m ,and then increased to 4.2 when loading backward in the third cycle (because of the load rate used when loading backward). In the fifth cycle, stiffness of specimen UD2 was twice that of specimen UD1.

The sharp reduction in stiffness of specimen UD1 is thought to be due to the type of transverse reinforcement used in the connection area which led to the deterioration of the joint region (cracking and crushing of concrete and pull-out of beam main bars) in the subsequent cycles. Another representation of stiffness degradation is given in Fig.6.1(b).

By correlating the stiffness of the hysteresis loops of specimens UD1 and UD2, it can be seen that the U-stirrups which covered the whole effective depth of the column reduce the slippage of beam and column main reinforcement in the joint region by increasing joint strength and by reducing the joint concrete cracking.

The U-stirrups mentioned above helped specimen UD2 improve its resistance by a change in the failure mode compared with specimen UD1.

Stiffness degradation of specimens EX2, UD1 and UD2 obtained from theory is illustrated in Fig.6.2. Specimen UD2 had almost the same stiffness in both studies. During cyclic loading, the reduction of this stiffness followed more or less the same pattern, as shown in Figs.6.1(a) and 6.2(a). Whereas stiffness of UD1 and EX2 were not well predicted, about 7 kN/m (experiment) and 5.5 kN/m (theory), and 6.5 kN/m (experiment) and 5 kN/m (theory), respectively. The loss of stiffness was well simulated for both specimens (UD1 and EX2). At the end of loading forward, stiffness of UD2 did drop to a value of 1.4 kN/m, which is twice that from experiment.

Comparing Figures 6.1 and 6.2, it appeared that the theory predicted rather well the overall behaviour of specimens in terms of stiffness.

6.2.2. Strains in Horizontal Reinforcement

The strains obtained from both experiment and analysis are illustrated in Table 6.1. These strains were recorded at a load level of 35 kN.The strains predicted in specimens EX2, UD1 and UD2 compared reasonably with those from experiments.

In general, the stirrups in all specimens in the joint region behaved rather well in comparing analysis and experiment, this is because none of these stirrups experienced any yielding in those locations and stayed in the linear range. The strain gauges locations are shown in Fig.6.3.

TABLE 6.1 COMPARISON OF EXPERIMENTAL AND THEORETICAL STRAINS IN JOINT STIRRUPS

SPECIMEN	EX2		UD1		UD2	
GAUGE	S1	S3	S2	S1	S9	S8
EXPERIMENTAL STRAINS (μs)	860	1003	711	335	1450	1645
THEORETICAL STRAINS (μs)	960	1300	1100	400	1600	1150

Note (1): The above strains were obtained at load level of 35 kN.

Note (2): Theoretical strains are not available for specimen EX1

6.3 COMPARISON WITH PUBLISHED RECOMMENDATIONS FOR JOINT DESIGN

It was noted in section 1.2 that the resistance of beam-column joint cores to shear in the horizontal direction may be considered as being supplied by two principal mechanisms. The first mechanism involves shear resisted by diagonal compression strut across the joint core and requires some confining reinforcement only in the joint core. The horizontal joint shear resisted by this mechanism is often described as the shear, V_{ch} , resisted by the joint concrete, although the mechanism involved is quite different from that associated with the shear resistance of concrete in flexural members. To resist the

remaining horizontal joint shear, V_{sh}, a truss mechanism which involves both horizontal and vertical joint reinforcement is necessary.

For design, the quantities V_{ch} and V_{sh} must be evaluated so that the necessary reinforcing for a particular joint can be detailed. Published recommendations for joint design include equations by means of which this may be achieved. Table 6.2 gives a comparison of values of V_{sh} and V_{ch} determined from the analytical and experimental test results, against the values used for design of the test units, and against values calculated using equations from the 'recommendations for design of beam-column joints in monolithic reinforced concrete structures' by the ACI-ASCE Committee 352 (1985), and from the draft New Zealand Concrete Code [DZ3101 (1978)].

The ACI-ASCE Recommendations give as the basic equation for the shear strength of joint concrete.

$$V_{ch} = 0.3\ \beta\ \gamma\sqrt{f_c'(1 + 0.3N_u/A_g)}\ \cdot[b' \cdot d_c] \qquad (6\text{-}1)$$

with $V_{ch} \leq 2/3\ V_{jh}$

where $\beta = 1.4$ for type 1 joints (no ductility requirement)

$\beta = 1.0$ for type 2 joints (ductility required)

$\gamma = 1.4$ if the joint is confined by beams in the transverse direction

$\gamma = 1.0$ otherwise.

f_c' = compressive strength of the concrete, N/mm^2

N_u = minimum compressive axial load, N

A_g = gross cross-section area of column, mm^2

b' = effective width of joint to outside of ties, *mm*

d_c = effective depth of column, *mm* (or d_{eff})

V_{jh} = total applied joint horizontal shear.

TABLE 6.2 RESISTANCE TO JOINT SHEAR PREDICTED BY PUBLISHED RECOMMENDATIONS

Specimen		EX-SPECIMENS		UD-SPECIMENS	
		EX1	EX2	UD1	UD2
f_c (N/mm)		80	37	42	40
N_u (kN)		150	100	700	50
Design horizontal shear strength	V_j	266	399	399	266
Horizontal shear strengths predicted by ACI-ASCE 352 Recommendations	V_{sh}	359	359	359	359
	V_{ch}	175	115	110	105
	V_{jh}	534	474	469	464
Horizontal shear strengths predicted by DZ3101	V_{sh}	500	500	500	500
	V_{ch}	22	0	0	0
	V_{jh}	522	500	500	500
Analytical horizontal shear (using ANSYS) (at 35 kN)	V_{sh}(from strains in stirrups)	250	243	189	198
	V_{ch}(from strains in concrete)	58	109	67	89
	V_{jh}	308	352	256	287
Experimental horizontal shear strength results (at 35 kN)	V_{sh}(estimated from stirrups strain)	250	242	188	210
	V_{ch}(estimated from Demec reading)	38	22	12	18
	V_{jh}	288	264	200	228

Notes: - All shear forces are in kN.

It is suggested in the Recommendations that for Type 2 joints under seismic loading the column axial load may be poorly defined, and should therefore be taken as zero. V_{ch} is therefore listed in Table 6.2 both as calculated with this assumption, and with the assumption that N_u is known to be at the level used in the tests.

The equation given in the Recommendations for the horizontal shear resisted by joint reinforcing

$$V_{sh} = \frac{A_v \cdot f_{yh} \cdot d_c}{s} \qquad (6\text{-}2)$$

where :

A_v = area of shear reinforcement within the distance s , mm^2

f_{yh} = yield strength of joint horizontal reinforcement, N/mm^2

s = spacing between sets of joints reinforcement, mm.

The equations given in the draft New Zealand Concrete Code for the horizontal shear strength of joints in plane frames are:

$$V_{ch} = 0.25 \left[1 + \frac{f'_c}{25}\right] \sqrt{\frac{N_u}{A_g} - \frac{f'_c}{10}} \, [b_j \cdot h_c] \qquad (6\text{-}3)$$

and $V_{ch} = 0$ if $N_u/A_g \leq f'_c/10$

and $V_{sh} = A_{jh} \cdot f_{yh}$ (6-4)

where :

b_j = effective joint width = (overall column width b_c), mm

h_c = overall depth of column, *mm*

A_{jh} = effective total area of horizontal joint reinforcement crossing the joint diagonal.

Values of joint horizontal shear strength calculated using equations (6-1) to (6-4) are compared in Table 6.2 to the values derived from the analysis data. Analytical values of V_{sh} were calculated by summing forces derived from strain measurements in the individual stirrup legs over the depth of the joint. Values of V_{ch} were then obtained as the difference between the applied horizontal shear, V_{jh}, and the derived values of V_{sh}.

It may be noted in Table 6.2 that there is reasonable agreement between the joint shear predicted by the analysis and the shears measured in the experiments. However, although these values are recorded when the load was 35 kN, which is close to ultimate in each case, the shears were considerably less than the shear capacities of the joints as evaluated by the Codes (see Table 6.2). This accords with the performance of the joints in the tests since the joint core was effectively intact after completion of each test. The specimens failed by plastic hinge formation at the end of the beam with minor damage to the joint core in each case.

Obviously the full strength of the joint horizontal reinforcement was not mobilized in any of the tests, but in all cases some limited yielding occurred in joint reinforcement, and it is considered that the design procedure for specimens EX1 and EX2 (see chapter two, section 2.1), which was in general accordance with that suggested in the ACI-ASCE Recommendations, resulted in efficient design. The joint

reinforcing was not required to undergo large inelastic strains, since the available strength of the joint was not fully utilized under the cyclic loading for all specimens. The low values of the horizontal shear resisted by the concrete mechanism determined at a late stage of loading (load step 28) give a good indication of the resistance which may be expected from this mechanism after severe seismic loading. Thus the zero recommendation given in the Draft New Zealand Concrete Code for joints with light axial loads is quite realistic. The values for V_{ch} given in the ACI-ASCE Recommendations are optimistic in these cases.

The vertical shears resisted by joint concrete and reinforcement mechanisms, V_{cv} and V_{sv} respectively was not taking into consideration, because in all specimens tested columns had no intermediate bars, and therefore $V_{cv} = V_{sh} = 0$, as can be seen in the following equations from the Draft New Zealand Concrete Code.

$$V_{cv} = \frac{A_{sc}}{A'_{sc}} \frac{V_{jv}}{2} \left(1 + \frac{N_u}{0.6 A_g f'_c}\right) \qquad (6\text{-}5)$$

where :

- A_{sc} = lesser area of column flexural steel in tensile or compressive face at the joint (mm^2)
- A'_{sc} = greater area of column flexural steel in tensile or compressive face at joint (mm^2)
- V_{jv} = total vertical shear force across the joint

and $$V_{sv} = A_{jv} \cdot f_{yv} \qquad (6\text{-}6)$$

where :

- A_{jv} = total area of vertical joint reinforcement (mm^2)
  (= area of intermediate column bars)
- f_{yv} = yield strength of vertical joint reinforcement.

The ACI-ASCE Recommendations make no provisions for resistance to vertical joint shear.

6.4 COMPARISON WITH POSTULATED MECHANISM OF RESISTANCE

A postulated mechanism of resistance to joint shear was outlined in chapter one, section 1.2. In the proposed mechanism part of the joint shear was resisted by the joint concrete acting as a direct diagonal strut, and part of the shear was resisted by joint reinforcement acting as a truss.

According to the postulated mode of joint concrete shear resistance for joints carrying little or no column axial load, the direct concrete strut acts between the concrete compression forces in the flexural members (see Fig.1.4, Chapter one). This implies that very little horizontal shear will be resisted by the joint concrete mechanism once cyclic loading in the inelastic range has started, due to the permanently open flexural cracks and the consequently small compression forces carried by the beam concrete. This prediction was substantiated in the tests of specimens UD1 and UD2 (i.e. stirrups strains increased).

It was further postulated in Chapter one, section 1.3 that when significant axial compression is applied to the joint, sufficient bond forces might be acquired from the beam bars to provide a horizontal

component for the direct concrete strut, even under cyclic conditions. This prediction was verified by specimen EX1, where significant proportions of the horizontal joint shear were found to be resisted by joint concrete during inelastic cycles, although the proportion decreased throughout the test as penetration of yield strain in the beam bars into the joint core increased.

In specimen EX2 the reduction in column axial load shifted the centre of concrete compression in the column sections above and below the joint core so that much less horizontal shear could be picked up from the beam bar bond forces to form an effective diagonal strut. This resulted in lower proportions of joint shear resisted by the joint concrete mechanism in this test.

From these results it appears that the crucial factors in promoting effective shear resistance by the joint concrete are the column axial load level and the extent of beam reinforcement yield penetration into the joint. In all cases of significant cyclic loading it is likely that some yield penetration will occur, while concrete compression forces in the beam plastic hinges will be small. However, if a significant part of the concrete compression forces in the column can act with bond forces from the beam flexural steel over which bond is still effective, then a valid direct diagonal strut mechanism may be formed.

The balance of the horizontal joint shear was resisted by horizontal joint reinforcement. As it was mentioned in section 1.2, this would be achieved by a truss mechanism involving joint stirrups as horizontal members, column bars and column axial load as vertical

members, and diagonal concrete struts as inclined members. The test results showed that the majority of the horizontal shear was resisted by this truss mechanism. During test and analysis of EX2, UD1 and UD2, additional compression strains were noted in the column bars, and this was considered to be due to the weakening of the surrounding joint concrete by cracking, which required the column bars to carry more of the compressive load.

6.5 RESPONSE OF EXTERIOR JOINTS TO SEISMIC LOADING

6.5.1 Mechanism of Shear Resistance

In accordance with recent practice [DZ3101 (1978) and ACI-ASCE (1976)], the beam flexural bars are terminated in hooked anchorages, either within the column core or in a separate anchorage block located beyond the outer face of the column. Then it is apparent that significant forces are available in the right direction and position at the root of the hook to provide appropriate end conditions for the operation of a direct concrete strut across the joint. Under negative moment loading, on the other hand, the bottom reinforcement is insufficient to carry all the compression necessary when tensile yielding of the top bars occurs. Thus some compression will be carried by the beam concrete when full negative moment is applied, and this provides a suitable end reaction for a diagonal strut, as shown in Fig.6.4(a). However the conditions at the diagonally opposite corner of the joint panel may not be so favorable. If the beam is asymmetrically reinforced, with a greater area of top reinforcement than of bottom reinforcement, then under loading producing positive bending (Fig.6.4) in the beam there will be no compression force in the concrete at the top of the beam after cyclic inelastic loading. This occurs because the yield forces of the bottom bars in tension

are insufficient to yield the top bars in compression, so that the cracks in the top of the beam can never close, and hence the concrete can carry very little compression. The end conditions for development of a direct diagonal strut are thus poor at the upper corner only, as shown in Fig.6.4(b), unless the presence of significant column axial load means that suitable horizontal forces can be transferred by bond from the top bars within the compressed depth of the column section above the joints.

The response of an exterior joint for which the beam is asymmetrically reinforced may therefore be expected to be better than that of a similar interior joint, because the presence of adequate anchorage hooks implies that suitable end conditions for the action of the direct diagonal strut are always available at both outer corners of the joint panel, and to a limited extent at one (bottom) inner corner. Thus it is suggested that for exterior joints with adequate anchorage for the beam flexural reinforcement, the joint horizontal reinforcement may be designed on the basis outlined for interior joints, considering only the lesser of the two possible design shear forces, i.e. the lesser of the shears resulting from either positive or negative bending moment. The direct concrete strut shown in Fig.6.4(a) is available to carry the remaining shear arising from the (reversed) larger moment.

6.5.2 Action on the Joint Core

As described in section 1.2, the horizontal shear, V_{jh}, applied to a beam-column joint may be calculated from the maximum likely overstrength of the beam flexural bars, less the shear in the column above.

$$V_{jh} = (A_{sb} + A_{st}) \cdot \alpha \cdot F_y - V_{col} \qquad (6\text{-}7)$$

where :

A_{st} = area of top reinforcement

A_{sb} = area of bottom reinforcement

α = overstrength factor

f_y = specified yield strength of beam reinforcement

V_{col} = column shear.

6.5.3 Requirements for Anchorage of Beam Flexural Reinforcement in Exterior Joints

Requirements for the anchorage of beam flexural bars at exterior joints are given in both sets of recommendations for joint design. The draft New Zealand Concrete Design Code [DZ3101 (1978)], in accordance with observed tests for exterior beam-column joints under cyclic loading [Park and Paulay (1973), and Blakeley (1975)], required that the development length, l_d, for beam flexural bars should be taken from the centreline of the column, or from $10d_b$ (d_b: beam bar diameter) inside the inner column face, whichever provides the smaller lead-in distance. The recommendations of ACI-ASCE Committee 352 (1976), on the other hand, suggest the development length may be taken from the line of the outermost layer of column bars. These two situations are illustrated in Fig.6.5.

The draft New Zealand Code also makes a more conservative assessment of the stress, f_h, able to be developed by a standard 90^0 hook than do the American recommendations. The draft New Zealand Code gives the expression:

$$f_h = 30\sqrt{f'_c} \qquad (6\text{-}8)$$

The ACI-ASCE Committee 352 give

$$f_h = 58.1(1-0.0118d_b)\sqrt{f_c'} \qquad (6\text{-}9)$$

and the ACI-318 committee give

$$f_h = 0.083\xi\sqrt{f_c'} \qquad (6\text{-}10)$$

The approach of ACI-ASCE Committee 352 appears to be based on the results of tests [Ismail and Jirsa (1972)], which did not include reversed cyclic loading, and it appears that the recommendations may not therefore be entirely appropriate for joints in frames subjected to earthquake loading.

For details about requirement lengths of anchorage, a comparative study between Americans and British codes can be found in Appendix A4.

6.6 SUMMARY OF RESEARCH FINDINGS

The principal part of the research reported in this thesis has been the testing under cyclic loading, simulating earthquake loading, and a finite element modelling of four full-scale reinforced concrete beam-column joint sub-assemblies from plane frames. The test results showed that beam-column joints can be designed so that the plastic deformation under seismic loading is restricted to the beam plastic hinges. Some stiffness degradation was observed under cyclic inelastic loading. The test units to which small column axial loads were applied displayed a secondary failure towards the end of each test when the beam flexural reinforcing bars slipped through the joint core. The slippage resulted in more serious stiffness degradation, with consequent loss of energy dissipating capacity.

The results obtained from the tests were shown to be consistent to some extent with those from the finite element analysis as it has been stated in chapter five, and with the mechanisms of joint shear resistance postulated in chapter one. According to these postulates, the applied joint shear is resisted partly by a concrete compression strut acting between diagonally opposite corners of the joint core, and partly by a truss which requires horizontal and vertical joint core reinforcement. For the concrete strut mechanism to be effective, suitable boundary conditions must be available to allow significant shear to be introduced at or near the corners of the joint core. After cyclic loading causing plastic hinging in the beams at the column faces the presence of full depth cracks in the beams means that suitable boundary conditions occur only for joint cores carrying moderate to heavy axial loads. In this case it was postulated that a greater depth of the concrete compression zone in the column sections would enable part of the bond force from the beam bars to combine with vertical forces from the column to allow a compression strut to develop between the corners of the joint core, even though no concrete compression forces were available in the beams. This behaviour was well illustrated in the tests, where the joint core of the test unit carrying relatively moderate axial loads performed much better than those of the units with low axial loads. This better behaviour occurred in spite of the fact that the unit to which moderate axial load was applied had less horizontal and vertical joint core reinforcement. In both cases the presence of beam concrete compressive forces provide favourable end conditions for the concrete compressive strut mechanism, and this was reflected by the low strains measured in joint core horizontal reinforcement during these parts of each test. As soon as reversed cyclic inelastic loading was applied, however, the

joint core tie strains increased, and the concrete mechanism became much less effective.

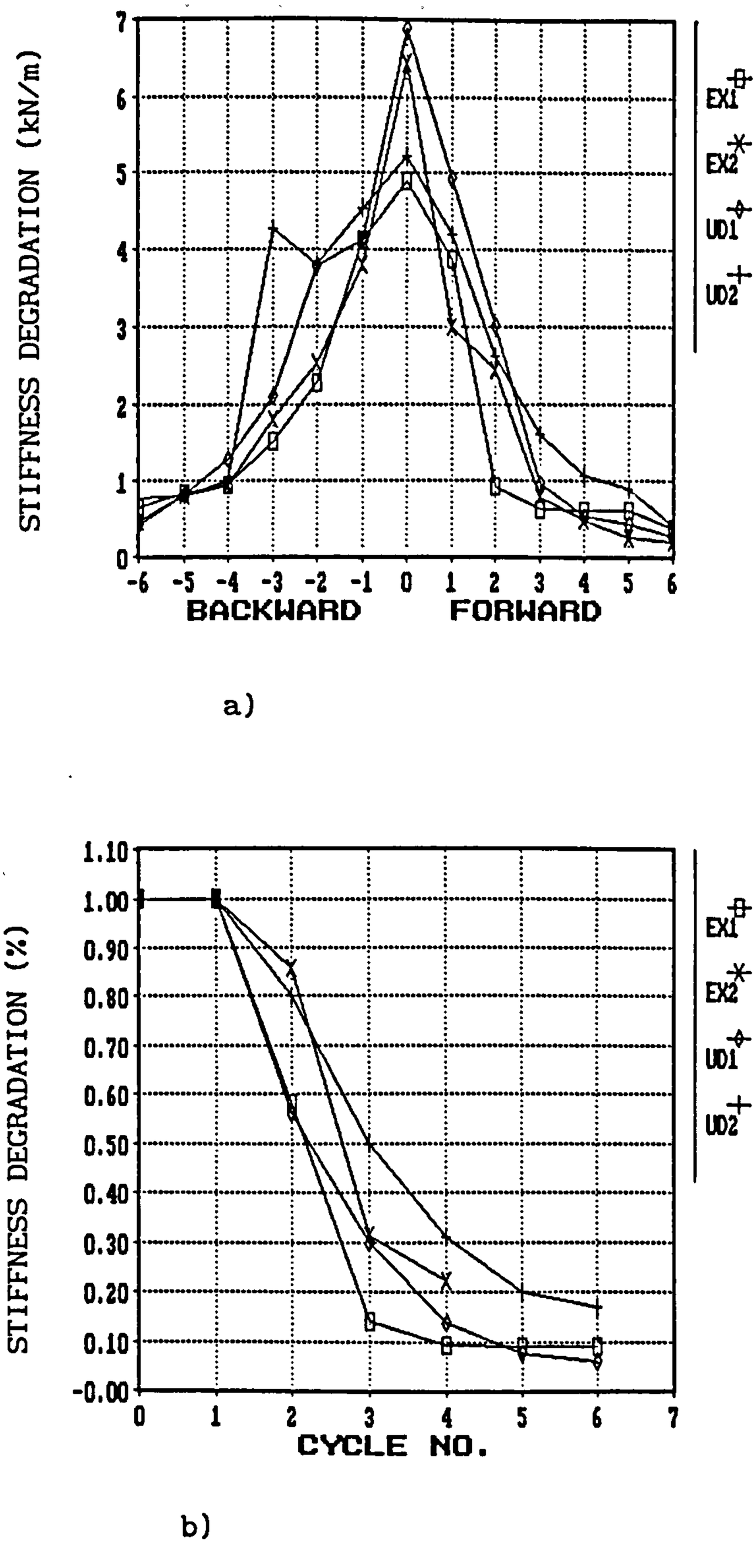

FIG.6.1 STIFFNESS VERSUS LOAD CYCLES

a) Stiffness degradation in kN/m

b) Stiffness degradation in percentage

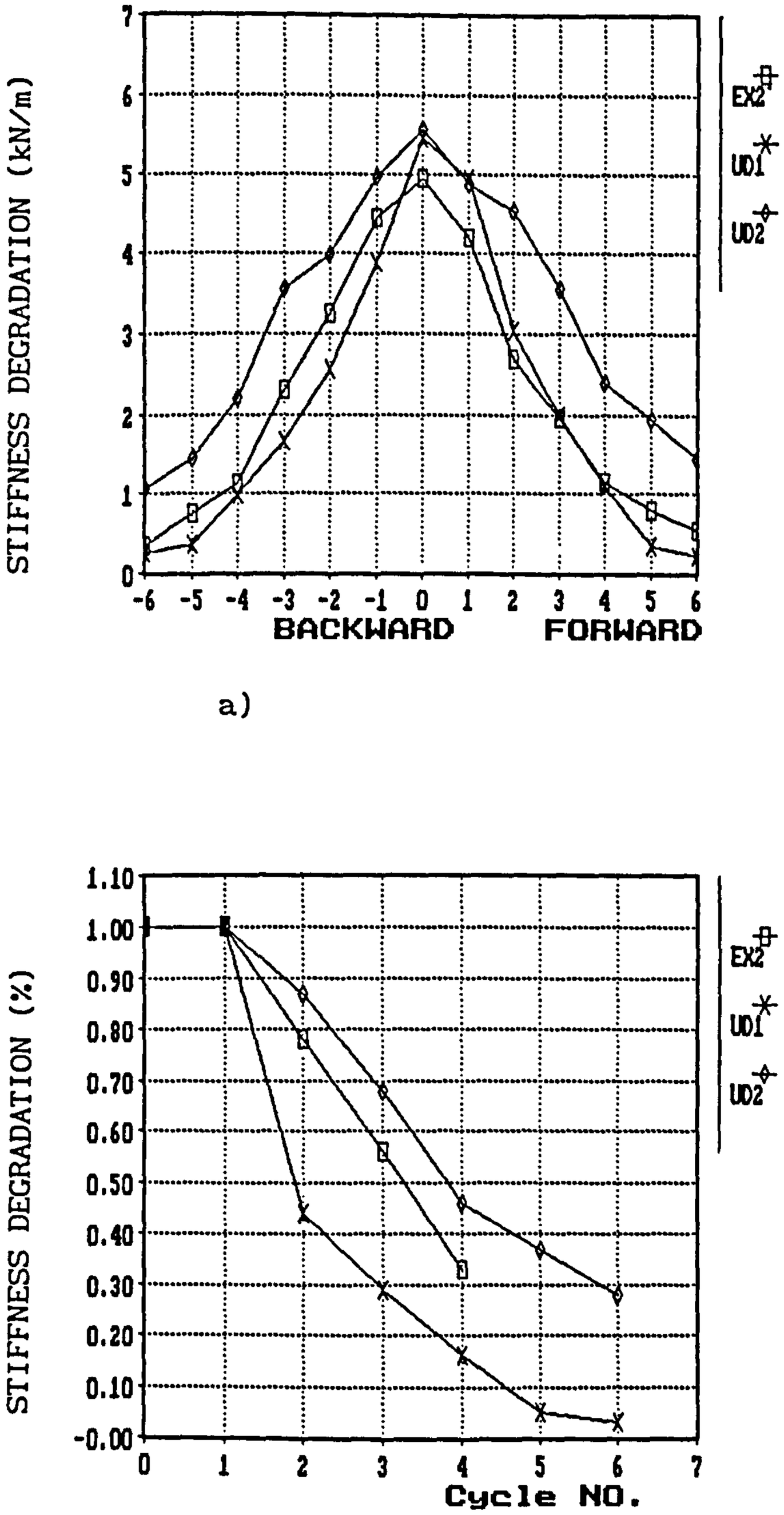

FIG.6.2 THEORETICAL STIFFNESS VERSUS LOAD CYCLES

a) Stiffness degradation in kN/m

b) Stiffness degradation in percentage

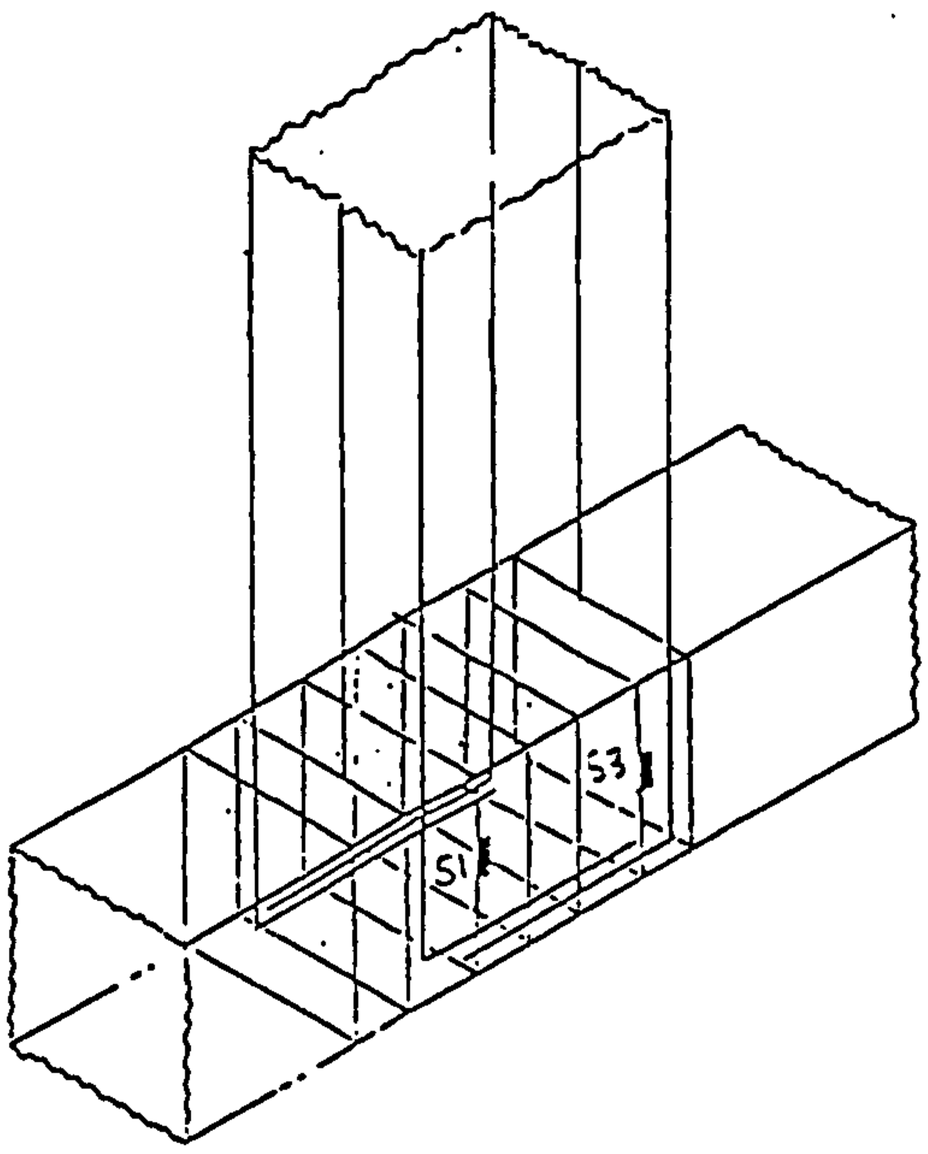

a) Specimen EX2

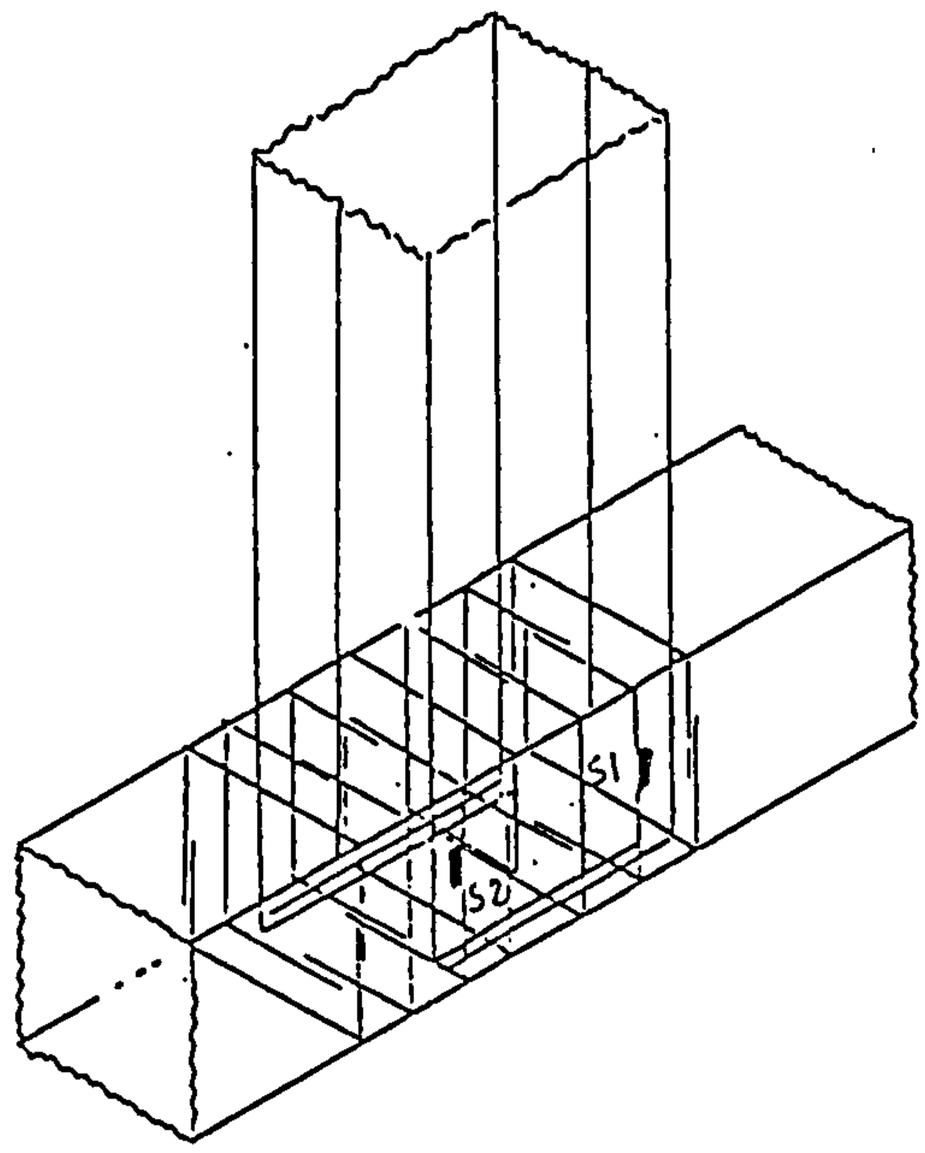

b) Specimen UD1

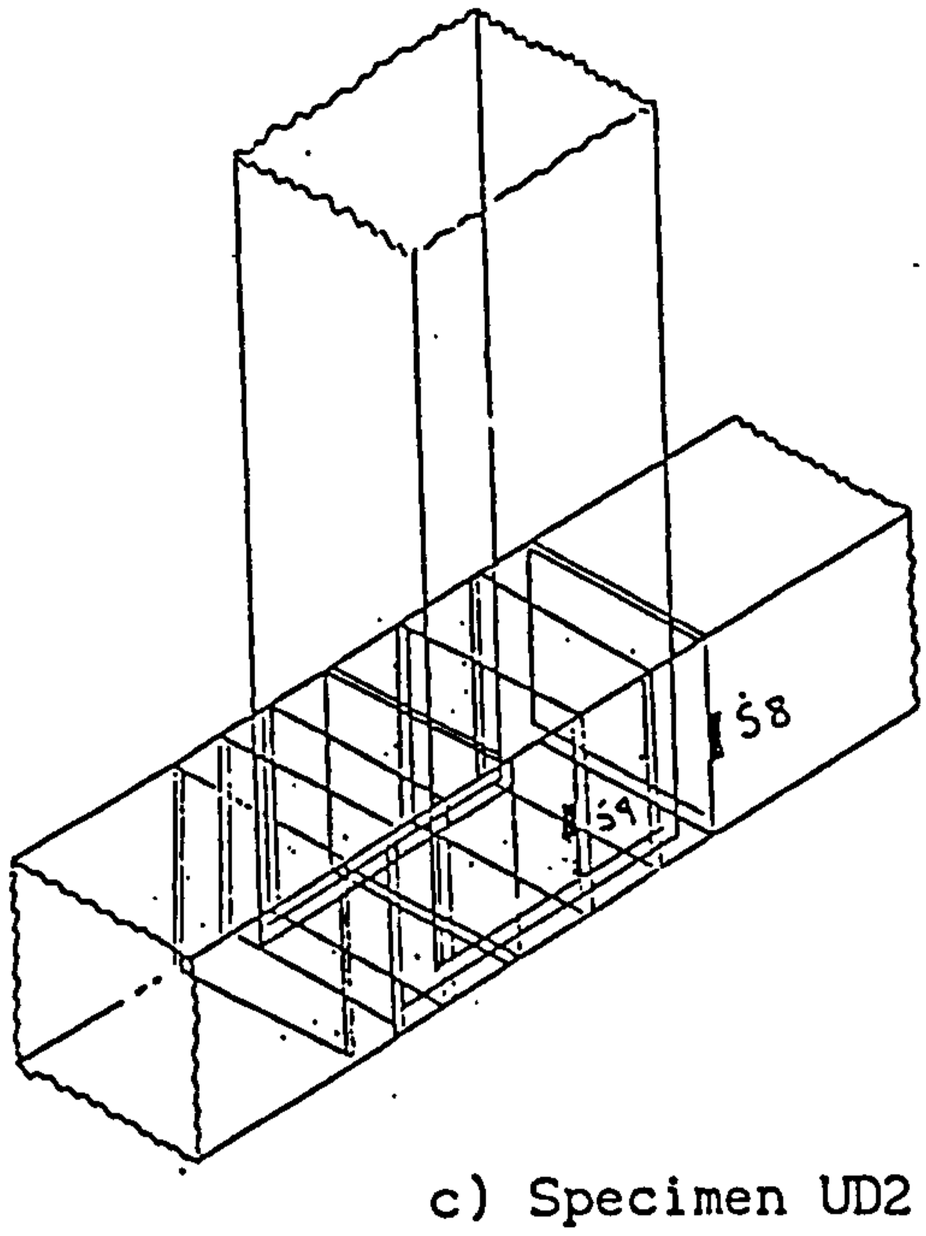

c) Specimen UD2

FIG. 6.3 STRAIN GAUGES LOCATIONS

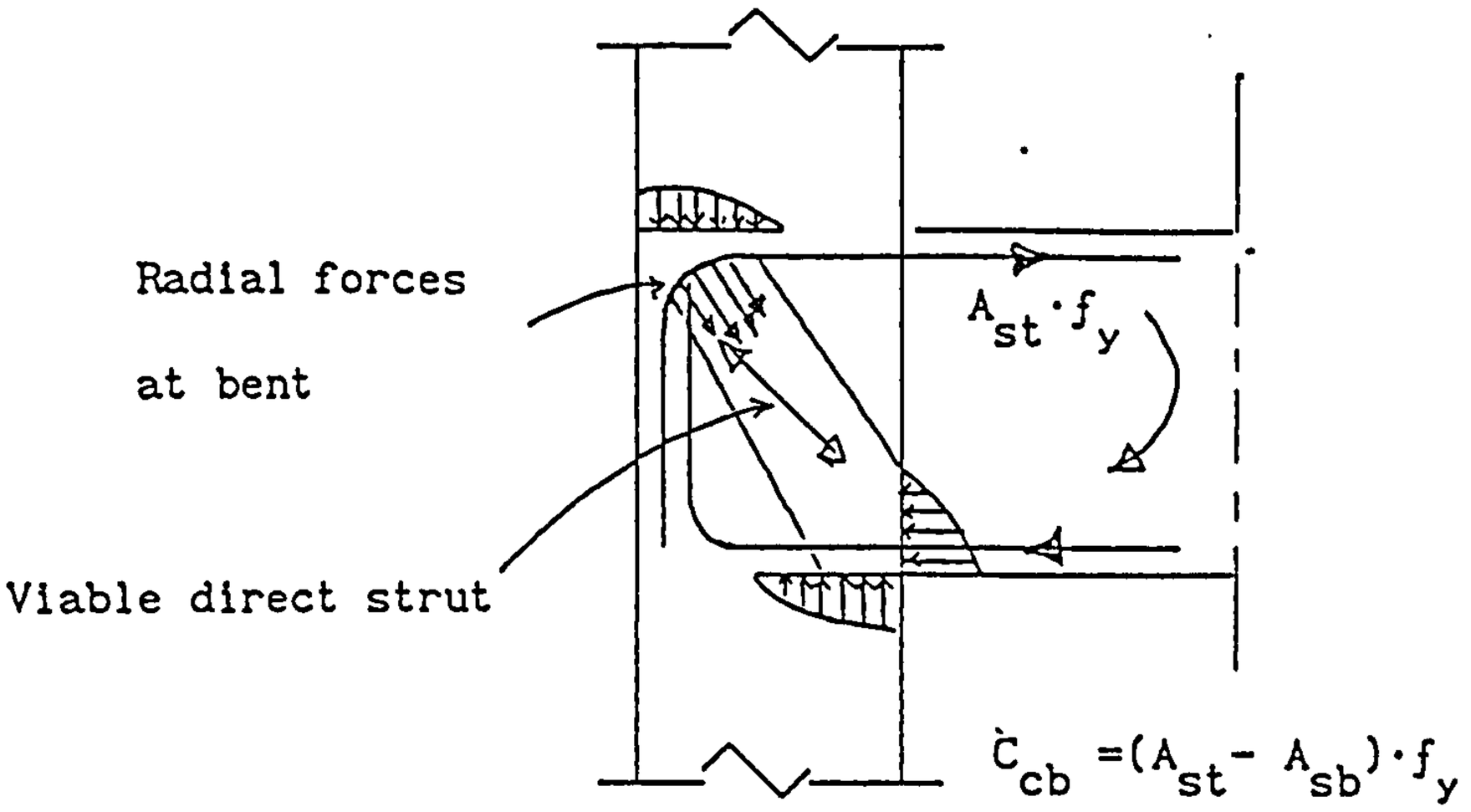

$A_{st} > A_{sb}$

a) Negative bending load

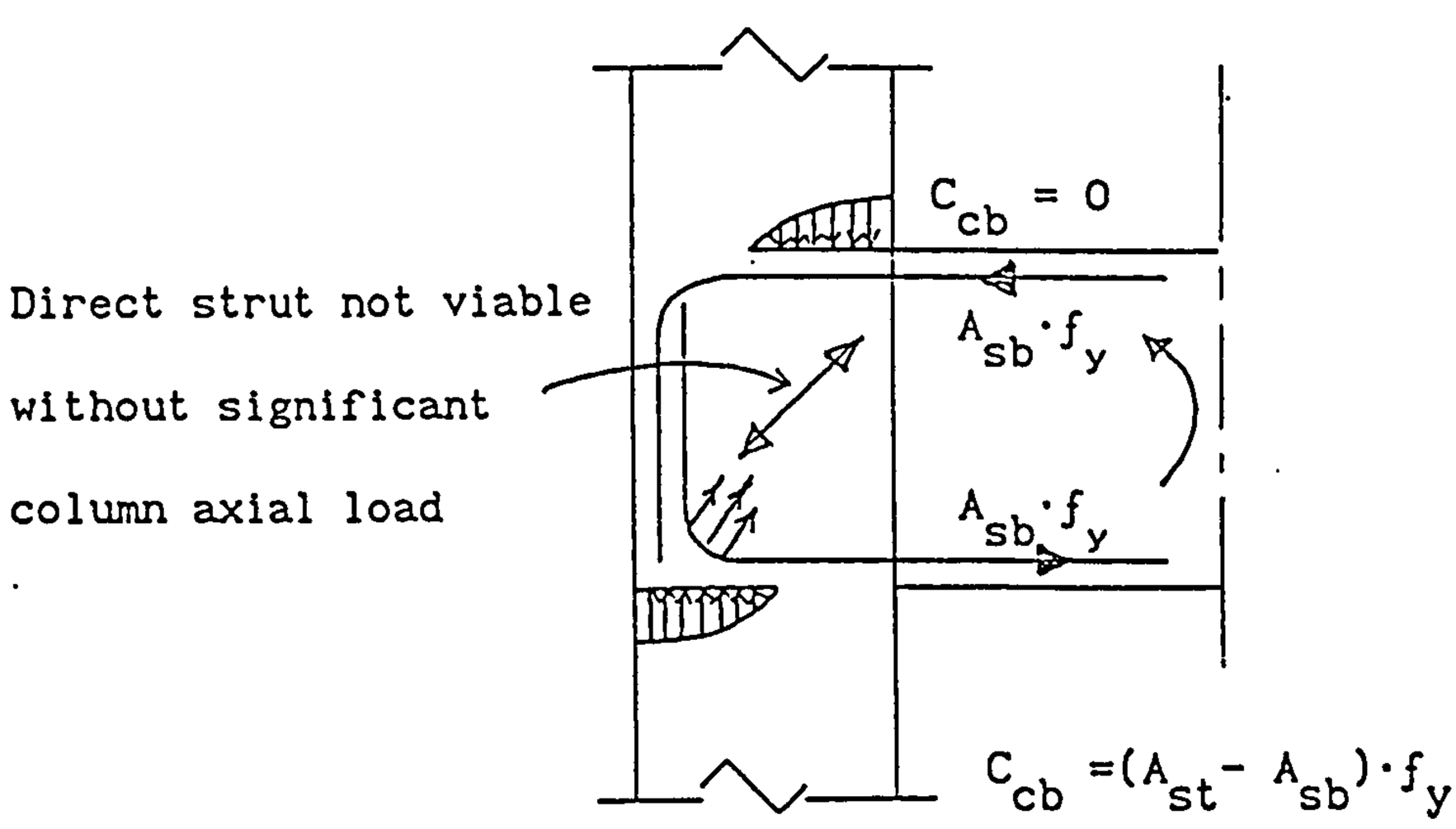

b) Positive bending load

FIG.6.4 DIRECT CONCRETE STRUT MECHANISM FOR SHEAR RESISTANCE IN EXTERIOR JOINTS

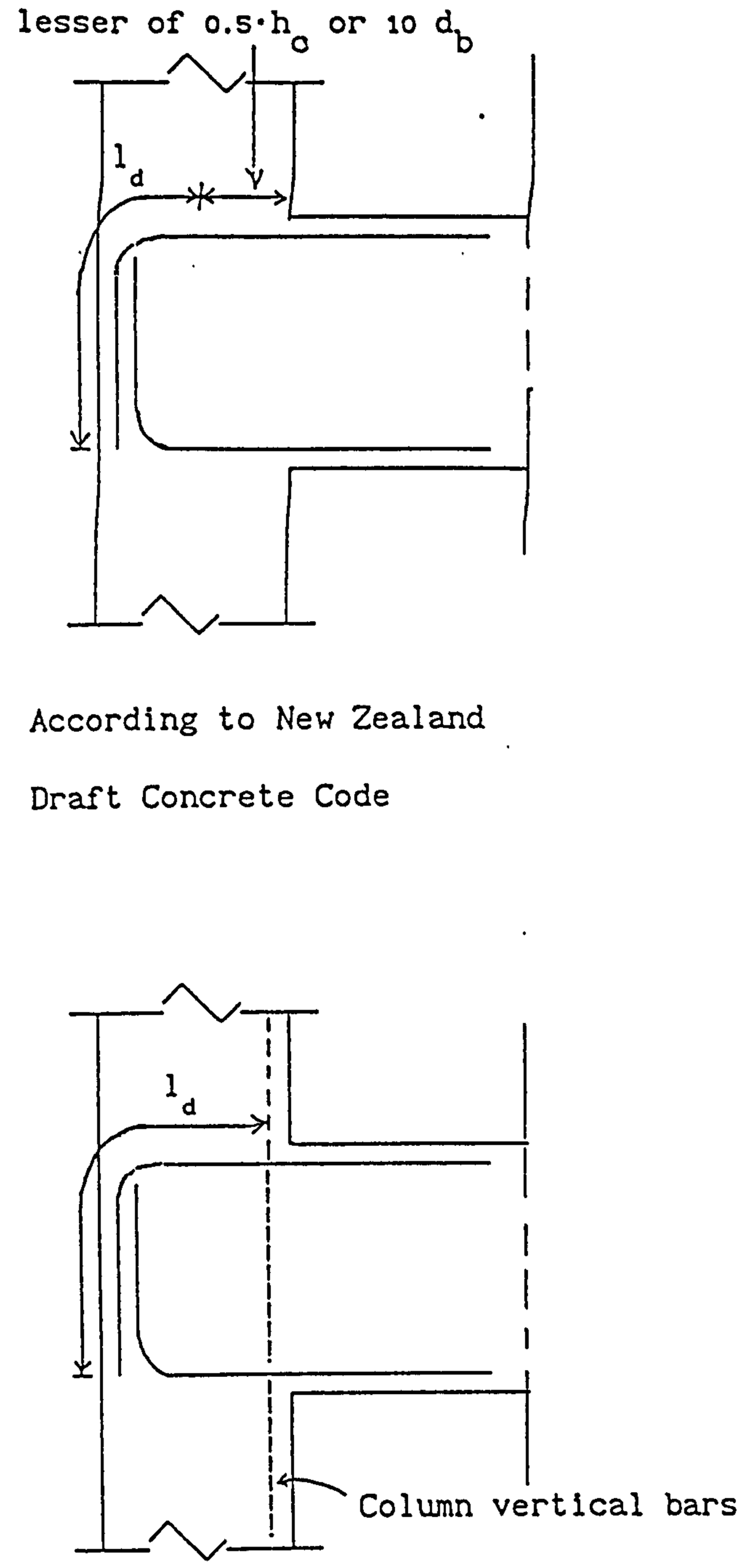

a) According to New Zealand

Draft Concrete Code

b) Recommendations of

ACI-ASCE Committee 352

FIG.6.5 RECOMMENDATIONS FOR ANCHORAGE OF BEAM FLEXURAL BARS

... AT EXTERIOR JOINTS

CHAPTER SEVEN SUMMARY AND CONCLUSIONS

7.1 SUMMARY

The primary objective of this research was to study the behaviour of exterior beam-to-column connections of reinforced concrete moment resisting frames. The investigation was divided into two parts:

a) The experimental investigation of beam-to-column connections.

b) The analytical study of beam-column sub-assemblies.

7.1.1 Experimental Investigation

The main purpose of the experimental investigation was:

1) To examine the effect of joint core reinforcement provided by a different type (U-stirrups) of joint hoops reinforcement on the behaviour of beam-to-column connections.

2) To compare the performance of U-stirrups and conventional hoops in beam-column connections when subjected to cyclic loading.

3) To investigate the influence of the flexural strength ratio on the response of beam-column connections.

4) To examine the influence of column axial load and concrete strength on the performance of the joint concrete strut mechanism.

To achieve these objectives, four full-scale exterior beam-column sub-assemblies were constructed. Two of the sub-assemblies had

conventional stirrups in the joint region (referred to as EX) and the other two which had a new type of transverse reinforcement in the connection area (referred to as UD). Of the two UD-specimens, one specimen (UD1) had the stirrups overlap length equal to one-half of the column effective depth, whereas the stirrups overlap length of the other specimen (UD2) covered the whole column depth.

The ratio of flexural strengths of columns to that of beams has been changed, in order to study the influence of this parameter on the behaviour of the sub-assemblies.

During testing, the columns were held horizontally in the testing frame with pin supports near the end of columns. An average of twenty electrical resistance strain gauges were placed on the reinforcement in and around the joint to continuously record the strain variations during the loading cycles. The specimens also had one LVDT placed at the tip of beams to measure its displacement. All specimens were subjected to six or more loading cycles, except specimen EX2 which had four cycles only. During the test, strain gauges and the LVDT were read by an amplifier connected to a PC computer. The crack development was recorded by means of Demec gauges.

Based on the effects of various parameters observed during the experimental investigation, some suggestions for design and detailing of joints are proposed.

7.1.2 Analytical Investigation

The analytical part of this research dealt with simulation of reinforced concrete sub-assemblies. The main objective of this study

was to obtain a good idea of the overall behaviour of beam-column sub-assemblies, especially, of the joints.

In order to have a clear insight of that behaviour, attention was focused on:

1) The investigation of the effectiveness of numerical modelling of reinforced beam-column connections subjected to cyclic loading up to failure.

2) Identification of some characteristics of structural performance that were not measured, or could not be measured in the experimental investigation, such as stress and (or) strain profile all along the reinforcing steel, the exact locations and the beginning of yielding in the reinforcement, stress distribution in concrete, crack patterns, etc.

In this respect, four analyses were carried out and these were direct simulations of the experiments. It is worth noting that when carrying out these analyses, two approximations had to be made, which were; the overlap length in specimen UD1 and the curvature of beams main bars of all specimens in the anchorage zone.

7.2 CONCLUSION

The following conclusions were reached from the results of the experimental and analytical investigations:

1) The joint shear stress significantly affected the behaviour of beam-column connections e.g. high joint shear stress led to more rapid

deterioration of the joint and an earlier pull-out of beam bars.

The type of transverse reinforcement used in the UD-specimens did affect the behaviour of these units generally, the overall response of the sub-assemblies and particularly the connection areas. Specimen UD1 which had intermediate longitudinal reinforcement in the beam developed a good hysteresis loop during the course of the test, but the U-stirrups with short legs used in the joint for confinement and to carry shear failed under high forces and the joint core began to deteriorate quickly at the end of experiment. On the other hand, specimen UD2 in which, the beam had no intermediate main bars and the joint was confined by U-stirrups with longer legs, maintained its strength throughout the test, and showed no serious degradation in the connection area.

2) The minimum column-to-beam flexural strength ratio in this study was 1.96 which is far superior to 1.5 suggested by the design Codes. This high strength ratio effectively, did not allow formation of plastic hinges to take place in the joint region. Therefore, the higher the flexural strength ratio, the better is the design for safety.

3) Confinement of the joint core by transverse hoop reinforcement improved the behaviour of specimens.

4) High strength of concrete affected the joint behaviour only prior to cracking. Specimens with a higher concrete strength dissipated more energy before cracking. In the post-cracking stage, the behaviour was mostly dependent upon the joint shear stress level

and the confinement of the joint.

Specimens which had intermediate longitudinal reinforcement in beams (EX2 and UD1) were more ductile and dissipated more energy than specimens without.

Although the understanding of the response of beam-column connection cores to seismic loading has recently been considerably improved, it is apparent that further testing of joint units would provide additional clarification. Further test results would allow the postulated mechanism of resistance to joint shear to be refined, with consequent further improvements to the design procedures.

The concept of 'elastic' joints, which are designed so that beam plastic hinges form away from the column faces, appears to provide a promising solution to the problem of congested joint core reinforcing, but test results appropriate to this type of joint are limited to date. Relevant parameters for further experimental programmes could include the distance at which the plastic hinges are located from the column faces, the method of reinforcing the hinges and the joint core, and the column axial load level.

The three-dimensional analysis was carried out in order to obtain an idea of the overall behaviour of the beam-column connection and, especially, of the joint.

Although the numerical simulation gave a good idea of the structural mechanism in the joint, more detailed research is still needed in this field. On the basis of the results of the present

analysis it is suggested that some parameters need a close examination. For example investigating the influence of the concrete quality, especially, the shear retention factor β, the curvature of the reinforcing beam bars (anchorage) in the joint, and the modelling of the stirrups' hooks.

Because of the limited nature of this investigation, it would appear that further work in the direction of the described work is necessary. Additional comparisons between experimental and analytical results are needed, and the significance of load history should be further explored.

REFERENCES

ABRAMS, D.P. (1987), "*Scale Relations for Reinforced Concrete Beam-Column Joints*," ACI, Structural Journal, Title no.84-S52, November-December,1987, pp.502-512.

ACI (1985), "*Recommendations for Design of Beam-Column Joints in Monolithic Concrete Structures*," ACI-ASCE Committee 352, ACI Journal, Vol. 82, NO. 3, May-June 1985, p226.

ACI (1977), "*Building Code Requirements for Reinforced Concrete*," American Concrete Institute, American Concrete Institute, Detroit, 318-77, 1977.

AHMAD, S., IRONS, B.M. and ZIENKIEWICZ, O.C. (1970), "*Analysis of Thick and Thin Shell Structures by Curved Finite Elements*," International Journal for Numerical Methods in Engineering, Vol. 2, NO. 3, 1970, pp. 419-451.

ANDERSON, J.C and **TOWNSEND, W.H.** (1977), "*Models for Reinforced Concrete Frames with Degrading Stiffness*," ASCE Proceedings, Vol.103, division ST, July-December, 1977, pp.2361-2369.

ASCE (1981), "*State-of-the-Art Report on Finite Element Analysis of Reinforced Concrete*," Task Committee on Concrete and Masonry Structures, ASCE, April 1981, 545pp.

BAHJAT, AB. and **WIGHT, J.K.** (1987), "*Study of Moving Beam Plastic Hinging for Earthquake-Resistant Design of Reinforced Concrete Buildings*," American Concrete Institute, ACI Structural Journal, No.84-S4, January-February, 1987, pp.31-39.

BATHE, K.J. (1982), "*Finite Element Procedures in Engineering Analysis*," Prentice-Hall, Englewood Cliffs, 1982.

BECKINGSALE, C.W. (1980), "*Post-Elastic Behaviour of Reinforced Concrete Beam-Column Joints*," Thesis submitted to the department of Civil Engineering, University of Canterbury, New Zealand for the degree of PhD. August 1980, pp.359.

BIOT, L.H. (1965), "*Mechanics of Incremental Deformation*," John Wiley and Sons, New York, 1965.

BIRSS, G.R. (1978), "*The Elastic Behaviour of Earthquake Resistant Reinforced Concrete Interior Beam-Column Joints*," Master Thesis, University of Canterbury, New Zealand, February, 1978.

BLAKELEY, R.W.G., MEGGET, L.M. and **PRIESTLEY, M.J.N.** (1975), "*Seismic Performance of two Full Size Reinforced Concrete Beam-Column Joint Units*,"Bulletin of the New Zealand National Society for Earthquake Engineering, Vol. 8, NO. 1, March 1975, pp.38-69.

CELEBI, M. and **PENZIEN, J.** (1973), "*Experimental Investigation into the Seismic Behaviour of Critical Regions of Reinforced Concrete Components as Influenced by Moment and Shear*," Report No. UCB/EERC, 73-4, Earthquake Engineering Research Center, University of California

Berkeley, California, January 1973.

CHEUNG, P.C., PAULAY, T. and **PARK, R.** (1993), "*Behaviour of Beam-Column Joints in Seismically-Loaded Reinforced Concrete Frames,*" The Structural Engineer, Vol.71, NO.8, 20 April, 1993, pp.129-138.

COPE, R.J., RAO, P.V., CLARK, L.A. and **NORRIS, P.** (1980), "*Modelling of Reinforced Concrete Behaviour for Finite Element Analysis of Bridge Slabs,*" Numerical Methods for Non-Linear Problems, Pinebridge Press, Swansea, September 1980, pp. 457-470.

DENN, M.M. (1969), "*Optimization by Variational Methods,*" McGraw-Hill, New York, 1969.

DeSALVO, G.J. (1987), "*ANSYS User's Manual,*" Swanson Analysis Systems, Inc., 1987.

DURRANI, A.J. and **WIGHT, J.K.** (1985), "*Behaviour of Interior Beam-Column Connections under Earthquake-Type Loading,*" American Concrete Institute, ACI Journal, May-June, 1985, pp.343-349.

DZ3101 (Draft New Zealand Standard) (1978), "*Code of Practice for the Design of Concrete Structures,*" Standards Association of New Zealand, Wellington, 1978.

EHSANI, M.R. and **WIGHT, J.K.** (1985), "*Exterior Reinforced Concrete Beam-Column Connections Subjected to Earthquake Type Loading,*" American Concrete Institute, ACI Journal, No.82-43, July-August, 1985.

EKHANDE, S.G., SELVAPPALAM, M. and **MADUGULA, M.S.** (1989), "*Stability Functions for Three-Dimensional Beam-Columns*," ASCE, Structural Journal, Vol.115, PTS.1-3, pp.467-479, 1989.

EL-METWALLY, S.E. and **CHEN, W.F** (1988), "*Moment-Rotation Modeling of Reinforced Concrete Beam-Column Connections*," ACI Structural Journal, July-August 1988, pp.384-394.

FENWICK, R.C. and **IRVINE, H.M.** (1977), "*Reinforced Concrete Beam-Column Joints for Seismic Loading*," Report NO. 142, Department of Civil Engineering, University of Auckland, New Zealand, March, 1977.

FILIPPOU, F.C., POPOV, E.P. and **BERTERO, V.** (1986), "*Analytical Studies of Hysteresis Behaviour of Reinforced Concrete Joints*," ASCE, Structural Journal, Vol.112 PTS.7-12, PP.1604-1622, 1986.

GEFKEN, P.R, and **RAMEY, M.R.** (1989), "*Increased Joint Hoop Spacing in Type 2 Seismic Joint using Fiber Reinforced Concrete*," American Concrete Institute, ACI Structural Journal, Vol.86, No.2, March-April, 1989, pp.168-172.

GRAYSON, R. and **STEVENS, L.K.** (1979), "*Non-Linear Analysis of Structural Systems of Steel and Concrete*," Proceedings of the Third International Conference on Finite Element Methods, The University of New South Wales, Sydney, Australia, July 2-6, 1979, Published by Unisearch Ltd, Kensington, New South Wales, Australia, 1979, pp. 147-157.

GROOTENBOER, H.J. (1981), "*Numerical Models for Reinforced Concrete*

Structures In Plane Stress," CONCRETE MECHANICS, Part C, HERON, Vol.26, 1981, NO.1c, pp. 57-61.

GEORGOUSSIS, G.K. and **PHIPPS, M.E.** (1981), "*The Influence of Low-Strength Concrete Beams on the Axial Load Capacity of Concrete Columns*," The Structural Engineer, Vol. 59B, No. 2, June 1981, pp. 17-26.

HA, G.-J, KIM, J.-K and **CHUNG, L.** (1992), "*Response of Reinforced High-Strength Concrete Beam-Column Joints under Load Reversals*," Magazine of Concrete Research, 1992, 44, No.160, September, 175-184.

HANSON, N.W. and **CONNER, H.W.** (1967), "*Seismic Resistance of Reinforced Concrete Beam-column Joints*," Journal of the Structural Division, ASCE, NO. ST5, October, 1967, pp. 533-560.

HANSON, N.W. (1971), "*Seismic Resistance of Concrete Frames with Grade 60 Reinforcement*," ASCE, Structural Journal, Vol.97, No. ST6, Proc. Paper 8180, June, 1971, pp.1685-1700.

HAWKINS, N.M. and **LIN, I.J.** (1979), "*Bond Characteristics of Reinforcing Bars for Seismic Loading*," Third Canadian Conference on Earthquake Engineering. Montreal, Que., Vol.II, 1979, pp.1225-1252.

HEMMATY, Y., DeROECK, G. and **VANDEWALLE, L.** (1992), "*Parametric Study of Reinforced Concrete Corner Joints Subjected to Positive Bending Moment by Non-linear Finite Element Method*," Proceedings, ANSYS Technology Conference, Vol.II, Swanson Analysis Systems, Pittsburgh, USA, June, 1992.

HIGHASHI, Y. and **OHWADA, Y.** (1969), "*Failing Behaviour of Reinforced Concrete Connections Subjected to Lateral Loads,*" Memoirs of Faculty of Technology, Tokyo Metropolitan University # 19, 1969.

HIKMAT, E.Z. and **DURRANI, A.J.** (1989), "*Seismic Response of Connections in Two-Bay Reinforced Concrete Frame Sub-Assemblies,*" ASCE, Journal of Structural Engineering, Vol. 115, No.11, November, 1989, paper No.24063.

HINTON, E., ROCK, A., and ZIENKIEWICZ, O. (1976), "*A Note on Mass Lumping and Related Process in the Finite Element Method,*" International Journal of Earthquake Engineering and structural Dynamics, Vol. 4, 1976, pp.245-249.

HOOSHANG, B., BIGGS, J.M. and **IRVINE, H.M.** (1981), "*Seismic Damage in Reinforced Concrete Frames,*" ASCE, Vol. 107, No. ST9, September 1981, pp.1713-1729.

HOUDE, J. (1973), "*Study of Force-Displacement Relationships for the Finite Element Analysis of Reinforced Concrete,*" Report No.73-2, Department of Civil Engineering and Applied Mechanics, McGill University, Montreal, 1973.

ICHINOSE, T. (1992), "*A Shear Design Equation for Ductile Reinforced Concrete Members,*" Earthquake Engineering & Structural Dynamics, Vol.21, No.3, March, 1992, pp.197-214.

IRONS, B.M. (1970), "*A Frontal Solution Program for Finite Element*

Analysis," International Journal for Numerical Methods in Engineering, Vol. 2, NO. 1, January, 1970, pp.5-23 (Discussion May, 1970, p. 149).

ISMAIL, M.A.F. and JIRSA, J.O. (1972), "*Behaviour of Anchored Bars Under Low Cycle Overloads Producing Inelastic Strains*," Journal of the American Concrete Institute, Vol. 69, NO. 7, July 1972, pp.433-438.

JIRSA, J.O., MEINHEIT, D.F. and **WOOLEN, J.W.** (1975), "*Factors Influencing the Shear Strength of Beam-Column Joints*," Proceedings U.S. National Conference on Earthquake Engineering, EERI, Ann Arbor, Michigan, June, 1975, pp.297-305.

KAAR, P.H, FIORATO, A.E., CARPENTER, J.E. and **CORELY, W.G.** (1978), "*Limiting Strains of Concrete Confined by Rectangular Hoops*," PCA Report No. RD 053. 01D, 1978.

KUPFER, H., HILSDORF, H.K. and **RUSCH, H.** (1969), "*Behaviour of Concrete under Biaxial Stresses*," ACI Journal, Vol. 66, No. 8, August 1969, pp.656-666.

KUPFER, H. and **GERSTLE, K.H.** (1973), "*Behaviour of Concrete under Biaxial Stresses*," ASCE, Journal of the Engineering Mechanics Division, Vol. 99, No. EM4, August 1973, pp.852-866.

LEE, D.L.N. (1976), " *Original and Repaired Beam-Column Sub-Assemblies Subjected to Earthquake Type Loading*," Report NO. UMEE 7654, Department of Civil Engineering, University of Michigan, April, 1976.

LEE, D.L.N., WIGHT, J.K. and **HANSON, R.D.** (1977), "*Reinforced Concrete*

Beam-Column Joints under Large Load Reversals," Journal of Structural Division, ASCE, Vol. 103, No.ST12, Dec., 1977, pp.2337-2350.

LIN, C.S. and **SCORDELIS, A.** (1975), "*Non-Linear Analysis of Reinforced Concrete Shells of General form*," Journal of the Structural Division, Vol. 101, March 1975, pp. 523-538.

MARQUES, J.G.L. and **JIRSA, J.O.** (1975), "*A Study of Hooked Bars Anchorage in Beam-Column Joints*," Proceedings, ACI, Vol.72, No.5, May, 1975, pp.198-209.

MATTOCK, A.H., KRIZ, L.B. and **HOGNESTAD, E.**, "*Rectangular Concrete Stress Distribution in Ultimate Strength Design*," Journal of the American Concrete Institute, Vol. 57, No. 8, February 1961, pp.875-926.

MEGGET, L.M. (1971), "*Anchorage of Beam Reinforcement in seismic Resistance Reinforced Concrete Frames*," Master of Engineering Report, Department of Civil Engineering, University of Canterbury, New Zealand, February, 1971.

MEGGET, L.M. and **PARK, R.** (1971), "*Reinforced Concrete Exterior Beam-Column Joints under Seismic Loading*," New Zealand Engineering, Wellington, New Zealand, Vol. 26, No. 11, Nov. 15, 1971, pp.341-353.

MEINHEIT, D.F. and **JIRSA, J.O.** (1977), "*The Shear Strength of Beam-Column Joints*," CESRL Report NO. 77-1, Department of Civil Engineering, University of Texas at Austin, January, 1977.

MELOSH, R.J. and BAMFORD, R.M. (1969), "*Efficient Solution of Load-Deflection Equations*," ASCE, Journal of the Structural Division, Vol. 95, NO. ST4, Proc. Paper 6510, Apr., 1969, pp. 661-676 (Discussion Dec., 1969, Jan., Feb., May, 1970, Closure, Feb., 1971)

MEINHEIT, D.F and JIRSA, J.O. (1981), "*Shear Strength of Reinforced Concrete Beam-Column Connection*," Proceedings, ASCE, Vol.107 ST11, November, 1981, pp.2227-2244.

MINOR, J. and JIRSA, J.O. (1975), "*Behaviour of Bent Bar Anchorages*," Proceedings, ACI, Vol.72, No.4, April, 1975, pp.141-149.

MORITA, S. and KAKU, T. (1984), "*Slippage of Reinforcement in Beam-Column Joint of Reinforced Concrete Frame*,". 8th WCEE, Vol.4, 1984, pp.477-484, San Francisco.

NAKATA, S. et al. (1980), "*Tests of Reinforced Concrete Beam-Column Sub-assemblies for U.S.-Japan Co-operative Research Program*," Building Research Institute, Ministry of Construction, Ibar-aki-Pref, October 1980, 112pp.

NGO, D. and SCORDELIS, A.C. (1967), "*Finite Element Analysis of Reinforced Concrete Beams*," Journal of the American Concrete Institute, Vol. 64, No. 3, March 1967, pp. 152-163.

NILSON, A.H. (1968), "*Non-Linear Analysis of Reinforced Concrete by the Finite Element Method*," Journal of the American Concrete Institute, Vol. 65, NO. 9, September, 1968, pp. 757-766.

NILSSON Ingvar, H.E., "*Reinforced Concrete Corners and Joints Subjected to Bending Moment - Design of Corners and Joints in Frame Structures*," Document No. D7: National Swedish Institute for Building Research, Stockholm, 1973, 249 pp.

NZS4203 (1976), "*Code of Practice for General Structural Design and Design Loadings for Buildings*," Standards Association of New Zealand, Wellington, 1976, 80p.

OTTOSEN, N.S. (1980), "*Non-Linear Finite Element Analysis of Concrete Structures*," Risφ-R-411, Risφ National Laboratory, DK -4000 Roskilde, Denmark May 1980, 186 pp.

PANAHSHAHI, N., WHITE, R.N. and **GERGELY, P.** (1992), "*Reinforced Concrete Compression under Inelastic Cyclic Loading*," ACI Structural Journal, Title no. 89-S18, March-April, 1992, pp.164-175.

PANTAZOPOULOU, S. and **BONACCI, J.** (1992), "*Consideration of Question about Beam-Column Joints*," ACI Structural Journal, Title no.89-S4, January-February 1992, pp.27-36.

PARK, R. and **PAULAY, T.** (1974), "*Behaviour of Reinforced Concrete External Beam-Column Joint under Cyclic Loading*," Proceedings, 5th World Conference on Earthquake Engineering, Vol.1, Rome, 1973, pp.772-781.

PARK, R. and **PAULAY, T.** (1975), "*Reinforced Concrete Structures*," John Wiley & Sons, New York, NY, 1975.

PARK, R. (1992), "*Capacity Design of Ductile Reinforced Concrete Building Structures for Earthquake Resistance*," The Structural Engineer, Vol.70, No.16, 18 August 1992.

PAULAY, T. et al. (1977), "*Capacity Design of Reinforced Concrete Ductile Frames*," Proceedings, Workshop on Earthquake-Resistant Reinforced Concrete Building Construction, University of California, Berkeley, CA, Vol.III, 1977, pp.1043-1075.

PAULAY, T., PARK, R. and **PRIESTLEY, M.J.N.** (1978), "*Reinforced Concrete Beam-Column Joints under Seismic Actions*," ACI Journal, November, 1978, pp. 588-593.

PETTON, R.N. (1972), "*Behaviour Under Seismic Loading of Reinforced Beam-Column Joints with Anchor Blocks*," Master of Engineering Report, Department of Civil Engineering, University of Canterbury, New Zealand, 1972.

POPOV, E.P. and **BERTERO, V.V.** (1973), "*On Seismic Behaviour of Two Reinforced Concrete Structural Systems for Tall Buildings*," Notes of Seminar on Simplified Design of Earthquake-Resistant Concrete Structures, PCA, San Francisco, June, 1993, pp. 117-139.

RENTON, G.W. (1972), "*The Behaviour of Beam-Column Joints under Cyclic Loading*," Master of Engineering Report, Department of Civil Engineering, University of Canterbury, New Zealand, 1972.

SARSAM, K.F. (1983), "*Strength and Deformation of Structural Concrete*

Joints," Ph.D Thesis Submitted to the University of Manchester Institute of Science and Technology, January 1983, pp.340.

SARSAM, K.F. and **PHIPPS, M.E.** (1985), "*The Shear Design of In situ Reinforced Concrete Beam-Column Joints Subjected to Monotonic Loading*," Magazine of Concrete Research, Vol. 37, No. 130, March 1985, pp. 17-27.

SCARPAS, A. (1981), "*The Inelastic Behaviour of Earthquake Resistant Reinforced Concrete Exterior Beam-Column Joints*," Report No. 81-2, Department of Civil Engineering, University of Canterbury, Christchurch, February 1981, 84 pp.

SCHNOBRICH, W.C. and **SUIDAN, M.** (1973), "*Finite Element Analysis of Reinforced Concrete*," ASCE, Journal of the Structural Division, ST10, PP. 2109-2122, October 1973.

SEAOC (1973), "*Recommended Lateral Force Requirements and Commentary*," Seismology Committee, Structural Engineers' Association of California, San Francisco, 1973, 146 pp.

SCOTT, R.H. (1992), "*The Effects of Detailing on Reinforced Concrete Beam-Column Connection Behaviour*," The Structural Engineer, Vol.70, No.18-15, September, 1992.

SCRIBNER, C.F. and **WIGHT, J.K.** (1978), "*Delaying Shear Strength Decay in Reinforced Concrete Flexural Members under Large Load Reversals*," Report NO. UMEE78R2, Department of Civil Engineering, University of Michigan, May, 1978.

SMITH, B.J. (1972), "*Exterior Reinforced Concrete Joints with Low Axial Load under Seismic Loading*," Master of Engineering Report, Department of Civil Engineering, University of Canterbury, New Zealand, 1972.

SOLEIMANI, D., POPOV, E. and **BERTERO, V.V.** (1979), "*Hysteretic Behaviour of Reinforced Concrete Beam-Column Sub-Assemblies*," ACI Journal, November, 1979, pp.1179-1195.

Stroband, J. and **Kolpa, J.J.**, "*The Behaviour of Reinforced Concrete Column-to-Beam Joints part2 - Corner Joints Subjected to positive Moments*," Delft University of Technology, Department of Civil Engineering, Report 5-83-9, Research No. 2.2.7417, April 1981, 104 pp.

TASUJI, M.E., SLATE, F.O. and **NILSON, A.H.** (1978), "*Stress-Strain Response and Fracture of Concrete in Biaxial Loading*," ACI Journal, Vol. 75, No. 7, July 1978, pp. 306-312.

TOWNSEND, W.H. and **HANSON, R.D.** (1972), "*The Inelastic Behaviour of Beam-Column Connections*," Doctoral Dissertation, University of Michigan, March, 1972.

TSANOS, I.G. et al. (1992), "*Seismic Resistance of Type 2 Exterior Beam-Column Joints Reinforced with Inclined Bars*," American Concrete Institute, ACI Structural Journal, No.89-S1, January-February, 1992.

UZUMERI, S.M. and **SECKIN, M.** (1974), "*Behaviour of Reinforced Concrete Beam-Column Joints Subjected to Slow Load Reversals*," Report NO.74-05,

Department of Civil Engineering, University of Toronto, March, 1974.

UZUMERI, S.M. (1977), "*Strength and Ductility of Cast-in-place Beam-Column Joints in Reinforced Concrete Structures in Seismic Zones*," Publication SP-53, ACI, Detroit, MI, 1977, pp. 293-350.

VAN MIER, J.G.M. (1987), "*Example of Non-Linear Analysis of Reinforced Concrete Structures with DIANA*," HERON, Volume 32, 1987, NO.3, pp.46-56.

VIWATHANATEPA, S., POPOV, E.P. and BERTERO, V.V. (1979), "*Seismic Behaviour of Reinforced Concrete Interior Beam-Column Sub-assemblies*," Report No. UCB/EERC-79/14, Earthquake Engineering Research Center, University of California, Berkeley, June 1979, 184pp.

YOUNG, S.C., MEYER, C. and **SHINOZUKA, M.** (1989), "*Modeling of Concrete Damage*," ACI Structural Journal, Vol. 86, No. 3, May-June, 1989, pp. 259-271.

YUNFEI, H., CHINGCHANG, H. and **YUFEN, C.** (1984), "*Further Studies on the Behaviour of Reinforced Concrete Beam-Column Joint under Reversed Cylic Loading*," 8th WCEE, Vol.4, pp.485-492, San Francisco, 1984.

ZHANG, L. and **JIRSA, J.O.** (1981), "*Shear Strength of Reinforced Concrete Beam-Column Joints*," presented at ACI Convention at Dallas, February, 1981.

ZHU, S. and **JIRSA, J.O.** (1983), "*A Study of Bond Deterioration in Reinforced Concrete Beam-Column Joints*," PMFSEL Report No.83-1, Phil

M. Ferguson structured Engineering Laboratory, The University of Texas at Austin, Austin, TX, 1983.

ZIENKIEWICZ, O.C. (1977), "*The Finite Element Method*," McGraw-Hill Company, London, 1977.

APPENDIX A

SAMPLE CALCULATIONS FOR SPECIMEN UD2

A1 ULTIMATE MOMENT CAPACITY OF BEAM (M_u)

A2 MOMENT CAPACITY OF COLUMN AT ULTIMATE BALANCED CONDITIONS (M_b)

A3 JOINT SHEAR STRESS (v_{jh})

A4 DEVELOPMENT LENGTH FOR ANCHORAGE (l_d)

A1 Calculation of Ultimate Moment Capacity of Beam (M_u)

A1.1 *Equivalent rectangular stress-block*

The equivalent rectangular stress block recommended by the ACI Code (1977) for the design of flexural members is based on extensive test [Mattock, Kriz and Hognestad (1961)]. The stress distribution assumed in the compressed part of the section is shown in Fig.A1. The maximum concrete compressive strain is 0.003, and the uniform stress across the depth of the stress block is $0.85 \cdot f'_c$, where f'_c is the cylinder crushing strength of the concrete. The proportion of the neutral axis depth over which uniform stress is assumed depends on the concrete strength.

if $f'_c < 27.6\ N/mm^2$, $\beta_1 = 0.85$

$f'_c > 27.6\ N/mm^2$, $\beta_1 = 0.85 - \dfrac{f'_c - 27.6}{6.9} \cdot 0.05$

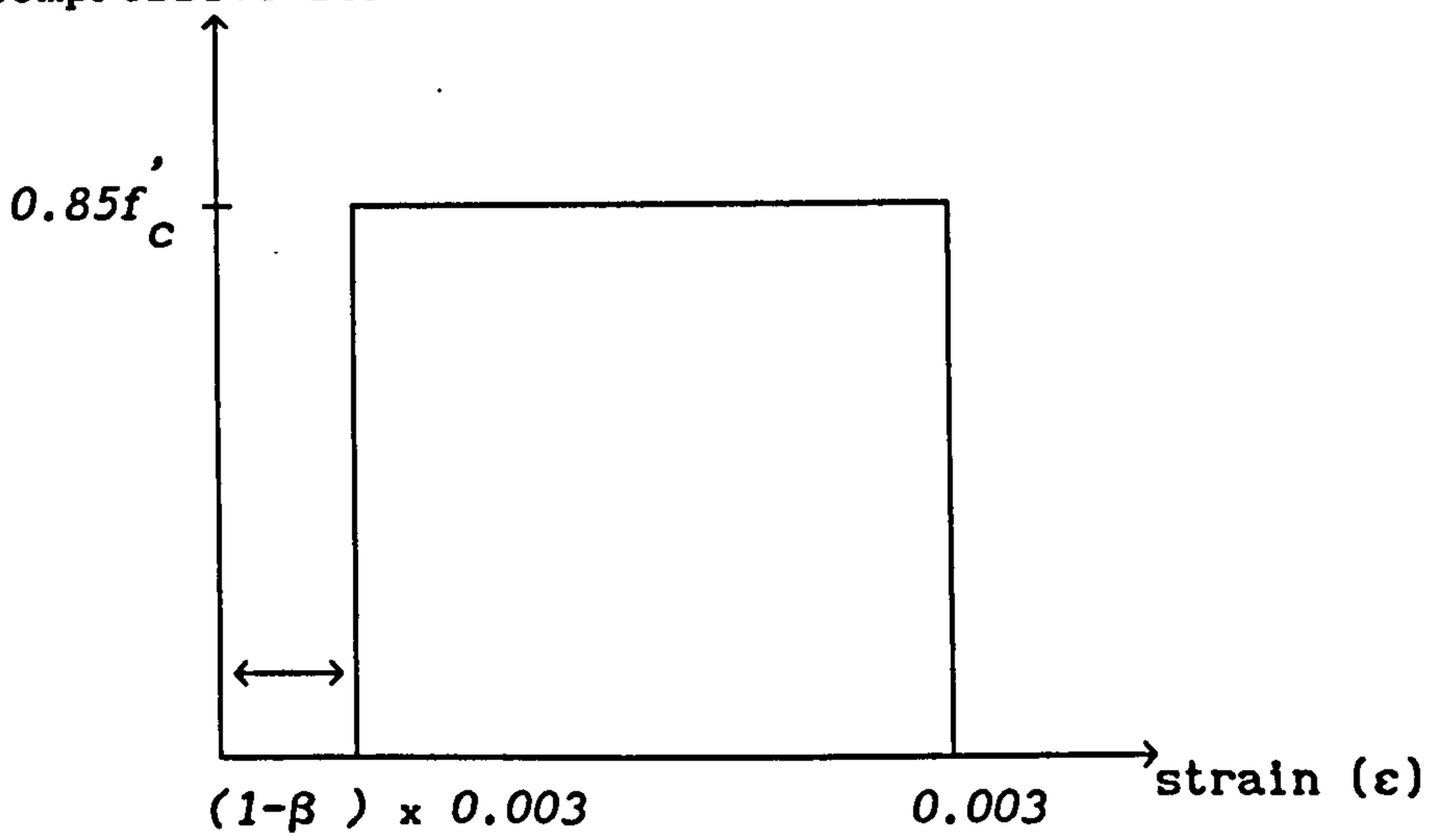

FIG.A1 ACI Rectangular Stress Block

The equivalent rectangular stress block is a design and analysis tool which has been shown [Mattock et al. (1961)] to predict very closely the strength of reinforced concrete beams and columns under uniaxial loading, since it is experimentally based on a rectangular compressed area of concrete.

Using The above ACI Committee 318 Recommendations, and the actual material properties of the specimen, see Fig.A2 for details.

From equilibrium: $C_c + C_s = T$

where:

$$C_c = 0.85 \cdot f'_c \cdot a \cdot b$$

$$C_s = A'_s \cdot \left[0.003 \cdot E'_s \left(\frac{x - d'}{x} \right) - 0.85 \cdot f'_c \right]$$

$$T = A_s \cdot f_y$$

Substituting:

$$0.85 \cdot f'_c \cdot a \cdot b + A'_s \cdot \left[0.003 \cdot E'_s \frac{(x - d')}{x} - 0.85 \cdot f'_c \right] = A_s \cdot f_y$$

Re-arranging, a quadratic equation is obtained for the neutral axis depth, x.

$$x^2 - \left[\frac{A_s \cdot f_y + 0.85 \cdot f'_c \cdot A'_s - 0.003 \cdot A'_s \cdot E'_s}{0.85 \cdot f'_c \cdot b \cdot \beta_1} \right] x - \frac{0.003 \cdot A'_s \cdot E'_s \cdot d'}{0.85 \cdot f'_c \cdot b \cdot \beta_1} = 0 \qquad \text{(A1)}$$

According to ACI-318 recommendations:

$$\beta_1 = 0.85, \text{ for } f'_c \leq 27.6 \ N/mm^2$$

or

$$\beta_1 = \left[0.85 - \frac{0.05}{6.895} (f'_c - 27.58) \right] \geq 0.65, \text{ for } f'_c > 27.58 \ N/mm^2$$

Substituting for UD2

$$\beta_1 = \left[0.85 - \frac{0.05}{6.895}(40 - 27.60)\right] \geq 0.65$$

$$= 0.76 \geq 0.65$$

therefore use $\beta_1 = 0.76$.

Substituting the actual material properties of specimen UD2 into equation A1, the following is obtained:

$$x^2 - \left[\frac{402 \cdot 472 + 0.85 \cdot 40 \cdot 226 - 0.003 \cdot 226 \cdot 198000}{0.85 \cdot 40 \cdot 250 \cdot 0.76}\right] x - \frac{0.003 \cdot 226 \cdot 198000 \cdot 15}{0.85 \cdot 40 \cdot 250 \cdot 0.76} = 0$$

Solving gives $x = 23.5\ mm$ the neutral axis depth.

$a = \beta_1 x = 0.76 \cdot 23.5 = 17.86\ mm$ the depth of the equivalent rectangular stress block.

$$\varepsilon'_s = 0.003 \cdot \frac{x - d'}{x} = 0.003 \cdot \frac{23.5 - 15}{23.5} = 0.00108$$

$$f'_s = \varepsilon'_s \cdot E'_s = 0.00108 \cdot 198000 = 215\ N/mm^2 < f'_y = 471\ N/mm^2$$

$$M_u = C_c \cdot (d - a/2) + A'_s \cdot (f'_s - 0.85 \cdot f'_c)\ (d - d')$$

where

$$C_c = 0.85 \cdot a \cdot b \cdot f'_c = 0.85 \cdot 17.86 \cdot 250 \cdot 40 = 151810$$

$$M_u = 151810\ (235 - 17.86/2) + 226\ (215 - 0.85 \cdot 40)\ (335 - 15)$$

$\therefore \quad M_u = 62.6\ kN.m$

the calculated beam ultimate moment capacity without material reduction.

A2 Ultimate Moment of Column at Balanced Conditions (M_b)

The method proposed in the ACI-318 Building Code will be used. For more details, see Fig. A3.

From the strain diagram:

$$x_b = \left[\frac{0.003}{0.003 + f_y/E_s}\right] d = \left[\frac{0.003}{0.003 + 471/198000}\right] \cdot 225 = 125 \text{ mm}$$

the neutral axis depth at the balanced conditions, when the tension steel yields simultaneously with the concrete strain reaching 0.003 in compression at the extreme fibre.

$$a_b = \beta_1 \cdot x_b = 0.76 \cdot 125 = 95 \text{ mm}$$

$$C_c = 0.85 \cdot f'_c \cdot b \cdot a_b = 0.85 \cdot 40 \cdot 250 \cdot 95 = 807.5 \text{ kN}$$

$$\varepsilon'_s = \left(\frac{x_b - d'}{x_b}\right) \cdot \varepsilon_c = \left(\frac{125 - 25}{125}\right) \cdot 0.003 = 0.0024$$

$$f'_s = \varepsilon'_s \cdot E'_s = 0.0024 \cdot 198000 = 475 \text{ N/mm}^2$$

$$C_s = f'_s \cdot A'_s = 475 \cdot 226 = 107 \text{ kN}$$

$$T = A_s \cdot f_y = 226.2 \cdot 471 = 106.5 \text{ kN}$$

therefore, the balanced column load, $N_b = C_c + C_s - T = 808$ kN

Taking moments with respect to the column centroid:

$$C_s \cdot \left[\frac{h - 2d'}{2}\right] + C_c \cdot \left[\frac{h - a_b}{2}\right] + T\ (d - h/2) - N_b \cdot e_b = 0$$

$$107 \cdot \left[\frac{250 - 2 \cdot 25}{2}\right] + 807.5 \cdot \left[\frac{250 - 95}{2}\right] + 106 \cdot (225 - 250/2) - \cdot 808 \cdot e_b = 0$$

therefore

$$e_b = 100 \text{ mm}$$

and

$M_b = 100 \cdot 808 \propto 80.8 \text{ kN.m}$, the moment capacity of the column at ultimate balanced conditions.

A3 Joint Shear Stress

The joint shear stress based on the nominal design values are given below:

beam:

top steel, $A_s' = 2\ \phi 12 = 226\ mm^2$

bottom steel, $A_s = 2\ \phi 16 = 402\ mm^2$

for the concrete compression strength of $f_c' = 40\ N/mm^2$, and steel yield strength of $471\ N/mm^2$, and the moment capacity of the beam ($62.6\ kN.m$) (Appendix A1), the column shear is

$$V_{col} = \frac{\Sigma\ M_b}{l_c} = 31.3\ kN$$

the joint shear force is

$$V_j = (A_s' + A_s) \cdot 1.25 \cdot f_y - (V_{col})/bh$$

$$V_j = (226 + 402) \cdot 1.25 \cdot 471 - (31.3)/(250 \cdot 250) = 369\ kN$$

where the factor 1.25 accounts for strain hardening in the beam reinforcement [DZ3101 (19780, Paulay et al. (1978)].

The joint shear stress is

$$v_{jh} = V_j/(bd)_{col} = \frac{369}{250 \cdot 225} = 6.5\ N/mm^2$$

$= 1.02\sqrt{f_c'}$, which is in good agreement with the recommendations outlined by different Codes of practice.

The following table summarizes the joint shear stress in all the test specimens.

Table A3 Joint Shear Stress in the Test Specimens

specimen	shear in column (V_{col}) (kN)	joint shear force (V_j) (kN)	joint shear stress (v_{jh}) (N/mm^2)	joint shear stress in term of $\sqrt{f'_c}$ (N/mm^2)
EX1	51	266	4.72	$0.52\sqrt{f'_c}$
EX2	41	399	7.09	$1.16\sqrt{f'_c}$
UD1	43.65	399	7.09	$1.10\sqrt{f'_c}$
UD2	31.3	369	6.50	$1.02\sqrt{f'_c}$

From the above table, it can be seen that the joint shear stress for specimens EX2, UD1 and UD2 are within the specified limit recommended by the United States, Canada and New Zealand design codes of practice [$0.7\sqrt{f'_c}$ to $1.2\sqrt{f'_c}$]. The lower limit could have any smaller value depending upon the design of beams and columns without compromising the safety of the connecting members. Specimen EX1, which had a high concrete strength also had a low joint shear stress.

A4 Development Length of Anchorage

The anchorage used for the beam main reinforcement is indicated in Fig. A4.

A4.1 ACI-318 Committee

Equivalent hook stress, $f_h = 0.083\xi\sqrt{f'_c}$

where $\xi = 540$ from table 12.5.1 of the code

$$f_h = 0.083 \cdot 540\sqrt{40} = 283.46 \ N/mm^2$$

The required total development length, l_d, is the greater of :

$$l_d \geq 0.019 \cdot A_b \cdot f_s/\sqrt{f'_c} = 0.019 \cdot 113 \cdot f_s/\sqrt{40} = 0.34 \ f_s \ mm$$

where A_b is the area of the bar

or

$$l_d \geq 0.058 \cdot d_b \cdot f_s = 0.058 \cdot 12 \cdot f_s = 0.696 \ f_s \ mm$$

Therefore,

Required $l_d = 0.696 \cdot 471 = 327.8 \ mm$ with a bar stress of f_y.

or

$l_d = 327.8 \cdot 1.25 = 409.75 \ mm$, for $f_s = 1.25 \ f_y$

Equivalent length of hook = $0.696 \cdot 283.45 = 197.28$

available anchorage, $A_p = 197.28+194 = 391.3 \ mm$

$$\frac{A_p}{l_d} = \frac{391.3}{327.8} = 1.19$$

$$\frac{A_p}{l_d} = \frac{391.3}{409.7} = 0.95$$

A4.2 ACI-ASCE Committee 352

Equivalent hook stress, $f_h = 58.1(1-0.0118d_b)\sqrt{f'_c}$

$f_h = 58.1(1-0.0118 \cdot 12)\sqrt{40} = 315.4\ N/mm^2$

The required anchorage length,

Required $l_d = 0.019 \cdot A_b \cdot f_s/\sqrt{f'_c} = 0.019 \cdot 113 \cdot 471/\sqrt{37} = 159\ mm$

or

Required $l_d = 1.25 \cdot 156 = 198.8\ mm$ with a bar stress of $1.25\ f_y$.

Equivalent length of hook $= 0.019 \cdot 113 \cdot 315.4/\sqrt{40} = 107\ mm$

available anchorage, $A_p = 107 + 180 = 287\ mm$.

Therefore,

$$\frac{A_p}{l_d} = \frac{287}{159} = 1.80$$

$$\frac{A_p}{l_d} = \frac{287}{198.8} = 1.40$$

A4.3 CP110:1972 Approach

$f_{bs} = 1.3 \cdot 2.6 = 3.38\ M/mm^2$ the allowable bond for type 2 deformed bars (Table 22 of the Code)

Required development length, $l_d = \dfrac{f_s \cdot \phi}{4\ f_{bs}}$

with $f_s = f_y$, $\quad l_d = \dfrac{471 \cdot 12}{4 \cdot 3.38} = 418\ mm$

with $f_s = 1.25\ f_y$, $\quad l_d = 1.25 \cdot 418 = 522.5\ mm$

For a 90° hook of an internal radius of 3ϕ, the equivalent length of the hook = $12\phi = 12 \cdot 12 = 144$ mm

available length in addition to the standard hook = 190 mm

available anchorage, $A_p = 190 + 350 - 8 \cdot 12 + 144 = 780$ mm

Therefore,

$$\frac{A_p}{l_d} = \frac{780}{418} = 1.86 \qquad \text{for } f_s = f_y$$

and

$$\frac{A_p}{l_d} = \frac{780}{522.5} = 1.49 \qquad \text{for } f_s = 1.25\, f_y$$

The following Table A4 summarises the results from the three different methods of anchorage calculations.

TABLE A4 Ratio of Provided to Required Anchorage

steel stress	$(A_p)/(l_d)$		
	CP110	ACI-318	ACI-ASCE C352
f_y	1.86	1.80	1.19
$1.25\, f_y$	1.49	1.40	0.95

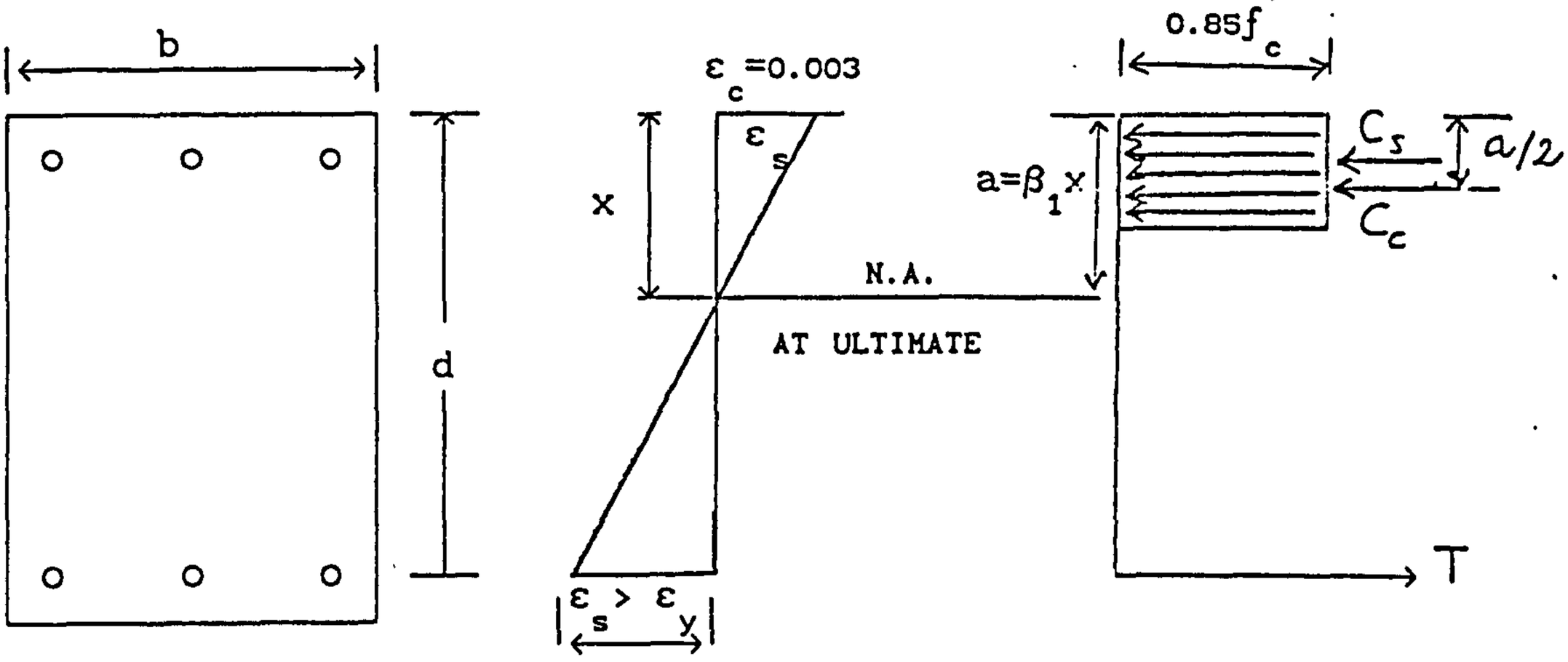

a) Ultimate Conditions in Flexure

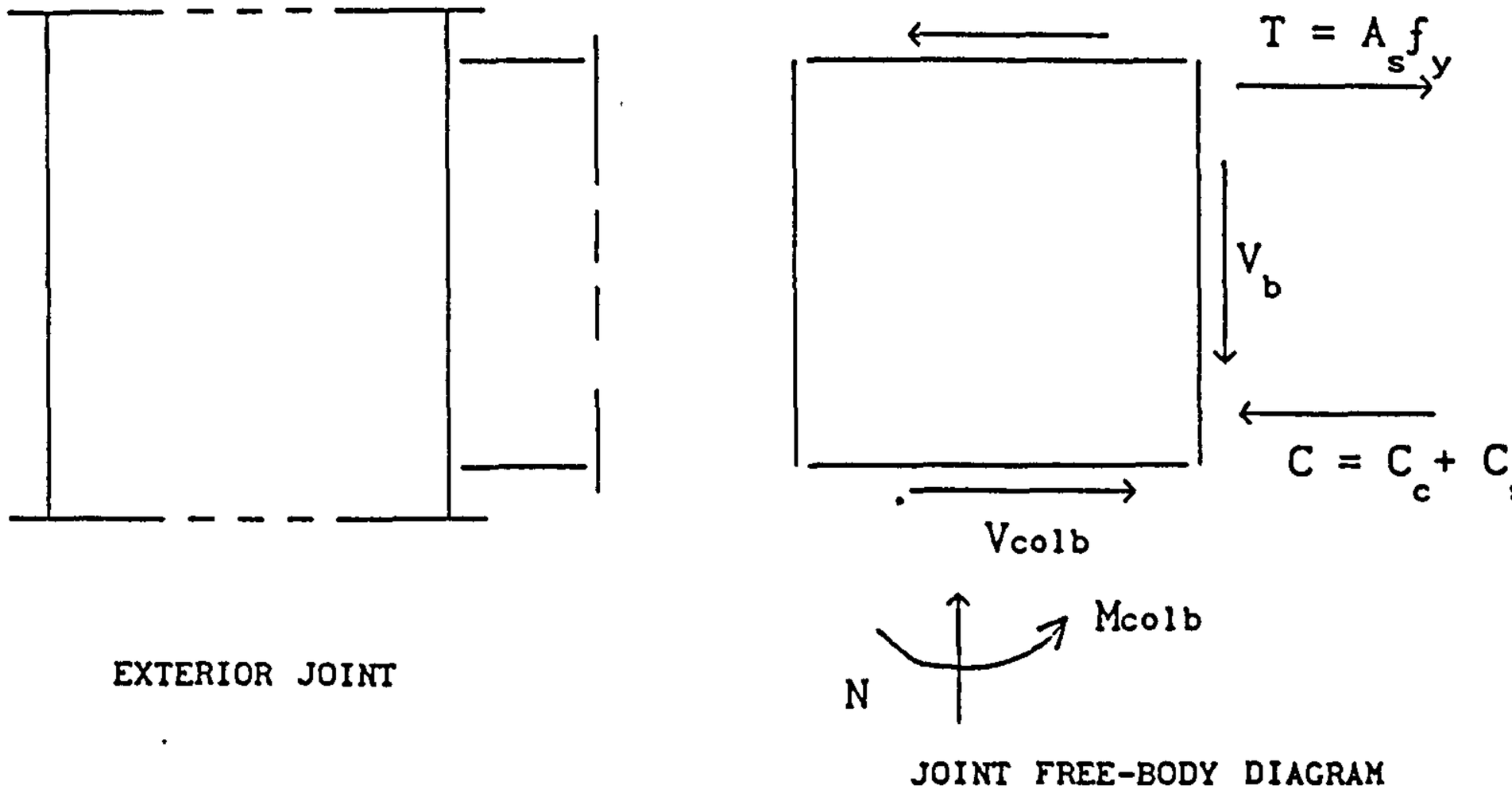

b) Joint Equilibrium

FIG. A2

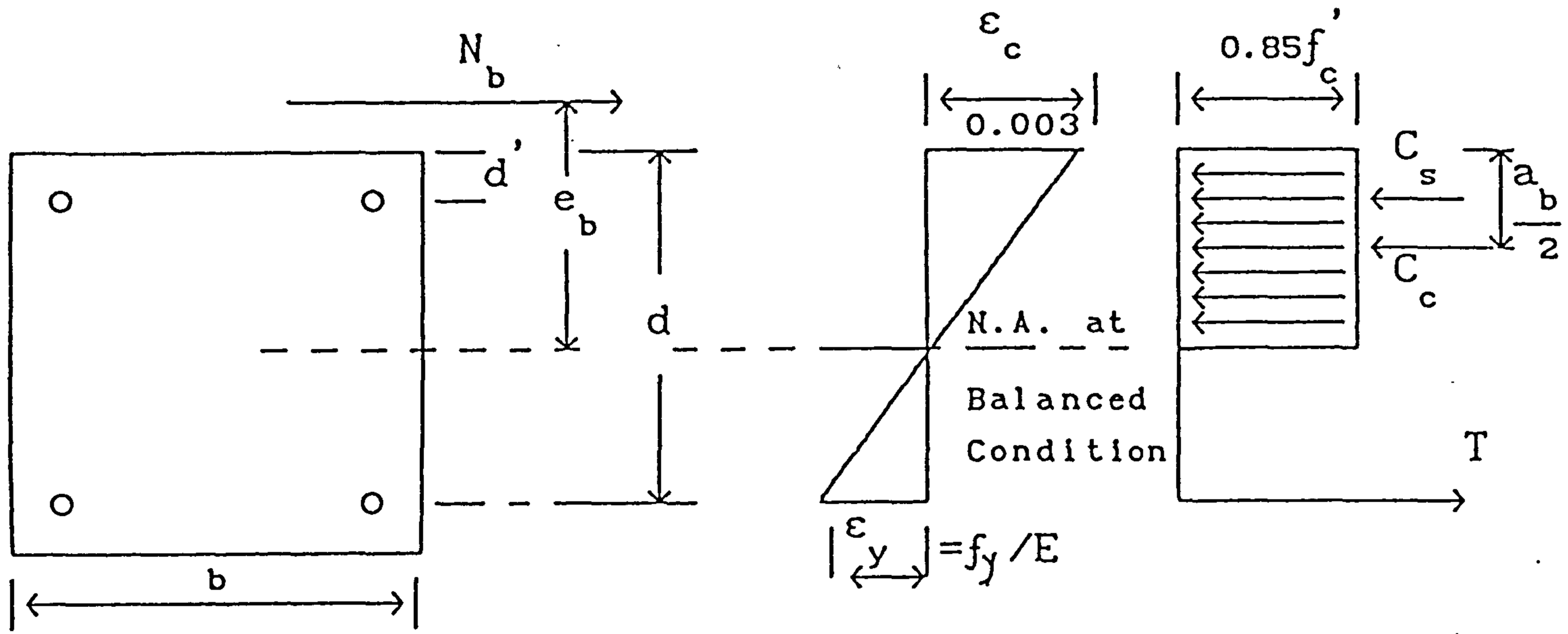
N_b
d'
e_b
d
b
ε_c
0.003
N.A. at
Balanced
Condition
ε_y = f_y / E
0.85f'_c
C_s
C_c
a_b/2
T
CROSS-SECTION
STRAINS
FORCES

FIG.A3

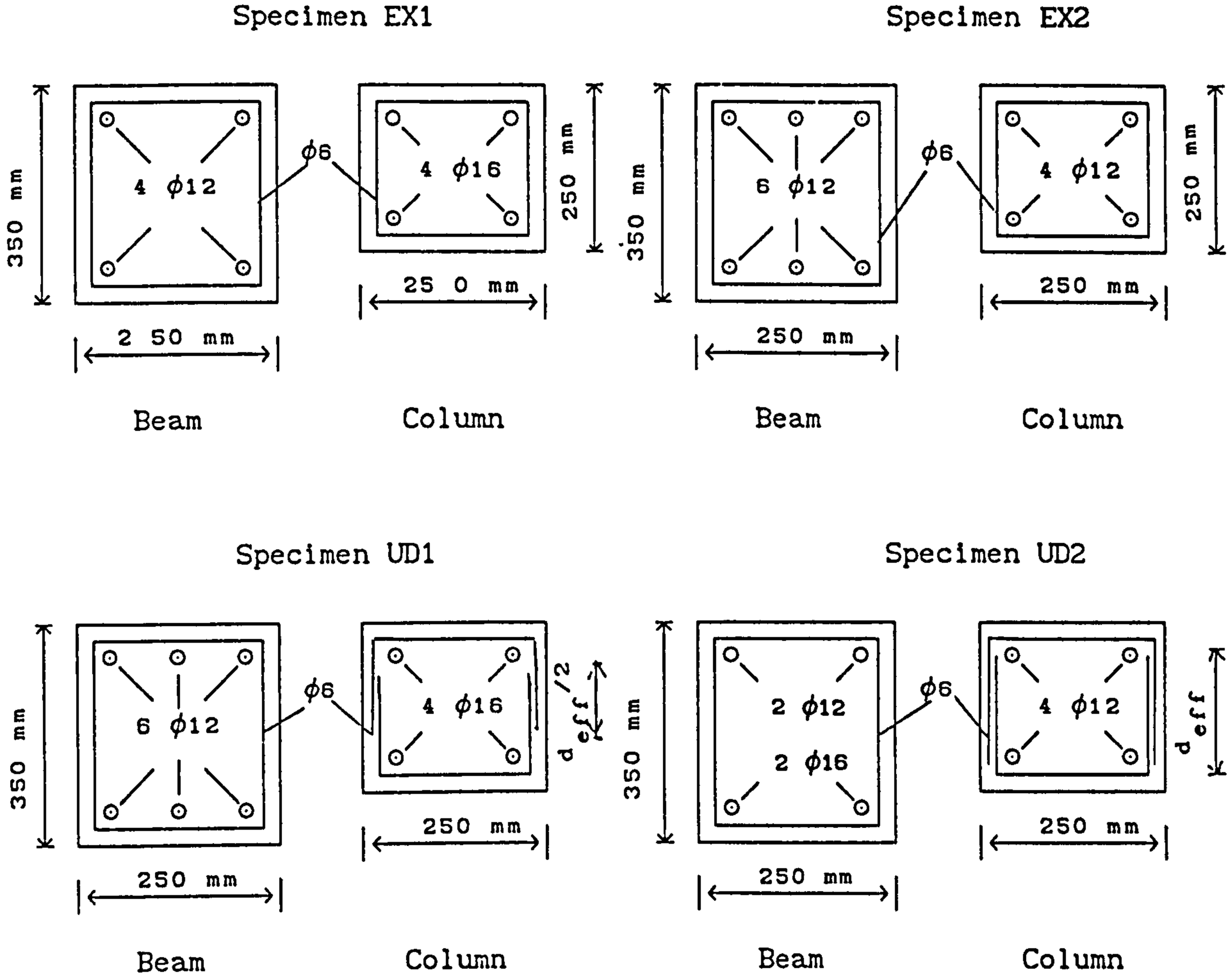

a) Beam and Column Cross-Section and Reinforcement Detail

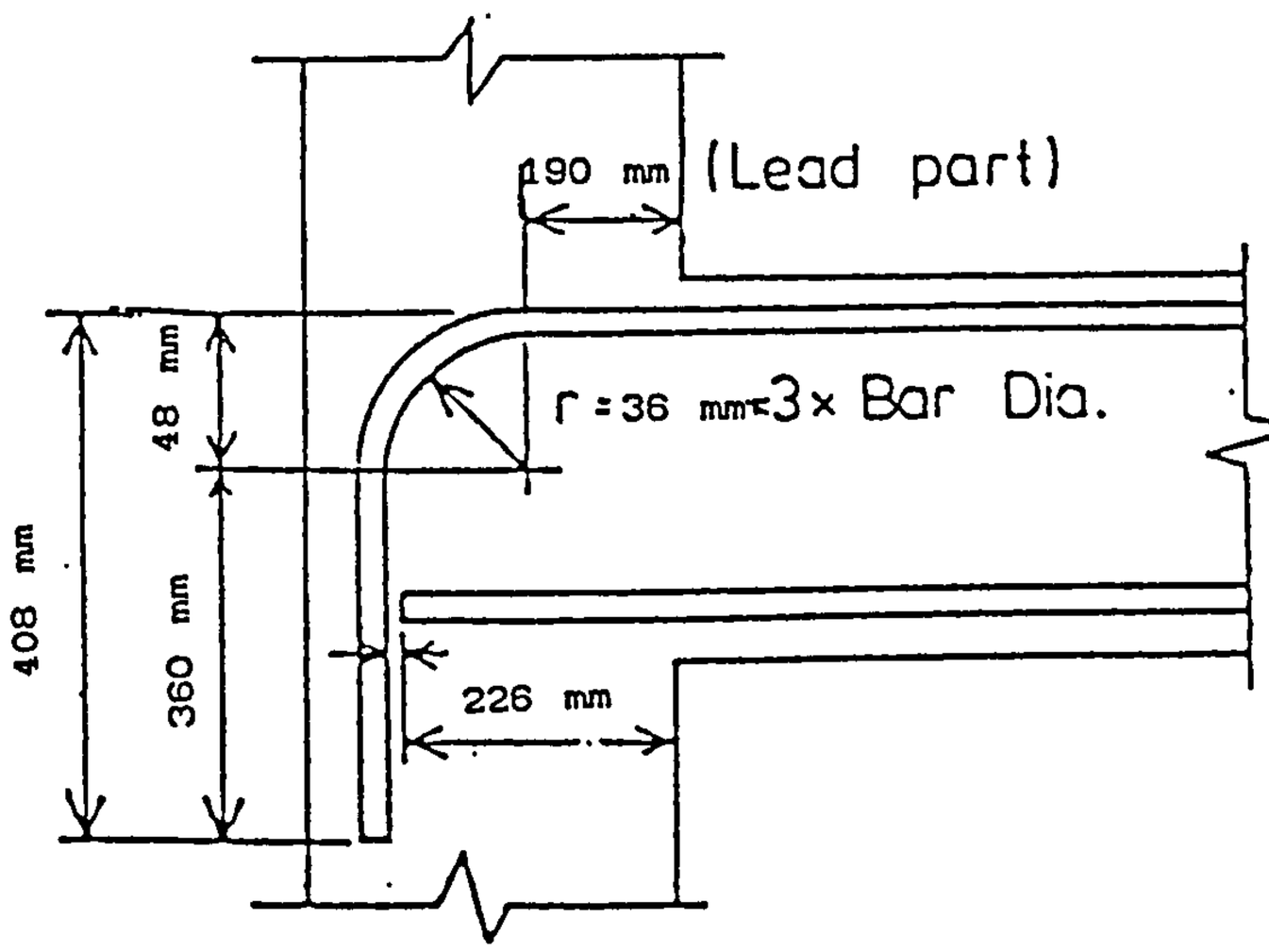

b) Anchorage of Beam Bars in Joint

FIG. A4

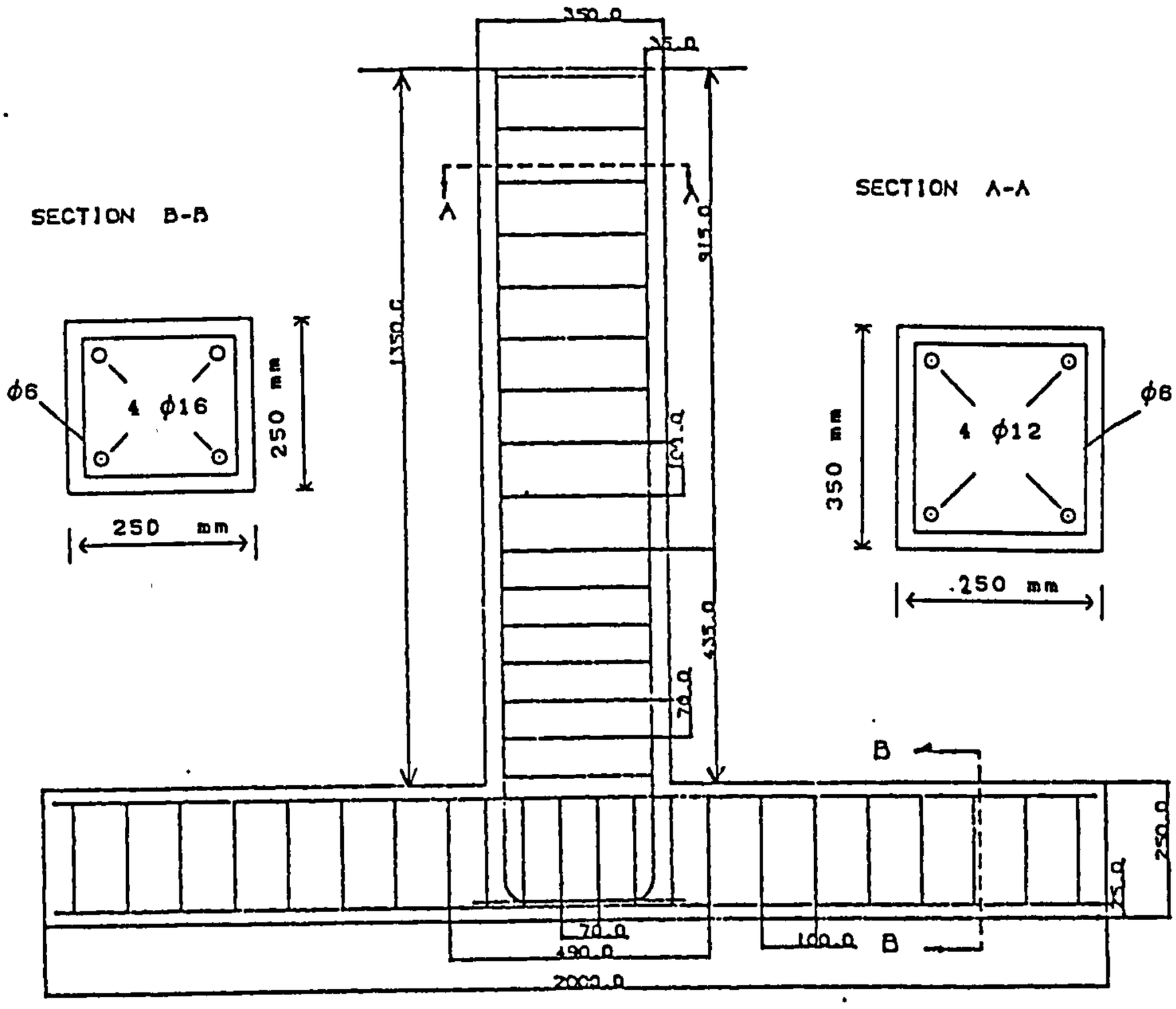

a) Detail of Specimen EX1

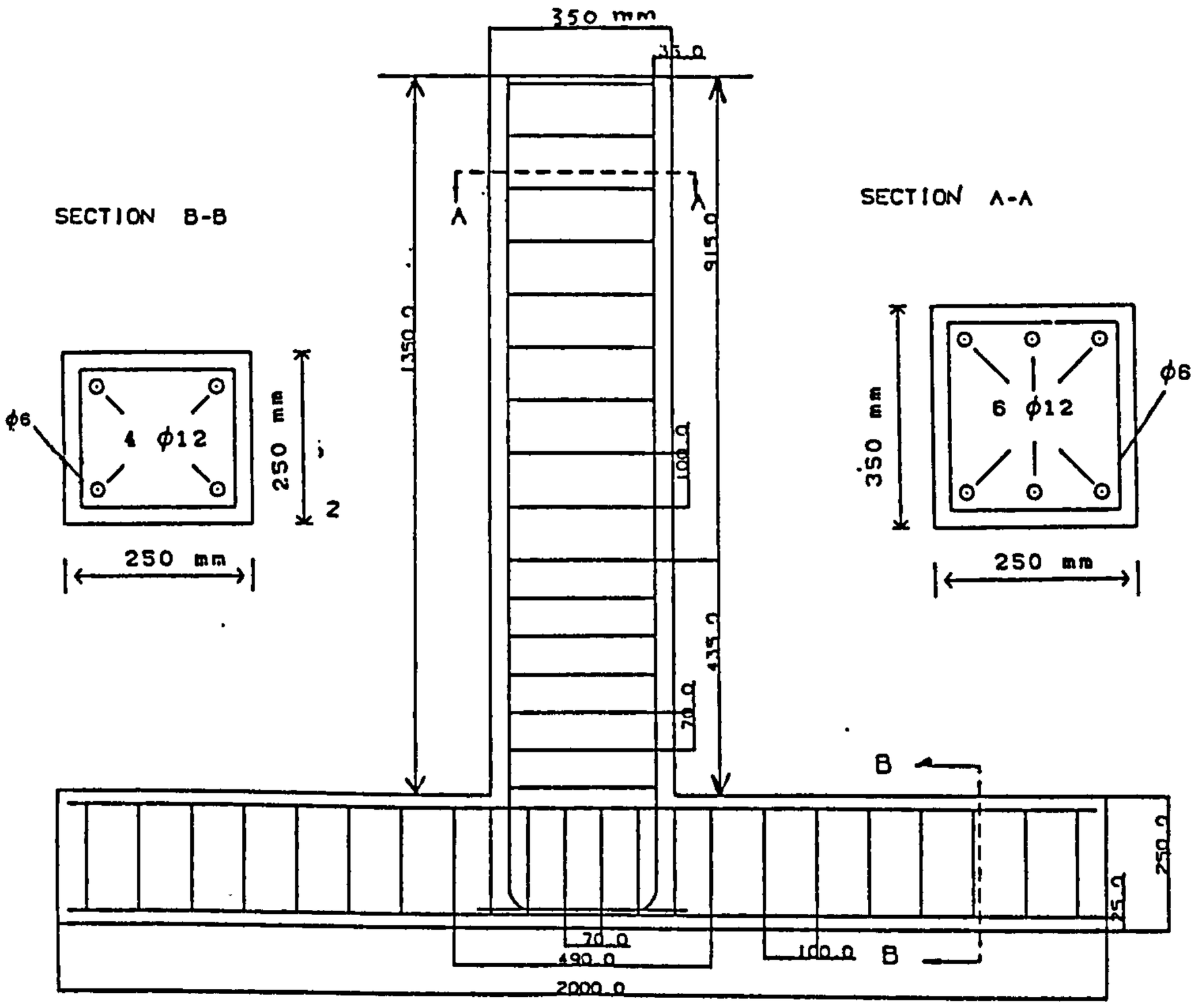

b) Detail of Specimen EX2

FIG. A5

c) Detail of Specimen UD1

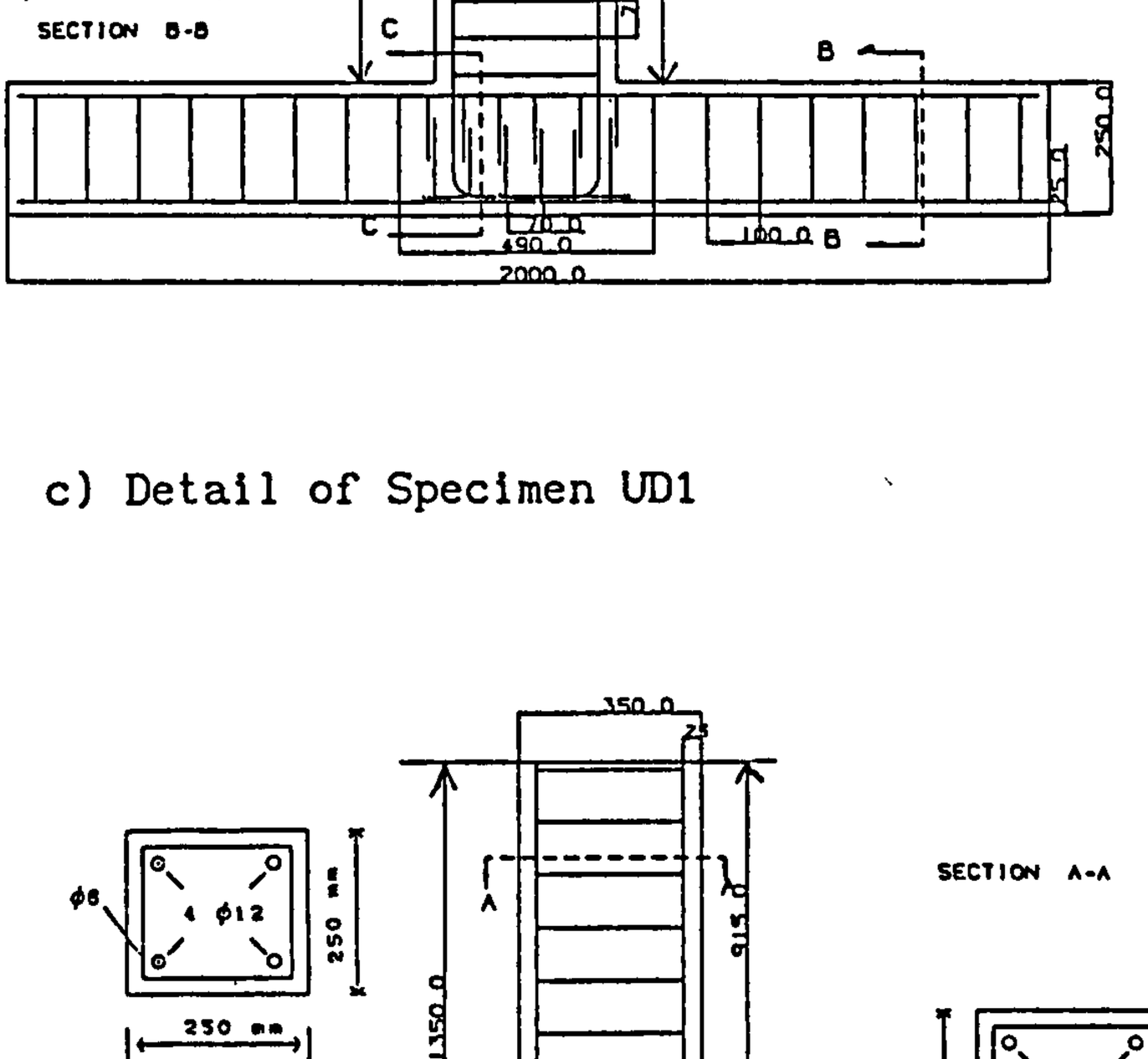

d) Detail of Specimen UD2

APPENDIX B

ANSYS INPUT DATA LISTING

Typical ANSYS program listing used in the analysis of beam-column sub-assemblies is given below. For the sake of simplification, only a listing of one analysis is presented. Command explanations can be obtained from the ANSYS user's manual [De Salvo and Swanson (1987].

B1 MODEL FOR THE ANALYSIS OF SPECIMEN UD2

```
/TITLE, R/C  BEAM-COLUMN EXTERIOR JOINT - UD2 -
/COM
/COM  FORCE IN NEWTONS
/COM  DISTANCE IN  MM
/COM
ET,1,65                          * CONCRETE ELEMENT
ET,2,8                           * LONGITUDINAL REINFORCEMENT
ET,3,8                           * STIRRUPS
/COM
/COM  CONCRETE LINEAR MATERIAL
/COM
EX,1,30E3
NUXY,1,.15
/COM  STEEL LINEAR MATERIAL
EX,2,204.5E3
NUXY,2,0.30
EX,3,198E3
NUXY,3,0.30
/COM  STEEL AND CONCRETE SECTIONS
R,1                              * CONCRETE ELEMENT (STIF65)
R,2,113.09                       * BEAM & COLUMN BARS (BARS #12)
R,3,28.27                        * STIRRUPS (#6)
/COM  CONCRETE NONLINEAR PROPERTIES
KNL,1                            * INVOKE NONLINEARITY PROCEDURE
NLTAB,1,2                        * CLASSICAL BILINEAR KINEMATIC HARDENING
NLY,DEFI,1,0,40.55               * YIELD STRESS AT 0 DEGREES
NLY,DEFI,1,100,40.55             * YIELD STRESS AT 100 DEGREES
```

```
NL,1,55,.01,.01                    * SHEAR COEFF. FOR OPEN CRACK (β)
NL,1,61,.5,.5                      * SHEAR COEFF. FOR CLOSED CRACK (β)
NL,1,67,6.21,6.21                  * TENSILE CRACKING STRESS
NL,1,73,40,40                      * TENSILE CRUSHING STRESS
/COM******STEEL NONLINEAR PROPERTIES ***************
/COM******MAIN REINFORCEMENT************
NLTAB,2,2                          * ELASTIC PLASTIC MODEL
NLY,DEFI,1,0,471                   * YIELD STRESS AT 0 DEGREES
NLY,DEFI,1,100,471                 * YIELD STRESS AT 100 DEGREES
/COM ******** STIRRUPS ************
NLTAB,3,2
NLY,DEFI,1,0,376
NLY,DEFI,1,100,376
/COM ************ NODE GENERATION **********************
/COM *** COLUMN ***
N,1
N,2,155
N,8,755
FILL,2,8
N,9,760  $N,10,825  $N,11,830  $N,12,895  $N,13,900  $N,14,965
N,15,970  $N,16,1035  $N,17,1040  $N,18,1105  $N,19,1110
N,20,1175  $N,21,1180  $N,22,1245  $N,23,1250
N,24,1345  $N,29,1845
FILL,24,29  $N,30,2000
NGEN,2,30,1,30,1,,,250  $NGEN,2,60,1,60,1,,250
/COM ***** ANCHORAGE *******
N,217,825  $N,218,830  $N,219,895  $N,220,900  $N,221,965  $N,222,970
N,223,1035  $N,224,1040  $N,225,1105  $N,226,1110  $N,227,1175
N,228,825,,250  $N,229,830,,250  $N,230,895,,250  $N,231,900,,250
```

```
N,232,965,,250   $N,233,970,,250   $N,234,1035,,250   $N,235,1040,,250
N,236,1105,,250   $N,237,1110,,250   $N,238,1175,,250
/COM ***** BEAM ******
N,121,825,280   $N,122,1175,280
NGEN,7,2,121,122,1,,70   $NGEN,10,2,133,134,1,,100
NGEN,3,32,121,152,1,,,125
/COM ************** ELEMENTS GENERATION ***********
/COM ***** COLUMN *******
TYPE,1   $MAT,1   $REAL,1            * CONCRETE ELEMENT
E,1,31,91,61,2,32,92,62   $EGEN,29,1,-1
/COM E,1,23,89,67,2,24,90,68   $EGEN,21,1,-1    $EGEN,2,22,-21
/COM ***** BEAM ********
E,70,100,185,121,80,110,186,122
E,121,153,155,123,122,154,156,124   $EGEN,15,2,-1   $EGEN,2,32,-15
/COM E,75,97,165,133,80,102,166,134
/COM E,97,119,197,165,102,124,198,166
/COM E,133,165,167,135,134,166,168,136
/COM EGEN,15,2,-1   $EGEN,2,32,-15
/COM ************  STEEL ELEMENTS ****************
TYPE,2   $MAT,2   $REAL,2
E,1,2   $EGEN,29,1,-1   $EGEN,2,30,-29   $EGEN,2,60,-58
TYPE,2   $MAT,2   $REAL,2
E,10,70   $E,70,121   $E,40,100   $E,100,185
E,20,80   $E,80,122   $E,50,110   $E,110,186
E,121,123   $EGEN,15,2,-1   $EGEN,2,1,-15   $EGEN,2,64,-30
TYPE,3    $MAT,3    $REAL,3
E,1,31   $E,31,91   $E,91,61   $E,61,1   $EGEN,7,1,-4
E,68,8   $E,8,38   $E,38,98   $E,9,69   $E,69,99   $E,99,39
E,100,70   $E,70,10   $E,10,40   $E,71,101   $E,101,41   $E,41,10
```

```
E,12,72   $E,72,102   $E,102,42   $E,73,13   $E,13,43   $E,43,103
E,104,74   $E,74,14   $E,14,44   $E,75,105   $E,105,45   $E,45,15
E,76,16   $E,16,46   $E,46,106   $E,17,77   $E,77,107   $E,107,47
E,108,78   $E,78,18   $E,18,48   $E,79,109   $E,109,49   $E,49,19
E,20,80   $E,80,110   $E,110,50   $E,81,21   $E,21,51   $E,51,111
E,112,82   $E,82,22   $E,22,52   $E,83,113   $E,113,53   $E,53,23
E,24,54   $E,54,114   $E,114,84   $E,84,24   $EGEN,7,1,-4
E,121,153   $E,153,185   $E,185,186   $E,186,154   $E,154,122   $E,122,121
EGEN,16,2,-6
/COM ************** BOUNDARY CONDITIONS *************
D,1,UX,,,91,30,UY
D,30,UY,,,120,30,UZ
/COM ************** DATA WRITE CONTROLS *************
WSORT,X                              * REORDER ELEMENTS IN X-DIRECTION
POSTR,1,1,6                          * POST STRESS INFORMATION LEVEL 6
CNVR, 0.05,,,300,1                   * SET CONVERGENCE CRITERIA
/COM ************** APPLIED FORCES ******************
F,30,FX,-12500,,120,30               * COLUMN AXIAL LOAD
F,149,FX,,,213,32                    * INITIAL APPLIED LOAD = 0 KN
AFWRITE                              * WRITE ANALYSIS FILE27
FINISH                               * EXIT PREP7 PREPROCESSING ROUTINE
/PREP6                               * ENTER PREP6 PREPROCESSING ROUTINE
NSTEPS,40                            * SET NUMBER OF LOAD STEPS TO 40
NTABLE,2                             * DEFINE TWO TABLES
FILL,1,1,4,1,-50                     * SET NUMBER OF ITERATIONS
FILL,2,1,4,1,2334,2334               * LOAD INCREMENT = 2.334 kN
NITTER,1                             * NUMBER OF ITERATIONS SET TO TABLE 1
FX,149,2                             * APPLIED LOAD SET TO TABLE 2
FX,181,2                                 =     =     =     =     =
```

```
FX,213,2                                =     =     =     =     =
FINISH                                * QUIT PREP6
/INPUT,27                             * EXECUTE FILE27
/INPUT,23                             * EXECUTE FILE23
FINISH
```